

# SUSTAINABLE MANUFACTURING PROCESSES

EDITED BY

R. GANESH NARAYANAN  
JAY S. GUNASEKERA



SUSTAINABLE  
MANUFACTURING PROCESSES

---

This page intentionally left blank

# SUSTAINABLE MANUFACTURING PROCESSES

---

*Edited by*

R. GANESH NARAYANAN

*Department of Mechanical Engineering, Indian Institute of Technology Guwahati,  
Guwahati, India*

JAY S. GUNASEKERA

*Department of Mechanical Engineering, University of Delaware, Newark,  
DE, United States*



ELSEVIER



**ACADEMIC PRESS**

An imprint of Elsevier

Academic Press is an imprint of Elsevier  
125 London Wall, London EC2Y 5AS, United Kingdom  
525 B Street, Suite 1650, San Diego, CA 92101, United States  
50 Hampshire Street, 5th Floor, Cambridge, MA 02139, United States  
The Boulevard, Langford Lane, Kidlington, Oxford OX5 1GB, United Kingdom

Copyright © 2023 Elsevier Inc. All rights reserved.

No part of this publication may be reproduced or transmitted in any form or by any means, electronic or mechanical, including photocopying, recording, or any information storage and retrieval system, without permission in writing from the publisher. Details on how to seek permission, further information about the Publisher's permissions policies and our arrangements with organizations such as the Copyright Clearance Center and the Copyright Licensing Agency, can be found at our website: [www.elsevier.com/permissions](http://www.elsevier.com/permissions).

This book and the individual contributions contained in it are protected under copyright by the Publisher (other than as may be noted herein).

Image of Harold Louis Gegel used with permission.

### Notices

Knowledge and best practice in this field are constantly changing. As new research and experience broaden our understanding, changes in research methods, professional practices, or medical treatment may become necessary.

Practitioners and researchers must always rely on their own experience and knowledge in evaluating and using any information, methods, compounds, or experiments described herein. In using such information or methods they should be mindful of their own safety and the safety of others, including parties for whom they have a professional responsibility.

To the fullest extent of the law, neither the Publisher nor the authors, contributors, or editors, assume any liability for any injury and/or damage to persons or property as a matter of products liability, negligence or otherwise, or from any use or operation of any methods, products, instructions, or ideas contained in the material herein.

ISBN: 978-0-323-99990-8

For information on all Academic Press publications visit our website at <https://www.elsevier.com/books-and-journals>

The Foreword by Katherine C. Morris is in the public domain as the foreword writer works for NIST., a US Government (Commerce Dept) agency.

2023 Published by Elsevier Inc.

*Publisher:* Matthew Deans

*Acquisitions Editor:* Brian Guerin

*Editorial Project Manager:* John Leonard

*Production Project Manager:* Surya Narayanan Jayachandran

*Cover Designer:* Mark Rogers



Typeset by TNQ Technologies

# Dedication

---

*Dedicated to the memory of  
our dear friend and great scientist*  
HAROLD LOUIS GEGEL, PHD, FASM  
(1933–2021)



Dr. Harold Louis Gegel was an internationally recognized Senior Scientist at the Materials Laboratory, Air Force Wright Aeronautical Laboratories, Dayton, Ohio. He led world-class materials processing research, which continues today to profoundly impact a wide range of manufacturing industries and applications. Dr. Gegel collaborated extensively with technical leaders from industry, universities, and other government agencies.

He received his doctorate degree from the Ohio State University. Dr. Gegel retired from his Air Force Senior Scientist position in 1988 and joined Universal Energy Systems, Inc., Dayton, Ohio, as Director of Processing Science Division until 1998. He received a Distinguished Life Member award from the American Society of Metals in 2004. Dr. Gegel was a great mentor, teacher, and role model for many researchers and technologists throughout the world including some authors and contributors of important work referenced in this book.

# Contents

---

<b>Contributors</b>	<b>xi</b>
<b>About the editors</b>	<b>xiii</b>
<b>Foreword</b>	<b>xv</b>
<b>Preface</b>	<b>xxi</b>
<b>Acknowledgment</b>	<b>xxiii</b>

## 1. Introduction to sustainable manufacturing processes

R. Ganesh Narayanan and Jay S. Gunasekera

1.1 Definition and importance	1
1.2 Manufacturing processes and sustainability implementation	3
1.3 Sustainability assessment	9
1.4 Computer-aided analyses and sustainable manufacturing	12
1.5 Industry 4.0 and sustainable manufacturing	16
1.6 Education for sustainability development	19
1.7 Summary	23
References	24

## 2. Sustainability in foundry and metal casting industry

Jatinder Madan and Prince Pal Singh

2.1 Introduction	29
2.2 What are foundry and metal casting processes?	30
2.3 Environmental issues in foundry and metal casting	32
2.4 Sustainability indicators for the foundry and metal casting industry	34
2.5 Concepts, technologies, management practices, and systems for sustainability assessment in the foundry and metal casting	38
2.6 IoT and Industry 4.0 in the foundry and metal casting	43
2.7 Summary	46
2.8 Disclosure	47
References	48

## 3. Sustainable manufacturing: material forming and joining

V. Satheeshkumar, R. Ganesh Narayanan, and Jay S. Gunasekera

3.1 Need for sustainable material forming	53
3.2 Extrusion and forging	55
3.3 Rolling and wire drawing	58

3.4 Sheet stamping	60
3.5 Flexible tooling	67
3.6 Green lubrication	69
3.7 Laser-based manufacturing	73
3.8 Need for sustainable joining processes	76
3.9 Sustainable fusion and solid-state welding processes	77
3.10 Mechanical joining	88
3.11 Adhesive bonding	91
3.12 Hybrid joining	92
3.13 Inclusive manufacturing	95
3.14 Summary	97
References	98
4. Sustainable manufacturing strategies in machining	
P. Sivaiah, D. Chakradhar, and R. Ganesh Narayanan	
4.1 Need for sustainable machining	113
4.2 Sustainable characteristics in machining	114
4.3 Sustainable machining techniques	115
4.4 Role of sustainable machining techniques in conventional machining processes	123
4.5 Sustainable nonconventional machining processes	133
4.6 Summary of recent developments, challenges, and future prospects	135
References	143
Further reading	153
5. Materials development for sustainable manufacturing	
R.J. Immanuel, S.K. Panigrahi, and James C. Malas	
5.1 Introduction	155
5.2 Need for development of materials	157
5.3 Classification of materials development	158
5.4 Microstructural modification of traditional materials	159
5.5 Optimization of material processing conditions	167
5.6 Material workability and microstructural control during deformation processes	169
5.7 Material processing maps	171
5.8 Role of activation energy	175
5.9 Role of stability	176
5.10 Increasing productivity of aluminum extrusion industry case study	180
5.11 Effects of prior processing history on workpiece behavior case study	182
5.12 Processing windows for different forms of Al-2024 materials case study	186
5.13 Stainless steel forging microstructure and property control case study	191
5.14 Summary	192
References	193

## 6. Sustainable product development process

Amer Ali and Jay S. Gunasekera

6.1 Innovation and product development	195
6.2 Product innovation strategy	196
6.3 Product life cycle	196
6.4 Product development process	198
6.5 Stage gate processes	199
6.6 NPD organization	201
6.7 Decision making process	201
6.8 Program release and launch	202
6.9 Proactive feedback mechanism and lessons learnt	203
6.10 Design processes, tools, and design for sustainability	203
6.11 Sustainability in remanufacturing	207
6.12 End of life design	207
6.13 Future outlook and direction	210
References	210

## 7. A case study on sustainable manufacture of Ti–6Al–4V ultralightweight structurally porous metallic materials by powder metallurgy route

Venugopal Srinivasan and James C. Malas

7.1 Introduction	213
7.2 ANTARES interface	220
7.3 Dynamic material model processing map	224
7.4 Summary	230
Further reading	230

## 8. Waste energy harvesting in sustainable manufacturing

Steve Zhengjie Jia

8.1 Introduction	231
8.2 Piezoelectric technology in sustainable manufacturing	235
8.3 Thermoelectric technology in sustainable manufacturing	242
8.4 Other energy harvesting technologies in sustainable manufacturing	249
8.5 Conclusion	254
References	254

## 9. Sustainability performance evaluation in manufacturing: theoretical and practical perspectives

N. Harikannan and S. Vinodh

9.1 Literature and state of art	257
9.2 Methodology	261

---

9.3 Case study	262
9.4 Results	278
9.5 Summary and recommendations	279
References	281
10. Additive manufacturing including laser-based manufacturing Soyeon Park, Kaiyue Deng and Kun Kelvin Fu	
10.1 Introduction and basic principles	285
10.2 Vat photopolymerization process (SLA)	290
10.3 Powder bed fusion process (PBF)	292
10.4 Extrusion-based process (FDM or FFF)	294
10.5 Jetting-based process (material jetting (MJ) and binder jetting (BJ))	296
10.6 Sheet lamination process (SL)	298
10.7 Directed energy deposition process (DED)	299
10.8 Hybrid manufacturing	300
10.9 Post-treatment processes	301
10.10 Sustainability issues in AM	304
10.11 Summary and future outlook	308
References	309
11. Computer integrated sustainable manufacturing Steve Zhengjie Jia, Jay S. Gunasekera, and James Glancey	
11.1 Introduction to computer integrated manufacturing	313
11.2 CAD/CAM/CAE in sustainable manufacturing	314
11.3 CAE in sustainable manufacturing	315
References	334
<b>Index</b>	<b>335</b>

# Contributors

---

- Amer Ali Management Consultant, Austin, TX, United States
- D. Chakradhar Department of Mechanical Engineering, IIT Palakkad, Palakkad, Kerala, India
- Kaiyue Deng Department of Mechanical Engineering, University of Delaware, Newark, DE, United States
- Kun Kelvin Fu Department of Mechanical Engineering, University of Delaware, Newark, DE, United States; Center for Composite Materials, University of Delaware, Newark, DE, United States
- James Glancey Mechanical Engineering, University of Delaware, Newark, DE, United States
- Jay S. Gunasekera Department of Mechanical Engineering, University of Delaware, Newark, DE, United States
- N. Harikannan Department of Production Engineering, National Institute of Technology, Tiruchirappalli, Tamil Nadu, India
- R.J. Immanuel Department of Mechanical Engineering, Indian Institute of Technology Bhilai, Sejbahar, Chhattisgarh, India
- Steve Zhengjie Jia Product Engineering, Litens Automotive Group, Toronto, ON, Canada
- Jatinder Madan Mechanical Engineering Department, Chandigarh College of Engineering and Technology (Degree Wing), Chandigarh, India
- James C. Malas Materials and Manufacturing Directorate, Air Force Research Laboratory, Dayton, OH, United States
- R. Ganesh Narayanan Department of Mechanical Engineering, Indian Institute of Technology Guwahati, Guwahati, Assam, India
- S.K. Panigrahi Department of Mechanical Engineering, Indian Institute of Technology Madras, Chennai, Tamil Nadu, India
- Soyeon Park Department of Mechanical Engineering, University of Delaware, Newark, DE, United States
- V. Satheeshkumar Department of Production Engineering, National Institute of Technology Tiruchirappalli, Tiruchirappalli, Tamil Nadu, India
- Prince Pal Singh Mechanical Engineering Department, I.K. Gujral Punjab Technical University, Kapurthala, Punjab, India

- P. Sivaiah Department of Mechanical Engineering, Madanapalle Institute of Technology & Science, Madanapalle, Andhra Pradesh, India
- Venugopal Srinivasan National Institute of Technology Nagaland, Chumukedima, Nagaland, India
- S. Vinodh Department of Production Engineering, National Institute of Technology, Tiruchirappalli, Tamil Nadu, India

# About the editors

---

## **R. Ganesh Naryanan**

Dr. R. Ganesh Narayanan is a Professor at the Department of Mechanical Engineering, Indian Institute of Technology (IIT), Guwahati, India. He received his Ph.D. from the IIT Bombay, India. His research areas of interest include Metal Forming and Joining. He has contributed many research articles in reputed journals and international conferences. He has edited several titles including: “*Sustainable Material Forming and Joining*” published by CRC press Boca Raton, “*Strengthening and Joining by Plastic Deformation*” published by Springer Singapore, “*Advances in Material Forming and Joining*” published by Springer India, and “*Metal Forming Technology and Process Modeling*” published by McGraw Hill Education, India. He has also edited several special journal issues including *Advances in Computational Methods in Manufacturing* in the *International Journal of Mechatronics and Manufacturing Systems*, and *Numerical Simulations in Manufacturing* in the *Journal of Machining and Forming Technologies*. He has organized three international conferences at IIT Guwahati, namely, the International Conference on Computational Methods in Manufacturing (ICMM) in 2011, the fifth International and 26th All India Manufacturing Technology, Design and Research (AIMTDR) Conference in 2014, and the second International Conference on Computational Methods in Manufacturing (ICMM) in 2019. He has also organized a GIAN course on “Green Material Forming and Joining” at IIT Guwahati in 2016.

## **Jay Gunasekera**

Jay Gunasekera is an Adjunct Professor in the Department of Mechanical Engineering of the University of Delaware, USA. He was previously the chair of the department of Mechanical Engineering at Ohio University, a Director of the SME/NAMRI board of the Society of Manufacturing Engineers, and North American editor of Elsevier’s *Journal of Materials Processing Technology*. He has undertaken research and consulting projects for the United States Air Force, General Electric, Pratt & Whitney, General Motors, and a large number of manufacturing companies in the US.

Dr. Gunasekera has published over 150 technical publications in refereed journals and conferences. He was awarded the highest doctorate (D.Sc.) Degree by the University of London in 1991 for his contribution in research and publications in the field of manufacturing engineering. He was made a Fellow of the City & Guilds of London, which is the highest honor conferred by that institution. He is a Fellow of SME & FRSA, past Fellow of IMechE, IProDE & IEE.

# Foreword

---

Dear Reader,

When I was asked to write the opening for this book, I was both delighted and humbled at the opportunity to be part of this important work. The focus of my own research at the National Institute of Standards and Technology (NIST) has been on propelling forward advances in sustainable manufacturing by creating repeatable practices using new technologies and standards for digital manufacturing. This book is a review of the results of efforts to create more Sustainable Manufacturing Processes over the last many years, and it encapsulates the foundations for the next evolutions to support this important area. My wish is that you find it an insightful reference as you venture on your own journey in the area of sustainable manufacturing.

The history of humankind is paved with ingenuity, cooperation, and competition. Some of the greatest technological leaps that have propelled us into the modern age were baited by competition and built on ingenuity and cooperation. Much of today's advanced manufacturing technologies started in the aftermath of World War II. During these times, our abilities and ingenuities were focused on new leaps in transportation, equipment, security, and space exploration. Using our deepest imaginations, we created the technologies that enabled man to go to the moon, robotic explorers to go to mars, telescopes to peer even deeper into the vast unknown expanse of space, satellites to provide instant communication around the world, and weapon systems to secure our nations. In those endeavors, we learned our strengths and our vulnerabilities as a human race.

The role of engineering and manufacturing in these undertakings cannot be overstated. The things we have achieved are the outcome of our collective and cooperative ingenuity applied to the pressing needs of the time and built on our imaginations to invent new products and solutions. The specification, precision, and certification of the capabilities needed to achieve such great feats are as vast as any scientific endeavor, and yet, in the reverse, the object under study is not purely a natural phenomenon but rather a complex system of human agreements, defined as a "discipline." These agreements enable us to construct and rely on a new kind of system—a system that incorporates natural phenomena together with a structured reality of our own making.

The engineers and manufacturers of today are being charged with forging ahead into a new world where our mission is one of global cooperation to ensure the survival of our species and ensure a continuously improving quality of life for the inhabitants of this world. As before, manufacturing is a pillar of this new society. While policy advocates may help to establish the will, it is the engineers and manufacturers who must define the way. From this challenge, sustainable manufacturing practices and principles emerge.

Sustainable manufacturing is one in which a carefully crafted balance of goals must not only be achievable but must also be manipulatable. The priorities of today will not be the same as those of tomorrow; the priorities in one locality may be different from those in others. Sustainable manufacturing will build on the digitalization of manufacturing in which the science behind the practice can be crafted and molded virtually before the actuality of production. Digitalization allows for focused experimentation to incrementally capture knowledge of the disciplines and add to our virtual understanding of the world. It enables exploration of yet unknown futures giving us the means to plan for desired outcomes and avoid crises.

This book is a story of sustainable manufacturing. It highlights the work developed in previous generations to enable the sophisticated manufacturing practices known today. It captures generations of learnings in how to manufacture more efficiently using a broad range of techniques by making the most of our resources—materials, energy, time, labor—while making the best achievable products. While the criteria that define these parameters are subject to shift, the systems must be such that they can adapt.

The challenge of the modern-day is how to sustain life on earth while continuing to improve the standard of living for the inhabitants. The world's population passed two billion inhabitants in 1928; in 2021 (less than 100 years later) that number was 7.9 billion and growing. Future projections by the UN indicate that growth rates will continue to rise and may pass 10 billion by the end of the century. In the meantime, standards of living around the world continue to increase. The result is growing demand for resources—food, energy, water, minerals, and other materials—pushing the bounds of the earth's capacities and threatening havoc for the environment.

Manufacturing must be part of the solution to provide good quality of life in an increasingly crowded world while managing available resources wisely. Currently, manufacturing and related supply chains account for a substantial portion of environmental impacts. Much of that is directly attributable to manufacturing production processes. Recent emphasis

toward decarbonization identified industrial emissions as one of the hardest sectors to address in terms of carbon reduction due in part to the diversity of manufacturing processes, where each will need to be addressed individually. To move toward global decarbonization, reductions in these emissions will be necessary. Some manufacturing processes will need to be adapted to account for new energy sources. Similar challenges exist with changing demands on material availability, particularly for critical minerals. Likewise, automobile manufacturing is being disrupted with the introduction of electric vehicles, and agri-food manufacturing is being transformed to improve efficiency and reduce waste in food processing and distribution.

The science that emerged to confront the challenges of the 20th century is being adapted to confront these growing strains on our natural environment. Virtual design and manufacturing developed to meet the needs for high-precision, high-value products. Equipment for the space race was characterized by single-use products that were costly, one of a kind, and irreplaceable. Little room for mistakes existed. Early attempts at space orbit were undertaken through the engagement of human “computers” who worked laboriously to calculate the data needed to validate the models. As “digital computers” came online advances happened much more rapidly. As a society, we learned how to use computers for much more than simple calculations.

Human ingenuity was brought to bear in creating models of new aerospace products so that manufacturing could be reasoned out before material was manipulated. Computer-aided design (CAD), finite element methods (FEM), computer integrated manufacturing (CIM), and other CAx technologies evolved along with the computer revolution. New software was developed to assist in forming the new models and to collect data necessary to validate capabilities against the real world in a systematic step-by-step fashion. Highly repeatable processes enabled new parts to be fully functional in the mind’s eye before they were forged, cast, or created by a growing set of manufacturing processes. Systems also emerged to integrate business processes inside an organization and through the supply chains.

Today, these approaches are growing to represent an even broader range of capabilities. Manufacturing is integral to modern living touching on things as useful as household goods and appliances, as fundamental as food, as varied as materials, and as indispensable as vaccines. The digital approaches and the manufacturing science developed for high-tech precision parts are being expanded to address this broad range of needs. Advances in computing technology including artificial intelligence (AI) and machine learning (ML) systems have evolved to manipulate the

abundance of data, identify patterns, and inform analyses across a range of production processes. Integration of analyses of different viewpoints on a single physical object has brought forth the concept of Digital Twins. Digital Twins coordinate a collection of virtual interdisciplinary models fed by data from today and expanded to imagine future possibilities.

The problems of the future take on a different scope than those from which these approaches emerged. We need to use manufacturing to the best of our abilities to create the products that will be needed by future generations to thrive within the resource constraints of our global ecosystem. Waste must become a thing of the past. Environmental impacts must be closely monitored, studied, and managed. The digital manufacturing capabilities that were born of the demanding high-tech needs of the 20th century must be brought to bear on the problems posed by human growth in the 21st century. Approaches to sustainable manufacturing through digitalization will be essential to addressing the needs of our future world.

As with the demands on engineering technologies, the demands on sustainable growth are many faceted and will rely on our institutions to see that technology continues to grow in the directions needed to address new challenges. Four distinct types of institutions form the pillars of support and growth for engineering and manufacturing:

- Academia provides for education for future generations of scientists and engineers to understand, maintain, and propel our capabilities forward.
- Trade associations, standards, and certification bodies are vanguards of the established, proven, and controlled disciplines of engineering and manufacturing with commitments to address the needs of tomorrow.
- The business community provides jobs and embodies the corporate values needed for our collective future. Already multinational corporations are beginning to rise to the sustainability challenge with the vast majority of the largest corporations working toward and reporting on more sustainability in their practices. Corporations must exist beyond a profit motive as they are the responsible party for executing toward our future outcomes.
- Governments represent societal interests in imagining and creating this new world, negotiating global and regional interests, directing resources, and establishing foundational capabilities and policies to move society in a positive direction.

Concerted efforts to bring together the perspectives of these diverse parties will result in a future as we need it to be. In the words of the late Dr. Hal Gegel to whom this book is dedicated:

Sustainability is a value shared by individuals and organizations who demonstrate this value in their management policies, daily activities, and social behavior. Individuals and organizations have played a key role in creating our current environmental and social circumstances. The denizens of today and future generations must create solutions and adapt them. The role of education in sustainability as a shared value is clear, education is a forever role that universities along with governments must provide for everyone. (*Dr. Gegel*)

Many great inventors of the world have credited their works to standing on the shoulders of giants. Each of us stands on the shoulders of not just those we have known and learned from, but every generation that came before those leaders and mentors. The knowledge passed down through the generations gives us the power to build and improve. For each person reading this book, my hope is that it is a source of conveying that power to collectively solve the shared challenges of future generations.

*KC Morris  
Engineering Laboratory Systems Integration Division  
Life Cycle Engineering Group Leader  
National Institute of Standards and Technology  
Gaithersburg, MD, USA  
April 2022*

This page intentionally left blank

# Preface

---

Metal casting, forming, machining, and joining are important manufacturing processes used to produce a variety of components existing in daily life. While these processes have seen significant developments in the last several decades, equivalent attention has not been provided toward sustainable manufacturing. Only in recent years has some emphasis been provided by policy makers, government bodies, industries, and academia on sustainability through enhanced use of renewable energy, establishment of sustainability practices, reduction in energy consumption and materials, reduction in emissions of wastes and effluents, and recycling of wastes and water. Research contributions have also improved in these domains.

The editors of the book organized a Global Initiative of Academic Networks (GIAN) course on “Green Material Forming and Joining” some years ago because they believed in the importance of sustainable manufacturing. They also organized a corresponding academic gathering to facilitate discussions, especially for students. The course provided the direction to edit the current book on *Sustainable Manufacturing Processes*.

There are *eleven chapters* in the book. The *first chapter* deals with an introduction to sustainable manufacturing processes by discussing the importance of sustainability, sustainability measures, the role of computational power, and Industry 4.0. The *second chapter* focuses on sustainability in foundry and metal casting industry, emphasizing environmental sustainability with consideration for industry important aspects. The *third chapter* is on “Sustainable material forming and joining,” which highlights the sustainable initiatives in material forming, and the developments in joining and welding in sustainable manufacturing. The *fourth chapter* deals with various methods of improving machining for sustainable manufacturing by the use of suitable cutting fluids, enhancing tool life, and reducing tool wear and workpiece distortion. The *fifth chapter* provides a summary of various sustainable material processing techniques accompanied by case studies. In *chapter six*, the use and development of processes, systems, organization, and tools in the product development process are discussed. The *seventh chapter* deals with a case study on sustainable manufacture of ultra-lightweight structurally porous metallic materials by powder metallurgy route. The common waste energy harvesting methods with the most potential to be adopted in sustainable manufacturing processes aims to improve energy efficiency has been

reported in *chapter eight*, along with conventional optimization-based strategies. Sustainability assessment is of paramount importance to quantify sustainability in industries. In this aspect, *chapter nine* accounts for sustainability performance evaluation using grey-based approach. Some of the recent developments in the field of additive manufacturing is presented in *chapter ten*. The *last chapter* provides a brief overview of computer-aided engineering techniques to demonstrate its importance in sustainable manufacturing with the help of industrial case studies.

The authors have provided bird's-eye view of the chosen topics. Further in-depth understanding can be gained by referring to the extensive reference database provided in the chapters. The authors and editors have taken great care in presenting the concepts and acknowledging the original sources. We believe that academia and industry experts will appreciate the contributions. Readers are encouraged to provide any constructive feedback for further improvement.

*R. Ganesh Narayanan, Jay S. Gunasekera*  
Editors

# Acknowledgment

---

The editors thank Ministry of Education, India, for introducing Global Initiative of Academic Networks (GIAN), which paved way for the professional collaboration between the editors that laid the foundation for the book. We are thankful to all the authors for their contributions in spite of their busy schedules. Their prompt email responses and chapter completion are acknowledged. We are grateful to Elsevier, Springer, ASM, NIST, EEA, and others for permitting to use the data in the journal articles, reports, and handbooks. We also thank the help rendered by the students of IIT Guwahati while formatting the figures in the book. Thanks to Arvind K. Agrawal, Tinu P. Saju, Pritam K. Rana, and Saibal K. Barik, who completed Ph.D. at IIT Guwahati, for helping us during GIAN course “Green Material Forming and Joining” in 2016. We also acknowledge the staff members of Elsevier for their patience and cooperation right from proposal stage to publication stage. Finally, we thank our spouses for showing patience during the book preparation and tolerating busy work schedules.

This page intentionally left blank

# Introduction to sustainable manufacturing processes

R. Ganesh Narayanan<sup>1</sup>, and Jay S. Gunasekera<sup>2</sup>

<sup>1</sup>Department of Mechanical Engineering, Indian Institute of Technology Guwahati, Guwahati, Assam, India; <sup>2</sup>Department of Mechanical Engineering, University of Delaware, Newark, DE, United States

## 1.1 Definition and importance

Some of the definitions of sustainable manufacturing (SM) are as follows.

- It is the design of human and industrial systems to ensure that humankind's use of natural resources and cycles do not lead to diminished quality of life due either to losses in future economic opportunities or to adverse impacts on social conditions, human health and the environment (Mihelcic et al., 2003).
- It is defined as the mass production of manufactured products through processes, which minimize negative environmental impacts, conserve energy, and natural resources, are safe for workers, communities, and consumers and are economically helpful (Gupta et al., 2016; Davim, 2010).
- It is the ability to smartly utilize available natural resources for manufacturing useful products and provide solutions that satisfy economic, environmental, and social objectives, without harming the environment, while continuing to improve the quality of human life (Garetti and Taisch, 2012). To achieve this, new technology, regulatory measures, and responsible social behavior are needed.

Although these are some definitions, an interesting observation by Moldavska and Welo (2017) reveals that SM has no unique definition. Some refer it as strategy or approach, whereas others define it as paradigm or system. According to their survey, several authors define SM as

creation or production of product and services in available literature. Other terms are provided in Fig. 1.1. Life cycle perspective that is predominantly discussed is not part of the definitions; however, total life cycle has been used in some of the articles for SM definitions. Moreover, as per UN, sustainable production is one of the sustainable development goals, which includes manufacturing as one of the measures toward sustainable development.

Sustainability and manufacturing are related in two sub-categories, namely, manufacturing for sustainability and sustainability of manufacturing, both are equally important as suggested in the literature in terms of number of articles (Moldavska and Welo, 2017). The sub-categories include both negative and positive aspects of manufacturing in day-to-day life. Manufacturing for sustainability mostly deals with development of products via new processes and materials that are better than conventional methods, while sustainability of manufacturing deals with maintaining sustainable production with conventional practices.

The importance of sustainable and green manufacturing lies in developing manufacturing technologies, raw materials, computational methods, policies for recycling and waste management, strategies for pollution control, effective business development, etc. with emphasis on appropriate use of resources without disrupting environment needs and reduce waste. This should include reduced use of hazardous raw materials, reduced energy utilization, and waste generation. The environmental concern while manufacturing a product was not there at all since the first industrial revolution. The development of processes did not take into account the effect of sustainability and green concepts, although there were innovations and novelty. Now-a-days, there are lots of importance

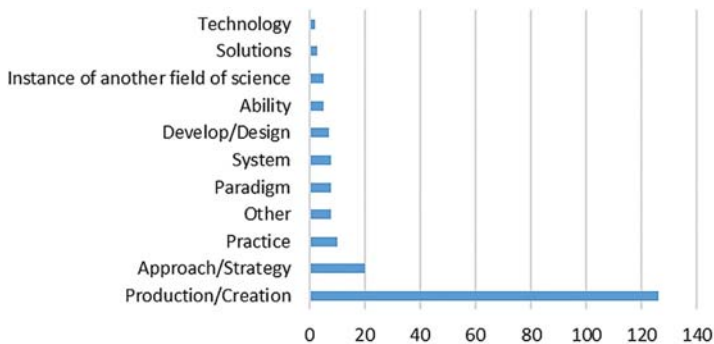


**FIGURE 1.1** Terms available in literature to define sustainable manufacturing concept. Used with permission from Moldavska, A., Welo, T., 2017. The concept of sustainable manufacturing and its definitions: a content-analysis based literature review. *Journal of Cleaner Production* 166, 744–755.

that the government bodies, nongovernment organizations, consumers, and top management of companies provide to involve sustainability as part of product and process development framework (Narayanan and Gunasekera, 2019). Such initiatives should be scientific in nature and should be validated on the shop floor for successful implementation and further improvements. To substantiate the importance of scientific interventions in implementing SM, a five-step guideline provided by Madan et al. (2015) to design an injection molding process can be referred. The framework suggest energy-based calculations and improvement for sustainable molding process. The decision support system predicted the experimental outputs reasonably well, and the difference is only 10%–30% considering the average inputs used for system development. Another example is fabrication of aluminum foam by powder metallurgy route using concentrated solar energy for sintering. The quality of solar sintered foams is good, and better mechanical properties such as compressive strength and impact energy absorption are achieved as compared with those made by conventional techniques. Such foams show impact-energy absorption of about  $25 \text{ MJ m}^{-3}$  and compressive strength of about 27 MPa (Canadilla et al., 2021).

## 1.2 Manufacturing processes and sustainability implementation

---

Casting, metal forming, welding and joining, machining, manufacturing by powder metallurgy, and recently, additive manufacturing (AM) are the major manufacturing processes through which components are fabricated. In casting, solidified metal blocks are manufactured through melting of raw materials and solidification after that. Sand casting, investment casting, die casting, and centrifugal casting are well-known casting processes. In metal forming, plastic deformation is utilized to provide permanent shape change to the raw material using rigid tools such as dies and punches. Some examples include rolling, extrusion, forging, wire drawing, sheet stamping, shearing, spinning, and tube forming. In joining, the raw materials or manufactured components are assembled, either permanently or temporarily, depending on the application. Welding, adhesive bonding, fastening, and riveting are some examples in joining processes. In machining, material removal forms the basis to attain the final shape of the product. Typical machining processes are turning, drilling, milling, shaping, broaching, sawing, etc. Powder metallurgy route is also well-known in which the raw material in the form of powder is consolidated and sintered to obtain mechanical and metallurgical bonding. Recently, AM is found to replace several conventional processes to make near-net shape components. In this, raw material in the form of powder or wire is

used to fabricate parts by adding layer by layer using a heat source. Almost in all situations, these processes are combined to manufacture engineering goods (Bastas, 2021). Since an elaborate discussion on sustainability aspects of such processes is provided in other chapters, a brief account is provided in this section with some examples. A book edited by Stark et al. (2017) on SM can also be referred for some specific case studies.

### 1.2.1 Sustainable reuse of spent foundry sand

Spent foundry sand (SFS) is the waste sand generated in foundry industries. Sustainable utilization of wastes in construction industries is an important pathway for sustainable production. In this context, in control concrete mix, natural sand in concrete is replaced with 5%–20% SFS (Siddique et al., 2018). Along with other advantages, using SFS increased compressive strength of concrete to 25–45 MPa as compared with 18–35 MPa for control concrete mix, and tensile strength improved to 2.5–4 MPa (Fig. 1.2). The variation depends on percentage composition of SFS in the control concrete mix. Above all, on introducing 20% SFS as replacement of sand, the cost of concrete is reduced by INR  $68\text{m}^{-3}$  in addition to reduction in  $\text{CO}_2$  emissions and saving in dumping expenditure of SFS. In another example, river sand is substituted by the discarded foundry sand obtained from steel molding industries for the production of lightweight concrete (Mailar et al., 2017). The crushed brick masonry aggregate is used as coarse aggregate for lab scale demonstration. Experimental observation reveals that the discarded foundry sand with 40% substitution level can be employed in constructing sloped roof slabs and architectural concrete blocks as these show good mechanical properties and durability.

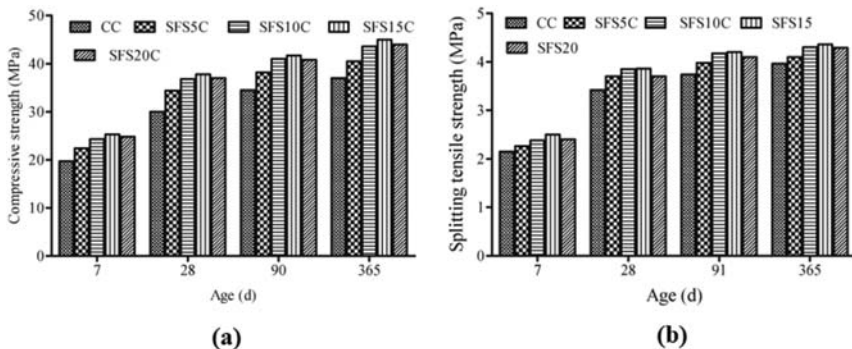


FIGURE 1.2 Influence of spent foundry sand on (A) compressive strength and (B) tensile strength of concrete. Used with permission from Siddique, R., Singh, G., Singh, M., 2018. Recycle option for metallurgical by-product (Spent Foundry Sand) in green concrete for sustainable construction. *Journal of Cleaner Production* 172, 1111–1120.

### 1.2.2 Sustainable fabrication of automotive components by metal forming route

Sustainable manufacturing of automotive components is possible by improving the efficiency of the manufacturing route, which can be achieved by resolving the ecological problems, achieving cost-saving, and adopting new standards and governmental policies. Hot forging of an automotive crankshaft can be made energy efficient by optimizing the in-line induction heating process prior to actual forging (Park and Dang, 2012). Seven heaters are involved in induction heating process, and as shown in Fig. 1.3A, the heaters are divided into three groups based on the temperature reached and penetration depth in the billet. Optimization of three variables such as voltage and two different frequencies is carried out through circuit coupled finite element modeling (Fig. 1.3B) and genetic algorithm. The finite element model includes four assumptions such as ignoring the helicity of the induction coil, adequacy of 2D model for a spiral inductor, ignoring the displacement of the heated billet, and ignoring the heat transfer by conduction in the axial direction. It is observed that the energy efficiency can be increased up to 6%, and the uniform heating of billet is possible as compared with the unoptimized case. By providing insulation in open spaces, about 4% of energy can be saved.

The impact of light weighting of automobile components is enormous in the context of SM. For example, a bumper beam of a compact car made of aluminum alloy saved approximately 210 and 190 MJ kg<sup>-1</sup> of aluminum in primary energy, and approximately, 16 and 15 CO<sub>2</sub> equivalent/kg of aluminum in greenhouse gas, in two different vehicles. Similarly, the aluminum front hood of a large passenger car saved

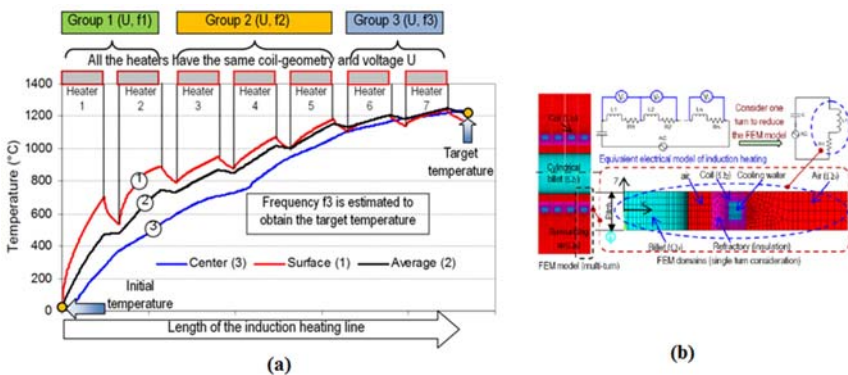


FIGURE 1.3 (A) Division of heaters into three groups and (B) circuit coupled finite element modeling of induction heating. Used with permission from Park, H.S., Dang, X.P., 2012. Optimization of the in-line induction heating process for hot forging in terms of saving operating energy. *International Journal of Precision Engineering and Manufacturing* 13(7), 1085–1093.

170 MJ kg<sup>-1</sup> of aluminum in primary energy and 13 CO<sub>2</sub> equivalent/kg of aluminum in greenhouse gas. The accident rate of passengers can also be reduced by weight reduction. Existing examples show that by light weighting, maintaining same size, the injury rate is reduced by 15%. Further reduction in injury rate is observed for the same weight but with increase in the size (<http://www.world-aluminium.org/>).

### 1.2.3 Fusion and solid-state welding and sustainability

Among fusion welding process, gas tungsten arc welding (GTAW) or tungsten inert gas welding (TIG) is extensively used to join thin sections of stainless steel, however, with lots of difficulties in case of thick sections in single pass. The difficulties disrupt maintaining sustainability in GTAW. Activated-TIG (A-TIG) is developed to improve the weld penetration up to 1.5–4 times in a single pass, helping us to maintain sustainability during welding. In A-TIG, a thin activated flux layer on the plates enhances the weld penetration. The activated flux is a paste, which is a mixture of an oxide or a halide powder and acetone or methanol. During welding, the paste evaporates, leaving a layer of the activated flux on the plate's surface (Pandya et al., 2021). There will be lots of energy savings in single pass A-TIG welding as compared to multi-pass TIG welding; however, it suffers from high amount of slug due to entrapment of oxide flux, which can be minimized by two modifications such as flux bounded TIG (FB-TIG) and flux zone TIG (FZ-TIG) welding processes.

Solid-state welding process, particularly friction stir welding (FSW), is a sustainable welding process (Mishra and Ma, 2005). It is energy efficient, ecofriendly, and flexible. Although there are several studies highlighting its efficiency (E.g. Shrivastava et al., 2015), a novel variant “friction welding of tube-to-tube plate using an external tool (FWTPET)” proposed by Senthil Kumaran et al. (2012) consumes lesser power of 0.1874 kWh as compared with TIG welding consuming 0.6755 kWh, reduces the power charge from Rs. 3.377 to Rs. 0.937, and reduces welding time from 16 min to 0.683 min. The joint formed is sufficiently strong as compared to TIG welding.

### 1.2.4 Sustainable machining

To achieve sustainable machining, all the aspects such as machining performance, materials behavior, lubricant type, lubrication method, production rate, and machine life expectancy have compounding effect. Cutting fluids reduce friction and force requirements and have potential to improve tool performance during machining is a good candidate for improving sustainability in machining. These fluids are predominantly introduced by flooding, and hence, minimum quality lubrication (MQL)

becomes crucial as part of clean and SM. Although this is the case, if the fluid consumption is excessive, cleaning costs and disposal costs of cutting fluids increase, which permits dry machining to become a good candidate. Tool cost is very high in this case. MQL scores well due to low raw material cost, fluid consumption, tool cost, cleaning costs, and disposal costs (Benedicto et al., 2017). Commercially available cutting fluids show harmful effects to our environment and also pose severe health related problems to workers. As an alternative, several green cutting fluids are developed. For example, Somashekaraiah et al. (2016) developed a new formulation for green cutting fluid, which is at par with that of commercial formulation, and results such as corrosion prevention, inhibition of microbial growth, and machining performance are encouraging. The cutting fluid is composed of coconut oil base (50 mass %), emulsifiers (40 mass%), and additives (10 mass %). It is mixed with deionized water at 1:20 ratio for testing and characterization. Mild steel turning and drilling experiments reveal that its performance is better than that of commercial fluid in several occasions.

Machining tool design, such as textured tools, enhances the tool life due to better heat transfer and continual supply of fluid into the mating surface (result of significant hydrodynamic lift force). Example provided by Gupta et al. (2021) during turning of Inconel 718, a hard-to-cut material, having a length of 100 mm and diameter of 30 mm showed that nanofluids with textured tool delivered superior results in comparison with other cooling conditions. One of the results on maximum flank wear shows that case C6 (hBN cooling with textured tool under MQL) showed minimum flank wear (Fig. 1.4) as compared with other cases such dry turning, nitrogen cooling, and hBN cooling with and without textured tool.

### 1.2.5 Sustainability of additive manufacturing

Near-net shape manufacturing of parts is feasible by AM with environmental benefits such as (i) improved efficiency and flexibility in product design, (ii) requirement of reduced raw material in the supply chain, (iii) a good replacement for energy-loaded, wasteful, and polluting processes, (iv) improved carbon footprint, and (v) decentralization of component manufacturing and production at the vicinity of consumption. However, it has limitations such as low productivity, surface integrity, repeatability and geometric accuracy. Environmental impact of AM, which is part of three sustainable dimensions along with economic and social impacts, can be assessed by resource consumption, waste management, and pollution control (Peng et al., 2018). Energy consumption by AM main equipment and auxiliary parts, and material consumption, from raw material to protective gas, are the two main agents in resource

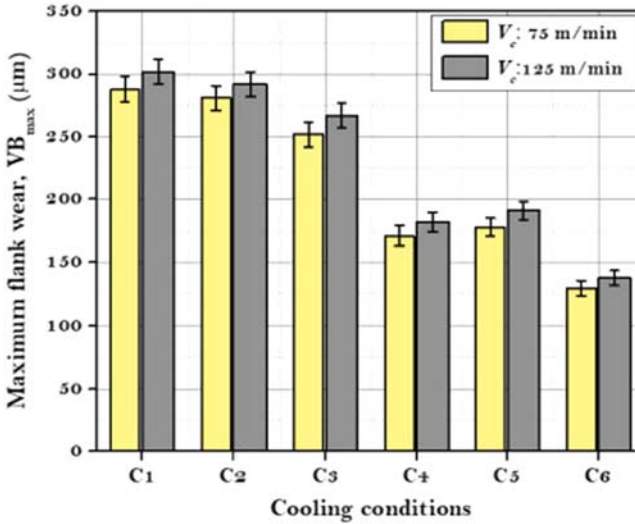


FIGURE 1.4 Flank wear during turning of Inconel 718 using textured and nontextured tools. Used with permission from Gupta, M.K., Song, Q., Liu, Z., Singh, R., Sarikaya, M., Khanna, N., 2021. Tribological behavior of textured tools in sustainable turning of nickel based super alloy. *Tribology International* 155, 106775–106788.

consumption. Resource wastages are seen specifically in lengthy product making schedule. Waste management in AM is crucial as there are nonrecyclable waste powder, scraps from defective parts, and support structures for making overhanging parts. Pollution control of AM is still in the rudimentary stage. A study made by Gebler et al. (2014) through model calculations reveal that by 2025 a.m. (or 3D printing, 3DP) has the potential to reduce costs by 170–593 billion USD, CO<sub>2</sub> emissions by 130.5–525.5 Mt, and total primary energy supply by 2.54–9.30 EJ. They have used the following models for calculations.

$$\text{Changes in costs: } \Delta C = \text{GDP}_{3\text{DP}} \times \Delta C_{3\text{DP}}$$

where  $\Delta C$  is the absolute change in costs,  $\text{GDP}_{3\text{DP}}$  is the market potential of 3DP, and  $\Delta C_{3\text{DP}}$  is the relative change in costs through 3DP compared with conventional processes.

$$\text{Changes in energy: } \Delta e = \frac{\text{GDP}_{3\text{DP}} \times \text{TPES}}{\text{GDP} \times \Delta e_{3\text{DP}}}$$

where  $\Delta e$  is the absolute change in energy, total primary energy supply-intensity (TPES)/gross domestic product (GDP) is the total primary

energy supply-intensity per GDP, and  $\Delta e_{3DP}$  is the relative change in energy through 3DP compared with conventional processes.

$$\text{Changes in CO}_2 \text{ emissions: } \Delta \text{CO}_2 = \frac{\text{GDP}_{3DP} \times \text{CO}_2}{\text{GDP} \times \Delta \text{CO}_{2,3DP}}$$

where  $\Delta \text{CO}_2$  is the absolute change in  $\text{CO}_2$  emissions,  $\text{CO}_2/\text{GDP}$  is the  $\text{CO}_2$  emission-intensity per GDP, and  $\Delta \text{CO}_{2,3DP}$  is the relative change in  $\text{CO}_2$  emissions through 3DP compared to conventional processes.

### 1.3 Sustainability assessment

There are several barriers to SM systems in industry practice specifically in micro, small and medium enterprises (MSME). [Virmani et al. \(2020\)](#) classified the barriers into four categories (specific to MSMEs in automobile industries) and ranked them as well in the order of importance: (i) production and operations related, (ii) organization related, (iii) collaboration-related barriers, and (iv) government rules and regulations. Production and operations barriers are more to do with lack of research facilities, lack of latest manufacturing facilities, weak operational information technology, underutilization of skilled manpower, and inert to accept changes. Barriers in organization are mainly due to top management team, lack of funds and corporate social responsibility, lack of policies, and initiatives for SM. Top management is the enabler of green supply chain in manufacturing practices. Nonintegration of suppliers and customers and passive industry networks lead to collaboration-related barriers. It is a good idea if supplier collaboration exists in providing better alternatives and solutions to difficulties met on the shop floor. Finally, government policies should support and propose strategies to implement green and sustainable initiatives efficiently. At the same time, government should be vigilant while imposing regulations ([Bag et al., 2018](#); [Modgil et al., 2020](#); [Koho et al., 2020](#); [Patala et al., 2014](#)). Currently, efforts are underway to promote more SM from a range of organizations including standards development organizations especially ISO and ASTM International, as well as efforts from the international community following through on the UN Sustainable Development Goals, and the investment community through the Sustainability Standards Accounting Board and others. These efforts are seeing a trickle down to even the small and medium size manufacturers (SMMs) ([Kibira et al., 2018](#); [Mani et al., 2016](#); [Komoto et al., 2020](#); [Escoto et al. 2022](#)). A paper by [Escoto et al. \(2022\)](#) expands on the global efforts toward more sustainable practices and highlights recent progress of SM toward inclusion of SMMs via standards. It argues a business case for SMM to move forward with SM at

this time. The study reviews the role that different standards fill and highlights those that are instrumental in pursuing manufacturing sustainability objectives.

In order to counteract such barriers, sustainability assessment and quantification are crucial. It avoids vagueness that aids in easy implementation of sustainability in manufacturing arena. Sustainability indicators (SIs) are helpful in this aspect, however, has no clear cut definition. As per [Heink and Kowarik \(2010\)](#), indicators have ambiguous definition and changes with context. In the context of ecology and environmental planning, a general definition of indicator is, It is a component or a measure of environmentally relevant phenomena used to depict or evaluate environmental conditions or changes or to set environmental goals [Heink and Kowarik \(2010\)](#)

To address these challenges, ASTM International E60.13 Subcommittee on Sustainable Manufacturing published a series of standards for SM.<sup>1</sup> At the core of these is a standard for representing “unit manufacturing processes” or UMPs ([ASTM 2020](#)). These specifications call for clear and precise formats for digitally representing manufacturing processes in terms of the inputs, outputs, resources, product and process information, and their transformation functions ([Mani et al., 2016](#)). Performance indicators are unique to each manufacturing process and the circumstances surrounding its operation. ASTM E3096-18 Standard Guide for Definition, Selection, and Organization of Key Performance Indicators for Environmental Aspects of Manufacturing Processes. [ASTM \(2018\)](#) specifies a consensus-based decision-making process, involving multiple stakeholders within a manufacturing organization, to set the indicators best suited to their particular situation ([Kibira et al., 2018](#)). A range of globally published indicator sets serves as input into this process. In SM, sustainability is measured via a number of publicly available indicator sets that are from various reports, unions, and policies ([Joung et al., 2013](#)).

- Global report initiative (GRI)
- Dow Jones Sustainability Indexes (DJSI)
- 2005 Environmental Sustainability Indicators (ESI)
- Environment Performance Index (EPfi)
- United Nations-Indicators of Sustainable Development (UN-CSD)
- Organization for Economic Cooperation and Development (OECD) Core Environmental Indicators (CEI)
- Ford Product Sustainability Index (Ford PSI)
- International Organization for Standardization (ISO) Environment Performance Evaluation (EPE) standard (ISO 14031)

<sup>1</sup><https://www.astm.org/get-involved/technical-committees/committee-e60/subcommittee-e60/jurisdiction-e6013>.

- Environmental Pressure Indicators for European Union (EPRI)
- Japan National Institute of Science and Technology Policy (NISTEP)
- European Environmental Agency Core Set of Indicators (EEA-CSI)

In 2018, the Sustainability Standards Accounting Board (SASB) published a set of 77 industry accounting standards in which the standards most relevant to the different industries were highlighted (“SASB” n.d.). Since that time, progress has been made toward a more comprehensive reporting standards through a collaboration of the five leading organizations in this space.

Generally, Triple Bottom Line (TBL) approach including environmental stewardship, economic growth, and social well-being are considered for sustainability assessment. A good example of this is provided by Sarkar et al. (2009), in which the following models (in Table 1.1) are used to evaluate the sustainability of manufacturing and selling packaged drinking water in a US-based company.

Three choices such as a 1-L mineral water bottle that is used and discarded for recycling, reusable aluminum bottles, repackaged water bottle with 1 USD incentive to those returning the used water bottle are attempted and tested for sustainability using the models (Equations 1–3). Finally, they demonstrated that selling repackaged water bottle is sustainable (Sarkar et al., 2009).

As per National Institute of Standards and Technology (NIST)’s categorization methodology, there are five dimensions to SM as listed in

TABLE 1.1 Models used to calculate environmental impact, economic benefit, and social value of the product (Sarkar et al., 2009).

Measurement	Models
Environmental impact (EI) of product	$EI = N(f(M_{new}, E_{new})) \text{ (1) where } M_{new} = \sum_{I=1}^{TM} M_{I-new}$ <p>and <math>E_{new} = \sum_{I=1}^{TE} E_{I-new}</math>. Here <math>M_{I-new}</math> includes various new materials added, <math>E_{I-new}</math> includes various new energies added, <math>TM</math> is the total number of different types of materials added and <math>TE</math> is the total number of different types of energies added.</p>
Economic benefit	$\text{Profit} = N(P-C) \text{ (2) where } N \text{ is the number of products sold by the company, } P \text{ is the price of the product, } C \text{ is the cost incurred on the product, which includes cost of manufacture, labor, transportation and other costs.}$
Social value (S)	$S = N(L \times F \times D \times \alpha) \text{ (3) where } N \text{ represents total number of products sold during a specific period, } L \text{ represents level of importance, } F \text{ for frequency of usage, } D \text{ for duration of benefit per usage, } \alpha \text{ is the average number of people using the same kind of product.}$

Fig. 1.5. As per NIST, along with environmental impact, economic benefit, and social value, technological advancement, and performance management are added. Each category has various sub-categories as well (Joung et al., 2013). They have also proposed sustainability evaluation process that involves eight different steps as shown in Fig. 1.6. Using such measurement process, a company can evaluate the level of sustainability by referring to some benchmark values, which are decided either based on past performance data, or standards, or by factor of safety. The sustainability level should either be equal to the benchmark or exceeding that (Fig. 1.7). Sustainability evaluation software tools help in quick assessment (Mani et al., 2012, 2013). Mani et al. (2014) have highlighted several avenues to characterize sustainability of AM parts that aid in developing benchmark for AM processes.

## 1.4 Computer-aided analyses and sustainable manufacturing

In several occasions, the shop floor trials are preceded by computational analyses. This helps in minimizing the cost and time involved in conducting the actual trials by materials savings, electric power savings, reduced machine utilization, minimizing defects and scrap, shortening time-to-market for manufactured goods, fuel savings, and pollution control. Enhancing computational power assists in successful implementation of sustainability in manufacturing environment. Narayanan

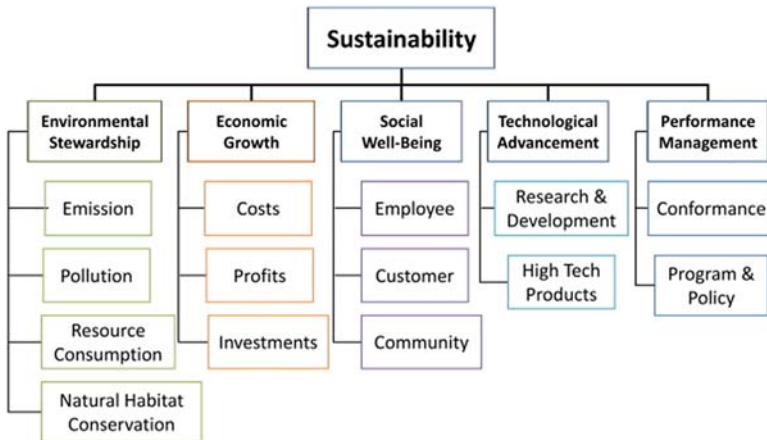


FIGURE 1.5 Sustainability categorization as per the National Institute of Standards and Technology. Used with permission from Joung, C.B., Carrell, J., Sarkar, P., Feng, S.C., 2013. Categorization of indicators for sustainable manufacturing. *Ecological Indicators* 24, 148–157.

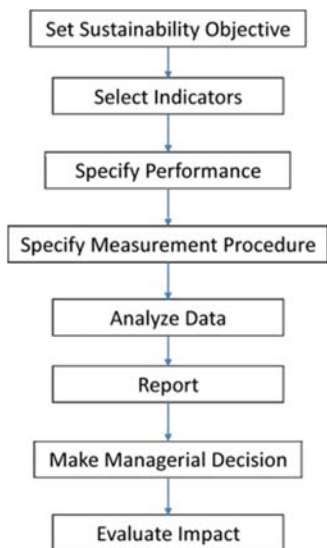


FIGURE 1.6 Sustainability evaluation process and steps. *Used with permission from Joung, C.B., Carrell, J., Sarkar, P., Feng, S.C., 2013. Categorization of indicators for sustainable manufacturing. Ecological Indicators 24, 148–157.*

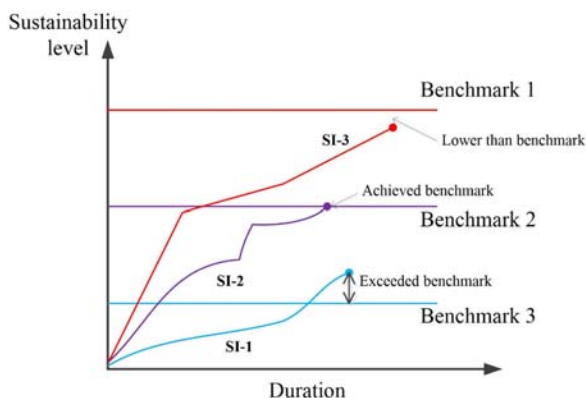


FIGURE 1.7 Proposed performance evaluation process.

and Das (2014) elaborately discussed how computations help in SM in real industries via several case studies. Although there are several such case studies, as rightly pointed out by Kibira and McLean (2008), the prime reason for building manufacturing simulations is to provide support tools that help the manufacturing decision-making process efficiently and effectively. Often such manufacturing simulation involves steps such as framing hypothesis and model the operation with validation, compare

the performance of current and proposed systems as per laid out metrics, and finally, implementing the proposed changes if the improvements suggested by simulations are acceptable. In traditional manufacturing, specific assistance rendered by computations and simulations are evaluating the manufacturability of new product designs, development, and validation of process data for new products, developing new production systems and processes, and developing benchmarks for continuous of manufacturing operations. When sustainability enters the framework, the scope of computations and simulations enlarges by the inclusion of environment aspects of manufacturing systems. Sustainability metrics such as energy utilization, pollution control, material wastes, workers safety, and social impact play as synergistic role in changing the framework of computations and simulations. In modeling SM, probably discrete modeling strategy may not work well. A combined, organized framework called as “system dynamic modeling framework” is required as suggested by [Kibira et al. \(2009\)](#). The framework includes four domains namely manufacturing, environmental, financial, and social domain. In such situations, multicriteria optimization and system dynamics optimization methods in combination with various modeling techniques (such as finite element method) are required, and the mathematical tool would be handy in modeling problems from the sustainability context ([Schenker et al., 2017](#); [Borndörfer et al., 2016](#)). Development of two solvers, PolySCIP and SD-SCIP, are presented to deal with applications from sustainability manufacturing, right from scheduling, manufacturing and production to planning subsidies and taxes, and furthermore in future. With the introduction of smart manufacturing technologies, where manufacturing systems are highly connected across an organization, standard-driven frameworks for sustainability assessment and optimization are evolving and allowing sustainability consideration to be incorporated in decision-making tools to address the complexity of competing objectives ([Bernstein et al., 2019, 2020](#); [Brodsky et al., 2016](#); [Lu et al. 2016](#); [Hatim et al., 2020](#)).

A virtual machining model for sustainable machining proposed by [Shao et al. \(2010\)](#) includes model inputs, the simulation model, and model outputs. Model inputs include NC program, workpiece, and cutting tool models. Along with machine tool and controller details like in traditional machining, energy consumption model, cutting tool status model, coolant/lubricant oil waste prediction model, metal chips model, etc. are the elements that should be included in the simulation model to make it suitable for sustainability prediction. Finally, model outputs will have sustainability report ([Shao et al., 2010](#)). Such a system-based modeling and sustainability calculation was also supported by [Lanz et al. \(2010\)](#) after conducting energy optimization during high-speed CNC machining of aluminum and titanium. They concluded that “it is more appropriate to

focus the energy saving goal on the system and facility level rather than optimizing locally to generate a win-win situation for the companies and the environment with lower cost and smaller environmental impact" (Lanz et al., 2010). Like virtual machining model, a computer-aided framework or system for sustainability analyses will be handy. These can be termed as sustainability analyzer. For instance, in a die casting industry, the sustainability analyzer should have facilities to select die casting metal or alloy, die casting process, process plan database, sub-process, output reports on fuel consumption, electric power consumed, raw material wastes, carbon emission (kg of CO<sub>2</sub>), and other sustainability outputs relevant to the process (Singh et al., 2012). For choosing process plan, a database is required. Similarly, for sustainability outputs, furnace database, die casting machines, and other database are mandatory. Manufacturing automotive piston by gravity die casting at Federal Mogul Goetze, Patiala, India, and making a tap knob by pressure die casting at HGI automotives, Faridabad, India, are the two case studies demonstrated by Singh et al. (2012). The sustainability analyzer predictions when compared with real-time data on fuel consumption, electric power consumed, raw material wastes, carbon emission (kg of CO<sub>2</sub>) reveal about 4%–7% differences between them, which are within acceptable level considering the industrial-scale production. Similarly, decision support system aids in improving sustainability of manufacturing processes (Shin et al., 2017).

Information models based on System Integration for Manufacturing Applications (SIMA) scheme and Green System Integration for Manufacturing Applications (Green SIMA) in the context of sustainability predictions would be helpful in capturing information to enable consistent computation and evaluation of sustainability performance indicators (Valivullah et al., 2014). Recent past embraced big data analytics to redefine the focus of the advanced manufacturing technology toward smart manufacturing, novel innovations and efficient handling of numerous data sets, which actually help SM in improving the life of people (E.g., developing materials like biodegradable materials) (Dubey et al., 2016; Kumar et al., 2018). Contribution of robot in SM is inevitable. Appropriate usage of robots in assembly lines leads to reduction in energy consumption and the overall energy requirements of shop floor. In such situations, optimization and simulation of the entire process cycle will be helpful to maintain sustainability. Cloud-based optimization proposed by Wang et al. (2018) resulted in optimized configuration leading to overall energy reduction by modeling inverse kinematics and dynamics of the robot from the cloud (Fig. 1.8).

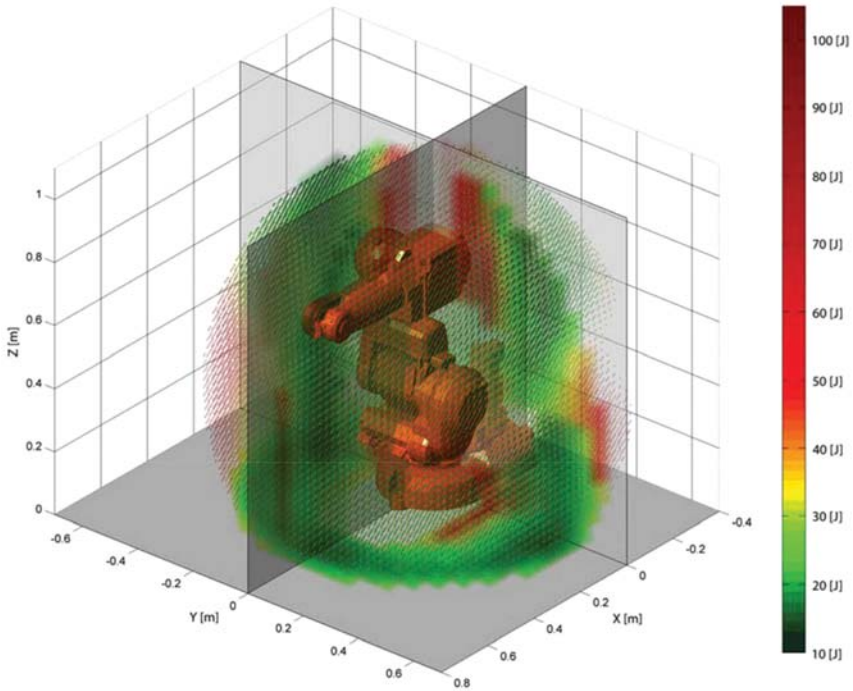


FIGURE 1.8 Energy map in the workspace of an ABB IRB 140 robot. *Used with permission from Wang, L., Mohammed, A., Wang, X.V., Schmidt, B., 2018. Energy-efficient robot applications towards sustainable manufacturing. International Journal of Computer Integrated Manufacturing 31 (8), 692–700.*

## 1.5 Industry 4.0 and sustainable manufacturing

The concept of Industry 4.0 (or Industry 4.0 Technologies, I4T) is to integrate Cyber-Physical-System (CPS) and Internet of Things (IoT) technologies into manufacturing operations at industry scale. Digitalization and automation are the main motives here. CPS and IoT help in vertical integration (integrating people, machines, and resources) and horizontal integration (integrating companies in supply chain), primarily IT driven, that are aimed to improve the overall efficiency of industry systems including sustainable manufacturing (Machado et al., 2020; Bakkari and Khatory, 2017; Lasi et al., 2014; Liao et al., 2017; Morrar et al., 2017). Micro perspective of I4T is provided in Fig. 1.9 (Stock and Seliger, 2016), which covers both horizontal integration and vertical integration of various activities in the form of smart factories. The NIST Smart manufacturing system landscape takes a similar approach but also looks at integration across three lifecycles: product system, production system, and supply chain (Lu et al. 2016).

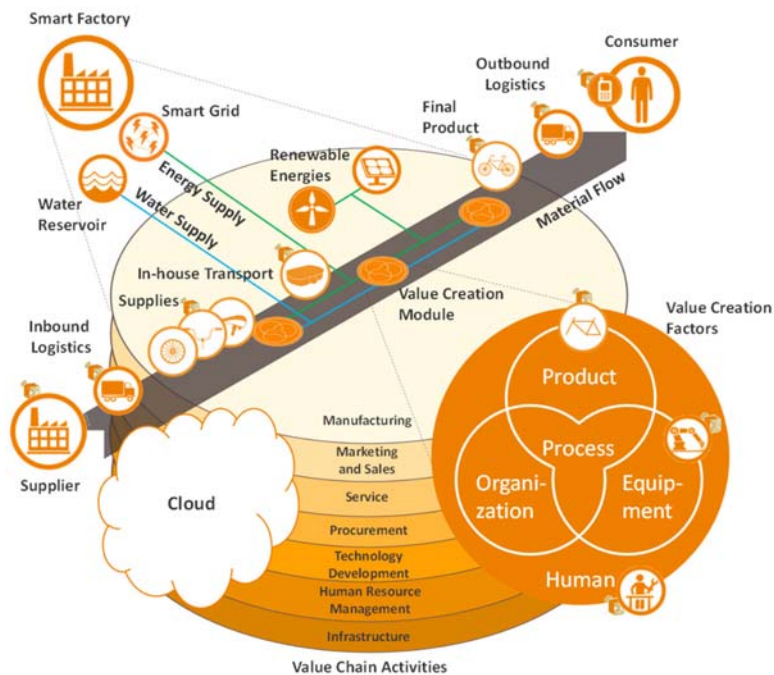


FIGURE 1.9 I4T: Microperspective. *Used with permission from Stock, T., Seliger, G., 2016. Opportunities of sustainable manufacturing in industry 4.0. Procedia CIRP 40, 536–541.*

The relation between supplier and consumer via logistics, raw material supplies, water and energy supplies, and final product making is clearly shown. The contribution of product, organization, equipment, and human factors is depicted in the form of value creation factors. In the meantime, [de Man and Strandhagen \(2017\)](#) showed how sustainability and I4T are related to business models. It covers all the contemporary topics such as autonomous robots, modeling simulation of plant operations, cloud services, AM, cybersecurity, big data analytics, etc. Sustainability provides helping hand, for example, in big data–driven predictive maintenance that improves productivity, energy consumption reduction, system-level coordination between machine, products, people, and companies, creating employment opportunities, etc., all part of scope of I4T. For instance, Purdue research foundation and researchers develop a cloud-based collaborative platform that aims to provide manufacturers with a detailed mapping of interindustrial dependence that helps to achieve manufacturing target based on material requirements (<https://manufacturingglobal.com/technology/purdue-university-drives-sustainable-manufacturing-processes>). With the introduction of these new technologies, the concept of sustainable

TABLE 1.2 Initiatives taken by Indian educational institutes for implementing courses related to sustainable development in their curricula.

Implementation details	Education institute	
Introduced sustainable development components into existing programs	IITs, IIMs, and some universities and colleges	
Created special programs such as		
(a)	Masters in Sustainable Development	Jadavpur University, University of Madras
(b)	Masters in Public Policy and Sustainable Development	TERI University
(c)	MBA in Business Sustainability	TERI University
(d)	Leadership Programme on Nutrition Security and Sustainable Development	Indira Gandhi Open National University
Included courses or modules on sustainable development in various subject areas such as		
(a)	Society and Environment in Department of Sociology	University of Hyderabad, Jammu University
(b)	Principles of Sustainable Development Course in ME Environmental Management	Anna University
(c)	Shodh Yatra	IIM, Ahmedabad
Green campus	TERI University	
Faculty organized community projects	University of Pune	
Student based activities such green colleges, symposia and action projects	South Asia youth Environment Network, Students at various HE institutions	
NGO conducted programs: curriculum reorientation and community engagement, teacher training	Centre for Environment Education	

TABLE 1.2 Initiatives taken by Indian educational institutes for implementing courses related to sustainable development in their curricula.—cont'd

Implementation details	Education institute
Based on law requirements on environmental studies with a sustainable development focus	Several undergraduate courses

*Used with permission from Chhokar, K.B., 2010. Higher education and curriculum innovation for sustainable development in India. International Journal of Sustainability in Higher Education 11 (2), 141–152.*

manufacturing has introduced the ability to share manufacturing data earlier in the product life cycle including at the design stage. Brundage et al. discuss the opportunities for introducing knowledge of manufacturing processes at different stages in the production lifecycle (Brundage et al., 2018). Ultimately, the data collected during manufacturing may be useful for upstream activities too, such as tracking material and processing information for evaluating use phase efficiency or end-of-use processing of products. This type of information will be necessary for transitioning to a Circular Economy where materials will be reintroduced into the marketplace after their intended purpose is met (Winans et al. 2017; Maya Reslan et al., 2022).

I4T is also related to lean manufacturing practices as preparing accurate value stream maps is the primary step in such practices. A value stream map is used to map a collection of activities that channelize a product or service from its initial stage to the customer. The main advantage of such a map is to design a future state with reduced lean waste (Kamble et al., 2020).

## 1.6 Education for sustainability development

The importance of disseminating the “sustainability” concept in academic community through education is significant. Education plays a larger role in making the academic community aware of the role of sustainability in manufacturing. The academic community should be ready to introduce curricula modification, create awareness among students through expert talks, seminars, group discussion, projects, change in attitude of staffs to consider such initiatives, develop centers, specializations, and departments on sustainable manufacturing in educational institutes. A survey study conducted by Chhokar (2010) on higher education and curriculum innovation for sustainable development in India attempts to present the initiatives geared to sustainable

**TABLE 1.3** Implemented modifications in Mechanical engineering curricula and in sustainable engineering in several universities (Kumar et al., 2005; Narayanan and Gunasekera, 2019).

Institution	Curricula modification
University of Delaware	<p>At the mechanical engineering department of U. of Delaware, a course on “sustainable manufacturing” meant for undergraduate and graduate students has been introduced recently. The course covers sustainability in material forming, joining, and foundry industries. It also covers the latest topics such as micro manufacturing, hydroforming, laser based manufacturing, and e-mobility. The assistance provided by computational aspects such as CAD/CAM, FEM, soft computing methods etc. are also highlighted. Several topics are listed for seminars from students.</p>
Villanova University	<p>A new department in sustainable engineering has been initiated in the university. Master’s degree program trains students to solve manufacturing problems from lifecycle point of view. The university also offers the Sustainable enterprise executive education and development program, a certificate program, and PhD focusing on sustainable engineering. Several research focus areas are suggested to students including energy studies, sustainable materials, and sustainable infrastructure and water resources. Minor in sustainable engineering or sustainability studies or humanitarian studies are also possible for undergraduate students.</p>
University of Kentucky College of Engineering	<p>Institute of sustainable manufacturing focus on research areas such as sustainable manufacturing processes, materials, manufacturing systems, product development, and economic analyses. The institute is home to a</p>

**TABLE 1.3** Implemented modifications in Mechanical engineering curricula and in sustainable engineering in several universities (Kumar et al., 2005; Narayanan and Gunasekera, 2019).—cont'd

Institution	Curricula modification
	journal, international journal of sustainable manufacturing, which emphasizes research articles based on science-based sustainability principles and their applications in fabricating innovative products and novel processes highlighting economic, environmental and societal aspects of sustainability.
John Hopkins University	Formulated a committee to monitor the changes in syllabus, incorporated nontechnical topics, floated new courses and modules in sustainability
University of Illinois at Chicago	Introduced computer science courses and methods to specialize in selected topics in computer science
University of Notre Dame	Created courses with industry collaborations that are oriented toward microprocessor based mechanical systems
Rice University	Introduced virtual laboratory courses to model dynamic systems
Kettering University, USA	Incorporated problem based learning by using computer simulations and animations to teach thermodynamics courses
Georgia Institute of Technology, USA	<p>Following are the initiatives in the institute for sustainable technology and development.</p> <ul style="list-style-type: none"> <li>• Inclusion of sustainability content in the existing courses</li> <li>• New courses in sustainability are not developed</li> <li>• Provides research and guidance support to help bringing about curricula change</li> </ul>
University of Washington, USA	<p>Under the design for environment lab,</p> <ul style="list-style-type: none"> <li>• Developed interdisciplinary courses on energy and environment</li> </ul>

*Continued*

**TABLE 1.3** Implemented modifications in Mechanical engineering curricula and in sustainable engineering in several universities (Kumar et al., 2005; Narayanan and Gunasekera, 2019).—cont'd

Institution	Curricula modification
University of Michigan, USA	<ul style="list-style-type: none"> <li>• Created discussion forum on environment issues to update the day-to-day requirements</li> </ul> <p>In center for sustainable systems,</p> <ul style="list-style-type: none"> <li>• Developed hydrogen technology in undergraduate curriculum</li> <li>• Initiated collaborative effort between School of natural resources and environment, and college of literature arts, and science, and developed a new curriculum in environment</li> </ul>
Michigan Tech, USA	<p>Conceived sustainable futures institute,</p> <ul style="list-style-type: none"> <li>• Focused on environment decision making by integrating eco-engineering, environment assessment and modeling, economic and human behavior elements of social sciences</li> <li>• Developed courses on engineering for environment, sustainable futures, life cycle engineering and environmentally responsible design and manufacturing for UG/PG students.</li> </ul>
University of Technology, Sydney	<p>Under institute of sustainable futures, they implemented,</p> <ul style="list-style-type: none"> <li>• Introduced sustainability related courses at graduate level, and conducted research in sustainability and green issues relevant to several engineering subjects</li> </ul>
Norwegian University of Science and Technology (NTNU)	<p>At NTNU, a 2 years M.Sc. program in sustainable manufacturing has been initiated. Students will get expertise in product development, project management, IT, I4T-CPS, design for sustainable manufacturing, and operations management. The courses are taught via lectures, group task,</p>

**TABLE 1.3** Implemented modifications in Mechanical engineering curricula and in sustainable engineering in several universities (Kumar et al., 2005; Narayanan and Gunasekera, 2019).—cont'd

Institution	Curricula modification
Cranfield University	seminars and laboratory based training.  Sustainable manufacturing systems center has been initiated focusing on manufacturing processes, systems, modeling, and simulation. Research themes that are of interest include sustainable materials and manufacturing, energy storage and harvesting, system-level modeling, biomanufacturing, data analytics, and several other advanced topics.

development in higher education in India. One important point concluded from the survey is in order to have a successful initiative to implement sustainability in education system, capacity among teachers should be improved by introducing them the links between environment and development. They should be trained to contextualize the sustainability content as per the discipline requirements and experiment the pedagogic methods to ascertain successful implementation of sustainability in curriculum. A summary of implementation of sustainability-related courses in Indian education system is provided in [Table 1.2](#).

The following case studies indicate the strategies followed in a few US educational institutes. [Kumar et al. \(2005\)](#) through a survey attempted to implement some changes in their university undergraduate mechanical engineering curriculum. They finally suggested that sustainability implementation should focus on the design and manufacture of products and systems. As per their analyses, [Table 1.3](#) lists some of the initiatives implemented by few US universities in mechanical engineering subject and, in general, in sustainable engineering.

## 1.7 Summary

The chapter attempts to present some salient topics in sustainable manufacturing with their importance. Some case studies are provided highlighting the importance of research behind implementing sustainability in manufacturing ecosystem. The relationship between concepts such as Industry 4.0 and sustainable manufacturing has been highlighted. It can be summarized that digitalization and automation that are core of

Industry 4.0 propeling the success of implanting sustainability in manufacturing field. The same has been evident from the discussion on role of computations and software tools in assessing sustainability in the form of indicators and in converting a nonsustainable process to sustainable and green. Education for sustainability development is also crucial, and several examples on subjects relevant to sustainability being implemented in various international universities are summarized. Several such initiatives are required at educational institutes to disseminate the sustainability concept and its importance in manufacturing.

## References

- ASTM, 2018. Standard Guide for Definition, Selection, and Organization of Key Performance Indicators for Environmental Aspects of Manufacturing Processes. ASTM International, West Conshohocken, PA. <https://doi.org/10.1520/E3096-18>.
- ASTM, 2020. Standard Guide for Characterizing Environmental Aspects of Manufacturing Processes. ASTM International, Conshohocken, PA. <https://doi.org/10.1520/E3012-20>. ASTM E3012-20).
- Bag, S., Gupta, S., Telukdarie, A., 2018. Importance of innovation and flexibility in configuring supply network sustainability. *Benchmarking: An International Journal* 25 (9), 3951–3985.
- Bakkari, M., Khatory, A., 2017. Industry 4.0: strategy for more sustainable industrial development in SMEs. In: *Proceedings of the IEOM 7th International Conference on Industrial Engineering and Operations Management*, pp. 11–13. Rabat, Morocco.
- Bastas, A., 2021. Sustainable manufacturing technologies: a systematic review of latest trends and themes. *Sustainability* 13 (8), 4271–4293.
- Benedicto, E., Carou, D., Rubio, E.M., 2017. Technical, economic and environmental review of the lubrication/cooling systems used in machining processes. *Procedia Engineering* 184, 99–116.
- Bernstein, W.Z., Tamayo, C.D., Lechevalier, D., Brundage, M.P., 2019. Incorporating unit manufacturing process models into life cycle assessment workflows. In: *Procedia CIRP*, 80:364–69. 26th CIRP Conference on Life Cycle Engineering (LCE) Purdue University, West Lafayette, IN, USA May 7–9, 2019. <https://doi.org/10.1016/j.procir.2019.01.019>.
- Bernstein, W.Z., Tensa, M., Praniewicz, M., Kwon, S., Ramanujan, D., 2020. An automated workflow for integrating environmental sustainability assessment into parametric Part Design through standard reference models. *Procedia CIRP*, 27th CIRP Life Cycle Engineering Conference (LCE2020) Advancing Life Cycle Engineering : From Technological Eco-Efficiency to Technology that Supports a World that Meets the Development Goals and the Absolute Sustainability 90 (January), 102–108. <https://doi.org/10.1016/j.procir.2020.02.058>.
- Borndörfer, R., Schenker, S., Skutella, M., Strunk, T., 2016. PolySCIP. In: Greuel, G.M., Koch, T., Paule, P., Sommese, A. (Eds.), *Mathematical Software – ICMS 2016*. ICMS 2016. Lecture Notes in Computer Science, vol 9725. Springer, Cham.
- Brodsky, A., Krishnamoorthy, M., Bernstein, W.Z., Omar Nachawati, M., 2016. A system and architecture for reusable abstractions of manufacturing processes. *IEEE International Conference on Big Data (Big Data)*, 2004–13. IEEE, Washington, DC, USA. <https://doi.org/10.1109/BigData.2016.7840823>.

- Brundage, M.P., Bernstein, W.Z., Hoffenson, S., Chang, Q., Nishi, H., Kliks, T., Morris, K.C., 2018. Analyzing environmental sustainability methods for use earlier in the product lifecycle. *Journal of Cleaner Production* 187 (June), 877–892. <https://doi.org/10.1016/j.jclepro.2018.03.187>.
- Cañadilla, A., Romero, A., Rodríguez, G.P., 2021. Sustainable production of powder metal-lurgy aluminum foams sintered by concentrated solar energy. *Metals* 11 (10), 1544–1562.
- Chhokar, K.B., 2010. Higher education and curriculum innovation for sustainable development in India. *International Journal of Sustainability in Higher Education* 11 (2), 141–152.
- Davim, J.P., 2010. *Sustainable Manufacturing*, first ed. John Wiley & Sons, Inc., New Jersey.
- de Man, J.C., Strandhagen, J.O., 2017. An Industry 4.0 research agenda for sustainable business models. *Procedia CIRP* 63, 721–726.
- Dubey, R., Gunasekaran, A., Childe, S.J., Wamba, S.F., Papadopoulos, T., 2016. The impact of big data on world-class sustainable manufacturing. *International Journal of Advanced Manufacturing Technology* 84 (1–4), 631–645.
- Escoto, X., Gebrehewot, D., Morris, K.C., 2022. Refocusing the barriers to sustainability for small and medium-sized manufacturers. *Journal of Cleaner Production* 338, 130589. <https://doi.org/10.1016/j.jclepro.2022.130589>.
- Garetti, M., Taisch, M., 2012. Sustainable manufacturing: trends and research challenges. *Production Planning & Control* 23 (2–3), 83–104.
- Gebler, M., Uiterkamp, A.J.S., Visser, C., 2014. A global sustainability perspective on 3D printing technologies. *Energy Policy* 74, 158–167.
- Gupta, K., Laubscher, R.F., Davim, J.P., Jain, N.K., 2016. Recent developments in sustainable manufacturing of gears: a review. *Journal of Cleaner Production* 112, 3320–3330.
- Gupta, M.K., Song, Q., Liu, Z., Singh, R., Sarikaya, M., Khanna, N., 2021. Tribological behavior of textured tools in sustainable turning of nickel based super alloy. *Tribology International* 155, 106775–106788.
- Hatim, Q.Y., Saldana, C., Shao, G., Bong Kim, D., Morris, K.C., Witherell, P., Rachuri, S., Kumara, S., 2020. A decision support methodology for integrated machining process and operation plans for sustainability and productivity assessment. *International Journal of Advanced Manufacturing Technology* 107 (7), 3207–3230. <https://doi.org/10.1007/s00170-019-04268-y>.
- Heink, U., Kowarik, I., 2010. What are indicators? On the definition of indicators in ecology and environmental planning. *Ecological Indicators* 10 (3), 584–593.
- Joung, C.B., Carrell, J., Sarkar, P., Feng, S.C., 2013. Categorization of indicators for sustainable manufacturing. *Ecological Indicators* 24, 148–157.
- Kamble, S., Gunasekaran, A., Dhone, N.C., 2020. Industry 4.0 and lean manufacturing practices for sustainable organisational performance in Indian manufacturing companies. *International Journal of Production Research* 58 (5), 1319–1337.
- Kibira, D., McLean, C., 2008. Modeling and simulation for sustainable manufacturing. In: *Proceedings of the 2nd IASTED 2008 Africa Conference on Modeling and Simulation*, p. 11.
- Kibira, D., Jain, S., McLean, C., 2009. A system dynamics modeling framework for sustainable manufacturing. *Proceedings of the 27th Annual System Dynamics Society Conference* 301, 1–22.
- Kibira, D., Brundage, M.P., Shaw, F., Morris, K.C., 2018. Procedure for selecting Key performance indicators for sustainable manufacturing. *Journal of Manufacturing Science and Engineering* 140 (1), 011005. <https://doi.org/10.1115/1.4037439>.
- Koho, M., Tapaninaho, M., Heilala, J., Torvinen, S., 2020. Towards a concept for realizing sustainability in the manufacturing industry. *Journal of Industrial and Production Engineering* 32 (1), 12–22.
- Komoto, H., Bernstein, W.Z., Kwon, S., Kimura, F., 2020. Standardizing environmental performance evaluation of manufacturing systems through ISO 20140. *27th CIRP life cycle*

- engineering conference (LCE2020)Advancing life cycle engineering : from technological eco-efficiency to technology that supports a world that meets the development goals and the absolute. *Sustainability* 90, 528–533. <https://doi.org/10.1016/j.procir.2020.02.043>.
- Kumar, V., Haapala, K.R., Rivera, J.L., Hutchins, M.J., Endres, W.J., Gershenson, J.K., Michalek, D.J., Sutherland, J.W., 2005. Infusing sustainability principles into manufacturing/Mechanical Engineering curricula. *Journal of Manufacturing Systems* 24, 215–225.
- Kumar, A., Shankar, R., Thakur, L.S., 2018. A big data driven sustainable manufacturing framework for condition-based maintenance prediction. *Journal of Computational Science* 27, 428–439.
- Lanz, M., Mani, M., Leong, S., Lyons, K., Ranta, A., Ikkala, K., Bengtsson, N., 2010. Impact of energy measurements in machining operations. *International Design Engineering Technical Conferences and Computers and Information in Engineering Conference* 44113, 867–873.
- Lasi, H., Fettke, P., Kemper, H.G., Feld, T., Hoffmann, M., 2014. Industry 4.0. *Business & Information Systems Engineering* 6 (4), 239–242.
- Liao, Y., Deschamps, F., Loures, E.F.R., Pierin Ramos, L.F., 2017. Past, present and future of Industry 4.0-a systematic literature review and research agenda proposal. *International Journal of Production Research* 55 (12), 3609–3629.
- Lu, Y., Morris, K.C., Frechette, S., 2016. Current Standards Landscape for Smart Manufacturing Systems." NIST IR 8107. National Institute of Standards and Technology. <https://doi.org/10.6028/NIST.IR.8107>.
- Machado, C.G., Winroth, M.P., Ribeiro da Silva, E.H.D., 2020. Sustainable manufacturing in Industry 4.0: an emerging research agenda. *International Journal of Production Research* 58 (5), 1462–1484.
- Madan, J., Mani, M., Lee, J.H., Lyons, K.W., 2015. Energy performance evaluation and improvement of unit-manufacturing processes: injection molding case study. *Journal of Cleaner Production* 105, 157–170.
- Mailar, G., Raghavendra, S.N., Hiremath, P., Sreedhara, B.M., Manu, D.S., 2017. Sustainable utilization of discarded foundry sand and crushed brick masonry aggregate in the production of lightweight concrete. *Engineering Structures and Technologies* 9 (1), 52–61.
- Mani, M., Madan, J., Lee, J.H., Lyons, K., Gupta, S.K., 2012. Characterizing sustainability for manufacturing performance assessment. *International Design Engineering Technical Conferences and Computers and Information in Engineering Conference* 45011, 1153–1162.
- Mani, M., Madan, J., Lee, J.H., Lyons, K.W., Gupta, S.K., 2013. Review on Sustainability Characterization for Manufacturing Processes. National Institute of Standards and Technology, Gaithersburg, MD. Report No. NISTIR 7913.
- Mani, M., Lyons, K.W., Gupta, S.K., 2014. Sustainability characterization for additive manufacturing. *Journal of Research of the National Institute of Standards and Technology* 119, 419–428.
- Mani, M., Larborn, J., Johansson, B., Lyons, K.W., Morris, K.C., 2016. Standard representations for sustainability characterization of industrial processes. *Journal of Manufacturing Science and Engineering* 138 (10). <https://doi.org/10.1115/1.4033922>.
- Mihelcic, J.R., Crittenden, J.C., Small, M.J., Shonnard, D.R., Hokanson, D.R., Zhang, Q., Chen, H., Sorby, S.A., James, V.U., Sutherland, J.W., Schnoor, J.L., 2003. Sustainability science and engineering: the emergence of a new metadiscipline. *Environmental Science and Technology* 37 (23), 5314–5324.
- Mishra, R.S., Ma, Z.Y., 2005. Friction stir welding and processing. *Materials Science and Engineering: R: Reports* 50 (1–2), 1–78.

- Modgil, S., Gupta, S., Bhushan, B., 2020. Building a living economy through modern information decision support system and UN sustainable development goals. *Production Planning & Control* 31 (1–2), 967–987.
- Moldavska, A., Welo, T., 2017. The concept of sustainable manufacturing and its definitions: a content-analysis based literature review. *Journal of Cleaner Production* 166, 744–755.
- Morrar, R., Arman, H., Mousa, S., 2017. The fourth industrial revolution (industry 4.0): a social innovation perspective. *Technology Innovation Management Review* 7 (11), 12–20.
- Narayanan, R.G., Das, S., 2014. Sustainable and green manufacturing and materials design through computations. *Proceedings of the Institution of Mechanical Engineers-Part C: Journal of Mechanical Engineering Science* 228 (9), 1581–1605.
- Narayanan, R.G., Gunasekera, J.S. (Eds.), 2019. *Sustainable Material Forming and Joining*, first ed. CRC Press. <https://doi.org/10.1201/9781315163147>.
- Pandya, D., Badgujar, A., Ghetiya, N., 2021. A novel perception toward welding of stainless steel by activated TIG welding: a review. *Materials and Manufacturing Processes* 36 (8), 877–903.
- Park, H.S., Dang, X.P., 2012. Optimization of the in-line induction heating process for hot forging in terms of saving operating energy. *International Journal of Precision Engineering and Manufacturing* 13 (7), 1085–1093.
- Patala, S., Hamalainen, S., Jalkala, A., Pesonen, H.-L., 2014. Towards a broader perspective on the forms of eco-industrial networks. *Journal of Cleaner Production* 82 (1), 166–178.
- Peng, T., Kellens, K., Tang, R., Chen, C., Chen, G., 2018. Sustainability of additive manufacturing: an overview on its energy demand and environmental impact. *Additive Manufacturing* 21, 694–704.
- Reslan, M., Last, N., Mathur, N., Morris, K.C., Ferrero, V., 2022. Circular economy: a product life cycle perspective on engineering and manufacturing practices. In: *29th CIRP Conference on Life Cycle Engineering*. Elsevier, Leuven.
- Sarkar, P., Rachuri, S., Suh, H.W., Lyons, K., Sriram, R.D., 2009. A measure of product sustainability based on triple bottom line. *International Design Engineering Technical Conferences and Computers and Information in Engineering Conference* 49057, 267–274.
- “SASB.” n.d. SASB. Accessed September 4, 2020. <https://www.sasb.org/>.
- Schenker, S., Vierhaus, I., Borndörfer, R., Fügenschuh, A., Skutella, M., 2017. Optimisation methods in sustainable manufacturing. In: *Sustainable Manufacturing*. Springer, Cham, pp. 239–253.
- Senthil Kumaran, S., Muthukumaran, S., Venkateswarlu, D., Balaji, G.K., Vinodh, S., 2012. Eco-friendly aspects associated with friction welding of tube-to-tube plate using an external tool process. *International Journal of Sustainable Engineering* 5 (2), 120–127.
- Shao, G., Kibira, D., Lyons, K., 2010. A virtual machining model for sustainability analysis. *International Design Engineering Technical Conferences and Computers and Information in Engineering Conference* 44113, 875–883.
- Shin, S.J., Kim, D.B., Shao, G., Brodsky, A., Lechevalier, D., 2017. Developing a decision support system for improving sustainability performance of manufacturing processes. *Journal of Intelligent Manufacturing* 28 (6), 1421–1440.
- Shrivastava, A., Krones, M., Pfefferkorn, F.E., 2015. Comparison of energy consumption and environmental impact of friction stir welding and gas metal arc welding for aluminium. *CIRP Journal of Manufacturing Science and Technology* 9, 159–168.
- Siddique, R., Singh, G., Singh, M., 2018. Recycle option for metallurgical by-product (Spent Foundry Sand) in green concrete for sustainable construction. *Journal of Cleaner Production* 172, 1111–1120.
- Singh, P., Madan, J., Singh, A., Mani, M., 2012. A computer-aided system for sustainability analysis for the die-casting process. *International Manufacturing Science and Engineering Conference* 54990, 1087–1096.

- Somashekaraiah, R., Gnanadhas, D.P., Kailas, S.V., Chakravorty, D., 2016. Eco-friendly, non-toxic cutting fluid for sustainable manufacturing and machining processes. *Tribology Online* 11 (5), 556–567.
- Stark, R., Seliger, G., Bonvoisin, J., 2017. *Sustainable Manufacturing: Challenges, Solutions and Implementation Perspectives*. Springer Nature, Cham, Switzerland.
- Stock, T., Seliger, G., 2016. Opportunities of sustainable manufacturing in industry 4.0. *Procedia CIRP* 40, 536–541.
- Valivullah, L., Mani, M., Lyons, K.W., Gupta, S.K., 2014. Manufacturing process information models for sustainable manufacturing. *International Manufacturing Science and Engineering Conference* 45806, 1–8.
- Virmani, N., Bera, S., Kumar, R., 2020. Identification and testing of barriers to sustainable manufacturing in the automobile industry: a focus on Indian MSMEs. *Benchmarking: An International Journal* 28 (3), 857–880.
- Wang, L., Mohammed, A., Wang, X.V., Schmidt, B., 2018. Energy-efficient robot applications towards sustainable manufacturing. *International Journal of Computer Integrated Manufacturing* 31 (8), 692–700.
- Winans, K., Kendall, A., Deng, H., 2017. The history and current applications of the circular economy concept. *Renewable and Sustainable Energy Reviews* 68 (February), 825–833. <https://doi.org/10.1016/j.rser.2016.09.123>.

# Sustainability in foundry and metal casting industry

*Jatinder Madan<sup>1</sup> and Prince Pal Singh<sup>2</sup>*

<sup>1</sup>Mechanical Engineering Department, Chandigarh College of Engineering and Technology (Degree Wing), Chandigarh, India; <sup>2</sup>Mechanical Engineering Department, I.K. Gujral Punjab Technical University, Kapurthala, Punjab, India

## 2.1 Introduction

Foundry and casting practices are among the oldest manufacturing methods; the first casting of metals can be traced way back to 4000 BCE. Casting of copper frog is the oldest existing casting believed to be produced in 3200 BCE in Mesopotamia (present-day Iraq) (Olsen, 2020). Signs of other metals being cast in history are available, the most prominent being bronze, cast iron, and gold. During 14th and 15th centuries, foundry industries were common in Europe and Russia, where bronze and iron bells, canons, and cannonballs were quite popular.

Even though numerous technological advancements have brought several other manufacturing processes to the industry, popularity of the foundry and metal casting industry is not waning, instead is aggressively serving automotive, general engineering, and construction sectors. This is primarily due to inherent capabilities that metal casting processes provide, such as low cost, flexibility to select a wide range of batch sizes, production of near net shape parts, and quality of parts produced. Market potential of metal casting industry is considerable, estimated to be US\$ 18.73 billion in 2016, which is projected to grow at a compound annual growth rate of 8.87% during the forecast period (2017–25) to reach US\$ 39.94 billion by 2025 (Markets and Markets, 2017).

A wide variety of metal casting processes is now available, the most notable being sand casting, gravity die casting, low-pressure die casting (LPDC) and high-pressure die casting (HPDC); on the top of that, many techniques and materials are available to prepare the molds, which are used to realize the metal casting process. Contemporary manufacturing industry employs metal casting processes to make a wide range of products useful for diverse applications, such as automobile, aerospace, consumer goods, defense and electronics, making use of different materials like steel, cast iron, aluminum, and magnesium, and many processes, such as sand casting and die casting, benefiting from a number of technologies available today. It would not be wrong to say that metal casting and foundry is indispensable part of the manufacturing industry.

## 2.2 What are foundry and metal casting processes?

A number of foundry and metal casting processes exist, which may be classified depending upon the type of metal and procedure adopted. They may be broadly classified into ferrous and nonferrous based on the type of metal used and collapsible mold and permanent mold based on the type of mold used. The foundry and metal casting processes possess a lot of similarities in the concepts they apply, as all of them use molten metal and a cavity to receive it, followed by solidification of the molten metal; vast differences exist in their methods, materials, processing conditions, and process capabilities. For example, sand mold casting makes use of collapsible mold made of molding sand to prepare the cavity, followed by pouring the molten metal at near atmospheric pressures. On the other hand, the HPDC process uses a permanent reusable metal mold also called die, pouring the metal at a very high pressure, and taking the solidified part out of the die.

The most common steps used in the foundry and metal casting processes are illustrated with the help of [Fig. 2.1](#). The operations within the system boundary, considered to be the factory walls, are melting, molding, pouring, cleaning, finishing, finished castings and packaging. Foundry shops often use fossil fuel-fired furnaces such as cupola and reverberatory furnaces to melt ingots and scrap materials. The furnaces remove moisture and other volatiles, such as paint, machining oils, and other contaminants from the charge, preventing the risk of an explosion in the furnace. These furnaces provide a large reservoir to ensure a steady and reliable supply of preheated molten metal to the plant. The preheated molten metal is withdrawn from the furnaces by tapping using a bull ladle. The preheated molten metal is then transferred to the induction furnace where molten metal is heated above pouring temperature and

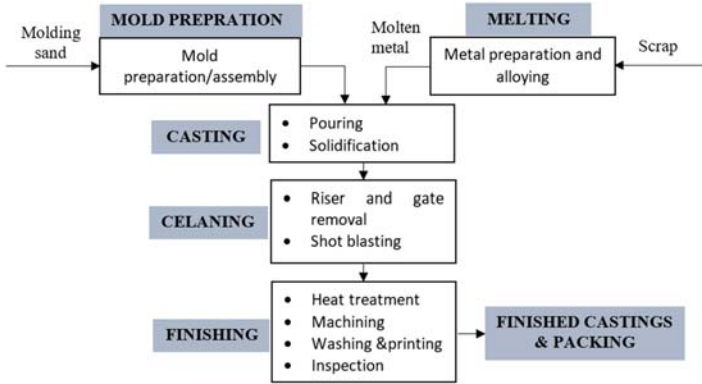


FIGURE 2.1 Steps in foundry and metal casting processes.

alloys, such as silicon, manganese, sulfur, and boron, are melted together in a precise combination to form a specific composition of the metal.

The metal composition is checked using spectroscopy, followed by its refinement and treatment using processes such as nodularization, inoculation, and deslagging. Thereafter, the molten metal is either poured into molds to get the final product in the form of metal ingots or transferred to crucible furnaces for casting products using different casting processes, such as gravity die casting and pressure die casting. Fig. 2.2 shows snapshots of the permanent molds used in gravity die casting.

In the casting shop, molten metal is poured into the mold cavity (collapsible or permanent) and taken out after solidification, which is further allowed to cool in air or water. The castings are transported using forklift trucks to the finishing shop, where riser-runner and sand are removed from the casting before applying deburring procedures, such as shot blasting on ferrous or nonferrous metal castings. Subsequently, metal castings are heat-treated (annealing, hardening, etc.) in electrical energy-operated furnaces. Later, several machining operations are carried out on the metal casting to get the desired features of a product.

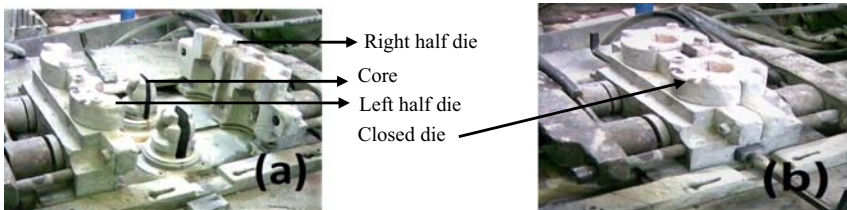


FIGURE 2.2 Gravity die casting process: die halves in (A) open position and (B) closed position.

Lastly, metal castings are washed and surface-treated to remove grease, oil, and dirt from the machined product, followed by stamping. The cast product is transported to the inspection shop for visual and automated quality checks for dimensions, tolerances, metal structure, surface, and defects, before final packing and dispatching.

### 2.3 Environmental issues in foundry and metal casting

The foundry processes depend upon a range of natural resources, such as sand, clay, and water. Besides finished castings, foundry processes generate emissions to air, solid waste, and liquid waste. Although foundry and metal casting processes are popular and have great potential, but they pose several environmental challenges. In order to assess environmental impacts of a manufacturing process, the system boundary and mapping of inputs and outputs is essential. The primary processes involved in the foundry and metal casting industry are mold preparation, metal preparation, pouring, cleaning, finishing, and packing, which have been considered to lie within the system boundary. Accordingly, Fig. 2.3 shows the flow diagram depicting the input and output of foundry and metal casting processes. The following paragraphs briefly discuss major processes within the system boundary as well as their inputs and outputs.

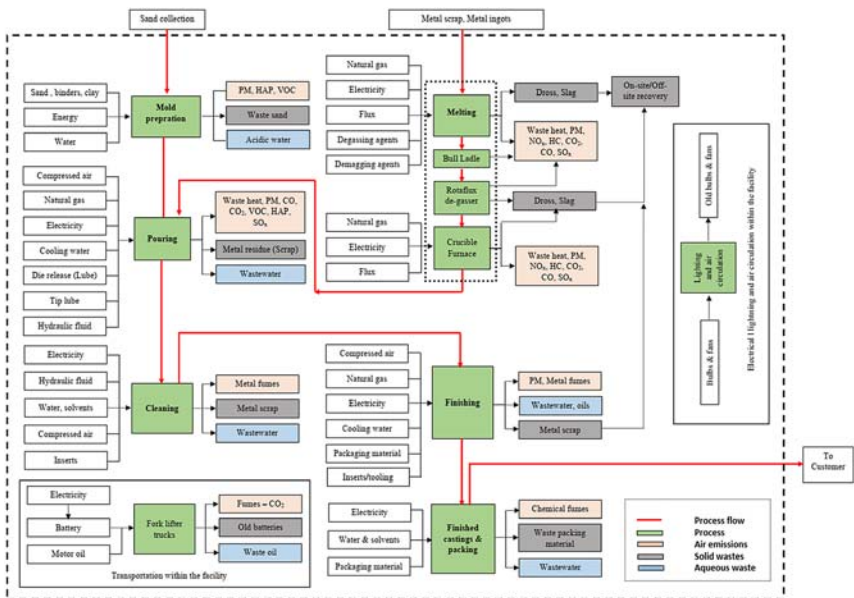


FIGURE 2.3 Major processes and their inputs–outputs in a foundry and casting facility.

*Melting* is the most energy-intensive process in foundry and metal casting responsible for 55%–80% of the total energy consumption. Metal preparation uses natural gas, energy from fuel, electrical energy, flux, degassing agents, and demagging agents and releases emissions to the air, namely, waste heat, metal fumes, and exhaust gases that contain combustion products, particularly particulate matters (PMs), nitrogen oxides ( $\text{NO}_x$ ), hydrocarbons (HC), carbon dioxide ( $\text{CO}_2$ ), carbon monoxide (CO), and sulfur dioxide ( $\text{SO}_2$ ). Furthermore, metal preparation generates solid waste in the form of dross and slag.

*Mold preparation* in a molding shop prepares cores and molds, which may either be a collapsible mold made of sand or permanent mold made of metals. The sand mold preparation harnesses sand, binders, clay, energy, and water. Furthermore, it makes use of a small amount of coke to prevent metal oxidation.

The pollutants released by *metal preparation* primarily consist of air emissions, residual wastes, and wastewater. Air emissions from the metal preparation comprise PMs, volatile organic compounds (VOCs), and hazardous air pollutants (HAP), such as benzene and phenols. Residual wastes contain metals, waste sand and residual chemical binders, wastewater, phenols, and acidic water.

The *pouring* of molten metal into a mold produces casting after solidification by making use of compressed air, natural gas, electrical energy, cooling water, and hydraulic fluid. The pollutant outputs due to the pouring stage include emissions to air, such as PMs, metal oxide fumes, VOCs, and  $\text{NO}_x$ , metal residue from pouring ladles and refractory materials from holding furnaces used for the molten metal. However, the pouring stage generates a little wastewater.

The *cleaning stage* uses inputs in the form of electrical energy, hydraulic fluid, water, solvents, compressed air, and inserts. The polluting outputs consist of emissions, namely, metal fumes, metal scrap, and wastewater containing oil, grease, and suspended solids.

Lastly, the *finishing stage* input consists of compressed air, natural gas, electrical energy, cooling water, solvents, and packaging materials. This stage generates emissions, such as PM, metal fumes, and chemical fumes to air, solid waste in the form of metal scrap and waste packaging material, and wastewater containing oil, dirt, and grease.

The above discussion indicates that air emissions are a significant environmental problem for the foundry and metal casting industry. The most significant releases to air are PM, HAP, VOCs, combustion gases, dust, and fumes. Emissions are released at each stage in the foundry that contains heavy metals and oxides, such as lead, tin, and cadmium. Solid waste includes waste sand, dross, slag, old batteries, and waste packaging material, which may be harmful to human health. The aqueous waste mainly consists of chemically contaminated water, organic compounds,

and inorganic metal compounds. It is observed that the foundry and metal casting processes cause global warming, eutrophication, acidification, eco-toxicity, and human toxicity, which impact the environment, economy, and society (Joshi et al., 2011) and beget several challenges related to their sustainability.

The new environmental regulations as well as increasing fuel and energy tariffs pose many challenges related to their sustainability; therefore, foundries and metal casting industries show a strong commitment for producing environmentally friendly metal castings by reducing industrial waste and emissions to the air (Page, 2019).

The sustainability assessment is often done by performing life cycle assessment (LCA) by making use of life cycle inventory (LCI) databases for material, energy, and processes. However, LCI databases related to the manufacturing processes are lacking. Since the LCI database is essential to carry out LCA of a product, manufactures often depend on material related information to find out the sustainability impact of a product. With the objective of gathering manufacturing processes related to LCI, a cooperative initiative involving different universities and organizations has been initiated (Kellens et al., 2012a, 2012b). The LCI database for the manufacturing processes by their cooperative initiative is also called Unit Process Life Cycle Inventory (UPLCI), which employs the concept of unit manufacturing process (UMP). UMP means an individual manufacturing process, such as injection molding, forging, machining, and die casting (National Research Council, 1995). Many researchers have found merit in further dividing a UMP into many subprocesses, which are considered to be identifiable and controllable steps of a manufacturing process (Madan et al., 2015). For example, injection molding, which is considered to be a UMP, can be further divided into controllable sub-processes, such as mold closing, injecting, and cooling. The concepts of UPLCI and sub-processes of a UMP are supposed to help in characterizing sustainability of manufacturing (Madan et al., 2015; Mani et al., 2012, 2014).

## 2.4 Sustainability indicators for the foundry and metal casting industry

---

According to US Department of Commerce, sustainable manufacturing is defined as “the creation of manufactured products that use processes that minimize negative environmental impacts, conserve energy and natural resources, are safe for employees, communities, and consumers and are economically sound” (Hauschild et al., 2014). Sustainable manufacturing itself focuses on the sustainability of the foundry and metal casting industry by focusing on three crucial aspects: social, economic, and environmental (Hendricks, 2019). The social aspects that

include factors, such as health, safety, community engagement, equity, and focus on the overall viability of the industry. The economic aspects focus on improving commercial profits. Alternatively, environmental aspects focus on protecting the environment by optimizing resource use and eliminating waste and pollution (Keeble, 1988). Although the three aspects of sustainability appear to stand apart, there are a lot of factors and data to suggest that they have many interdependencies (Camilleri, 2017). It has been reported that employing environmental sustainability in manufacturing increases its profitability and other benefits that are often related to credibility and reputation in the society (Fisher et al., 2021). Hence, the discussion in this chapter will focus on the environmental sustainability of the foundry and metal casting industry.

There are several factors to be looked into to know the environmental sustainability performance of an enterprise. Environmental sustainability factors are greenhouse gas emissions (GHGs), solid waste, water contamination, and air pollution. The manufacturers seek sets and indicators to determine environmental sustainability associated with their activities (Ahmad et al., 2019; Hutchins et al., 2013). Many published frameworks, such as Global Reporting Initiative (GRI) guidelines, Dow Jones Sustainability Index, sustainability metrics from Britain's Institution of Chemical Engineers (IChemE), United Nations Commission on Sustainable Development, International Labor Organization, General Motors metrics for sustainable manufacturing, Ford product sustainability index, and OECD sustainable manufacturing toolkit provide generic indicators derived by experts, policymakers, and other stakeholders.

The above-mentioned packages of indicators suggested by leading organizations provide generic pathways for the industry to improve its sustainability; however, selection of suitable indicators often depends on the type of industrial sector. Furthermore, many researchers have proposed indicators for the assessment of sustainability for the manufacturing industry. Veleva and Ellenbecker (2001) presented core and supplemental indicators for the manufacturing industry. Azapagic (2004) developed sustainability indicators for the mining industry. Krajnc and Glavic (2003, 2005) developed a standardized set of indexes for sustainable manufacturing focusing on the manufacturing industry. Jung et al. (2013) categorized sustainability indicators for the manufacturing industry. Garbie (2014) developed a sustainability assessment index using indicators from the three dimensions of sustainable manufacturing.

In the context of the foundry and metal casting industry, attempts have been made to identify suitable sustainability indicators. Gopal and Ramesh (2014) used seven indicators to measure the sustainability performance of a foundry cluster at Kolhapur, Maharashtra, India, namely, process yield, production efficiency, capacity utilization, energy consumption, fresh sand consumption, freshwater consumption, and labor

productivity. Singh and Madan (2016) focus on environmental indicators such as energy consumption and air emissions for sustainability assessment of the die casting industry. AFS Environmental Health and Safety Division (2017) uses air emissions, water use, and material and resources to assess the performance of a foundry enterprise.

Most of the sets and frameworks have a long list of indicators; hence, identifying suitable indicators for the foundry and metal casting industry need to be done carefully to accurately represent the operations. Since all the foundry and metal casting processes go through metal preparation, preparation of mold and cavity, pouring of molten metal, cooling, solidification, retrieving the solid part, heat treatment, and lastly its post-processing, a set of sustainability indicators, which can be applied uniformly to the foundry and metal casting industry, are highly desirable. Fig. 2.4 shows important environmental sustainability indicators for the foundry and metal casting industry, which are discussed in the following paragraphs.

*Energy use:* Ample energy for the melting and other allied operations is required in the entire foundry and metal casting industry. Therefore, energy intensity becomes an important indicator across all the foundry and metal casting industries. It includes sub-indicators, such as fuel use

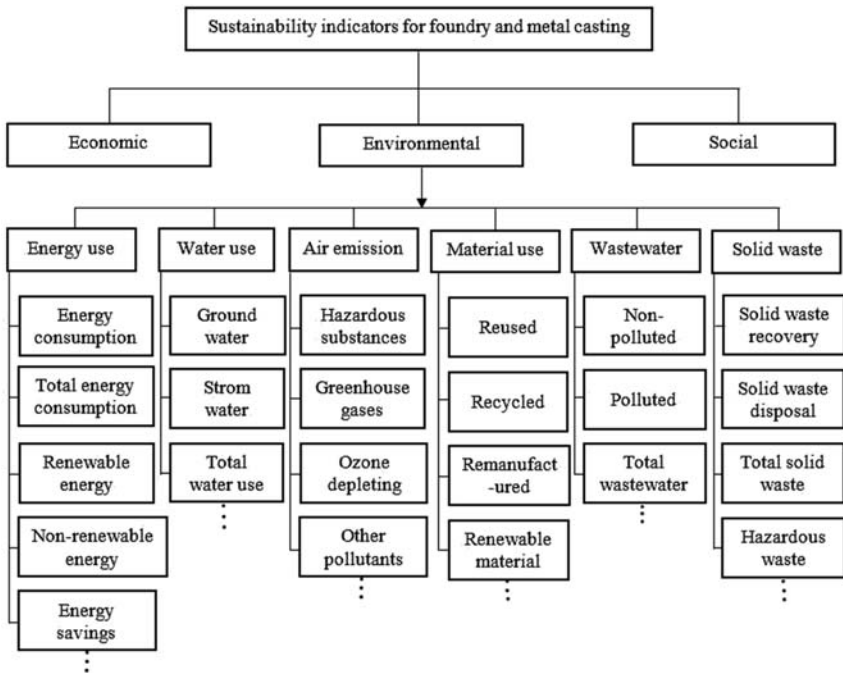


FIGURE 2.4 Structure of sustainability indicators.

(diesel, petrol, etc.), coal, electricity, liquefied petroleum gas, and natural gas (Djekic et al., 2014).

*Water use:* Water is used in the foundry and metal casting industry for several purposes, such as preparation of molding sand and increasing the rate of cooling. Therefore, indicators related to the overall water use as well as recycling of water need to be considered when selecting suitable sustainability indicators.

*Air emission:* Research has been going on to use environmentally friendly inputs, such as renewable sources of energy and materials for the foundry and metal casting industry. Foundry and metal casting release emissions to the air, such as CO<sub>2</sub>, CO, SO<sub>x</sub>, NO<sub>x</sub>, VOCs, sulfur dioxide, ammonia, PM, dust, waste heat, and smoke, which are used to track the air emissions aspect (Ahmad et al., 2019).

*Material use:* The foundry and metal casting industry in addition to the raw material used for producing parts also employs several other ingredients. For example, the foundry industry uses molding sand, clay, and binders for expandable green sand molding and core making. Similarly, permanent metal casting processes also use a number of materials, such as steel for die making, lubricants, and releasing agents. The materials can be reused or recycled, which also needs consideration for selection of suitable indicators.

*Wastewater:* Water is required in the foundry and metal casting in several processes. Moreover, there are chances of it being contaminated when it gets to mix with the suspended particles, metals, ethylene glycol, lubricants, and other materials (Gao et al., 2009). Wastewater is generally transferred to sewers through pipes to public treatment plants, which generally lack treatment methods to treat industrial wastewater causing water pollution.

*Solid waste:* Foundry and metal casting industry consumes many scrap materials. However, recycling of solid wastes generates hazardous materials, such as waste residue containing heavy metals, sludge, sand residue, spent solvents, and paints (Ahmad et al., 2019). Solid waste is a sign of inadequacy in the production process and product design. Hence, solid waste indicator helps in tracking the environmental sustainability of the foundry and metal casting processes by eliminating waste.

The above-discussed indicators may be considered as the most important for evaluating the environmental sustainability of the foundry and metal casting industry. In addition to the in-house operations, the boundary of the environmental assessment can also be extended to include impacts associated with the supply chain. For example, water intensity, energy intensity, and greenhouse intensity of the products used, which are procured directly from outside or the services availed, can be considered to have an accurate picture of sustainability assessment of the foundry and metal casting industry.

## 2.5 Concepts, technologies, management practices, and systems for sustainability assessment in the foundry and metal casting

---

The foundry and metal casting industry benefits from many concepts, technologies, management practices, and systems for sustainability assessment, which are discussed in the following sections.

### 2.5.1 Sustainability concepts

The foundry and metal casting industry makes use of several concepts related to sustainability. One of the most important concepts is lean and green practices, which are considered highly beneficial for the industry in general. The lean concept is a critical way to improve productivity and eliminate seven wastes, namely, defects, overproduction, transport, waiting, inventory, motion, and excess-processing by using a number of techniques, such as Kaizen, Value stream mapping, Workplace Organization, 5S, and Total Preventive Maintenance (Saetta and Caldarelli, 2020). Studies have shown that lean approach modifications improve the environmental state of the foundry and metal casting industry by reducing waste and optimizing resource utilization. For example, reducing transportation means reducing the release of greenhouse gases and energy.

It is suggested that green manufacturing should be adopted to achieve higher sustainability (Pinto Junior and Mendes, 2017). Green manufacturing focuses on manufacturing environmentally friendly products using materials with minimal resources and processes that minimize energy consumption, material use, waste, and hazardous substances (Abualfaraa et al., 2020). For realizing green manufacturing, techniques like eco-balance and LCA are used to conduct an in-depth evaluation of environmental state of the foundry and metal casting. Furthermore, techniques such as Design for Environment, End of Life strategies (reuse, recycle, remanufacture, etc.) help in improving sustainability (Ciceri et al., 2010). Many foundries are improving their environmental sustainability by waste reuse and recycling. For example, waste foundry sand has been used as affordable floor bedding for cow farms. Waste (iron slag) from cupola furnace is used for impermeable construction material in pipe and road construction (American Foundry Society, 2015). Another notable example is the use of scrap metal collection barrels, instead of sending the scrap to landfill, it is recycled and reused. Similarly, installing a new cupola injection system that eliminates the handling, storage, and shipping of dropout material results in reduced environmental regulatory reporting liability. Recycling zinc from brass baghouse systems preventing hazardous landfills is also helpful to reduce environmental impact. Many researchers combined lean and green

concepts with the continuous improvement culture in the foundry and metal casting industries. For example, value stream mapping has been applied in the foundry to address environmental and production wastes (Larson and Greenwood, 2004).

### 2.5.2 Sustainable technologies

Sustainable technologies have several benefits over conventional technologies and therefore help improve sustainability rating of the foundry and metal casting industry. In the following paragraphs, we discuss a few technologies that have paved the way for the improvement of sustainable foundry and metal casting industry.

*Inorganic binders:* Organic binders used in the foundry and metal casting industry are an essential evil that provides requisite strength to the mold albeit are responsible for releasing pollutants into the air. Therefore, inorganic binder technologies, such as GEOPOL and geopolymer binder systems for the production of molds and cores in the foundry, have been found to be more environment friendly (SANDTEAM, 2021).

*Dust collection:* Industry produces high dust pollution; therefore, casting industry uses modern dust collection technologies, such as baghouse dust filters and wet scrubbers, that control air pollution and remove PM from the air (Hossiney et al., 2018). Moreover, industries have installed baghouse leak detection systems to improve efficiency of the filtration system (American Foundry Society, 2016a).

*Reduce volatile organic compounds:* The foundry and metal casting industry can reduce VOCs by 58% by variety of means, such as using less thinner and solvent-based asphalt paints, as well as replacing solvent-based asphalt paint with the technologically advanced water-based asphalt emulsion paint (American Foundry Society, 2021).

*Improved ventilation systems:* Installation of modern ventilation systems, such as push-pull ventilation systems, increases the collection of fugitive and visible emissions from the melting operations in the foundry industry, thereby improving the air quality (Kulmala et al., 2006).

*Efficient water use:* The American Foundry Society (AFS) has highlighted a 30%–95% reduction in the use of water by employing closed-loop cooling water equipment, improving stormwater by naturally filtering heavy metals and solids from stormwater runoff (American Foundry Society, 2016b).

*Recycling and reuse:* Sustainable technologies help to recycle and conserve energy and material consumption through optimized processes. For example, waste sand from the foundry is either reused or reclaimed. Furthermore, instead of fresh clay, waste sand is used as: cover material over PVC liner of a landfill closure project, subbase fill for an airport runway and residential home construction (American Foundry

Society, 2017). Another good example is recovering cupola waste heat and reusing it for heating various zones within the industry, such as providing hot water facilities throughout the year (Amstedrail, 2021).

*Clean source of energy:* Diesel fueled forklift trucks can be replaced with those using sustainable energy sources, such as fuel cells and lithium-ion batteries, which are both economical and environment friendly (Mancini et al., 2011; Stambouli, 2011). Rooftop solar power, which is considered a reliable source of cleaner energy for the industry, can meet a significant percentage of the foundry's electricity requirement (Mango, 2014). Making use of solar cells, such as perovskite solar cells that provide high power conversion efficiency, also led to improved environmental sustainability (Gong et al., 2015).

*Clean energy storage systems:* Storing renewable energy is more challenging than producing it. Hence, energy storage technologies (Akinyele and Rayudu, 2014), such as supercapacitors for electrical energy, pumped hydro storage systems, compressed air storage systems, and thermal energy storage systems, such as solar water heating and heat pump systems, help improve energy efficiency and reduce the use of nonrenewable resources.

*Recyclable packaging:* Paper-based packaging products used for metal casting are recyclable (Lokahita et al., 2017), thus making them both economically and environmentally friendly for use.

*Energy-saving:* Foundries are also practicing replacing fluorescent bulbs with light-emitting diode (LED) bulbs, which can save up to 75%–80% of the electricity consumption. Furthermore, variable speed motors, efficient compressors, and compressed air system upgrade offer good energy savings opportunities with better management of services (Noro and Lazzarin, 2016).

*Process improvement:* Sustainable castings manufactured using optimized process parameters reduce energy consumption and casting defects (Zheng et al., 2018), improve resource efficiency (Salonitis et al., 2016), and reduce environmental impacts, such as solid waste, carbon emissions, and human toxicity (Neto et al., 2008).

*Hybrid additive manufacturing:* 3D printing technology has been combined with the metal casting by using rapid prototyping to fabricate sand molds in the foundry industry (Hodder and Chalaturnyk, 2019). These hybrid technologies help improve overall sustainability of the foundry and metal casting industry.

### 2.5.3 Sustainable management practices

Sustainable management practices play a crucial role in achieving a better sustainability assessment of the foundry and metal casting industry. Environmentally safe products improve brand value, improve

stakeholder relations, and increase their profitability by making changes to be more environmentally responsible, which at the same time leads to improved efficiency (AFS Environmental Health and Safety Division, 2017). From implementing management systems and metrics to waste management and beneficial reuse, metal casters can play a vital role in the saving of natural resources. There are general management practices for environmental management in the manufacturing industry that can be applied across all industries including the foundry and metal casting. Some of the management practices that can be applied to the foundry and metal casting industry are below mentioned.

Manufacturers commonly use an Environmental Management System (EMS) (Environmental Protection Agency, 2021) to reduce their environmental footprints. EMS focuses on managing environmental aspects by systems, procedures, practices, and services to set new targets and eliminate or control adverse environmental impacts and wastes. Implementation of EMS uses standard ISO 14001:2015 (Bravi et al., 2020) or EU ECO-Management and Audit Scheme (EMAS) (Strachan et al., 1997). Foundry and metal casting management also practices Environmental Audit (E.A.) (Stefana et al., 2019) to identify environmental compliance and management system implementation gaps with corrective action plans. Management conducts E.A. according to the standard ISO 19011 (Prytulaska et al., 2019).

Environmental monitoring, measurement, and control (EMMC) concentrate on quantifying, monitoring, and controlling resources consumption, waster wastage, and emissions in the industry. The EMMC practice intends to know where and how resource use produces waste and emissions (Stefana et al., 2019).

Metal casting industry also practices environmental benchmarking (O'Rourke et al., 2012) tool to compare the environmental performance of its processes with those of others. Furthermore, it identifies processes and practices that impact the environmental performance of the industry (Mani et al., 2012; Ribeiro and Sarsfield, 2006).

Management practices programs, such as Plan-Do-Check-Act (PDCA) (Do, 2017), are used for continuous improvement in quality and environmental management of cast alloys produced in the foundry and metal casting industry. Environmental modeling and simulation are commonly used tools practiced by the managements that employ computers and software tools. The model evaluates and predicts the actual use of resource consumption and emissions, such as carbon emissions, to identify sustainability opportunities. In addition to the above-mentioned practices, the foundry and metal casting industry management ensures training the workers on environmental management to make them aware of environmental aspects of their work culture. Industry managements

also set up environment management teams, which help in implementing EMS for achieving environmental sustainability (Eppich and Naranjo, 2007).

### 2.5.4 Sustainability assessment tools

Sustainability assessment tools are gaining importance because of their easy-to-use graphical user interface and ready access to databases, which help in prompt assessment of sustainability footprint of the industry. Sustainability assessment of the foundry and metal casting processes is generally done with the help of available LCA software tools, such as OpenLCA, SimaPro, GaBi, and Umberto. Liu et al. (2020) used OpenLCA to identify environmental production hotspots for one ton of ferrous metal castings produced or traded at the country level. Zeng et al. (2013) used SimaPro to compare environmental sustainability of Constrained Rapid Induction Melting Single Shot Up–Casting with the traditional sand casting using Eco-Indicator 99 (Baayen, 2000) and Ecopoint score (Zeng et al., 2013) as a single metric for comparison of their environmental sustainability. Swedish foundry association commissioned Swerea SWE-CAST (a research group from Swedish Institute of Casting Technology, Sweden) to analyze the CO<sub>2</sub> emissions for the foundry producing countries, such as India, Denmark, and China. Wänerholm (Wänerholm, 2017) used the EcoInvent LCI database (Ecoinvent, 2021) and GaBi LCA software tool (GaBi, 2021) to determine energy-based carbon emissions from the foundries. Yadav et al. (2021) determined the environmental impact in terms of global warming potential, eutrophication potential, acidification potential, human toxicity potential, ozone depletion potential, and photochemical ozone creation potential for sand casting process. They used GaBi LCA tool to consider raw material use, energy consumption, waste, and emissions during the manufacturing phase. Nörmann and Maier-Speredelozzi (2016) demonstrated the use of Umberto to account for environmental impacts, such as human toxicity, global warming potential, waste generation, and energy use in the casting process.

In addition to the generic LCA software, which can be used for sustainability assessment of manufacturing, including the metal casting process, other software systems that are especially useful for the foundry and the metal casting industry are also available. These systems are advantageous as they provide process specific databases related to material and manufacturing resources and need limited information from the user. Singh et al. (2012) developed a computer-aided system named Sustainability Assessor for the Die Casting process, which determines the CO<sub>2</sub> emissions, solid waste, and energy use based on the process plan information. The system is capable of handling gravity die casting and pressure die casting processes. The system depends on the database of materials and manufacturing resources and provides sustainability

assessment for comparison and decision-making on the basis of minimal user input invited through its GUI. [Pagone et al. \(2016\)](#) developed a tool to perform a sustainability analysis of the casting process by minimizing material and energy wastage. It provides information about the material and energy flow with the help of sankey diagram to identify suitable candidates for improvement activities.

Sustainability of metal casting processes is often linked to the lesser defects and lower rejection rate. Nowadays, with the help of process simulation software, it is possible to predict the characteristics of the final cast products such as residual stresses and defective locations without performing costly and time-consuming trial and error experiments ([Khan and Sheikh, 2016](#)). In this context, the industry uses several domain-specific software systems for flow and solidification simulation to support design for manufacturing to realize material and cost savings. Examples of such software systems are MagmaSoft ([MagmaSoft, 2021](#)), ProCAST ([PESI, 2021](#)); MoldFlow ([AutoDesk, 2021](#)), Flow3D Cast ([Flow3D, 2021](#)), and Altair Inspire CAST Casting Simulation Software ([Altair, 2021](#)).

## 2.6 IoT and Industry 4.0 in the foundry and metal casting

Internet of things or IoT, as they are called in short, are described physical objects that have sensors embedded and employ software and other assistive technologies to connect and exchange data with other devices and systems with the help of the internet and communication networks. They are supposed to pave the way for Industry 4.0, which is considered the fourth industrial revolution and depends on automation of processes and services for better control and efficiency of industrial operations.

Application of IoT in the foundry and metal casting industry will be helpful by way of interconnected machines equipped with sensors and actuators, efficient casting plants, increased quality control in production, more accessible machinery, downtime tracking, and improved resource management ([Radley, 2018](#)). It has been reported that the application of Industry 4.0 and enabling technologies like Industrial IoT (IIoT) to the selected industries was possible with minimal investment and personnel training with encouraging results, such as 5% reduction in maintenance costs, 18% reduction in downtime in the targeted areas, and 10% improvement in mold production ([Wenson et al., 2021](#)).

IoT-enabled approach has been used in the die casting industry for energy monitoring and analysis. The approach captures energy data with the help of digital power meters and PLCs for transferring it to a central server using real-time Ethernet ([Liu et al., 2018](#)). It uses energy per part

and energy per action as the indicator to develop and interpret the data and evaluate the performance of a die casting machine. The approach has been demonstrated with the help of a case study showcasing energy monitoring and analysis.

Presently, the application of Industry 4.0 in the foundry and metal casting industry is considered in its nascent stage. Many more metal casting industries now want to implement Industry 4.0, for which, the suppliers need to develop the right set of equipment and technology. The foundry and metal casting industry needs to appreciate that a lot of value can be realized with the application of Industry 4.0 (Anand, 2017). Many solutions for automation of the foundry processes are available by different suppliers, such as Smartsense (Rhina, 2021) and Wimera foundry solution (Wimera, 2021). Fig. 2.5 illustrates a general IoT solution structure in the foundry and metal casting industry.

Another IoT platform for the foundry helps the industry by providing analytics, reporting, and alerts under the platform where it accesses real-

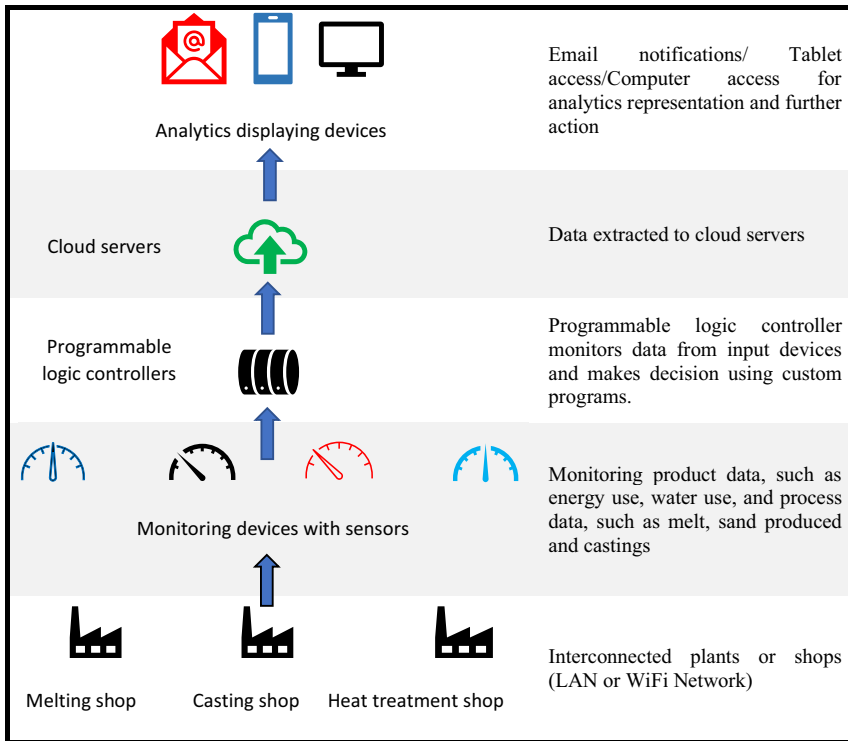


FIGURE 2.5 A general framework of an Internet of Things system in the foundry and casting industry.

time data for energy consumption, material use, and production rate. Moreover, it creates alerts for issues related to hardware reliability on a real-time basis. Furthermore, such IoT platforms have the capabilities of data analytics, centralized monitoring, breakdown, and preventive maintenance alerts in different shops, such as melting, molding, sand, core, fettling, painting, and despatch (Kothari, 2016).

Fig. 2.6 shows the information flow of an IoT system that helps in the raw material handling for the foundry and metal casting industry. IoT foundry solution helps operators to handle raw materials at different bays efficiently, live dashboards help improve overall efficiency, automatic alerts on set parameters help in preventive maintenance and avoid breakdowns, and energy monitoring improves energy usage efficiency alongside reducing environmental emissions and energy costs.

Attempts have been made by many researchers to enhance the capabilities of the IoT systems for their application in the foundry and metal casting industry. Pastor-López et al. (2019) used IoT machine learning techniques coupled with computer vision to predict the quality of castings from their digital images. Lee et al. (2018) developed an integrated framework for the foundry and metal casting that includes IoT equipment, such as sensors and actuators. The above-mentioned equipment systematically gathers data for implementing machine learning algorithms that predict casting defects, such as porosity and cold shut, in pressure die casting. Aneiba and Brown (2018) developed a smart die casting model for the HPDC machines that can sense real-time heat distribution rate inside the die-cavity zone. It helps in adjusting the

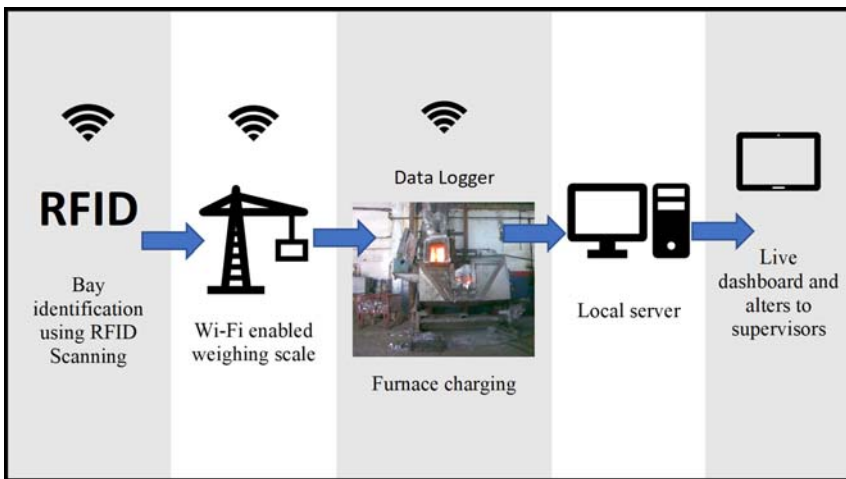


FIGURE 2.6 Raw material handling using Internet of Things in the foundry and metal casting industry.

temperature and other process parameters, such as pressure and filling velocity using PLCs and actuators. [Scharf et al. \(2021\)](#) developed Foundry 4.0 technology to increase sustainability in the foundry and metal casting processes by reducing production costs, increasing energy efficiency, improving automation of the process, and lowering carbon emissions. They used a novel burner technology based on natural gas, mobile crucible ladles, and sensors. This helped in process monitoring facilitating control of metal quantity and heat required for fully automated operation using communication technology.

Recent efforts for sustainability evaluation and improvement by way of big data and data analytics have also gained significance. They help capture the data from the foundry and metal casting to apply approaches, such as machine learning and artificial intelligence to produce sustainable products ([Kovačević et al., 2020](#)). Cyber-physical production systems help connect physical processes with the cyber world for processing the data from the foundry industry. Many software companies are developing autonomous optimization software that can perform tedious and repetitive tasks without the assistance of engineers, such as identification of optimal process and tooling layout in the foundry and metal casting industry ([Heisser, 2016](#)). IoT-enabling technologies, such as virtual and augmented reality, can be used in the foundry and metal casting industry for the training of new workers, such as virtual die casting machine simulators. Rapid prototyping technologies, such as sand 3D printing, have helped in improving the environmental sustainability of the foundry processes by facilitating making of molds. Use of smart solutions, such as cloud computing, is also helping to enhance the sustainability of the foundry and metal casting industry.

Contemporary industries are taking advantages of the digital twins ([Boychenko, 2021](#)) that help mimic the physical processes and manufacturing resources for remote monitoring, training, manufacturing optimization thereby saving cost, and improving operational efficiency alongside helping the industry to prevent transmission risk of COVID-19 ([Alrashed et al., 2022](#)). We are hopeful that the concepts of Industry 4.0, digital twins, UMPs, and their controllable sub-processes with the help of enabling technologies, such as IoTs can be used to significantly improve sustainability of the foundry and metal casting industry.

---

## 2.7 Summary

Foundry and metal casting industry is a very important manufacturing process even though it is very old, and several new manufacturing

methods, such as additive manufacturing, have been developed over time. However, the foundry and metal casting industry always remained a target of environmental bashing due to their high energy intensity of operations as well as release of air emissions, water contamination, and solid waste. Therefore, this chapter outlines sustainability-related challenges being faced by the foundry and metal casting industry and sails through the important aspects for making the industry sustainable.

Sections 2.1 and 2.2 of the chapter introduced the historical background and provided an understanding of the foundry and metal casting processes. Section 2.3 of the chapter discussed different operations happening in the foundry and metal casting industry to identify inputs and outputs. The section details input pertaining to material and energy alongside outputs in different forms, i.e., gaseous, liquid, and solid, helping understand important environmental issues. Section 2.4 discusses sustainability indicators that are considered important for the foundry and metal casting industry. As discussed earlier, the foundry and metal casting processes are quite old and benefited from the expertise available and industry best practices that have evolved over time. Therefore, Section 2.5 of the chapter details useful concepts, technologies, management practices, and assessment tools related to the sustainability of the foundry and metal casting industry. Lastly, Section 2.6 of the chapter provides an overview of the latest technological advancements that apply Industry 4.0 concepts and IoTs in the foundry and metal casting industry with the objective of making the industry more sustainable.

The discussions made in the chapter rely on research work on concepts, technological advancements, management practices, assessment tools, IoT-based smart solutions, Industry 4.0, and digital twins, relevant to the foundry and metal casting industry. We are hopeful that the chapter will provide important leads to the foundry and metal casting industry for meeting the sustainability-related challenges thereby contributing toward sustainable development goals (SDGs) as per agenda of the United Nations.

---

## 2.8 Disclosure

---

The authors declare that they have no relevant or material financial interests that relate to the discussions made in this chapter. Further, the names of any commercial product mentioned in the chapter are merely for the sake of discussion only and should not be considered as a recommendation.

## References

- Abualfaraa, W., Saloniitis, K., Al-Ashaab, A., Ala'raj, M., 2020. Lean-green manufacturing practices and their link with sustainability: a critical review. *Sustainability* 12, 981.
- AFS Environmental Health & Safety Division, 2017. Sustainability in metalcasting: the green foundry project. *Modern Casting Magazine* 1–6.
- Ahmad, S., Wong, K.Y., Rajoo, S., 2019. Sustainability indicators for manufacturing sectors. *Journal of Manufacturing Technology Management* 30, 312–334.
- Akinyele, D.O., Rayudu, R.K., 2014. Review of energy storage technologies for sustainable power networks. *Sustainable Energy Technologies and Assessments* 8, 74–91.
- Alrashed, S., Min-Allah, N., Ali, I., Mehmood, R., 2022. COVID-19 outbreak and the role of digital twin. *Multimedia Tools and Applications* 1–15.
- Altair, 2021. Altair Inspire Cast [WWW Document]. Streamlined Casting Simulation Software (accessed November 27, 2021). <https://www.altair.com/inspire-cast>.
- American Foundry Society. Waste Management and Benifical Use: Foundry By-Product Benifical Reuse [WWW Document]. Green Foundry Case Studies. <https://afsinc.s3.amazonaws.com/Documents/EHS/012%20Foundry%20By-Product%20Benifical%20Reuse.pdf>.
- American Foundry Society, 2016a. Air Emissions: Baghouse Leak Detection [WWW Document]. Green Foundry Case Studies (accessed December 30, 2021). <https://afsinc.s3.amazonaws.com/Documents/EHS/001BaghouseLeakDetection.pdf>.
- American Foundry Society, 2016b. Water: Eliminating the Generation and Discharge of Non-contact Cooling Water [WWW Document]. Green Foundry Case Studies (accessed March 1, 2022). <https://afsinc.s3.amazonaws.com/Documents/EHS/007EliminatingtheGenerationandDischargeofNon-ContactCoolingWater.pdf>.
- American Foundry Society, 2017. Case Studies [WWW Document]. Green Foundry Case Studies (accessed December 26, 2021). <https://afsinc.s3.amazonaws.com/Documents/FIRST/20091214.pdf>.
- American Foundry Society, 2021. Air Emissions: Volatile Organic Compound (VOC) Reduction with Switch to Water Based Paint [WWW Document]. Green Foundry Case Studies (accessed December 25, 2021). <https://afsinc.s3.amazonaws.com/Documents/EHS/002VolatileOrganicCompoundsReduction-SwitchtoWater-BasedPaint.pdf>.
- Amstedrail, 2021. Sustainability [WWW Document]. Our Commitment to the Environment (accessed November 30, 2021). <https://www.amstedrail.com/sustainability/environment/>.
- Anand, A.K., 2017. Industry 4.0 and the Foundry Industry [WWW Document]. *Industrial Automation Magazine* (accessed December 20, 2021). <https://www.industrialautomationindia.in/articleitm/7263/Industry-4.0-and-the-Foundry-Industry-articles>.
- Aneiba, A., Brown, S., 2018. Smart die casting: a new approach. *Innovation in Manufacturing through Digital Technologies and Applications: Thoughts and Reflections on Industry 4.0*, pp. 80–90.
- AutoDesk, 2021. MoldFlow [WWW Document]. AutoDesk (accessed October 18, 2021). <https://www.autodesk.in/products/moldflow/overview>.
- Azapagic, A., 2004. Developing a framework for sustainable development indicators for the mining and minerals industry. *Journal of Cleaner Production* 12, 639–662.
- Baayen, H., 2000. *Eco-indicator 99 Manual for Designers*, Ministry of Housing, Spatial Planning and the Environment. The Hague, Netherlands.
- Bravi, L., Santos, G., Pagano, A., Murmura, F., 2020. Environmental management system according to ISO 14001:2015 as a driver to sustainable development. *Corporate Social Responsibility and Environmental Management* 27, 2599–2614.
- Boychenko, M., 2021. Powering Industry with Digital Twins : Infinite Foundry Joins EIT Digital Accelerator [WWW Document]. EIT Digital (accessed January 17, 2022). <https://www.eitdigital.eu/newsroom/news/2021/powering-industry-with-digital-twins-infinite-foundry-joins-eit-digital-accelerator/>.

- Camilleri, M.A., 2017. Corporate sustainability and responsibility: creating value for business, society and the environment. *Asian Journal of Sustainability and Social Responsibility* 2, 59–74.
- Ciceri, N.D., Garetti, M., Sperandio, S., 2010. *Advances in Production Management Systems. New Challenges, New Approaches*, IFIP Advances in Information and Communication Technology, IFIP Advances in Information and Communication Technology. Springer, Berlin, Heidelberg.
- Djekic, I., Miocinovic, J., Tomasevic, I., Smigic, N., Tomic, N., 2014. Environmental life-cycle assessment of various dairy products. *Journal of Cleaner Production* 68, 64–72.
- Do, D., 2017. 11 Steps to Build a Continuous Improvement Culture [WWW Document]. *The Lean Way* (accessed November 25, 2021). <https://theleanway.net/11-Steps-to-Building-a-Continuous-Improvement-Culture>.
- Ecoinvent, 2021. Ecoinvent 3.8 [WWW Document]. Database (accessed November 27, 2021). <https://ecoinvent.org/the-ecoinvent-database/data-releases/ecoinvent-3-8/#1610466712441-9948416b-c529>.
- Environmental Protection Agency, 2021. Environmental Management Systems (EMS) [WWW Document]. United States Environmental Protection Agency (accessed November 26, 2021). <https://www.epa.gov/ems>.
- Eppich, R., Naranjo, R.D., 2007. *Implementation of Metal Casting Best Practices*. Report of US Department of Energy.
- Fisher, J., Arora, P., Chen, S., Rhee, S., Blaine, T., Simangan, D., 2021. Four propositions on integrated sustainability: toward a theoretical framework to understand the environment, peace, and sustainability nexus. *Sustainability Science* 16, 1125–1145.
- Flow3D, 2021. FLOW-3D [WWW Document]. Flow Science (accessed October 13, 2021). <https://www.flow3d.com>.
- GaBi, 2021. Improve Your Product Sustainability Performance [WWW Document]. GaBi Software (accessed October 12, 2021). <https://gabi.sphera.com/international/index/>.
- Gao, L., Ren, N., Wang, A., 2009. Pollution mechanism and control strategies of corn deep processing industry. In: 2009 International Conference on Management and Service Science. IEEE, Beijing, China, pp. 1–4.
- Garbie, I.H., 2014. An analytical technique to model and assess sustainable development index in manufacturing enterprises. *International Journal of Production Research* 52, 4876–4915.
- Gong, J., Darling, S.B., You, F., 2015. Perovskite photovoltaics: life-cycle assessment of energy and environmental impacts. *Energy & Environmental Science* 8, 1953–1968.
- Gopal, E.N., Ramesh, D., 2014. Resource efficiency for sustainability in ferrous foundry—a case of Kolhapur msme cluster. *Indian Foundry Journal* 60, 30–39.
- Hauschild, M., Dornfeld, D., Hutchins, M., Kara, S., Jovane, F., 2014. Sustainable manufacturing. In: *CIRP Encyclopedia of Production Engineering*. Springer, Berlin, Heidelberg, pp. 1208–1214.
- Heisser, C., 2016. Autonomous Optimization : A New Approach to Increased Efficiencies [WWW Document]. *Foundry Management and Technology* (accessed October 12, 2021). <https://www.foundrymag.com/simulation-it/article/21928815/autonomous-optimization-a-new-approach-to-increased-efficiencies>.
- Hendricks, C., 2019. Tremendous potential - environmental, economical and social sustainability in foundries. GIFA, METEC, THERMPROCESS, NEWCAST 2019 1–5.
- Hodder, K.J., Chalaturnyk, R.J., 2019. Bridging additive manufacturing and sand casting: utilizing foundry sand. *Additive Manufacturing* 28, 649–660.
- Hossiney, N., Das, P., Mohan, M.K., George, J., 2018. In-plant production of bricks containing waste foundry sand—a study with Belgaum foundry industry. *Case Studies in Construction Materials* 9, 1–26.

- Hutchins, M.J., Robinson, S.L., Dornfeld, D., 2013. Understanding life cycle social impacts in manufacturing: a processed-based approach. *Journal of Manufacturing Systems* 32, 536–542.
- Joshi, D., Modi, Y., Ravi, B., 2011. Evaluating environmental impacts of sand cast products using life cycle assessment. In: *Research into Design—Supporting Sustainable Product Development*. Indian Institute of Science, Bangalore, India, pp. 978–981. Research Publishing, Bangalore, India.
- Joung, C.B., Carrell, J., Sarkar, P., Feng, S.C., 2013. Categorization of indicators for sustainable manufacturing. *Ecological Indicators* 24, 148–157.
- Keeble, B.R., 1988. The Brundtland report: 'Our common future'. *Medicine and War* 4, 17–25.
- Kellens, K., Dewulf, W., Overcash, M., Hauschild, M.Z., Dufloy, J.R., 2012a. Methodology for systematic analysis and improvement of manufacturing unit process life-cycle inventory (UPLCI)-CO2PE! initiative (cooperative effort on process emissions in manufacturing). Part 1: methodology description. *International Journal of Life Cycle Assessment* 17, 69–78.
- Kellens, K., Dewulf, W., Overcash, M., Hauschild, M.Z., Dufloy, J.R., 2012b. Methodology for systematic analysis and improvement of manufacturing unit process life cycle inventory (UPLCI) CO2PE! initiative (cooperative effort on process emissions in manufacturing). Part 2: case studies. *International Journal of Life Cycle Assessment* 17, 242–251.
- Khan, M.A.A., Sheikh, A.K., 2016. Simulation tools in enhancing metal casting productivity and quality: a review. *Proceedings of the Institution of Mechanical Engineers - Part B: Journal of Engineering Manufacture* 230, 1799–1817.
- Kothari, M., 2016. Eyes in the sky. *Industrial Business Mart* 13, 1–3.
- Kovačević, L., Oliveira, R., Terek, P., Terek, V., 2020. The direction of foundry industry: toward the foundry 4.0. *Journal of Mechatronics, Automation and Identification Technology* 5, 23–28.
- Krajnc, D., Glavic, P., 2003. Indicators of sustainable production. *Clean Technologies and Environmental Policy* 5, 279–288.
- Krajnc, D., Glavic, P., 2005. How to compare companies on relevant dimensions of sustainability. *Ecological Economics* 55, 551–563.
- Kulmala, I., Hynynen, P., Welling, I., Säämänen, A., 2006. Local ventilation solution for large, warm emission sources. *Annals of Occupational Hygiene* 51, 35–43.
- Larson, T., Greenwood, R., 2004. Perfect complements: synergies between lean production and eco-sustainability initiatives. *Environmental Quality Management* 13, 27–36.
- Lee, J., Noh, S., Kim, H.-J., Kang, Y.-S., 2018. Implementation of cyber-physical production systems for quality prediction and operation control in metal casting. *Sensors* 18, 1428.
- Liu, W., Tang, R., Peng, T., 2018. An IoT-enabled approach for energy monitoring and analysis of die casting machines. *Procedia CIRP* 69, 656–661.
- Liu, Y., Li, H., Huang, S., An, H., Santagata, R., Ulgiati, S., 2020. Environmental and economic-related impact assessment of iron and steel production. A call for shared responsibility in global trade. *Journal of Cleaner Production* 269, 122239.
- Lokahita, B., Aziz, M., Yoshikawa, K., Takahashi, F., 2017. Energy and resource recovery from Tetra Pak waste using hydrothermal treatment. *Applied Energy* 207, 107–113.
- Madan, J., Mani, M., Lee, J.H., Lyons, K.W., 2015. Energy performance evaluation and improvement of unit-manufacturing processes: injection molding case study. *Journal of Cleaner Production* 105, 157–170.
- Magmasoft, 2021. MAGMASOFT-Autonomous Engineering [WWW Document]. MAGMA (accessed November 12, 2021). <https://www.magmasoft.co.in/en/>.
- Mancini, M., Nobili, F., Tossici, R., Wohlfahrt-mehrens, M., Marassi, R., 2011. High performance, environmentally friendly and low cost anodes for lithium-ion battery based on TiO<sub>2</sub> anatase and water soluble binder carboxymethyl cellulose. *Journal of Power Sources* 196, 9665–9671.

- Mango, S., 2014. Solar for Foundries [WWW Document] (accessed November 28, 2021). <https://www.solarmango.com/in/sector/foundries>.
- Mani, M., Madan, J., Lee, J.H., Lyons, K., Gupta, S.K., 2012. Characterizing sustainability for manufacturing performance assessment. In: 32nd Computers and Information in Engineering Conference, Parts A and B, vol 2. American Society of Mechanical Engineers, pp. 1153–1162.
- Mani, M., Madan, J., Lee, J.H., Lyons, K.W., Gupta, S.K., 2014. Sustainability characterisation for manufacturing processes. *International Journal of Production Research* 52, 5895–5912.
- Markets and Markets, 2017. Metal Casting Market-Forecast to 2025 (Dublin, Ireland).
- National Research Council, 1995. *Unit Manufacturing Processes : Issues and Opportunities in Research*. The National Academies Press, Washington, DC (National Academies Press, Washington, D.C).
- Neto, B., Kroeze, C., Hordijk, L., Costa, C., 2008. Modelling the environmental impact of an aluminium pressure die casting plant and options for control. *Environmental Modelling & Software* 23, 147–168.
- Nörmann, N., Maier-Speredelozzi, V., 2016. Cost and environmental impacts in manufacturing: a case study approach. *Procedia Manufacturing* 5, 58–74.
- Noro, M., Lazzarin, R.M., 2016. Energy audit experiences in foundries. *International Journal of Energy and Environmental Engineering* 7, 409–423.
- O'Rourke, L., Santalucia, P., Papson, A., Brickett, J., Beshers, E., Cronin, C., Gentle, J.A., Blanco, E., 2012. Environmental benchmarking: overview of the process and benefits. In: *Handbook on Applying Environmental Benchmarking in Freight Transportation*, pp. 7–9.
- Olsen, D., 2020. History of Metal Casting [WWW Document]. MetalTek (accessed October 8, 2021). <https://www.metaltek.com/blog/history-of-metal-casting/>.
- Page, I., 2019. Environmental , Economic and Social Sustainability in Foundries [WWW Document]. GIFA (accessed December 30, 2021). <https://www.spotlightmetal.com/environmental-economic-and-social-sustainability-in-foundries-a-806710/>.
- Pagone, E., Jolly, M., Salonitis, K., 2016. The development of a tool to promote sustainability in casting processes. *Procedia CIRP* 55, 53–58.
- Pastor-López, I., la Puerta, J.G., de Sanz, B., Goti, A., Bringas, P.G., 2019. How IoT and computer vision could improve the casting quality. In: *Proceedings of the 9th International Conference on the Internet of Things*. ACM, New York, NY, USA, pp. 1–8.
- PESI, 2021. Cavitation [WWW Document]. Pacific ESI (accessed December 31, 2021). <https://www.esi.com.au/>.
- Pinto Junior, M.J.A., Mendes, J.V., 2017. Operational practices of lean manufacturing: potentiating environmental improvements. *Journal of Industrial Engineering and Management* 10, 550–580.
- Prytulska, N., Antiushko, D., Gusarevich, N., 2019. International standard ISO 19011:2018: perspectives of implementation. ISSN 1998-2666. *Товари і ринки 2019*, 5–15.
- Radley, 2018. The Future of Metal Casting with the Industrial Internet of Things ( IIoT ) [WWW Document]. Manufacturing Industry (accessed December 18, 2021). <https://www.radley.com/the-future-of-metal-casting-with-the-industrial-internet-of-things-iiot/>.
- Rhina, 2021. SmartSense Platform [WWW Document]. Smartsense (accessed December 10, 2021). [https://www.rhinomachines.net/index.php/product/single\\_product/24](https://www.rhinomachines.net/index.php/product/single_product/24).
- Ribeiro, L.M.M., Sarsfield Cabral, J.A., 2006. A benchmarking methodology for metalcasting industry. *Benchmarking: An International Journal* 13, 23–35.
- Saetta, S., Caldarelli, V., 2020. Lean production as a tool for green production: the Green Foundry case study. *Procedia Manufacturing* 42, 498–502.

- Salonitis, K., Jolly, M.R., Zeng, B., Mehrabi, H., 2016. Improvements in energy consumption and environmental impact by novel single shot melting process for casting. *Journal of Cleaner Production* 137, 1532–1542.
- SANDTEAM, 2021. The Environmentally-Friendly Inorganic Binder System: GEOPOL [WWW Document]. Foundry Corporate News (accessed December 9, 2021). <https://www.foundry-planet.com/d/the-environmentally-friendly-inorganic-binder-system-geopolR/>.
- Scharf, S., Sander, B., Kujath, M., Richter, H., Riedel, E., Stein, H., Tom Felde, J., 2021. Foundry 4.0: an innovative technology for sustainable and flexible process design in foundries. *Procedia CIRP* 98, 73–78.
- Singh, P., Madan, J., Singh, A., Mani, M., 2012. A computer-aided system for sustainability analysis for the diecasting process. In: ASME 2012 International Manufacturing Science and Engineering Conference. American Society of Mechanical Engineers, Notre Dame, Indiana, USA, pp. 1087–1096.
- Singh, P.P., Madan, J., 2016. A computer-aided system for sustainability assessment for the diecasting process planning. *International Journal of Advanced Manufacturing Technology* 87, 1283–1298.
- Stambouli, A.B., 2011. Fuel cells : the expectations for an environmental-friendly and sustainable source of energy. *Renewable and Sustainable Energy Reviews* 15, 4507–4520.
- Stefana, E., Cocca, P., Marciano, F., Rossi, D., Tomasoni, G., 2019. A review of energy and environmental management practices in cast iron foundries to increase sustainability. *Sustainability* 11, 7245.
- Strachan, P., Haque, M., McCulloch, A., Moxen, J., 1997. The eco-management and audit scheme: recent experiences of UK participating organizations. *European Environment* 7, 25–33.
- Veleva, V., Ellenbecker, M., 2001. Indicators of sustainable production: framework and methodology. *Journal of Cleaner Production* 9, 519–549.
- Wänerholm, M., 2017. Climate Impact of Metal-Casting. Jönköping.
- Wenson, J., Nelson, E., Balliet, L.M., 2021. A Practical Implementation of Industry 4.0 in Foundries [WWW Document]. Industry 4.0 at the World Economic Forum (accessed December 10, 2021). <https://www.moderncasting.com/articles/2021/04/20/practical-implementation-industry-40-foundries>.
- Wimera, 2021. Digital Foundry [WWW Document] (accessed November 30, 2021). <https://www.wimerasys.com/digital-foundry/>.
- Yadav, A., Jamwal, A., Agrawal, R., Kumar, A., 2021. Environmental impacts assessment during sand casting of Aluminium LM04 product: a case of Indian manufacturing industry. *Procedia CIRP* 98, 181–186.
- Zeng, B., Salonitis, K., Jolly, M., 2013. Comparison of the environmental impact of the CRIMSON process with normal sand casting process. In: Proceedings of the 11th International Conference on Manufacturing Research (ICMR2013). Cranfield, Bedfordshire, UK, pp. 1–6.
- Zheng, J., Huang, B., Zhou, X., 2018. A low carbon process design method of sand casting based on process design parameters. *Journal of Cleaner Production* 197, 1408–1422.

# Sustainable manufacturing: material forming and joining

V. Satheeshkumar<sup>1</sup>, R. Ganesh Narayanan<sup>2</sup>, and  
Jay S. Gunasekera<sup>3</sup>

<sup>1</sup>Department of Production Engineering, National Institute of Technology Tiruchirappalli, Tiruchirappalli, Tamil Nadu, India; <sup>2</sup>Department of Mechanical Engineering, Indian Institute of Technology Guwahati, Guwahati, Assam, India; <sup>3</sup>Department of Mechanical Engineering, University of Delaware, Newark, DE, United States

## 3.1 Need for sustainable material forming

Several products in automotive, aerospace, defense, food packaging, construction, and agriculture sectors are manufactured through plastic deformation (or forming) of high-strength metals such as steel and cast iron. Energy consumption is significantly high during the formation of such materials as compared with processing nonmetals. As a result, use of lightweight materials like aluminum and magnesium alloys is observed. However, still steel grades are utilized as raw materials in tonnes.

Sustainable material forming is a mandatory requirement to minimize the overall environmental impact, in addition to the traditional requirements such as lower cost, better quality, and faster to market. Considering the requirements, today, sophisticated and efficient computations such as finite element method (FEM)/finite element analyses (FEA) and virtual metal forming have replaced trial-and-error try-outs. Such methods include design for product quality, production economy, and environmental impact, along with traditional deliverables. Reduction of carbon foot print and average CO<sub>2</sub> emissions is aimed through alliances between raw material manufacturers and users (Eg. ultralight steel automotive body (ULSAB) concept). The European Union regulators have imposed to reduce average CO<sub>2</sub> emission to about 130 gCO<sub>2</sub>/km by 2015 and 95 gCO<sub>2</sub>/km in 2020 across all new vehicles (Fig. 3.1A). The available

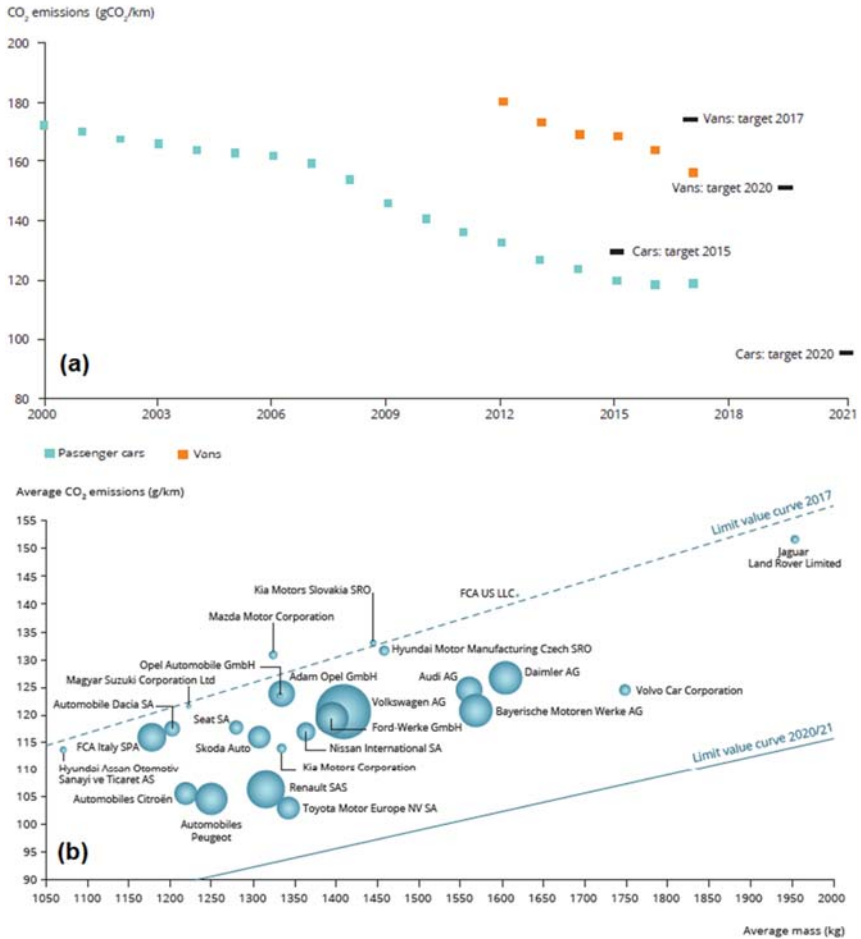


FIGURE 3.1 (A) Evolution of CO<sub>2</sub> emissions for new passenger cars and vans in EU-28 and (B) target achieved by individual manufacturer registering more than 100,000 vehicles/year in 2017. Reused with permission from EEA; EEA Report, No 15/2018, Monitoring CO<sub>2</sub> emissions from new passenger cars and vans in 2017.

test data show that a weight reduction of 100 kg corresponds to 8–12 g km<sup>-1</sup> reduction of CO<sub>2</sub> emission. As per report from European Environment Agency (EEA) in 2017, with increase in vehicle weight, the CO<sub>2</sub> emission increases significantly (Fig. 3.1B). In 2017, Toyota Motor Europe had the lowest CO<sub>2</sub> emissions of all larger manufacturers, as it managed to reduce average CO<sub>2</sub> emissions by more than 2 gCO<sub>2</sub>/km from the previous year. In 2018, once again, Toyota Motor Europe had the lowest average CO<sub>2</sub> emissions of about 102 gCO<sub>2</sub>/km and managed to reduce average CO<sub>2</sub> emissions by one gCO<sub>2</sub>/km compared to 2017 (EEA

Report, No 02/2020, Monitoring CO<sub>2</sub> emissions from passenger cars and vans in 2018). Although weight reduction is the objective, increased strength is favorable in terms of safety and crash resistance.

Sustainable material forming is possible via system-level eco-design, optimization of energy consumption, water usage and materials wastage, virtual forming process development, integrate virtual-physical forming process design, and use of novel and efficient material forming technologies and materials. The following sections detail some of the attempts in this aspect.

### 3.2 Extrusion and forging

Extrusion and forging are bulk-forming processes useful in producing several automotive and aerospace components of varying sizes and quality. Bulk forming processes are usually characterized by large load requirements, and hence stronger tools and dies are needed as compared to other metal forming processes. The interface contact stress are high as there is a continuous movement of material relative to tools. Billet and tool lubrication in the form of coating and lubricants play a crucial role in determining the quality of products. Design modifications in tool and process result in sustainable and green forging and extrusion with improvement in product quality. Sustainability can be achieved in several routes such as material modifications, process modifications, tool design, lubrication, etc., during extrusion and forging. Jeong et al. (2014) by following a different homogenization method during porthole extrusion of Al6063 billet and with the help of finite element (FE) simulation, a defect free extruded cylindrical tube was produced. The energy consumption can be reduced by 25% compared to the conventional porthole extrusion process. In another study, Jeong et al. (2013) manufactured helical pinion gear by cold extrusion process, which is a scrap reducing and energy saving method as compared to machining. FE simulations help in optimizing friction factor and heat treatments (isothermal annealing and spheroidizing) improved the formability of the billet material, all finally yielded a defect free gear. To substantiate the importance of cold extrusion over machining to produce gears, Yun et al. (2014) through life cycle assessment (LCA) technique showed that the cold extrusion process minimized the energy consumption in the manufacturing of single-type and double-type gears by 25% and 49%, respectively, in comparison to conventional machining, and also reduced CO<sub>2</sub> emissions. The material recovery rate improved by about 91% when compared to machining. Instead of manufacturing a hollow helical gear by conventional material, Kim et al. (2015) utilized the superplastic behavior of Zn-22wt%Al eutectoid alloy to

make the component by the powder extrusion route. SEM pictures revealed that fine-grained and equiaxed structure produced by solution treatment is maintained during the extrusion without microcracks. A barrel, made of Mg alloy, in a digital camera can be manufactured by hot backward extrusion process, and thoughtful optimization of temperature, lubricating conditions, and tool temperature using FE simulations resulted in defect free component (Fig. 3.2) (Park and Kim, 2012). Generally, this is performed by machining with significant loss of material, and recycling becomes mandatory. In recent times, 3D printing methods play a vital role in manufacturing industries either in terms of product fabrication or in terms of tool fabrication. Significant reduction in material, energy, and number of stages is documented. Extrusion die fabricated by selective laser melting provided flexibility to integrate multidirectional cooling channels within die during hot extrusion of components. The die cooling helped in reduction of process temperature of the tool as well as of the extrudate during thin square hollow profile (Holker et al., 2013). Energy estimation in all factory level would improve the sustainability through proper accounting of energy requirement for each operation (Schmidt et al., 2015). Another energy efficient process known as “friction stir back extrusion” reduces energy consumption and CO<sub>2</sub> emissions when compared to conventional extrusion making it ecofriendly and sustainable. The overall sustainability score for the process is 94.3%, which is about three times better compared to conventional extrusion (Saad et al., 2020). Direct recycling of aluminum chips by hot extrusion is another energy efficient and sustainable manufacturing route for metallic rods (Wagiman et al., 2020).

The following are examples in forging operations involving process and material modifications resulting in sustainable manufacturing and energy savings. Ku and Kang (2014) proposed a multistage cold forging and



**FIGURE 3.2** Digital camera barrel made of AZ31B alloy by hot extrusion. Reused with permission from Park, C.W., Kim, Y.H., 2012. A study on the manufacturing of digital camera barrel using magnesium alloy. *International Journal of Precision Engineering and Manufacturing* 13, 1047–1052. <https://doi.org/10.1007/s12541-012-0136-x>; springer.

process for manufacturing the outer race of a constant velocity (CV) joint, which is actually made by the multistage warm forging process consisting of nine operations. The process has been simplified to achieve an environmentally friendly multistage cold forging technology with only six operations such as initial billet cutting, forward extrusion, upsetting, backward extrusion, necking-ironing-sizing, and final component stage. Two important decisions including raw material spheroidizing to reduce its strength and increase the formability and redesign of tools to relieve forged part after necking-ironing-sizing are considered to complete the stages successfully (Fig. 3.3). Manufacturing of steering system output shaft by multistage forging operation (Choi et al., 2015), differential case in automobile transmission by warm forging of a Mg alloy (Yoon and Lee, 2015), cam ring gear parts of large diameter for truck clutch by hot-cold forge method (Park et al., 2019), aluminum piston forging process with different lubricating conditions (Lee et al., 2019), and automobile engine mounting parts by hot-cold forging technology (Park and Kwon, 2016) are some case studies showing modifications in process design yielding light weight products with potential reduction in CO<sub>2</sub> emissions and improved fuel economy. Other case studies have shown that FE simulations and analytical modeling helped in prediction of forging defects, die design, and tool life during multistage forging operations (Kim et al., 2012; Kim and Choi, 2009; Kwon and Park, 2011). Bimetallic ring components are generally fabricated by forging. In a recent attempt by Mondal et al. (2020), friction stir (FS)-assisted forging in solid state was implemented to fabricate a bimetallic ring made of Mg–Al alloys, a unique move toward sustainable manufacturing. Fig. 3.4 explains the stages in the process. Since heat generation during FSP assists in fabrication, there is no need of external heating like in warm and hot forging reducing the overall energy requirement and furnace usage.



FIGURE 3.3 Fabrication of outer race using multistage cold forging process. Reused with permission from Ku, T.-W., Kang, B.-S., 2014. Tool design and experimental verification for multistage cold forging process of the outer race. *International Journal of Precision Engineering and Manufacturing* 15, 1995–2004. <https://doi.org/10.1007/s12541-014-0556-x>; Springer.

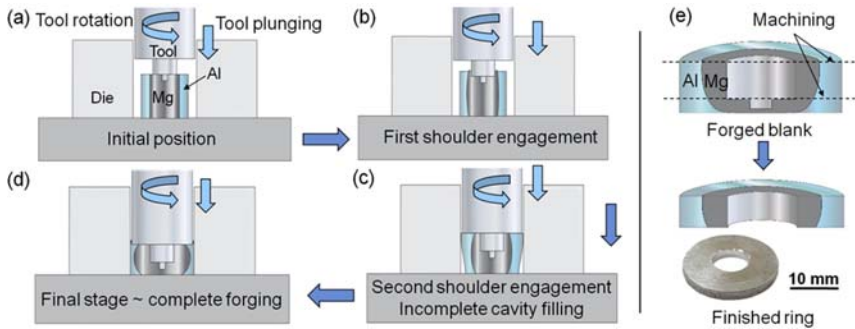


**FIGURE 3.4** Fabrication of bimetallic ring using friction stir (FS)-assisted forging process [(A)–(D): FS forging stages and (E): forged blank and a bimetallic ring]. *Reused with permission from Mondal, M., Basak, S., Das, H., Hong, S.-T., Choi, H., Park, J.-W., Han, H.N., 2020. Manufacturing of magnesium/aluminum bimetallic ring components by friction stir assisted simultaneous forging and solid-state joining. International Journal of Precision Engineering and Manufacturing - Green Technology. <https://doi.org/10.1007/s40684-020-00244-0>; springer.*

Die design in forging and extrusion is of prime importance. Several computational methods such as upper bound method and finite element method are developed based on well-established plasticity theories for modeling processes such as ring rolling. Neural network models are also developed for such predictions. Hybrid neural network-finite element models are efficient in industry-scale applications. Such methods are useful in predicting defects during extrusion and forging (Gunasekera and Hoshino, 1982; Gunasekera et al., 1984, 1998; Rachakonda et al., 1991; Alfozan and Gunasekera, 2003; Ranatunga and Gunasekera, 2006; Parvizi and Rohani Raftar, 2019).

### 3.3 Rolling and wire drawing

Rolling strategies such as differential speed rolling, structure controlled rolling, change in rolling temperature, and rolling direction influence the microstructure and mechanical properties of sheets. The following examples highlight the same in terms of formability of sheets.

In *differential speed rolling* (DSR), sheet is rolled by asymmetric rolling process with the help of upper and lower rolls having different rotational speeds. Roll speed ratio, which is the ratio of speed of upper roll to speed of lower roll, is the controlling parameter in DSR. Rolls with different diameters and materials creating varied friction conditions are other ways to perform asymmetric rolling. DSR is meant to introduce grain refinement through high plastic-strain accumulation resulting in strengthening of sheets and control the deformation texture influencing anisotropy of

sheets (Polkowski, 2016). In comparison to conventional sheet rolling, deformation geometry is changed in DSR. For slow roll, the neutral points move toward the entry of the roll gap, while for fast roll, it moves toward the exit. This results in lowering the roll force and imparting high through thickness shear strain on the sheet. DSR on hot extruded AZ31B sheet of 4 mm thickness improved the elongation to failure and  $n$  value. As a result, the Erichsen values, obtained from Erichsen cup tests, of the DSR processed sheet improved from 2.6 to 4 in room temperature rolling and from 4.1 to 7.6 at 423 K rolling temperature, when compared to conventionally rolled sheets (Huang et al., 2009). Kim et al. (2007) also revealed similar results when maintaining roll speed ratio at 3:1 and with appropriate annealing in AZ31 plates. DSR on CP titanium sheets improved the Erichsen values from 12.2 to 12.7 for the conventionally rolled sheets and from 12.9 to 14.7 in the case of DSRed sheets (Huang et al., 2010). As observed, the improvement is significant in case of sheets that experienced DSR.

In *single roller drive rolling*, which is another asymmetric rolling method, one roll is driven by a motor, and another roll (idle roll) is allowed to rotate freely to establish larger shear deformation in through thickness direction of the sheet (Sakai et al., 2001). The work done by Sakai et al. (2001) on AA5052 sheet of 3 mm thickness and Chino et al. (2002) on AZ31 Mg alloy showed improvement in press formability along with inducing lower planar anisotropy.

*Cross-rolling of sheets* is another method in which shear rolling improves the press-formability of sheets (Fig. 3.5). The rolls are positioned at " $\theta$ " angle ( $\approx 7$  degrees) to TD in the sheet plane (TD-RD). Due to thrust force along the axial direction of the roll, intense shear deformation is

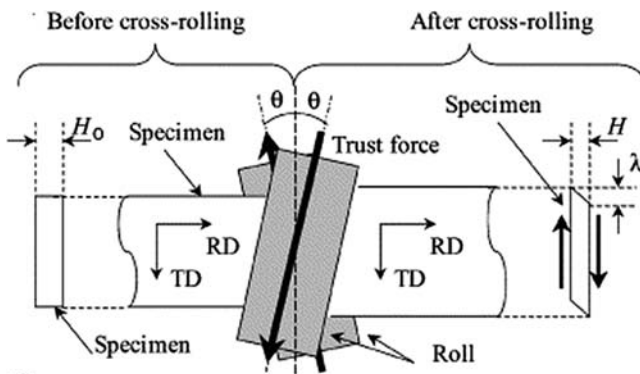


FIGURE 3.5 Cross-rolling of sheets. (where RD - Rolling Direction and TD - Transverse Direction). Reused with permission from Chino, Y., Sassa, K., Kamiya, A., Mabuchi, M., 2007. Microstructure and press formability of a cross-rolled magnesium alloy sheet. *Materials Letters* 61, 1504–1506, Elsevier.

introduced in the through thickness (ND) of the sheet. Press formability evaluated by Erichsen cup tests showed doubling of formability for cross-rolled AZ31 Mg alloy sheets of 6 and 5 mm thickness (Chino et al., 2006a, 2007). Four cases such as as-cross-rolled specimen, as-normal-rolled specimen, cross-rolled specimen, annealed at 673 K for 30 min, and normal-rolled specimen annealed at 673 K for 30 min are compared to show the effect of annealing.

*Rolling direction* can be changed after each rolling pass to enhance the formability and fracture elongation of AZ31 Mg alloy sheets (Zhang et al., 2013; Chino et al., 2006b); however, it depends on the scheme of rolling. Changing the rolling direction after each pass by 45 or 90 degrees to the RD produced fine-grained microstructure, higher strength, and larger fracture elongation. Erichsen cup tests reveal improvement in formability by about 28%–31%. In *equal channel angular rolling (ECAR)*, the sheet is rolled in a normal twin roller, and at the end of the rolling operation, it is passed through a channel having a change in deformation angle. AZ31 Mg alloy of 1.6 mm thickness showed reduction in yield strength and improvement in elongation with increase in number of rolling passes (Chen et al., 2007). The limiting drawing ratio has increased from 1.2 to 1.6 after ECAR.

Similar approaches are also followed in wire drawing for sustainable wire quality, efficient lubrication, material modifications, die design, process design, etc (Martinez et al., 2020; Prisco et al., 2020; Wang et al., 2018; Amine et al., 2018; Xu et al., 2020).

---

### 3.4 Sheet stamping

---

Improving the stamping quality of sheets is part of sustainable manufacturing. Replacing existing material grade to a new grade is beneficial, and it enhances the overall performance of the parts and tools. For instance, (i) replacing ZStE 420 (microalloyed steel with  $C \% \leq 0.10$ ) with TRIP 700 steel resulted in a formed sheet part without fracture, (ii) using multiphase steel as electrode material instead of normal steel in resistance spot welding, the diameter of electrode increased with increase in electrode forces, and weldability range became adaptable, and (iii) a deep drawing tool for TRIP 700 provided flexibility in tool requirement with CVD-coated and hardened inserts and cooling channels (Refer The Application of Multiphase Steel in the Body-in-White by Markus Pfesstorf). However, such changes are not always possible; sometimes, it may not be beneficial as well. In such situations, the existing materials need modifications in their structure with the help of approaches in materials processing, forming processes, tooling, and lubrication to enhance their

forming quality. Forming at elevated temperature, FS processing, incremental forming, hydroforming, sandwich sheets structures, and lubrication methods are presented here in the context.

Warm forming, deformation of sheets done at elevated temperatures less than recrystallization temperature, and hot forming, generally done at above recrystallization temperature of the material are the two methods of forming quality improvement. The response of sheet materials to change in temperature depends on its quality. Aluminum alloys such as Al 5754, Al 5182 containing 1% Mn, and Al 6111-T4 are formed in biaxial mode of deformation at temperature range of 200–350 °C (Li and Ghosh, 2004). Al 5754 shows significant improvement in forming limit with increase in the temperature as observed from forming limit curve (FLC) data, while not much difference is seen in case of Al 5182 containing 1% Mn between 300 °C and 350 °C. Temperature has a minimal effect on forming limit in case of Al 6111-T4 sheets. Attempts made by Sen and Kurgan (2016) show improved deep drawability of HC300LA sheet via warm deep drawing. The draw ratio increased by 22% in case of 1.2 mm thick sheet and about 20% for 1.5 mm thick sheet in the temperature range of 170–295 °C. Limiting draw ratio improvement with an increase in temperature is also witnessed in AZ31 alloy sheets as well (Hariharasudhan et al., 2004). Numerical simulations of round cup and rectangular pan helped in process design and predicted the thinning and force requirements acceptably (Fig. 3.6). Improvement in forming limit of AZ31 sheets with an increase in temperature and significant effect of

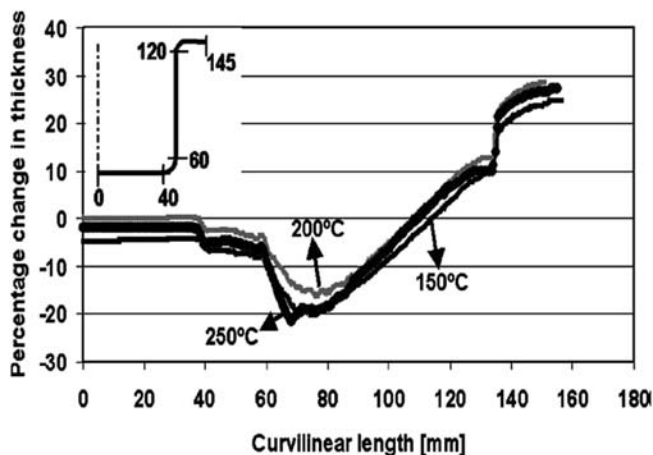


FIGURE 3.6 Thinning prediction and experimental comparison at different forming temperatures. Reused with permission from Hariharasudhan, P., Ngaile, G., Altan, T., 2004. Finite element simulation of magnesium alloy sheet forming at elevated temperatures. *Journal of Material Processing Technology* 146, 52–60, Elsevier.

strain rate at higher temperature are presented in [Chan and Lu \(2014\)](#) work. Strain rate sensitivity index plays a significant role in case of the effect of the strain rate. A camera casing was designed for optimizing the process temperature by finite element simulations, and at 300 °C, a crack free part was fabricated ([Chan and Lu, 2014](#)). Other materials also show change in formability and springback with change in forming temperature, and such changes are beneficial for part manufacturing, such as wheel base ([Chen et al., 2020](#); [Gerstein et al., 2021](#); [Caro et al., 2021](#); [Yang et al., 2020](#)). Selection of lubricants during hot forming is crucial. The use of lubricants such as vitreous enamel (commercial lead borosilicate glass) and devitrifying enamel (commercial lead zinc borate glass) in case of AA5083 ([Riahi et al., 2008](#)), a number of vegetable oil-based lubricants in case of magnesium sheet ([Ramezani and Schmid, 2015](#)), addition of swellable and nonswellable mica, melamine cyanuric acid, potassium titanate, and cellulose powder to a commercial lubricant made of hydrophilic polymer and a mineral salt in case of Al-coated 22MnB5 steel ([Uda et al., 2016](#)) improved the drawability of sheets, reduced coefficient of friction, and enhanced lubricity.

In friction stir welding (FSW) and friction stir processing (FSP), a rigid rotating tool is plunged into the sheet parts to be joined/processed and traversed at a particular velocity so that stirring and mixing of materials occur at elevated temperatures ([Mishra and Ma, 2005](#); [Ma, 2008](#)). At the end of the process, the sheets are welded in case of FSW, while these are processed in case of FSP. The microstructure and properties of the welded and processed zones are altered resulting in formability improvement. Formability improvement is an indication of improved materials behavior resulting in sustainable forming. Some examples are presented here.

The effect of tool shoulder diameters, 12 and 18 mm, on the forming limit of FSW sheets made of an aluminum alloy shows that in near plane-strain condition, the forming limit of the raw sheet and FSW sheets are almost same, while it improved significantly in stretching strain paths, improving the overall formability ([Ramulu, 2012](#); [Ramulu et al., 2013a](#)). In another attempt, [Ramulu et al. \(2013b\)](#) revealed that with increase in the tool rotation speed from 1300 to 1400 rpm, the forming limit of FSW sheet has improved, and with increase in feed rate from 90 to 100 mm min<sup>-1</sup>, it has decreased ([Fig. 3.7](#)). Out of all weld orientations and locations, weld at center and longitudinal weld are preferable ([Ramulu, 2012](#); [Ramulu et al., 2015](#)) ([Fig. 3.8](#)). In [Miles et al. work \(2004, 2005\)](#), FSWed sheets made of 5182-O, 5754-O, and 6022-T4 grades are fabricated, and a decreasing forming limit is seen in stretching limit as compared to that in plane strain for similar and dissimilar material combinations. [Miles et al. \(2006\)](#) also showed that tailor-made DP steel (DP 590) sheets fabricated by FSW exhibit better formability as compared to laser-welded sheets by about 20%. Other than DP 590 steel, transformation-induced plasticity (TRIP)

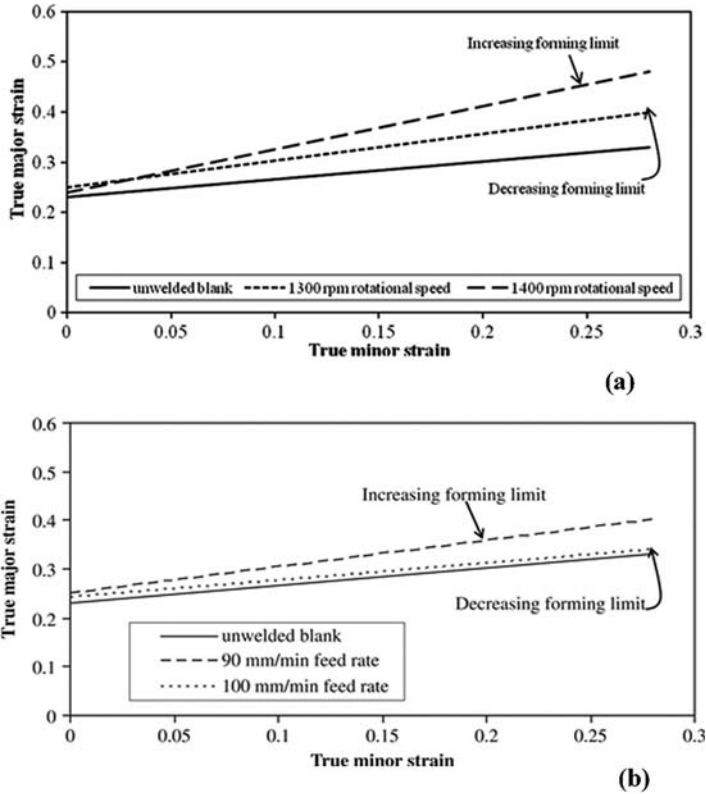


FIGURE 3.7 Improvement in forming limit of friction stir welding (FSW) Al6xxx sheets with change in (A) rotational speed and (B) feed rate. (Reused with permission from Ramulu, P.J., 2012. *Forming Behavior of Friction Stir Welded Sheets Ph.D. thesis IIT Guwahati, India*; Reused with permission from Ramulu, P.J., Narayanan, R.G., Kailas, S.V., 2013a. *Forming limit investigation of friction stir welded sheets: influence of shoulder diameter and plunge depth. International Journal of Advanced Manufacturing Technology* 69, 2757–2772).

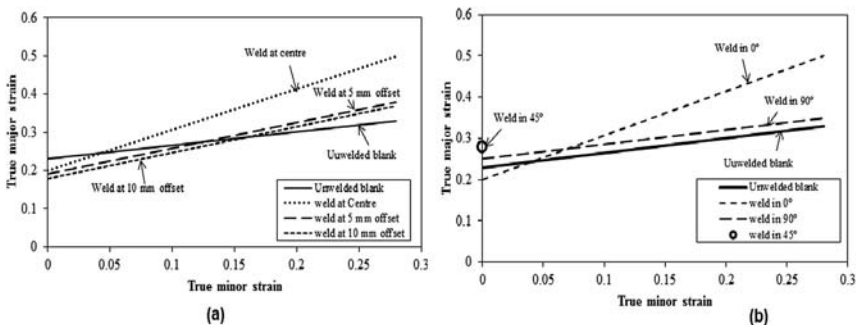


FIGURE 3.8 Forming limit improvement of friction stir welding (FSW) sheets at different (A) weld locations and (B) weld orientations. (Reused with permission from Ramulu, P.J., 2012. *Forming Behavior of Friction Stir Welded Sheets Ph.D. thesis IIT Guwahati, India*).

590 steel and DP 980 steels are also possible as suggested by Miles et al. (2009). Forming limit data of FSW sheets made of 1.4 and 1.2 mm thick stainless steel sheets reveal that (i) in uniaxial mode of deformation, transverse weld orientation is better, (ii) in plane-strain mode of deformation, longitudinal weld orientation is acceptable, and (iii) in biaxial tension, weld orientation has no role on formability (Moayedi et al., 2020) (Fig. 3.9). FSP resulted in significant improvement in superplastic properties of Al–4Mg–1Zr alloy characterized by improved superplastic ductility and reduced flow stress. A maximum ductility of 1280% was achieved at  $1 \times 10^{-1} \text{ s}^{-1}$  and  $525^\circ\text{C}$ , which considerably larger than that of rolled sheets (Ma et al., 2003). The microstructure having fine grains is also thermally stable at elevated temperatures. It is understood from the examples that FSW not only improves the formability of welded sheets but also provides scope for optimizing the forming deliverables based on various welding and tool parameters.

Hydroforming of sheets and tubes involves plastic deformation of materials with the help of fluid pressure. Hydroforming technology exhibits several merits such as higher drawing ratio, improved surface characteristics, minimized springback, improved dimensional accuracy, and ability to fabricate complicated shapes in less stages, when compared with conventional forming (like deep drawing, tube expansion, etc.). A multistage forming process can be converted to a single-stage process by utilizing the advantages (Zhang et al., 2004). The forming limit of sheets can be increased with the help of hydroforming. Various applications in

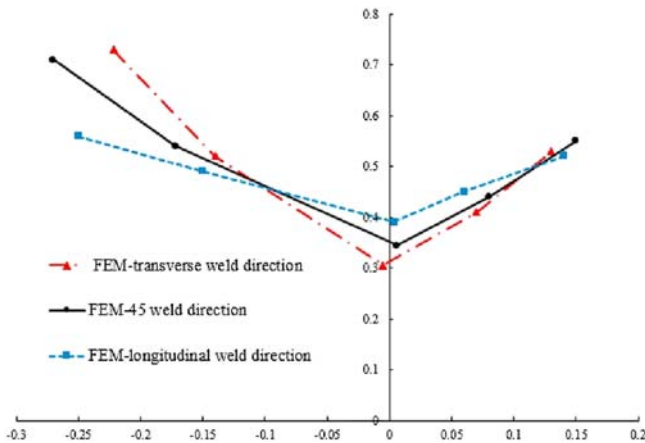


FIGURE 3.9 Forming limit diagram of friction stir welding (FSW) stainless steel sheets at different weld orientations. Reused with permission from Moayedi, H., Darabi, R., Ghabussi, A., Habibi, M., Foong, L.K., 2020. Weld orientation effects on the formability of tailor welded thin steel sheets. *Thin-Walled Structures* 149, 106669, Elsevier.

the automotive sector include radiator frames, exhaust components, engine parts, camshafts, axles, crankshafts, seat structures, etc (Ahmetoglu and Altan, 2000). Various other hydroformed components as projected by Tolazzi (2010) include cooling tube for FIAT FGP, tubes, and profiles in the new Opel GT, dashboard cowl on the Porsche Panamera. Recently, Kucharska and Moraczyński (2020) demonstrated that a car exhaust system piping made of chromium–nickel steel (AISI304L) can be fabricated by hydroforming technology.

There are several ways to modify the technology for the benefit of sustainable manufacturing. Pulsating hydroforming is one such method to improve the forming limit of tubes by oscillating the internal pressure. It is demonstrated by Mori et al. (2004, 2007) that tube formability improves due to uniform expansion during pulsating hydroforming. For a tube of 38 mm outer diameter, 1.1 mm wall thickness, and 200 mm tube length, the internal pressure was varied at  $17.7 \pm 3$  MPa with 0.67 cycles per unit punch displacement. Wrinkles during tube hydroforming, which are generally considered as defect, can be used to improve the forming quality. Optimized loading path (axial distance vs. internal pressure) and number of wrinkles not only improved the formability of tubes but also reduced the thinning rate (Yuan et al., 2007). Instead of conventional mineral oil as pressurizing fluid, *magnetorheological fluid* (MRF) can be used to improve the formability of tube with reduced thinning (Rosel and Merklein, 2014). Hydroforming at elevated temperature (Seyedkashi et al., 2014; Lang et al., 2012) and electromagnetic assisted hydroforming are other variants to improve the formability of sheets and tubes, reduce thinning, and improve corner filling (Chu and Liu, 2013).

Incremental sheet forming (ISF) is one recent advancement to improve the forming limit of sheets with the help of rigid tool with hemispherical head imparting localized deformation. Tool path, friction conditions, material quality, tool type, tool size, feed rate, tool rotational speed, and incremental depth, all affect the forming quality in a compounding fashion. ISF can be implemented with die or without die (called as single-point ISF). ISF with double tools (called as two-point ISF) are also used for sheet forming. ISF is a flexible forming process as it does not require specialized tooling (Jackson and Allwood, 2009). ISF improves forming limit of sheets due to through thickness shear as proposed by Allwood et al. (2007) or serrated strain paths because of cyclic, local plastic deformation (Eyckens et al., 2007). Forming limit curve describing the loci of necking limit is insufficient, and fracture forming limit curves are required to quantify formability in ISF (Silva et al., 2008). Other than metallic materials like copper (Jackson and Allwood, 2009), aluminum alloys (Jeswiet and Young, 2005), pure titanium (Gatea et al., 2018), ISF of polymers (polyvinylchloride (PVC)) (Fig. 3.10) proposed by Silva et al. (2010), carbon fiber–reinforced plastics (CFRP) (Fig. 3.11) proposed by

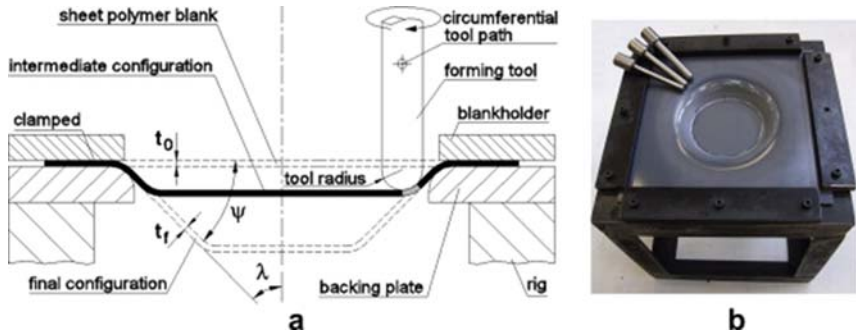


FIGURE 3.10 Single-point incremental sheet forming (ISF) of polymer sheet (A) schematic and (B) actual setup. Reused with permission from Silva, M.B., Alves, L.M., Martins, P.A.F., 2010. Single point incremental forming of PVC: Experimental findings and theoretical interpretation. *Eur. J. Mech. – A Solids* 29, 557–566, Elsevier Masson SAS. All rights reserved.

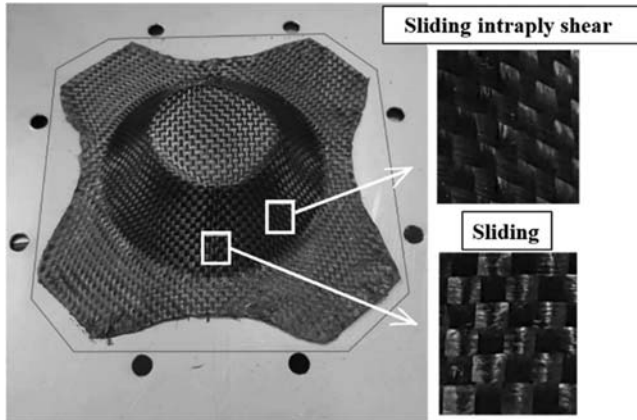


FIGURE 3.11 Incremental sheet forming (ISF) of carbon fiber-reinforced plastics (CFRP) (60 degrees cone shape with four layers of prepreg). Reused with permission from Xiao, X., Kim, J.-J., Oh, S.-H., Kim, Y.-S., 2021. Study on the incremental sheet forming of CFRP sheet. *Composites Part A: Applied Science and Manufacturing* 141, 106209. <https://doi.org/10.1016/j.compositesa.2020.106209>, Elsevier.

(Xiao et al., 2021) are also possible. In Kim and Park (2002) work, improvement in forming limit of 1050 Al sheet of 0.3 mm thickness is presented. Forming limit is higher for a tool with rotating head without friction, for smaller tools of 10 and 5 mm diameter, and at lower feed rates of 0.1 mm as compared to 0.3 and 0.5 mm.

Converting a monolithic sheet to sandwich sheet, use of variable blank holding force (BHF), developing lubricants and coatings improve the forming quality of sheets. Satheshkumar and Narayanan (2014 2015a,b) showed that ductility, an index to quantify formability, of adhesive

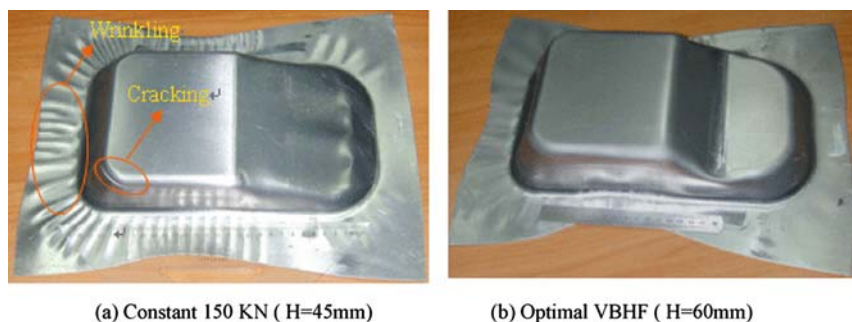


FIGURE 3.12 Stepped rectangular box fabricated by constant and optimum variable blank holding force (BHF). (A) Constant 150 kN ( $H = 45$  mm), and (B) Optional VBHF ( $H = 60$  mm). Reused with permission from Zhong-qin, L., Wu-rong, W., Guan-long, C., 2007. A new strategy to optimize variable blank holder force towards improving the forming limits of aluminum sheet metal forming. *Journal of Materials Processing Technology* 183, 339–346, Elsevier.

bonded sheets can be improved by changing epoxy and acrylic adhesive properties. Ductility of epoxy adhesive with 1:1 hardener to resin ratio is better than 0.6:1 ratio, and in case of acrylic adhesive, 1.2:1 ratio shows better ductility as compared to 0.8:1. Formability limit developed by Kim et al. (2003) for AA5182/polypropylene/AA5182 sandwich sheets, Liu et al. (2013) for AA5052/polyethylene/AA5052 sandwich sheet, and Aghchai et al. (2008) for two layers AA1100-st12 sheets bonded by polyurethane adhesive reveals improvement of forming limit of sandwich sheets as compared to monolithic sheets.

Optimized variable BHF reduces wrinkling and tearing, and improves the forming height as compared to constant 150 kN BHF (Zhong-qin et al., 2007) while fabricating a step rectangular box made of 5754 aluminum alloy (Fig. 3.12). In the category of new lubricants and coatings, mixture of boric acid crystals and canola oil (Lovell et al., 2006), use of wheat flour particles dispersed in water for sheet drawing (Yoshimura et al., 2002), boric acid dry films (Rao and Wei, 2001) for drawing and stretching applications of aluminum alloys, forming dies coated with titanium nitride (TiN) or vanadium carbide (VC) for stamping high strength steel sheets (Abe et al., 2014) and diamond like carbon (DLC) coating on Al5052 sheets (Horiuchi et al., 2012) are examples demonstrating improvement in the forming quality sheets in terms of better surface characteristics, reduced coefficient of friction and drawing load, increased formability level, etc.

### 3.5 Flexible tooling

Flexible tooling is commonly used to fabricate sheet components. Multipoint forming and rubber pad forming are two prominent methods

of flexible tooling. There is no need of die and related design and fabrication operations while using multipoint forming making it advantageous as compared to traditional stamping. A set of punches, which are simple in shape and easy to fabricate, is used in place of traditional large punch. Thus, the cost involved in designing expensive traditional punch is minimized. However, movement of punch in multipoint forming is achieved by computer interface. Real-time control of each punch to attain the shape of part is crucial, and standard design procedures need to be established. Only a small region below the punch is plastically deformed as opposed to conventional large punch. A slight change in part shape is possible at a later stage using some of the punches instead of fabricating another die for the purpose. With these advantages, multipoint forming helps in sustainable manufacturing of sheet parts.

Dimpling and buckling are the commonly observed defects during multipoint forming. Dimples are formed due to the severe thinning of sheet at a location as a result of localized pressure provided on the sheet. These can act as a source of failure during application. Buckling of sheet occurs between two adjacent contact regions established by punches and sheet, which are deprived of clamping pressure (Li et al., 1999). Multipoint die forming, multipoint half die forming, multipoint press forming, and multipoint half press forming are the four types in multipoint forming (Fig. 3.13) (Li et al., 1999). Multipoint forming with variable blank holding force (BHF) and sectional multipoint forming are proposed by Li et al. (2002) as new varieties. Use of multipoint forming with variable BHF helped in forming an aluminum sheet of 1 mm thickness without wrinkles. In the sectional multipoint forming, the sheet is deformed in parts using a press with smaller bed size. For instance, a sheet of 3 m size can be formed with the forming area of about  $140 \times 140$  mm only. Cai et al. (2008) presented numerical simulation of multipoint forming of steel, copper, and aluminum sheets and predicted buckling, dimpling, and springback. Peng et al. (2013) demonstrated multipoint forming of polycarbonate sheet, and titanium alloy cranial prosthesis can be formed with multipoint forming as demonstrated by Tan et al. (2007).

Rubber pad forming of sheets is another category of flexible tooling in which a rubber pad is used instead of rigid punch to deform sheets with the help of rigid die. Some of the merits are uniform distribution of strain during sheet deformation enhances its formability, design of rigid die is sufficient, reduction in fabrication cost, and precise assembly of rigid die is not required. Bipolar plate (used in fuel cells) fabricated by rubber pad forming (Talebi-Ghadikolaee et al., 2020; Liu and Hua, 2010; Lim et al., 2013; Jeong et al., 2014) is a good example in which the role of rubber hardness, rubber thickness, punch speed and pressure, internal and external radii of die, and draft angle of the die on the product quality are highlighted. A prototype of support rib for an aircraft wing made of an

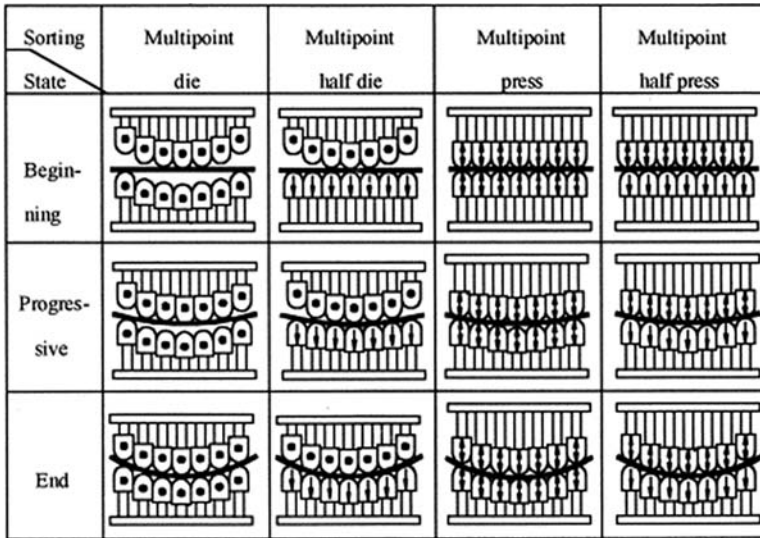


FIGURE 3.13 Types of multipoint forming. Reused with permission from Li, M., Liu, Y., Su, S., Li, G., 1999. Multi-point forming: a flexible manufacturing method for a 3-d surface sheet. *Journal of Materials Processing Technology* 87, 277–280, Elsevier.

aluminum alloy has been fabricated by rubber pad forming exhibits less thinning and good surface finish (Browne and Battikha, 1995). Forming of adhesive-bonded sandwich sheet with improved formability using rubber pad forming is also possible (Kukreja and Narayanan, 2019).

### 3.6 Green lubrication

In metal forming, friction exists between deforming body (like billet or sheet) and rigid tools (like die, punch, holder, etc.). Lubricants are used to minimize friction. Material flow, load requirement, defect formation, and finally, product quality are controlled by friction and lubricants. Selecting lubricants and lubrication systems are equally important to tool design and selection of other process requirements and that depends on material quality, forming temperature, interface pressure, and sliding speed. Similar situation and requirements prevail in joining processes based on plastic deformation. The prime function of lubricant is to control friction and prevent tool wear. There are other functions such as aiding appropriate die filling, reducing surface pressures to enhance tool life, minimizing adhesion in hot and cold forming situations, provide insulating effect to avoid die chill, reduce health related risks, and permit easy removal (ASM handbook, 1992). Fluid lubricants contain oils, water, and

synthetic compounds along with additives as primary ingredients to improve the effectiveness of lubrication. The fluid lubricants are in the form of solutions, emulsions, and pastes. Viscosity, density, and compressibility of the fluid lubricants are the crucial properties of concern. Additives such as film-strength additives, extreme pressure (EP) additives, suspended solids, corrosion inhibitors, oxidation inhibitors, defoamers, and antimicrobial agents help in the applicability of lubricants during metal working and mainly in controlling lubricity ([ASM handbook, 1992](#)). Controlling lubricity is vital for sustainable lubrication and forming as it minimizes friction and wear, protect contacting surfaces of workpiece, prevent tool and workpiece from corrosion, and lubricate equipment. Solid lubricants such as polyethylene, polyvinylchloride, and polytetrafluoroethylene, MoS<sub>2</sub>, graphite, sodium carbonate, teflon, nylon, etc. are preferred when lubricant film strength requirements are more than what is possible with liquid lubricants ([ASM handbook, 1998](#)). Dry soaps, thermoplastic polymer coatings like polyethylene, polypropylene, polytetrafluoroethylene (PTFE), PVC, polystyrene, polyimide, polymethyl methacrylate (PMMA), metal coatings made of tin and zinc, hard coatings like TiN, TiC, Al<sub>2</sub>O<sub>3</sub>, and multilayer coatings like TiC/Al<sub>2</sub>O<sub>3</sub>/TiN are also used as lubricants ([ASM handbook, 1998](#)). An example at lab scale demonstrated by [Erdin and Ozdilli \(2019\)](#) showed that the polyester polymer coating on steel sheets improved the surface quality of the test specimens, and as a consequence, molding forces reduced, deep drawing ratios improved, and defects such as tearing and wrinkling are lessened. Microextrusion of 6063 aluminum alloy with various tool coatings such as CrN, TiN, DLC-PVD, and DLC-CVD with definite range of hardness, thickness, and coefficient of friction reveals (i) decrease in energy consumption with reduction in coefficient of friction and (ii) possibility of tool life extension by high hardness of the tool surface and low bearing lengths ([Sucharitpwatskul et al., 2020](#)).

Selection of lubricants is a complicated task as it depends on several factors including contacting material pair, type of forming process, forming conditions like speed, pressure, temperature, actual normal contact stresses, and workpiece surface characteristics. The recommended lubricants in cold forming and hot forming conditions for different materials are listed in [Table 3.1](#).

Maintaining sustainability and green manufacturing are given special emphasis in industries. Development of new materials and processes resulted in developing new lubricants that are ecofriendly and are derived from natural resources. Biodegradable lubricants from vegetables, crops, edible items, etc. and their characteristics suit the requirements of sustainable and green manufacturing ([Nagendramma and Kaul, 2012](#)). Vegetable oils are renewable, biodegradable, and human friendly. Palm, soya bean, sunflower, coconut, safflower, rapeseed, cotton

TABLE 3.1 Lubricants used for various sheet materials in hot and cold working states.

Material	Cold forming lubricant	Hot forming lubricant
Aluminum alloys	Synthetic solutions, emulsions, lanolin suspensions, water suspensions, soap solutions, mineral oil, fatty oils	Graphite suspension
Copper alloys	Emulsion, fatty oils, mineral oils, soap suspensions, water suspensions, tallow suspensions, synthetic solutions	Pigmented pastes, graphite suspensions
Magnesium alloys	Solvent plus fatty compounds, mineral oils plus fatty compounds	Graphite plus molybdenum disulfide, soap plus water, tallow plus graphite
Nickel and Nickel alloys	Emulsions, mineral oils plus EP additives, water plus chlorine additives, conversion coatings plus soap	Graphite suspension, molybdenum disulfide suspension, resin coating plus salts
Refractory metals and alloys	Copper plating	Molybdenum disulfide suspension
Carbon steels and low alloy steels	Emulsions, soap pastes, water, fatty oils plus, mineral oils, polymers, conversion coating, molybdenum disulfide, graphite in grease, synthetic solutions	Graphite suspension
Stainless steels	Fatty oils, mineral oil, water, polymers, conversion coating plus soap, mineral oil plus additives, pigmented soaps	Graphite suspension
Titanium and Titanium alloys	Water, pigmented soaps, polymers, conversion coating plus soap	Graphite suspension, MoS <sub>2</sub> suspension

Reprinted with permission from ASM international, All rights reserved, [www.asminternational.org](http://www.asminternational.org) (ASM Handbook, 1998. Forming and Forging, vol. 14, Ed. Semiatin, S.L.

seed, and peanuts are potential sources of bio lubricants. Oils from species such as Jatropha, Neem, Karanja, Castor, Mahua, Linseed, and Moringa are categorized under nonedible oils and have about 30%–50% (of volume) oil content (Mobarak et al., 2014). Out of these, coconut has about 60% oil content, higher than other species. Table 3.2 compares the properties of vegetable oils and mineral oils (Mobarak et al., 2014). It can be understood from the table that vegetable oils possess a higher viscosity index ensuring efficiency at elevated temperatures and the increased load bearing ability, have low pour point providing good lubrication for cold starts, exhibit higher flash point ensuring safe environment without catching fire, and the ability to maintain lubricant properties at elevated temperatures. They also have good resistance to corrosive and rust environment. Vegetable oil–based lubricants have disadvantages like low oxidative stability (oil will oxidize quickly during use if unprocessed) and have low temperature limitations, unfriendly smell, bad compatibility with paints and sealants (Mobarak et al., 2014). Above all, the demanding concern of safe and clean work environment is satisfied by vegetable-based biolubricants due to nontoxic nature and easy disposal. Data on physio-chemical properties provided by Mobarak et al. (2014) indicate vegetable oils possess good properties.

TABLE 3.2 Comparison of properties of vegetable oils with mineral oils.

Properties	Vegetable oils	Mineral oils
Density in $\text{kg m}^{-3}$ at 20°C	940	880
Viscosity index	100 to 200	100
Shear stability	Good	Good
Pour point, °C	–20 to +10	–15
Cloud flow	Poor	Poor
Miscibility with mineral oils	Good	NA
Solubility in water	No	No
Hydrolytic stability	Poor	Good
Oxidation stability	Moderate	Good
Seal swelling tendency	Slight	Slight
Sludge formation	Poor	Good

Reused with permission from Mobarak H.M., Mohamad E.N., Masjuki H.H., Kalam M.A., Al Mahmud K.A.H., Habibullah, M., Ashraf A.M., 2014. The prospects of bio-lubricants as alternatives in automotive applications. *Renewable and Sustainable Energy Reviews* 33, 34–43, Elsevier.

Self-lubricating tool coating is another sustainable approach followed to maintain sustainability in metal forming operations. In this case, external lubricants are not used; instead, ceramic and other coatings on the die surface or self-lubricating systems are used. For example, for high-temperature applications and massive cold forming, TiCN, TiC–TiN, and diamond-like carbon (DLC) coatings are used (Reisel et al., 2003, 2005; Wank et al., 2006). Further, the coated tools not only improve the drawability in deep drawing by delaying fracture but also enhance the die life and galling performance (Murakawa et al., 1995, 1999; Podgornik et al., 2004).

### 3.7 Laser-based manufacturing

Metallic and nonmetallic components are fabricated traditionally by injection molding, forging, extrusion, and sheet stamping operations using tools such as die, punch, mold, etc. Tool production is expensive because of long process time, involves technical difficulties, and is labor intensive. The lead time required for tool fabrication is about 11 weeks, and it is about 1 year in case of large, complicated tools used in the automotive sector. Moreover, severe processing conditions, corrosive environment, thermal cycling, mechanical loading, etc. restrict the life of tools during actual applications. New methods of producing tools by new processes are required to enhance the service life of tools. The claim can be substantiated with the help of unsustainable tool life cycle (Fig. 3.14) and environment impact of various manufacturing operations involved in traditional manufacturing route (Table 3.3) (Morrow et al., 2007).

Recent scientific and research advancements in laser-based manufacturing such as laser-based additive manufacturing ensure remanufacture of tools by repairing it. The strategy significantly reduces

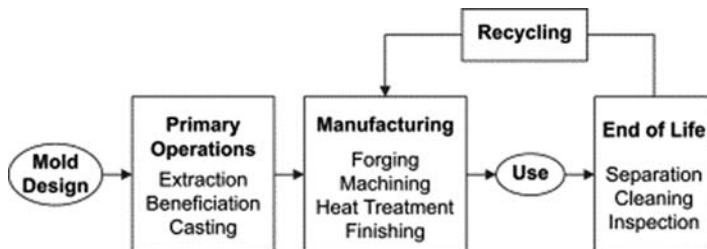


FIGURE 3.14 Life cycle of tools in traditional operations. Reused with permission from Morrow, W.R., Qi, H., Kim, I., Mazumder, J., Skerlos, S.J., 2007. Environmental aspects of laser-based and conventional tool and die manufacturing. *Journal of Cleaner Production* 15, 932–943. <https://doi.org/10.1016/j.jclepro.2005.11.030>, Elsevier.

TABLE 3.3 Environmental impact of traditional operations.

Manufacturing operations	Candidates for reducing environmental burden
Casting	Air/water emissions and energy consumption from furnace and mold material handling operations; solid waste from discarded mold material; general footprint of factory operation and associated overhead.
Forging	Energy consumption; hydraulic fluid use and spills; conversion coating use; metalworking lubricants and fluids; footprint/overhead; tool production and disposal.
Machining	Energy consumption; production and handling of waste chips; metalworking fluids; tool production and use; on-site wastewater treatment.

Reused with permission from Morrow, W.R., Qi, H., Kim, I., Mazumder, J., Skerlos, S.J., 2007. Environmental aspects of laser-based and conventional tool and die manufacturing. *Journal of Cleaner Production* 15, 932–943. <https://doi.org/10.1016/j.jclepro.2005.11.030>, Elsevier.

the lead time and tool fabrication cost along with reducing environmental impact as there is no polluting stages that are observed in the traditional route. Improvement in industrial competitiveness is also observed. Morrow et al. (2007) provided three case studies including a mold insert design, mirror design, and stamping tool remanufacture, all attempted by conventional CNC machining route and direct metal deposition (DMD) (a laser additive manufacture method) route. The energy consumption results reveal that the performance of CNC and DMD routes depends on solid to cavity volume ratio. DMD performs better in case to low ratios, while CNC is acceptable in high ratios (Fig. 3.15). Electricity consumption in stamping tool repairing/remanufacture is lower than in the CNC route (Fig. 3.15). Wilson et al. (2014) also showed that energy consumption and carbon footprint (kg of CO<sub>2</sub>) are much lesser in case of turbine blade repaired by laser direct deposition (LDD) as compared to investment casting. The total energy needed in LDD was acceptable in cases when less than 18% of the total blade volume needs overhauling (Fig. 3.16). However, Yoon et al. (2014), through case studies, concluded that by considering specific energy consumption as reference, injection molding and machining are highly recommended for fabrication. Only when the quantity of parts is small, fused deposition modeling (FDM) is beneficial over conventional manufacturing processes.

In powder bed fusion (PBF) method, several parts can be made via the additive manufacturing route. The total energy consumed for fabricating

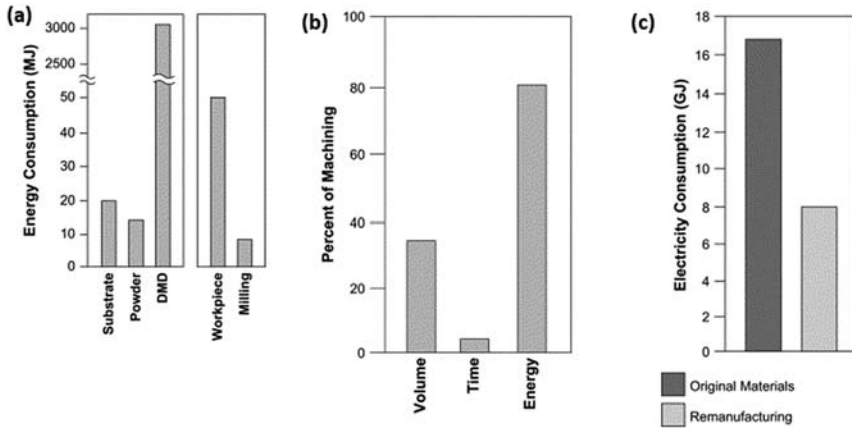


FIGURE 3.15 (A) Energy consumption comparison in mold insert design, (B) comparison in mirror design, and (C) electricity consumption in remanufacture. *Reused with permission from Morrow, W.R., Qi, H., Kim, I., Mazumder, J., Skerlos, S.J., 2007. Environmental aspects of laser-based and conventional tool and die manufacturing. Journal of Cleaner Production 15, 932–943. <https://doi.org/10.1016/j.jclepro.2005.11.030>, Elsevier.*

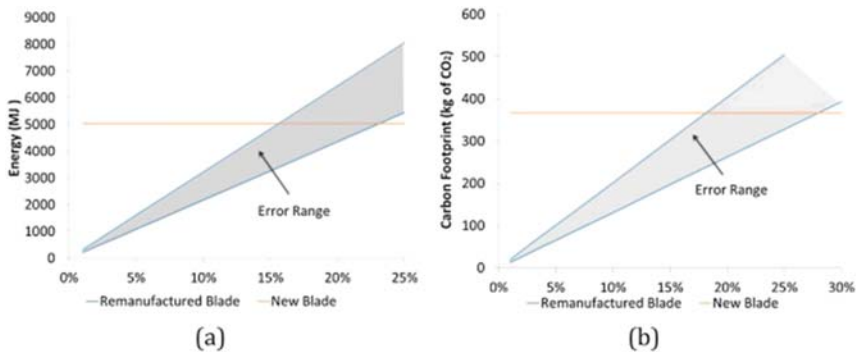


FIGURE 3.16 (A) Total energy consumption and (B) carbon footprint comparison between laser direct deposition and investment casting at different repair stages. *Reused with permission from Wilson, J.M., Piya, C., Shin, Y.C., Zhao, F., Ramani, K., 2014. Remanufacturing of turbine blades by laser direct deposition with its energy and environmental impact analysis. Journal of Cleaner Production 80, 170–178. <https://doi.org/10.1016/j.jclepro.2014.05.084>, Elsevier.*

a medical product, tibia fixation plate, or implant, by laser-PBF, which has got 7540 mm<sup>3</sup> of total volume of fabrication, is about 63 MJ. The unit process life cycle inventory methodology has been followed for calculations (Ramirez-Cedillo et al., 2021), which can be used a choice for improving the process efficiency with energy minimization. Another important issue in the context of sustainable manufacturing is recyclability of powder particles during PBF. Recently, Gorji et al. (2020) studied

the effect of using SS316L recycled powder particles in pore formation. They found that the recycled powders show slightly more porosity that is confirmed by X-ray computing tomography results. Due to this, the recycled powders exhibit lower hardness and higher modulus at different indentation depths as compared to virgin powders. Finally, they suggested to record the powder bed area used for printing the product for every machine. More details on 3DP of variety of stainless steel can be obtained elsewhere (Zitelli et al., 2019).

Laser forming is a recent development toward sustainable manufacturing. In this process, laser heat source is used to bend sheets and plates through which uncomplicated and complicated shapes can be fabricated. Due to laser heat, local softening occurs and leads to plastic strain because of rise in temperature and subsequent cooling. Monolithic sheets, double-layered sheets, metallic materials, composites, tubes, etc. can be formed without the use of rigid tools. It is a contactless process making it sustainable. Scan distance, number of passes per scan line, number of scan lines on the profile of the bend, and overlapping of the laser beam paths are essential parameters to fabricate a continuous smooth bend (Safari et al., 2020a). Three different mechanisms such as temperature gradient mechanism (TGM), buckling mechanism (BM), and upsetting mechanism (UM) are proposed during laser beam irradiation of metallic structures (Shi et al., 2007; Safari et al., 2020a). Steel, aluminum alloys, magnesium alloys, and titanium alloys are common among sheet materials that are laser formed. Some examples are shown in Fig. 3.17. Sheets can be bent and converted to dome shape and saddle shape structures as proposed by Chakraborty et al. (2018), Safari et al. (2020b), Shahabad et al. (2017), Thomsen (2020). Laser forming of bimetallic sheets (Nejad et al., 2021; Kotobi et al., 2019) and laminated composites (Seyedkashi et al., 2016) are practically possible and applicable in electronic device manufacturing industries.

### 3.8 Need for sustainable joining processes

In this section, need for sustainable joining processes, strategies to develop green and sustainable processes in fusion welding, solid-state welding, adhesive bonding, mechanical joining and hybrid joining, and inclusive manufacturing from materials joining point of view are discussed with examples from literature. In order to reduce CO<sub>2</sub> emissions, which has increased by about 57% between 1990 and 2017, several industries all over the world have started to strive toward clean, green, and energy-efficient production (Halkos et al., 2021; Ali et al., 2018). Material joining is a broad area in manufacturing wherein there is a lot of scope for

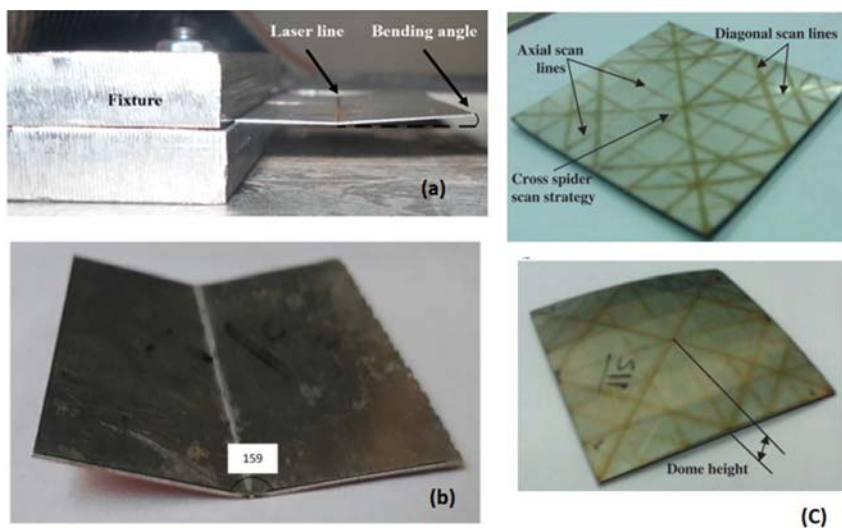


FIGURE 3.17 Laser-formed sheets: (A) stainless steel sheet (reused with permission from [Abedi and Gollo, 2019](#); Elsevier), (B) aluminum-copper bimetallic sheet (reused with permission from [Nejad et al., 2021](#); Elsevier), and (C) dome-shaped stainless sheet (reused with permission from [Maji et al., 2014](#); Elsevier).

developing sustainable methods including optimizing energy consumption and resources, recycling waste, repairing welded structures, remanufacturing of worn out parts, eliminating defects, reducing harmful emissions, efficient protection strategies, agile joining, increasing productivity, development of green tools, computations based optimization, and so on. To achieve such objectives, several new joining processes are introduced and traditional processes are modified. Moreover, such developments are propelled by discovery of new materials.

### 3.9 Sustainable fusion and solid-state welding processes

Various sustainable strategies and practices developed in welding, mechanical joining, materials deposition, and hybrid joining are discussed as follows.

#### 3.9.1 Fusion welding

In the case of fusion welding processes, reducing particulate fumes, reducing energy consumption, enhancement of mechanical performance, reducing defects, power loss management, utilization of consumables, and improving weldment efficiency are focused. In shielded metal arc

welding (SMAW) process, coating the electrode with  $ZrO_2$  nanoparticles improved the impact toughness of the weld (Dabiri et al., 2015), using austenitic stainless steel fillers enhanced the ballistic performance of armor steel joints (Balakrishnan et al., 2011), using external magnetic field for achieving acceptable weld geometry (Singh et al., 2021a), usage of Ni-based austenitic welding electrode (ENiCrMo-6), the matching ferritic welding electrode ENi11 for betterment of tensile strength of 9%Ni ferritic steel (El-Batahgy et al., 2020), and development of welding torch for absorbing hydrogen in gas shielded arc welding (Kawabe et al., 2016) are some important developments to achieve sustainability. Through life cycle assessment, Vimal et al. (2015) proved that 100% recycling of wire is possible for sustainable SMAW process.

In order to minimize spatter and fumes during  $CO_2$  gas-shielded arc welding, the proposals by Yamazaki et al. (2012) to regulate the globular transfer of molten droplets in which each droplet is squeezed at its upper part in peak current duration and detached in base current duration, and Tsuyama et al. (2014) to use an electrically heated filler wire, referred as F-metal active gas (F-MAG), are noteworthy. The deposition rate of F-MAG is 1.5 times more than  $CO_2$  arc welding under the same heat input resulting in savings in welding time and energy.

Gas tungsten arc welding (GTAW) is well understood and easily controllable because filler material is not necessary. There are several attempts to attain sustainable joining in the past and a few are summarized in Table 3.4.

Gas metal arc welding (GMAW) is used to weld a wide range of metals in many industrial fields because of its high efficiency, low cost, and significant potential. The welding setup can be used for additive manufacturing as well. Table 3.5 presents contributions to make GMAW a sustainable joining method.

Plasma arc welding (PAW) is advantageous in terms of high welding speed, produces better weld quality, and imparts longer electrode life during welding. The three major types of plasma arc welding processes are (i) microplasma arc welding, (ii) melt-in mode plasma arc welding, and (iii) keyhole mode plasma arc welding. Microplasma welding is carried out at current less than 15 A, and it produces low energy density and low plasma velocity for welding thin sheets. Melt-in mode plasma arc welding is used for welding sheets with thickness of about 2.5 mm wherein current varies between 15 and 400 A. Keyhole mode plasma arc welding is used for welding materials with thickness more than 2.5 mm and current more than 400 A. Apart from these types, the other variants like variable polarity plasma arc welding (VPPAW) process, pulsed plasma gas welding (PPGW), double pulsed plasma arc welding (DPPAW) are widely used for joining steels with thickness between 9.5 and 12.5 mm. PAW exhibits better weld penetration and minimized

TABLE 3.4 Attempts entertained to achieve sustainable GTAW.

Reference	Strategies/ improvements implemented in GTAW	Improved outputs toward sustainable joining
Baskoro et al. (2018)	Generating external magnetic field around the welding area	<ul style="list-style-type: none"> <li>• Improved the weld penetration and welding efficiency.</li> <li>• Reduces power consumption.</li> </ul>
Wagner et al. (2018)	Using helium gas at a concentration of more than 80%	Reduces UV radiation.
Feng et al. (2021)	Postweld treatment of GTAWed titanium alloy by warm laser shock peening	<ul style="list-style-type: none"> <li>• Increases 42.3% of high cycle vibration fatigue limit.</li> <li>• Decreases the compressive residual stress in weld zone and HAZ by 14% and 17%, respectively.</li> </ul>
Lee et al. (2020)	Water cooling during GTAW	<ul style="list-style-type: none"> <li>• Prevents solidification cracking in weldment.</li> <li>• Reduces the thermal stress and strain in the weld bead</li> </ul>
Guo et al. (2021)	Gas tungsten wire arc additive manufacturing (GT-WAAM) of thin wall with AZ80M magnesium alloy	UTS of the structure is close to that of the as-extruded AZ80M and better than as-cast AZ80M.
Srikanth and Manikandan (2017)	Pulsed current GTAW of nickel-based superalloy C-276 using filler wires like ERNiCr-3, ERNiCrMo-3, and ERNiCrMo-14 and faster cooling rate	<ul style="list-style-type: none"> <li>• Improves metallurgical and mechanical properties by reducing the microsegregation of alloying elements.</li> <li>• Refining grain structure as compared to GTAW.</li> </ul>

Continued

TABLE 3.4 Attempts entertained to achieve sustainable GTAW.—cont'd

Reference	Strategies/ improvements implemented in GTAW	Improved outputs toward sustainable joining
Chen et al. (2020a)	Pulsed ultrasonic–assisted gas tungsten arc welding	Refines grains and microstructure, improves crystal isotropy and hardness of the weld region

angular distortion, residual stress, and smaller HAZ when compared to other arc welding processes resulting in sustainable welding. Filler material is not required for thin sections, which is an added advantage. Energy density of PAW is more than GTAW (Sahoo and Tripathy, 2021) and acceptable microstructure characteristics as well (Huang, 2010).

Submerged arc welding (SAW) finds a lot of sustainable applications in fabrication industries as it is reliable and provides deep penetration, smooth and sound weld, and high productivity. An envelope of molten granular flux used to shield the arc protects the weld pool from atmospheric contamination. Cladding is also possible with SAW for which hard material could be deposited on a softer substrate. Sustainability can be achieved by controlling the parameters like arc voltage, welding current, welding speed, wire diameter, granular flux, and extended length. Improvement in joint tensile and impact strengths by optimized arc voltage or current (Aman and Singh, 2020), improvement in tensile strength and toughness by adopting an organic adhesive assisted underwater SAW (Dong et al., 2020), preheating of wire reducing distortion, and improvement of mechanical properties of the welded joint (Abhishek et al., 2020) are some examples in the direction.

While comparing the performance of GMAW, SMAW, GTAW, and flux core arc welding (FCAW) during welding of carbon steel plates with 25 mm thickness having U and V groove configurations, GMAW performs better than the other processes. Merits of GMAW include lower energy consumption and filler material usage and lower environmental load due to less quantity of shielding gas used at high speed. On the other hand, GTAW requires high power, has low welding speed, and has high shielding gas consumption. However, it presents the lowest emission of fumes, when compared to FCAW and SMAW. FCAW exhibits a lower deposition efficiency of about 86% that leads to a higher consumption of fillers. SMAW has low deposition efficiency of 60%, which results in high consumption of fillers and welding energy (Favi et al., 2019).

TABLE 3.5 Attempts entertained to achieve sustainable GMAW.

Reference	Strategies/ Improvements implemented in GMAW	Improved outputs toward sustainable joining
Zong et al. (2020)	Double shielded pulsed GMAW to feed the shielding gas of argon and CO <sub>2</sub> with two independent coaxial channels.	<ul style="list-style-type: none"> <li>• Improves weld stability.</li> <li>• Increases content of CO<sub>2</sub> up to 50%.</li> <li>• Helps avoid short circuit and spatter.</li> </ul>
Schafranski et al. (2017)	Adding H <sub>2</sub> and CO <sub>2</sub> in argon gas mixtures in GMAW.	<p>Ar+8%CO<sub>2</sub> mixture exhibits superior deposition efficiency and weld bead wettability.</p> <p>Ar+5%H<sub>2</sub>+7%CO<sub>2</sub> mixture increases wire melting rate and weld bead wettability similar to Ar+ 8% CO<sub>2</sub>.</p>
Chen et al. (2020b)	Pulsed power ultrasonic-assisted GMAW	<ul style="list-style-type: none"> <li>• Increases the weld penetration, weld area and microhardness of welded joint.</li> <li>• Refines grains.</li> </ul>
Shi et al. (2014, 2016)	Pulsed double-electrode GMAW for joining of aluminum to galvanized steel sheets.	<ul style="list-style-type: none"> <li>• Reduces heat input and increases energy required to melt the filler metal.</li> <li>• Helps in achieving welded joint having about 89% of shear-tensile strength of base metal.</li> </ul>
Hadadzadeh et al. (2017)	Employing pulsed current GMAW of Al-6.7 Mg alloy by maintaining low peak current of 120 A and increasing the frequency (0.5–2.0 Hz).	<ul style="list-style-type: none"> <li>• Improves weld strength.</li> <li>• Reduces HAZ softening of strain hardened Al-6.7 Mg alloy.</li> </ul>

Continued

TABLE 3.5 Attempts entertained to achieve sustainable GMAW.—cont'd

Reference	Strategies/ Improvements implemented in GMAW	Improved outputs toward sustainable joining
Khan and Madhukar (2020)	Utilization of different heat sources in WAAM.	GMAW and GTAW are preferred as an economical choice.
Derekar et al. (2020)	WAAM of AA5183 by pulsed-metal inert gas (MIG) and cold metal transfer techniques.	Pulsed-MIG samples show increased number of pores and volume fraction of porosity, and absorb more hydrogen than CMTed samples.
Kumaran et al. (2020)	Pulsed and normal cold metal transfer (PCMT, NCMT), and GMAW of AA7475 using ER5356 and ER4043 fillers.	The PCMT using ER5356 filler exhibits superior performance at a specific set of welding conditions.

Laser beam welding (LBW) exhibits high flexibility, quality, and energy density, and it is widely applied in the fields of automobile, aerospace, and so on. There are different types of laser welding processes based on laser heat sources like neodymium-doped yttrium aluminum garnet (Nd:YAG) laser, CO<sub>2</sub> laser, diode laser, disk laser, and fiber laser. The most widespread lasers for welding are the solid-state lasers of Nd:YAG, and the gas lasers of CO<sub>2</sub>. Laser power, welding speed, and pulse rate are the major influential parameters in LBW that affect the weld configuration and quality, and provide scopes for sustainable welding as described in Table 3.6.

Electron beam welding (EBW) ensures high energy efficiency, high-quality, and deep penetrated welded joints in structural metals in a wide range of thickness from 0.025 to 300 mm. Material range includes different grades of steel, refractory metals like tungsten, molybdenum, niobium, and chemically active metals like titanium, zirconium, and beryllium. It is also used for the production of films, coatings by deposition, surface modification, rapid prototyping, texturing surface, cladding with wire and powder, and alloying. EBW is influenced by the parameters like accelerating voltage, beam and lens current, focal position, welding speed, beam oscillation, and pulsing. Considering deep weld penetration, welding wide variety of materials, and useful in variety of applications, EBW is a good candidate for sustainable joining (Weglowski et al., 2016; Liu et al., 2021; Slobodyan, 2021).

TABLE 3.6 Attempts entertained to achieve sustainable laser welding.

Reference	Strategies/ improvements implemented in laser welding	Improved outputs toward sustainable joining
Auwal et al. (2018a)	Laser power, welding speed, and pulse rate are the major influential parameters in LBW of different alloys that affect the weld configuration and quality.	Even a high-power laser over 5 kW can be focused on a spot as small as 0.1 mm.
Auwal et al. (2018a, b)	Utilizing continuous wave in laser welding of titanium alloys and copper alloys.	<ul style="list-style-type: none"> <li>• Improves the keyhole stability.</li> <li>• Increases penetration depth and bead width increase with increase in laser power and decrease in welding speed.</li> <li>• High laser power and high welding speed reduce spatter and material loss.</li> </ul>
Oladimeji and Taban (2016)	Dual-beam laser welding and double-pulse laser welding of aluminum alloys.	Reduces solidification cracking and porosity.
Sakate et al. (2021)	Utilizing a parallel water jet in underwater wet laser welding.	<ul style="list-style-type: none"> <li>• Enhances the removal of water vapor formed at the laser-water-workpiece interface without creating hindrance to the molten weld bead.</li> <li>• Reduces energy loss and enhances the laser energy coupling efficiency, deep penetration and fine grain formation.</li> </ul>

*Continued*

TABLE 3.6 Attempts entertained to achieve sustainable laser welding.—cont'd

Reference	Strategies/ improvements implemented in laser welding	Improved outputs toward sustainable joining
Wei et al. (2015)	Hot and cold wire laser welding	Hot-wire laser welding exhibits a maximum energy saving of 16%.
Huang et al. (2021)	Carbon emission (CE) evaluation in a fiber laser welding of 2.5 mm thick AA sheets.	<ul style="list-style-type: none"> <li>• <math>CE_{(\text{Cooling system})} = 1.78 * CE_{(\text{laser devices})}</math>.</li> <li>• The auxiliary equipment and the cooling system are actually responsible for total carbon emissions.</li> </ul>

Other than the welding process described above, gas welding and resistance welding are also utilized significantly for welding a variety of metallic materials, and several attempts are made for sustainable fabrication of structures (Singh et al., 2021b; Li et al., 2015a; Khan et al., 2015; Pan et al., 2021). The comparison of geometry of butt weld joint made using various fusion welding technologies, the deep penetration, and weld width are shown in Fig. 3.18.

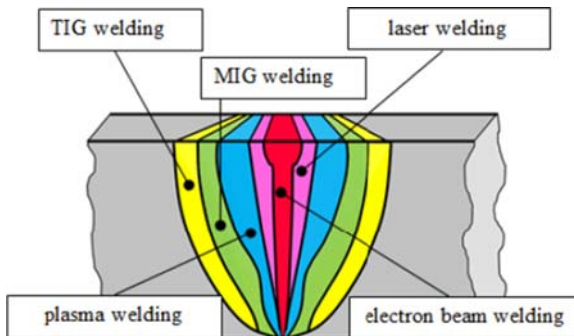


FIGURE 3.18 Geometry of a butt joint by various welding technologies. MIG-metal inert gas; TIG-tungsten inert gas. Reused with permission from Weglowski, M.S., Błacha, S., Phillips, A., 2016. *Electron beam welding – techniques and trends – Review. Vacuum 130*, 72–92; Elsevier.

### 3.9.2 Solid-state welding

In this section, sustainable strategies developed in low heat input and high heat input solid-state welding processes are discussed. Low heat input solid-state welding processes include ultrasonic welding, magnetic pulse welding and explosive welding (detonation speed ranges from 2400 to 3600 m s<sup>-1</sup>), and high heat input welding processes include friction welding (shaft or pipe rotation speed as high as 900 m min<sup>-1</sup>), FS welding, forge welding (50%–90% of melting temperature), and diffusion bonding (0.5×melting point of material) (Kalpakjian and Schmid, 2018; Matthew, 2000).

In the case of ultrasonic welding, frequency of vibration can be in the range of 15–70 kHz, and the most common frequency ranges from 20 to 40 kHz (Troughton, 2009). Liu and Cao (2021) demonstrated dissimilar joining of copper and aluminum alloy by electric current–assisted ultrasonic welding. The electric current helps promoting the plastic flow at the welding interface owing to the electroplastic effect and the generation of resistance heat by the electric Joule effect. As a result, quality of material mixing improved with enhancement in tensile strength of 12% and fracture energy of 21% as compared to traditional ultrasonic welding. Ma et al. (2021) proposed a nanoparticle-accelerated ultrasonic welding technique using a Cu nanoparticle (Cu NP) interlayer. The addition of interlayer drastically increases the load carrying capacity by 253% for Cu–Cu joints welded with an ultrasonic energy as low as 200 J, reducing the energy input to half of that without Cu NPs. Simply applying ethanol to the faying surface during USW of Al–Mg alloys and preheating specimens help improving weld strength (Hiraishi and Watanabe, 2004). Welding energy and time can be optimized to realize improvement in USW of ZEK100 Mg alloy used for vehicle body structures (Macwan and Chen, 2016). Using bigger sonotrode in USW of thermoplastic composite structures can enhance welding efficiency and load carrying capability at reduced welding time (Zhao et al., 2021).

Explosion welding offers high strength bonding during high-speed oblique collision of workpieces caused by the detonation of explosives and helps in achieving desirable physical and mechanical properties of joints. Some sustainable joining routes include heavy-ion irradiation of welded joints (like CuCrZr/316LN joints) delivering good structural integrity and void less joints (Yi et al., 2021), explosive welding of brass L63 with Invar 36N at throwing speed of 440 m s<sup>-1</sup> and impact angle of 12 degrees provide solid phase with 100% continuity of adhesion layers, separation strength at par with brass strength, and high-quality welding zone (Saikov et al., 2020) and using emulsion explosives in the case of low thickness sheets of 1 mm or less up to 0.3 mm without buffers and avoid crack formation (Zlobin et al., 2018).

Magnetic pulse welding (MPW) integrates the advantages of high-speed forming and solid-phase welding. The discharge pulse frequency depends on the parameters of the electromagnetic circuit and which lies in between 10 and 200 kHz, but usual operational frequencies are in between 10 and 20 kHz during the applications (Sapanathan et al., 2016). Joining of dissimilar metals is achieved through severe plastic deformation. MPW is applied to the welding of aluminum, magnesium, and copper, and their alloys to other dissimilar metals with good strength and corrosion resistance. The interfacial width of MPW joint is in the order of microns, and there is no HAZ as well. Lightweight tubular assembly is fabricated by MPW attributing to high toughness, high efficiency, good accuracy, and low cost. The key parameters include radial gap, relative lap length (RLL), and discharge voltage. Use of optimum welding conditions while welding 5A02 aluminum tube and SS304 steel tube yielded a maximum shear strength of 48.9 MPa (Yu et al., 2020), and using uniform pressure electromagnetic actuator in case of an aluminum alloy to Q235 steel sheet resulted in higher joint strength as compared to the weaker parent metal (Yu and Tong, 2017). Similar sustainable strategies are attempted by others as well.

In the case of high heat input solid-state welding processes, friction welding is a well-known method to produce dissimilar joints between Cu and its alloys, and steels including stainless steel. The advantages include no fumes and harmful radiation, and protecting atmosphere is not necessary. Welding of Cu alloys is not so easy, because the high heat input in a short time is necessary due to the high electrical and thermal conductivities. The major weld parameters include rotational speed and time, and friction and forging pressure. The main strategy for sustainable joining in this case is to optimize the welding conditions as shown in welding pure copper and austenitic stainless steel (Kimura et al., 2020), process modifications like introducing welding ring as a filler material to join longer tubes (Faes et al., 2009), and sample design like using conical end cylindrical rods to reduce the intermetallic compound layer thickness (Zhang et al., 2021). Linear friction welding (LFW) offers self-cleaning effect to remove surface contaminants for achieving a better property of the welded joints. The inclusions in the joints could be fully cleaned with increase in axial shortening length (Geng et al., 2021).

Friction stir welding (FSW) is a sustainable permanent solid-state joining process in which a nonconsumable rotating tool with a shoulder and pin is used to mechanically stir soften workpieces at the interface due to frictional heat. The temperature ranges from 230 °C to 260 °C at the tip of the rotating tool during welding process (Kalpakjian and Schmid, 2018). Eventually, a continuous joint is produced by a translational motion along the interface. It has the advantages like reduced porosity defect and mechanical distortion, no requirement of shielding gas, desired

microstructural characteristics, and eco-friendly. The major parameters that influence FSW include tool design, rotational speed, welding speed, axial force, plunge depth, and tool tilt angle. In FSW of AA5754, higher feed rate produces smaller grain size and higher low-angle grain boundaries, which results in improvement in yield strength and tensile strength of the welded joints (El-Rayes et al., 2019). FSW of AA 6061 and AZ31 sheets at higher rotational and transverse speeds increases the intensity of plastic deformation and dynamic recrystallization. Fine equiaxed grains are generated in stir zone, thereby improving the strength and hardness (Verma et al., 2018). Postweld heat treatment of FSWed AZ31 Mg alloy imparts superior tensile strength of 199 MPa at 1200 rpm and 300 mm min<sup>-1</sup> and provides scope for sustainable joining process (Wang et al., 2017). Underwater FSW helped AA6082 welded joints to retain 79% of weld efficiency of the base metal tensile strength, which is 10% more than traditional FSW (Wahid et al., 2018). Reinforcement of nugget zone with nanoparticles such as Al<sub>2</sub>O<sub>3</sub>, TiO<sub>2</sub>, TiB<sub>2</sub>, and SiC by friction stir processing (FSP) is in practice mainly to enhance the mechanical properties (El-Sayed et al., 2021). Friction stir spot welding (FSSW), predominantly used for fabricating joints, is performed in three stages namely plunging, stirring, and retracting of tool. FSSW has many advantages over conventional joining methods such as reduced distortion, improved fatigue life, no consumable requirement, and environment-friendly. There are several examples toward sustainable joining including FSSW of sandwich sheets (AA5052-H32/HDPE/AA5052-H32) by Pritam et al. (2019). It is shown that sandwich sheets can be made by FSSW-like bimetallic sheets and found increase in hardness of the joints with increase in plunge speed. Further, Saju and Narayanan (2020) investigated the role of hole diameter on mechanical behavior and joint formation of dieless FS lap joints in aluminum alloys. The joints produced exhibit lap shear fracture load of about 42%, 86%, and 25% higher than FS forming, FSSW with pin, and pinless FSSW samples respectively. Considering environmental impact of FSW, Buffa et al. (2019) proposed the control strategies for reducing electrical energy consumption of FSW process. The wall plug electric energy is converted into welding energy, conversion losses, and low-grade heat. An increase in tool feed rate with a fixed tool rotation results in a decreased energy demand. Proper choice of both machine and process parameters significantly influence the energy efficiency of the process and the overall environmental impact of the FSW process. Maximum energy saving of about 28% could be achieved when a traditional milling machine is substituted with a dedicated FSW machine. Using the bobbin tool in FS welding of Mg alloy resulted in joints having 91%–95% of tensile strength of parent metal (Li et al., 2020). Similarly, the FSW tools like Flared-Triflute probe and a Skew probe exhibit welds of 190% of the plate thickness, improvement in weld integrity, a reduction in

upper plate thinning, and an increased welding speed over current practice (Thomas et al., 2003). In friction spot joining, surface pre-treatments improve the bonding mechanisms and mechanical properties by changing aluminum surface topography and/or surface chemistry (Goushegir, 2016).

### 3.10 Mechanical joining

In mechanical joining, fasteners are used for temporary joints and for permanent and semipermanent joints, the processes like riveting, stitching, stapling, nailing, different fits, crimping, clinching, and seaming are used. In this section, a few variants of mechanical joining toward sustainable manufacturing have been discussed. For joining of aluminum and other materials used in automotive vehicles, self-pierce riveting (SPR) (Fig. 3.19A), and clinching (Fig. 3.19B) are utilized. In order to fulfill demands like lower cycle time, or more material and thickness flexibility, joining by forming techniques like flowdrill screwing and high-speed bolt joining (Fig. 3.19C) are used. High-speed bolt (RIVTAC) (Fig. 3.19C) is an auxiliary joining element driven by a pneumatic-accelerated piston into

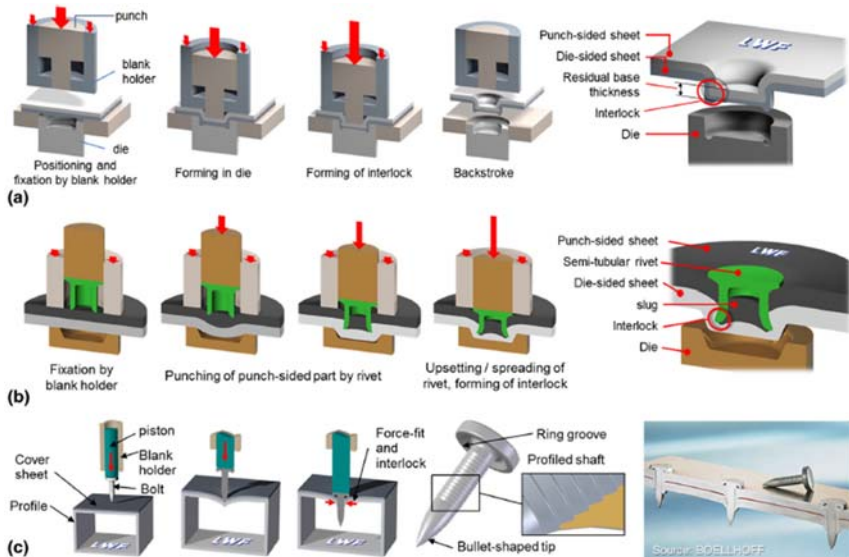


FIGURE 3.19 Illustration of selected mechanical joining processes for automotive applications. (A) Clinching with static die, (B) self-pierce riveting (SPR), and (C) high-speed bolt joining. Reused with permission from Meschut, G., Janzen, V., Olfemann, T., 2014a. *Innovative and highly productive joining technologies for multi-material lightweight car body structures. Journal of Materials Engineering and Performance* 23(5), 1515–1523; Springer Nature.

the workpieces at speeds between 20 and 40 m s<sup>-1</sup> (Meschut et al., 2014a). Steel sheets with tensile strength of up to ~700 MPa and a ductility of at least 8% could be clinched, clinch-bonded, and clinch-riveted with significant load capacity. SPR joint strength increases with the increase in the sheet material thickness or the stack thickness. Generally, joints with larger-diameter rivets exhibit higher strength than smaller-diameter rivets. In joining of stack of varying thickness of sheets, it is advisable if the thick sheet is used at the bottom. Prestraining of sheet materials prior to riveting helps in increasing the joint strength (Li et al., 2017).

Considering challenges when joining boron steels with aluminum, SPR with solid-rivets (Fig. 3.20A), resistance element welding (REW) (Fig. 3.20B), and friction element welding (FEW) processes (Fig. 3.20C) are suitable. In SPR with solid rivets, a positive lock is created by forming the die-sided aluminum sheet into a ring groove at the rivet (Mucha, 2014). Thermal–mechanical joining processes like REW and FEW processes are suitable for joining low-ductile and high-strength materials in multi-material joints. In these processes, an auxiliary joining element made of

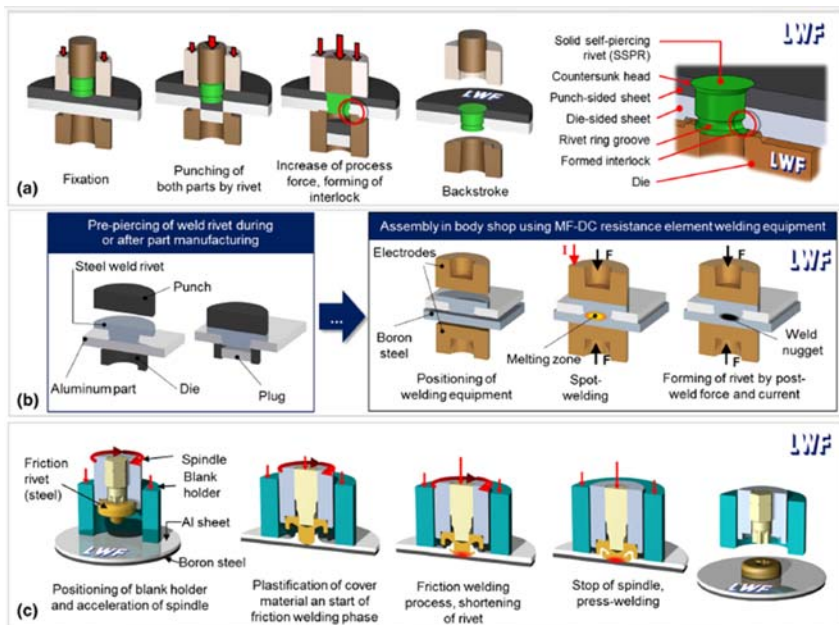


FIGURE 3.20 Illustration of selected innovative joining methods for UHSS-aluminum combinations. (A) Self-pierce riveting with solid rivets (SSPR); (B) resistance element welding (REW); and (C) friction element welding (FEW). Reused with permission from Meschut, G., Janzen, V., Olfermann, T., 2014a. Innovative and highly productive joining technologies for multi-material lightweight car body structures. *Journal of Materials Engineering and Performance* 23(5), 1515–1523; Springer Nature.

steel is commonly used to overcome welding incompatibility of dissimilar material joints (Meschut et al., 2014b). The processes are highly suitable for all kinds of advanced high-strength steels with moderate ductility and tensile strength of more than 1800 MPa (Meschut et al., 2013).

There are other unique sustainable methods such as the one proposed by Narayanan (2018) joining a rod (metal or nonmetal) to a sheet using a simple lathe machine (Fig. 3.21). The method involves plastic deformation of the rod and joining happens by material accumulation. During accumulation, the material not only gets sheared, but also gets curled, before joining occurs. Tool geometry also influences this joining process. The joints produced by this process performs equivalent to a welded joint. Green friction riveting using polymer rivets by Xie et al. (2020) and laser shock clinching of pure copper foil and prepierced stainless steel sheet by Zheng et al. (2020) are noteworthy. Meibner et al. (2018) developed smart human–robot SPR joining tool useful for aircraft final assembly. The smart tool is operated through networking and the mobile devices assisting employees smartly. The smart tool utilized in the fuselage reduced time up to 50% for assembly compared to the conventional riveting process.

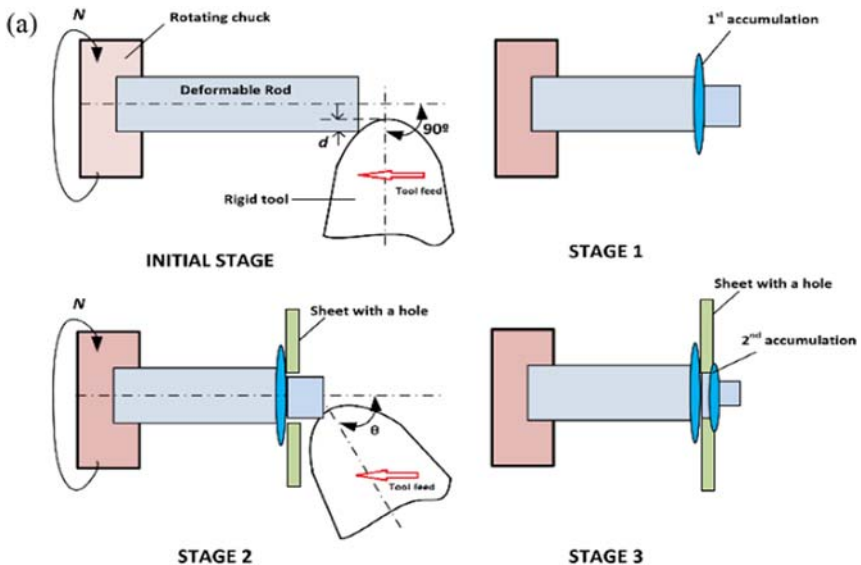


FIGURE 3.21 Joining by material accumulation. Reused with permission from Narayanan, R.G., 2018. A novel method of joining a rod to a sheet by end deformation: a preliminary experimental study. *International Journal of Precision Engineering and Manufacturing* 19(5), 773–779; Springer Nature.

### 3.11 Adhesive bonding

Adhesive bonding is a promising technology for joining dissimilar materials and geometries and more suitable in aspects like high strength to weight ratio, design flexibility, damage tolerance, fatigue resistance, and so on. Adhesive-bonded joints are influenced by joint configuration, material and geometrical properties, surface preparation, failure mode, and bonding methods. The geometry of adhesive-bonded joint plays an important role for the significant stress state. Fig. 3.22 shows a general overview of a few topologies (Kupski and Freitas, 2021). Out of two adherent layouts,  $[0/90/0/90]_{2s}$  and  $[90/0/90/0]_{2s}$ , wavy joint shows 100% higher the average lap shear strength for layout  $[90/0/90/0]_{2s}$  and about 50% higher for layout  $[0/90/0/90]_{2s}$  than that of conventional single lap joints (Zeng and Sun, 2001). Similarly, change in adhesive quality, joint configuration, and material combinations help in sustainable adhesive bonding with enhanced mechanical performance (Avila and Bueno, 2004a, 2004b; Da Silva et al., 2007; Canyurt et al., 2010). The local surface toughening concept helps to increase overall joint strength and outperforms other existing concepts. About 84% of the joint strength could be increased with surface toughening specimens as compared to the reference design.

Mixed adhesive joint shows better strength than brittle or ductile adhesive, and load carrying capacity of brittle adhesive is higher than ductile adhesive (Da Silva et al., 2009). Varying the hardener to resin ratio of adhesive influences the mechanical properties of adhesive-

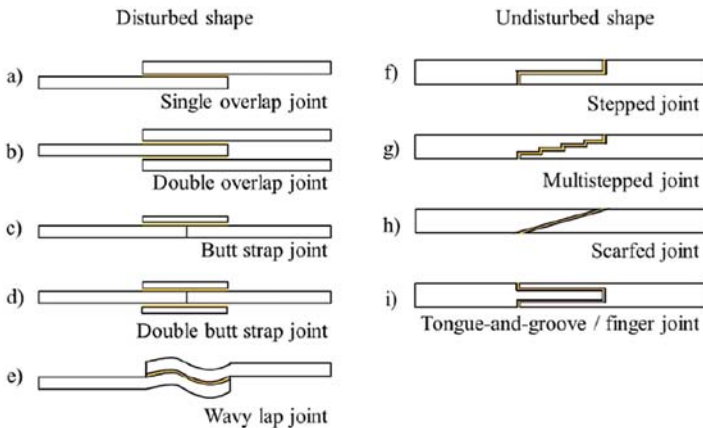


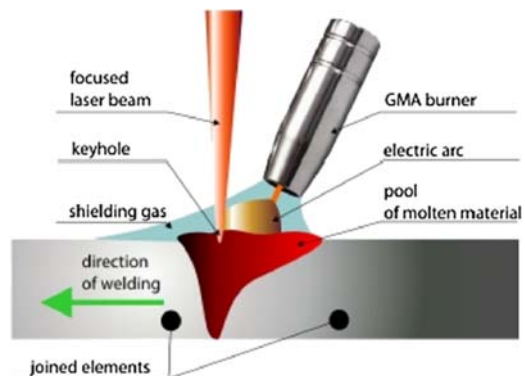
FIGURE 3.22 Global joint topologies (A) Single overlap joint, (B) Double overlap joint, (C) Butt strap joint, (D) Double butt strap joint, (E) Wavy lap joint, (F) Stepped joint, (G) Multistep joint, (H) Scarfed joint, and (I) Finger joint. Reused with permission from Kupski, J., de Freitas, S.T., 2021. Design of adhesively bonded lap joints with laminated CFRP adherends: review, challenges and new opportunities for aerospace structures. *Composite Structures*, 268, 113923–113935; Elsevier (Open Access).

bonded sheets. Utilizing two-part adhesive with hardener-rich formulation, filling carbon black powder at a suitable wt.% in adhesive, and reinforcement of high ductile wire in low ductile adhesive help increasing the ductility of adhesive and thereby improved the formability of adhesive-bonded steel sheets. Even in a two-part adhesive system, the green performance toward better strength with resin formulation, and better ductility with hardener rich formulation could be achieved (Satheeshkumar and Narayanan, 2014, 2015a,b, 2016). Surface preparation of adherents plays an important role, and it directly influences the quality of the bonded joint. In order to obtain a strong and durable joint, removal of all contaminants like lubricants, dusts, loose corrosion layers, and micro-organisms from the surfaces improves surface wettability and surface energy, and activation of surfaces being bonded is observed (Budhe et al., 2017). Wang et al. (2021) proposed an ultrasonic vibration–assisted adhesive bonding process for laser ablated carbon fiber–reinforced polymers. The bond strength was improved by 234% with laser ablation and by 340% with both laser ablation and ultrasonic treatment with reference to the untreated joint. It is also seen that the tensile strength of the adhesive weld bond joints of the coated and uncoated DP steel is higher than that of the adhesive bonded and resistance spot welded joints (Hayat, 2011).

### 3.12 Hybrid joining

Hybrid joining utilizes the combined advantages of different welding processes. In hybrid laser-arc welding process, the combined effect and interaction of laser beam and the electric arc are utilized (Fig. 3.23) to produce a deep and narrow weld with better mechanical properties, weld efficiency, and increased production rate (Acherjee, 2018). Just to

FIGURE 3.23 Scheme of hybrid laser arc welding process. Reused with permission from Acherjee, B., 2018. *Hybrid laser arc welding: state-of-art review. Optics & Laser Technology* 99, 60–71; Elsevier.



elaborate, the ability of laser beam to produce narrow and deep weld pool by focusing on a tiny area and the advantages of arc welding like excellent gap bridging ability, high electrical efficiency, and efficient weldability of high reflective materials provide a hybridization effect (Fig. 3.24) compensating the drawbacks of both the processes leading to sustainability (Ascari et al., 2012). Lasers like CO<sub>2</sub>, Nd:YAG, fiber, and arc welding processes like GMAW, GTAW, and PAW are mostly employed in laser-arc hybrid welding processes (Li et al., 2011; Liu et al., 2017; Frostevarg and Kaplan, 2014; Gureev et al., 1989), and tailor-made advantages are possible with suitable combination. In hybrid laser-TIG welding, the laser energy absorption in the base material could be improved by preheating of base materials through advancing TIG arc, and thereby arc gets stabilized (Dilthey and Wiesschemann, 2002). The metal deposition rate of hybrid laser GTAW is less than that of hybrid laser GMAW because only a fraction of heat of the arc is used to melt the filler wire during hybrid laser-GTAW process (Seyffarth and Krivtsun, 2002). Hybrid laser-PAW shows higher penetration depth than that of laser welding for the same energy input per unit length of the weld

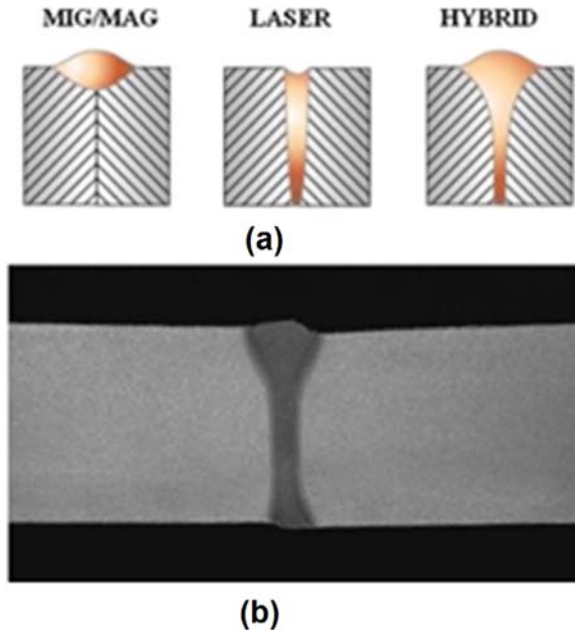


**FIGURE 3.24** (A) Weld beads during arc welding, laser welding, and hybrid laser-arc welding, respectively and (B) sectional view of weld bead produced from hybrid laser arc welding. Reused with permission from Acherjee, B., 2018. *Hybrid laser arc welding: state-of-art review. Optics & Laser Technology* 99, 60–71; Elsevier.

(Emmelmann et al., 2011). The heat input from the arc could be reduced up to 40% with hybrid laser-PAW as compared to the hybrid laser-GTAW (Kim et al., 2011). The hybrid plasma-GTAW of 12 mm thick modified 12% Cr ferritic stainless steel shows sound weld and good mechanical properties (Taban et al., 2009).

In hybrid laser-arc welding, paraxial and coaxial arrangements are used. In paraxial arrangement, either arc welding torch or laser beam is positioned as a leading heat source in such a way they follow the same weld line and interact at a common weld zone. In coaxial arrangement, the laser beam is passed through a hollow arc welding nonconsumable electrode in such a way both laser beam and electric arc follow a common central axis (Acherjee, 2018). Sustainable joining of thick plates with sound weld properties are observed with the arrangements in shorter time (Bagger et al., 2003). The hybrid laser arc welding helps reduce the cost up to 50%, improve the productivity up to 50%, produce defect free weld, offer high welding speed, impart quality seam, improve mechanical and fatigue properties, reduce number of passes due to deep penetration, and are also economical than autogenous laser welding (Acherjee, 2018). Hybrid MIG-SMAW, hybrid brazing-GTAW, and hybrid GTAW-GMAW are other possibilities in hybrid joining (Narasimhan et al., 2019; Pouranvari and Abbasi, 2018; Hernandez et al., 2020). Mori et al. (2020) developed a combined hot stamping and mechanical joining process for producing ultrahigh-strength steel patchwork components. Uniform heating, patch formed by mechanical joining within the die-punch setup, and laser welding as finishing process, all completed in a sequence, producing joint with acceptable fracture load (Fig. 3.25).

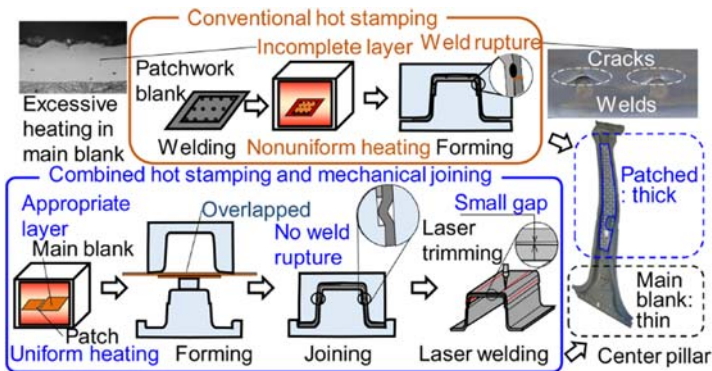


FIGURE 3.25 Conventional hot stamping process, combined process of hot stamping and mechanical joining for producing ultrahigh-strength steel patchwork components. Reused with permission from Mori, K.I., Kaido, T., Suzuki, Y., Nakagawa, Y., Abe, Y., 2020. Combined process of hot stamping and mechanical joining for producing ultra-high strength steel patchwork components. *Journal of Manufacturing Processes* 59, 444–455; Elsevier.

Another example of hybrid joining is to combine adhesive bonding (AB) and magnetic pulse welding (MPW) to introduce magnetic pulse weld bonding (MPWB) and MPWB produced joint made of AA 5052 sheet with 91% increase in lap-shear load and 6 times improvement in energy absorption over MPW joint (Peng et al., 2019). Tong et al. (2020) demonstrated the advantage of using modified FS clinching-brazing (MFSC-B) and FS spot welding-brazing (FSSW-B) of AA5083-H321 and pure Cu alloys using a thin Zn intermediate layer.

### 3.13 Inclusive manufacturing

Manufacturing firms are aware of the sustainable hierarchy and green approaches, which focus on several R's that include reduce, reuse, recycle, redesign, remanufacturing, and recovery to promote sustainable manufacturing. Sustainable manufacturing is also referred as inclusive manufacturing that encompasses three perspectives like people-, environment-, and technology-oriented innovations. In terms of people, it is important to include all categories of people in various manufacturing activities to improve the skill set of future workforce, encourage rural innovation and open-source designs, and develop new business models. Environment concern redirects companies to contemplate product life cycle and safe handling of end-of-life products. The technology perspective includes the role of technology like cloud computing, Internet of Things (IoT), and big data algorithms (Gunasekaran et al., 2018).

Inclusive and sustainable industrial development (ISID) promotes minimization of environmental hazards, social integration, and equity (Yuan et al., 2020). For a successful ISID, it is important to develop an environmental friendly framework including economic and social growth, innovation, and technology and to distribute the benefits of industrial growth equally to all stakeholders. To evaluate the progression in the promotion of ISID and in the raise of industry's share of employment and GDP, the United Nations use two indicators like (i) manufacturing value-added products as a proportion of GDP and per capita and (ii) manufacturing employment as a proportion of total employment. Another indicator to evaluate the progression of the sustainable industries is CO<sub>2</sub> emissions per unit of value added products (Halkos et al., 2021). Green industries could be promoted to deliver important environmental goods and services along with their products possibly. Thus, not only contributing to environmental sustainability, but also supporting for the transition toward clean energy, low-carbon development and sustainable production and consumption patterns (Li, 2015). There has been a significant contribution in material joining toward sustainable

**TABLE 3.7** Contribution of material joining to sustainable manufacturing and promoting ISID.

<b>Contribution of joining processes</b>	<b>References</b>
Utilization and development of experts and operator skills	Zeng and Sun (2001)
Development of operators' protection strategies and aids	Zong et al. (2020)
Development of expertise in modeling, innovations in joining	Ma et al. (2021); Faes et al. (2009); Meschut et al. (2014a); Meschut et al. (2014b); Zheng et al. (2020)
Improvisation in joining methods	Singh et al. (2021a); Kawabe et al. (2016); Balakrishnan et al. (2011); El-Batahgy et al. (2020); Yamazaki et al. (2012); Tsuyama et al. (2014); Baskoro et al. (2018); Lee et al. (2020); Zong et al. (2020); Derekar et al. (2020); Dong et al. (2020); Abhishek et al. (2020); Goushegir (2016); Wang et al. (2017); Pritam et al. (2019); Saju and Narayanan (2020); Satheeshkumar and Narayanan (2014, 2015a,b, 2016); Da Silva et al. (2009); Kupski and Freitas (2021)
Carbon efficient joining	Huang et al. (2021); Taban et al. (2009); Acherjee (2018)
Energy efficient technologies and strategies	Huang et al. (2021); Shi et al. (2014, 2016); Huang (2010); Favi et al. (2019); Kim et al. (2011)
Innovative practices	Sakate et al. (2021); Da Silva et al. (2007); Canyon et al. (2010)
Influence of technology including hybrid joining	Feng et al. (2021); Chen et al. (2020a); Chen et al. (2020b); Oladimeji and Taban (2016); Wang et al. (2021); Liu et al. (2017); Frostevarg and Kaplan (2014); Acherjee (2018)
Computer integrated joining technologies and automation including robot assisted joining	Meibner et al. (2018); Kupski and Freitas (2021)

**TABLE 3.7** Contribution of material joining to sustainable manufacturing and promoting ISID.—cont'd

<b>Contribution of joining processes</b>	<b>References</b>
Flexibility of joining methods in modern manufacturing	Guo et al., (2021); Khan and Madhukar (2020); Derekar et al. (2020)
Utilization of green tools	Li et al. (2020); Thomas et al. (2003); Wang et al. (2021)
Environmental management practices	Vimal et al. (2015); Favi et al. (2019); Buffa et al. (2019)
Remanufacturing strategies include repair ability of adhesive bonded sheets and mechanical fastening methods	Da Silva et al. (2007, 2009); Meschut et al. (2014a, b)
Development of eco-friendly joining strategies	Narayanan (2018); Xie et al. (2020); Kupski and Freitas (2021)
Economic and lifecycle strategies	Vimal et al. (2015); Favi et al. (2019)

manufacturing and encompassing the perspectives of inclusive manufacturing. Example references listed in [Table 3.7](#) support promoting ISID in material joining field.

### 3.14 Summary

In the current chapter, importance of developing sustainable forming and joining processes is emphasized with examples from existing case studies. It is observed that a numerous strategies and practices have been developed in forming and joining processes toward sustainable manufacturing with variety of merits and demerits. Such practices resulted in sustainable forging, extrusion, rolling, sheet stamping, flexible tooling, laser manufacturing, fusion and solid state welding, adhesive bonding, and mechanical joining. Optimization of material and process conditions helps in achieving energy reduction, processes with no fumes, enhanced performance with desired properties, and use of lightweight materials. Specifically in joining, hybrid processes yielded improved energy efficiency, reduced emission, and resource utilization and contributes significantly to sustainable manufacturing. In addition, automation

including robot-assisted forming and joining processes enabled reduction in operator fatigue, cycle time, and productivity. Beyond such remarkable achievements, there is a wide scope for promoting endless inclusive and sustainable industrial development.

## References

- Abe, Y., Ohmi, T., Mori, K., Masuda, T., 2014. Improvement of formability in deep drawing of ultra-high strength steel sheets by coating of die. *Journal of Materials Processing Technology* 214, 1838–1843.
- Abedi, H.R., Gollo, M.H., 2019. An experimental study of the effects of surface roughness and coating of Cr<sub>2</sub>O<sub>3</sub> layer on the laser-forming process. *Optics & Laser Technology* 109, 336–347.
- Abhishek, K.P., Dixit, A., Sunil, P., Pandey, P.M., 2020. Distortion control in welded structure with advanced submerged arc welding. *Materials Today Proceedings* 26, 1492–1495.
- Acherjee, B., 2018. Hybrid laser arc welding: state-of-art review. *Optics & Laser Technology* 99, 60–71.
- Aghchai, A.J., Shakeri, M., Mollaei-Dariani, B., 2008. Theoretical and experimental formability study of two-layer metallic sheet (Al1100/St12). *Proc. IMechE Part B: Journal of Engineering Manufacture* 222, 1131–1138.
- Ahmetoglu, M., Altan, T., 2000. Tube hydroforming: state-of-the-art and future trends. *Journal of Materials Processing Technology* 98 (1), 25–33.
- Alfozan, A., Gunasekera, J.S., 2003. An upper bound element technique approach to the process design of axisymmetric forging by forward and backward simulation. *Journal of Materials Processing Technology* 142, 619–627.
- Ali, S.S., Kaur, R., Ersoz, F., Lotero, L., Weber, G.W., 2018. Evaluation of the effectiveness of green practices in manufacturing sector using CHAID analysis. *Journal of Remanufacturing* 9 (1), 3–27.
- Allwood, J.M., Shouler, D.R., Tekkaya, A.E., 2007. The increased forming limits of incremental sheet forming processes. In: *SheMet '07 International Conference on Sheet Metal*, Palermo, Italy, pp. 621–628.
- Aman, S., Singh, R.P., 2020. A review of effect of welding parameters on the mechanical properties of weld in submerged arc welding process. *Materials Today Proceedings* 26, 1714–1717.
- Amine, K.E., Larsson, J., Pejryd, L., 2018. Experimental comparison of roller die and conventional wire drawing. *Journal of Materials Processing Technology* 257, 7–14. <https://doi.org/10.1016/j.jmatprotec.2018.02.012>.
- Ascari, A., Fortunato, A., Orazi, L., Campana, G., 2012. The influence of process parameters on porosity formation in hybrid laser-GMA welding of AA6082 aluminum alloy. *Optics & Laser Technology* 44 (5), 1485–1490.
- ASM Handbook, 1992. *Friction, Lubrication, and Wear Technology*, Volume 18, *Metal Working Lubricants* by Joseph T, pp. 255–277. Laemmler.
- ASM Handbook, 1998. In: Semiatin, S.L. (Ed.), *Forming and Forging*, vol 14.
- Auwal, S.T., Ramesh, S., Yusof, F., Manladan, S.M., 2018a. A review on laser beam welding of copper alloys. *International Journal of Advanced Manufacturing Technology* 96, 475–490.
- Auwal, S.T., Ramesh, S., Yusof, F., Manladan, S.M., 2018b. A review on laser beam welding of titanium alloys. *International Journal of Advanced Manufacturing Technology* 97, 1071–1098.
- Avila, A.F., Bueno, P.D., 2004a. An experimental and numerical study on adhesive joints for composites. *Composite Structures* 64 (3–4), 531–537.

- Avila, A.F., Bueno, P.D., 2004b. Stress analysis on a wavy-lap bonded joint for composites. *International Journal of Adhesion and Adhesives* 24 (5), 407–414.
- Bagger, C., Olsen, F.O., Wiwe, B.D., Paulin, N.A., 2003. Closing the weld gap with laser/MIG hybrid welding process. In *NOLAMP 9* (Institut for Produktion og Ledelse, DTU).
- Balakrishnan, M., Balasubramanian, V., Madhusuhan, R.G., Sivakumar, K., 2011. Effect of buttering and hardfacing on ballistic performance of shielded metal arc welded armour steel joints. *Materials and Design* 32, 469–479.
- Baskoro, A.S., Fauzian, A., Basalamah, H., Kiswanto, G., Winarto, W., 2018. Improving weld penetration by employing of magnetic poles' configurations to an autogenous tungsten inert gas (TIG) welding. *International Journal of Advanced Manufacturing Technology* 99, 1603–1613.
- Browne, D.J., Battikha, E., 1995. Optimization of aluminium sheet forming using a flexible die. *Journal of Materials Processing Technology* 55, 218–223.
- Budhe, S., Banea, M.D., De Barros, S., Da Silva, L.F., 2017. An updated review of adhesively bonded joints in composite materials. *International Journal of Adhesion and Adhesives* 72, 30–42.
- Buffa, G., Ingarao, G., Campanella, D., Lorenzo, R.D., Micari, F., Fratini, L., 2019. An insight into the electrical energy demand of friction stir welding processes: the role of process parameters, material and machine tool architecture. *International Journal of Advanced Manufacturing Technology* 100, 3013–3024.
- Cai, Z.-Y., Wang, S.-H., Li, M.-Z., 2008. Numerical investigation of multi-point forming process for sheet metal: wrinkling, dimpling and springback. *International Journal of Advanced Manufacturing Technology* 37, 927–936. <https://doi.org/10.1007/s00170-007-1045-5>.
- Canyurt, O.E., Meran, C., Uslu, M., 2010. Strength estimation of adhesively bonded tongue and groove joint of thick composite sandwich structures using genetic algorithm approach. *International Journal of Adhesion and Adhesives* 30 (5), 281–287.
- Caro, L.P., Odenberger, E.-L., Schill, M., Niklasson, F., Åkerfeldt, P., Oldenburg, M., 2021. Springback prediction and validation in hot forming of a double-curved component in alloy 718. *International Journal of Material Forming* 14, 1355–1373. <https://doi.org/10.1007/s12289-021-01615-x>.
- Chakraborty, S.S., Racherla, V., Nath, A.K., 2018. Thermo-mechanical finite element study on deformation mechanics during radial scan line laser forming of a bowl shaped surface out of a thin sheet. *Journal of Manufacturing Processes* 31, 593–604. <https://doi.org/10.1016/j.jmapro.2017.12.025>.
- Chan, L.C., Lu, X.Z., 2014. Material sensitivity and formability prediction of warm-forming magnesium alloy sheets with experimental verification. *International Journal of Advanced Manufacturing Technology* 71, 253–262.
- Chen, Z.H., Cheng, Y.Q., Xia, W.J., 2007. Effect of equal-channel angular rolling pass on microstructure and properties of magnesium alloy sheets. *Materials and Manufacturing Processes* 22, 51–56.
- Chen, W., Song, H., Lazarescu, L., Xu, Y., Zhang, S.-H., Banabic, D., 2020. Formability analysis of hot-rolled dual-phase steel during the multistage stamping process of wheel disc. *International Journal of Advanced Manufacturing Technology* 110, 1563–1573. <https://doi.org/10.1007/s00170-020-05963-x>.
- Chen, C., Fan, C., Cai, X., Lin, S., Yang, C., Zhuo, Y., 2020a. Microstructure and mechanical properties of Q235 steel welded joint in pulsed and un-pulsed ultrasonic assisted gas tungsten arc welding. *Journal of Materials Processing Technology* 275, 116335–116341.
- Chen, C., Fan, C., Liu, C., Cai, X., Lin, S., Zhuo, Y., 2020b. Microstructure evolutions and properties of Al–Cu alloy joint in the pulsed power ultrasonic-assisted GMAW. *Acta Metallurgica Sinica* 33, 1397–1406.

- Chino, Y., Mabuchi, M., Kishihara, R., Hosokawa, H., Yamada, Y., Wen, C., Shimojima, K., Iwasaki, H., 2002. Mechanical properties and press formability at room temperature of AZ31 Mg alloy processed by single roller drive rolling. *Materials Transactions* 43, 2554–2560.
- Chino, Y., Sassa, K., Kamiya, A., Mabuchi, M., 2006a. Enhanced formability at elevated temperature of a cross-rolled magnesium alloy sheet. *Materials Science and Engineering A* 441, 349–356.
- Chino, Y., Lee, J.S., Sassa, K., Kamiya, A., Mabuchi, M., 2006b. Press formability of a rolled AZ31 Mg alloy sheet with controlled texture. *Materials Letters* 60, 173–176.
- Chino, Y., Sassa, K., Kamiya, A., Mabuchi, M., 2007. Microstructure and press formability of a cross-rolled magnesium alloy sheet. *Materials Letters* 61, 1504–1506.
- Choi, Y.-J., Lee, S.-K., Lee, I.-K., Cho, Y.-J., Lee, J.-W., Cho, J.-W., Jeong, M.-S., 2015. Multi-stage forging process design of steering system output shaft for reduction of energy consumption. *International Journal of Precision Engineering and Manufacturing* 16, 1455–1460. <https://doi.org/10.1007/s12541-015-0192-0>.
- Chu, G., Liu, W., 2013. Experimental observations of 5A02 aluminum alloy in electromagnetically assisted tube hydroforming. *Journal of Occupational Medicine* 65, 599–603. <https://doi.org/10.1007/s11837-013-0578-3>.
- Da Silva, L.F., Adams, R.D., 2007. Techniques to reduce the peel stresses in adhesive joints with composites. *International Journal of Adhesion and Adhesives* 27 (3), 227–235.
- Da Silva, L.F., Lopes, M.J., 2009. Joint strength optimization by the mixed-adhesive technique. *International Journal of Adhesion and Adhesives* 29 (5), 509–514.
- Dabiri, A.R., Mojjallal, R.Y., Ahmadi, E., Fattahi, M., Amirkhanlou, S., Fattahi, Y., 2015. Effect of ZrO<sub>2</sub> nanoparticles on the impact properties of shielded metal arc welds. *Materials Letters* 158, 325–328.
- Derekar, K.S., Addison, A., Joshi, S.S., Zhang, X., Lawrence, J., Xu, L., Melton, G., Griffiths, D., 2020. Effect of pulsed metal inert gas (pulsed-MIG) and cold metal transfer (CMT) techniques on hydrogen dissolution in wire arc additive manufacturing (WAAM) of aluminium. *International Journal of Advanced Manufacturing Technology* 107, 311–331.
- Dilthey, U., Wiesschemann, U., 2002. Prospectives offered by combining and coupling laser beam and arc welding. *Welding International* 9, 711–719.
- Dong, S., Han, Y., Jia, C., Wu, C., Zhang, M., Yang, Q., Yang, J., 2020. Organic adhesive assisted underwater submerged-arc welding. *Journal of Materials Processing Technology* 284, 116739–116747.
- El-Batahgy, A., Saiyah, A., Khafagi, S., Gumenyuk, A., Gook, S., Rethmeier, M., 2020. Shielded metal arc welding of 9%Ni steel using matching ferritic filler metal. *Science and Technology of Welding & Joining* 26 (2), 116–122.
- El-Rayes, M.M., Soliman, M.S., Abbas, A.T., Pimenov, D.Y., Erdakov, I.N., Abdel-Mawla, M.M., 2019. Effect of feed rate in FSW on the mechanical and microstructural properties of AA5754 joints. *Advances in Materials Science and Engineering* 2019, 1–12.
- El-Sayed, M.M., Shash, A.Y., Abd-Rabou, M., ElSherbiny, M.G., 2021. Welding and processing of metallic materials by using friction stir technique: a review. *Journal of Advanced Joining Processes* 3, 100059–100078.
- Emmelmann, C., Kirchoff, M., Petri, N., 2011. Development of plasma-laser-hybrid welding process. *Physics Procedia* 12, 194–200.
- Erdin, M.E., Ozdilli, O., 2019. Deep drawing of polymer coated metal sheets. *Journal of Mechanical Science and Technology* 33, 5383–5392. <https://doi.org/10.1007/s12206-019-1032-4>.
- Eyckens, P., He, S., Van Bael, A., Van Houtte, P., Duflou, J., 2007. Forming limit predictions for the serrated strain paths in single point incremental sheet forming. *AIP Conference Proceedings* 908, 141–146. <https://doi.org/10.1063/1.2740802>.

- Faes, K., Dhooge, A., De Baets, P., Afschrift, P., 2009. New friction welding process for pipeline girth welds—welding time optimisation. *International Journal of Advanced Manufacturing Technology* 43 (9), 982–992.
- Favi, C., Campi, F., Germani, M., 2019. Comparative life cycle assessment of metal arc welding technologies by using engineering design documentation. *International Journal of Life Cycle Assessment* 24, 2140–2172.
- Feng, X., Pan, X., He, W., Liu, P., An, Z., Zhou, L., 2021. Improving high cycle fatigue performance of gas tungsten arc welded Ti6Al4V titanium alloy by warm laser shock peening. *International Journal of Fatigue* 149, 106270–106282.
- Frostevarg, J., Kaplan, A.F., 2014. Undercuts in laser arc hybrid welding. *Physics Procedia* 56, 663–672.
- Gatea, S., Xu, D., Ou, H., McCartney, G., 2018. Evaluation of formability and fracture of pure titanium in incremental sheet forming. *International Journal of Advanced Manufacturing Technology* 95, 625–641. <https://doi.org/10.1007/s00170-017-1195-z>.
- Geng, P., Qin, G., Ma, H., Zhou, J., Zhang, C., Ma, N., 2021. Numerical modelling on the plastic flow and interfacial self-cleaning in linear friction welding of super alloys. *Journal of Materials Processing Technology* 296, 117198–117211.
- Gerstein, G., Kahra, C., Golovko, O., Schäfer, F., Klose, C., Herbst, S., Nürnberger, F., Maier, H.J., 2021. Hot forming of shape memory alloys in steel shells: formability, interface, bonding quality. *Production Engineering* 15, 271–283. <https://doi.org/10.1007/s11740-021-01024-8>.
- Gorji, N.E., Saxena, P., Corfield, M., Clare, A., Rueff, J.-P., Bogan, J., González, P.G.M., Snelgrove, M., Hughes, G., O'Connor, R., Raghavendra, R., Brabazon, D., 2020. A new method for assessing the recyclability of powders within Powder Bed Fusion process. *Materials Characterization* 161, 110167. <https://doi.org/10.1016/j.matchar.2020.110167>.
- Goushegir, S.M., 2016. Friction spot joining (FSJ) of aluminum-CFRP hybrid structures. *Welding in the World* 60, 1073–1093.
- Gunasekaran, A., Subramanian, N., Yusuf, Y., 2018. Strategies and practices for inclusive manufacturing: twenty-first-century sustainable manufacturing competitiveness. *International Journal of Computer Integrated Manufacturing* 31 (6), 490–493.
- Gunasekera, J.S., Hoshino, S., 1982. Analysis of extrusion or drawing of polygonal sections through straightly converging dies. *ASME Journal of Engineering for Industry* 104 (1), 38–45.
- Gunasekera, J.S., Gegel, H.L., Doraivelu, S.M., Malas, J.C., Graham, J.C., Altan, T., 1984. Computer aided design of “multi-holed”. *Streamlined Extrusion Dies*. *CIRP Annals* 33 (1), 129–131.
- Gunasekera, J.S., Jia, Z., Malas, J.C., Rabelo, L., 1998. Development of a neural network model for a cold rolling process. *Engineering Applications of Artificial Intelligence* 11 (5), 597–603.
- Guo, Y., Quan, G., Jiang, Y., Ren, L., Fan, L., Pan, H., 2021. Formability, microstructure evolution and mechanical properties of wire arc additively manufactured AZ80M magnesium alloy using gas tungsten arc welding. *Journal of Magnesium and Alloys* 9, 192–201.
- Gureev, D.M., Zaikin, A.E., Zolotarevsky, A.B., 1989. Method of laser-arc material processing and its application. In: *Transactions of the Physical Institute of the USSR Academy of Science*, vol 198. Nauka, Moscow, pp. 41–61.
- Hadadzadeh, A., Ghaznavi, M.A., Kokabi, A.H., 2017. HAZ softening behavior of strain-hardened Al-6.7Mg alloy welded by GMAW and pulsed GMAW processes. *International Journal of Advanced Manufacturing Technology* 92, 2255–2265.
- Halkos, G., Alba, J.M., Todorov, V., 2021. Economies' inclusive and green industrial performance: an evidence based proposed index. *Journal of Cleaner Production* 279, 123516–123530.

- Hariharasudhan, P., Ngaile, G., Altan, T., 2004. Finite element simulation of magnesium alloy sheet forming at elevated temperatures. *Journal of Materials Processing Technology* 146, 52–60.
- Hayat, F., 2011. Comparing properties of adhesive bonding, resistance spot welding, and adhesive weld bonding of coated and uncoated DP 600 steel. *Journal of iron and steel research international* 18 (9), 70–78.
- Hernández, R.T., Hernández, C.V.L., García-Rentería, M.A., Torres-Gonzalez, R., García-Villarreal, S., Curiel-López, F.F., Falcón-Franco, L.A., 2020. First assessment on the microstructure and mechanical properties of GTAW-GMAW hybrid welding of 6061-T6 AA. *Journal of Manufacturing Processes* 59, 658–667.
- Hiraishi, M., Watanabe, T., 2004. Improvement of ultrasonic weld strength of Al–Mg alloys by alcohol adhesion–ultrasonic welding of Al–Mg alloys. *Welding International* 18 (5), 357–363.
- Hölker, R., Jäger, A., Ben Khalifa, N., Tekkaya, A.E., 2013. Controlling heat balance in hot aluminum extrusion by additive manufactured extrusion dies with conformal cooling channels. *International Journal of Precision Engineering and Manufacturing* 14, 1487–1493. <https://doi.org/10.1007/s12541-013-0200-1>.
- Horiuchi, T., Yoshihara, S., Iriyama, Y., 2012. Dry deep drawability of A5052 aluminum alloy sheet with DLC-coating. *Wear* 286–287, 79–83.
- Huang, H.Y., 2010. Research on the activating flux gas tungsten arc welding and plasma arc welding for stainless steel. *Metals and Materials International* 16 (5), 819–825.
- Huang, X., Suzuki, K., Watazu, A., Shigematsu, I., Saito, N., 2009. Improvement of formability of Mg–Al–Zn alloy sheet at low temperatures using differential speed rolling. *Journal of Alloys and Compounds* 470, 263–268.
- Huang, X., Suzuki, K., Chino, Y., 2010. Improvement of stretch formability of pure titanium sheet by differential speed rolling. *Scripta Materialia* 63, 473–476.
- Huang, Z., Cao, H., Zeng, D., Ge, W., Duan, C., 2021. A carbon efficiency approach for laser welding environmental performance assessment and the process parameters decision-making. *International Journal of Advanced Manufacturing Technology* 114, 2433–2446.
- Jackson, K., Allwood, J., 2009. The mechanics of incremental sheet forming. *Journal of Materials Processing Technology* 209, 1158–1174. <https://doi.org/10.1016/j.jmatprotec.2008.03.025>.
- Jeong, M.-S., Lee, S.-K., Yun, J.-H., Sung, J.H., Kim, D.H., Lee, S., Choi, T.-H., 2013. Green manufacturing process for helical pinion gear using cold extrusion process. *International Journal of Precision Engineering and Manufacturing* 14, 1007–1011. <https://doi.org/10.1007/s12541-013-0134-7>.
- Jeong, M.G., Jin, C.K., Hwang, G.W., Kang, C.G., 2014. Formability evaluation of stainless steel bipolar plate considering draft angle of die and process parameters by rubber forming. *International Journal of Precision Engineering and Manufacturing* 15, 913–919.
- Jeong, M.-S., Lee, S.-Y., Lee, I.-K., Lee, S.-K., Kim, D.H., Cho, Y.-J., Ko, D.-C., 2014. Green alternative aluminum extrusion process through process convergence. *International Journal of Precision Engineering and Manufacturing* 15, 1173–1177. <https://doi.org/10.1007/s12541-014-0453-3>.
- Jeswiet, J., Young, D., 2005. Forming limit diagrams for single-point incremental forming of aluminium sheet. *Proceedings - Institution of Mechanical Engineers Part B Journal of Engineering Manufacture* 219, 359–364. <https://doi.org/10.1243/095440505X32210>.
- Kalpakjian, S., Schmid, S.R., 2018. *Manufacturing Processes for Engineering Materials*, sixth ed. Pearson, USA.
- Kawabe, N., Maruyama, T., Yamazaki, K., Suzuki, R., 2016. Development of gas shielded arc welding process to achieve a very low diffusible hydrogen content in weld metals. *Welding in the World* 60, 383–392.

- Khan, A.U., Madhukar, Y.M., 2020. An economic design and development of the wire arc additive manufacturing setup. *Procedia CIRP* 91, 182–187.
- Khan, M.F., Sharma, G., Dwivedi, D., 2015. Weld-bonding of 6061 aluminium alloy. *The International Journal of Advanced Manufacturing* 78 (5–8), 863–873.
- Kim, Y.-J., Choi, C.-H., 2009. A study on life estimation of hot forging die. *International Journal of Precision Engineering and Manufacturing* 10, 105–113. <https://doi.org/10.1007/s12541-009-0054-8>.
- Kim, Y.H., Park, J.J., 2002. Effect of process parameters on formability in incremental forming of sheet metal. *Journal of Materials Processing Technology* 130 (131), 42–46.
- Kim, K.J., Kim, D., Choi, S.H., Chung, K., Shin, K.S., Barlat, F., Oh, K.H., Youn, J.R., 2003. Formability of AA5182/polypropylene/AA5182 sandwich sheets. *Journal of Materials Processing Technology* 139, 1–7.
- Kim, W.J., Lee, J.B., Kim, W.Y., Jeong, H.T., Jeong, H.G., 2007. Microstructure and mechanical properties of Mg–Al–Zn alloy sheets severely deformed by asymmetrical rolling. *Scripta Materialia* 56, 309–312.
- Kim, C.H., Ahn, Y.N., Kim, J.H., 2011. CO<sub>2</sub> laser-micro plasma arc hybrid welding for galvanized steel sheets. *Transactions of Nonferrous Metals Society of China* 21, s47–s53.
- Kim, J.-B., Seo, W.-S., Park, K., 2012. Damage prediction in the multistep forging process of subminiature screws. *International Journal of Precision Engineering and Manufacturing* 13, 1619–1624. <https://doi.org/10.1007/s12541-012-0212-2>.
- Kim, B.-M., Ko, D.-C., Kim, D.-H., Lee, S.-B., Hwang, D.-W., Lee, K.-H., 2015. Fabrication of miniature hollow helical gear by powder extrusion of gas-atomized Zn-22wt%Al powder. *International Journal of Precision Engineering and Manufacturing* 16, 1429–1433. <https://doi.org/10.1007/s12541-015-0188-9>.
- Kimura, M., Ohara, K., Kusaka, M., Kaizu, K., Hayashida, K., 2020. Effects of tensile strength on friction welding condition and weld faying surface properties of friction welded joints between pure copper and austenitic stainless steel. *Journal of Advanced Joining Processes* 2, 100028–100038.
- Kotobi, M., Mansouri, H., Honarpisheh, M., 2019. Investigation of laser bending parameters on the residual stress and bending angle of St-Ti bimetal using FEM and neural network. *Optics & Laser Technology* 116, 265–275.
- Ku, T.-W., Kang, B.-S., 2014. Tool design and experimental verification for multi-stage cold forging process of the outer race. *International Journal of Precision Engineering and Manufacturing* 15, 1995–2004. <https://doi.org/10.1007/s12541-014-0556-x>.
- Kucharska, B., Moraczyński, O., 2020. Exhaust system piping made by hydroforming: relations between stresses, microstructure, mechanical properties and surface. *Archives of Civil and Mechanical Engineering* 20, 141.
- Kukreja, G., Narayanan, R.G., 2019. Forming of adhesive-bonded sandwich sheets with a rubber pad. *Metallurgical and Materials Transactions A* 50, 2155–2168. <https://doi.org/10.1007/s11661-019-05168-2>.
- Kumaran, T.A.V., Reddy, S.A.N.J., Jerome, S., Anbarasan, N., Arivazhagan, N., Manikandan, M., Sathishkumar, M., 2020. Development of pulsed cold metal transfer and gas metal arc welding techniques on high-strength aerospace-grade Aa7475-T761. *JMEPEG* 29, 7270–7290.
- Kupski, J., de Freitas, S.T., 2021. Design of adhesively bonded lap joints with laminated CFRP adherends: review, challenges and new opportunities for aerospace structures. *Composite Structures* 268, 113923–113935.
- Kwon, I.-K., Park, H.-S., 2011. Design of die forging process of thrust shaft for large marine diesel engine using floating die concept. *International Journal of Precision Engineering and Manufacturing* 12, 527–535. <https://doi.org/10.1007/s12541-011-0066-z>.

- Lang, L., Liu, B., Li, T., Zhao, X., Zeng, Y., 2012. Experimental investigation on hydromechanical deep drawing of aluminum alloy with heated media. *Steel Research International* 83, 230–237.
- Lee, S.-W., Jo, J.-W., Joun, M.-S., Lee, J.-M., 2019. Effect of friction conditions on material flow in FE analysis of Al piston forging process. *International Journal of Precision Engineering and Manufacturing* 20, 1643–1652. <https://doi.org/10.1007/s12541-019-00189-8>.
- Lee, J.H., Yamashita, S., Ogura, T., Saida, K., 2020. Solidification cracking prevention by thermal strain control via water cooled gas tungsten arc welding. *Materials Today Communications* 23, 101109–101119.
- Li, Y., 2015. Towards inclusive and sustainable industrial development. *Development* 58 (4), 446–451.
- Li, D., Ghosh, A.K., 2004. Biaxial warm forming behavior of aluminum sheet alloys. *Journal of Materials Processing Technology* 145, 281–293.
- Li, M., Liu, Y., Su, S., Li, G., 1999. Multi-point forming: a flexible manufacturing method for a 3-d surface sheet. *Journal of Materials Processing Technology* 87, 277–280.
- Li, M.Z., Cai, Z.Y., Sui, Z., Yan, Q.G., 2002. Multi-point forming technology of sheet metal. *Journal of Materials Processing Technology* 129, 333–338.
- Li, R., Li, Z., Zhu, Y., Rong, L., 2011. A comparative study of laser beam welding and laser–MIG hybrid welding of Ti–Al–Zr–Fe titanium alloy. *Materials Science and Engineering* 528 (3), 1138–1142.
- Li, Y., Zhang, Y., Bi, J., Luo, Z., 2015. Impact of electromagnetic stirring upon weld quality of Al/Ti dissimilar materials resistance spot welding. *Materials & Design* 83, 577–586.
- Li, D., Chrysanthou, A., Patel, I., Williams, G., 2017. Self-piercing riveting—a review. *International Journal of Advanced Manufacturing Technology* 92 (5), 177–824.
- Li, G., Li, Z., Zhang, J., Luo, S., Guo, N., 2020. Macrostructure, microstructure and mechanical properties of bobbin tool friction stir welded ZK60 Mg alloy joints. *Journal of Materials Research and Technology* 9 (4), 9348–9361.
- Lim, S.S., Kim, Y.T., Kang, C.G., 2013. Fabrication of aluminum 1050 micro-channel proton exchange membrane fuel cell bipolar plate using rubber-pad-forming process. *International Journal of Advanced Manufacturing Technology* 65, 231–238.
- Liu, J., Cao, B., 2021. Microstructure characteristics and mechanical properties of the Cu/Al dissimilar joints by electric current assisted ultrasonic welding. *Journal of Materials Processing Technology* 297, 117239–117248.
- Liu, Y., Hua, L., 2010. Fabrication of metallic bipolar plate for proton exchange membrane fuel cells by rubber pad forming. *Journal of Power Sources* 195, 3529–3535.
- Liu, J., Liu, W., Xue, W., 2013. Forming limit diagram prediction of AA5052/polyethylene/AA5052 sandwich sheets. *Materials and Design* 46, 112–120.
- Liu, S., Chen, S., Wang, Q., Li, Y., Zhang, H., Ding, H., 2017. Analysis of plasma characteristics and conductive mechanism of laser assisted pulsed arc welding. *Optics and Lasers in Engineering* 92, 39–47.
- Liu, X., Dong, Q., Wang, P., Chen, H., 2021. Review of electron beam welding technology in space environment. *Optik* 225, 165720–165731.
- Lovell, M., Higgs, C.F., Deshmukh, P., Mobley, A., 2006. Increasing formability in sheet metal stamping operations using environmentally friendly lubricants. *Journal of Materials Processing Technology* 177, 87–90.
- Ma, Z., 2008. Friction stir processing technology: a review. *Metallurgical and Materials Transactions A* 39, 642–658. <https://doi.org/10.1007/s11661-007-9459-0>.
- Ma, Z.Y., Mishra, R.S., Mahoney, M.W., Grimes, R., 2003. High strain rate super plasticity in friction stir processed Al–Mg–Zr alloy. *Materials Science and Engineering A* 351, 148–153.
- Ma, Q., Cao, Y., Zhang, W., Zhao, W., Chen, H., Li, M., Liang, Z., Xiao, Y., Ji, H., 2021. Low energy ultrasonic welding for Cu–Cu joining accelerated via Cu nanoparticles. *Journal of Materials Processing Technology* 296, 117210–117219.

- Macwan, A., Chen, D.L., 2016. Ultrasonic spot welding of a rare-earth containing ZEK100 magnesium alloy: effect of welding energy. *Metallurgical and Materials Transactions A* 47 (4), 1686–1697.
- Maji, K., Pratihari, D.K., Nath, A.K., 2014. Laser forming of a dome shaped surface: experimental investigations, statistical analysis and neural network modelling. *Optics and Lasers in Engineering* 53, 31–42.
- Martinez, G.A.S., Qian, W.-L., Kabayama, L.K., Prisco, U., 2020. Effect of process parameters in copper-wire drawing. *Metals* 10, 105. <https://doi.org/10.3390/met10010105>.
- Matthew, J.D., 2000. *Titanium: A Technical Guide*, second ed., vol 76. ASM International.
- Meibner, J., Schmatz, F., Beu, F., Sender, J., Flugge, W., Gorr, E., 2018. Smart human-robot-collaboration in mechanical joining processes. *Procedia Manufacturing* 24, 264–270.
- Meschut, G., Hahn, O., Janzen, V., Olfemann, T., Matzke, M., 2013. Comparison of innovative thermal joining technologies for joining ultra-high-strength steels in multi-material structures. *DVS-berichte* 296. VS Media GmbH, Düsseldorf, Germany, 2013. ISBN: 978-3-87155-614-2.
- Meschut, G., Janzen, V., Olfemann, T., 2014a. Innovative and highly productive joining technologies for multi-material lightweight car body structures. *Journal of Materials Engineering and Performance* 23 (5), 1515–1523.
- Meschut, G., Hahn, O., Janzen, V., Olfemann, T., 2014b. Innovative joining technologies for multi-material structures. *Welding in the World* 58 (1), 65–75.
- Miles, M.P., Nelson, T.W., Decker, B.J., 2004. Formability and strength of friction-stir-welded aluminum sheets. *Metallurgical and Materials Transactions A* 35, 3461–3468. <https://doi.org/10.1007/s11661-004-0183-8>.
- Miles, M.P., Nelson, T.W., Melton, D.W., 2005. Formability of friction-stir-welded dissimilar-aluminum-alloy sheets. *Metallurgical and Materials Transactions A* 36, 3335–3342.
- Miles, M.P., Pew, J., Nelson, T.W., Li, M., 2006. Comparison of formability of friction stir welded and laser welded dual phase 590 steel sheets. *Science and Technology of Welding & Joining* 11 (4), 384–388.
- Miles, M.P., Nelson, T.W., Steel, R., Olsen, E., Gallagher, M., 2009. Effect of friction stir welding conditions on properties and microstructures of high strength automotive steel. *Science and Technology of Welding & Joining* 14 (3), 228–232.
- Mishra, R.S., Ma, Z.Y., 2005. Friction stir welding and processing. *Materials Science and Engineering: R: Reports* 50 (1–2), 1–78.
- Moayedi, H., Darabi, R., Ghabussi, A., Habibi, M., Foong, L.K., 2020. Weld orientation effects on the formability of tailor welded thin steel sheets. *Thin-Walled Structures* 149, 106669.
- Mobarak, H.M., Mohamad, E.N., Masjuki, H.H., Kalam, M.A., Al Mahmud, K.A.H., Habibullah, M., Ashraful, A.M., 2014. The prospects of bio-lubricants as alternatives in automotive applications. *Renewable and Sustainable Energy Reviews* 33, 34–43.
- Mondal, M., Basak, S., Das, H., Hong, S.-T., Choi, H., Park, J.-W., Han, H.N., 2020. Manufacturing of magnesium/aluminum bimetallic ring components by friction stir assisted simultaneous forging and solid-state joining. *International Journal of Precision Engineering and Manufacturing - Green Technology* 8, 1429–1438. <https://doi.org/10.1007/s40684-020-00244-0>.
- Mori, K., Patwari, A.U., Maki, S., 2004. Improvement of formability by oscillation of internal pressure in pulsating hydroforming of tube. *CIRP Annals - Manufacturing Technology* 53, 215–218.
- Mori, K., Maeno, T., Maki, S., 2007. Mechanism of improvement of formability in pulsating hydroforming of tubes. *International Journal of Machine Tools and Manufacture* 47, 978–984.
- Mori, K.I., Kaido, T., Suzuki, Y., Nakagawa, Y., Abe, Y., 2020. Combined process of hot stamping and mechanical joining for producing ultra-high strength steel patchwork components. *Journal of Manufacturing Processes* 59, 444–455.

- Morrow, W.R., Qi, H., Kim, I., Mazumder, J., Skerlos, S.J., 2007. Environmental aspects of laser-based and conventional tool and die manufacturing. *Journal of Cleaner Production* 15, 932–943. <https://doi.org/10.1016/j.jclepro.2005.11.030>.
- Mucha, J., 2014. The numerical analysis of the effect of the joining process parameters on self-piercing riveting using the solid rivet. *Archives of Civil and Mechanical Engineering* 14, 444–454.
- Murakawa, M., Koga, N., Kumagai, T., 1995. Deep drawing of aluminium sheets without lubricant by use of diamond-like carbon coated dies. *Surface and Coatings Technology* 76–77, 553–558.
- Murakawa, M., Koga, N., Takeuchi, S., 1999. Diamond like carbon-coated dies for deep drawing of aluminum sheets. *ASME The Journal of Manufacturing Science and Engineering* 121 (4), 674–678.
- Nagendramma, P., Kaul, S., 2012. Development of ecofriendly/biodegradable lubricants: an overview. *Renewable and Sustainable Energy Reviews* 16 (1), 764–774.
- Narasimhan, P.N., Mehrotra, S., Raja, A.R., Vashista, M., Yusufzai, M.Z., 2019. Development of hybrid welding processes incorporating GMAW and SMAW. *Materials Today Proceedings* 18, 2924–2932.
- Narayanan, R.G., 2018. A novel method of joining a rod to a sheet by end deformation: a preliminary experimental study. *International Journal of Precision Engineering and Manufacturing* 19 (5), 773–779.
- Nejad, R.M., Shojaati, Z.S.H., Wheatley, G., Moghadam, D.G., 2021. On the bending angle of aluminum-copper two-layer sheets in laser forming process. *Optics & Laser Technology* 142, 107233.
- Oladimeji, O.O., Taban, E., 2016. Trend and innovations in laser beam welding of wrought aluminum alloys. *Welding in the World* 60, 415–457.
- Pan, C., Zhang, R., Wang, D., Li, Y., Yamaguchi, T., Fan, X., Zhao, D., Wang, W., 2021. Preparation of high performance Fe-based amorphous coating by resistance seam welding. *Surface and Coatings Technology* 408, 126813.
- Park, C.W., Kim, Y.H., 2012. A study on the manufacturing of digital camera barrel using magnesium alloy. *International Journal of Precision Engineering and Manufacturing* 13, 1047–1052. <https://doi.org/10.1007/s12541-012-0136-x>.
- Park, D.-H., Kwon, H.-H., 2016. Development of automobile engine mounting parts using hot-cold complex forging technology. *International Journal of Precision Engineering and Manufacturing - Green Technology* 3, 179–184. <https://doi.org/10.1007/s40684-016-0023-5>.
- Park, D.-H., Kwon, H.-D., Kwon, H.-H., 2019. Development of cam ring gear parts of large diameter for truck clutch using hot–cold complex forging technology of small bar. *International Journal of Precision Engineering and Manufacturing* 20, 827–836. <https://doi.org/10.1007/s12541-019-00100-5>.
- Parvizi, A., Rohani Raftar, H.R., 2019. Application of artificial neural network and genetic algorithm to predict and optimize load and torque in T-section profile ring rolling. *Proceedings of the Institution of Mechanical Engineers - Part C: Journal of Mechanical Engineering Science* 233 (17), 5966–5976.
- Peng, H., Li, M., Liu, C., Cao, J., 2013. Study of multi-point forming for polycarbonate sheet. *International Journal of Advanced Manufacturing Technology* 67, 2811–2817. <https://doi.org/10.1007/s00170-012-4694-y>.
- Peng, D., Liu, Q., Li, G., Cui, J., 2019. Investigation on hybrid joining of aluminum alloy sheets: magnetic pulse weld bonding. *International Journal of Advanced Manufacturing Technology* 104 (9), 4255–4264.
- Podgornik, B., Hogmark, S., Sandberg, O., 2004. Influence of surface roughness and coating type on the galling properties of coated forming tool steel. *Surface and Coatings Technology* 184 (2–3), 338–348.

- Polkowski, W., 2016. In: Glebovsky, V. (Ed.), *Differential Speed Rolling: A New Method for a Fabrication of Metallic Sheets with Enhanced Mechanical Properties*. Chapter 5, *Progress in Metallic Alloys*. InTech. <https://doi.org/10.5772/64418>.
- Pouranvari, M., Abbasi, M., 2018. Dissimilar gas tungsten arc weld-brazing of Al/steel using Al-Si filler metal: microstructure and strengthening mechanisms. *Journal of Alloys and Compounds* 749, 121–127.
- Prisco, U., Martinez, G.A.S., Kabayama, L.K., 2020. Effect of die pressure on the lubricating regimes achieved in wire drawing. *Production Engineering* 14, 667–676. <https://doi.org/10.1007/s11740-020-00985-6>.
- Pritam, R.K., Narayanan, R.G., Kailas, S.V., 2019. Friction stir spot welding of AA5052-H32/HDPE/AA5052-H32 sandwich sheets at varying plunge speeds. *Thin-Walled Structures* 138, 415–429.
- Rachakonda, S., Gengusamy, S., Gunasekera, J.S., Dwivedi, S.N., 1991. Computer-aided process design for the manufacture of rolled rings. *International Journal of Computer Integrated Manufacturing* 4 (2), 97–104.
- Ramezani, M., Schmid, S.R., 2015. Bio-based lubricants for forming of magnesium. *Journal of Manufacturing Processes* 19, 112–117. <https://doi.org/10.1016/j.jmapro.2015.06.008>.
- Ramirez-Cedillo, E., García-López, E., Ruiz-Huerta, L., Rodriguez, C.A., Siller, H.R., 2021. Reusable unit process life cycle inventory (UPLCI) for manufacturing: laser powder bed fusion (L-PBF). *Production Engineering* (15), 701–716. <https://doi.org/10.1007/s11740-021-01050-6>.
- Ramulu, P.J., 2012. *Forming Behavior of Friction Stir Welded Sheets*. Ph.D. thesis. IIT Guwahati, India.
- Ramulu, P.J., Narayanan, R.G., Kailas, S.V., 2013a. Forming limit investigation of friction stir welded sheets: influence of shoulder diameter and plunge depth. *International Journal of Advanced Manufacturing Technology* 69, 2757–2772.
- Ramulu, P.J., Kailas, S.V., Narayanan, R.G., 2013b. Influence of tool rotation speed and feed rate on the forming limit of friction stir welded AA6061-T6 sheets. *Proc IMechE Part C: Journal of Mechanical Engineering Science* 227, 520–541.
- Ramulu, P.J., Kailas, S.V., Narayanan, R.G., 2015. Formability of friction stir welded sheets made of AA 6061-T6 at different weld orientations and weld locations. *International Journal of Materials and Product Technology* 50 (2), 147–160.
- Ranatunga, V., Gunasekera, J.S., 2006. UBET based numerical modeling of bulk deformation processes. *Journal of Materials Engineering and Performance* 15 (1), 47–52.
- Rao, K.P., Wei, J.J., 2001. Performance of a new dry lubricant in the forming of aluminum alloy sheets. *Wear* 249, 86–93.
- Reisel, G., Wielage, B., Steinhäuser, S., Hartwig, H., 2003. DLC for tool protection in warm massive forming. *Diamond and Related Materials* 12, 1024–1029.
- Reisel, G., Dorner-Reisel, A., Wielage, B., 2005. Silicon doped diamond like carbon as substitute for lubrication in spin-extrusion. *Diamond and Related Materials* 14, 1810–1814. <https://doi.org/10.1016/j.diamond.2005.06.014>.
- Riahi, A.R., Morales, A.T., Alpas, A.T., 2008. Evaluation of vitreous and devitrifying enamels as hot forming lubricants for aluminum AA5083 alloy. *Journal of Materials Engineering and Performance* 17, 387–394. <https://doi.org/10.1007/s11665-008-9208-6>.
- Rosel, S., Merklein, M., 2014. Improving formability due to an enhancement of sealing limits caused by using a smart fluid as active fluid medium for hydroforming. *Production Engineering. Research and Development* 8, 7–15.
- Saad, M.H., Jarrah, O.M., Nazzal, M.A., Darras, B.M., Kishawy, H.A., 2020. Sustainability-based evaluation of friction stir back extrusion of seamless tubular shapes. *Journal of Cleaner Production* 267, 121972. <https://doi.org/10.1016/j.jclepro.2020.121972>.

- Safari, M., Alves de Sousa, R., Joudaki, J., 2020a. Fabrication of saddle-shaped surfaces by a laser forming process: an experimental and statistical investigation. *Metals* 10, 883. <https://doi.org/10.3390/met10070883>.
- Safari, M., Alves de Sousa, R., Joudaki, J., 2020b. Recent advances in the laser forming process: a review. *Metals* 10, 1472. <https://doi.org/10.3390/met10111472>.
- Sahoo, A., Tripathy, S., 2021. Development in plasma arc welding process: a review. *Materials Today Proceedings* 41, 363–368.
- Saikov, I.V., Malakhov, A.Y., Saikova, G.R., Denisov, I.V., Gulyaev, P.Y., 2020. Influence of explosive welding parameters on the structure of interface in brass–invar thermobimetals. *Inorganic Materials: Applied Research* 11, 448–452.
- Saju, T.P., Narayanan, R.G., 2020. Dieless friction stir lap joining of AA 5050-H32 with AA 6061-T6 at varying pre-drilled hole diameters. *Journal of Manufacturing Processes* 53, 21–33.
- Sakai, T., Hamada, S., Saito, Y., 2001. Improvement of the r-value in 5052 aluminum alloy sheets having through-thickness shear texture by 2-pass single-roll drive unidirectional shear rolling. *Scripta Materialia* 44, 2569–2573.
- Sakate, P.M., Mullick, S., Gopinath, M., 2021. An investigation on physical phenomena of water-jet assisted underwater wet laser welding technique under continuous and pulsed mode operation. *Optik - International Journal for Light and Electron Optics* 242, 167272–167283.
- Sapanathan, T., Raelison, R.N., Buiron, N., Rachik, M., 2016. Magnetic pulse welding: an innovative joining technology for similar and dissimilar metal pairs. *Joining Technologies*, Mahadzir Ishak, IntechOpen. <https://doi.org/10.5772/63525>.
- Satheeshkumar, V., Narayanan, R.G., 2014. Investigation on the influence of adhesive properties on the formability of adhesive-bonded steel sheets. *Proceedings of the Institution of Mechanical Engineers - Part C: Journal of Mechanical Engineering Science* 228 (3), 405–425.
- Satheeshkumar, V., Narayanan, R.G., 2015a. Forming performance of adhesive bonded steel sheets reinforced with metallic wires. *Welding in the World* 59 (6), 883–900.
- Satheeshkumar, V., Narayanan, R.G., 2015b. In-plane plane strain formability of adhesive-bonded steel sheets: influence of adhesive properties. *International Journal of Advanced Manufacturing Technology* 76, 993–1009.
- Satheeshkumar, V., Narayanan, R.G., 2016. Experimental evaluation and prediction of formability of adhesive bonded steel sheets at different adhesive properties. *Journal of Testing and Evaluation* 44 (3), 1294–1306.
- Schafranski, L.L., Cunha, T.V.D., Bohórquez, C.E.N., 2017. Benefits from H<sub>2</sub> and CO<sub>2</sub> additions in argon gas mixtures in GMAW. *Journal of Materials Processing Technology* 249, 158–166.
- Schmidt, C., Li, W., Thiede, S., Kara, S., Herrmann, C., 2015. A methodology for customized prediction of energy consumption in manufacturing industries. *International Journal of Precision Engineering and Manufacturing - Green Technology* 2, 163–172. <https://doi.org/10.1007/s40684-015-0021-z>.
- Sen, N., Kurgan, N., 2016. Improving deep drawability of HC300LA sheet metal by warm forming. *International Journal of Advanced Manufacturing Technology* 82, 985–995.
- Seyedkashi, S.M.H., Moslemi Naeini, H., Moon, Y.H., 2014. Feasibility study on optimized process conditions in warm tube hydroforming. *Journal of Mechanical Science and Technology* 28, 2845–2852.
- Seyedkashi, H., Gollo, M.H., Biao, J., Moon, Y.H., 2016. Laser bendability of SUS430/C11000/SUS430 laminated composite and its constituent layers. *Metals and Materials International* 22, 527–534.
- Seyffarth, P., Krivtsun, I., 2002. *Laser-arc Processes and Their Applications in Welding and Material Treatment*. CRC Press, ISBN 9780415269612.

- Shahabad, S.I., Naeini, H.M., Roohi, A.H., Tavakoli, A., Nasrollahzade, M., 2017. Experimental investigation of laser forming process to produce dome-shaped products. *International Journal of Advanced Manufacturing Technology* 90, 1051–1057. <https://doi.org/10.1007/s00170-016-9437-z>.
- Shi, Y., Shen, H., Yao, Z., Hu, J., 2007. Temperature gradient mechanism in laser forming of thin plates. *Optics & Laser Technology* 39 (4), 858–863.
- Shi, Y., Zhang, G., Huang, Y., Lu, L., Huang, J., Shao, Y., 2014. Pulsed double-electrode GMAW-brazing for joining of aluminum to steel. *Welding Journal* 93, 216s–224s.
- Shi, Y., Li, J., Zhang, G., Huang, J., Gu, Y., 2016. Corrosion behavior of aluminum-steel weld-brazing joint. *Journal of Materials Engineering and Performance* 25, 1916–1923.
- Silva, M.B., Skjoedt, M., Atkins, A.G., Bay, N., Martins, P.A.F., 2008. Single-point incremental forming and formability—failure diagrams. *The Journal of Strain Analysis for Engineering Design* 43, 15–35. <https://doi.org/10.1243/03093247JSA340>.
- Silva, M.B., Alves, L.M., Martins, P.A.F., 2010. Single point incremental forming of PVC: experimental findings and theoretical interpretation. *European Journal of Mechanics ASolids* 29, 557–566. <https://doi.org/10.1016/j.euromechsol.2010.03.008>.
- Singh, R.P., Raghuvanshi, D., Pal, A., 2021a. Effect of external magnetic field on weld width and reinforcement height of shielded metal arc welded joints. *Materials Today Proceedings* 38, 112–115.
- Singh, R.P., Kumar, S., Dubey, S., 2021b. A review on working and applications of oxy-acetylene gas welding. *Materials Today Proceedings* 38 (1), 34–39.
- Slobodyan, M., 2021. Resistance, electron- and laser-beam welding of zirconium alloys for nuclear applications: a review. *Nuclear Engineering and Technology* 53, 1049–1078.
- Srikanth, A., Manikandan, M., 2017. Development of welding technique to avoid the sensitization in the alloy 600 by conventional gas tungsten arc welding method. *Journal of Manufacturing Processes* 30, 452–466.
- Sucharitpawatskul, S., Mahayotsanun, N., Bureerat, S., Dohda, K., 2020. Effects of tool coatings on energy consumption in micro-extrusion of aluminum alloy 6063. *Coatings* 10 (4), 381. <https://doi.org/10.3390/coatings10040381>.
- Taban, E., Kaluc, E., Dhooge, A., 2009. Hybrid (plasma+ gas tungsten arc) weldability of modified 12% Cr ferritic stainless steel. *Materials and Design* 30 (10), 4236–4242.
- Talebi-Ghadikolae, H., Elyasi, M., Mirnia, M.J., 2020. Investigation of failure during rubber pad forming of metallic bipolar plates. *Thin-Walled Structures* 150, 106671. <https://doi.org/10.1016/j.tws.2020.106671>.
- Tan, F.X., Li, M.Z., Cai, Z.Y., 2007. Research on the process of multi-point forming for the customized titanium alloy cranial prosthesis. *Journal of Materials Processing Technology* 187–188, 453–457. <https://doi.org/10.1016/j.jmatprotec.2006.11.149>.
- Thomas, W.M., Staines, D.G., Norris, I.M., de Frias, R., 2003. Friction stir welding tools and developments. *Welding in the World* 47, 10–17.
- Thomsen, A.N., 2020. Laser Forming of Sheet Metal. Ph.D. thesis. Aalborg University, Denmark, 2020.
- Tolazzi, M., 2010. Hydroforming applications in automotive: a review. *International Journal of Material Forming* 3, 307–310. <https://doi.org/10.1007/s12289-010-0768-2>.
- Tong, L., Xie, J., Liu, L., Chang, G., Ojo, O.O., 2020. Microscopic appraisal and mechanical behavior of hybrid Cu/Al joints fabricated via friction stir spot welding-brazing and modified friction stir clinching-brazing. *Journal of Materials Research and Technology* 9 (6), 13239–13249.
- Troughton, M.J., 2009. Chapter 2: ultrasonic welding. In: *Handbook of Plastics Joining*, second ed. William Andrew Publishing, ISBN 9780815515814, pp. 15–35.
- Tsuyama, T., Yuda, M., Nakai, K., 2014. Effects of hot wire on mechanical properties of weld metal using gas-shielded arc welding with CO<sub>2</sub> gas. *Welding in the World* 58, 77–83.

- Uda, K., Azushima, A., Yanagida, A., 2016. Development of new lubricants for hot stamping of Al-coated 22MnB5 steel. *Journal of Materials Processing Technology* 228, 112–116. <https://doi.org/10.1016/j.jmatprotec.2015.10.033>.
- Verma, J., Taiwade, R.V., Reddy, C., Khatirkar, R.K., 2018. Effect of friction stir welding process parameters on Mg-AZ31B/Al-AA6061 joints. *Materials and Manufacturing Processes* 33 (3), 308–314.
- Vimal, K.E.K., Vinodh, S., Raja, A., 2015. Modelling assessment and deployment of strategies for ensuring sustainable shielded metal arc welding process - a case study. *Journal of Cleaner Production* 93, 364–377.
- Wagiman, A., Mustapa, M.S., Asmawi, R., Shamsudin, S., Lajis, M.A., Mutoh, Y., 2020. A review on direct hot extrusion technique in recycling of aluminium chips. *International Journal of Advanced Manufacturing Technology* 106, 641–653. <https://doi.org/10.1007/s00170-019-04629-7>.
- Wagner, R., Siewert, E., Schein, J., Hussary, N., Jäckel, S., 2018. Shielding gas influence on emissions in arc welding. *Welding in the World* 62, 647–652.
- Wahid, M.A., Siddiquee, A.N., Khan, Z.A., Sharma, N., 2018. Analysis of cooling media effects on microstructure and mechanical properties during FSW/UFSW of AA 6082-T6. *Materials Research Express* 5 (4), 046512–046529.
- Wang, G., Yan, Z., Zhang, H., Zhang, X., Liu, F., Wang, X., Su, Y., 2017. Improved properties of friction stir-welded AZ31 magnesium alloy by post-weld heat treatment. *Materials Science and Technology* 33 (7), 854–863.
- Wang, X., Wang, C., Shen, X., Sun, F., 2018. High-speed drawing of Al alloy wire by diamond-coated drawing die under environmentally friendly water-based emulsion lubrication. *Journal of Manufacturing Science and Engineering* 140, 124502. <https://doi.org/10.1115/1.4041477>.
- Wang, H., Tong, X., Chen, Y., Hua, L., Wu, M., Ji, W., 2021. Study on ultrasonic vibration-assisted adhesive bonding of CFRP laminates with laser ablation-treated surfaces. *Composite Structures* 268, 113983–113992.
- Wank, A., Reisel, G., Wielage, B., 2006. Behavior of DLC coatings in lubricant free cold massive forming of aluminum. *Surface and Coatings Technology* 201, 822–827. <https://doi.org/10.1016/j.surfcoat.2005.12.043>.
- Weglowski, M.S., Błacha, S., Phillips, A., 2016. Electron beam welding – techniques and trends – Review. *Vacuum* 130, 72–92.
- Wei, H., Zhang, Y., Tan, L., Zhong, Z., 2015. Energy efficiency evaluation of hot-wire laser welding based on process characteristic and power consumption. *Journal of Cleaner Production* 87, 255–262.
- Wilson, J.M., Piya, C., Shin, Y.C., Zhao, F., Ramani, K., 2014. Remanufacturing of turbine blades by laser direct deposition with its energy and environmental impact analysis. *Journal of Cleaner Production* 80, 170–178. <https://doi.org/10.1016/j.jclepro.2014.05.084>.
- Xiao, X., Kim, J.-J., Oh, S.-H., Kim, Y.-S., 2021. Study on the incremental sheet forming of CFRP sheet. *Composites Part A: Applied Science and Manufacturing* 141, 106209. <https://doi.org/10.1016/j.compositesa.2020.106209>.
- Xie, Y., Huang, Y., Meng, X., Wang, F., Wan, L., Dong, Z., Cao, J., 2020. Friction rivet joining towards high-performance wood-metal hybrid structures. *Composite Structures* 247, 112472–112481.
- Xu, D.-C., Zhai, S.-Y., Cheng, H.-Y., Guadie, A., Wang, H.-C., Han, J.-L., Liu, C.-Y., Wang, A.-J., 2020. Wire-drawing process with graphite lubricant as an industrializable approach to prepare graphite coated stainless-steel anode for bioelectrochemical systems. *Environmental Research* 191, 110093. <https://doi.org/10.1016/j.envres.2020.110093>.
- Yamazaki, K., Suzuki, R., Yamazaki, K., Suzuki, R., Shimizu, H., Koshiishi, F., 2012. Spatter and fume reduction in CO<sub>2</sub> Gas-shielded arc welding by regulated globular transfer. *Welding in the World* 56, 9–10.

- Yang, X., Wang, B., Zhou, J., 2020. Numerical and experimental study on formability of TC4 alloy in a novel multi-layer sheet hot stamping process. *International Journal of Advanced Manufacturing Technology* 110, 1233–1247. <https://doi.org/10.1007/s00170-020-05802-z>.
- Yi, X., Du, Y., Geng, D., Li, Z., Han, W., Liu, P., Chen, J., Yabuuchi, K., Yoshida, K., Ohnuki, S., Zhan, Q., 2021. Heavy-ion irradiation and post-irradiation annealing effects in explosion-welded CuCrZr/316LN joints for ITER application. *Materials Characterization* 178, 111252–111261.
- Yoon, J., Lee, J., 2015. Process design of Warm-Forging with extruded Mg-8Al-0.5Zn alloy for differential case in automobile transmission. *International Journal of Precision Engineering and Manufacturing* 16, 841–846. <https://doi.org/10.1007/s12541-015-0110-5>.
- Yoon, H.-S., Lee, J.-Y., Kim, H.-S., Kim, M.-S., Kim, E.-S., Shin, Y.-J., Chu, W.-S., Ahn, S.-H., 2014. A comparison of energy consumption in bulk forming, subtractive, and additive processes: review and case study. *International Journal of Precision Engineering and Manufacturing - Green Technology* 1, 261–279. <https://doi.org/10.1007/s40684-014-0033-0>.
- Yoshimura, H., Torikai, S., Nishihara, T., Toshiji, N., Inouchi, N., 2002. Application of wheat flour lubricants to the press forming process. *Journal of Materials Processing Technology* 125–126, 375–378.
- Yu, H., Tong, Y., 2017. Magnetic pulse welding of aluminum to steel using uniform pressure electromagnetic actuator. *International Journal of Advanced Manufacturing Technology* 91 (5), 2257–2265.
- Yu, H., Dang, H., Qiu, Y., Zhang, W., 2020. Effects of key parameters on magnetic pulse welding of 5A02 tube and SS304 tube. *International Journal of Advanced Manufacturing Technology* 110 (9), 2529–2540.
- Yuan, S., Wang, X., Liu, G., Wang, Z.R., 2007. Control and use of wrinkles in tube hydroforming. *Journal of Materials Processing Technology* 182, 6–11.
- Yuan, Q., Cheng, C.F.C., Wang, J., Zhu, T.T., Wang, K., 2020. Inclusive and sustainable industrial development in China: an efficiency-based analysis for current status and improving potentials. *Applied Energy* 268, 114876–114893.
- Yun, J.-H., Jeong, M.-S., Lee, S.-K., Jeon, J.-W., Park, J.-Y., Kim, G.M., 2014. Sustainable production of helical pinion gears: environmental effects and product quality. *International Journal of Precision Engineering and Manufacturing - Green Technology* 1, 37–41. <https://doi.org/10.1007/s40684-014-0006-3>.
- Zeng, Q., Sun, C., 2001. Novel design of a bonded lap joint. *American Institute of Aeronautics and Astronautics Journal* 39, 1991–1996.
- Zhang, L., 2021. Filler metals, brazing processing and reliability for diamond tools brazing: a review. *Journal of Manufacturing Processes* 66, 651–668.
- Zhang, S.H., Wang, Z.R., Xu, Y., Wang, Z.T., Zhou, L.X., 2004. Recent developments in sheet hydroforming technology. *Journal of Materials Processing Technology* 151 (1–3), 237–241.
- Zhang, H., Huang, G., Roven, H.J., Wang, L., Pan, F., 2013. Influence of different rolling routes on the microstructure evolution and properties of AZ31 magnesium alloy sheets. *Materials and Design* 50, 667–673.
- Zhao, T., Zhao, Q., Wu, W., Xi, L., Li, Y., Wan, Z., Villegas, I.F., Benedictus, R., 2021. Enhancing weld attributes in ultrasonic spot welding of carbon fibre-reinforced thermoplastic composites: effect of sonotrode configurations and process control. *Composites Part B* 211, 108648–108658.
- Zheng, C., Pan, C., Wang, J., Zhao, G., Ji, Z., 2020. Mechanical joining behavior of Cu–Fe dissimilar metallic foils in laser shock clinching. *International Journal of Advanced Manufacturing Technology* 110 (3), 1001–1014.

- Zhong-qin, L., Wu-rong, W., Guan-long, C., 2007. A new strategy to optimize variable blank holder force towards improving the forming limits of aluminum sheet metal forming. *Journal of Materials Processing Technology* 183, 339–346.
- Zitelli, C., Folgarait, P., Schino, A.D., 2019. Laser powder bed fusion of stainless steel Grades: a review. *Metals* 9, 731. <https://doi.org/10.3390/met9070731>.
- Zlobin, B.S., Kiselev, V.V., Shterzer, A.A., Plastinin, A.V., 2018. Use of emulsion explosives in experimental studies of flows in the bonding zone in explosive welding. *Combustion, Explosion and Shock Waves* 54 (2), 231–237.
- Zong, R., Chen, J., Wu, C., 2020. A comparison of double shielded GMAW-P with conventional GMAW-P in the arc, droplet and bead formation. *Journal of Materials Processing Technology* 285, 116781–116794.

# Sustainable manufacturing strategies in machining

*P. Sivaiah<sup>1</sup>, D. Chakradhar<sup>2</sup>, and R. Ganesh Narayanan<sup>3</sup>*

<sup>1</sup>Department of Mechanical Engineering, Madanapalle Institute of Technology & Science, Madanapalle, Andra Pradesh, India; <sup>2</sup>Department of Mechanical Engineering, IIT Palakkad, Palakkad, Kerala, India; <sup>3</sup>Department of Mechanical Engineering, Indian Institute of Technology Guwahati, Guwahati, Assam, India

## 4.1 Need for sustainable machining

Machining of metallic materials involves temperature development at the cutting zone due to contact between the tool and workpiece. Especially, machining of hard-to-cut materials develops higher cutting temperature because of greater mechanical properties (Ulutan and Ozel, 2011; Pusavec et al., 2014). Therefore, utilization of cutting fluids at the cutting zone is obligatory to control the cutting temperature. The conventional cooling method delivers poor performance characteristics due to failure in the control of high cutting temperatures at the higher cutting condition (Shaw and Richardson, 1951; Cassin and Boothroyd, 1965). However, the conventional cooling method uses chemically contaminated cutting fluids, which affect the machinist health, environmental pollution, and manufacturing cost negatively (Baradie, 1996; Feng and Hattori, 2000; Hong and Broomer, 2000; Shokrani et al., 2016). Consequently, many environmental conscious regulations imposed stringent restrictions to the metal cutting industries on the usage of cutting fluid and disposal of cutting fluids into the atmosphere (Marksberry, 2007; Rao, 2011; Shokrani et al., 2012). So, metal cutting industries, focused on sustainable machining techniques to fulfill the environmental conscious regulations without compromising productivity. In this connection, many researchers focused on various sustainable machining techniques to meet the demand

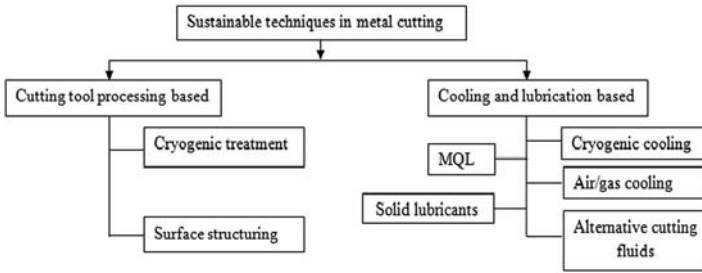
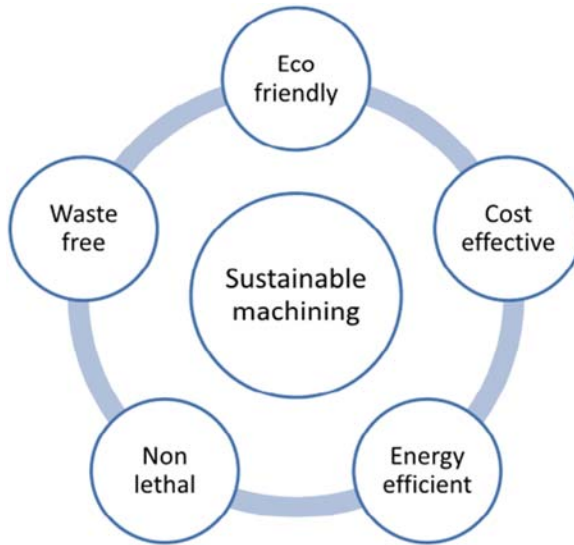


FIGURE 4.1 Sustainable machining techniques for cleaner production. Used with permission from Chetan G.S., Rao, P.V., 2015. Application of sustainable techniques in metal cutting for enhanced machinability: a review. *Journal of Cleaner Production*, 100, 17–34.

of metal cutting industries as shown in Fig. 4.1. Shokrani et al. (2012) reviewed the different machining techniques to reduce or eliminate the use of conventional coolants in metal material and concluded that dry machining, minimum quantity lubricant (MQL), and cryogenic machining techniques reduce or avoid cutting fluid to meet the industry requirements. In recent times, usage of surface texturing of the tool in machining has been increasing due to the increased process performance in different machining processes (Pratap and Patra, 2020). Therefore, the present chapter discusses the recent advancements in the different conventional and nonconventional machining processes under dry, MQL, machining with surface textured tools and cryogenic cutting conditions. Brief discussion on green cutting fluids is also provided. Finally, recent advances, challenging problems, and future prospects are summarized.

## 4.2 Sustainable characteristics in machining

The characteristics required for sustainable machining are shown in Fig. 4.2. A sustainable manufacturing process is defined as the process, which produces the product by using less energy, less cost, and without creating a problem for the operator and environment (Jayal et al., 2010). Dry machining involves no coolant usage; therefore, it avoids coolant waste, chip recycling cost, and coolant associated costs. Since there is no coolant involved in this process, there is no coolant disposal cost thereby no damage to the environment. MQL cooling method uses cutting fluid 1000 times lower than conventional cooling method. In this method, there is no coolant collection and coolant disposal; hence, it is an environmentally friendly cooling method. The cryogenic cooling method uses cryogenic coolants, which evaporate easily at the atmosphere condition. Therefore, no chip cleaning cost, no disposal of coolants, and low energy consumption. Machining with textured tools does not require cutting



**FIGURE 4.2** Characteristics of sustainable machining. *Used with permission from Chetan G.S., Rao, P.V., 2015. Application of sustainable techniques in metal cutting for enhanced machinability: a review. Journal of Cleaner Production, 100, 17–34.*

fluids during machining. Hence, it is an environmentally friendly machining approach because of no coolant disposal into the atmosphere (Chetan et al., 2015).

## 4.3 Sustainable machining techniques

### 4.3.1 Dry machining

The meaning of dry machining is conducting machining operations without coolant supply. It absolutely avoids the coolant-associated costs and chip recycling cost. Since there is no coolant involved in dry machining, there is no health risk to the working machinist. Klocke and Eisenblätter (1998) recommended dry machining to improve the machinability of gray cast iron material in turning and milling operations. The benefits of dry machining are shown in Fig. 4.3. However, dry machining of hard-to-cut material results in high cutting temperature resulting in poor machining performance (Behera et al., 2016; Bordin et al., 2017). Further, rapid adhesion tool wear mechanism is observed in dry cutting of aluminum alloy due to high ductility and low melting point of the workpiece material. Therefore, other sustainable machining

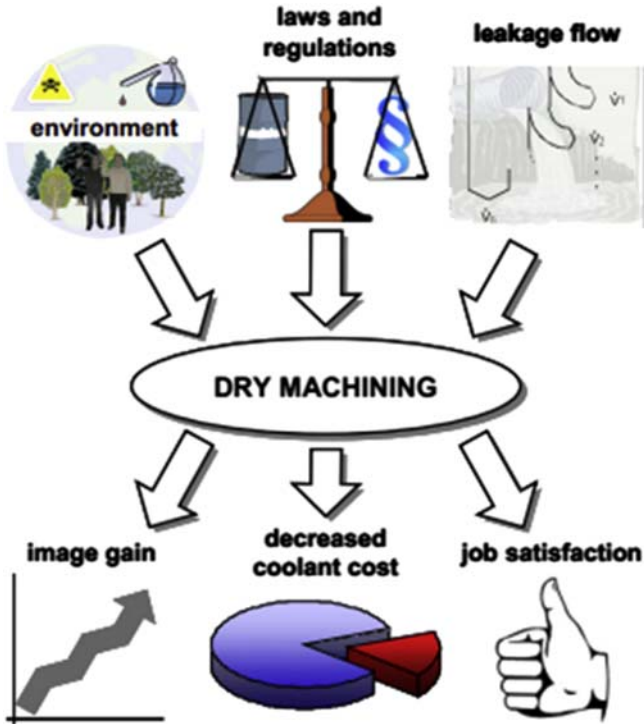


FIGURE 4.3 Benefits of dry machining. *Used with permission from Weinert, K., Inasaki, I., Sutherland, J.W., Wakabayashi, T., 2004. Dry machining and minimum quantity lubrication. CIRP annals, 53(2), 511–537.*

techniques has been adopted to meet the high machining performance of hard-to-cut material.

### 4.3.2 Minimum quantity lubrication machining

Minimum quantity lubrication cooling technique is an eco-friendly machining technique. In MQL machining, small quantity lubrication ( $50\text{--}450\text{ mL h}^{-1}$ ) is supplied along with compressed air, resulting in MQL mist at the machining zone. The coolant cost in the MQL cooling method is 1000 times less than the conventional cooling method. In this method, no coolant disposal to the atmosphere and no coolant disposal cost are involved. The schematic of the MQL setup used in the machining process is shown in Fig. 4.4. MQL mist generation at the cutting zone is shown in Fig. 4.5. In MQL, cutting zone temperature reduction is mainly due to the convective heat transfer mechanism of the compressed air and cutting oil (Ezugwu, 2005). It was proved that the addition of nanoparticles in MQL

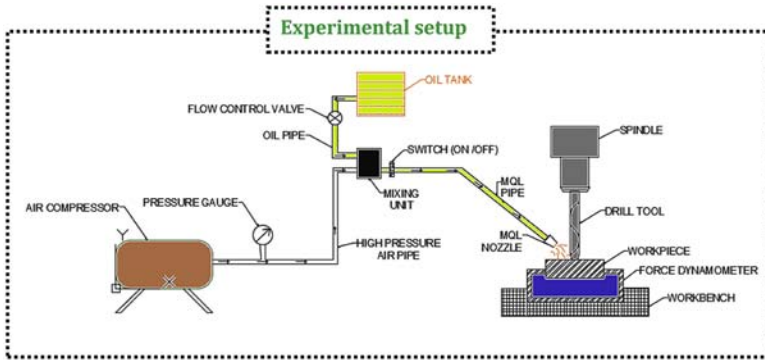


FIGURE 4.4 Schematic of minimum quantity lubrication setup in drilling process. Used with permission from Pal, A., Chatha, S.S., Sidhu, H.S., 2020. Experimental investigation on the performance of MQL drilling of AISI 321 stainless steel using nano-graphene enhanced vegetable-oil-based cutting fluid. *Tribology International*, 151, 106508..

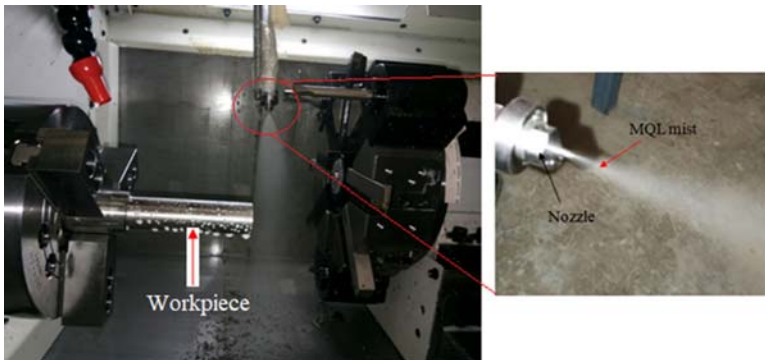


FIGURE 4.5 Minimum quantity lubrication mist at the machining zone in turning operation. Used with permission from Sivaiah, P., & Bodicherla, U., 2020. Effect of surface texture tools and minimum quantity lubrication (MQL) on tool wear and surface roughness in CNC turning of AISI 52100 steel. *Journal of The Institution of Engineers (India): Series C*, 101(1), 85-95.

cooling methods significantly improves the metal cutting process performance (Pal et al., 2020). The mechanism of the nanofluid MQL system in the metal cutting process can be understood by using Fig. 4.6. The drawback of MQL cooling is it fails to control the machining zone temperatures at the industrial cutting conditions (Attanasio et al., 2006; Obikawa et al., 2006). Nevertheless, still, MQL generates coolant mist at the machining surroundings, affecting the operator health (Aoyama et al., 2008).

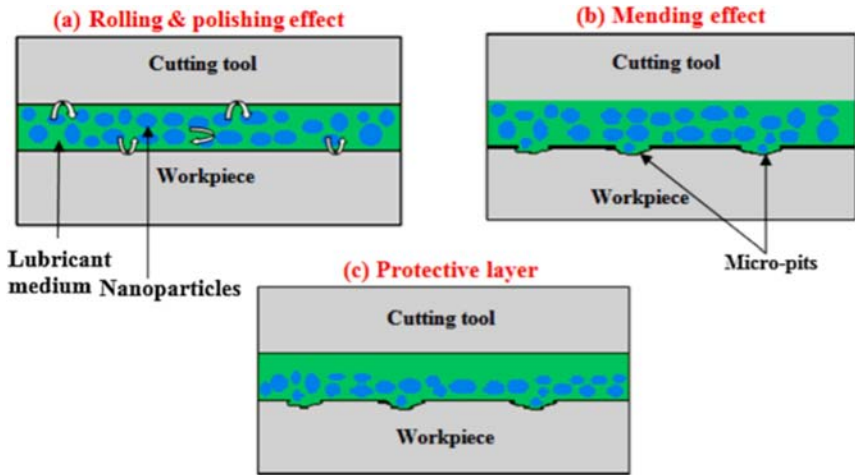


FIGURE 4.6 A schematic of lubrication mechanism by the application of nano-oil between tool–workpiece interfaces. Used with permission from Pal, A., Chatha, S.S., Sidhu, H.S., 2021. Performance evaluation of the minimum quantity lubrication with  $Al_2O_3$ -mixed vegetable-oil-based cutting fluid in drilling of AISI 321 stainless steel. *Journal of Manufacturing Processes*, 66, 238–249.

### 4.3.3 Cryogenic machining

Compared to all techniques, the application of cryogenic fluids at the machining zone is one of the novel sustainable machining techniques to fulfill the stringent new environmental conscious regulations and superior product functional performance (Yildiz and Nalbant, 2008). The commonly used cryogenic fluids are liquid nitrogen ( $LN_2$ ) and liquid carbon dioxide ( $LCO_2$ ) in the metal cutting processes. Since these fluids evaporate quickly after reaching the machining zone, the use of these coolants eliminates the cost incurred in chip cleaning and coolant maintenance. There are four types of cryogenic machining approaches as follows.

1. Cryogenic precooling of the workpiece
2. Indirect cryogenic cooling
3. Cryogenic treatment of tool
4. Cryogenic spray cooling/cryogenic jet cooling

The method of cooling in four cryogenic machining approaches is illustrated in Fig. 4.7. In the cryogenic precooling approach, cryogenic fluid is supplied in an enclosed bath or general flooding way to cool down the workpiece before machining. In the indirect cryogenic cooling approach, cryogenic fluid cools the cutting tool, however, without direct contact between the cryogenic fluid and machining zone. Cryogenic

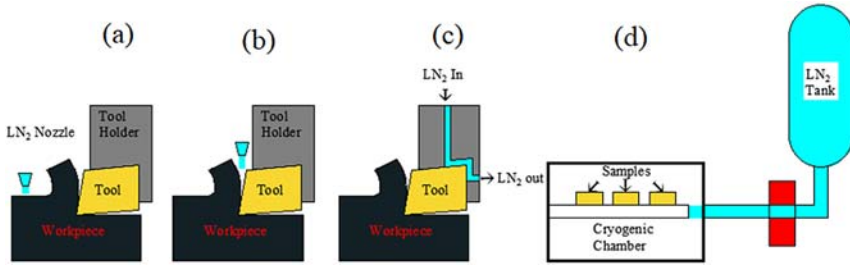


FIGURE 4.7 Different cryogenic cooling approaches (A) precooling, (B) spray cooling, (C) indirect cooling, and (D) cryogenic treatment.

treatment of tools means cooling of cutting tools at a low-temperature process, which is similar to heat-treatment process, cryogenic treatment done at lower temperatures (between  $-148$  and  $-196^{\circ}\text{C}$ ). In the cryogenic jet cooling approach, cryogenic fluids are supplied to the machining zone with help of nozzles having a small diameter.

Sivaiah and Chakradhar carried out extensive work during the turning of 17-4 PH steel material under external cryogenic cooling condition and noticed superior results with cryogenic cooling over dry, wet, and MQL conditions (Sivaiah and Chakradhar, 2017a, 2017b, 2018a, 2018b, 2019). In their work, they have supplied  $\text{LN}_2$  at the cutting zone using a cryogenic machining setup. The schematic view of the cryogenic machining setup is shown in Fig. 4.8. It was reported that majorly  $\text{LN}_2$  serves the three

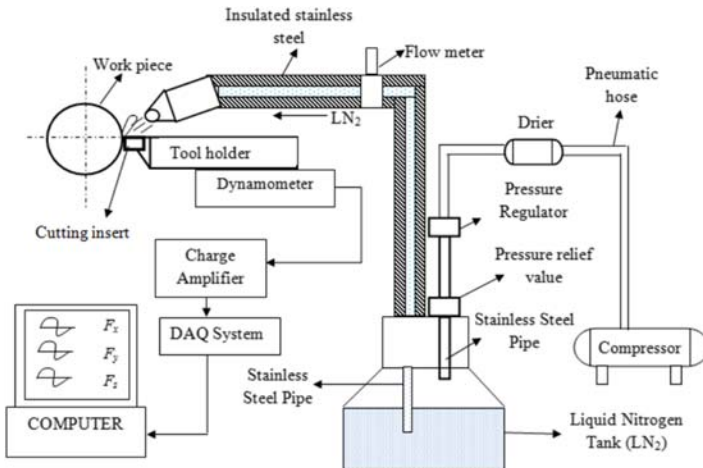


FIGURE 4.8 Schematic of external cryogenic jet machining experimental setup. Used with permission from. Sivaiah, P., Chakradhar, D. 2019. The effectiveness of a novel cryogenic cooling approach on turning performance characteristics during machining of 17-4 PH stainless steel material. *Silicon*, 11(1), 25–38.

mechanisms in external cryogenic cooling at the cutting zone (Hong, 2006). The first one is when  $\text{LN}_2$  is sprayed at the tool–workpiece interface, it reduces the ductility of workpiece material thus improves the chip breakability leads to the control of coefficient of friction between the contact asperities. The second one is when  $\text{LN}_2$  is injected between the cutting zone. The coolant forms a thin hydrodynamic lubrication film, resulting in low friction between the contact asperities. The third one is when  $\text{LN}_2$  is supplied at the cutting zone—it contacts the chip and controls the plastic deformation in the chip, thereby improving the chip breakability.

Recently, Sivaiah and Chakradhar (2020) carried out a review on novel cooling techniques in direct and indirect cryogenic cooling approaches during the turning of various difficult-to-cut materials. It was reported that the position of the  $\text{LN}_2$  nozzle plays an important role in turning process performance. Further, the research gap was explained in the cryogenic turning process. Sivaiah and Chakradhar (2018b) supplied  $\text{LN}_2$  to the rake and flank face of the tool using a modified tool holder as shown in Fig. 4.9A and noticed a substantial increment in the turning process performance over external  $\text{LN}_2$  cooling using one nozzle (Fig. 4.9B). They mentioned that the additional cooling effect with  $\text{LN}_2$  in the modified tool holder contributed to better results.

#### 4.3.4 Surface texturing of tools

Surface texturing of the cutting tool is one of the emerging sustainable machining techniques to machine various difficult-to-cut materials. Unlike cryogenic and MQL cooling, in this technique, there is no need for compulsory supply of coolant at the cutting zone to improve any machining performance. Surface texturing can be done by using many

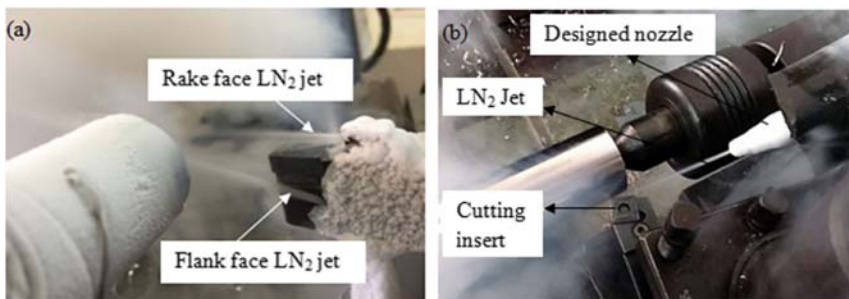


FIGURE 4.9 Machining zone at the (A) with modified tool holder and (B) with external nozzle. Used with permission from Sivaiah, P., Chakradhar, D. 2019. The effectiveness of a novel cryogenic cooling approach and turning performance characteristics during machining of 17-4 PH stainless steel material. *Silicon*, 11(1), 25–38.

conventional and nonconventional machining processes (Arslan et al., 2016). Su et al. (2017) used fiber laser machining technology to develop linear microgrooves on the flank face of the tool and conducted dry turning experiments on Ti6Al4V material. Results indicated that textured tools significantly reduced the friction at the cutting due to low tool-chip contact length when compared with untextured tools, respectively. Duan et al. (2019) developed linear microgrooves on the rake face of the tool and AISI H13 steel was machined with the developed tool. They observed a derivative cutting mechanism with the textured tool as shown in Fig. 4.10.

Likewise, Kawasegi et al. (2019) noticed low friction, cutting force, and low surface roughness with the textured tool during turning of aluminum alloy and nickel-phosphorus (NiP) due to the derivative cutting mechanism. Sivaiah et al. (2020) fabricated linear microgrooves at different angles on the rake side of the tool and investigated the machinability characteristics during turning of AISI 304 material with developed tools under MQL cooling conditions, respectively. Compared with the results of untextured tools, textured tools substantially improved the turning process performance under MQL condition because of coolant storage in the microgrooves. The schematic interpretation of the cutting mechanism in a single pattern textured tool under MQL is shown in Fig. 4.11.

Similarly, hybrid-textured tools were developed with a combination of microgrooves and circular dimple holes over the rake side of the tool. Hybrid textured tools showed greater turning performance over single pattern textured tools and untextured tools under the MQL cooling method due to substantial reduction of cutting zone temperature through convection heat transfer mode and storage of coolant in the microgrooves (Sivaiah, 2019; Sivaiah et al., 2020). Fig. 4.12 depicts the schematic understanding of MQL coolant assistance in a hybrid-textured tool.

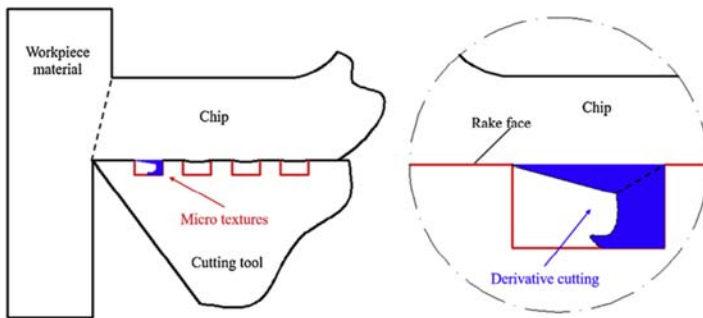


FIGURE 4.10 Schematic of derivative cutting mechanism. Used with permission from Duan, R., Deng, J., Lei, S., Ge, D., Liu, Y., Li, X., 2019. Effect of derivative cutting on machining performance of micro textured tools. *Journal of Manufacturing Processes*, 45, 544–556.

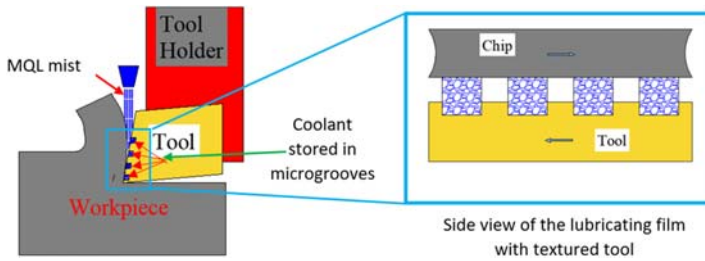


FIGURE 4.11 Schematic interpretations concerning influencing mechanism at the single pattern textured tool-workpiece under minimum quantity lubricant condition.

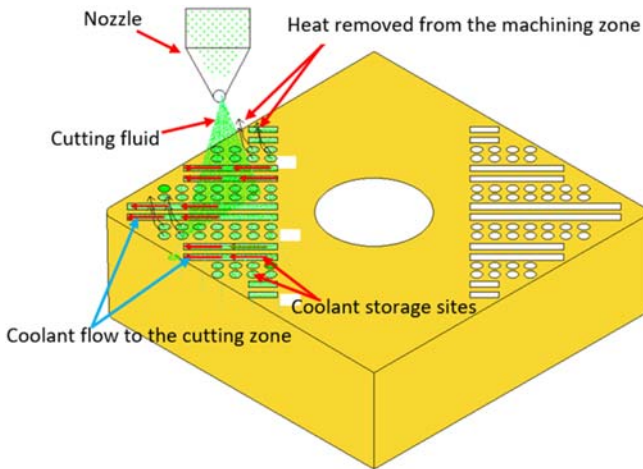


FIGURE 4.12 Schematic interpretation of role of coolant in the hybrid texture tool during cutting operation.

Hao et al. (2018) performed experiments with hybrid textured tools under MQL and dry cutting conditions and compared the turning process performance with untextured and different textured tools during turning of titanium alloy under dry and MQL conditions. They noticed paramount turning performance with hybrid textured tools compared with other tools under considered cutting environments, respectively. They reported that hybrid textured tools facilitate the uniform lubrication film and interfacial pressure of the lubrication film resulting in greater turning process performance. Surface textured tool-assisted machining significantly improves the turning, drilling, grinding, and milling process performance by satisfying the sustainable machining requirement during machining of various difficult-to-cut materials.

## 4.4 Role of sustainable machining techniques in conventional machining processes

### 4.4.1 Cryogenic cooling

Recently, a significant amount of research work has been carried out in different conventional and nonconventional machining processes under external cryogenic cooling and indirect cryogenic cooling as follows.

#### 4.4.1.1 Cryogenic turning operation

Agrawal et al. (2021) supplied the LN<sub>2</sub> at the rake and flank faces of the tool using two external nozzles during CNC turning of titanium alloy at different cutting velocity conditions. Results show that cryogenic cooling significantly improved the turning process performance over wet cooling conditions respectively at all the cutting velocity conditions. They mentioned that the efficient cooling effect of LN<sub>2</sub> contributed to favorable results in the cryogenic cooling conditions. Further, it was reported that cryogenic machining contributed to 27% and 22% reduction of total machining cost and total emissions over wet cooling at the higher cutting velocity conditions, respectively. Gupta et al. (2021) recommended the LN<sub>2</sub> coolant to improve the machinability characteristics of  $\alpha$ - $\beta$  titanium alloy in CNC turning operation when compared to dry and LCO<sub>2</sub> cutting conditions, respectively. They identified that LN<sub>2</sub> contributed to low friction at the cutting zone results in improved turning process performance. Jadhav et al. (2020) applied TOPSIS-based artificial neural networks (ANN-GA) approach to optimize the CNC turning process during machining of Nimonic C-263 alloy under external cryogenic cooling environments. Further, observed outstanding performance with cryo-treated tools under external cryogenic cooling environment due to rise in tool hardness compared to dry cutting conditions. Kara et al. (2020) noticed superior turning process performance in cryo-treated tools because of the refinement of grain size compared to conventional treated tools. Further, ANN was applied to predict the surface roughness and validated with experimental runs. They observed a good correlation between the predicted and experimental results. Jamil et al. (2019) carried out experiments on  $\alpha$ - $\beta$  titanium in CNC turning operation under cryogenic, MQL, and dry environments at different cutting velocity and feed rate conditions. They found that machining cost and tool life is significantly improved with the cryogenic cooling condition.

#### 4.4.1.2 Cryogenic drilling operation

Available literature shows that investigation on the drilling process is extensively carried out only under two different cryogenic cooling approaches, namely, cryogenic jet/spray cooling environment and

cryogenic treatment. [Ahmed and Kumar \(2016\)](#) determined the optimum cutting conditions for multiple objective optimization of the drilling process during making holes in titanium alloy using the TOPSIS method. [Khanna et al. \(2020a,b,c\)](#) observed superior hole quality in external cryogenic jet cooling conditions because of low plastic deformation of the workpiece compared to dry conditions during CNC drilling of CFRP composites. However, results showed that increased Young's modulus and tensile strength of the workpiece under cryogenic condition responsible for high cutting forces over dry condition respectively. In another work, [Khanna et al. \(2020a\)](#) reported that external cryogenic spray cooling conditions result in superior CNC drilling performance characteristics owing to low temperature during CNC drilling of Inconel 718 material compared to dry condition. However, low cutting forces were recorded during measurement in cryogenic conditions due to changes in mechanical properties over the dry conditions. [Giasin \(2018\)](#) performed CNC drilling experiments on GLARE under dry, MQL, and external cryogenic jet cooling conditions, respectively. From observed results, they concluded that cryogenic and MQL techniques are not recommendable to improve the hole quality due to avoidance of expansion in GLARE constituents. [Raj and Karunamoorthy \(2019\)](#) studied the effect of deep cryogenic treatment WC tools on tool wear and surface roughness during drilling of CFRP composite material, and results were compared with untreated WC tools. From the experimental study, it was observed that cryogenically treated tools performed better in reducing the tool wear and surface roughness when compared to untreated WC drills. Further, a 7% increase of microhardness was observed on drill surface of cryogenic treated tools over untreated tools, respectively.

[Arun et al. \(2018\)](#) studied the impact of deep and shallow cryogenic treatment of drill tools during CNC drilling of AISI 304 stainless steel and evaluated the drilling performance in terms of maximum thrust force, average surface roughness, circularity error, and exit burr height. Superior drilling performance was observed with the deep cryogenic treated tool over shallow cryogenic-treated tools. Furthermore, mathematical models were developed to predict all responses, and models were validated with confirmation tests. [Dix et al. \(2014\)](#) developed simulation models for different cryogenic cooling approaches in the drilling process to predict the cutting temperature and cutting forces using DEFORM 3D software. Soon after, simulated results were compared with the experimental results during CNC drilling of normalized 42CrMo4 steel with WC drill and observed a good correlation between them. [Impero et al. \(2018\)](#) investigated the cutting force and torque under cryogenic and wet cooling conditions respectively in CNC drilling of CFRP composite/titanium stacks. They supplied liquid nitrogen using an external nozzle and found a significant reduction in the results under cryogenic cooling

conditions due to the easy removal of the chip resulting in superior chip embrittlement. [Joshi et al. \(2018\)](#) observed low surface roughness and low delamination factor for drilled CFRP holes in cryogenic cooling when compared to dry machining at both cutting speed and feed rate varying conditions. Additionally, simulation studies were carried to predict the delamination factor and predicted findings agreed with the experimental results accurately.

#### **4.4.1.3 Cryogenic milling operation**

[Ravi and Kumar \(2011\)](#) hardened AISI H13 tool steel was machined during milling operation under dry, cryogenic, and conventional cooling conditions at different cutting velocity conditions, respectively. The cryogenic external jet cooling method was used and evaluated the milling process performance in terms of cutting temperature, tool flank wear, surface roughness, and chip morphology. Results of the study indicated that a maximum of 60% reduction in cutting temperature was found with cryogenic cooling over other cutting environments. In another work, [observed a maximum reduction of temperature 48% and cutting force of 50% in cryogenic cooling condition over dry and wet cooling condition during milling of AISI D3 tool steel. This is due to efficient and effective penetration of LN<sub>2</sub> coolant during milling \(\[Ravi and Kumar, 2012\]\(#\)\). \[Mia \\(2017\\)\]\(#\) supplied the cryogenic coolant \(LN<sub>2</sub>\) through the internal hole of the tool during milling of tempered medium carbon steel and observed low surface roughness and low cutting force over dry and wet cooling conditions. In their work, experiments were conducted based on the L27 orthogonal array experimental design and optimum cutting conditions were identified using desirable analysis. Further, mathematical models were developed using response surface methodology \(RSM\). Furthermore, the cooling condition is identified as the most influential factor on milling process performance. In contrast to these results, \[Nalbant and Yildiz \\(2011\\)\]\(#\) observed high cutting force in cryogenic cooling due to a rise in the hardness of the machined workpiece during CNC milling of AISI 304 stainless steel.](#)

[Varghese et al. \(2019\)](#) compared the performance of cryogenically treated tools and untreated tools during milling of Maraging steel under dry conditions. Cryogenically treated tools had enhanced tool life compared to untreated tools due to grain refinement. [Sadik and Isakson \(2017\)](#) investigated the effect of cooling environment on tool life in face milling of Ti–6Al–4V alloy. In their work, LCO<sub>2</sub> was utilized as a cryogenic coolant and emulsion-based coolant was used in the conventional cooling method. It was realistic to achieve 6 times tool life improvement in cryogenic cooling compared to conventional cooling due to the low friction between the tool–workpiece interfaces. Further, low chipping of the cutting edge was noticed in cryogenic cooling. [Anburaj and Kumar](#)

(2021b) applied the LCO<sub>2</sub> and LN<sub>2</sub> using the external cryogenic cooling method and studied its influence on tool wear, chip morphology, and surface integrity while face milling Inconel 625 superalloy. The cryogenic coolants outperformed dry and wet cooling conditions in improving the milling performance. However, better surface quality characteristics were noticed while using LCO<sub>2</sub> over LN<sub>2</sub> cooling, whereas residual stress and microhardness significantly improved with LN<sub>2</sub> cooling over LCO<sub>2</sub> because of favorable tool-chip contact nature. In another work, optimum cutting parameters indicate cryogenic cooling method as eco-friendly method compared to dry and wet cooling cutting conditions during face milling of Inconel 625 (Anburaj and Pradeep Kumar, 2021a). Jebaraj et al. (2021) observed a significant improvement in the end milling process performance in LCO<sub>2</sub> cooling conditions over wet cooling conditions during SKT4 die steel milling due to a significant drop in the cutting temperatures. Shokrani et al. (2016) performed experiments on Ti–6Al–4V during CNC milling operation under cryogenic cooling, dry, and wet cooling conditions, respectively. In their work, cryogenic coolant (LN<sub>2</sub>) is supplied at the cutting zone using an external spray jet cooling method. A significant improvement in the surface integrity characteristics is observed in cryogenic machining condition when compared to other cutting environments. Further, observed reduction of surface defects in the machined surface in cryogenic cooling conditions due to low cutting zone temperature.

Okafor and Jasra (2018) evaluated the performance of the CNC milling process during machining of Inconel 718 material under different cooling strategies like MQL, external cryogenic cooling (LN<sub>2</sub>), and hybrid cooling (MQL + LN<sub>2</sub>) using different coated and uncoated tools. It was noticed high cutting forces in LN<sub>2</sub> cooling were due to the hardening of workpiece material and increased friction at the contact asperities when compared to the other two cooling strategies. Lee et al. (2015) studied the effect of different cutting conditions such as dry, LN<sub>2</sub> cooling, and hybrid cooling approach (combination of LN<sub>2</sub>+ heating of workpiece) on tool life and cutting force during CNC milling of Ti–6Al–4V. High cutting force and high tool wear were seen in LN<sub>2</sub> cooling over hybrid cooling approach. The major tool wear observed in LN<sub>2</sub> cooling was due to chipping of cutting edge, whereas in the hybrid approach, it was due to rubbing action. Sivalingam et al. (2018) carried out experiments on Ti–6Al–4V alloy in the CNC milling process using cryo-treated and untreated tools at different cutting speed conditions, respectively. It was revealed that tool wear, surface roughness, and cutting force were significantly low in cryo-treated tools compared to untreated tools. It was mentioned that low tool wear was responsible for low cutting force and surface roughness in cryo-treated tools. Wang et al. (2016) analyzed the surface roughness and cutting force during CNC milling of aramid fiber composite materials

under cryogenic cooling and dry cutting environments at different cutting speeds and depth of cut conditions, respectively. They found that brittle shearing cutting action caused significant improvement in the milling process. Further, they recommended that high surface quality was restricted up to cutting speed of 5000 RPM in dry cutting, whereas it was more than 5000 RPM in cryogenic cooling conditions. [Huang et al. \(2014\)](#) found good stability in the CNC end milling process with cryogenic cooling during machining of AA7075 compared to dry cutting conditions. It was described that resistance in workpiece deformation and improved chip breakability contributed to low cutting force in the cryogenic cooling method. A significant improvement in machinability characteristics were observed in the CNC milling process during machining of titanium alloy in cryogenic cooling method over conventional cooling ([Shokrani et al., 2016](#)). They stated that positive chemical reactivity between the contact asperities attributed to advantageous results in cryogenic machining. There are other notable efforts by [Kumar and Gururaja \(2020\)](#), [Şirin et al. \(2021\)](#), [Jamil et al. \(2021\)](#), [Wang and Wang \(2021\)](#), and [Albertelli et al. \(2021\)](#) depicting cryogenic milling as sustainable machining process.

#### **4.4.1.4 Cryogenic grinding, boring, and broaching operations**

[Elanchezian and Kumar \(2018\)](#) observed a significant reduction of grinding temperature, cutting force, and surface roughness during grinding of Ti–6Al–4V material in LCO<sub>2</sub> condition over wet cooling condition respectively at different nozzle positions and depth of cut conditions, respectively. They stated that the reduction of breakage of grit particles at low grinding temperatures in cryogenic cooling contributed to favorable results in the grinding process. [Manimaran et al. \(2013a\)](#) studied the effect of LN<sub>2</sub> delivery pressure and depth of cut on the grinding force, surface roughness, and chip morphology in the grinding process while machining of EN31 material, and results were compared with dry and wet cooling conditions, respectively. Results indicated that cryogenic cooling significantly improved the grinding process performance compared to other cutting conditions, respectively. Further, it was reported that the high delivery pressure of LN<sub>2</sub> coolant increased the machining performance greatly over the low delivery pressure of LN<sub>2</sub> coolant. In another work, optimum conditions were determined for the grinding process during machining of AISI 316 material using the multiobjective optimization technique ([Manimaran and Kumar, 2013b](#)). [Zhang et al. \(2018\)](#) hybrid cooling approach (MQL + nano fluids + LN<sub>2</sub>) was used to supply the at the machining zone during grinding of Ti–6 Al–4V alloy and found substantial improvement in the grinding process due to effective cooling and lubrication effect compared to LN<sub>2</sub> and MQL environments, respectively. Further, simulation has been carried out and validated with experimental results. [Zhou et al. \(2014\)](#) noticed high

grinding forces in cryogenic cooling owing to constraint in the plastic deformation of material at low temperature when compared to wet cooling conditions during grinding of SiCp/Al composites. However, a reduction in surface roughness was found with cryogenic cooling due to avoid of softening effect of material in cryogenic cooling. [Khoran et al. \(2020\)](#) improved the performance of the grinding process during grinding of polyether ether ketone (PEEK) material under cryogenic cooling conditions because of grinding wheel shape retainment at low temperatures compared to compact air conditions. Paul et al. carried out extensive research work in the grinding process during machining of different difficult-to-cut materials and concluded that cryogenic cooling was the promising technique to improve the grinding process performance compared to dry and wet cooling conditions, respectively ([Paul and Chattopadhyay, 1995, 2006](#)). The contributions from [Sastry et al. \(2020\)](#) on boring of gunmetal under cryogenic, dry, and wet cooling conditions and [Navukkarasan et al. \(2020\)](#) on broaching of AISI 4340 steel under cryogenic and dry cutting conditions showed superiority of cryogenic environment in the final part making.

## 4.4.2 MQL machining

### 4.4.2.1 MQL turning operation

Various researchers have applied the MQL during the machining of difficult-to-cut materials to the machining zone at different manufacturing processes. [Kuzu et al. \(2015\)](#) conducted an experimental study on compacted graphite iron material under dry and MQL cutting conditions. They have observed that MQL machining substantially reduced the tool wear, surface roughness, and cutting force by 10%, 25%, and 5%, respectively, over the wet machining. They found that the reason for turning performance improvement in MQL was due to the substantial decrease of a coefficient of friction between contact asperities. [Amini et al. \(2015\)](#), in the first stage of their work, determined optimum MQL process parameters in terms of flow rate, nozzle position, and nozzle effective distance from the machining zone for conducting the experiments on AISI 4142 material. They have observed significant improvement in the turning performance (like in tool wear, surface roughness, and cutting force) under the MQL condition due to the control of built-up edge formation at the cutting tool. [Chinchanikar and Choudhury \(2014\)](#) obtained superior tool life in the MQL environment over the dry environment due to the better lubrication effect. [Sohrabpoor et al. \(2015\)](#) carried out the experiments on AISI 4340 material under the MQL, wet, dry, and air coolant conditions and investigated the tool wear and surface roughness, respectively. In their study, they supplied the MQL at both flank, rake

faces of the tool, and they found that MQL machining provided favorable results compared to other conditions due to the substantial decrement of cutting zone temperature. Kouam et al. (2015) achieved advantageous turning performance results in MQL machining while machining of 7075-T6 aluminum alloy over the dry machining. The importance of MQL environment over dry condition was also demonstrated by Sarikaya et al. (2016) in machining of Hayness 25 superalloy, Khan et al. (2009) using vegetable-based coolant during machining of AISI 9310 and Sharma and Sidhu (2014) during turning of AISI D2 steel.

#### **4.4.2.2 MQL drilling operation**

Pal et al. (2021) noticed paramount performance with 1.5% wt. nano-MoS<sub>2</sub> MQL in drilling process while machining of AISI 321 stainless steel compared to dry, wet, and MQL cooling conditions, respectively. It was reported that efficient tribofilm layer formation and reduced friction at the cutting zone with nano MQL coolant were responsible for better results in the nanofluid MQL cooling method. Further, they found a significant reduction in the adhesion of the workpiece to the drill bit in nano-MQL cooling method due to the high viscosity of cutting fluid used. Zhu et al. (2020) noticed maximum temperature at the center of the drill than corners during drilling of AA2024-T351 material under MQL and dry cutting conditions. Further, noticed changes in tool wear mechanism. Pal et al. (2020) concluded that the quantity of nanoparticles in the MQL cooling method significantly affects the drilling performance while machining AISI 321 stainless steel. Overall, outstanding performance with nanofluid MQL method has been observed due to adequate lubrication compared to the pure MQL cooling method.

#### **4.4.2.3 MQL milling operation**

Race et al. (2021) performed milling operation on carbon steel (SA516) material under MQL, dry, and wet cooling conditions, respectively. They found noteworthy improvement in tool wear and surface integrity with MQL condition due to the efficient cooling lubrication at the tool–workpiece interface. Further, they concluded that both dry and MQL have cost-effective and environmental advantages when compared to conventional cooling respectively. An et al. (2020) observed abrasion and chipping as the major tool wear mechanisms in LCO<sub>2</sub> cooling because of aggravated friction between the contact asperities. However, hybrid-cooling approach (MQL + LCO<sub>2</sub>) substantially improved the milling process performance over LCO<sub>2</sub> and dry conditions respectively during side milling of titanium alloy. The ultrasonic-assisted milling with MQL (UAMMQL) cooling promoted uniform fine droplets on the machined surface during milling of TC4 alloy results in significant improvement in the process performance compared to ultrasonic assisted milling and

milling process (Ni and Zhu, 2020). Ul Haq et al. (2021) included nanofluid in the MQL cooling method and applied it at the cutting zone using an external nozzle during milling of Inconel 718 and deliverables were compared with the MQL method. Nanofluid MQL method significantly improved the milling performance compared to the MQL method because of the added lubrication effect of nanofluids in the MQL system. Likewise, Sirin et al. (2021a,b) also found improved performance with the hBN nanofluid MQL cooling method in milling of X-750 nickel alloy compared to the dry condition. Günan et al. (2020) found similar improvement during milling of Hastelloy C276 alloy.

#### **4.4.2.4 MQL grinding operation**

De Souza et al. (2020) auxiliary cleaning system Coupled MQL (CSMQL) cooling method was investigated to evaluate the performance of grinding of AISI 4340 steel, and results were compared with pure MQL and conventional cooling method. From the results, noteworthy improvement in grinding process performance was found compared to other cooling methods. Al<sub>2</sub>O<sub>3</sub>-based nanofluid MQL with sunflower oil as base oil was identified as the best cooling method by Viridi et al. (2020) to improve the grinding performance of Inconel-718 compared to pure MQL cooling method. Formation of strong lubrication film at the grinding zone was responsible for better results in case of the nanofluid MQL cooling method. The chip removal phenomenon in flood cooling and nanofluid MQL is shown in Fig. 4.13.

In Li et al. (2020), MQL cooling was used with graphene-based nanofluid during grinding of TC4 alloy and found superior grinding performance with it due to low friction. In addition, they concluded that the concentration of nanopowder in MQL fluid significantly affects the grinding process performance. In this context, contributions from Adibi et al. (2018) and Jia et al. (2014) should be noted. In these studies, MQL cooling was attempted during grinding of ceramic matrix composites and a hardened steel grade.

### **4.4.3 Machining with surface textured tools**

#### **4.4.3.1 Texture tools in turning operation**

Reddy et al. (2021) carried out experiments on AISI304 material using two different textured tools (linear microgrooves and circular dimples) under MQL conditions. Untextured tools were also used. A substantial reduction of temperature with linear microgrooves compared to other tools was observed due to effective lubrication conditions leading to better turning performance characteristics. Elias et al. (2021) showed that pyramid shape texture on the flank face of the turning tool is the best

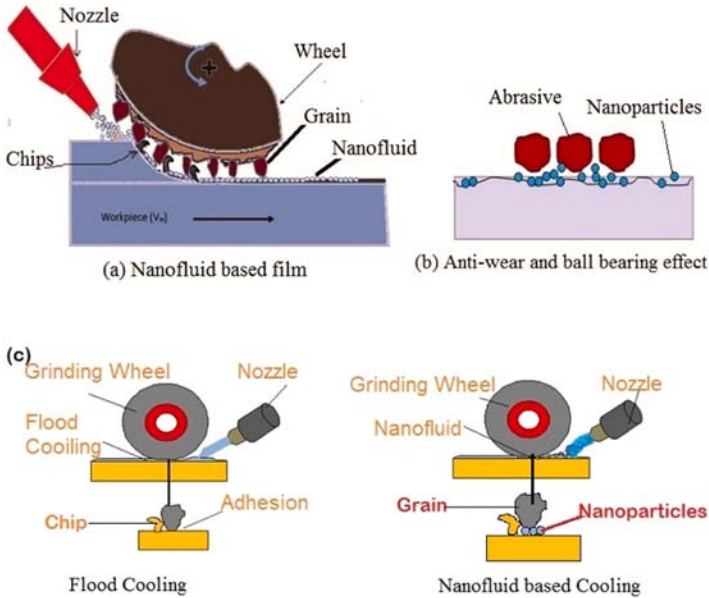


FIGURE 4.13 (A, B) Schematic of nano fluid minimum quantity lubrication (NFMQL) surface grinding showing tribological properties of nanoparticles. (C) Schematic shows the chip removal phenomenon in case of flood and nanofluid grinding. Used with permission from Virdi, R.L., Chatha, S.S., Singh, H., 2020. Machining performance of Inconel-718 alloy under the influence of nanoparticles based minimum quantity lubrication grinding. *Journal of Manufacturing Processes*, 59, 355–365.

choice for Ti alloy micro turning under MQL cooling conditions. They mentioned that coolant storage in the texture design and derivative cutting mechanism is responsible for better results in textured tools. Dinesh et al. (2017) observed similar reasons for improved turning performance of a magnesium alloy. A few research works have been reported on the hybrid textured tools under different cutting environments. Hybrid textured tools significantly improved the turning process performance as compared to single pattern textured tools under different cutting environments (Sharma and Pandey, 2016a,b; Sun et al., 2016).

#### 4.4.3.2 Texture tools in drilling operation

Niketh and Samuel (2018) have made circular dimple microgrooves on the flute and margin side of the drill bits (Fig. 4.14) and performed experiments Ti–6Al–4V under MQL, dry, and wet cooling conditions. Tools having texture design performed better in all the working conditions. Niketh and Samuel (2017) also found less clogging of chip at the cutting zone with the textured drill tool while drilling Ti–6Al–4V. Textured drill tools with designs such as pit holes, linear grooves, and convex micro

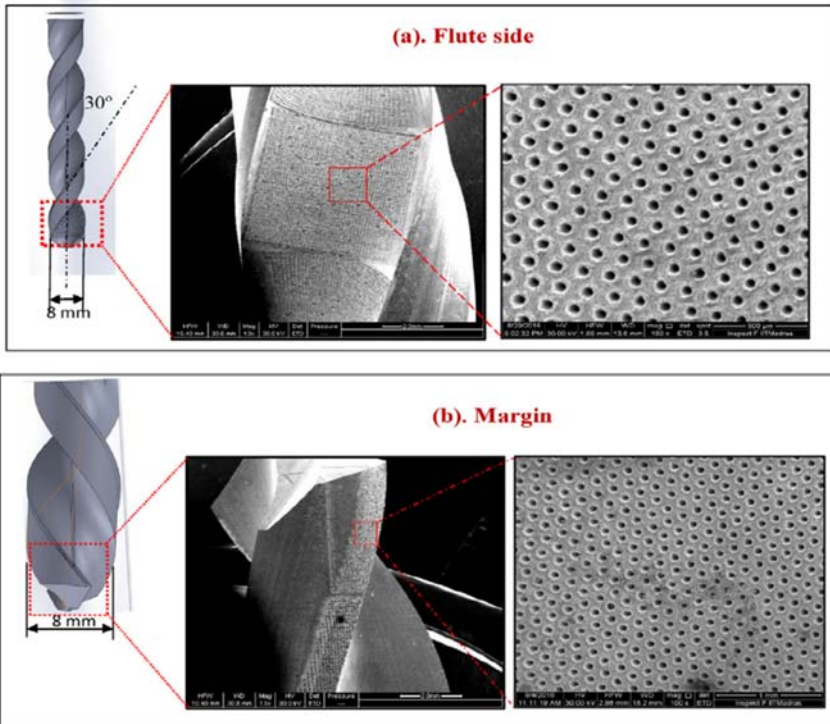


FIGURE 4.14 (A) Microdimples at the flute side and (B) microdimples at the margin side. Used with permission from Niketh, S., Samuel, G.L., 2018. Drilling performance of micro textured tools under dry, wet and MQL condition. *Journal of Manufacturing Processes*, 32, 254–268.

dimples performed better during drilling of Inconel 718 as highlighted by Pang and Wang (2020). An increase of heat transfer area and increase of air convection on tool surfaces are reported as reasons for such improvement. The contributions from Ling et al. (2013) and Guo et al. (2019) on drilling of Ti alloy using textured tools are also worth noting. In this, Guo et al. (2019) used an internal cooling twist drill with surface texture and compared the outputs with untextured drill tool having an internal cooling arrangement. The internal cooling system helped in flushing of chips from the machining zone and control of cutting temperatures.

#### 4.4.3.3 Texture tools in milling and grinding operations

Arumugaprabu et al. (2019) fabricated textured end mill tools with different pitches and depths and investigated their performance during milling of AISI 1045 steel. A significant improvement in the milling

process performance is noticed with textured tools and geometry of texture design. Peña-Parás et al. (2020) and Chen et al. (2019) also highlighted the benefit of milling of AISI 1018 steel and CFRP with textured tools having microgrooves. An improvement in performance has been observed. Chen et al. also showed that textured tools having grooves parallel to cutting edge outperformed other textured tools due to the advantage of chip bending and desirable shear direction. Pratap and Patra (2020) performed microgrinding on BK7 glass with textured tools under MQL condition (Fig. 4.15) and compared results with untextured tools. Textured tools, due to easy chip removal and effective lubrication supply at the cutting zone performed better. Further, they recommended that MQL droplet size should be close to texture geometry.

## 4.5 Sustainable nonconventional machining processes

Nonconventional machining processes are considered as a good alternative for conventional machining processes due to their special characteristics and ability to make intricate shapes, features, and micro-components. However, they generate toxic fumes, contamination, thermal damage to parts, etc., resulting in unclean ecosystem. Electric discharge machining (EDM), electrochemical machining (ECM), abrasive water jet machining (AJM/AJWM), laser beam machining (LBM), and ultrasonic machining (USM) are some important types in this category (Gupta, 2020; Gupta and Gupta, 2019). Table 4.1 shows a summary of contributions to make nonconventional machining processes green and sustainable.

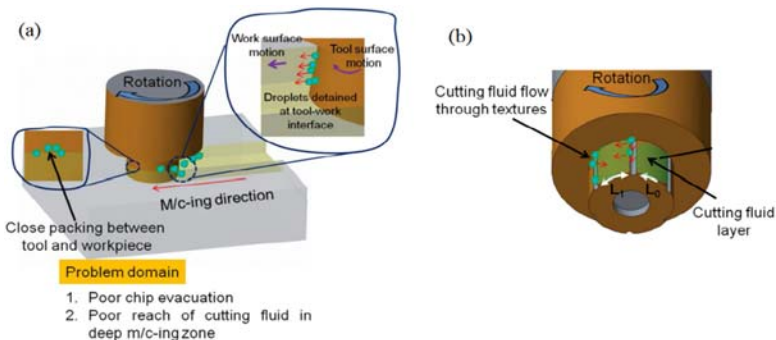


FIGURE 4.15 (A) Untextured tool and (B) textured tool used in microgrinding of BK7 glass. Used with permission from Pratap, A., Patra, K., 2020. Combined effects of tool surface texturing, cutting parameters and minimum quantity lubrication (MQL) pressure on microgrinding of BK7 glass. *Journal of Manufacturing Processes*, 54, 374–392.

TABLE 4.1 Summary of contributions in sustainable nonconventional machining processes.

Process	References	Contributions
EDM	Valaki and Rathod (2016a); Leao (2004); Valaki and Rathod (2016b); Zhang et al. (2013); Ishfaq et al. (2021); Paswan et al. (2020); Kumar and Kumar (2015); Srivastava and Pandey (2012); Srivastava and Pandey (2013); Goyal et al. (2018); Manivannan and Kumar (2018); Manivannan and Kumar (2017); Gill and Singh (2010)	<ul style="list-style-type: none"> <li>• application of vegetable oil-based biodielectric fluids for EDM of M238 HH grade steel</li> <li>• review of various sustainable eco-friendly dielectric fluids</li> <li>• use of waste vegetable oil for EDM of M238 HH grade steel</li> <li>• use of Jatropha curcas oil based bio dielectric fluid</li> <li>• new type of dielectric namely water-in-oil emulsion used in sinking EDM of mild steel</li> <li>• use of graphene-based dielectric for EDM of Ti–6Al–4V</li> <li>• use of steam as dielectric medium during sink EDM of aluminum-based MMC</li> <li>• analysis on cryogenic EDM</li> <li>• machining performance for sustainable EDM process with ultrasonic assisted cryogenically cooled electrode</li> <li>• analysis on cryogenic micro EDM</li> <li>• feasibility of deep cryogenic treatment on machinability of Ti alloy in ED drilling</li> </ul>
ECM	Fang et al. (2014); Ryu (2015); Yang et al. (2011); Sekar et al. (2016)	<ul style="list-style-type: none"> <li>• Pulsed-ECM (PECM) as a superior environmentally friendly variant of ECM</li> <li>• use of anhydrous citric acid as a green electrolyte in PECM (micro) of SS 304</li> <li>• usage of everyday mineral water as an electrolyte in ECM as eco-friendly, non-corrosive, and low cost electrolyte</li> <li>• nano-fluid-based ECM as an alternative to improve the performance and sustainability aspects of ECM</li> </ul>
AJM/ AJWM	Sabarinathan et al. (2020); Pradhan et al. (2021); Gupta et al. (2017); Melentiev and Fang (2018); Karkalos et al. (2021); Yuvaraj and Kumar (2016); Zhang et al. (2021)	<ul style="list-style-type: none"> <li>• recycling and reusing of alumina grinding wheel waste as abrasive grain in AJWM</li> <li>• sustainability assessment of hot-AJM hardstone quartz using hot silicon carbide abrasives</li> <li>• introduction to ice jet machining – a variant of AJWM</li> <li>• advances and challenges in AJM</li> <li>• sustainability assessment of AWJ machining of Ti–6Al–4V using glass beads abrasive particles</li> <li>• cryogenic AJWM of aluminum alloy</li> </ul>

**TABLE 4.1** Summary of contributions in sustainable nonconventional machining processes.—cont'd

Process	References	Contributions
LBM	<a href="#">Apostolos et al. (2012)</a> ; <a href="#">Loktionov et al. (2010)</a> ; <a href="#">Darwish et al. (2016)</a> ; <a href="#">Kruusing (2004)</a> ; <a href="#">Alahmari et al. (2016)</a>	<ul style="list-style-type: none"> <li>• optimizing parameters for sustainable energy consumption during laser drilling of ST37 mild steel</li> <li>• introduction of underwater and water assisted laser processing</li> <li>• improving the energy efficiency of femtosecond laser ablation of refractory metals</li> <li>• fabrication of sustainable burr free micro-channels in underwater (distilled) laser machining of inconel 718</li> </ul>
USM	<a href="#">Sharma and Pandey (2016a,b)</a> ; <a href="#">Airao et al. (2020)</a> ; <a href="#">Khanna et al. (2020a,b,c)</a>	<ul style="list-style-type: none"> <li>• design and analysis of horn toward sustainable USM</li> <li>• highlight advantages of ultrasonic assisted turning toward cost effective and eco-friendly machining</li> <li>• sustainability assessment of ultrasonic assisted turning of Nimonic 90</li> <li>• sustainability assessment of cryogenic ultrasonic assisted turning of inconel 718</li> </ul>

## 4.6 Summary of recent developments, challenges, and future prospects

Machining is an important step in manufacturing, and hence, it should be sustainable in all forms like machining performance, materials behavior, lubricant type, lubrication method, production rate, and machine life expectancy. Cutting fluid is provided to reduce friction and improve surface integrity of the products and to increase production rate by reducing cutting forces. Cutting fluids are predominantly introduced by flooding, and hence, MQL becomes crucial as part of “clean” manufacturing. Several recent developments attempt to address the importance of MQL, and not following it results in wastage of fluid making waste disposal cumbersome. It also has tremendous effect of workers health. Hence, MQL and choice of cutting fluid are of recent focus. Dry machining and cryogenic machining are also studied in recent times. Several examples are provided in the previous sub-sections of the chapter. One important step in sustainable machining is to perform cost analysis considering all the recent developments. [Benedicto et al. \(2017\)](#) did the exercise as given in [Table 4.2](#). The following points should be noted.

TABLE 4.2 Comparison of costs for various lubricating and cooling systems.

Cost category	Raw material cost	Fluid consumption	Equipment costs	Tool cost	Cleaning costs	Disposal costs
Fluid application type						
Cutting fluids	2	5	4	3	5	5
Dry machining	1	1	1	5	1	1
MQL	2	2	3	2	2	2
Solid lubricant	4	3	3	3	3	4
Cryogenic cooling	3	3	5	3	1	1
Gaseous cooling	3	3	4	4	1	1
Sustainable cutting fluids	3	4	4	2	4	3
Nanofluids	5	4	4	3	4	5

1, very low; 2, low; 3, medium; 4, high; 5, very high.

Used with permission from Benedicto, E., Carou, D., Rubio, E.M., 2017. Technical, economic and environmental review of the lubrication/cooling systems used in machining processes. *Procedia Engineering*, 184, 99–116.

- Due to very high fluid consumption, cleaning costs, and disposal costs of cutting fluids, dry machining scores are encouraging in all aspects except tool cost. Tool cost is very high in this case due to wear and tear of cutting tools.
- MQL scores are also encouraging due to low raw material cost, fluid consumption, tool cost, cleaning costs, and disposal costs.
- Use of nanoparticles to enhance the cutting fluid performance is expensive in all aspects.

In MQL machining, type of cutting fluid, whether it is mineral oil or vegetable oil or synthetic ester, is vital due to the requirements of non-toxicity, biodegradability, stability, and lubricity. Vegetable oils and synthetic esters satisfy some of the requirements. Analyses done by [Khan and Dhar \(2006\)](#), [Ginting et al. \(2015\)](#), [Islam \(2013\)](#), [Sani et al. \(2019\)](#), and [Boswell et al. \(2017\)](#) are some case studies and reviews available on this aspect. Despite several advantages and second best in terms of cost benefits ([Table 4.2](#)), four different bottlenecks are observed for MQL advancements. They are incompetent cooling ability, limitations of machining difficult-to-machine workpiece, inefficient chips removal, and lack of studies on optimization of machining parameters ([Nor Hamran et al., 2020](#)). Although this is the case, MQL advancements are in the form of combinations with additives, cooled air/gas, and restructuring methods in the last few years ([Fig. 4.17](#)). The combinations of MQL with solid lubricants and cryogenic and solid lubricants and cold compressed air are the new routes of developments. In the category of restructuring MQL, researchers focus on new nozzle design including number of nozzles ([Zaman and Dhar, 2019](#); [Maruda et al., 2017](#); [Naresh Babu et al., 2017](#)), nozzle adapter, nozzle diameter, and nozzle holder. Several customized MQL system or modified MQL system with a cleaning jet, electrostatic technology, and ultrasonic vibration are also developed ([De Souza et al., 2017, 2020](#); [Ni and Zhu, 2020](#); [Su et al., 2019](#)). External MQL system using an ejector nozzle and conventional nozzle, and internal MQL system using single channel and dual channels are some arrangements available in practice ([Fig. 4.16](#)) ([Nor Hamran et al., 2020](#)).

Dry machining is an ideal situation as it avoids use of cutting fluid and economically acceptable as well ([Table 4.2](#)). It poses no health problems for workers as well. However, issues are tool life should be compromised, difficult to achieve desired product geometry, deterioration of surface properties of machined parts, difficulty in machining materials such as austenitic stainless steel, nickel and titanium alloys, etc., difficulty in evacuating chips in machining operations like key-way milling, drilling of long holes, grooving, etc ([Goindi and Sarkar, 2017](#)). To solve the issues, various approaches are explored by researchers as summarized in [Table 4.3](#). Other than these strategies, MQL machining, and cryogenic

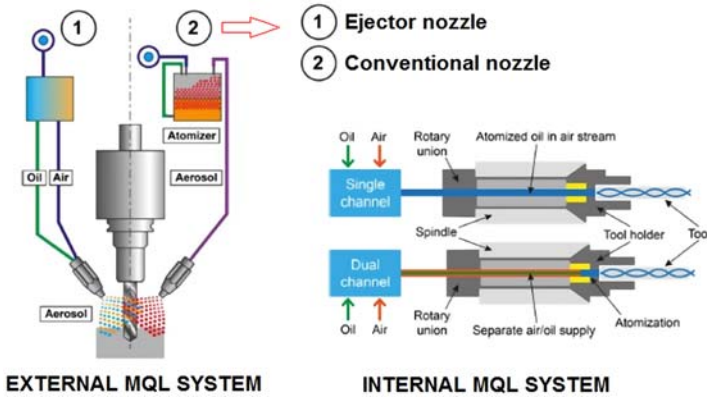


FIGURE 4.16 Description of external and internal minimum quantity lubrication systems. Used with permission from Hamran, N.N., Ghani, J.A., Ramli, R., Haron, C.C., 2020. A review on recent development of minimum quantity lubrication for sustainable machining. *Journal of Cleaner Production*, 268, 122165; Elsevier.

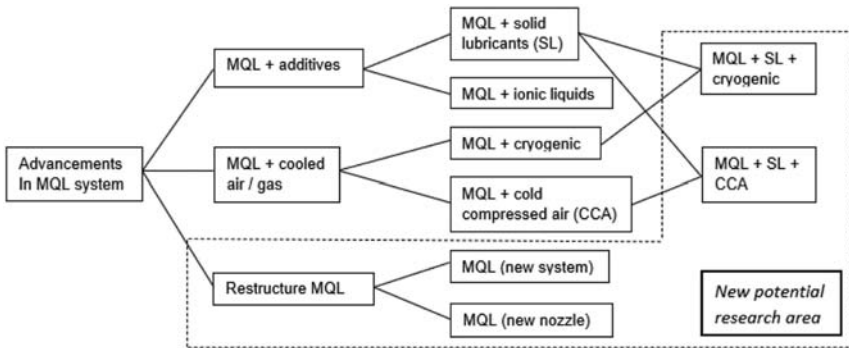


FIGURE 4.17 Minimum quantity lubrication advancements. Used with permission from Hamran, N.N., Ghani, J.A., Ramli, R., Haron, C.C., 2020. A review on recent development of minimum quantity lubrication for sustainable machining. *Journal of Cleaner Production*, 268, 122165; Elsevier.

machining are also adopted to solve problems as discussed in the previous sub-sections.

Another challenging issue in sustainable machining is the use of mineral oil (petroleum based) in the form of flood, mist, or jet. Disposal methods and occupational safety are of great concerns in this case. During disposal, the challenges are biodegradability, compatibility with sustainable disposal methods, and toxic nature. The available disposal methods (chemical, mechanical, electrochemical, and biological) involve high operational cost and complex reactions (Lee et al., 2017), which may not

TABLE 4.3 Approaches for solving problems in dry machining.

Approach	Developments	Recent contributions
Selection of tool materials	Use of carbides of tungsten, titanium, and tantalum; cermets based on titanium carbonitride; ceramics; cubic boron nitride; diamond are observed	Uddin et al. (2021)
Use of tool coating	Coatings made from hard materials such as TiN, TiCN, CrN, CBN, diamond, etc.; use of multilayered nanocoatings and self-lubricated coatings, cubic boron nitride and diamond coatings are observed.	Kumar et al. (2020); Sahoo and Datta (2020); Gomez et al. (2012)
Changes in tool geometry	Use of high rake angles, small wedge angles, and sharp cutting edges in cutting tools	Sadeghifar et al. (2020); Kuo et al. (2021)
Assisted machining	Vibration-assisted machining; laser-assisted and plasma-assisted machining; hybrid cooling-assisted machining	Yang et al. (2020); Gupta et al. (2020); Khan et al. (2020); You et al. (2020)

meet sustainability requirements. Occupational safety of workers against skin injuries, chronic illness, etc. is of prime importance. As an alternative to mineral oils, vegetable oils that can be disposed in a sustainable and eco-friendly manner are focused these days. From existing contributions, it is observed that vegetable oil-based metal working fluids show minimal social, environmental, and economic effects as compared to mineral oil based. Vegetable oil-based fluids are easily broken down into eco-friendly substances that are less toxic and can be disposed in a sustainable fashion. However, they have limitations in terms of oxidation stability, hydrolytic stability, and heat bearing ability due to their chemical structure. Canola oil, a vegetable oil, has excellent biodegradability, low toxicity, excelled lubrication, good viscosity index, affordable and acceptable thermal stability, and seal compatibility as compared to ester-based metal working fluids and mineral oils (Wickramasinghe et al., 2020). Other vegetable oils used for drilling, turning, grinding, and milling operations are coconut oil, food-grade vegetable oil, palm oil, sunflower oil, sesame oil, soyabean oil, rapeseed oil, and Jatropa oil (Wickramasinghe et al., 2020). Fig. 4.18 lists the vegetable oils used in cutting operations (Sankaranarayanan et al., 2021). The market share of

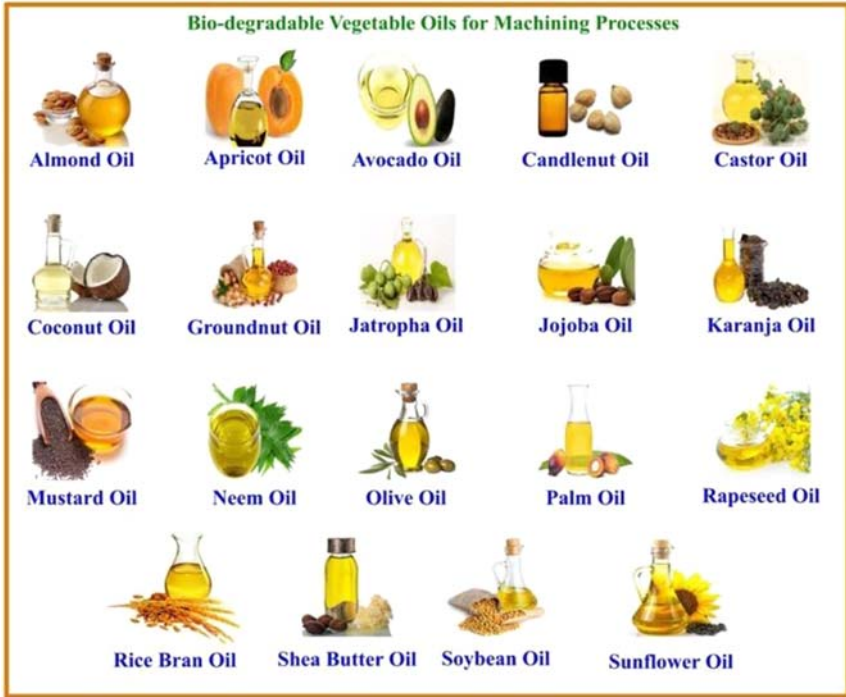


**FIGURE 4.18** Eco-friendly biodegradable vegetable oils for cutting applications. *Used with permission from Sankaranarayanan, R., Hynes, R.J.N., Kumar, S.J. Krolczyk, G.M., 2021. A comprehensive review on research developments of vegetable-oil based cutting fluids for sustainable machining challenges. Journal of Manufacturing Processes, 67, 286–313.*

vegetable oils increased significantly in recent past and predicted to improve in the same fashion in US as presented in Fig. 4.19 (Sankaranarayanan et al., 2021). This indicates effective utilization of vegetable oil-based metal working fluids in machining operations. Although these are expensive, considering the long-term benefits such as eco-friendliness and affordable disposal methods, it is worth investing in such metal working fluids. There are evidences showing better cutting practices when nanoparticles are added to base fluids (vegetable or mineral) in appropriate concentrations (like 0.1 to 1 wt%).

Optimization of machining processes is inevitable, and focus is moved to optimization of sustainable machining processes in the last several years. In this, 3E-based (Ecological, Economical, and Equity) optimization is required. This means the parameters affecting ecological impact, economic impact, and social impact that should be considered for optimization (Alvarez et al., 2016). Recently, a similar strategy for sustainable machining process optimization is also proposed by Salem et al. (2021)

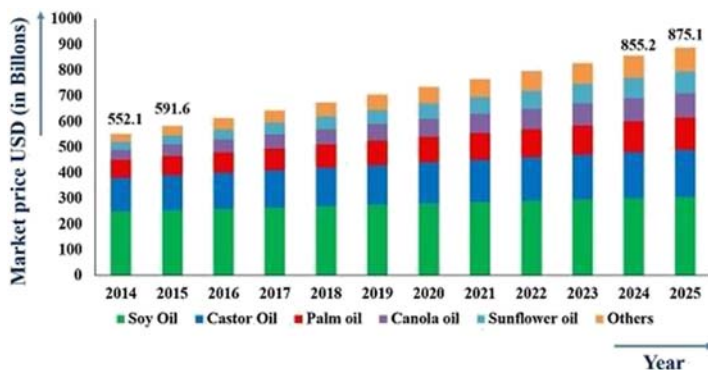


FIGURE 4.19 Market share of vegetable oils. Used with permission from Sankaranarayanan, R., Hynes, R.J.N., Kumar, S.J. & Krolczyk, G.M., 2021. A comprehensive review on research developments of vegetable-oil based cutting fluids for sustainable machining challenges. *Journal of Manufacturing Processes*, 67, 286–313.

(Fig. 4.20). It is clearly pointed out by Jawahir et al. (2020) in their comprehensive review that economic models should be considered while optimizing machining processes and developing such models lack agility. They have also concluded that inaccurate material models and simplified assumptions in numerical modeling of machining are barriers in developing robust modeling approaches. On the other hand, as per Sen et al. (2021), incorporation of thermal analyses with sustainability analysis is an important step in green machining along with advantages of data science.

Considering all the aspects discussed above, the following are proposed as points of concerns and further research should progress in the direction to implement sustainable machining in lab scale and large scale.

- Machining ductile material with dry machining is a difficult task due to the adhesion wear mechanism. Therefore, further studies should focus on identifying the impact of different types of coating tools and tool geometries on machining performance in conventional machining.
- MQL machining of difficult-to-cut material yielded poor performance at severe conditions. MQL mist formation and continuous MQL mist generation at the nozzle are difficult tasks. Further investigation is required on MQL process parameters to understand the effectiveness of the MQL cooling method during machining of difficult-to-cut materials. Special attention is required in optimizing nanoparticles when nanofluid MQL cooling method is used for machining of various difficult-to-cut materials.
- In cryogenic machining, storage/maintain of cryogenic coolant for a long time at the cutting zone using the conventional cutting tool is a

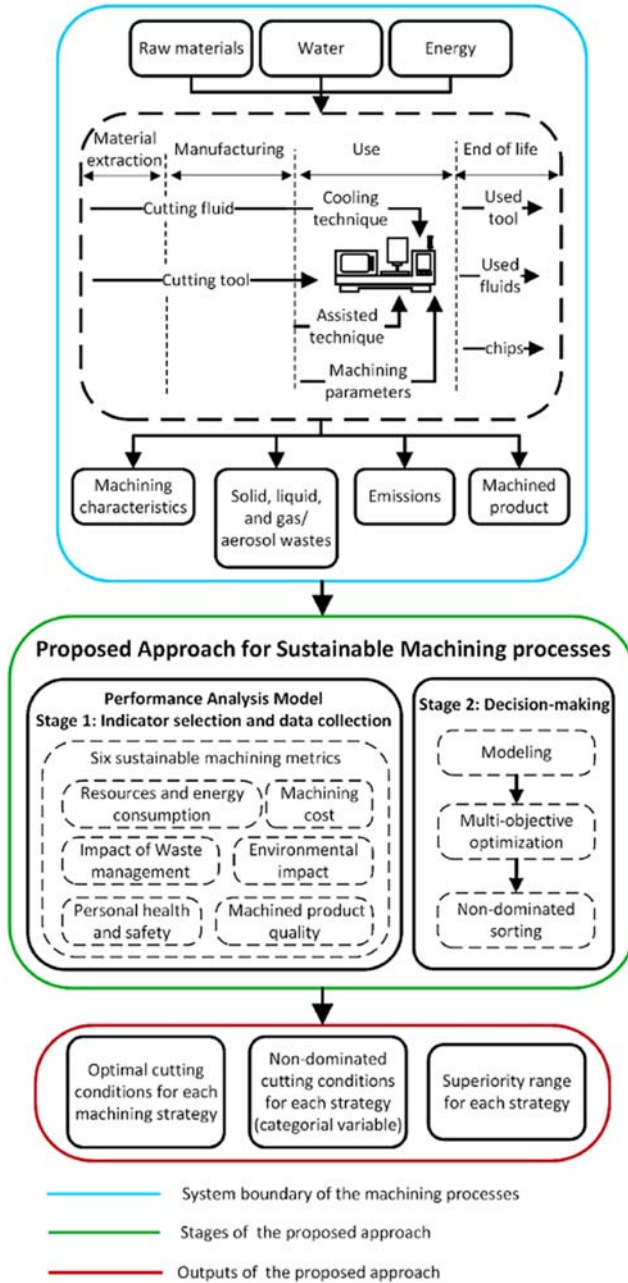


FIGURE 4.20 Strategy for sustainable machining processes optimization. *Used with permission from Salem, A., Hegab, H., Kishawy, H.A., 2021. An integrated approach for sustainable machining processes: assessment, performance analysis, and optimization. Sustainable Production and Consumption, 25, 450–470.*

challenging task. Detailed studies are required to optimize nozzle position parameters such as nozzle angle, nozzle distance from machining zone, and nozzle diameter in the conventional and nonconventional machining. Surface integrity should be given prominence in such investigations.

- The textured tool performance was significantly affected by the texture design and its geometry, position of texture design, and cooling method. However, developing MQL mist size smaller than the geometry of the texture is a challenging job. Therefore, the effect of texture design and texture position can be studied to understand the cutting mechanism under dry, MQL, and cryogenic cooling conditions.
- Development and use of biodegradable cutting fluids for safe and efficient machining leading to sustainable manufacturing

In nonconventional machining processes, the following should be attempted for sustainable and green manufacturing.

- In EDM, utilizing alternate environmentally nonthreatening dielectric fluids such as vegetable oils and bio-diesel, using dry and near-dry EDM, possibilities of using hybrid variants like electric discharge grinding, abrasive-assisted EDM, and magnetic-field-assisted EDM would be highly beneficial.
- In ECM, utilizing PECM, using environmentally friendly electrolytes, and implementing hybrid processes (including ECM combined with EDM, USM, mechanical grinding, etc.) results in sustainable and green machining.
- In LBM, identifying various laser sources, underwater LBM, and optimization of process conditions for maximizing energy efficiency would result in green machining.
- Ice jet machining, an energy efficient variant of AJWM, offers benefits such as good work surface quality, enhanced productivity, no adverse machining effects, no tool repairing and cooling requirements, and toxic fume generation, along with reduced wastes.

## References

- Adibi, H., Esmaeili, H., Rezaei, S.M., 2018. Study on minimum quantity lubrication (MQL) in grinding of carbon fiber-reinforced SiC matrix composites (CMCs). *International Journal of Advanced Manufacturing Technology* 95 (9), 3753–3767.
- Agrawal, C., Wadhwa, J., Pitroda, A., Pruncu, C.I., Sarikaya, M., Khanna, N., 2021. Comprehensive analysis of tool wear, tool life, surface roughness, costing and carbon emissions in turning Ti–6Al–4V titanium alloy: cryogenic versus wet machining. *Tribology International* 153, 106597.

- Ahmed, L.S., Kumar, M.P., 2016. Multiresponse optimization of cryogenic drilling on Ti-6Al-4V alloy using topsis method. *Journal of Mechanical Science and Technology* 30 (4), 1835–1841.
- Airao, J., Khanna, N., Roy, A., Hegab, H., 2020. Comprehensive experimental analysis and sustainability assessment of machining Nimonic 90 using ultrasonic-assisted turning facility. *International Journal of Advanced Manufacturing Technology* 109 (5), 1447–1462.
- Alahmari, A.M., Ahmed, N., Darwish, S., 2016. Laser beam micro-machining under water immersion. *International Journal of Advanced Manufacturing Technology* 83 (9–12), 1671–1681.
- Albertelli, P., Mussi, V., Strano, M., Monno, M., 2021. Experimental investigation of the effects of cryogenic cooling on tool life in Ti6Al4V milling. *International Journal of Advanced Manufacturing Technology* 1–13.
- Alvarez, M.E.P., Bárcena, M.M., González, F.A., 2016. A review of sustainable machining engineering: optimization process through triple bottom line. *Journal of Manufacturing Science and Engineering* 138 (10), 100801-1–100801-100816.
- Amini, S., Khakbaz, H., Barani, A., 2015. Improvement of near-dry machining and its effect on tool wear in turning of AISI 4142. *Materials and Manufacturing Processes* 30 (2), 241–247.
- An, Q., Cai, C., Zou, F., Liang, X., Chen, M., 2020. Tool wear and machined surface characteristics in side milling Ti6Al4V under dry and supercritical CO<sub>2</sub> with MQL conditions. *Tribology International* 151, 106511.
- Anburaj, R., Pradeep Kumar, M., 2021a. Experimental studies on cryogenic CO<sub>2</sub> face milling of Inconel 625 superalloy. *Materials and Manufacturing Processes* 36 (7), 814–826.
- Anburaj, R., Pradeep Kumar, M., 2021b. Influences of cryogenic CO<sub>2</sub> and LN<sub>2</sub> on surface integrity of inconel 625 during face milling. *Materials and Manufacturing Processes* 1–11.
- Aoyama, T., Kakinuma, Y., Yamashita, M., Aoki, M., 2008. Development of a new lean lubrication system for near dry machining process. *CIRP annals* 57 (1), 125–128.
- Apostolos, E., Panagiotis, S., Konstantinos, S., George, C., 2012. Energy efficiency assessment of laser drilling process. *Physics Procedia* 39, 776–783.
- Arslan, A., Masjuki, H.H., Kalam, M.A., Varman, M., Mufti, R.A., Mosarof, M.H., Quazi, M.M., 2016. Surface texture manufacturing techniques and tribological effect of surface texturing on cutting tool performance: a review. *Critical Reviews in Solid State and Materials Sciences* 41 (6), 447–481.
- Arumugaprabu, V., Ko, T.J., Kumaran, S.T., Kurniawan, R., Kwak, Y., Yu, Z., Uthayakumar, M., 2019. Performance of surface-textured end-mill insert on AISI 1045 steel. *Materials and Manufacturing Processes* 34 (1), 18–29.
- Arun, M., Arunkumar, N., Vijayaraj, R., Ramesh, B., 2018. Investigation on the performance of deep and shallow cryogenic treated tungsten carbide drills in austenitic stainless steel. *Measurement* 125, 687–693.
- Attanasio, A., Gelfi, M., Giardini, C., Remino, C.A.R.L.O., 2006. Minimal quantity lubrication in turning: effect on tool wear. *Wear* 260 (3), 333–338.
- Babu, M.N., Manimaran, G., Muthukrishnan, N., 2017. Experimental estimation of minimum quantity lubrication in turning on AISI 410 stainless steel. *International Journal of Machining and Machinability of Materials* 19 (6), 522–537.
- Baradie El, M.A., 1996. Cutting fluids: Part II. Recycling and clean machining. *Journal of Materials Processing Technology* 56 (1–4), 798–806.
- Behera, B.C., Ghosh, S., Rao, P.V., 2016. Wear behavior of PVD TiN coated carbide inserts during machining of Nimonic 90 and Ti6Al4V superalloys under dry and MQL conditions. *Ceramics International* 42 (13), 14873–14885.
- Benedicto, E., Carou, D., Rubio, E.M., 2017. Technical, economic and environmental review of the lubrication/cooling systems used in machining processes. *Procedia Engineering* 184, 99–116.

- Bordin, A., Sartori, S., Bruschi, S., Ghiotti, A., 2017. Experimental investigation on the feasibility of dry and cryogenic machining as sustainable strategies when turning Ti6Al4V produced by Additive Manufacturing. *Journal of Cleaner Production* 142, 4142–4151.
- Boswell, B., Islam, M.N., Davies, I.J., Ginting, Y.R., Ong, A.K., 2017. A review identifying the effectiveness of minimum quantity lubrication (MQL) during conventional machining. *International Journal of Advanced Manufacturing Technology* 92 (1), 321–340.
- Cassin, C., Boothroyd, G., 1965. Lubricating action of cutting fluids. *Journal of Mechanical Engineering Science* 7 (1), 67–81.
- Chen, Y., Guo, X., Zhang, K., Guo, D., Zhou, C., Gai, L., 2019. Study on the surface quality of CFRP machined by micro-textured milling tools. *Journal of Manufacturing Processes* 37, 114–123.
- Chetan, G.S., Rao, P.V., 2015. Application of sustainable techniques in metal cutting for enhanced machinability: a review. *Journal of Cleaner Production* 100, 17–34.
- Chinchanikar, S., Choudhury, S.K., 2014. Hard turning using HiPIMS-coated carbide tools: wear behavior under dry and minimum quantity lubrication (MQL). *Measurement* 55, 536–548.
- Darwish, S., Ahmed, N., Alahmari, A.M., Mufti, N.A., 2016. A comparison of laser beam machining of micro-channels under dry and wet mediums. *International Journal of Advanced Manufacturing Technology* 83 (9–12), 1539–1555.
- De Souza Ruzzi, R., de Mello Belentani, R., de Mello, H.J., Canarim, R.C., D'Addona, D.M., Diniz, A.E., de Aguiar, P.R., Bianchi, E.C., 2017. MQL with water in cylindrical plunge grinding of hardened steels using CBN wheels, with and without wheel cleaning by compressed air. *International Journal of Advanced Manufacturing Technology* 90 (1–4), 329–338.
- De Souza Ruzzi, R., de Andrade, R.B., da Silva, R.B., de Paiva, R.L., Abrão, A.M., de Aguiar, P.R., Bianchi, E.C., 2020. Effects of grinding-wheel cleaning system in application of minimum quantity lubrication technique. *Journal of Manufacturing Processes* 58, 116–128.
- Dinesh, S., Senthilkumar, V., Asokan, P., 2017. Experimental studies on the cryogenic machining of biodegradable ZK60 Mg alloy using micro-textured tools. *Materials and Manufacturing Processes* 32 (9), 979–987.
- Dix, M., Wertheim, R., Schmidt, G., Hochmuth, C., 2014. Modeling of drilling assisted by cryogenic cooling for higher efficiency. *CIRP Annals* 63 (1), 73–76.
- Duan, R., Deng, J., Lei, S., Ge, D., Liu, Y., Li, X., 2019. Effect of derivative cutting on machining performance of micro textured tools. *Journal of Manufacturing Processes* 45, 544–556.
- Elanchezian, J., Pradeep Kumar, M., 2018. Effect of nozzle angle and depth of cut on grinding titanium under cryogenic CO<sub>2</sub>. *Materials and Manufacturing Processes* 33 (13), 1466–1470.
- Elias, J.V., Venkatesh N, P., Lawrence, K.,D., Mathew, J., 2021. Tool texturing for micro-turning applications—an approach using mechanical micro indentation. *Materials and Manufacturing Processes* 36 (1), 84–93.
- Ezugwu, E.O., 2005. Key improvements in the machining of difficult-to-cut aerospace superalloys. *International Journal of Machine Tools and Manufacture* 45 (12–13), 1353–1367.
- Fang, X., Qu, N., Zhang, Y., Xu, Z., Zhu, D., 2014. Effects of pulsating electrolyte flow in electrochemical machining. *Journal of Materials Processing Technology* 214 (1), 36–43.
- Feng, S.C., Hattori, M., 2000. October). Cost and process information modeling for dry machining. In: *Proc. Of the International Workshop for Environment Conscious Manufacturing-ICEM-2000*, pp. 1–8.

- Giasin, K., 2018. The effect of drilling parameters, cooling technology, and fiber orientation on hole perpendicularity error in fiber metal laminates. *International Journal of Advanced Manufacturing Technology* 97 (9), 4081–4099.
- Gill, S.S., Singh, J., 2010. Effect of deep cryogenic treatment on machinability of titanium alloy (Ti-6246) in electric discharge drilling. *Materials and Manufacturing Processes* 25 (6), 378–385.
- Ginting, Y.R., Boswell, B., Biswas, W., Islam, N., 2015. Advancing environmentally conscious machining. *Procedia Cirp* 26, 391–396.
- Goindi, G.S., Sarkar, P., 2017. Dry machining: a step towards sustainable machining—challenges and future directions. *Journal of Cleaner Production* 165, 1557–1571.
- Gomez, H., Durham, D., Xiao, X., Lukitsch, M., Lu, P., Chou, K., Sachdev, A., Kumar, A., 2012. Adhesion analysis and dry machining performance of CVD diamond coatings deposited on surface modified WC–Co turning inserts. *Journal of Materials Processing Technology* 212 (2), 523–533.
- Goyal, R., Sng, S., Kumar, H., 2018. Performance evaluation of cryogenically assisted electric discharge machining (CEDM) process. *Materials and Manufacturing Processes* 33 (4), 433–443.
- Günan, F., Kivak, T., Yıldırım, Ç.V., Sarıkaya, M., 2020. Performance evaluation of MQL with  $Al_2O_3$  mixed nanofluids prepared at different concentrations in milling of Hastelloy C276 alloy. *Journal of Materials Research and Technology* 9 (5), 10386–10400.
- Guo, D., Guo, X., Zhang, K., Chen, Y., Zhou, C., Gai, L., 2019. Improving cutting performance of carbide twist drill combined internal cooling and micro-groove textures in high-speed drilling Ti6Al4V. *International Journal of Advanced Manufacturing Technology* 100 (1–4), 381–389.
- Gupta, K., 2020. A review on green machining techniques. *Procedia Manufacturing* 51, 1730–1736.
- Gupta, K., Gupta, M.K., 2019. Developments in nonconventional machining for sustainable production: a state-of-the-art review. *Proceedings of the Institution of Mechanical Engineers - Part C: Journal of Mechanical Engineering Science* 233 (12), 4213–4232.
- Gupta, K., Avvari, M., Mashamba, A., Mallaiah, M., 2017. Ice jet machining: a sustainable variant of abrasive water jet machining. In: *Sustainable Machining*. Springer, Cham, pp. 67–78.
- Gupta, M.K., Song, Q., Liu, Z., Sarıkaya, M., Jamil, M., Mia, M., Kushvaha, V., Singla, A.K., Li, Z., 2020. Ecological, economical and technological perspectives based sustainability assessment in hybrid-cooling assisted machining of Ti-6Al-4 V alloy. *Sustainable Materials and Technologies* 26, e00218.
- Gupta, M.K., Song, Q., Liu, Z., Sarıkaya, M., Mia, M., Jamil, M., Singla, A.K., Bansal, A., Pimenov, D.Y., Kuntoglu, M., 2021. Tribological performance based machinability investigations in cryogenic cooling assisted turning of  $\alpha$ - $\beta$  titanium alloy. *Tribology International* 160, 107032.
- Hamran, N.N., Ghani, J.A., Ramli, R., Haron, C.C., 2020. A review on recent development of minimum quantity lubrication for sustainable machining. *Journal of Cleaner Production* 268, 122165.
- Hao, X., Chen, X., Xiao, S., Li, L., He, N., 2018. Cutting performance of carbide tools with hybrid texture. *International Journal of Advanced Manufacturing Technology* 97 (9), 3547–3556.
- Hong, S.Y., 2006. Lubrication mechanisms of LN<sub>2</sub> in ecological cryogenic machining. *Machining Science and Technology* 10 (1), 133–155.
- Hong, S.Y., Broomer, M., 2000. Economical and ecological cryogenic machining of AISI 304 austenitic stainless steel. *Clean Products and Processes* 2 (3), 157–166.
- Huang, X., Zhang, X., Mou, H., Zhang, X., Ding, H., 2014. The influence of cryogenic cooling on milling stability. *Journal of Materials Processing Technology* 214 (12), 3169–3178.

- Impero, F., Dix, M., Squillace, A., Prisco, U., Palumbo, B., Tagliaferri, F., 2018. A comparison between wet and cryogenic drilling of CFRP/Ti stacks. *Materials and Manufacturing Processes* 33 (12), 1354–1360.
- Ishfaq, K., Asad, M., Anwar, S., Pruncu, C.I., Saleh, M., Ahmad, S., 2021. A comprehensive analysis of the effect of graphene-based dielectric for sustainable electric discharge machining of Ti-6Al-4V. *Materials* 14 (1), 23.
- Islam, M.N., 2013. Effect of additional factors on dimensional accuracy and surface finish of turned parts. *Machining Science and Technology* 17 (1), 145–162.
- Jadhav, P.S., Mohanty, C.P., Hotta, T.K., Gupta, M., 2020. An optimal approach for improving the machinability of Nimonic C-263 superalloy during cryogenic assisted turning. *Journal of Manufacturing Processes* 58, 693–705.
- Jamil, M., Khan, A.M., He, N., Li, L., Iqbal, A., Mia, M., 2019. Evaluation of machinability and economic performance in cryogenic-assisted hard turning of  $\alpha$ - $\beta$  titanium: a step towards sustainable manufacturing. *Machining Science and Technology* 23 (6), 1022–1046.
- Jamil, M., Zhao, W., He, N., Gupta, M.K., Sarikaya, M., Khan, A.M., Siengchin, S., Pimenov, D.Y., 2021. Sustainable milling of Ti-6Al-4V: a trade-off between energy efficiency, carbon emissions and machining characteristics under MQL and cryogenic environment. *Journal of Cleaner Production* 281, 125374.
- Jawahir, I.S., Schoop, J., Kaynak, Y., Balaji, A.K., Ghosh, R., Lu, T., 2020. Progress toward modeling and optimization of sustainable machining processes. *Journal of Manufacturing Science and Engineering* 142 (11), 110811.
- Jayal, A.D., Badurdeen, F., Dillon Jr., O.W., Jawahir, I.S., 2010. Sustainable manufacturing: modeling and optimization challenges at the product, process and system levels. *CIRP Journal of Manufacturing Science and Technology* 2 (3), 144–152.
- Jebaraj, M., Pradeep Kumar, M., Anburaj, R., 2021. Investigations on milling SKT4 steel by using cryogenic carbon-dioxide. *Materials and Manufacturing Processes* 1–7.
- Jia, D., Li, C., Zhang, D., Zhang, Y., Zhang, X., 2014. Experimental verification of nanoparticle jet minimum quantity lubrication effectiveness in grinding. *Journal of Nanoparticle Research* 16 (12), 1–15.
- Joshi, S., Rawat, K., Balan, A.S.S., 2018. A novel approach to predict the delamination factor for dry and cryogenic drilling of CFRP. *Journal of Materials Processing Technology* 262, 521–531.
- Kara, F., Karabatak, M., Ayyıldız, M., Nas, E., 2020. Effect of machinability, microstructure and hardness of deep cryogenic treatment in hard turning of AISI D2 steel with ceramic cutting. *Journal of Materials Research and Technology* 9 (1), 969–983.
- Karkalos, N.E., Karmiris-Obratański, P., Kudelski, R., Markopoulos, A.P., 2021. Experimental study on the sustainability assessment of AWJ machining of Ti-6Al-4V using glass beads abrasive particles. *Sustainability* 13 (16), 8917.
- Kawasegi, N., Kawashima, T., Morita, N., Nishimura, K., Yamaguchi, M., Takano, N., 2019. Effect of texture shape on machining performance of textured diamond cutting tool. *Precision Engineering* 60, 21–27.
- Khan, M.M.A., Dhar, N.R., 2006. Performance evaluation of minimum quantity lubrication by vegetable oil in terms of cutting force, cutting zone temperature, tool wear, job dimension and surface finish in turning AISI-1060 steel. *Journal of Zhejiang University - Science* 7 (11), 1790–1799.
- Khan, M.M.A., Mithu, M.A.H., Dhar, N.R., 2009. Effects of minimum quantity lubrication on turning AISI 9310 alloy steel using vegetable oil-based cutting fluid. *Journal of Materials Processing Technology* 209 (15–16), 5573–5583.
- Khan, A.M., Jamil, M., Mia, M., He, N., Zhao, W., Gong, L., 2020. Sustainability-based performance evaluation of hybrid nanofluid assisted machining. *Journal of Cleaner Production* 257, 120541.

- Khanna, N., Agrawal, C., Gupta, M.K., Song, Q., 2020a. Tool wear and hole quality evaluation in cryogenic Drilling of Inconel 718 superalloy. *Tribology International* 143, 106084.
- Khanna, N., Shah, P., Agrawal, C., Pusavec, F., Hegab, H., 2020b. Inconel 718 machining performance evaluation using indigenously developed hybrid machining facilities: experimental investigation and sustainability assessment. *International Journal of Advanced Manufacturing Technology* 106 (11), 4987–4999.
- Khanna, N., Pusavec, F., Agrawal, C., Krolczyk, G.M., 2020c. Measurement and evaluation of hole attributes for drilling CFRP composites using an indigenously developed cryogenic machining facility. *Measurement* 154, 107504.
- Khoran, M., Amirabadi, H., Azarhoushang, B., 2020. The effects of cryogenic cooling on the grinding process of polyether ether ketone (PEEK). *Journal of Manufacturing Processes* 56, 1075–1087.
- Klocke, F., Eisenblätter, G., 1998. Dry cutting-State of research. *VDI-Berichte* 1399, 159–188.
- Kouam, J., Songmene, V., Balazinski, M., Hendrick, P., 2015. Effects of minimum quantity lubricating (MQL) conditions on machining of 7075-T6 aluminum alloy. *International Journal of Advanced Manufacturing Technology* 79 (5), 1325–1334.
- Kruusing, A., 2004. Underwater and water-assisted laser processing: Part 2—etching, cutting and rarely used methods. *Optics and Lasers in Engineering* 41 (2), 329–352.
- Kumar, D., Gururaja, S., 2020. Machining damage and surface integrity evaluation during milling of UD-CFRP laminates: dry vs. cryogenic. *Composite Structures* 247, 112504.
- Kumar, S.V., Kumar, M.P., 2015. Machining process parameter and surface integrity in conventional EDM and cryogenic EDM of Al–SiCp MMC. *Journal of Manufacturing Processes* 20, 70–78.
- Kumar, C.S., Majumder, H., Khan, A., Patel, S.K., 2020. Applicability of DLC and WC/C low friction coatings on Al<sub>2</sub>O<sub>3</sub>/TiCN mixed ceramic cutting tools for dry machining of hardened 52100 steel. *Ceramics International* 46 (8), 11889–11897.
- Kuo, C., Liu, J., Chang, T., Ko, S., 2021. The effects of cutting conditions and tool geometry on mechanics, tool wear and machined surface integrity when routing CFRP composites. *Journal of Manufacturing Processes* 64, 113–129.
- Kuzu, A.T., Bijanzad, A., Bakkal, M., 2015. Experimental investigations of machinability in the turning of compacted graphite iron using minimum quantity lubrication. *Machining Science and Technology* 19 (4), 559–576.
- Leão, F.N., Pashby, I.R., 2004. A review on the use of environmentally-friendly dielectric fluids in electrical discharge machining. *Journal of Materials Processing Technology* 149 (1–3), 341–346.
- Lee, I., Bajpai, V., Moon, S., Byun, J., Lee, Y., Park, H.W., 2015. Tool life improvement in cryogenic cooled milling of the preheated Ti–6Al–4V. *International Journal of Advanced Manufacturing Technology* 79 (1–4), 665–673.
- Lee, C.M., Choi, Y.H., Ha, J.H., Woo, W.S., 2017. Eco-friendly technology for recycling of cutting fluids and metal chips: a review. *International Journal of Precision Engineering and Manufacturing-Green Technology* 4 (4), 457–468.
- Li, M., Yu, T., Zhang, R., Yang, L., Ma, Z., Li, B., Zhao, J., 2020. Experimental evaluation of an eco-friendly grinding process combining minimum quantity lubrication and graphene-enhanced plant-oil-based cutting fluid. *Journal of Cleaner Production* 244, 118747.
- Ling, T.D., Liu, P., Xiong, S., Grzina, D., Cao, J., Wang, Q.J., Xia, Z.C., Talwar, R., 2013. Surface texturing of drill bits for adhesion reduction and tool life enhancement. *Tribology Letters* 52 (1), 113–122.
- Loktionov, E.Y., Ovchinnikov, A.V., Protasov, Y.Y., Sitnikov, D.S., 2010. Energy efficiency of femtosecond laser ablation of refractory metals. *Journal of Applied Spectroscopy* 77 (4), 561–568.
- Manimaran, G., Kumar, M.P., 2013a. Investigation of cooling environments in grinding EN 31 steel. *Materials and Manufacturing Processes* 28 (4), 424–429.

- Manimaran, G., Kumar, M.P., 2013b. Multiresponse optimization of grinding AISI 316 stainless steel using grey relational analysis. *Materials and Manufacturing Processes* 28 (4), 418–423.
- Manivannan, R., Kumar, M.P., 2017. Multi-attribute decision-making of cryogenically cooled micro-EDM drilling process parameters using TOPSIS method. *Materials and Manufacturing Processes* 32 (2), 209–215.
- Manivannan, R., Pradeep Kumar, M., 2018. Improving the machining performance characteristics of the  $\mu$ EDM drilling process by the online cryogenic cooling approach. *Materials and Manufacturing Processes* 33 (4), 390–396.
- Marksberry, P.W., 2007. Micro-flood (MF) technology for sustainable manufacturing operations that are coolant less and occupationally friendly. *Journal of Cleaner Production* 15 (10), 958–971.
- Maruda, R.W., Krolczyk, G.M., Michalski, M., Nieslony, P., Wojciechowski, S., 2017. Structural and microhardness changes after turning of the AISI 1045 steel for minimum quantity cooling lubrication. *Journal of Materials Engineering and Performance* 26 (1), 431–438.
- Melentiev, R., Fang, F., 2018. Recent advances and challenges of abrasive jet machining. *CIRP Journal of Manufacturing Science and Technology* 22, 1–20.
- Mia, M., 2017. Multi-response optimization of end milling parameters under through-tool cryogenic cooling condition. *Measurement* 111, 134–145.
- Nalbant, M., Yildiz, Y., 2011. Effect of cryogenic cooling in milling process of AISI 304 stainless steel. *Transactions of Nonferrous Metals Society of China* 21 (1), 72–79.
- Navukkarasan, A., Kumar, M.P., Sastry, C.C., 2020. Experimental investigation of dry and cryogenic broaching of AISI 4340 steel. *Materials and Manufacturing Processes* 35 (14), 1584–1597.
- Ni, C., Zhu, L., 2020. Investigation on machining characteristics of TC4 alloy by simultaneous application of ultrasonic vibration assisted milling (UVAM) and economical-environmental MQL technology. *Journal of Materials Processing Technology* 278, 116518.
- Niketh, S., Samuel, G.L., 2017. Surface texturing for tribology enhancement and its application on drill tool for the sustainable machining of titanium alloy. *Journal of Cleaner Production* 167, 253–270.
- Niketh, S., Samuel, G.L., 2018. Drilling performance of micro textured tools under dry, wet and MQL condition. *Journal of Manufacturing Processes* 32, 254–268.
- Obikawa, T., Kamata, Y., Shinozuka, J., 2006. High-speed grooving with applying MQL. *International Journal of Machine Tools and Manufacture* 46 (14), 1854–1861.
- Okafor, A.C., Jasra, P.M., 2018. Effects of cooling strategies and tool coatings on cutting forces and tooth frequency in high-speed down-milling of Inconel-718 using helical bull-nose solid carbide end mills. *International Journal of Advanced Manufacturing Technology* 97 (5–8), 2301–2318.
- Pal, A., Chatha, S.S., Sidhu, H.S., 2020. Experimental investigation on the performance of MQL drilling of AISI 321 stainless steel using nano-graphene enhanced vegetable-oil-based cutting fluid. *Tribology International* 151, 106508.
- Pal, A., Chatha, S.S., Sidhu, H.S., 2021. Performance evaluation of the minimum quantity lubrication with  $\text{Al}_2\text{O}_3$ -mixed vegetable-oil-based cutting fluid in drilling of AISI 321 stainless steel. *Journal of Manufacturing Processes* 66, 238–249.
- Pang, K., Wang, D., 2020. Study on the performances of the drilling process of nickel-based superalloy Inconel 718 with differently micro-textured drilling tools. *International Journal of Mechanical Sciences* 180, 105658.
- Paswan, K., Pramanik, A., Chattopadhyaya, S., Basak, A.K., 2020. A novel approach towards sustainable electrical discharge machining of metal matrix composites (MMCs). *International Journal of Advanced Manufacturing Technology* 106 (3), 1477–1486.

- Paul, S., Chattopadhyay, A.B., 1995. Effects of cryogenic cooling by liquid nitrogen jet on forces, temperature and surface residual stresses in grinding steels. *Cryogenics* 35 (8), 515–523.
- Paul, S., Chattopadhyay, A.B., 2006. Environmentally conscious machining and grinding with cryogenic cooling. *Machining Science and Technology* 10 (1), 87–131.
- Peña-Parás, L., Maldonado-Cortés, D., Rodríguez-Villalobos, M., Romero-Cantú, A.G., Montemayor, O.E., 2020. Enhancing tool life, and reducing power consumption and surface roughness in milling processes by nanolubricants and laser surface texturing. *Journal of Cleaner Production* 253, 119836.
- Pradhan, S., Das, S.R., Dhupal, D., 2021. Performance evaluation of recently developed new process HAJM during machining hardstone quartz using hot silicon carbide abrasives: an experimental investigation and sustainability assessment. *Silicon* 13 (9), 2895–2919.
- Pratap, A., Patra, K., 2020. Combined effects of tool surface texturing, cutting parameters and minimum quantity lubrication (MQL) pressure on micro-grinding of BK7 glass. *Journal of Manufacturing Processes* 54, 374–392.
- Pusavec, F., Deshpande, A., Yang, S., M'Saoubi, R., Kopac, J., Dillon Jr., O.W., Jawahir, I.S., 2014. Sustainable machining of high temperature Nickel alloy–Inconel 718: part 1–predictive performance models. *Journal of Cleaner Production* 81, 255–269.
- Race, A., Zwierzak, I., Secker, J., Walsh, J., Carrell, J., Slatter, T., Maurotto, A., 2021. Environmentally sustainable cooling strategies in milling of SA516: effects on surface integrity of dry, flood and MQL machining. *Journal of Cleaner Production* 288, 125580.
- Raj, D.S., Karunamoorthy, L., 2019. Performance of cryogenically treated WC drill using tool wear measurements on the cutting edge and hole surface topography when drilling CFRP. *International Journal of Refractory Metals and Hard Materials* 78, 32–44.
- Rao, R.V., 2011. *Advanced Modeling and Optimization of Manufacturing Processes: International Research and Development*. Springer, London, pp. 339–357.
- Ravi, S., Kumar, M.P., 2011. Experimental investigations on cryogenic cooling by liquid nitrogen in the end milling of hardened steel. *Cryogenics* 51 (9), 509–515.
- Ravi, S., Kumar, M.P., 2012. Experimental investigation of cryogenic cooling in milling of AISI D3 tool steel. *Materials and Manufacturing Processes* 27 (10), 1017–1021.
- Reddy, V.C., Venkaiah, T., Nishkala, T., Yadav, G.M.P., 2021. Effect of textured tools in turning operation: a comparison with conventional tools. *Transactions of the Indian National Academy of Engineering* 1–12.
- Ryu, S.H., 2015. Eco-friendly ECM in citric acid electrolyte with microwire and microfoil electrodes. *International Journal of Precision Engineering and Manufacturing* 16 (2), 233–239.
- Sabarinathan, P., Annamalai, V.E., Rajkumar, K., 2020. Sustainable application of grinding wheel waste as abrasive for abrasive water jet machining process. *Journal of Cleaner Production* 261, 121225.
- Sadeghifar, M., Javidikia, M., Songmene, V., Jahazi, M., 2020. Finite element simulation-based predictive regression modeling and optimum solution for grain size in machining of Ti6Al4V alloy: influence of tool geometry and cutting conditions. *Simulation Modelling Practice and Theory* 104, 102141.
- Sadik, M.I., Isakson, S., 2017. The role of PVD coating and coolant nature in wear development and tool performance in cryogenic and wet milling of Ti-6Al-4V. *Wear* 386, 204–210.
- Sahoo, S.P., Datta, S., 2020. Dry machining performance of AA7075-T6 alloy using uncoated carbide and MT-CVD TiCN-Al<sub>2</sub>O<sub>3</sub>-coated carbide inserts. *Arabian Journal for Science and Engineering* 45 (11), 9777–9791.
- Salem, A., Hegab, H., Kishawy, H.A., 2021. An integrated approach for sustainable machining processes: assessment, performance analysis, and optimization. *Sustainable Production and Consumption* 25, 450–470.

- Sani, A.S.A., Abd Rahim, E., Sharif, S., Sasahara, H., 2019. Machining performance of vegetable oil with phosphonium-and ammonium-based ionic liquids via MQL technique. *Journal of Cleaner Production* 209, 947–964.
- Sankaranarayanan, R., Hynes, R.J.N., Kumar, S.J., Krolczyk, G.M., 2021. A comprehensive review on research developments of vegetable-oil based cutting fluids for sustainable machining challenges. *Journal of Manufacturing Processes* 67, 286–313.
- Sarikaya, M., Yılmaz, V., Güllü, A., 2016. Analysis of cutting parameters and cooling/lubrication methods for sustainable machining in turning of Haynes 25 superalloy. *Journal of Cleaner Production* 133, 172–181.
- Sastry, C.C., Gokulakrishnan, K., Hariharan, P., Kumar, M.P., Boopathy, S.R., 2020. Investigation of boring on gunmetal in dry, wet and cryogenic conditions. *Journal of the Brazilian Society of Mechanical Sciences and Engineering* 42 (1), 1–24.
- Sekar, T., Arularasu, M., Sathiyamoorthy, V., 2016. Investigations on the effects of Nano-fluid in ECM of die steel. *Measurement* 83, 38–43.
- Sen, B., Mia, M., Krolczyk, G.M., Mandal, U.K., Mondal, S.P., 2021. Eco-friendly cutting fluids in minimum quantity lubrication assisted machining: a review on the perception of sustainable manufacturing. *International Journal of Precision Engineering and Manufacturing-Green Technology* 8 (1), 249–280.
- Sharma, V., Pandey, P.M., 2016a. Comparative study of turning of 4340 hardened steel with hybrid textured self-lubricating cutting inserts. *Materials and Manufacturing Processes* 31 (14), 1904–1916.
- Sharma, V., Pandey, P.M., 2016b. Recent advances in ultrasonic assisted turning: a step towards sustainability. *Cogent Engineering* 3 (1), 1222776.
- Sharma, J., Sidhu, B.S., 2014. Investigation of effects of dry and near dry machining on AISI D2 steel using vegetable oil. *Journal of Cleaner Production* 66, 619–623.
- Shaw, M.C., Pigott, J.D., Richardson, L.P., 1951. Effect of cutting fluid upon chip–tool interface temperature. *Transactions of the American Society of Mechanical Engineers* 71 (2), 45–56.
- Shokrani, A., Dhokia, V., Newman, S.T., 2012. Environmentally conscious machining of difficult-to-machine materials with regard to cutting fluids. *International Journal of Machine Tools and Manufacture* 57, 83–101.
- Shokrani, A., Dhokia, V., Newman, S.T., 2016. Investigation of the effects of cryogenic machining on surface integrity in CNC end milling of Ti–6Al–4V titanium alloy. *Journal of Manufacturing Processes* 21, 172–179.
- Sirin, S., Sarikaya, M., Yildirim, C.V., Kivak, T., 2021a. Machinability performance of nickel alloy X-750 with SiAlON ceramic cutting tool under dry, MQL and hBN mixed nanofluid-MQL. *Tribology International* 153, 106673.
- Sirin, S., Yildirim, C.V., Kivak, T., Sarikaya, M., 2021b. Performance of cryogenically treated carbide inserts under sustainable cryo-lubrication assisted milling of Inconel X750 alloy. *Sustainable Materials and Technologies* 29, e00314.
- Sivaiah, P., 2019. Evaluation of hybrid textured tool performance under minimum quantity lubrication while turning of AISI 304 steel. *Journal of the Brazilian Society of Mechanical Sciences and Engineering* 41 (12), 1–8.
- Sivaiah, P., Chakradhar, D., 2017a. Influence of cryogenic coolant on turning performance characteristics: a comparison with wet machining. *Materials and Manufacturing Processes* 32 (13), 1475–1485.
- Sivaiah, P., Chakradhar, D., 2017b. Machinability studies on 17-4 PH stainless steel under cryogenic cooling environment. *Materials and Manufacturing Processes* 32 (15), 1775–1788.
- Sivaiah, P., Chakradhar, D., 2018a. Comparative evaluations of machining performance during turning of 17-4 PH stainless steel under cryogenic and wet machining conditions. *Machining Science and Technology* 22 (1), 147–162.

- Sivaiah, P., Chakradhar, D., 2018b. Effect of cryogenic coolant on turning performance characteristics during machining of 17-4 PH stainless steel: a comparison with MQL, wet, dry machining. *CIRP Journal of Manufacturing Science and Technology* 21, 86–96.
- Sivaiah, P., Chakradhar, D., 2019. The effectiveness of a novel cryogenic cooling approach on turning performance characteristics during machining of 17-4 PH stainless steel material. *Silicon* 11 (1), 25–38.
- Sivaiah, P., Chakradhar, D., 2020. Identifying the effectiveness of manner of cryogenic coolant supply in different cryogenic cooling techniques in turning process—a review. *Machining Science and Technology* 24 (6), 948–999.
- Sivaiah, P., Ajay Kumar G, V., Singh, M.M., Kumar, H., 2020. Effect of novel hybrid texture tool on turning process performance in MQL machining of Inconel 718 superalloy. *Materials and Manufacturing Processes* 35 (1), 61–71.
- Sivalingam, V., Sun, J., Yang, B., Liu, K., Raju, R., 2018. Machining performance and tool wear analysis on cryogenic treated insert during end milling of Ti-6Al-4V alloy. *Journal of Manufacturing Processes* 36, 188–196.
- Sohrabpoor, H., Khanghah, S.P., Teimouri, R., 2015. Investigation of lubricant condition and machining parameters while turning of AISI 4340. *International Journal of Advanced Manufacturing Technology* 76 (9–12), 2099–2116.
- Srivastava, V., Pandey, P.M., 2012. Effect of process parameters on the performance of EDM process with ultrasonic assisted cryogenically cooled electrode. *Journal of Manufacturing Processes* 14 (3), 393–402.
- Srivastava, V., Pandey, P.M., 2013. Study of ultrasonic assisted cryogenically cooled EDM process using sintered (Cu–TiC) tooltip. *Journal of Manufacturing Processes* 15 (1), 158–166.
- Su, Y., Li, Z., Li, L., Wang, J., Gao, H., Wang, G., 2017. Cutting performance of micro-textured polycrystalline diamond tool in dry cutting. *Journal of Manufacturing Processes* 27, 1–7.
- Su, Y., Lu, Q., Yu, T., Liu, Z., Zhang, C., 2019. Machining and environmental effects of electrostatic atomization lubrication in milling operation. *International Journal of Advanced Manufacturing Technology* 104 (5), 2773–2782.
- Sun, J., Zhou, Y., Deng, J., Zhao, J., 2016. Effect of hybrid texture combining micro-pits and micro-grooves on cutting performance of WC/Co-based tools. *International Journal of Advanced Manufacturing Technology* 86 (9), 3383–3394.
- Uddin, G.M., Joyia, F.M., Ghufuran, M., Khan, S.A., Raza, M.A., Faisal, M., Arafat, S.M., Zubair, S.W.H., Jawad, M., Zafar, M.Q., Zeid, I., 2021. Comparative performance analysis of cemented carbide, TiN, TiAlN, and PCD coated inserts in dry machining of Al 2024 alloy. *International Journal of Advanced Manufacturing Technology* 112 (5), 1461–1481.
- ul Haq, M.A., Hussain, S., Ali, M.A., Farooq, M.U., Mufti, N.A., Pruncu, C.I., Wasim, A., 2021. Evaluating the effects of nano-fluids based MQL milling of IN718 associated to sustainable productions. *Journal of Cleaner Production* 310, 127463.
- Ulutan, D., Ozel, T., 2011. Machining induced surface integrity in titanium and nickel alloys: a review. *International Journal of Machine Tools and Manufacture* 51 (3), 250–280.
- Valaki, J.B., Rathod, P.P., 2016a. Assessment of operational feasibility of waste vegetable oil based bio-dielectric fluid for sustainable electric discharge machining (EDM). *International Journal of Advanced Manufacturing Technology* 87 (5), 1509–1518.
- Valaki, J.B., Rathod, P.P., 2016b. Investigating feasibility through performance analysis of green dielectrics for sustainable electric discharge machining. *Materials and Manufacturing Processes* 31 (4), 541–549.
- Varghese, V., Ramesh, M.R., Chakradhar, D., 2019. Influence of deep cryogenic treatment on performance of cemented carbide (WC-Co) inserts during dry end milling of maraging steel. *Journal of Manufacturing Processes* 37, 242–250.

- Virdi, R.L., Chatha, S.S., Singh, H., 2020. Machining performance of Inconel-718 alloy under the influence of nanoparticles based minimum quantity lubrication grinding. *Journal of Manufacturing Processes* 59, 355–365.
- Wang, F., Wang, Y., 2021. Comparison of cryogenic cooling strategy effects on machinability of milling nickel-based alloy. *Journal of Manufacturing Processes* 66, 623–635.
- Weinert, K., Inasaki, I., Sutherland, J.W., Wakabayashi, T., 2004. Dry machining and minimum quantity lubrication. *CIRP annals* 53 (2), 511–537.
- Wickramasinghe, K.C., Sasahara, H., Abd Rahim, E., Perera, G.I.P., 2020. Green Metalworking Fluids for sustainable machining applications: a review. *Journal of Cleaner Production* 257, 120552.
- Yang, Y., Natsu, W., Zhao, W., 2011. Realization of eco-friendly electrochemical micromachining using mineral water as an electrolyte. *Precision Engineering* 35 (2), 204–213.
- Yang, Z., Zhu, L., Zhang, G., Ni, C., Lin, B., 2020. Review of ultrasonic vibration-assisted machining in advanced materials. *International Journal of Machine Tools and Manufacture* 103594.
- Yildiz, Y., Nalbant, M., 2008. A review of cryogenic cooling in machining processes. *International Journal of Machine Tools and Manufacture* 48 (9), 947–964.
- You, K., Yan, G., Luo, X., Gilchrist, M.D., Fang, F., 2020. Advances in laser assisted machining of hard and brittle materials. *Journal of Manufacturing Processes* 58, 677–692.
- Yuvaraj, N., Kumar, M.P., 2016. Cutting of aluminium alloy with abrasive water jet and cryogenic assisted abrasive water jet: a comparative study of the surface integrity approach. *Wear* 362, 18–32.
- Zaman, P.B., Dhar, N.R., 2019. Design and evaluation of an embedded double jet nozzle for MQL delivery intending machinability improvement in turning operation. *Journal of Manufacturing Processes* 44, 179–196.
- Zhang, Y., Liu, Y., Ji, R., Cai, B., Shen, Y., 2013. Sinking EDM in water-in-oil emulsion. *International Journal of Advanced Manufacturing Technology* 65 (5–8), 705–716.
- Zhang, J., Li, C., Zhang, Y., Yang, M., Jia, D., Hou, Y., Li, R., 2018. Temperature field model and experimental verification on cryogenic air nanofluid minimum quantity lubrication grinding. *International Journal of Advanced Manufacturing Technology* 97 (1–4), 209–228.
- Zhang, G., Sun, Y., Gao, H., Liu, X., Zuo, D., 2021. PDMS material embrittlement and its effect on machinability characteristics by cryogenic abrasive air-jet machining. *Journal of Manufacturing Processes* 67, 116–127.
- Zhou, L., Huang, S., Yu, X., 2014. Machining characteristics in cryogenic grinding of SiCp/Al composites. *Acta Metallurgica Sinica* 27 (5), 869–874.
- Zhu, Z., He, B., Chen, J., 2020. Evaluation of tool temperature distribution in MQL drilling of aluminum 2024-T351. *Journal of Manufacturing Processes* 56, 757–765.

## Further reading

- Potta, S., 2019. Effect of cryogenic coolant on turning performance: a comparative study. *SN Applied Sciences* 1 (1), 1–9.
- Sivaiah, P., Bodicherla, U., 2020. Effect of surface texture tools and minimum quantity lubrication (MQL) on tool wear and surface roughness in CNC turning of AISI 52100 steel. *Journal of the Institution of Engineers: Series C* 101 (1), 85–95.
- Ray, A., 2018. Design and performance analysis of ultrasonic horn with a longitudinally changing rectangular cross section for USM using finite element analysis. *Journal of the Brazilian Society of Mechanical Sciences and Engineering* 40 (7), 1–11.
- Sivaiah, P., Revantha Kumar, M., Bala Subramanyam, S., Prasad, K.L.V., 2021. A comparative study on different textured and untextured tools performance in turning process. *Materials and Manufacturing Processes* 36 (8), 926–935.

- Valaki, J.B., Rathod, P.P., Sankhvara, C.D., 2016. Investigations on technical feasibility of *Jatropha curcas* oil based bio dielectric fluid for sustainable electric discharge machining (EDM). *Journal of Manufacturing Processes* 22, 151–160.
- Wang, F., Wang, Y., Hou, B., Zhang, J., Li, Y., 2016. Effect of cryogenic conditions on the milling performance of aramid fiber. *International Journal of Advanced Manufacturing Technology* 83 (1–4), 429–439.

# Materials development for sustainable manufacturing

*R.J. Immanuel<sup>1</sup>, S.K. Panigrahi<sup>2</sup>, and James C. Malas<sup>3</sup>*

<sup>1</sup>Department of Mechanical Engineering, Indian Institute of Technology Bhilai, Sejbahar, Chhattisgarh, India; <sup>2</sup>Department of Mechanical Engineering, Indian Institute of Technology Madras, Chennai, Tamil Nadu, India; <sup>3</sup>Materials and Manufacturing Directorate, Air Force Research Laboratory, Dayton, OH, United States

## 5.1 Introduction

Sustainability is a nature-driven phenomenon meant to endure the living capability in earth. The natural process of sustainability is a simple use-recycle-reuse phenomenon as presented in Fig. 5.1. The concept and definition of sustainability are changed with the large intervention of human into this process. Usage of natural resources beyond the nature's ability to reproduce the used resource is the main reason for decline of nature-driven sustainability.

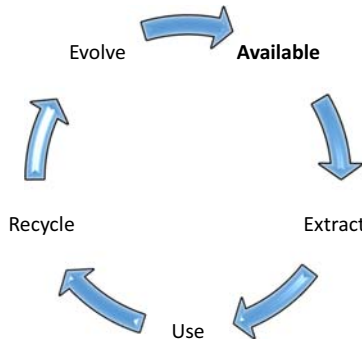


FIGURE 5.1 Sustainability cycle.

This has been realized in the recent decades as the unplanned human usage of resources has led to near extinction of many naturally occurring resources. Hence, the term sustainability is redefined to preserve the adversarial effect of resources' overusage on environment, economy, and society. Across the world, large focus in the recent days is given toward establishing a sustainable environment in all these domains. The research attention in the field of sustainability is also evident from the number of publications in the recent years as shown in Fig. 5.2.

One major aspect on sustainability is in the domain of manufacturing, which is the focus of this book. Manufacturing, as a process, does not have a direct implication on sustainability, but the components of manufacturing processes, such as casting, machining, raw materials, lubricants, etc., make the system more complex to understand in terms of sustainability. A systematic reading on various domains of manufacturing is required to understand its overall role on sustainability. Looking into the research work published within the engineering domain in the field of sustainable manufacturing presented in Fig. 5.3, the number is found to be significantly low, though there is an essential need for research on sustainable manufacturing.

One reason for the less attention in the field of sustainable manufacturing could be the lack of resources available to understand the fundamentals and future perspective of sustainable manufacturing. This chapter presents a concise information on the need for focus on material development toward sustainable manufacturing.

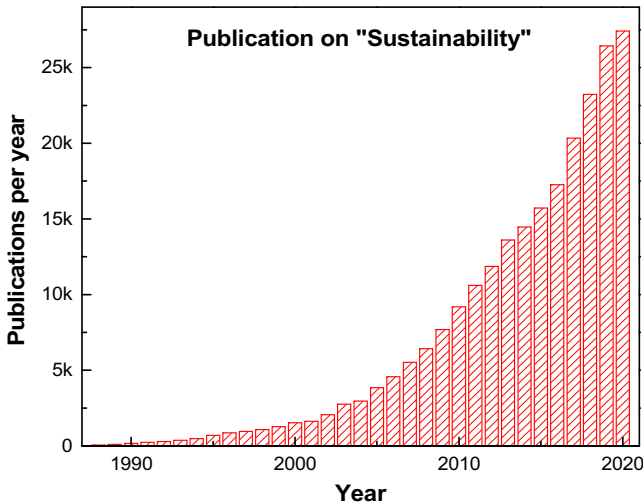


FIGURE 5.2 Number of Scopus indexed articles on sustainability [as on November 21, 2020].

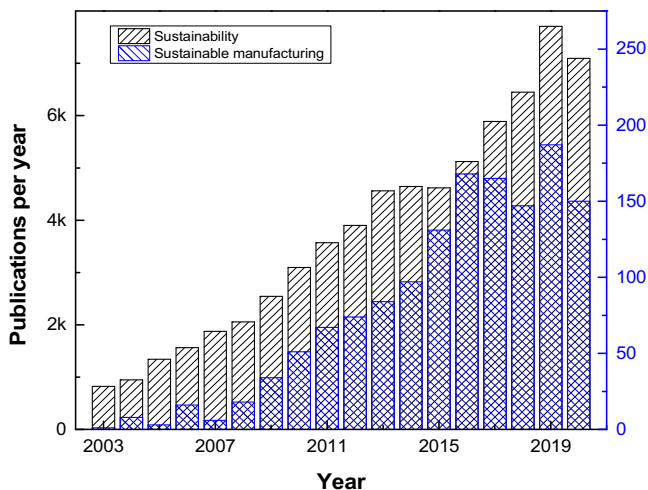


FIGURE 5.3 Number of Scopus indexed articles on sustainability and sustainable manufacturing considering only the publications in the domain of engineering [as on November 21, 2020].

## 5.2 Need for development of materials

Materials drive the society toward development in various fields. Looking back at the history, it is evident that new materials are always a need whenever mankind takes a leap in technological forefront. Even today, many countries pay attention toward development of newer materials and have this agenda as part of their national development policies.

New material development is driven by the end-application, which poses challenges to existing materials. For example, superalloys came as an alternative to certain class of steel when there arose a need to have higher working temperature that improves the system efficiency. Similarly, various such conditions and needs are constantly driving the materials domain to develop new and novel materials.

When scientists intend to develop new material to meet the application challenges, the primary focus is on properties and performance of the new materials. The impact of new materials' development and processing on the environment is often ignored. As an example, developing a new material that has higher melting point in place of an existing material requires a melting furnace with higher temperature, if the conventional casting route is preferred. This has an indirect impact on energy consumption, usage of supplementary materials to aid the high-temperature casting, and various other aspects. The development of newer materials

with superior properties also leads to various challenges on secondary manufacturing processes. Therefore, the development of materials should be made keeping in mind, the sustainability of development process, and the postdevelopment manufacturing processes involved in the final product development.

The present chapter focuses on some key processing techniques that are being explored in the recent times toward development of new materials, their fundamental principles, advantages, and limitations. These techniques may be either novel by itself or an adaptation of existing manufacturing processes. Such exploration on the new processes and materials will drive the materials and manufacturing industries toward a sustainable business.

### 5.3 Classification of materials development

Material development is always driven by the necessity demanded of industries. Among various factors more crucial are the improvement in mechanical performance, reduction in the overall cost, and sometimes a synergy of both.

Conventionally, every metallic materials follow a casting route at the material development stage. Based on the application, it may be further subjected to metal working process or directly taken to the product development stage. However, with the current need in terms of properties, there is a large deviation from the traditional casting-based material development route.

While the available methods employed for development of materials are many, they can be broadly categorized under two domains (Fig. 5.4): (i) methods employed to modify the existing material to perform better by tailoring the microstructure and (ii) methods to change the material chemistry so as to fit the demanded requirement.

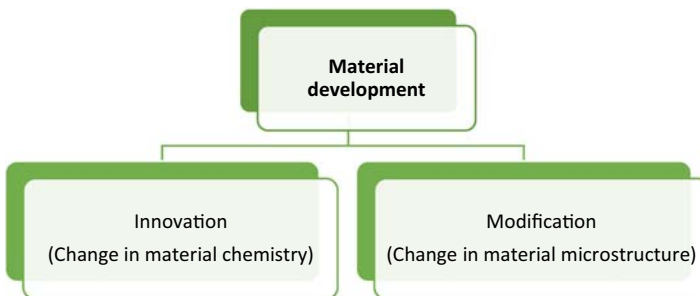


FIGURE 5.4 Classification of material development strategies.

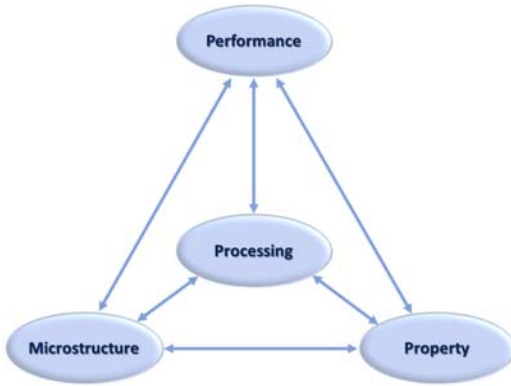


FIGURE 5.5 Tetrahedron of materials science.

## 5.4 Microstructural modification of traditional materials

The interdependence of materials' performance on the microstructure is a well-established fact. The famous tetrahedron of material science (Fig. 5.5) brings out the fact that the properties of the material are direct resultants of the microstructure.

The microstructure of materials can be tailored by subjecting the material to thermal, mechanical, and/or thermo-mechanical treatments. Some standard treatments are presented in Fig. 5.6. By microstructural modification, the properties of conventional materials can be enhanced, eliminating the need to go for alternate advanced materials.

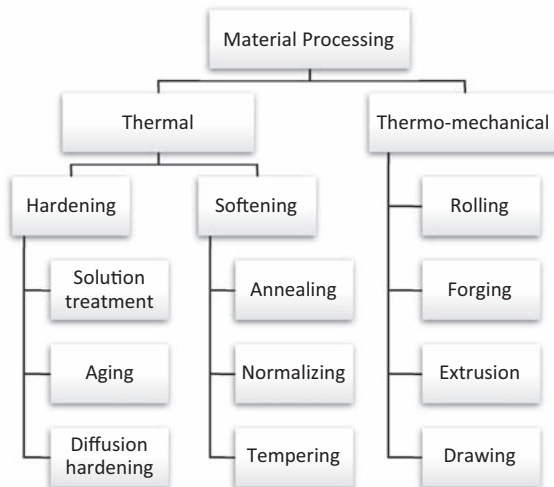


FIGURE 5.6 Commonly practiced thermal and thermo-mechanical treatments.

Conventionally metal working processes are classified as shaping processes, which are primarily used to shape the material as desired for the application. The material is subjected to mechanical strain to modify the shape of the material. The imposed strain is accommodated within the material as a metallurgical defect called as dislocation. Increase in the dislocation (technically, dislocation density) improves the strength of the material, which is called as dislocation strengthening or strain hardening. This is achieved at the cost of ductility.

The metal working processes are performed either at room temperature or at high temperature. When performed at high temperature, along with the addition of dislocations, a competing mechanism is activated to reduce the increase in dislocation, which is called as recovery. The process of recovery helps the material to regain the ductility lost due to the strain hardening. When the accumulated dislocation is higher and the metal working temperature is at least one-third of the melting point of the material, the grain structure of the material rearranges, which leads to improved ductility, and the process is termed as recrystallization. The effect of recrystallization on the material is more similar to that of recovery.

These are the basic strengthening and softening mechanisms that tailor the properties during thermo-mechanical treatment. However, with increased complexity in the material's microstructure, many other mechanisms get involved, which the readers can be acquainted with, by reading any standard book on the basic metallurgy.

Conventional thermal treatment and thermomechanical treatments lead to certain level of microstructural modification. However, special forms of thermo-mechanical treatments are required to significantly modify the microstructure and thereby the mechanical properties of the materials, that are discussed in the present section.

### 5.4.1 Severe plastic deformation

Severe plastic deformation (SPD) processes are special class of thermo-mechanical treatments used to alter the microstructure of the materials. By definition, SPD processes are those that impose large amount of plastic strain on the material with negligible shape change. These techniques are derived from conventional metal forming processes like forging, extrusion, rolling, etc. As the conventional metal forming processes are shape-changing processes, special fixtures are deigned to impart very large plastic strain without notable change in the shape to the stock material.

The strain induced by the SPD processes results in the formation of nanostructures. These nanostructures are not synonymous to nano-grained microstructure. This is because, in most of the SPD processes, the end microstructure without any postprocess heat treatment is highly strained, i.e., the microstructure is densely packed with dislocations. With

partial recovery and dynamic recrystallization during the SPD processes, the dislocation networks are transformed to fine structures with low-angled boundaries (Figs. 5.7 and 5.8).

Because of this distinct microstructure, the strength of the material is significantly high as compared with the standard material processed through any conventional thermo-mechanical processes. The primary strengthening factors in all the SPD processes are grain-boundary strengthening and strain hardening. With the addition of post-SPD heat treatments, the stored strain energy can be partially relieved by further recrystallization, thereby improving the ductility of the material at the cost of strength.

Practically, the microstructure of materials processed through SPD and post-SPD thermal treatment has grain size ranging from sub-micrometer size to few hundreds of nanometers. This type of microstructures are specifically called as ultrafine grains (UFG). These UFG materials have more stable microstructure and hence finds a huge potential in various engineering application. Also, the mechanical properties of UFG materials are better than the conventional materials and hence a potential alternative for new advanced materials.

Researchers have explored a huge number of SPD processes that can significantly alter the microstructure and improve the material properties. Few of them emerged to be more prominent and scalable to industrial level. Prominent SPD processes are discussed further.

### 5.4.2 Equal channel angular extrusion

Equal channel angular extrusion (ECAE), is popularly known as equal channel angular pressing (ECAP). This is a modified extrusion process (Fig. 5.9). Conventionally extrusion is a metal forming process used to

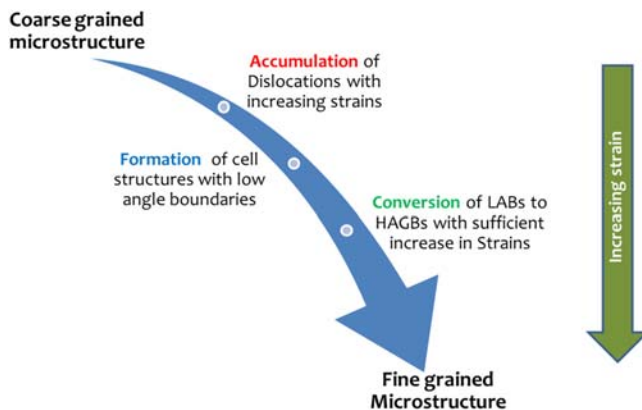


FIGURE 5.7 Evolution of microstructure in SPD process. Low angle boundary (LAB); High angle grain boundary (HAGB).

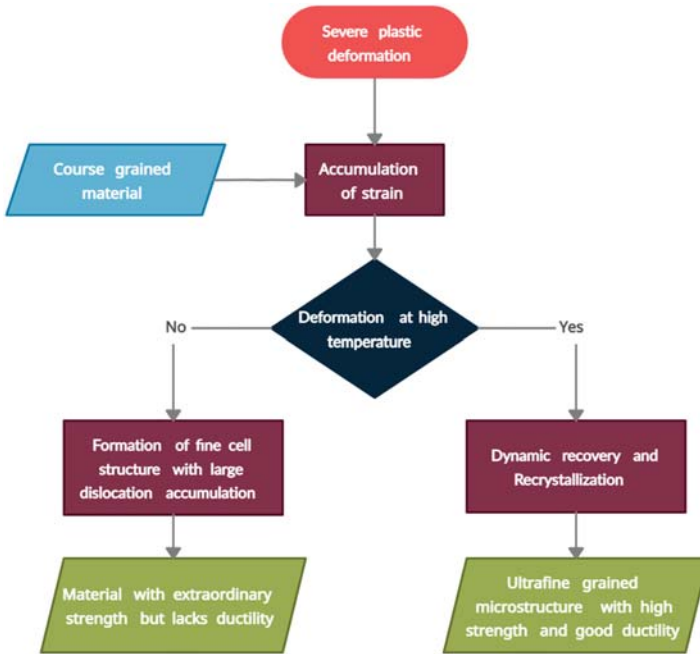


FIGURE 5.8 A schematic demonstrating the role of thermal and mechanical treatment on material's microstructure and performance.

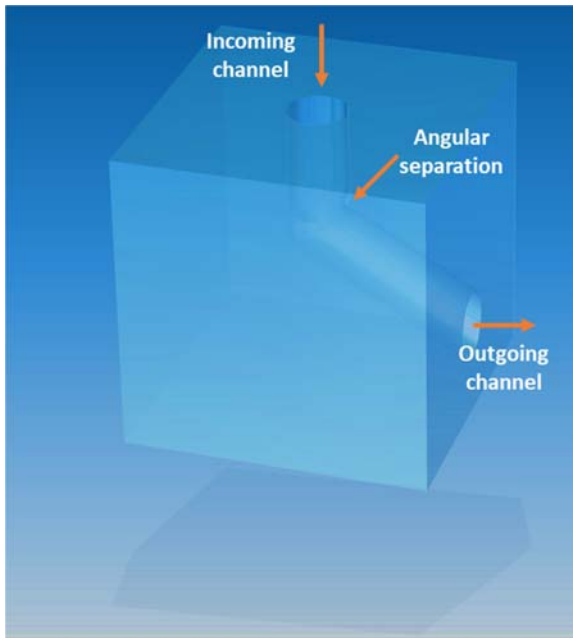


FIGURE 5.9 Schematic diagram of equal channel angular extrusion (ECAP).

reduce the lateral dimension of long objects. The change in shape is achieved by a combination of shear and compression strain components.

Equal channel angular pressing is a shape-preserving plastic deformation process. As the name indicates, the ECAP die composes of multiple channels (minimum two) for the material to pass through. The incoming and outgoing channels are deflected by a definite angle. When the material crosses this angular boundary, it is subjected to shear strain. The strain imposed on the material does not cause any shape change on the material since the shape of incoming and outgoing channels remain the same. Therefore, the strain imparted on the material is termed as equivalent strain. The equivalent strain imposed on the material per pass is mathematically presented as:

$$\epsilon_{\text{equivalent}} = \frac{1}{\sqrt{3} \left[ 2 \cot\left(\theta/2 + \phi/2\right) + 2 \operatorname{cosec}\left(\theta/2 + \phi/2\right) \right]} \quad (5.1)$$

For a simple “L”-type fixture design, the equivalent strain per pass is about **0.3**. The overall resultant strain is the equivalent strain per pass multiplied by the number of passes. Since, the process does not impose any shape change, there is no process-based constraint on the number of passes. The deciding factors for the total number of passes of ECAP are the initial and final material properties, requirement in property improvement, cost- and time-related constraints, etc.

### 5.4.3 High-pressure torsion

High-pressure torsion, abbreviated as HPT, is an SPD process that uses a combination of compression and shear strain to impose large plastic strain on the material. The fixture for HPT includes a die with circular groove to accommodate the material to be processed (Fig. 5.10). The groove present in the die constraints the lateral flow of material during the HPT process. The punch assembly of the process contains the positive replica of the groove that completely encapsulates the material with close to nil clearance.

The punch-die assembly is subjected to a combination of pressure and twist. The high-pressure combined with the torsional stress plasticizes the encapsulated material, imposing large plastic strain. Similar to ECAP, the material processed by HPT does not undergo any shape change because of the constrained plastic deformation imposed through shear and compression. The equivalent strain imposed on the material during HPT is given as

$$\epsilon_{\text{equivalent}} = \frac{\pi \times d \times n}{\sqrt{3} \times t} \quad (5.2)$$

FIGURE 5.10 Schematic layout of high-pressure torsion process.



where  $d$  and  $t$  are the material's diameter and thickness, respectively, and  $n$  is the number of torsional rotation applied in HPT.

Experimentally, it is observed that the HPT process is more efficient in refining the microstructure of material as compared with ECAP. With less than one full rotation of the HPT, one can achieve UFG microstructure with HPT, whereas in ECAP, one has to go for multiple number of ECAP passes. However, the drawback of HPT lies with the limitation in the size of material, it can process. Since the punch and die arrangement of HPT should encapsulate the material to be processed, it is practically limited to disc-shaped material, with limitation in both thickness and diameter. Therefore, usage of HPT process is very limited in practical applications.

#### 5.4.4 Accumulative roll bonding

Conventionally, rolling is a commonly employed process to convert the material from cast to wrought form. During rolling, large strain is imposed on the material, which results in significant microstructural modification, the removing the dendritic form of microstructure and cast

porosity. Due to the imposed strain, rolling also leads to improvement in the mechanical properties.

However, the imposed strain and resultant change in the microstructure is not strong enough to classify rolling process under SPD processes. On the other hand, roll bonding is a special joining process that helps in joining two sheets of similar dimension by strain-induced diffusion.

Accumulative roll bonding (ARB) is a process evolved by the combination of conventional rolling process and roll-bonding process (Fig. 5.11).

First, the sheet/plate material is rolled in a conventional rolling mill to 50% thickness reduction either by multiple passes or by single pass. The reduced sheets are then cut into half and stacked to bring back to the original thickness. Before stacking, the surfaces are brushed to remove any oxide layer formation and to improve the bonding efficiency. The stacked sheet is again rolled to 50% thickness reduction. The process of stacking and rolling can be repeated as many times required so as to achieve the desired UFG microstructure.

ARB process can be employed to achieve significant improvement in the mechanical properties. The limitation of the process is that it can be applied only to sheet metals.

#### 5.4.5 Special rolling techniques

As mentioned in the previous section, rolling is an effective process to impart large strain on the material. However, the rate of strain accumulation through dislocations is compensated during rolling by partial recovery. When the rolling is performed at high temperature, dynamic recrystallization also takes place that partially preserve the initial microstructure, thereby, preventing large strain accumulation.

Several techniques were adapted in the recent years to increase the rate of dislocation accumulation and to arrest the softening phenomena like

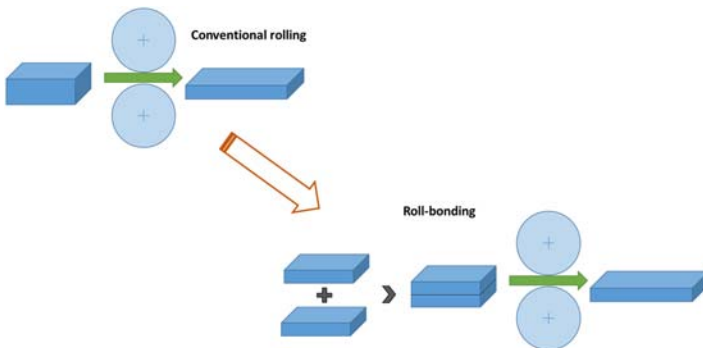


FIGURE 5.11 Schematic showing the evolution of roll bonding from rolling process.

recovery and recrystallization. Two of such techniques are more prominent. They are:

- i. Cryorolling
- ii. Asymmetric rolling

### 5.4.6 Cryorolling

Cryorolling is similar to conventional rolling by principle, except for the working temperature. It is clearly understood that the processing temperature plays a critical role in controlling the dynamic recovery and recrystallization mechanisms. Higher the temperature, more is the rate of dynamic recovery and recrystallization. By suppressing the recovery and recrystallization phenomena during the plastic deformation process, large amount of strain energy can be stored in the material in the form of dislocations. The stored dislocations help in improving the strength of the material.

In cryorolling, the temperature of the material is maintained within sub-zero degree centigrade domain throughout the process. There are many ways to do this. However, one prominent methodology that emerged to be more successful is by holding the material in liquid nitrogen for a definite period of time before rolling (Fig. 5.12). The holding time depends on the sample thickness and material's thermal conductivity. It will be higher for material with larger dimension and lower thermal conductivity.

Once taken out of liquid nitrogen, the sample may immediately rolled to avoid increase in the temperature. Liquid nitrogen immersion is mandatory before every rolling pass to maintain uniformity in rolling temperature.

Experimental results show that the strength improvement achieved through cryorolling is much higher as compared with that of other SPD processed materials. Applicability of cryorolling for improving the material properties is dependent on the material characteristics.

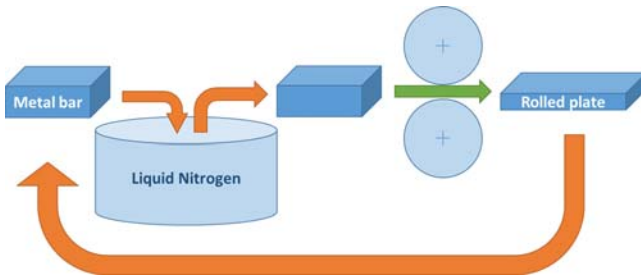


FIGURE 5.12 Schematic layout of cryorolling process.

### 5.4.7 Asymmetric rolling

The conventional rolling process has a symmetry in processing. In conventional rolling, both the rollers have the same surface velocity. This helps in keeping the neutral point at both the surface of the plate at a line perpendicular to the linear movement of the rolling operation. In asymmetric rolling, the surface velocity of both the surface of the plate is unequal. This differential surface velocity is achieved by either of the following.

1. Both the rollers have different rotational speed. This is performed either by having individual drive for the rollers or by connecting the rollers through a gear train that can vary the speed of driver roller from the driven roller.
2. Both the rollers have same rotational speed but different radius. Difference in the radius leads to different surface velocity for a given rotational speed.

The differential velocity of rolling at the surfaces enhances the rate of dislocation accumulating in the material. This leads to improved microstructural refinement in the material as compared with that of conventional rolling. However, as described earlier, the refinement is not as severe as in case of cryorolling, since the process of asymmetric rolling is done at higher temperatures, which leads to partial recovery of generated dislocations.

However, as an alternative, a hybrid process, synergizing the potential of asymmetric rolling and cryorolling, can be framed. The increased strain accumulation from asymmetric rolling along with the suppression effect of cryorolling on the dynamic recovery results in significant microstructural refinement in this hybrid process. While few reports exist, standing as a proof of this extraordinary performance, a wider exploration was not carried out in this aspect.

## 5.5 Optimization of material processing conditions

Manufacturing supply chains face increasing demands for sustainable manufactured products created using economically sound processes that minimize negative environmental impacts while conserving energy and natural resources. Original equipment manufacturers (OEMs), part suppliers, and primary material suppliers have been challenged to meet stringent cost requirements, complex geometrical shapes, mechanical property requirements, and rapid delivery constraints (Fig. 5.13). Materials and energy consumption are greatly reduced from new and improved processes that utilize full capabilities of manufacturing equipment and eliminate waste from costly trial-and-error process

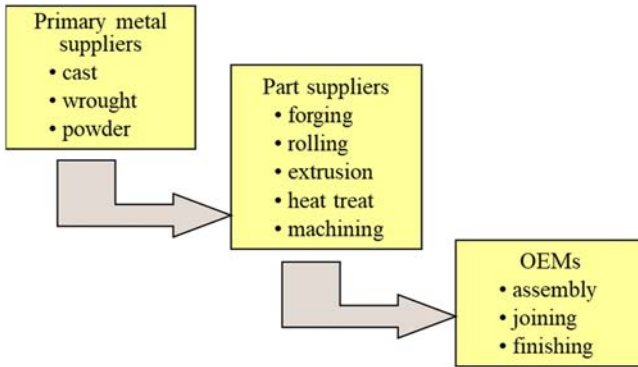


FIGURE 5.13 Example supply chain for metal products.

optimization approaches. There is a wide variety of approaches to achieving sustainable manufacturing capabilities including methods that improve material processing conditions for increasing productivity, reducing scrap materials, reducing die trials and set-ups, and increasing product quality with defect and microstructure control. The workpiece material pedigree, as determined by its composition, defects, microstructure, properties, and thermomechanical history, has major impacts on production yields, material utilization, and product durability. Sustainability benefits are also realized by resolving common metal processing problems such as internal and surface defects in products, which are caused by poor material behavior and nonuniform deformation. Typical material issues during cold forming operations are the formation of edge cracks, waviness, and sliver defects, and specific hot working issues include the formation of undesirable phases, surface imperfections, nonuniform microstructure, and wedge cracking.

The selection and control of material processing conditions throughout the supply chain have a significant impact on quality, cost, and delivery of the manufactured products. Sustainable manufacturing considerations that reduce consumption of materials and energy or reduce the carbon footprint will generally require modified processing conditions or different manufacturing processes. Specific knowledge about the workpiece material behavior under processing conditions is an important input to the product and process design activities. Product design tasks involve specifying workpiece composition, properties, geometries, and tolerances. Process design tasks include specifying the initial billet size and microstructure and the number and sequence of manufacturing operations. For each manufacturing operation, material processing conditions such as temperature, tooling geometry, die/workpiece lubrication, and ram speed are selected.

Optimization is essentially one method for performing a design, and whether the resulting design is the best design depends entirely on the criteria specified by the designer. Optimization techniques require the specification of two types of criteria: objectives (wants) and constraints (needs). To achieve the desired goals, the designer must specify all relevant criteria and must carefully determine which criteria are objectives and which are constraints. As an example, it may be desired to minimize production costs [objective] while maintaining specified product quality standards [constraint]. On the other hand, the opposite scenario may be desired (i.e., maximize the product quality [objective] while not exceeding a specified a specified cost [constraint]). Effective optimization strategies consider the entire manufacturing process design problem.

Most process design and optimization approaches used for maximizing production and profit rates do not give adequate consideration to the role of materials and sustainability. Process design and production planning activities are mainly concerned with the ease of obtaining the finished shape and size of the final product, and specific information concerning the material behavior is lacking for achieving sustainable manufacturing. For example, total production time may be minimized with little regard for ability of the material to respond favorably at the imposed production rate. These approaches have been suitable for conventional materials such as steels, copper, and aluminum-based alloys which can be processed successfully under a wide range of processing conditions. In other words, these materials can be said to possess wide "processing windows" in terms of workpiece temperature and strain rate. Materials such as superalloys, intermetallics, ordered alloys, and metal-matrix composites have restricted or narrow "processing windows." During processing of these materials, variables such as temperature and strain rate must be monitored and controlled continuously, let the material exhibit different types of instabilities. In the extreme case, these materials may undergo dynamic fracture if processed at high deformation rates; this problem can generally be overcome by selection of higher processing temperatures. Thus, knowledge of material behavior must be explicitly taken into account in the optimization and control of manufacturing processes, especially for difficult-to-process materials.

## 5.6 Material workability and microstructural control during deformation processes

---

It is important to understand metallurgical phenomena associated with the workpiece under processing conditions for effective design and control of thermomechanical processes. Fundamental material processing characteristics such as plastic flow and fracture behavior and operative

microstructural mechanisms strongly influence product qualities such as shape, size, and mechanical properties. In the case of deformation processes, knowledge of constitutive behavior, hot workability, and metallurgical mechanisms is needed for process design and control to achieve high-quality, complex-shaped components. Similarly in heat-treatment processes, knowledge of time-temperature-transformation behavior and the kinetics of microstructure development is required for controlling the microstructure and properties of the product.

The relative ease with which a metal can be shaped by deformation processes such as forging, extrusion, rolling, pressing, and drawing is generally referred to as workability. It is also defined as the degree of deformation that can be achieved in a particular metal working process without causing cracking or fracture or poor mechanical properties. Workability depends on the state-of-stress, strain, strain rate, and temperature in combination with metallurgical factors such as resistance of the material to ductile fracture. Therefore, the workability may be classified as (1) state-of-stress-related workability, which depends on the workpiece geometry, die design, and friction conditions and (2) intrinsic workability, which depends on the previous history of the material, temperature, strain, and strain rate conditions.

Understanding both the demands of the manufacturing process on the workpiece material and how the workpiece material can intrinsically respond to the process demands provides the fundamental insights for optimizing workability. Process demands on the workpiece material are manifested via the state-of-stress and the severity of deformation, speed of deformation, and thermal conditions. They are governed by selected manufacturing equipment systems, tooling and die design, and die/workpiece interface conditions. If stress components in a deforming workpiece become tensile, then weak interfaces within the material can open up and cause surface or internal fractures. Also material flow patterns with abrupt changes such as rigid body rotations can cause discontinuities in velocity field and cracking. Thermal gradients in the deformation zone foster nonuniform deformation and defects such as internal shear banding. The severity of the material process conditions can be evaluated using finite element analyses of field quantities such as stress, strain, strain-rate, temperature, and heating/cooling rate and their gradients in deformation zones. Fig. 5.14 illustrates an example of the correlation between finite element predictions of tensile stresses during an isothermal cylindrical compression test and resulting material surface fractures in bulge regions produced from workpiece/tooling friction conditions. The shaded areas show where the hydrostatic stress-to-effective stress ratio values are positive, and thereby, a tensile state of stress exists. The demands of the process should be minimized for sustainable manufacturing applications.

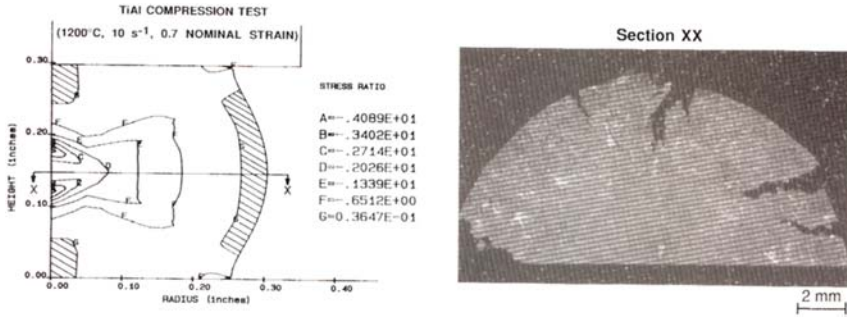


FIGURE 5.14 Example fractures caused by tensile stresses in bulge regions of cylindrical compression test. Material is titanium aluminide (Malas, 1999).

Consideration of intrinsic workability is also important for producing high yield, sound-manufactured products, while reducing the overall waste of materials and energy. Intrinsic workability is defined as a material property, which is independent of changes in geometry, die design, press characteristics, and lubrication conditions. Consider the case of chevron cracking (central burst) phenomena shown in Fig. 5.15 for extrusion of 6061 aluminum, which is a commonly used aluminum alloy. This internal defect is very difficult to detect and is caused by tensile stresses along the workpiece centerline during extrusion. Fig. 5.15 (a) exhibits severe chevron defects and strongly suggests poor workability for the workpiece material. However, for the same material and die geometry, center bursting is not observed, as shown in Fig. 5.15B, for a different extrusion speed (i.e., strain rate) conditions. Favorable workability in case (b) can be attributed to the intrinsic ability of the material to mitigate tensile stresses through favorable metallurgical mechanisms, which avoid fracture and plastic instability.

## 5.7 Material processing maps

Material processing maps provide a useful framework for optimization of hot deformation processing conditions in terms of workpiece temperature and strain rate. In hot deformation there are “safe” and “damage” mechanisms that occur in different strain rate-temperature regimes. For example, the “safe” mechanisms involve dynamic recovery and dynamic recrystallization, while the “damage” mechanisms are wedge cracking (dominant at lower strain rates and higher temperatures) and void formation at hard particles (dominant at high strain rates and lower temperatures). Frost and Ashby (1982) and Raj (1981) and other researchers have developed various atomistic and phenomenological approaches

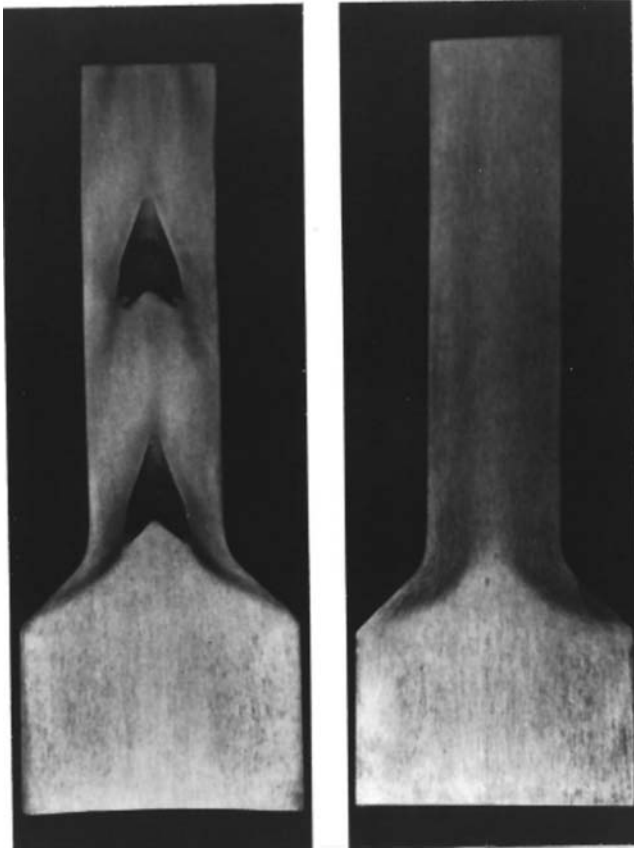


FIGURE 5.15 Example of round-to-round extrusion of 6061 aluminum alloy extruded at temperature of 500°F and speeds of (A) 1.5 in/min, (B) 0.9 in/min (Gurney, 1978).

identifying dominant deformation and damage mechanisms over a range of processing conditions. Gegel et al. (1988) and Prasad et al. (1984) developed a continuum approach material processing map methodology called “dynamic material modeling” (DMM), and the workpiece material is considered to be a dissipator of power. Constitutive relationships for plastic flow describe the manner in which the power is converted at any instant into two forms: thermal and microstructural, which are not recoverable by the system. The dependence of the workpiece flow stress on strain, strain rate, temperature, and thermomechanical history provides the essential constitutive properties for DMM. Material data from hot deformation tests such as isothermal compression or torsion tests conducted at different temperatures and strain rates are used to generate the required constitutive relationships. DMM was developed was in

response to the need for a macroscopic description of flow, fracture, and workability of complex engineering materials under hot working conditions. A compendium of DMM processing maps was developed by Prasad et al. (2015) that identifies the desired material processing windows for a wide range of metallic systems including, conventional alloys, special purpose alloys, intermetallics, ordered alloys, and metal-matrix composites.

The DMM approach provides an effective methodology investigated by Malas et al. (1992) for utilizing relationships among constitutive behavior, hot workability, and microstructure development, which are needed for process optimization. Flow stress ( $\sigma$ ) is the necessary material property that links constitutive behavior to hot workability via DMM. In the case of constitutive relations, flow stress values describe the inherent resistance of the material to plastic deformation as well as the hardening and softening behavior of the material. Flow stress sensitivity to changes in temperature and strain rate is fundamentally related to intrinsic workability in terms of mechanical stability, material stability, and power partitioning. At large plastic strains, the flow stress value has a negligible dependence upon strain. This phenomenon coincides with a basic premise of DMM—that steady state is the attractor for irreversibility and material stability by means of entropy production. Hence, flow stress and the accuracy with which they are measured are important to the understanding of the interrelationships of material behavior.

Workability and microstructure development under hot-working conditions are strongly influenced by the deformation mechanism(s) governing the material system. Typically, several metallurgical mechanisms are operative during processing, especially in the case of complex engineering materials. This situation contributes to the stochastic nature of the material behavior, which leads to nonuniform microstructures and inhomogeneous plastic deformation. For most metallic systems, these complicated situations are mitigated under certain processing conditions where a particular softening mechanism dominates. Determining the location of these desirable regions is important for producing controlled microstructures and enhanced plastic flow.

The DMM approach makes use of the constitutive equations for plastic flow determined from hot deformation tests performed at different temperatures and strain rates. Parameters such as the strain rate sensitivity and temperature sensitivity of the flow stress are related to the manner in which the workpiece dissipates energy instantaneously during hot deformation. The rate of change of stress with strain rate at constant levels of strain ( $\epsilon$ ) and temperature ( $T$ ) is the strain-rate sensitivity parameter ( $m$ ), which is defined as follows:

$$m = [\partial(\log\sigma)/\partial(\log\dot{\epsilon})]_{\epsilon, T} \quad (5.3)$$

The temperature sensitivity of the flow stress is analyzed in terms of a parameter ( $s$ ):

$$s = -1/T \left[ \frac{\partial(\ln\sigma)}{\partial\left(\frac{1}{T}\right)} \right] \varepsilon, \dot{\varepsilon} \quad (5.4)$$

Furthermore, an apparent activation energy parameter ( $Q_{app}$ ), which correlates with dominant deformation mechanisms, can be determined from computations of  $m$ - and  $s$ -values, namely

$$Q_{app} = \frac{sRT}{m} \quad (5.5)$$

where  $R$  is the universal gas constant.

Gegel (1988) derived DMM stability criteria that are expressed in terms on the magnitude of  $m$ - and  $s$ -values and how they change with strain rate. Four criteria material stability are given as:

$$0 < m \leq 1 \quad (5.6)$$

$$\frac{\partial m}{\partial(\log\dot{\varepsilon})} < 0 \quad (5.7)$$

$$S \geq 1 \quad (5.8)$$

$$\frac{\partial s}{\partial(\log\dot{\varepsilon})} < 0 \quad (5.9)$$

The DMM provides useful macroscopic information for identifying processing regimes where desirable softening mechanisms are in operation and the material behavior is essentially deterministic. As shown schematically in Fig. 5.16, the processing window of a given metallic system is defined as the design range of processing conditions under which material behavior is stable and a desirable and relatively constant value of apparent activation energy ( $Q^*$ ) exists. The shaded region satisfies all four DMM stability criteria. Metal-forming equipment speed and temperature capabilities can constrain and reduce the optimal processing window. Hence, the DMM processing mapping approach for process optimization involves the superposition mapping of the following information over a given range of processing conditions.

- Stability analyses for determining safe processing conditions
- Activation energy analyses for determining where deformation mechanisms are operative and dominant
- Sensitivity analyses for determining desired processing window for deterministic and robust microstructure control

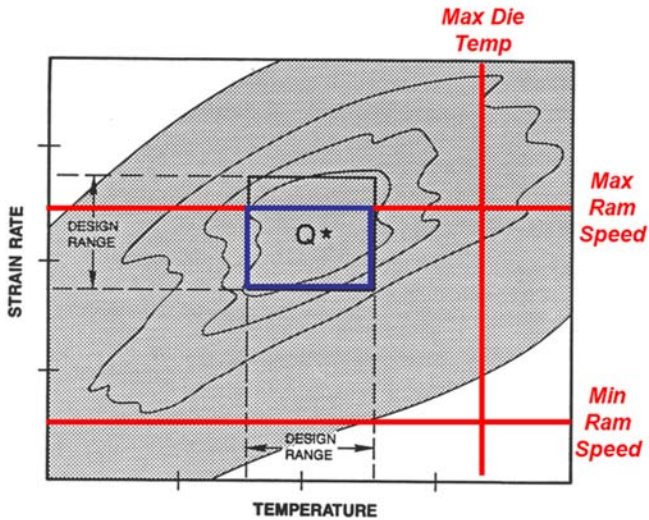


FIGURE 5.16 Conceptual dynamic material modeling (DMM) processing map for hot-working processes showing contours of activation energy with the desirable one identified as  $Q^*$ , shaded region that satisfies all four DMM stability criteria, and manufacturing equipment limitations. *Used with permission from Malas, J.C. & Seetharamen, V., 1992. Using material behavior models to develop process control strategies, Journal of The Minerals, Metals & Materials Society 44, 8–13.; Springer Nature.*

- Identify manufacturing equipment characteristics and limitations for determining processing conditions

## 5.8 Role of activation energy

Deformation mechanisms can be identified by the amount of potential free energy required for their activation. Microstructural transformations require atomic mobility; to activate this mobility, an increase in energy must be provided to transport the atoms from one site to another according to Martin et al. (1976) During a thermomechanical process, a material system changes its state in accordance with the imposed conditions of temperature, strain, and strain rate for dissipating energy. In order for a system to achieve a more stable, lower energy state, it must first pass through an intermediate, less stable, and higher energy state that acts as a barrier to the transformation unless the necessary activation can be provided. As shown schematically in Fig. 5.17, a material system can lower its free energy by transitioning through a series of dissipative energy states and microstructures. Typically, for a given free-energy state of the material system, the potential exists for a number of possible dissipative paths.

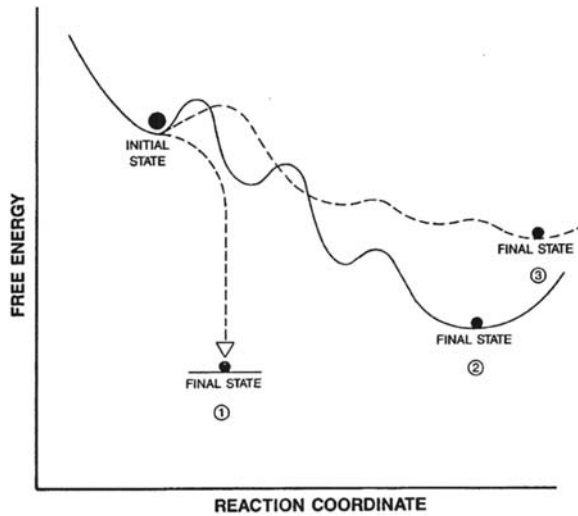


FIGURE 5.17 Notional illustration of three possible dissipative paths. Reaction coordinates are process control parameters such as temperature and strain rate.

In this situation, the material response must be controlled such that the microstructure will transform in a stable and efficient way. Three possible dissipative paths and final states, namely, (1) fracture, (2) recrystallization, and (3) recovery, are notionally illustrated in Fig. 5.17. Using computations of  $m$ - and  $s$ -values, the apparent activation energy ( $Q_{app}$ ) associated with a prevailing deformation mechanism is mapped over a given range of processing conditions.

## 5.9 Role of stability

Stable workpiece material behavior during any manufacturing operation is critical for production of high quality, reproducible products. Stability is a fundamental requirement for material process control. Typical types of material instabilities include dynamic strain aging, formation of new phases, adiabatic shear deformation, or regions of localized deformation, grain boundary and triple point cracks, void generation (cavitation), and hot shortness. Material damage and flow instabilities cause inhomogeneous deformation and produce defects like nonuniform microstructures, shear bands, and strain markings. Typical cracking and shear band defects are shown in Fig. 5.18. Inhomogeneous deformation is detrimental to the mechanical properties of the product in particular the ductility, fracture toughness, and fatigue crack growth rate. The phenomena, which cause inhomogeneous deformation during forming, can

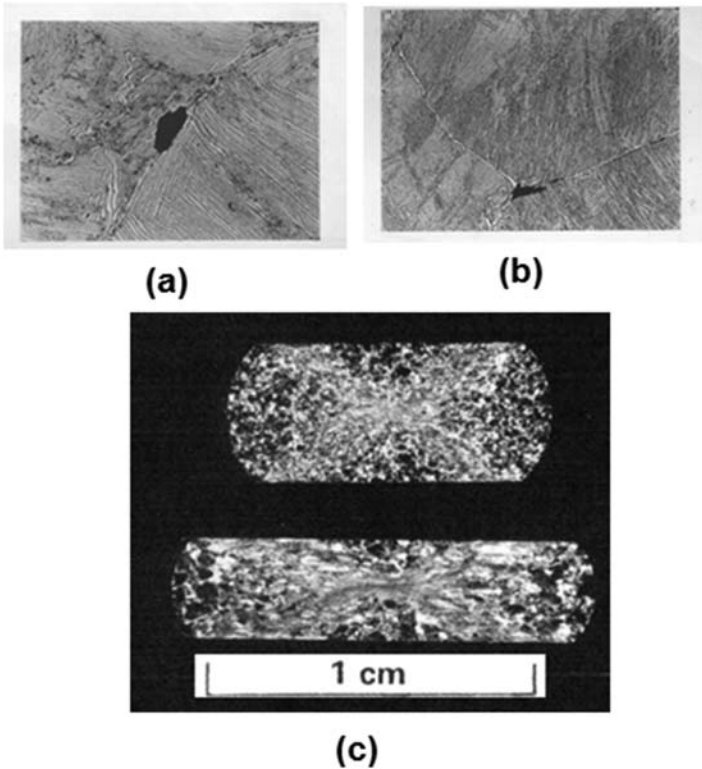


FIGURE 5.18 Examples of Ti-6242 instabilities. Top photos (A, B) show grain boundary cracking and void formation. Bottom photo (C) shows macroscopic shear band defect. [(B): Used with permission from [Gegel et al., 1980](#), Elsevier (C) Used with permission from [Semiatin and Lahoti, 1982](#); Springer Nature].

be termed as “flow instabilities” and the regimes of temperature and strain rate where deformation is not homogeneous can be termed as “instability” regions. It is therefore necessary to avoid processing regimes where the instabilities are likely to occur. The DMM stability criteria (given in [Eq. \(5.4\) through 5.7](#)) provide the necessary—but not sufficient—conditions for avoiding process-induced material instabilities. Violations of the DMM stability amplify stochastic behavior and results in nonuniform microstructures and deformation.

The stable range of strain-rate sensitivity ( $m$ ) values was derived by [Gegel et al. \(1988\)](#) from theoretical considerations of maximum rate of power dissipation by material systems and experimental observations. Metals and alloys generally satisfy this criterion ([Eq. 5.6](#)) under hot working conditions. Negative  $m$ -values are obtained under conditions promoting strain aging (a product of the interaction of mobile dislocations

and solute atoms). However, the imposed strain rates for hot working operations are generally too high for strain aging phenomena to occur and are thereby avoided. Another mechanism that can lead to negative  $m$  values is the dynamic propagation of pre-existing or newly formed microcracks, which eventually lead to fracture of the workpiece. As the value of “ $m$ ” increases, the tendency for localized deformation decreases, enabling extensive elongation of the workpiece under tensile loading without necking. Similarly, the occurrence of shear band formation can be inhibited very effectively at high  $m$  values. For metals and alloys,  $m = 1$  represents ideal superplastic behavior resulting from Newtonian flow typical of a glass material.

The stability criterion related to the variation of  $m$  with  $\log \dot{\epsilon}$  (Eq. 5.7) stems from the theoretical requirement for the material system to continuously lower its total energy. If fracture stress is assumed to be independent of strain rate, then an increasing  $m(\dot{\epsilon})$  will probably lead to catastrophic failure at high strain rates. In contrast, a decreasing  $m(\dot{\epsilon})$  has a lower probability of inducing fracture in the workpiece. Fig. 5.19 describes both of these cases. Hence, this stability criterion leads to more uniform stress fields across the workpiece and a decreased tendency for strain localization, which is clearly desirable.

The lower limit of  $s$ -values (Eq. 5.8) is derived from the premise that the net entropy production rate associated with irreversible processes must

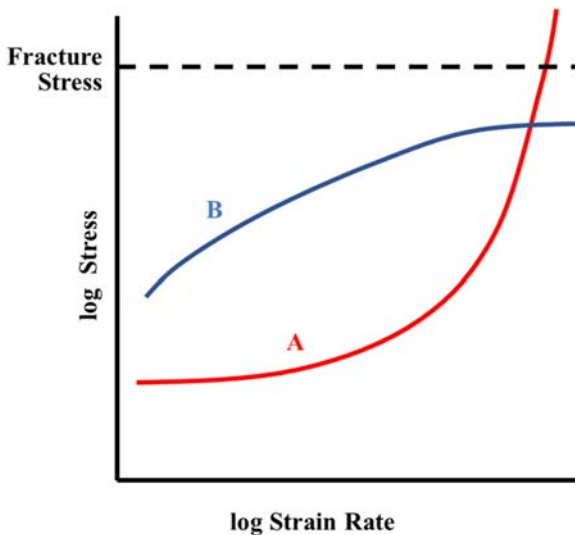


FIGURE 5.19 Schematic representations of two cases: type-A behavior shows instability condition when  $\frac{\partial m}{\partial(\log \dot{\epsilon})} > 0$  and type-B behavior shows stable condition when  $\frac{\partial m}{\partial(\log \dot{\epsilon})} < 0$ .

be positive for stable conditions. It is well established that when dynamic recovery alone operates as a softening mechanism, the temperature dependence of the flow stress is relatively weak. In contrast, when both dynamic recrystallization and dynamic recovery are in operation, the flow stress varies markedly with temperature. Thus, low values of  $s$  are indicative of the dynamic recovery processes, while high values of  $s$  are usually associated with dynamic recrystallization processes.

The stability criterion relating to the variation of  $s$  with  $\log \dot{\epsilon}$  (Eq. 5.9) arises from the necessity for the material system to continuously lower its total energy. As the strain rate increases, the extent of adiabatic heating in local regions increases significantly. Hence, in any particular region of the workpiece, if the local strain rate increases above the nominal value, then it is accompanied by a reduction in the local flow stress. However, if  $s(\dot{\epsilon})$  increases with the strain rate, then a very significant thermal softening will be encountered in the regime of high strain rates, which will produce severe strain localization and adiabatic shear bands. This autocatalytic process is likely to lead to severe cracking of the workpiece if the material has poor resistance to nucleation and growth of cracks. On the other hand, compliance with this stability criterion has a mitigating influence upon this tendency for flow localization. Fig. 5.20 schematically illustrates the implication of  $s$ -value variations with the strain rate. The  $s$ -values are proportional to the slopes of the  $\ln \sigma$  versus  $T^{-1}$  curves, and for a given temperature,  $s$ -values must increase with a decreasing strain rate to avoid localized thermal softening phenomena. Hence, this stability criterion leads to more uniform stress fields across the workpiece and a decreased tendency for strain localization, which is clearly desirable.

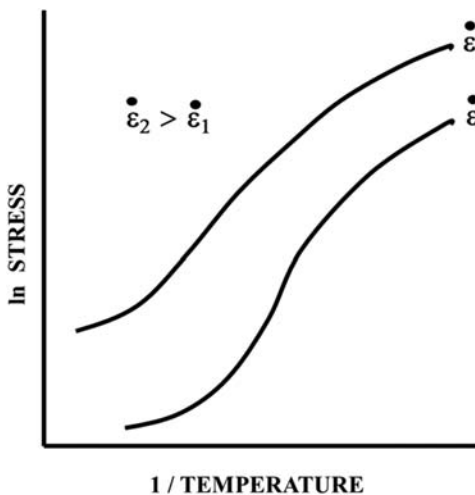


FIGURE 5.20 Schematic illustration of stability implications of  $s$ -value variations with strain rate using notional  $\ln \sigma$  versus  $T^{-1}$  curves for two different strain rates conditions.

Thus, the four stability criteria of the DMM approach have a sound metallurgical basis. Since the material is both dynamic and stochastic, these criteria should be regarded as probabilistic indicators of the behavioral trends exhibited by a material during hot working. The effects of these instabilities upon the workability of a material can be alleviated substantially by proper process control and die design. For instance, die designs that produce negative mean stresses or significant compressive stress components in the workpiece during processing can, in part, offset the adverse effect of positive values of  $\partial m/\partial(\log \dot{\epsilon})$ . This observation is exemplified by the remarkable successes associated with processes such as hydrostatic extrusion, pack rolling, and closed-die forging.

### 5.10 Increasing productivity of aluminum extrusion industry case study

Dynamic material model processing maps and streamlined die design methods have been applied extensively to industrial extrusion processes. Significant improvements in producibility, product quality, and manufacturing productivity were reported by [Pecchia \(1993\)](#) and [Ashley \(1994\)](#) in the case involving a group of small aluminum extrusion companies and tool and die makers near Youngstown, Ohio. The focus of this study is Al 6063 and conventional flat-faced shear die designs. Al 6063 is the most common alloy used for aluminum extrusion, and it is used for making ladders, bicycle rims, and window frames. The flat-faced shear die produces severe velocity changes in metal flow, which create major demands on material workability. However, shear dies produce very smooth surface finish on extruded products, which are desirable for aesthetic reasons. The aluminum extrusion companies were interested in upgrading their production methods with improvements that effectively address the follow aluminum extrusion problems:

- Eliminate internal defects in products, which are caused by poor material behavior and nonuniform deformation
- Eliminate surface defects of products caused by poor die design and temperature control
- Utilize the full capabilities of the extrusion presses
- Avoid the costly trial-and-error approach used to design extrusion dies

A DMM processing map was developed for selecting extrusion temperatures and ram speeds, which allowed extrusion companies to determine the best conditions for processing an alloy with respect to material behavior. The AL 6063 processing map shown in [Fig. 5.21](#) was generated using hot compression test data for the billet material. The

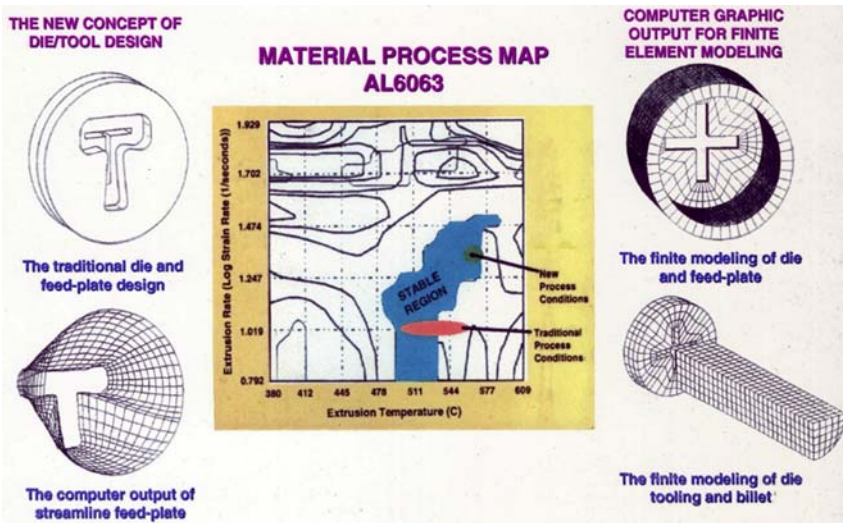


FIGURE 5.21 Dynamic material model and streamlined die design approach for improving aluminum extrusion industry.

traditional processing conditions used by the extrusion companies are speeds that correspond to approximate strain-rates of 10 per second and temperatures that range from 500 to 550°C. Note that this temperature range includes both stable and unstable conditions, which would cause internal and surface defects and variability in product qualities. The improved processing conditions were determined to be extrusion speeds that are two times faster (approximate strain-rates of 20 per second) and increased temperature of 560°C that is closely controlled.

Extrusion die design configurations were also improved using finite element modeling and geometric modeling. Traditional feeder plates such as the T-section die shown in Fig. 5.21 were designed using geometric model for streamlined dies. Feeder plates help control material flow through the die orifice. While it is cost prohibitive to make the ideal streamlined feed-plate shown in the figure, a simple flat-faced plate can be made using the wire-frame coordinates of the streamlined geometric model. Using feeder plates based on streamlined die design reduces the severity of localized deformation, abrupt changes to material flow paths, and the overall demands of the process on the workpiece material.

Significant benefits in product quality, cost, and productivity were realized from the implementation of these DMM processing map results and streamline feed-plate designs. As shown in Fig. 5.22, AL 6063 products with solid cross-sections are extruded nearly 2 times faster without deterioration of the product quality. AL 6063 products with hollow cross-section products are extruded 1.5 times faster. Also,

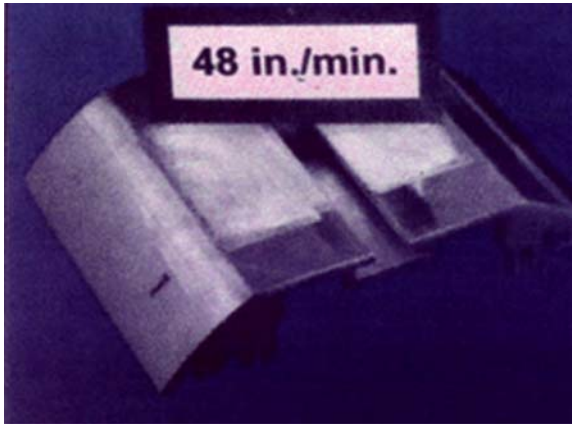


FIGURE 5.22 Section of Al 6063 extruded light bar for emergency vehicles. Process improvements increased extrusion speed from 25 to 48 in./min.

extrusion companies improved their product qualities by eliminating surface defects and by increasing dimensional control capabilities from 5 mils to 3 mils (0.005–0.003 inch) tolerances. Extrusion companies estimated 40% reduction in start-up scrap metal requirements, a 25% reduction in extrusion costs, and a 25% increase in overall productivity.

### 5.11 Effects of prior processing history on workpiece behavior case study

---

The processing behavior and mechanical properties of most engineering materials are strongly influenced by the thermomechanical history of the workpiece. The relationship among microstructure, processing, and properties of a given material system must be considered for sustainable manufactured products. The processing history of workpieces change for a variety of reasons including changes in the material supply chain or design modifications for optimizing microstructures and properties in the finished product. In these cases, a single processing map is not valid for the multiple variants of a given composition of material. Samples should be tested and analyzed, and a DMM processing map generated for each starting condition of the workpiece material.

The microstructure of titanium alloys can be varied and controlled by thermomechanical processing. The nature and degree of microstructure control that can be obtained depends on the alloy class and type. Ti-6242 (Ti-6Al-2Sn-4Zr-2Mo-0.1Si) is near- $\alpha$ ,  $\alpha + \beta$  titanium alloy whose hot working characteristics are very sensitive to the initial preform microstructure and processing variables. For evaluating the constitutive

behavior of this material, two different preform microstructures, equiaxed  $\alpha + \beta$  and acicular  $\beta$  or transformed  $\beta$  were investigated by Dadras & Thomas as shown in Fig. 5.23. The equiaxed  $\alpha + \beta$  microstructure has high tensile and high low-cycle fatigue properties, and the acicular  $\beta$  microstructure has good creep and high stress rupture properties. The prior material processing history of both preform microstructures is given in Table 5.1.

In general, deformation-induced flow softening is observed under most hot working conditions for both equiaxed  $\alpha + \beta$  and acicular  $\beta$  preform test samples. The acicular  $\beta$  preform samples are typically characterized by higher initial flow stress followed by more extensive softening. For any particular temperature and strain rate, the acicular  $\beta$  preform flow stress approaches that of the Equiaxed  $\alpha + \beta$  preform at strains in excess of  $\epsilon = 0.6$ . This is illustrated in the flow stress curves for both Ti-6242 preform microstructures shown in Fig. 5.24.

The prior material processing history of a Ti-6242 workpiece has significant effects on its microstructures and flow stress properties. And these major differences are also observed in the DMM processing maps for both preform microstructures. As shown in Fig. 5.25, acicular  $\beta$  preform exhibits instabilities, namely, grain boundary cracking and kinking

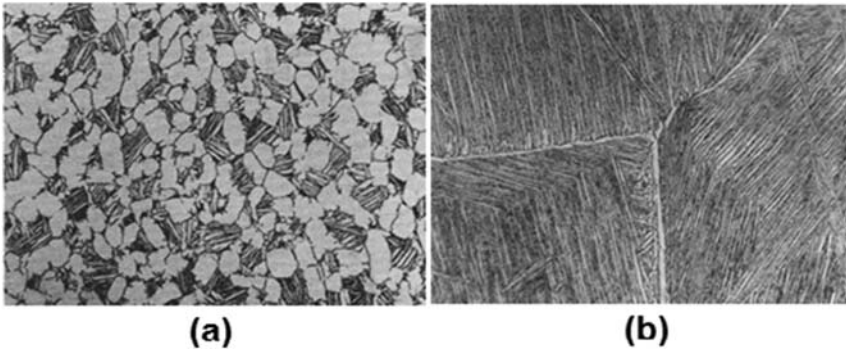


FIGURE 5.23 Ti-6242 preform microstructures (500 $\times$ ), (A) Equiaxed  $\alpha + \beta$ ; (B) Acicular  $\beta$

TABLE 5.1 Prior processing history of Ti-6242 preforms (Dadras and Thomas, 1981).

	Forge conditions	Heat treat conditions
Equiaxed $\alpha + \beta$ preform	954 C (1750 F)/Air cool	968 C (1775 F)/2 h/Air cool
Acicular $\beta$ preform	1037 C (1900 F)/Air cool	1024 C (1875 F)/2 h/Air cool

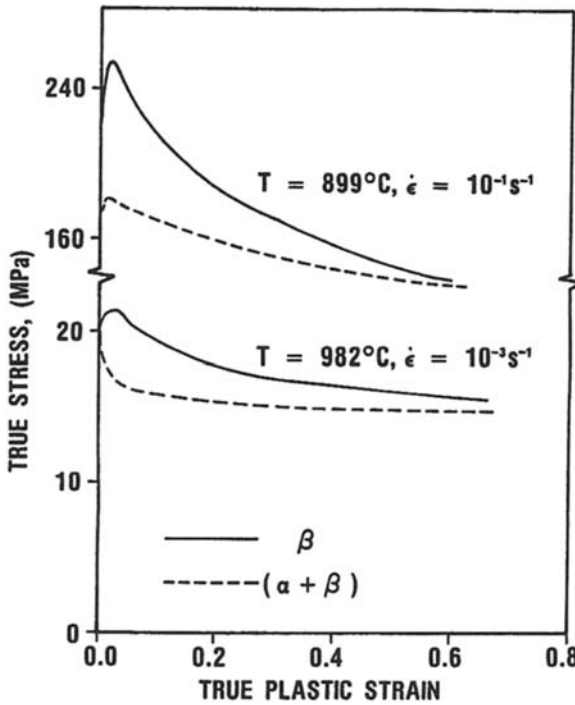


FIGURE 5.24 Dependence of flow stress on preform microstructure for Ti-6242. Used with permissions from Dadras, P. & Thomas, J.F., 1981. *Metallurgical Transactions A*, 12A, 1867; Springer Nature.

and stable behavior where the deformation damage mechanisms are mitigated by diffusional processes. Contours of efficiency of power dissipation ( $\eta$ ) shown on this map provide empirical correlations to deformation and fracture mechanisms.

The relationships among hot forming, heat treatment, microstructure, and physical properties in the production of titanium and its alloys are very complex. Processing maps simplify and clarify material behavior and provide top-down perspective for identifying safe and unsafe processing conditions. Effects of prior material processing history are clearly demonstrated in Fig. 5.26, which compares the processing maps of both Ti-6242 preform microstructures. As shown, the deformation and fracture mechanisms are very different for titanium preforms with the same chemical composition. The acicular  $\beta$  preform exhibits kinking, plastic instability, dynamic grain growth, and spheroidization of acicular  $\alpha$  structure. And the equiaxed  $\alpha + \beta$  preform exhibits adiabatic shear bands, superplasticity, and dynamic recrystallization of  $\alpha$ -phase. The safe processing window for the equiaxed  $\alpha + \beta$  preform is larger than the acicular

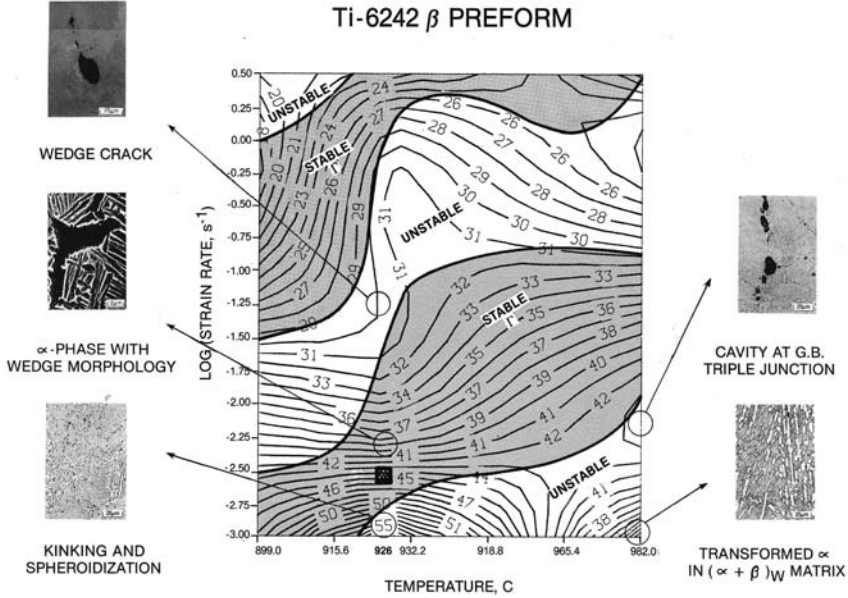


FIGURE 5.25 Processing map of Ti-6242 (acicular  $\beta$  Preform) at a strain of 0.6. Contours of efficiency of power dissipation ( $\eta$ ) are shown. Shaded regions correspond to stable material behavior (Gegel, 1988; Reprinted with permission of ASM International. All rights reserved. [www.asminternational.org](http://www.asminternational.org)).

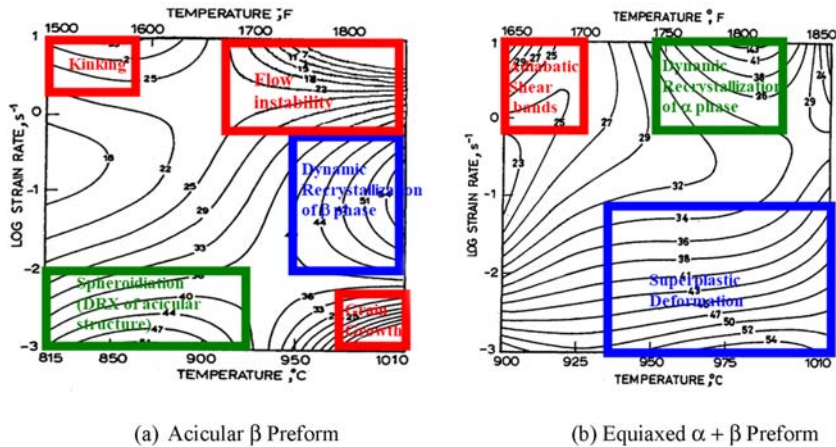


FIGURE 5.26 Processing maps for Ti-6242 preform microstructures at a strain of 0.6. (a) Acicular  $\beta$  preform and (b) Equiaxed  $\alpha + \beta$  preform. Contours of efficiency of power dissipation ( $\eta$ ) are shown (Prasad et al., 2015; reprinted with permission of ASM International. All rights reserved. [www.asminternational.org](http://www.asminternational.org)).token=1e42ab1302472d9a1dbe40be2de91a

$\beta$  preform. This also implies that the equiaxed  $\alpha + \beta$  preform can be worked with a greater variety metal forming equipment such as slow hydraulic presses, hydraulic presses, mechanical presses, and hammer forge presses. The typical average strain rates of mechanical presses and hammer forge presses are 1–30 per second and 10 to 200 per second, respectively, and are too fast for stable processing of acicular  $\beta$  preform materials.

Prasad et al. (2015) identified the optimum processing conditions to be 985°C (1805°F) and 10 per second for equiaxed  $\alpha + \beta$  preform materials and to be 875°C (1607°F) and 0.001 per second for acicular  $\beta$  preform materials. Additional research studies and interpretation of Ti-6242 processing maps were contributed by Gegel (1988) and Prasad et al. (1984). In summary, any changes to the thermomechanical history of the workpiece material must be evaluated in order avoid undesired material behavior and waste from costly trial-and-error process optimization approaches.

## 5.12 Processing windows for different forms of Al-2024 materials case study

---

Aluminum alloy 2024 (Al-2024) is among the class of Al-Cu-Mg age hardenable alloys developed for use in aerospace applications due to its low density and good damage tolerance. The high strength in this alloy is primarily derived from the precipitation and redistribution of fine  $\text{Al}_2\text{CuMg}$  particles. This alloy is produced in various forms by thermo-mechanical processing techniques, which give rise to a variety of starting microstructures. Typical applications of this alloy include aircraft structures, rivets, and truck wheels. Included in the Al-2024 family is a rapidly solidified powder metallurgy (P/M) product reinforced with silicon-carbide whiskers ( $\text{SiC}_w$ ). The addition of whiskers significantly enhances the specific strength and stiffness, which make this material suitable for critical structural components. However, these materials are difficult to shape using conventional processing techniques because of intricate microstructural features developed by rapid solidification and addition of ceramic reinforcements. Furthermore, since their mechanical properties are strongly dependent upon microstructural characteristics such as volume fraction and aspect ratio of whiskers, it is essential that manufacturing of structural shapes be accomplished without fracturing whiskers or changing their aspect ratio. This case study examines microstructural complexities and how they tend to reduce the size of the safe and optimal processing windows.

The microstructures of different forms of Al-2024 are shown in Fig. 5.27. The ingot Al-2024 has a multiphase microstructure (Fig. 5.27A) consisted of soluble fine  $\text{Al}_2\text{CuMg}$  precipitates along with iron-rich

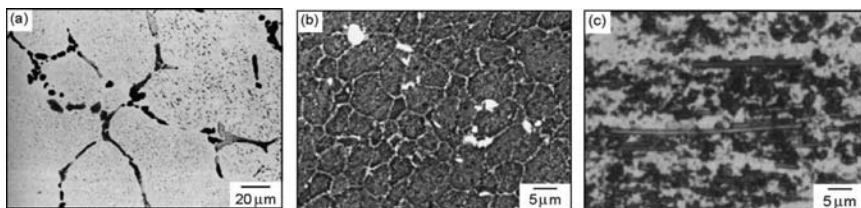


FIGURE 5.27 Microstructures of Al-2024 in different forms: (A) ingot (optical), (B) P/M (backscatter scanning electron microscopy (SEM)), and (C) P/M with 20 v/o SiC<sub>w</sub> (optical) (Used with permission from Malas et al., 2004; Elsevier).

phases. The wrought Al-2024 microstructure has large elongated grains with coarse, uniformly distributed Al<sub>2</sub>CuMg precipitates within the grains and at grain boundaries. The P/M Al-2024 microstructure (Fig. 5.27B) consists of fine equiaxed grains with uniformly distributed fine precipitates of Al<sub>2</sub>CuMg at grain boundaries and triple junctions. The P/M Al-2024 with 20 v/o SiC<sub>w</sub> microstructure (Fig. 5.27C) also has a fine grain size with SiC whiskers aligned in the extrusion direction.

The hot working behavior of wrought Al-2024 has been investigated extensively. Flow softening due to dynamic recovery at temperatures above 250°C with apparent activation energy values in the range of 90–200 kJ per mol was reported by Charpentier et al. (1986). Microstructures of samples deformed at 425°C revealed the presence of fine equiaxed grains near the alignments of (Cu, Al) particles and transverse subgrains, which are indicative of static or dynamic recrystallization. At high temperatures (482°C), precipitate dissolution, banded structures, and abnormal grain growth were recorded, which are the manifestations of microstructural instabilities. Hence, the wrought material can be ideally formed in the broad temperature range of 250–450°C and strain rate range of 0.001–1.1 per second.

As expected, the processing window of the wrought Al-2024 is wider than that of the ingot Al-2024 due to homogenization and reconstitution of the microstructure as a result of prior thermomechanical treatments (rolling, forging, and temper treatments). The processing map for steady-state behavior of ingot Al-2024 is shown in Fig. 5.28A. In this figure, the contour numbers represent the apparent activation energy ( $Q_{app}$ ), and the shaded region corresponds to microstructural instability evaluated using the stability criteria (Eqs. 5.6–5.9). The map for ingot Al-2024 form exhibits an activation energy plateau of  $\sim 140$  kJ per mol in the range 325–450°C and 0.001 to 0.1 per second. Microstructures of deformed test samples revealed that dynamic recovery is the dominant mechanism under these processing conditions. Furthermore, the value of  $Q_{app}$  is comparable to that for self-diffusion in pure aluminum (142 kJ per mol) suggesting that dislocation climb is the rate-controlling step. The large

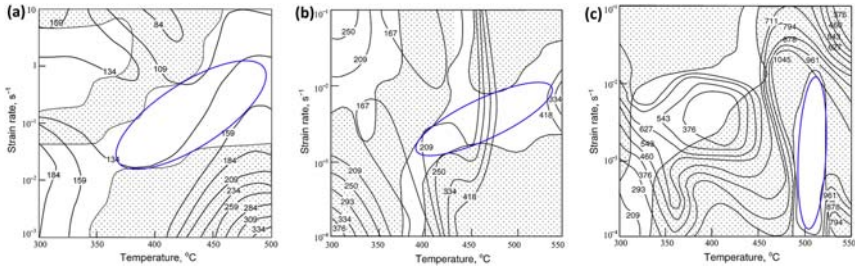


FIGURE 5.28 Optimal processing windows at a strain of 0.3 for different forms of Al-2024. (a) Ingot, (b) P/M and (c) P/M with 20 v/o SiC<sub>w</sub> Used with permission from Malas, J.C., Venugopal, S., Seshacharyulu, T., 2004. Effect of microstructural complexity on the hot deformation behavior of aluminum alloy 2024, *Materials Science and Engineering* 368, no. 1–2. p.41–47.; Elsevier.

stable region compares well with the safe processing region for commercial purity aluminum in Raj's atomistic mechanism map reported by Raj (1981). The unstable conditions at high temperatures (400–500°C) and low strain rates (0.005–0.05 per second) are associated with wedge cracking phenomenon. In this region,  $Q_{app}$  increases rapidly from 160 to 335 kJ per mol. Instability region at high strain rates is associated with adiabatic heating, which causes flow localization and cracking. The rather small variability of  $Q_{app}$  and a wide region of stability imply that ingot Al-2024 exhibits simple flow behavior with a relatively large processing window.

The P/M Al-2024 processing shown in Fig. 5.28B clearly shows different and more complex behavior than that of the ingot Al-2024 shown in Fig. 5.28A. The increased variability of  $Q_{app}$  and the reduced regions of stability are due to nonequilibrium microstructure along with prior particle boundary (PPB) defects produced during powder processing. In the testing ranges,  $Q_{app}$  values are in the range 167–418 kJ per mol. Microstructural evidence showed that at low temperatures (<375°C), cracking at the PPBs occurs at low strain rates, while adiabatic shear banding occurs at high strain rates. Manifestation of high temperature—low strain rate instability identified in the processing map was in the form of wedge cracking. The material undergoes dynamic recovery at temperatures below 400°C while dynamic recrystallization was observed in the ranges 400–450°C and 0.0001 to 0.01 per second. The process of dynamic recrystallization is considered to be highly beneficial in eliminating the PPBs and reconstituting the microstructure, which gives rise to significant improvements in mechanical properties. This analysis shows that the safe and optimal processing window for hot working of P/M Al-2024 is more restricted than that of the wrought or ingot material due to increased microstructural complexity introduced by rapid solidification.

The plastic flow behavior of P/M Al-2024 is further complicated by the addition of  $\text{SiC}_w$ , which is a rigid ceramic phase in a plastically deforming matrix. The processing map for P/M Al-2024 with 20 v/o  $\text{SiC}_w$  is shown in Fig. 5.28C. Comparison of this map with that of the P/M Al-2024 (Fig. 5.28B) reveals that the  $\text{SiC}_w$  dispersion significantly restricts the processing window. The  $Q_{\text{app}}$  values estimated for the composite are in the range 377–1047 kJ per mol and vary sharply throughout the temperature and strain rate ranges of testing. Safe processing range for the composite occurs over a narrow range of temperature (475–525°C) and strain rate (0.0001–0.01 per second) in which dynamic recrystallization of the matrix is the dominant microstructural mechanism. The addition of  $\text{SiC}_w$  is found to promote dynamic recrystallization by increasing the dislocation density in the matrix during deformation. Detailed microstructural analysis revealed that several damage processes occur under various processing conditions. Cavitation and whisker fracture occurs around 300°C/0.1 per second, cracking at the prior particle at 300°C/0.0001 per second, matrix kinking in the region of 550°C/0.1 per second, and dynamic grain growth around 550°C/0.0001 per second.

The narrow processing window for P/M Al-2024-20 v/o  $\text{SiC}_w$  composite material is validated through scaled up extrusion experiments using 76.2 mm diameter x 152.4 mm length billets. Fig. 5.29A shows the photograph of the product after extrusion at 500°C and a nominal strain rate of 0.01 per second. Under these processing conditions, dynamic recrystallization of the matrix material occurs, which allows the  $\text{SiC}$  whiskers to flow without fracture. It was also observed that a critical whisker aspect ratio of approximately 20:1 is maintained when deformed in the design range, which holds key in providing improved balance of mechanical properties in the composite. The whisker-matrix plastic flow behavior under these processing conditions can be visualized analogous to that of “logs flowing in a stream.” Fig. 5.29B shows photograph of a product extruded at 500°C and a strain rate of 0.1 per second, which exhibits gross unstable flow resulting in fir-tree cracking. These experiments demonstrate that the safe processing window predictions made in the previous section are accurate, and greater care should be exercised in controlling the process parameters during hot working of the composite to avoid defects.

Increases in microstructural complexity tend to reduce the size of the safe processing window. This fact is well known and established in Metals Handbook by Dieter (1988). This was demonstrated in this case study using processing maps for different forms of Al-2024 materials. The influence of microstructural complexity on the safe hot working range is illustrated in Fig. 5.30. Relatively, the microstructural complexity increases in the order wrought, ingot, P/M, and P/M with  $\text{SiC}_w$ . Fig. 5.30 shows the upper ( $T_{\text{upper}}$ ) and lower ( $T_{\text{lower}}$ ) temperature limits for safe hot

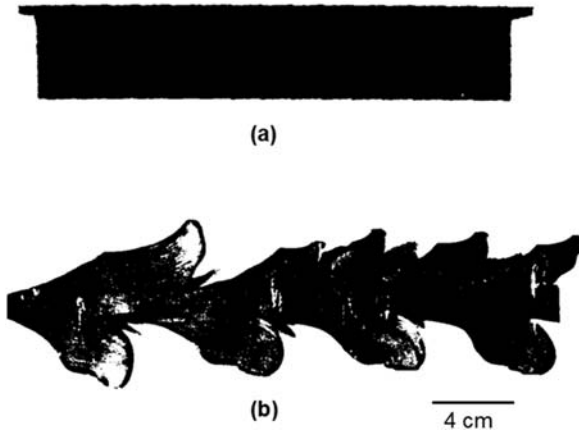


FIGURE 5.29 Photographs of P/M Al-2024 with 20 v/o  $\text{SiC}_w$  composite products extruded at (A) 500°C and 0.01 per second and (B) 500°C and 0.1 per second (Used with permission from [Malas et al., 2004](#); Elsevier).

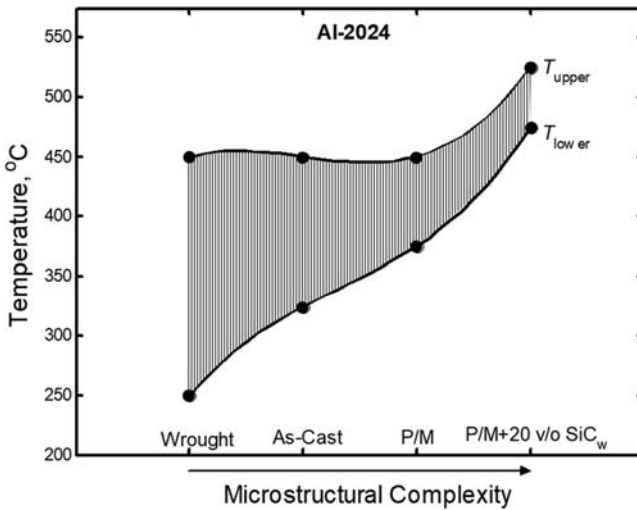


FIGURE 5.30 Influence of microstructural complexity on the safe hot working temperature range for Al-2024 material systems (Used with permission from [Malas et al., 2004](#); Elsevier).

working of these different Al-2024 conditions. This figure clearly reveals that the safe processing temperature range narrows as the microstructural complexity increases and correspondingly demands greater process control.

## 5.13 Stainless steel forging microstructure and property control case study

AISI 316 stainless steel is a very common austenitic stainless steel, and its primary alloying constituents after iron are chromium, nickel, molybdenum, and small quantities of silicon, phosphorus, and sulfur. The hot deformation behavior of austenitic stainless steels have been studied extensively. Venugopal (1996) conducted an industrial validation of 316L stainless steel (SS) processing maps using hot forging, rolling, and extrusion processes. 316L is an extra low carbon version of 316 SS.

The processing map shown in Fig. 5.31A is for 316L SS workpiece in the solution-annealed condition with an equiaxed grain structure. The processing window highlighted on the map corresponds to a stable region where the activation energy is fairly flat and corresponds to dynamic recrystallization. These processing conditions are desirable because microstructure can be controlled much more precisely, and there is reduced sensitivity to process variation. Fig. 5.31B shows the grain size variance to be 7  $\mu\text{m}$  within the temperature range of the process design window. The grain size variance increases to more than 20  $\mu\text{m}$  as processing conditions move further away these ideal conditions. Materials with uniform microstructures possess reduced statistical variability in the mechanical properties of the final product. This result is substantiated (Fig. 5.32) using tensile strength measurements on 316L samples that were forged over a range of temperatures.

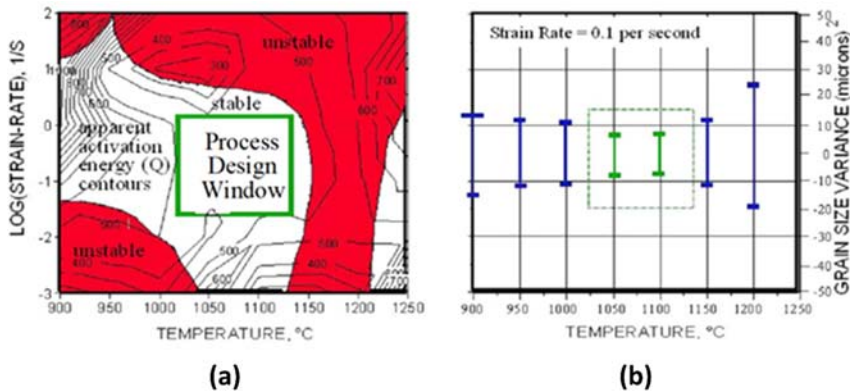


FIGURE 5.31 316 SS processing map with design window and measured grain size variations over range of temperatures and 0.1 per second conditions (copyright 1998 from optimal design of thermomechanical processes using ideal forming concepts by Malas and Frazier (1998); Reproduced by permission of Taylor and Francis Group, LLC, a division of Informa plc.).

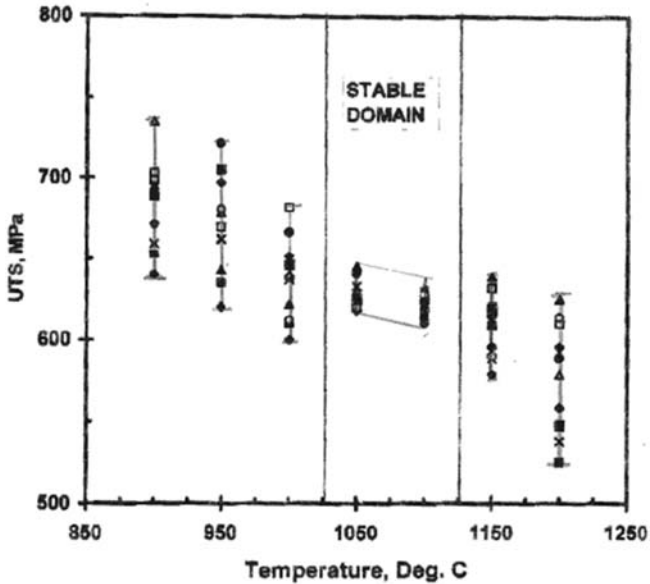


FIGURE 5.32 Room temperature tensile strength properties of 316L Stainless steel products forged at strain rate = 0.15 per second over a range of hot working temperatures (Venugopal, 1997).

This case study demonstrated how the optimal processing windows can be used to more precisely control microstructures and properties in the final products. Significant gains in sustainable manufacturing are realized from both the reduced uncertainty of material properties and the increased robustness with respect to process variations. For example, less material could be required to cover factors of safety in product design, and less scrap material would be needed for manufacturing process development on the shop floor.

## 5.14 Summary

Material development and the proper selection of new or improved manufacturing processes have major impacts on energy and natural resources conservation, as well as reducing the overall carbon emission outputs. Sustainable manufacturing requires changes to traditional approaches that are driven by cost and product performance. More efficient ways for making parts must be explored. Special processing techniques such as equal channel angular extrusion, high-pressure torsion, cryo-rolling, and asymmetric rolling could significantly reduce the number of processing steps for making products.

The selection and control of material processing conditions throughout the supply chain have significant impact on quality, cost, and delivery of the manufactured products. Specific knowledge about the workpiece material behavior under processing conditions is an important input to the product and process design activities. Material processing maps provide a useful framework for optimization of hot deformation processing conditions in terms of workpiece temperature and strain rate. The DMM approach was explained for identifying processing regimes where desirable material behavior exists and damage mechanisms are avoided. Case studies are examined to show productivity benefits and the importance of understanding material pedigree for process optimization and sustainable manufacturing.

## References

- Ashley, S., 1994. Improved aluminum extrusions. *Mechanical Engineering-CIME* 116 (6), 20. June.
- Charpentier, P.L., et al., 1986. *Metallurgical Transactions A* 17A, 2227.
- Dadras, P., Thomas, J.F., 1981. *Metallurgical Transactions A* 12A, 1867.
- Dieter, G.E., 1988. *Metals Handbook*, vol 14. ASM, Metals Park, OH, p. 367.
- Frost, H.J., Ashby, M.F., 1982. *Deformation Mechanism Maps*. Pergamen Press, New York.
- Gegel, H.L., 1988. In: Arsenault, R.J., Beeler, J.R., Easterling, D.M. (Eds.), *Synthesis of Atomistics and Continuum Modeling to Describe Microstructure, Computer Simulations in Material Science*. ASM Metals, Park, OH, pp. 291–344.
- Gegel, H., Nadiiv, S., Raj, R., 1980. Dynamic effects on flow and fracture during isothermal forging of a titanium alloy. *Scripta Metallurgica* 14, 241.
- Gegel, H.L., et al., 1988. *Modeling Techniques Used in Forging Process Design, Metals Handbook, ninth ed.*, vol 14. ASM International, Metals Park, Ohio, pp. 417–438.
- Grant, P., Mason, T., 2013. Section A: new and advanced materials and section B. Chemistry input into the manufacturing of novel materials and future trends in food manufacturing 1–56.
- Gurney, F.J., 1978. A Phenomenological Mechanism for the Occurrence of the Extrusion Central Burst Defect, Air Force Materials Laboratory Technical Report. AFML TR-79-4031.
- Malas, J.C., 1999. Unpublished Research at Materials & Manufacturing Directorate. Air Force Research Laboratory, Ohio.
- Malas, J.C., Frazier, W.G., 1998. Optimal design of thermomechanical processes using ideal forming concepts, *Integration of Material. Process and Product Design* 229–236.
- Malas, J.C., Seetharamen, V., 1992. Using material behavior models to develop process control strategies. *Journal of Occupational Medicine* 44, 8–13.
- Malas, J.C., Venugopal, S., Seshacharyulu, T., 2004. Effect of microstructural complexity on the hot deformation behavior of aluminum alloy 2024. *Materials Science and Engineering* 368 (1–2), 41–47.
- Martin, J.W., Doherty, R.D., 1976. *Stability of Microstructure in Metallic Systems*. Cambridge University Press, New York.
- Pecchia, D., 1993. Air Force Deal to Aid Aluminum Makers, *The Vindicator* (Ohio Newspaper). Youngstown, Ohio, 4 July 1993.
- Prasad, Y.V.R.K., et al., 1984. *Metallurgical Transactions A* 15A, 1883–1891.
- Prasad, Y.V.R.K., Rao, K.P., Sasidhar, S. (Eds.), 2015. *Hot Working Guide: A Compendium of Processing Maps*, second ed. ASM International.

- Raj, R., 1981. *Metallurgical Transactions A* 12A, 1089.
- Riahi, M., Ehsanian, M.H., Asgari, A., Djavanroodi, F., 2017. On a novel severe plastic deformation method: severe forward extrusion (SFE). *International Journal of Advanced Manufacturing Technology* 93, 1041–1050. <https://doi.org/10.1007/s00170-017-0561-1>.
- Semiatin, S.L., Lahoti, G.D., 1982. The occurrence of shear bands in isothermal hot forging. *Metallurgical Transactions A* 13, 275.
- Sutherland, J.W., Richter, J.S., Hutchins, M.J., Dornfeld, D., Dzombak, R., Mangold, J., Robinson, S., Hauschild, M.Z., Bonou, A., Schönsleben, P., Friemann, F., 2016. The role of manufacturing in affecting the social dimension of sustainability. *CIRP Annals - Manufacturing Technology* 65, 689–712. <https://doi.org/10.1016/j.cirp.2016.05.003>.
- Valiev, R.Z., Estrin, Y., Horita, Z., Langdon, T.G., Zehetbauer, M.J., Zhu, Y.T., 2015. Fundamentals of superior properties in bulk NanoSPD materials. *Materials Research Letters* 1–21. <https://doi.org/10.1080/21663831.2015.1060543>.
- Venugopal, S., 1997. Unpublished Research at Indira Gandhi Centre for Atomic Research, India.
- Venugopal, S., et al., 1996. Industrial validation of processing maps of 316L stainless steel using hot forging, rolling, and extrusion. *Materials Science and Technology* 12, 11.
- Verlinden, B., Leuven, K.U., Engineering, M., 2004. Severe plastic deformation of metals. *Metals Metallurgy*.
- Xu, Q., 2019. Thoughts on the development of new material technology. *IOP Conference Series: Materials Science and Engineering* 493. <https://doi.org/10.1088/1757-899X/493/1/012122>.
- Yu, H., Lu, C., Tieu, K., Liu, X., Sun, Y., Yu, Q., Kong, C., 2012. Asymmetric cryorolling for fabrication of nanostructural aluminum sheets. *Scientific Reports* 2. <https://doi.org/10.1038/srep00772>.

# Sustainable product development process

*Amer Ali<sup>1</sup>, and Jay S. Gunasekera<sup>2</sup>*

<sup>1</sup> Management Consultant, Austin, TX, United States; <sup>2</sup> Department of Mechanical Engineering, University of Delaware, Newark, DE, United States

## 6.1 Innovation and product development

Product development is a central part of new product introductions in a competitive market environment. This activity or phase is termed as the most critical in the growth and expansion of businesses and corporations. Through novel products and ideas, new companies are formed, become household names, and set the foundation for subsequent growth and innovation. There are numerous companies that have followed this pattern and many of them are case studies in product development and innovation.

While we have seen many companies that have risen to fame, garnered accolades, and generated immense benefits for all stakeholders, they have all had product development as a central strategy for these actions and growth. Kodak, IBM, Apple, GE, and Xerox are all examples of the development, new products, growth, and market dominance to an extent. However, when the strategies and the focus on product development and innovation stutter, some dominant players become stagnant giving rise to newer and more nimble competition.

Materials, ferrous or nonferrous, and manufacturing processes are instrumental in creating innovations in industrial, residential, commercial, retail, and service industries. Material development and manufacturing process development are generally at the forefront in facilitating disruptive technologies and innovations. Because of the importance of sustainability and the formulation of product goals, these need to be addressed up-front in a product development scheme. Hence, sustainability and sustainable manufacturing processes need to be a

major activity at the concept phase of any project and will require a cross-functional team working on it throughout the product development cycle (Cooper, 2004; McGrath, 1996). This chapter describes the elements of the product development process with a view on manufacturing processes and sustainability development in a new product.

## **6.2 Product innovation strategy**

Innovations drive sustainable growth and a potential winning path to lead the market in respective areas. Having product innovation and product strategy is critical to outline the life cycle of current and future products, taking into account customer feedback, market needs, differentiation, and market share. This activity, when carefully analyzed in the various industries, is tied to the New Product Development (NPD) function, the robustness of the system, and the efficacy of execution (Christensen, 2000). Some of elements that are critical are outlined below:

- Product Vision
- Voice of Customer
- Product and Platform Strategy
- Key Metrics Development

## **6.3 Product life cycle**

Product life cycles have been defined in various methodologies in literature and practice. A better approach to the product life cycle is to concatenate the product life cycles in a circular pattern with the next generation improvements, or introduction and replacement of a new product. The previous stages provide for design ideas, thought leadership, strategic continuity, and learnings. An example of the product life cycle is illustrated in Fig. 6.1.

The product cycle commences with the concept phase which is developed with inputs from customer and business needs. This is enhanced further with a business feasibility study, setting up of marketing requirements, the product operational metrics, financial assumptions, timeline estimates, and resources required. This is generally the stage in which high-level product needs, the product development time, the potential costs, the key performance requirements, etc., get outlined. Hence, this is a critical step for manufacturing processes and material selection to identify business and performance matching materials, processes, and attributes.

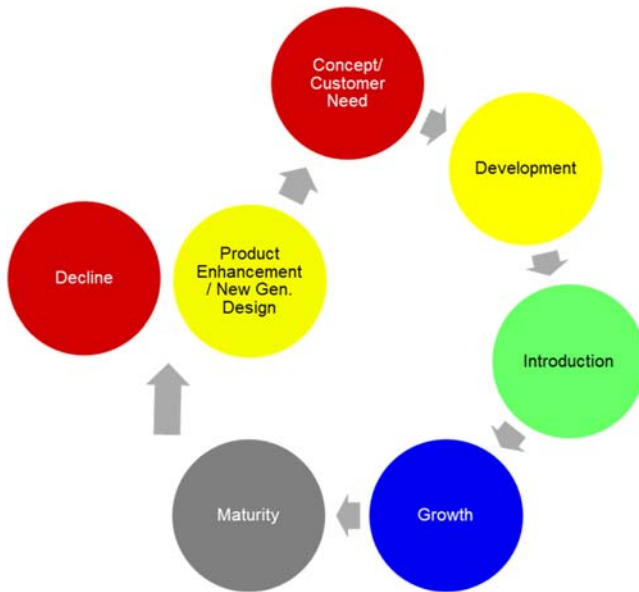


FIGURE 6.1 Schematic of a product life cycle.

Material selections are critical and have to be considered across the complete life cycle and even potentially into the net phases of product enhancement. This will be discussed further, but one of the requirements being stipulated by some countries is the “product take back” or product recyclability initiative. This is also referred to as Extended Producer Responsibility (EPR) laws. Per this rule, manufacturers will be required to take back the product at the end of the product life and utilize sustainable separating techniques for recyclability, reuse, etc. In other words, manufacturers will be responsible for the collection and proper disposal of their products. As the responsibility of the product utilized will lie on the manufacturer, it will be imperative to design and select materials and processes that will meet the longer-term criteria.

This stage should have adequate representation from the design team, the material scientists, the operations team, etc., to help define the initial concept, the development of the targets, resource requirements, KPIs, etc., that would feed and stay with the product development and the product life cycles.

The next stages of the product life cycle include the following:

- **Introduction:** This is the launch of the product after the successful culmination of the development cycle. The product is introduced to the market and exposed to the customers during this cycle.

- Growth: A product ramp-up, depending on the success, would require expansion of the manufacturing operations, capacity, and support infrastructure. Also, important in this phase are aftermarket, service, customer support, warranty, and quality.
- Maturity: A product reaches steady state production and consumption during the maturity stage. Any potential issues during ramp-up, quality improvement, and performance improvement, marketing campaigns, have been undertaken and resolved at this point.
- Decline: While most all products may have a decline, ideally this phase is one that should be perceived before its occurrence, and the potential next step in the circular life cycle is invoked to avoid this step. This could be a product enhancement or developing a replacement product, depending on the business case, and developed through a similar process.
- Preplanning and Lessons Learned: One of the aspects is to have a product feedback loop to tabulate and collect the product benefits, customer likes, improvements needed, growth prospect, and competitive landscape comparison. The feedback is employed to make next level improvements, devising sales, and marketing strategies, developing technologies and solutions for a potentially new product.
- Next Generation Product Goals: Astute technical and business professionals have an incubator of technologies and product ideas that could be developed and deployed at the optimum time, especially, to expand and launch the next generation of products. Ideation processes combined with strategic product road mapping and market needs add to the technology and product incubator of ideas.

The product life cycle is a cyclical process throughout the multiple generations of the product. Adhering to such a system with discipline provides the tools to keep the product fresh and competitive.

## 6.4 Product development process

A formal product development process is part of the operational system of most all companies involved in developing products and solutions. Various acronyms and names are used to describe the development process that include New Product Introduction (NPI), Product Development Process (PDP), New Product Development (NPD), Staged Gate Process, etc., with many organizations using internal acronyms or names.

Generally, the product development process is to facilitate:

- Concurrent development
- Risk identification, management, and reduction
- Timeline and financial control and management
- Management decision at critical phases/stages

The result of this approach, if followed properly, is a product that is launched on-time, meeting the desired financial metrics, the risks are managed and mitigated, environmental health and safety (EH&S) and sustainability targets are achieved, the operations are geared up for delivery, customer support is established, and marketing collaterals, after market, service, spare parts, operational manuals, etc., are setup for performance excellence.

There are many factors that lead to the successful product development and execution of the process. Following are some of the more important aspects:

- Senior management involvement
- Discipline
- Multifunction teams and involvement
- Scalable, lean, and flexible approach and organization

There are a couple of product development process approaches. One is a Waterfall method and the other is an Agile process. Agile is an iterative process to develop and deliver product in short bursts to customers. Software development generally employs the Agile development process with multiple teams working on different aspects simultaneously. The waterfall method is more sequential and a linear process, with one development phase leading to the next. The end product is delivered at the culmination of the project. This is the general process employed in automotive, aerospace, industrial, and consumer industries.

---

## 6.5 Stage gate processes

---

A stage gate process (also called NPD, NPI, PDP, etc.) is designed and broken up into stages or phases in the development cycle. This process may start many years before the product enters the marketplace. The project duration depends on the complexity of the product and the development involved. For example, aerospace and automotive are more complex and will have a longer development time.

An example of a stage gate process is shown in [Fig. 6.2](#). The stage gate process commences with a concept stage. This is followed by development stages, product launch, and product feedback stages. An important part of the process is to involve all the key internal organizations and functionalities that touch or may interface with the product. Each stage

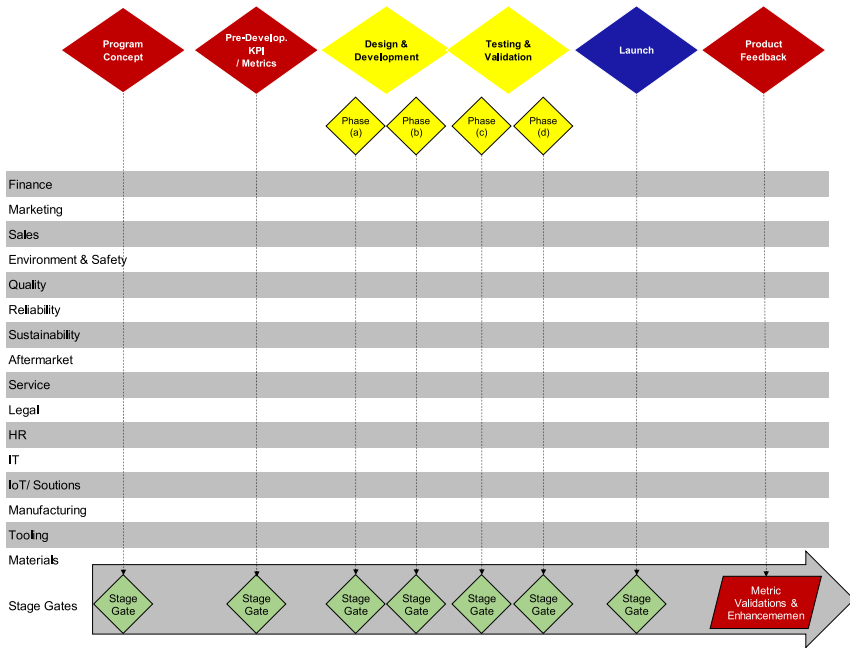


FIGURE 6.2 Stage gate process.

culminates with a stage gate or a management review process, generally involving the senior managers with the project team. It is important to mention that there may be senior management representative or representatives who own and sponsor the project.

The organizations listed on the left in Fig. 6.2 are examples that are involved in the product development process. It is critical to have all key functionalities involved concurrently in the product development process. In actual practice, organizational layout of companies will likely be different and tailored for their operations. In addition, the program phases and the stage gates may be classified differently in some organizations, or may have additional or fewer phases and stage gates.

The concept development phase culminates by presenting the business case for a new product. A heavy amount of work is required by marketing and finance organizations to develop the business plan, the product road maps, product characteristics, and the financial plan along with the other functionalities. Involvement of human resources along with other groups for resource planning for the development, ramp-up, and postdevelopment is identified at this stage.

An important part in each phase is the use of appropriate tools. Some tools that can be employed will be mentioned later. These tools could be utilized for risk identification and management, financial calculations,

design analyses, manufacturability, serviceability, etc. The purpose of the tools is to help develop a “business model” or baseline of the product. Thereafter, these tools help establish go-forward criteria and assist in determining and managing key program metrics. The tools and metrics are developed and updated throughout the program development process and a summary is presented at stage gates.

The second stage may be a preliminary stage to the development phase. Proof-of-concept demonstration, technology, and product market readiness questions, resource allocation and approvals, technology road map, operations development, training, and customer support tools are outlined. A viable proof of concept and prototype presented at the stage gate will help successfully complete this stage. The later stages will use this preliminary design and will be refined, enhanced, and addressed in each phase.

The program development stage and the testing stage are generally the longer phases. These phases go through the steps of actual product design, build, testing, tooling development, operations/factory readiness, etc.

Prior to the stage gate for product launch, the product team through the stage gate process demonstrates the functionality of the product, operations readiness, certification of quality function requirements, and formation of customer support infrastructure—all that would support the ramp-up and operations of the product.

---

## 6.6 NPD organization

---

The new product development (NPD) process should be disciplined having a formal hierarchical structure. This of course depends on the size of the project. Some of the smaller sized projects may not require a full-time project manager, but may have a matrix organization that is led by a project leader. The structure is generally lean to facilitate efficacious decision-making and operations. A general organization structure for a large new product development project can be illustrated in [Fig. 6.3](#).

---

## 6.7 Decision making process

---

The stage gates hold the decision-making process to approve and commence work for the subsequent next phase. This approval may trigger other subapprovals for project funding, capital requirements, resource planning, layout changes, intellectual property, legal approvals, etc.

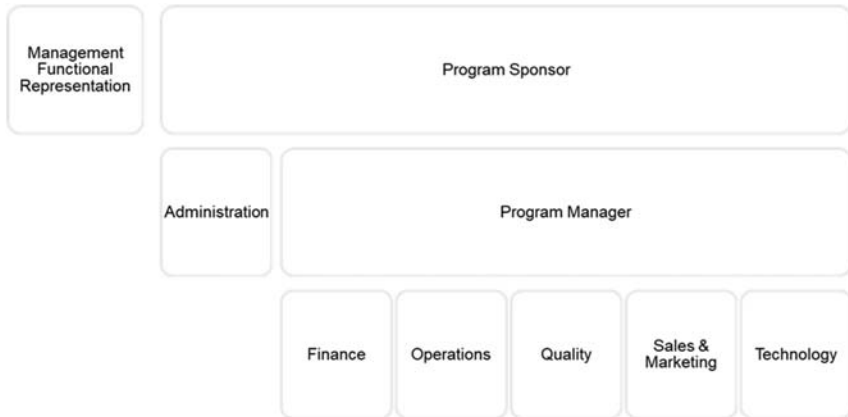


FIGURE 6.3 Example organization of a product development project.

At each phase of the new product development process phase, the project team develops and outlines the program KPIs (Key Performance Indicators), the updated timeline, capital, expense, resource status, and the projected next steps. It is important to identify the major risks at each phase and manage and mitigate them as a team. In addition, the business target updates are to be affirmed along with the timeline. These outputs are the responsibility of the project team. Any critical issues or any risks that require the sponsor and the management team intervention are separately presented for succinct guidance and approval.

## 6.8 Program release and launch

The product launch is initiated after the successful completion of the launch Stage Gate. The project team demonstrates successful completion of the following:

- Product launch plan
- Product verification
- Quality metrics adherence
- Manufacturing readiness
- Product ramp-up management
- Marketing and sales plan
- Risk control and mitigation demonstration
- Financial roadmap confirmation

At this stage, the original target and metrics for the product are compared and reverified. Any deviation from the target may require

additional work or may require a remedial action plan, if approved by the management team and if it is not deemed critical to the product launch.

## 6.9 Proactive feedback mechanism and lessons learnt

The product development cycle, in a broader sense, is a subset of the product life cycle. The product life cycle is circular and periodic. In the same manner, the product development process dove-tails into the circular product life cycle process. In the initial period, perhaps a year or so after the product launch, the feedback and learning are handled by the project team to address issues effectively and expeditiously. Thereafter, the product becomes a part of normal operations. Any subsequent development, enhancements, or improvements are handled as part of normal sustaining operations for the products.

The product life cycle is a living process, as is the maintenance of the product through this process. Through market feedback, marketing insights, continuous improvement programs, operational improvements, and quality enhancements, the product is continually upgraded so that it maintains and/or achieves market leadership.

## 6.10 Design processes, tools, and design for sustainability

Various tools and methodologies have been developed that are used to develop and enhance products. While many tools and techniques can be applied to a product or process in its life cycle, it makes good sense to use and employ them especially for a new product as part of the new product development process. A new product represents a clean sheet and is easier to baseline, assign targets, and build the design based on these techniques.

There are a number of tools that are used, but only a few are mentioned. Tools are simply a technique in a larger tool box. A good practitioner uses the best and most appropriate tool for the job at hand. This does not mean that all tools need to be employed at all times if they are not practical. However, some of the tools below, or their equivalent, will likely be used for new products.

- Design for X (DFX)

Design for X is an approach to optimize the total cost, manufacturing, service, performance, safety, supply chain, and the environmental footprint. The “X” in DFX represents all the functional organizations, similar to those presented in [Fig. 6.2](#) in the stage gate process. The approach is to

analyze the complete value stream of the product in a cross-functional methodology. This approach may use additional tools or subtools, but relies on the cooperation of the organization. A cross-functional linkage of DFX is shown in Fig. 6.4. DFX sessions are carried throughout the new product development process. The list of actions and ideas from a DFX are prioritized based on impact, risk, ease of implementation, and savings opportunity. Each subsequent DFX in the next phase of the stage gate process uses the previous session as an input, analyzing the action items and identifying new ideas for improvement. The results from DFX can result in impacting the following:

- Cost
- Quality
- Service
- Manufacturing
- Lean
- Environmental footprint
- Make versus Buy
- Design for Manufacturing and Assembly (DFMA)

This is a widely employed tool for products that emphasizes on the ease of manufacturing and optimized assembly operations. This is a part of two-pronged processes: Design for Manufacturing and Design for Assembly. This approach was initially promulgated by Geoffery Boothroyd of the University of Massachusetts (Boothroyd et al., 2011). It focuses on reducing the production cost and the time to manufacture. This is accomplished by reducing the number of components and the ease of manufacturing of parts. Part number proliferation in not only complex but indirectly has a large cost associated with it. By reducing the number of parts, the cost is impacted and reduced. The ease of fabrication makes

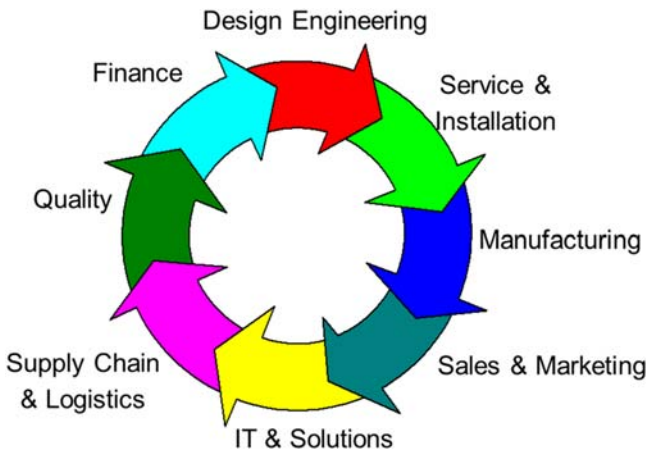


FIGURE 6.4 Dfx cross functionality.

for faster time to market and less operations time, combining functionalities, which can result in further reduced costs. At the same time, the product is designed to have a less complex manufacturing process that helps in operations.

- Design for Serviceability

Service and aftermarket roughly may contribute up to 40% of the product revenue. In some products, such as the aerospace industry, it may be higher over the product life cycle. In addition, ease of service is a direct correlation with customer needs for service and reliability. Taking the service aspect of the product, one facilitates the maintenance and use phase in the product life cycle. The purpose of this approach is to:

- Enhance the product life
- Reduce operational cost
- Reduce repair and service time
- Improve quality and reliability
- Ease of issue detection

Some of the guiding principles involved in this approach include part standardization, simplification, ease of access, ergonomics, safety, training, and ease of operations.

- Design for Safety and Quality

It is widely known that quality cannot be inspected. Rather, quality is designed and embedded in the product. The new product development process facilitates this approach to design safety and quality starting from scratch in the concept phase. This entails that quality is embedded in the product value stream from material handling, manufacturing processes and subprocesses, packaging and unpackaging, installation, service, and use by customer. Hence, all the safety and quality guidelines and metrics are identified and addressed in the development process.

Quality and safety must have a set of objectives that are identifiable or quantifiable to be measured and tracked. Some of the examples include product dimensions, fit, form and function, sharp edges, ergonomics, etc. The quality metrics include key quantifiable attributes of a product that satisfy customer, production, or process limits. By employing this methodology and using appropriate tools, quality and safety features and performance characteristics are embedded into the product operation and into the product value stream.

Some of the common tools employed include the following:

- Six sigma
- Statistical process design
- Design of experiments
- Mistake proofing
- Critical to quality

- Design simplification
- Failure mode and effects analysis (FMEA)
- Design for environment

The Design for Environment (DfE) principal entails quantifying and reducing the environmental impact of the product through its value stream and product life cycle. As shown in Fig. 6.5, the approach deals with minimizing environmental impact by analyzing material selections, material extraction, and amount of recycled material from an initial standpoint. The objective is to identify materials that are less energy intensive to extract and produce, the materials are recyclable, and some recycled material can be employed in material production. Production, product use, energy consumption, material handling, and transportation are optimized in development and use phase. The emphasis in this exercise is to have a lower energy consumption profile, minimal packaging requirements, and decrease emissions and avoid environmentally harmful emissions. Finally, it is desirable to have products with enhanced life in the life cycle. At the end of product life, the product, components, and materials should be easily segregated. Further, the components and

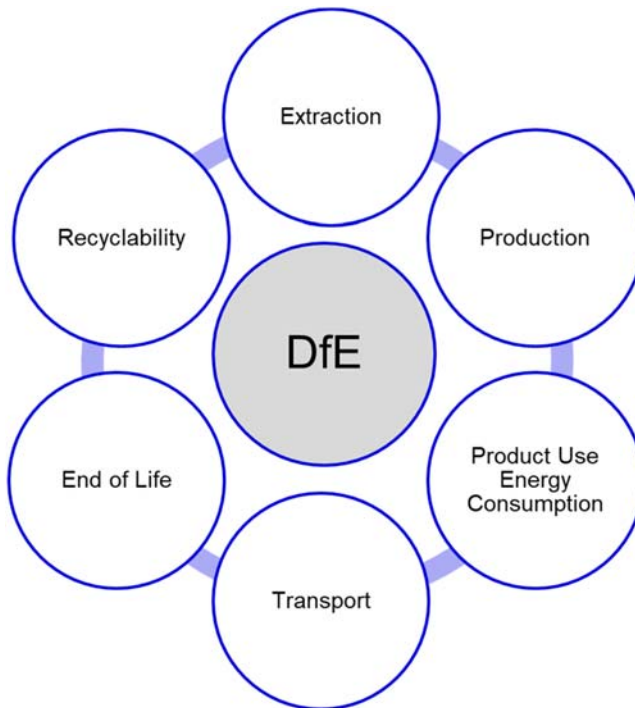


FIGURE 6.5 Design for environment (DfE) approach.

materials should be designed such that they are safe, and could be recycled or reused with lower energy transformation costs.

Commercial software are available that have built-in material libraries with relevant information or new material profiles can be added. These software can interface with other design systems and packages to determine the DfE and environmental impact on a normalized scale. In this manner, better environmental selections can be employed in selecting materials, processes, and design.

## **6.11 Sustainability in remanufacturing**

Remanufacturing is a process to reformulate and utilize nonfunctional, used, and dismantled products. These are transformed into new functional products or sub-assemblies with the same or longer life span. Remanufacturing is an environmentally friendly process. It supports products to be reutilized rather than being sent to a landfill. This helps in supporting the circular economy.

Life cycle analysis (LCA) or DfE evaluates environmental compliance and performance through the product life cycle. The potential contribution to the environment is assessed by collating the resources employed, contribution to climate change, air emissions, and toxicity impact. LCA links the product's environmental performance and the ultimate impact to the environment and society.

It is important to have measurable tools to quantify the remanufacturing content. Several attempts have been presented to quantify and link the life cycle content or remanufacturing content. Normalized scales have been developed and deployed to discern between different approaches, materials, and remanufacturing content (Han et al., 2021).

The material flows of circular product life cycle are shown in Fig. 6.6, starting from raw material extraction to disposal. Important considerations in the remanufacturing process include the following:

- Input requirements
- Materials recovery
- Waste management
- Remanufacturing economics

## **6.12 End of life design**

Product take back or EPR laws are an important part of the circular life cycle economy. To incentivize sustainable practices through design, education, innovation, reuse, and remanufacturing, many organizations and

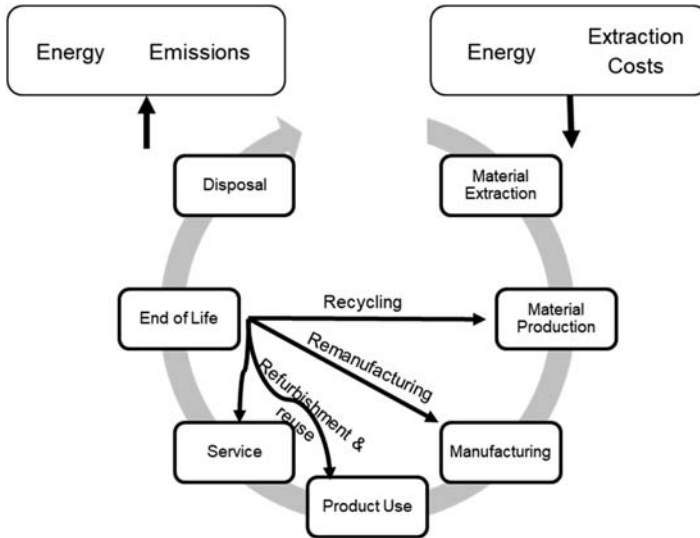


FIGURE 6.6 Product life cycle material flows.

governments are formulating laws that would make the manufacturer and producer responsible for the end-of life disposal, reuse, refurbishment, and recycling of the product. These approaches, designs, and laws aim at preventing waste at the source, the discernible selection of optimum materials and processes, and cost-effective operation and use of the product, with an environmentally and economical life cycle through product end-life (Johnson et al., 2014).

End-of-life design makes the product development process more critical in thinking and designing the product through sustainable operations, making for easy disassembly and recycling for reuse, as needed.

- Country and Regional Regulatory Requirements

In the electronics industry and under their guidance, the U.S. Environmental Protection Agency (EPA) hosted a forum to “harness the collective power of the electronics community and identify shared priorities that will advance domestic end-of-life electronics management” (EPA, 2014). In addition, there are currently 25 US states that have passed electronic waste laws and take back laws (Quinn, 2021).

About a dozen US states are also formulating laws on EPR on packaging. These laws are designed to hold the producers accountable for managing packaging materials through the use and recycling phases.

The European Union currently has product take back laws and policies on managing the end of life and recycling of many products and materials (OECD, 2001), such as the following:

- Batteries and accumulators
- Construction and demolition waste
- Vehicles
- Mining
- Electrical and electronic equipment (RoHS).
- Waste from electrical and electronic equipment (WEEE)

Japan and Korea also have end-of-life vehicle directives holding producers and importers responsible for use of resources. The laws address the collection and recycling of vehicles, as well as the recycling and use of hazardous substances. Many of these EPR and product take back laws are extending into other consumer products.

- Recyclability

EPR is being added throughout the product life cycle in the area of recycling and waste management. The financial impact is currently borne by customers, citizens, governments, organizations, and producers.

EPR and take back laws and regulations, mentioned earlier, have a heavy emphasis on the end-use of consumer products with the aim to minimize the environmental impact. Many of the laws entail waste management, tire recycling, electronics usage and disposal, collection of batteries, plastics and postage disposal, oil waste management, chemical collection and disposition, etc.

Hence, there is a need to develop strategies in the product development process to account for the complete product life cycle. Selection of materials, processes, designs, tooling, use condition, serviceability, etc., all impact the life cycle cost and help in making the product more sustainable.

- Remanufacturing

Remanufacturing is a process which can transform a previously used, worn, or even a nonfunctional product to be reused, recovered, and rebuilt. The process entails the collection of end-of-life products and components and processing them to make them useable, meeting the performance and specifications of the original part or component. Remanufacturing is an integral part of the circular economy designed to reduce waste and cost, by extending the life of products (Haziri et al., 2019; Paterson et al., 2017).

Some of the basic steps in a remanufacturing operation include the following:

- Collection of components and products
- Part inspection
- Disassembly
- Removal of hazardous materials, chemicals, and fluids (if any)

- Part refurbishment
- Quality and specification verification
- Component assembly
- Component testing and approval

### **6.13 Future outlook and direction**

A futuristic and strategic outlook is imperative in product management to keep the product refreshed, relevant, and aimed at having a leading position in the marketplace. This is a part of product life cycle management and the product development process. Some of the pertinent areas include technology management and future development and preparation.

Technology is at the core of most products. Products gain a leading position or keep the differentiation through technical innovation and leadership. Innovation and technology upgrades are properly managed through a robust technology management process. The objective is to create and have a technology incubator of ideas that are generated through an ideation process, as well as feedback from customers, ideas generated from operations, etc. Next generation materials, processes, and manufacturing would be a part of this process. The ideation process facilitates new ideas, assigns priorities, recommends a development path forward, and identifies commercialization potential. An offensive strategy includes intellectual property and implementation of an approach to commercialize ideas and protect innovative ideas from proliferating. Some aspects of the technology management process are listed below:

- Ideation process
- Idea incubator
- Technology readiness roadmap
- Intellectual property strategy
- Phased development
- Parallel execution
- Product development velocity
- Design and management tools
- Regulatory landscape
- Safety and design requirements
- Customer preference evolution

### **References**

Boothroyd, G., Dewhurst, P., Knight, W., 2011. Product Design for Manufacture and Assembly. CRC Press.

- Christensen, C., 2000. *The Innovator's Dilemma: When New Technologies Cause Great Firms to Fail*. Harper Business Publishers.
- Cooper, R., 2004. *Product Leadership: Pathways to Profitable Innovation*. Perseus Book Group.
- Han, J., Pingfei, J., Childs, P., 2021. Metrics for measuring sustainable product design concepts. *Energies* 14 (12), 3469. <https://doi.org/10.3390/en14123469>.
- Haziri, L., Sundin, E., Sakao, T., 2019. Feedback from remanufacturing: its unexploited potential to Improve future product design. *Sustainability* 11 (24), 4037.
- Johnson, M.R., McCarthy, I.P., 2014. Product recovery decisions within the context of extended producer responsibility. *Journal of Engineering and Technology Management. Engineering and Technology Management for Sustainable Business Development* 34, 9–28.
- McGrath, M., 1996. *Setting the Pace in Product Development: A Guide to Product and Cycle-Time Excellence*. Butterworth-Heinemann.
- OECD, 2001. *Extended Producer Responsibility: A Guidance Manual for Governments*. OECD Publishing, Paris. <https://doi.org/10.1787/9789264189867-en>.
- Paterson, D., Ijomah, W., Windmill, J., 2017. End-of-Life decision tool with emphasis on Remanufacturing. *Journal of Cleaner Production* 148, 653–664.
- Quinn, M., 2021. Could be year for packaging EPR, nearly a dozen state bills in play. *Waste Dive*. [www.wastedive.com](http://www.wastedive.com).
- United States Environmental Protection Agency (EPA), September 2014. , *Sustainable Materials Management (SMM) Electronics Reuse and Recycling Forum*. Arlington, VA.

This page intentionally left blank

# A case study on sustainable manufacture of Ti–6Al–4V ultralightweight structurally porous metallic materials by powder metallurgy route

*Venugopal Srinivasan<sup>1</sup>, and James C. Malas<sup>2</sup>*

<sup>1</sup>National Institute of Technology Nagaland, Chumukedima, Nagaland, India; <sup>2</sup>Materials and Manufacturing Directorate, Air Force Research Laboratory, Dayton, OH, United States

## 7.1 Introduction

The weight of the components or parts is a major concern in automotive, aerospace, marine, and medical for bioimplantation applications. In order to cater to the demand of these applications, a few critical components made up of ultralightweight materials are being manufactured and used. There are numerous methods and fabrication techniques have been developed in the manufacturing of the components of ultralightweight materials. The advancements in the development of Structurally Porous Materials (SPM) are also progressing in phase with the requirements through extensive research. A new class of Ti–6Al–4V alloy ultralightweight SPM has been developed through powder metallurgical route for aero-space applications. In practice, the billets of ultra-lightweight SPM are being produced through Powder Metallurgy (P/M) route and near-net-shape and net-shape components are manufactured through deformation processing (forming) of the billets of ultra-lightweight SPM. The P/M route can be divided into three general steps: (i) powder making, (ii) preform or blank making (consolidation) and (iii) Plastic working of

blanks or preforms. These three steps are instructive on different manufacturing methods and techniques and they have major impact on sustainability. Each step in the P/M process is important because defects, which occur during these steps generally, cannot be removed by sintering or heat treatment. The powder-making step is the topmost important one because the fundamental powder characteristics of the individual particle such as composition, size shape, microstructure, and surface structure are controlled by the particular powder making process used to produce the particles. These powder characteristics, in turn, control the technological properties, especially the aggregate properties of the consolidated material. The manufacturing of powders through Rapid Solidification Technology (RST) followed by hot-consolidation and subsequent plastic working is a preferred route for manufacturing SPM billets because this route ensures the required shape with desired mechanical properties. Two of the factors most strongly influencing the subsequent consolidation and plastic deformation are: (i) the particle size distribution and (ii) the environment which controls the average cooling rate besides the particle shape, particle contamination, surface layer and specific surface area of the powders produced through RST. The particle size controls the hardness, composition gradient, surface layer and microstructure. In the case of high-temperature alloys systems, the discrete quenching rate for each particle associated with a particular particle size distribution leads to the development of wide range of microstructures because of the formation of intermetallic compounds. The surface layers of metal-alloy powders are enriched with impurities and therefore, the physical properties may differ considerably from those of the base material. This layer may be enriched with some solute element, an oxide layer, a hydrated oxide layer, a metallic carbide, an intermetallic compound, or a combination of these, e.g., an oxide layer plus an intermetallic compound. During consolidation, the preform or billet/blank-making process is controlled largely by the powder-making process and by the physical properties of the individual particles. A powder compact before application of external pressure consists of many physical particles, which are uniform in composition. At tap density, these powders usually retain their shape and they can exert pressure on the surrounding medium. However, they cannot resist tensile stresses. The compact at tap density occupies a position somewhere between a liquid and a solid. The technological characteristics of this powder depend upon the resistance of the individual particles to compression, shearing and bending. The properties of this compact continuously change during pressing. The bonds between individual particles in contact with other particles are due to adhesion at the contact surfaces. Particles, which are soft and plastic form strong adhesion bonds during cold compaction, while those, which are hard and less ductile do not. The compacting pressure tends to cause the particles to

shift and occupy the most stable geometric position; this is accompanied by contact distortion and shearing of the particles. The basic particle shape tends to remain undistorted. The green strength is principally controlled by the strength of local adhesion. Vacuum hot pressing (VHP) or hot isostatic pressing (HIP) must be used to densify a compact when the particles are hard and resist compression. The aggregate properties of the compacts produced by VHP or HIP should be equivalent to the service properties of the components. If the aggregate properties of the billets are to be enhanced further forming operations are required on the compacts. In this case, the aggregate properties of the billet should be at least equivalent to the plastic-working properties. Plastic working of P/M preforms is being used for shaping and strengthening the finished product. Plastic working has been observed to improve markedly the strength of the matrix and imparting a better surface finish. Besides, controlled plastic working of preforms or billets is now being considered as a means of strengthening and increasing their workability. This additional working is also thought to be essential for controlling the properties in the finished shape. Plastic working is required for overcoming powder making defects such as discrete foreign particles and size-distribution-related defects. In view of the inherent advantages, the deformation processing routes on the P/M preforms/billets are always preferred for manufacturing components. Rolling and forging routes are being preferred for manufacturing of SPMs because of amenability of controlling the development of microstructure for achieving desired strength and quality in the components in these processes. Further, the Rolling and forging routes offer conservation of materials, adoptability for automation, sustainability and ability to produce economically a near-net-shape parts possessing a required set of service properties. The SPM is sandwiched between two Ti/Ni/Stainless Steel face sheets for manufacturing of sheet metal components. The blistering formation between the SPM core material and the face-sheet material is the severe defect observed during the rolling of Ti-6Al-4V SPM and the formation of blister shall be avoided to maintain the porosity level without any decrease (i.e., lower relative density). Materials modeling of the behavior of materials under processing conditions and process modeling and simulation are being done for the purpose of understanding and designing of forming operations. A finite element method (FEM) forming simulation capability and material modeling for the Ti-6Al-4V alloy ultralightweight SPM have been developed for designing rolling process for this new class of materials.

Process modeling for microstructure and shape optimization is required to achieve both engineering and manufacturing functional objectives. Since the rheological behavior of this new class of Ti-6Al-4V alloy ultralightweight SPM is envisioned to have both plastic and fluid

flow behavior, a new yield criterion was developed that takes these two factors into account. The forming model for the new class of low-density structural materials made it necessary to extend the current yield function for porous materials in ANTARES FEA application to account for the incompressibility of the gas contained in the workpiece material.

Axisymmetric compression tests were done using the samples of 5 mm diameter and 7.5 mm height in the temperature range from 200°C to 1000°C at isothermal condition and at the strain-rates of 0.0001 s<sup>-1</sup>, 0.001 s<sup>-1</sup>, 0.01 s<sup>-1</sup>, 0.1 s<sup>-1</sup>, 1 s<sup>-1</sup>, and 10 s<sup>-1</sup>. Table 7.1 provides the data on the flow stress in the temperature range from 700 to 1000°C at the strain-rates of 0.0001 s<sup>-1</sup>, 0.001 s<sup>-1</sup>, 0.01 s<sup>-1</sup>, 0.1 s<sup>-1</sup>, 1 s<sup>-1</sup>, and 10 s<sup>-1</sup>.

Table 7.2 provides the data on the flow stress at 0.2 plastic strain in the temperature range from 200 to 1000°C at the strain-rates of 0.25 s<sup>-1</sup>, 1 s<sup>-1</sup>, 2.5 s<sup>-1</sup>, 10 s<sup>-1</sup>, and 16 s<sup>-1</sup>.

The constitutive equation and the yield criterion for the Ti–6Al–4V SPM have been developed using the above flow stress data. The constitutive behavior model of SPM was implemented in the ANTARES FEA application. Metallurgical analysis of 64% relative density SPM alloy compression test specimens and rolled sheet specimens show blistering formation between the SPM core material and the face-sheet material. A Dynamic Material Model (DMM) processing map for the 64% relative density SPM alloy was developed for the purpose of defining the processing parameters of temperature and strain rate for achieving good rolled product without the development of gas blisters. The results for the microstructure and dynamic material modeling show how understanding the fundamental mechanical and microstructural stability characteristics of the material may help in selecting the process parameters.

### 7.1.1 Modeling of SPM by the finite element method

The constitutive behavior model of SPM was implemented in the ANTARES FEA application. The main difference between rigid viscoplastic (incompressible material) FEA and this version of ANTARES FEA is that the P/M version allows for compressibility because the material is porous. The von-Mises yield criteria was also enhanced by adding  $J_1$  (Hydrostatic stress) in addition to the typical  $J_2$  (Shear stresses) used for incompressible material plasticity. The general constitutive equation in FEM formulation is given by the following:

$$\sigma^* = 2\mu\dot{\epsilon} + m\lambda m^T \dot{\epsilon} \quad (7.1)$$

where

$\sigma^*$  is the stress vector

TABLE 7.1 Flow curves (MPa) of Ti-6Al-4V Structurally Porous Material (64% relative density).

Strain rate, s <sup>-1</sup>	Temperature, °C	Strain								
		0.00	0.0125	0.025	0.05	0.1	0.2	0.3	0.4	0.5
0.0001	700	111.90	130.00	140.48	142.86	140.00	134.52	126.19	119.05	116.67
	750	47.02	67.86	72.50	75.30	76.39	75.00	70.80	70.24	70.24
	800	25.00	32.14	35.71	39.29	43.75	45.24	45.24	44.64	44.05
	850	13.69	17.86	20.24	22.62	24.50	25.00	25.00	25.00	25.00
	900	7.14	10.71	12.25	13.00	14.25	14.88	14.88	14.88	14.88
	950	5.95	8.34	9.50	10.14	10.74	10.74	10.74	10.74	10.74
	1000	4.5	5.30	6.25	7.14	8.33	7.85	7.14	7.14	7.14
0.001	700	165.52	195.45	205.68	211.36	219.32	214.77	211.36	204.55	202.27
	750	73.91	127.27	140.91	146.59	150.00	146.59	140.91	135.23	132.95
	800	58.70	82.95	88.64	94.32	96.59	97.43	95.91	90.91	86.36
	850	27.27	45.45	49.89	51.25	54.55	56.82	55.68	55.00	54.55
	900	27.00	27.70	28.25	29.55	30.75	31.82	31.82	31.82	31.82
	950	10.22	11.37	11.75	12.50	13.63	15.75	15.91	15.91	15.91
	1000	10.00	10.22	10.5	11.00	11.36	11.36	11.36	11.36	11.36
0.01	700	232.00	262.50	271.88	281.25	291.67	297.92	296.88	294.79	293.60
	750	150.00	169.79	178.33	197.50	210.42	219.17	219.17	219.17	219.17
	800	90.00	100.00	104.17	114.58	125.00	142.71	146.88	150.00	150.00
	850	65.00	77.08	80.21	83.33	89.58	95.83	100.00	103.13	103.13
	900	54.00	54.12	54.15	54.16	54.17	54.17	54.17	54.17	54.17
	950	24.00	26.50	27.00	27.08	27.48	27.08	27.08	27.08	27.08
	1000	18.00	19.79	20.26	20.83	20.83	20.83	20.83	20.83	20.83
0.1	700		310.42	318.75	327.08	331.25	329.17	325.00	320.83	320.83

Continued

TABLE 7.1 Flow curves (MPa) of Ti–6Al–4V Structurally Porous Material (64% relative density).—cont'd

Strain rate, s <sup>-1</sup>	Temperature, °C	Strain								
		0.00	0.0125	0.025	0.05	0.1	0.2	0.3	0.4	0.5
1	750		252.08	268.75	287.50	300.00	306.25	310.42	316.67	320.23
	800		178.13	184.00	194.00	208.33	213.54	218.75	226.04	230.00
	850		154.17	160.42	168.75	181.04	202.08	210.42	218.75	226.04
	900		66.70	67.71	65.63	64.58	68.75	69.79	72.92	75.00
	950		46.80	46.88	46.88	46.88	46.88	46.88	46.88	46.88
	1000		31.25	32.00	33.70	37.50	40.50	41.00	41.67	41.67
	700		360.53	373.68	389.47	400.00	395.26	380.26	367.10	365.50
	750		306.00	326.00	350.00	364.00	364.00	350.00	344.00	342.00
	800		270.00	292.00	310.50	321.00	326.00	320.00	314.00	312.00
	850		195.00	202.00	210.00	214.00	217.00	218.00	218.00	218.00
10	900		132.00	138.00	143.00	145.00	146.00	146.00	146.00	146.00
	950		76.00	78.00	80.00	82.00	82.00	82.00	82.00	82.00
	1000		63.50	67.50	70.00	72.50	74.00	74.00	74.00	74.00
	700		411.76	423.53	444.12	461.77	458.83	447.06	438.23	438.23
	750		347.06	364.71	382.35	400.00	400.00	397.06	394.12	385.29
	800		297.06	310.00	323.35	350.00	351.47	344.12	338.24	335.29
	850		276.17	283.82	294.12	307.35	314.71	311.73	308.82	308.82
	900		188.64	190.91	195.59	200.00	204.41	205.88	207.35	208.82
	950		130.88	132.35	132.40	133.82	138.23	138.23	138.24	138.24
	1000		100.00	97.95	100.00	105.88	110.00	111.76	114.71	117.64

TABLE 7.2 Flow stress at 0.2 plastic strain in the temperature range from 200 to 1000°C at the strain-rates of 0.25 s<sup>-1</sup>, 1 s<sup>-1</sup>, 2.5 s<sup>-1</sup>, 10 s<sup>-1</sup>, and 16 s<sup>-1</sup>.

Ti-6Al-4V flow stress (ksi) values at 0.2 plastic strain					
Temperature, °C	Strain rate, s <sup>-1</sup>				
	0.25	1.0	2.5	10.0	16.0
200	146.67	151.00	153.93	158.48	160.05
400	123.77	127.60	130.20	134.23	135.63
600	86.57	94.60	100.31	109.62	112.97
800	41.90	51.30	58.64	71.80	76.80
900	19.11	23.30	26.56	32.39	34.64
1000	7.92	9.50	10.71	12.85	13.66

$\dot{\epsilon}$  is the strain rate vector

$\mu$  and  $\lambda$  are the Lamé's Constants and will be functions of temperature, strain, strain-rate, relative density, and flow stress in general.

$$m = \begin{bmatrix} 1 \\ 1 \\ 1 \\ 0 \\ 0 \\ 0 \end{bmatrix} \text{ for the 3D problem.}$$

The elemental velocity field in the FEM is approximated as follows:

$$u = N^T v \quad (7.2)$$

where  $v$  is the nodal velocity and  $N$  is the shape function matrix. By differentiating Eq. (7.2), we get the following:

$$\dot{\epsilon} = Bv \quad (7.3)$$

where  $B$  is called the strain-rate matrix.

Therefore, by substituting Eq. (7.3) into Eq. (7.1), we get the following:

$$\sigma^* = (2\mu\dot{\epsilon} + m\lambda m^T)Bv \quad (7.4)$$

For SPM we found from the constitutive equation developed as

$$\mu = \frac{Y_{SPM}}{2\dot{\epsilon}_p A} \quad (7.5)$$

$$\mu = \frac{Y_{SPM}}{2\dot{\epsilon}_p(3-A)} \quad (7.6)$$

where  $Y_{SPM}$  is to be calculated from the yield criterion developed and

$$A = 2(1 + \nu) \quad (7.7)$$

$\nu$  is the Poisson's ratio and is related to the relative density.

To incorporate the SPM behavior into ANTARES, it is assumed that the total stress for SPM will be additive of the general stress  $\sigma^*$  and the pressure inside the pores  $p$ , that is,

$$\sigma = \sigma^* + mp \quad (7.8)$$

where  $\sigma$  is the total stress for SPM. Now substituting Eq. (7.8) into Eq. (7.4), we get the following:

$$\sigma = (2\mu + m\lambda m^T)Bv + mp \quad (7.9)$$

For the numerical calculation, within each time step, the pressure inside the pores  $p$  will be considered to be constant and it will be updated after each time step;  $p$  will be calculated from the volume change of the pores. With the above finite element model and the yield criterion developed for SPM, the SPM behavior is implemented in to ANTARES, but to run and verify the model, the relation of Poisson's ratio with the relative density and pressure inside the pores need to be found out and also the flow curves for the representative SPM material. The simulation of deformation process is being carried out on the ANTARES 3D tetrahedral element to solve problems with complex tool geometry which requires continuous remeshing of the finite element model. ANTARES has got the automatic remeshing capability.

## 7.2 ANTARES interface

A new graphical user interface for ANTARES has been developed. This new interface will add functionality for solving such problems as those associated with creating multielement groups for simulation of billet with mixed materials and generating multistage control for simulations that involve tool changes and changes of boundary conditions during the forming processes. These new capabilities are important for simulations of forming with SPMs, because SPM billet consists of porous materials in the center and the dense material as the frame or face-plate sheet on the outer layer.

### 7.2.1 Material behavior modeling

Material behavior modeling has been done using a Ti–6Al–4V SPM. The relative density of this material was 64% although the relative density of this particular SPM alloy was less than the relative density that the SPM developers will use in a production environment; it does reveal some very important characteristics of this class of materials. The microstructure of the material in its as-received condition was characterized using quantitative metallography, and its morphological characteristics were compared to the microstructure of the specimens, which were deformed by constant temperature and strain-rate compression testing. The morphology of the gas pores provided very useful information about the deformation mechanisms during processing of the SPM. The microstructure of rolled SPM in the vicinity of where large gas bubbles formed between the face sheet and the SPM core material was studied metallographically and compared to the SPM microstructure which evolved as a result of compression testing. A possible mechanism for bubble formation was deduced from these studies.

A DMM processing map was developed to provide a framework for understanding the deformation process. This map is based on the flow stress behavior as a function of temperature, strain-rate, and strain, which was determined by constant temperature and strain-rate compression testing. This map defines the intrinsic stability of the work piece material as it undergoes forced dissipative flow during metal forming. This map will be discussed later with respect to the microstructures that were observed, but it is apparent from the DMM processing map that the workpiece material during rolling was being deformed by unstable deformation processes.

### 7.2.2 Microstructure comparisons

As-received Ti–6Al–4V SPM (64% relative density).

These comparisons will be based on the gas pore morphology. The as-received gas pore morphology of the hot isostatically pressed material has two basic features:

1. The gas pores have an irregular surface.
2. The gas pores are randomly distributed.

These characteristics are believed to be typical of all the as-received hot isostatically pressed SPM. Fig. 7.1 shows the microstructure of as-received SPM.

Compression Tested Specimens:

The morphological characteristics of the compression-tested specimens are as follows:

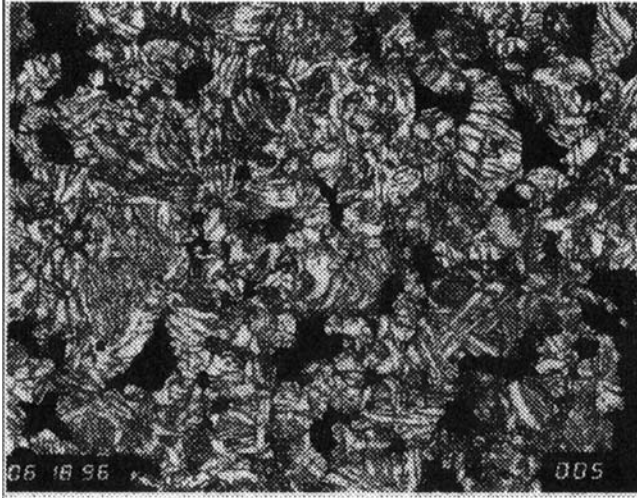


FIGURE 7.1 The microstructure of as-received SPM at 100 X.

1. The surface of the gas pores is irregular. Inside the pore, part of the surface is concave, indicating that the gas pressure inside the pore is increasing. Another part of the pore surface has the appearance of finger-like structure. This structure is a result of the matrix phase material that is flowing into the gas pore structure. The occurrence of the finger-like structure suggests that the flow stress of the matrix phase is greater than the pressure of the gas pore under the observed conditions of deformation temperature and strain-rate.
2. The orientation of the gas pores is in the direction of the stress axis.

Fig. 7.2 shows typical microstructure showing morphology of gas pores in the sample deformed at  $850^{\circ}\text{C}$  and strain-rate of  $1\text{ s}^{-1}$ . During deformation, both the matrix material and the gas pores deform during deformation, and the pore morphology indicates that pressure is increased inside the gas pores during deformation, which is indicative of an SPM that is increasing in relative density as a result of deformation.

### 7.2.3 Rolled specimens

The rolled specimens had a relative density that was greater than the compression tested specimens. The relative density of these specimens was about 85%. The important feature of the rolled material is the distribution of the gas pores and their morphology relative to the morphology of the compression tested material. The characteristics of the gas pores are as follows:

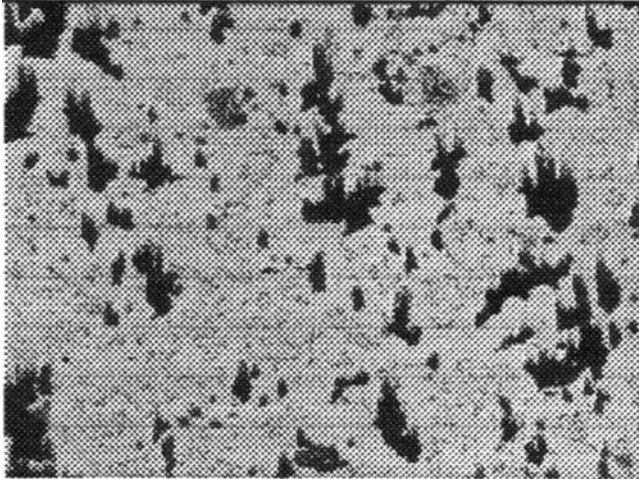


FIGURE 7.2 Typical microstructure showing morphology of gas pores in the sample deformed at 850°C and strain-rate of  $1 \text{ s}^{-1}$  at 200 X.

1. The pores remain uniform during rolling.
2. The deformation of the pores during rolling appears to be less than the deformation associated with compression testing.
3. The pores line-up in bands along the maximum shear stress lines. The bands form as a result of flow localization. It can be deduced that the banding structure results because of the matrix material which is being deformed under temperature and strain-rate conditions, which produce unstable flow localization conditions. In contrast, these processing parameters are stable conditions for the gas pores. It is believed that flow localization provides a mechanism for the gas to escape from the surface of the rolled product to form a blister between the SPM core material and the face-plate material. Fig. 7.3 is schematic diagram showing the state of stress during the rolling process and the variation of density of the porous material across the thickness of the rolled product. Fig. 7.4 provides a schematic diagram of the flow localization phenomena occurring during rolling of SPM.

Fig. 7.5A and B and Fig. 7.6A and B show the temperature distribution in the billet of SPM during the first pass (10% reduction on thickness on each pass) and second pass, respectively.

4. The volume fraction of gas pores is reduced in the region below the surface where gas bubble formed.

Fig. 7.7 exhibits the microstructure in the shear band devoid of gas pores and Fig. 7.8 depicts the microstructure adjacent to shear band

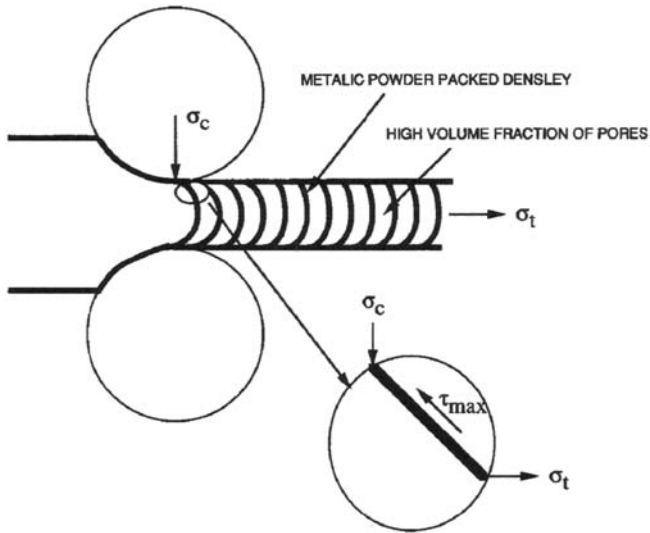


FIGURE 7.3 Schematic diagram showing the state of stress during the rolling process and the variation of density of the porous material across the thickness of the rolled product.

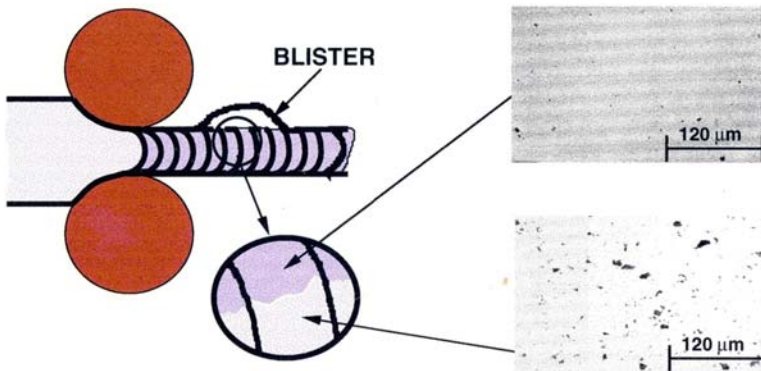


FIGURE 7.4 Schematic diagram of the flow localization phenomena occurring during rolling of SPM.

showing high volume of gas pores. The microstructure near the surface of the rolled SPM sheet below the surface where the gas bubble formed is shown in Fig. 7.9. Fig. 7.10 clearly shows that the gas has escaped from the SPM workpiece material.

### 7.3 Dynamic material model processing map

#### 7.3.1 DMM processing map

A DMM processing map was constructed from the material stability information, which is contained in a set of compression tests done as a

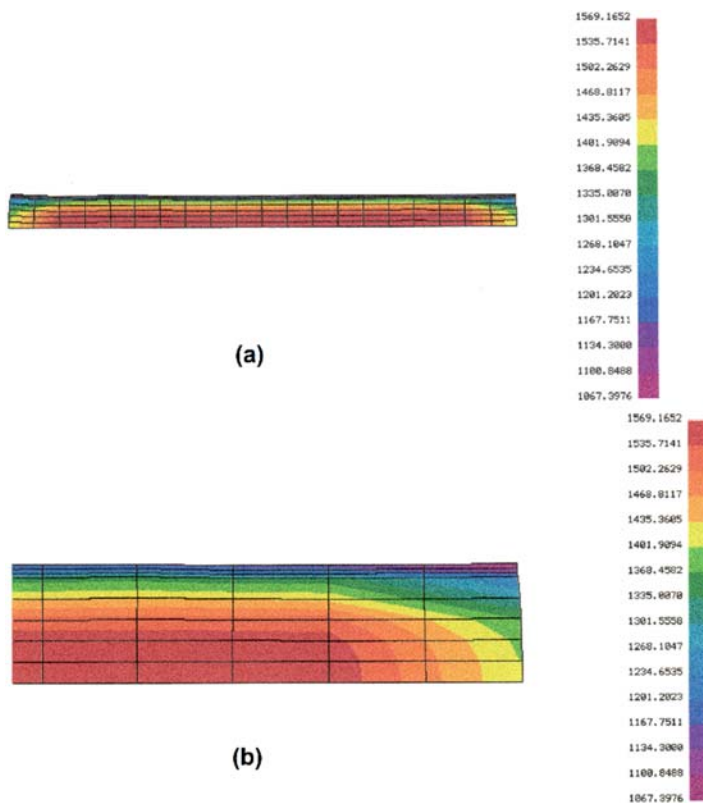


FIGURE 7.5 (A) The temperature distribution in the billet of SPM during the first pass (10% reduction on thickness on each pass) and (B) Magnified view of 5(A).

function of constant temperature, constant effective strain-rate, and deformation time. The DMM stability maps of Ti–6Al–4V SPM for 64% and 91% relative densities are given in Figs. 7.11 and 7.12, respectively. The DMM can present the following stability criteria:

1. Mechanical stability of the workpiece material
2. Microstructural stability of the workpiece material
3. Phase diagram stability (first-order phase transformation and singularities)
4. Activation energy criterion.

The DMM processing map shows the stable and unstable regions for the low-density (64%) SPM alloy. The microstructure investigations indicate that it is necessary to establish a balance between the mechanical stability of the matrix material and the mechanical stability of gas pores. To achieve this balance, the SPM material should be subjected to

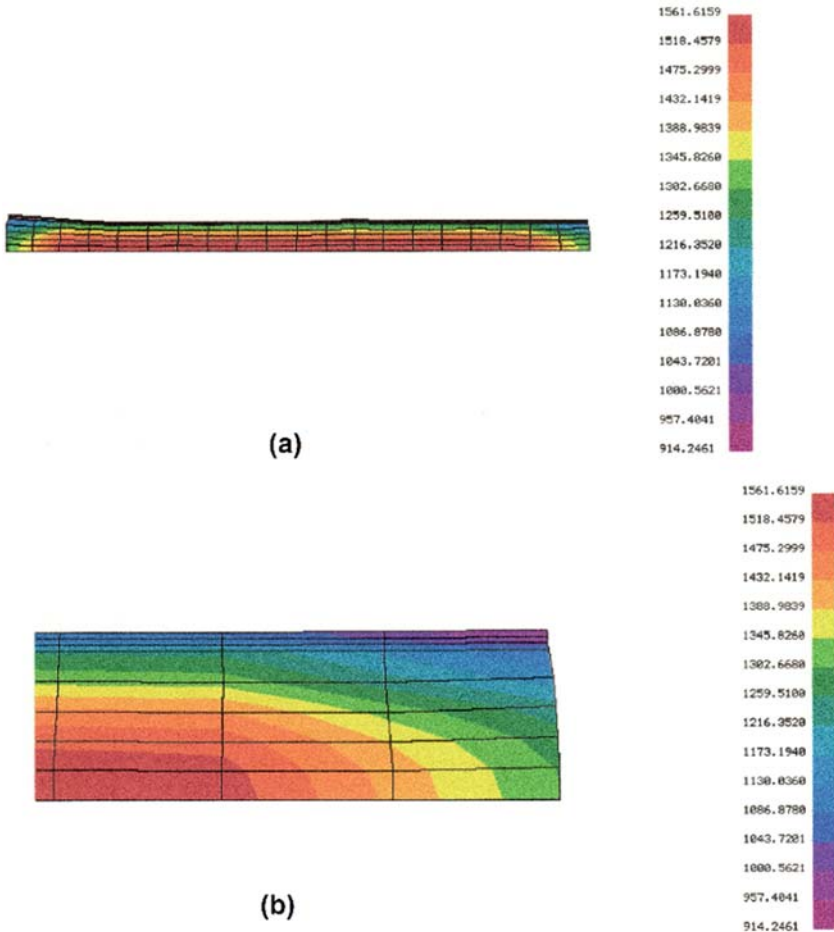


FIGURE 7.6 (A) The temperature distribution in the billet of SPM during the second pass (10% reduction on thickness on each pass) and (B) Magnified view of 6(A).

processing parameters, which cause stability for the forming process to lie on the boundary of the stable region, where the deformation process is bimodal in the sense of stability. When processing parameters of temperature and strain-rate line on this boundary, the flow stress of the continuous matrix material is approximately equal to the pressure in the gas pores, and this condition will result in a stable material flow process.

Calculations of the effective strain-rate in the subscale rolling process show this strain-rate to be of the order of  $10 \text{ s}^{-1}$ . Based on the DMM processing map, the rolling processes are being operated under unstable processing conditions. This statement can be rationalized also by considering the behavior of the flow curves for the workpiece material as the strain-rate is progressively increased.

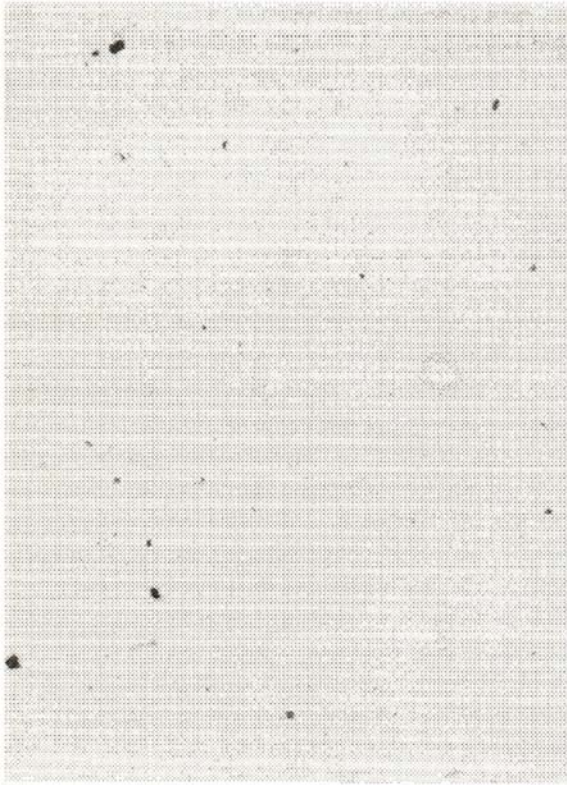


FIGURE 7.7 The microstructure in the shear band devoid of gas pores at 200 X.



FIGURE 7.8 The microstructure adjacent to shear band showing high volume of gas pores at 200 X.



FIGURE 7.9 The microstructure near the surface of the rolled SPM sheet below the surface where the formation of gas bubble is evident 200 X.

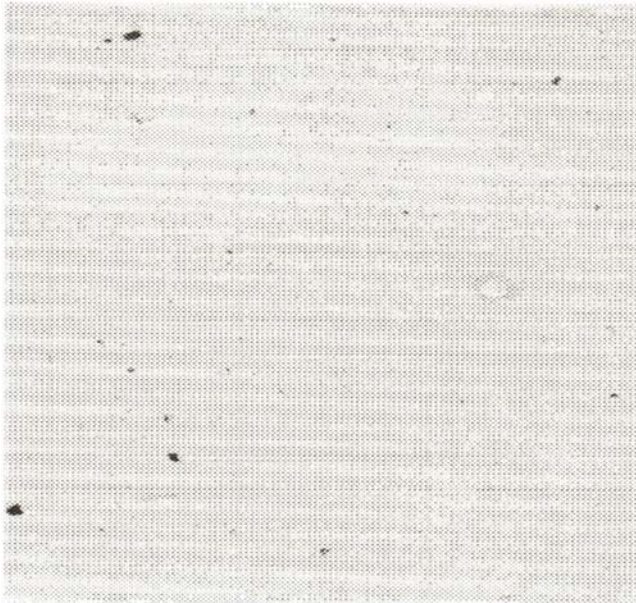


FIGURE 7.10 The microstructure of the rolled product free from gas pores; it clearly shows that the gas has escaped from the SPM workpiece material at 200 X.

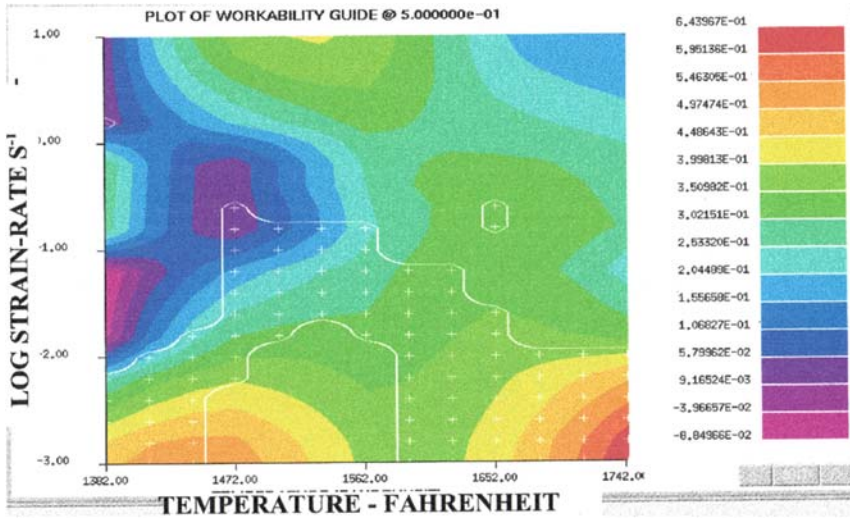


FIGURE 7.11 The DMM stability maps of Ti-6Al-4V SPM for 64% relative density.

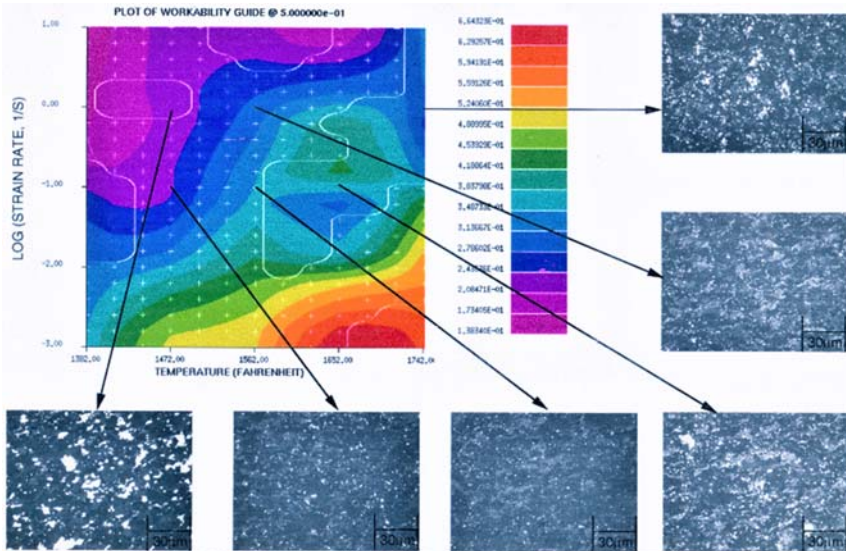


FIGURE 7.12 The DMM processing map for 91% relative density and the microstructure recorded on the samples deformed at various combinations of temperature and strain-rate exhibiting morphology of pores.

The flow curves for this material show smooth flow curves for all strain-rates until the strain-rate reaches 1 or higher. At these strain-rates, the flow curves become serrated as soon as the workpiece materials start to flow. The serrations are believed to be associated with the emission of gas due to the instability of the workpiece material. Since flow localization

was observed in the cross-section of the rolled sheet just below where a gas blister is formed during the rolling operation, the assumption of gas emission during unstable workpiece material flow and leading to blister formation appears to be reasonable.

The shape of the flow curves also shows a continuous rise in the flow stress as a function of strain during stable flow. With this type of flow stress behavior, the shape of the stability map will not change with time (deformation). Therefore, a possible solution for managing the emission of gas during rolling and the elimination of gas blisters is to operate the rolling process on the boundary of the processing map. Each roll pass shall be designed to preserve the stability conditions necessary to achieve stable forced dissipative plastic flow. The currently used processing parameters for the SPM material produce a strain-rate, which is about two orders of magnitude too large.

---

## 7.4 Summary

---

Materials modeling of the behavior of Ti–6Al–4V SPM under processing conditions using DMM processing maps and process modeling and simulation have been carried out. The plastic flow behavior of Ti–6Al–4V SPM has been evaluated in the temperature range from 200 to 1000°C and at strain-rates from 0.0001 s<sup>-1</sup> to 10 s<sup>-1</sup>. Rolling process has been modeled using FEM technique for the simulation of rolling of Ti–6Al–4V SPM. Using the above-mentioned material and process models, the formation of blister during rolling of Ti–6Al–4V SPM has been studied. This investigation suggests a possible solution for managing the emission of gas during rolling and the elimination of gas blisters to operate the rolling process on the boundary of the processing map. Each roll pass shall be designed to preserve the stability conditions necessary to achieve stable forced dissipative plastic flow. This case study on sustainable manufacture of Ti–6Al–4V ultralightweight structurally porous metallic materials by powder metallurgy route shows productivity benefits from understanding material behavior and process optimization analyses.

### Further reading

- Gegel, H.L., Gunasekera, J.S., Doraivelu, S.M., Malas, J.C., Morgan, J.T., Matson, L.E., 1982. Consolidation and Forming of P/M Porous Billets. Proc. of the III Conference on Rapid Solidification Processing. Gaithersberg, Maryland.
- Gegel, H.L., 1988. In: Arsenault, R.J., Beeler, J.R., Easterling, D.M. (Eds.), *Synthesis of Atomistics and Continuum Modeling to Describe Microstructure*, Computer Simulations in Material Science. ASM Metals, Park, OH, pp. 291–344.
- Malas, J.C., Seetharamen, V., 1992. Using material behavior models to develop process control strategies. *Journal of Occupational Medicine* 44, 8–13.

# Waste energy harvesting in sustainable manufacturing

*Steve Zhengjie Jia*

Product Engineering, Litens Automotive Group, Toronto, ON, Canada

## 8.1 Introduction

In the past decade, the sustainability issues in manufacturing industry have become a fundamental requirement, in addition to the traditional requirements for lower cost, better quality, and faster to market. More and more stringent standards and policies have come into effect to accomplish the task. The manufacturing industry is now required to minimize the overall environmental impact to society under a life cycle perspective. The sustainability in manufacturing industry generally includes three aspects (Narayanan and Gunasekera, 2019) such as (i) environmental sustainability—about planet, (ii) economic sustainability—about profit, and (iii) social sustainability—about people. Extensive research has been done to investigate the manufacturing sustainability including how to efficiently use materials and resources, and how to effectively reduce the energy consumption and wastes in the manufacturing processes. The manufacturing processes should be designed, optimized, and controlled with environmental sustainability in mind and the products produced from manufacturing should not be harmful to people during production and use in terms of health and safety.

Sustainability assessment in manufacturing processes is a multiobjective and interdisciplinary task, and a great challenge due to its inherent complexity and uncertainty. Sustainability is a concept and difficult to measure. A directly precise comparison of sustainability of different manufacturing processes/sectors can be impractical, but the reduction of energy consumption is a measurable target. Fig. 8.1 shows the world total final energy consumption over five main sectors (IEA, 2019). The industrial sector is the largest user of energy and accounts for 37% of the total global energy consumption in 2017. The energy consumption within the

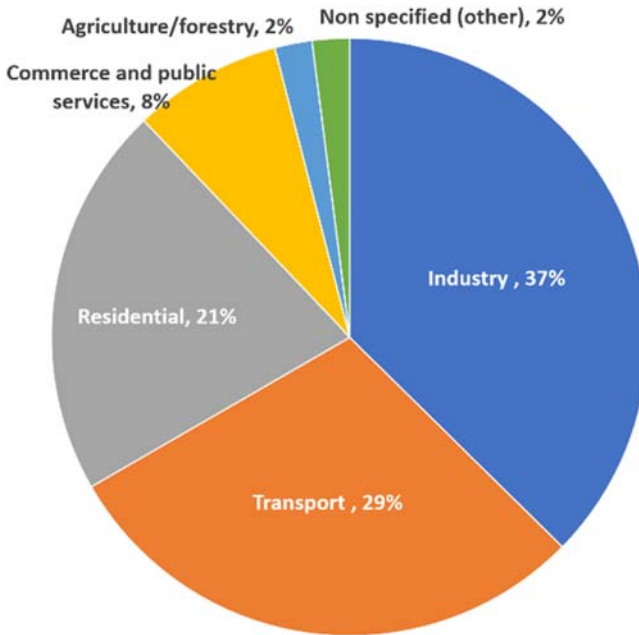


FIGURE 8.1 World total final consumption by sector 2017. Reproduced from: IEA, 2019. *World Energy Balances, an Overview*. [https://iea.blob.core.windows.net/assets/8bd626f1-a403-4b14-964f-f8d0f61e0677/World\\_Energy\\_Balances\\_2019\\_Overview.pdf](https://iea.blob.core.windows.net/assets/8bd626f1-a403-4b14-964f-f8d0f61e0677/World_Energy_Balances_2019_Overview.pdf).

industrial sector is shown in Fig. 8.2 (Fawkes et al., 2016). The chemicals and petrochemicals, iron and steel, nonmetallic minerals, and pulp and paper are the four industrial subsectors having the most energy consumption, which account for nearly two thirds of all industrial energy consumption. Therefore, improving the energy efficiency of these industrial subsectors should be prioritized. The energy efficiency is usually defined as the ratio of the useful energy output over the associated energy input. Improving energy efficiency in manufacturing processes is a process of technical advancement and the fundamental energy efficiencies tend to improve over time as the advancement and the invention of manufacturing technologies.

On the other hand, the renewable energy sources can be, wherever possible, used to replace the nonrenewable energy sources to reduce the “energy consumption,” which can help improve the overall energy efficiency and may bring economic and greenhouse gas benefits in certain situations, but does not improve the basic efficiency in any end-use process. Both the renewables and energy efficiency can contribute to achieving energy cost and environmental objectives. However, it has been reported that installing renewables is more expensive than improving energy

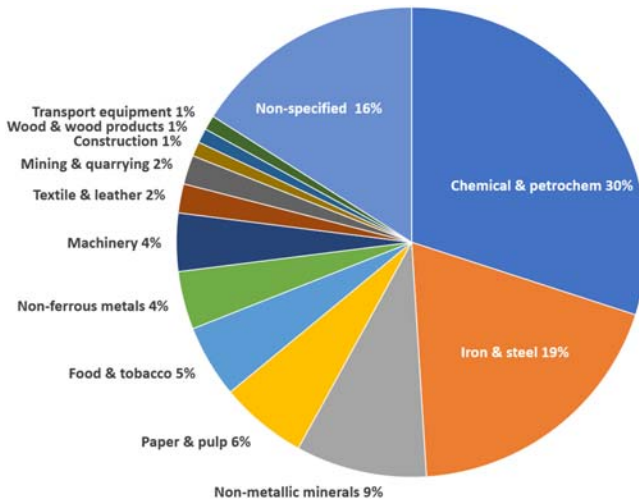


FIGURE 8.2 Breakdown of industrial energy use by sector 2004. Used with permission from Fawkes, S., Oung, K., Thorpe, D., 2016. *Best Practices and Case Studies for Industrial Energy Efficiency Improvement – an Introduction for Policy Makers*. UNEP DTU Partnership, Copenhagen. <https://europa.eu/capacity4dev/file/31409/download?token=kOYq7O5T>.

efficiency in term of a price-per-energy-unit basis (Fawkes et al., 2016). Therefore, improving energy efficiency may be implemented first and then to consider renewables. However, for any energy conversion process, there is a fundamental limit set by the laws of thermodynamics. Practically, there is no real-life technology that can reach that limit. In other word, the energy efficiency has a limit. Based on Cullen et al. (2011) research, 475 EJ of global primary energy resources including oil, coal, renewables, and nuclear were consumed, only 11% of which, 55 EJ were converted into useful energy for services such as motion, heat, cooling, light, and sound. In addition, as the reduction of the energy consumption by applying the renewable energy sources is not considered as the efficiency improvement, and as the efficiency improvement by advancing the technologies and/or invention of the new technologies has a limit, the waste energy harvesting can be an effective third means to further reduce the energy consumption, which is equivalent to the efficiency improvement.

### 8.1.1 Energy harvesting technologies

In the past years, the wasted energy harvesting has attracted a great attention and the wasted energy harvesting technologies have gained a great advancement. The energy harvesting technology has been now widely used to collect small amounts of energy from the environment to power various autonomous wireless, portable devices, especially for

long-term, low-power, and self-sustaining electronic systems. For example, to enable the emerging Internet of Things (IoT), energy harvesting is a key supporting technology to be used to power many wireless nodes that make up the IoT, as where batteries are impractical. Energy harvesting technology provides an attractive alternative to battery-operated systems in these situations. Energy harvesting technology using solar cells is another example that has been reported in many scientific papers and explained in excellent review articles by various researchers.

Different harvesting technologies and materials are needed to capture the different types of waste energy. This chapter is intended to provide a brief introduction to the most common used waste energy harvesting technologies, including the following:

**Piezoelectric Energy Harvesting Technology:** A piezoelectric material can be used to convert mechanical kinetic energy into electrical energy. Strain or deformation of a piezoelectric material causes charge separation across the device, producing an electric field and consequently a voltage drop proportional to the stress applied. Under resonant vibration conditions, the output electric energy from a mechanically excited piezoelectric element can be dramatically increased as the peak tip displacement of the bimorph is much greater, which significantly increases the stress in the piezoelectric layers.

**Thermoelectric and Pyroelectric Energy Harvesting Technologies:** Thermal energy can be obtained from waste heat generated during manufacturing processes. Either thermoelectric or pyroelectric effects can be used to harvest thermal energy as long as a heat source is present. Thermoelectric effect requires a temperature gradient to generate electricity, whereas pyroelectric effect requires a varying temperature to generate electricity. The thermal–electricity energy conversion efficiency mainly depends on the temperature difference between the heat source and the environment. A greater temperature difference leads to a better output.

### 8.1.2 Waste energy harvesting in sustainable manufacturing

In manufacturing industry, great work has been done for the improvement of the energy efficiency in the past decades, but not much work has been reported on harvesting waste energy released in manufacturing processes. There is a huge amount of energy in manufacturing processes dissipated into the environment as waste in the form of thermal energy such as heat and temperature gradients, mechanical energy such as vibration and motion, sound, light, ... etc., which are usually called as the “waste energy.” This waste energy represents a large portion of the total energy consumed in manufacturing processes. Recovering even a fraction of this waste energy would have a great economic and environmental

impact. Harvesting this waste energy will not only reduce the energy costs to achieve the economic sustainability, but also improve the energy efficiency to achieve an environmentally sustainable manufacturing. This harvested energy from the waste energy in manufacturing processes can be considered as a special form of “renewable” energy in manufacturing processes or as an additional improvement of the overall energy efficiency.

This chapter mainly focuses on the waste energy harvesting technologies that have a great potential to be adopted in sustainable manufacturing processes to further improve overall energy efficiency, in addition to the traditional methods, such as the optimization of manufacturing processes for better energy efficiency.

Energy harvesting is highly relevant to smart manufacturing operations. These technologies could enable more intelligence in large-scale manufacturing operations resulting in improved efficiency. Therefore, the effect of energy harvesting technologies in reducing greenhouse gas emissions reaches far beyond the immediate energy harvested by the devices themselves.

The energy harvesting technologies in sustainable manufacturing may include four processes: (1) harvesting waste energy produced during manufacturing processes, (2) converting the harvested energy into electric energy, (3) processing the energy in power conversion devices, and (4) storing the harvested energy (electricity) into the energy storage (battery) for the use late or immediately utilizing the harvested energy (electricity) for the systems, such as IIoT system including wireless sensors and network communication.

## **8.2 Piezoelectric technology in sustainable manufacturing**

There is a wide range of the mechanical waste energy sources available in manufacturing processes, such as turbine engine, rolling mills, motors, compressor, chillers, pumps, fans, vibrations, cutting and dicing, noise, etc. Mechanical waste energy is usually about the kinetic energy in mechanical vibration and motion, which can be harvested by three basic vibration-to-electricity mechanisms: piezoelectric, electromagnetic, and electrostatic transductions. Piezoelectric harvesting technology has received the most attention as piezoelectric materials have a higher power density and the piezoelectric energy harvester output voltage can be directly used.

### **8.2.1 Piezoelectric effects**

The “piezo” in the Greek is “to press.” The piezoelectric phenomena were found by Pierre and Jacques in 1880 that mechanical stresses were

accompanied by macroscopic polarization and produced the electric surface charges. Later, it was discovered that an imposed voltage produces mechanical strains or deformation in a piezoelectric material (Kong et al., 2014; Rafique, 2018). When a piece of piezoelectric material under mechanical stresses generates an electric charge, and when a piece of piezoelectric material under a voltage experiences a mechanical deformation or dimensional change, this reversible piezoelectric effects can be used to convert mechanical deformation into electricity as a generator or to convert electricity into mechanical deformation as an actuator.

The relationships between mechanical force applied to the piezoelectric component and the electricity produced by the piezoelectric component depend on several factors, including piezoelectric material properties, the size and shape of the piezoelectric component, the direction of the piezoelectric and mechanical excitation, etc.

**Electric polarization:** Under the influence of an external electric field, a piezoelectric material component experiences a dynamical change of the positions of the nuclei and the electrons resulting in dipoles, which is called the polarization. There are three main sources of polarization: electronic, ionic, and dipolar or orientation. Electronic polarization results from the displacement of the center of the negatively charged electron cloud. Ionic polarization occurs only in ionic materials. Orientation polarization is only found in substances with a permanent dipole moment. The sum of these three polarizations gives the total electric polarization (Kong et al., 2014).

PZT is lead zirconate titanate ( $\text{PbZr}_{1-x}\text{Ti}_x\text{O}_3$ ), one of the world's most widely used piezoelectric ceramic materials. PZT is a polycrystalline material with random orientation of polar domains as shown in Fig. 8.3A. Under a strong DC electric field, the randomly oriented polar domains turn to align with the external electric field to a well-polarized orientation as shown in Fig. 8.3B. After the external electric field is removed, this polarization almost remains as shown in Fig. 8.3C.

**Piezoelectric effect:** The electric charge can be generated by an externally applied force on the piezoelectric component, where the material is polarized, and which is called direct piezoelectric effect. Thus, this piezoelectric effect can be used to convert the mechanical energy into electrical energy. On the other hand, some materials exhibit the reverse piezoelectric effect, a mechanical deformation can be generated by applying voltages on the component. This reverse piezoelectric effect can be used to convert the electric energy into mechanical energy, such as actuator and positioning devices. Since the piezoelectric materials are anisotropic in nature, their electrical and mechanical properties are different for the excitations (Kong et al., 2014).

**Piezoelectric linear constitutive equations:** According to the linear theory of piezoelectricity, the coupling relation between electric field  $E$ ,

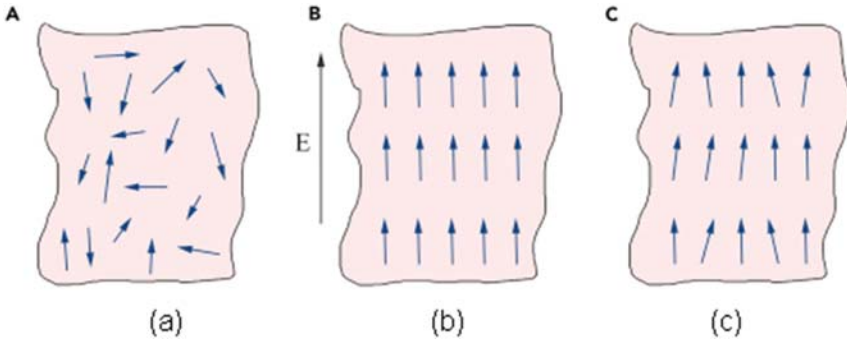


**FIGURE 8.3** Polarization of polycrystalline piezoelectric ceramic (A) Random orientation of polar domains prior to poling, (B) Poling under a constant electric field, (C) Remnant polarization after the removal of the electric field. *Used with permission from Yang, A., Zhou, S., Zu, J., Inman, D., 2018. High-performance piezoelectric energy harvesters and their applications, Joule 2 (4), 642–697, Elsevier.*

electric charge density  $D$ , mechanical stress  $T$ , and strain  $S$  is given by the following (Kong et al., 2014):

$$S_p = s_{pq}^E \cdot T_q + d_{pk} \cdot E_k$$

$$D_i = d_{iq} \cdot T_q + \epsilon_{ik}^T \cdot E_k$$

where  $s_{pq}^E$  is elastic compliance tensor at constant electric field,  $\epsilon_{ik}^T$  is dielectric constant tensor under constant stress,  $d_{pk}$  is piezoelectric constant tensor,  $S_p$  is the mechanical strain in  $p$  direction,  $D_i$  is electric displacement in  $i$  direction,  $T_q$  is mechanical stress in  $q$  direction, and  $E_k$  is the electric field in  $k$  direction. The electromechanical coupling factor  $k$  is the measurement of the ability of a piezoelectric material to convert electrical and mechanical energy and is defined by Kong et al. (2014). The detailed theory on piezoelectricity can be found in many literatures (Kong et al., 2014; Rafique, 2018; Ikeda, 1996).

$$k^2 = \frac{\text{converted mechanical energy}}{\text{input electrical energy}} \quad \text{or}$$

$$k^2 = \frac{\text{converted electrical energy}}{\text{input mechanical energy}}$$

### 8.2.2 Piezoelectric energy harvesting

Energy harvesting has become a critical technology to achieve long-lifespan self-powered operations of millions wireless sensor networks in IoT, portable devices, and medical implants. Since the late 1990s,

piezoelectric energy harvesting has been intensively investigated. The piezoelectric effect has been nowadays widely used to convert mechanical energy into electric energy. This mechanical energy comes from many different sources, including mechanical vibration and human motion. The key factor is whether an energy harvester can generate sufficient electricity power for the applications under variable excitation conditions. Most piezoelectric energy harvesting devices produce power on the order of milliwatts, which is just enough for some microscale devices such as wristwatches by converting motion from the human body into electrical power. The first microscale piezoelectric energy harvester was developed by the researchers at MIT using thin film PZT in 2005 (Jeon et al., 2005). The piezoelectric cantilever energy harvester is a typical energy harvesting device and the most common used configuration of the piezoelectric harvester as shown in Fig. 8.4. But it has a drawback that the piezoelectric cantilever is not uniformly deformed, resulting in the piezoelectric material not fully utilized to convert strain into electricity. Thus, some triangle-shaped and L-shaped cantilevers are suggested for a better uniform deformation distribution.

### 8.2.3 Piezoelectric technology in sustainable manufacturing

Mechanical vibrations exist in many manufacturing processes. This mechanical vibration is usually harmful to the system and must be controlled and damped using a damping device. This mechanical vibrational kinetic energy is usually converted (or dissipated) into heat (thermal energy) that is removed from the system and released into environment to achieve the control of the mechanical vibration. The dissipated energy is wasted and reduces the overall energy efficiency of the system. Harvesting this mechanical vibrational energy is a viable application of the piezoelectric technology since these mechanical vibrational kinetic energy sources are widely available in manufacturing processes for energy harvesting, ranging from industrial machinery to motors, from giant rolling mills to forging presses, and from large-scale

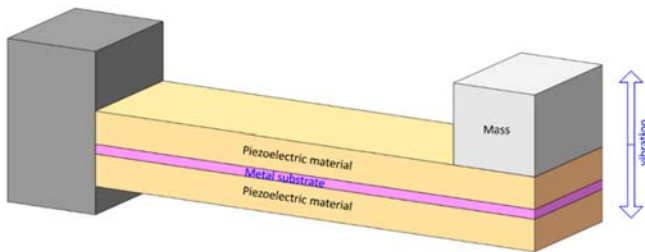


FIGURE 8.4 Cantilever piezoelectric energy harvester.

automotive assembly lines to power generations. Harvesting this waste energy not only improves the overall energy efficiency to achieve the sustainable manufacturing, but also protects the system and reduces the energy costs to achieve the economic sustainability.

As an example, an engine crankshaft fatigue failure is mainly caused by torsional vibration. A torsional vibration damper must be used to control and damp this torsional vibration to protect the crankshaft. The torsional vibration damper is usually made of the rubber or viscous damping components. The torsional vibration (kinetic) energy is dissipated by rubber/viscous materials into heat (thermo-elastic) to be released into environment to achieve the vibration control, where heat energy is wasted, which reduces the overall energy efficiency of the system.

A new patented damping device has been invented by the author, published in United States Patent US11,028,897B2 (Jia and Litens Automotive Group, 2021) as shown in Fig. 8.5. In this new damping device, a piezoelectric torsional vibration energy harvester is to function as a torsional vibration damper simultaneously, where the torsional vibration (kinetic) energy is converted by piezoelectric beam into electric energy to be stored in an electric energy storage component for the use late. The new damping device does both harvesting and damping the torsional vibration energy simultaneously. Harvesting the dissipated energy is an additional benefit of this new piezoelectric torsional vibration energy harvesting device, in addition to its simultaneous damping function. In addition, the piezoelectric element and the load resistance can be tuned for the max

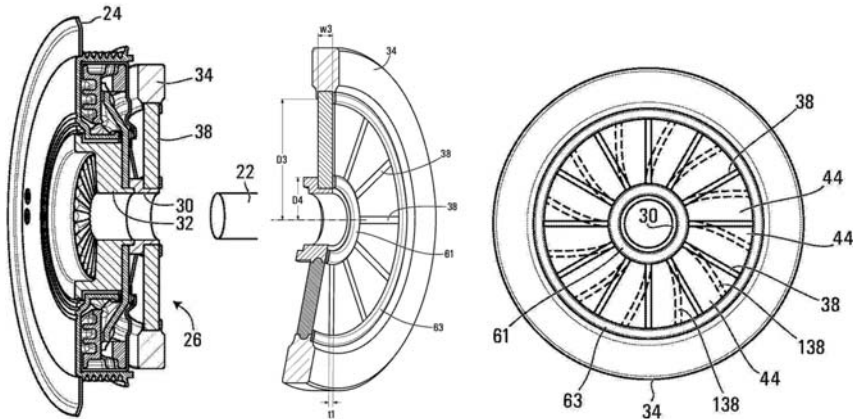


FIGURE 8.5 New patented damping device (United States Patent US11,028,897B2). Used with permission from Jia, Z., Litens Automotive Group, 2021. Torsional Vibration Damper and Method of Making Same, United States Patent US11,028,897B2, United States Patent and Trademark Office, June 8, 2021, <https://patents.google.com/patent/US11028897B2/en?q=US11%2c028%2c897B2>.

electric power output for a wide frequency range. In general, a higher strain (or deflection) and higher frequency produces a higher electric output and a higher damping. This makes this new piezoelectric energy harvesting device a very viable application of the piezoelectric vibration damper.

In the piezoelectric torsional vibration energy harvester/damper, the angular vibration of the outer inertial ring induces the bending deflection to the piezoelectric strip spring element. Multiple piezoelectric layers arranged on each side of the strip spring are in serial connection, and the piezoelectric layers on both sides can be arranged in serial or parallel connection depending on the polarization direction. The mechanism of this harvester/damper is explained in Fig. 8.6. The natural frequency of the harvester structure is tuned to the excitation frequency of the torsional vibration source to achieve a resonance condition for the highest harvesting electric energy.

The piezoelectric FEA model as shown in Fig. 8.7 can be used to investigate the characteristics of the piezoelectric torsional vibration energy harvester. The results are shown in Figs. 8.8 and 8.9. The effects of piezo-material properties on power output are shown in Fig. 8.8. For the single unit piezoelectric power output for PZT-4 and PVDF, Piezo 2 is much more effective to generate electricity than Piezo 1. The effects of piezo layer thickness on power output are shown in Fig. 8.9.

In summary, the piezoelectric torsional vibration energy harvester/damper has five major benefits: (1) One device two functions: mechanical—electric shunt damping and energy harvesting; (2) Highest

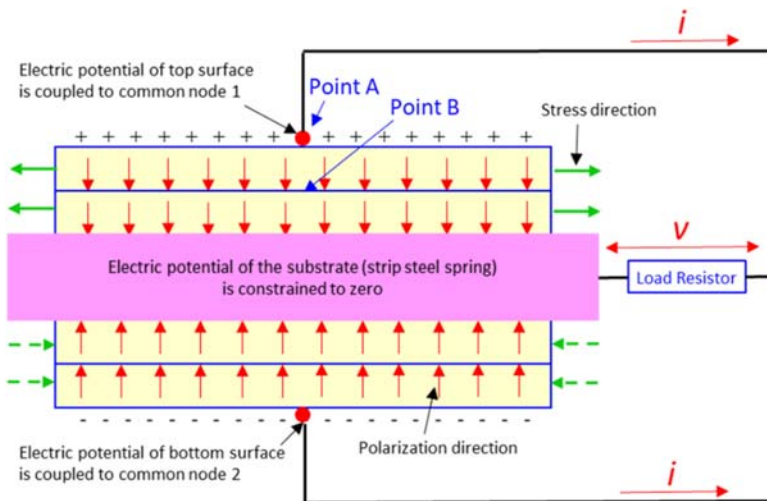


FIGURE 8.6 One strip spring with 2 piezoelectric layers on each side.

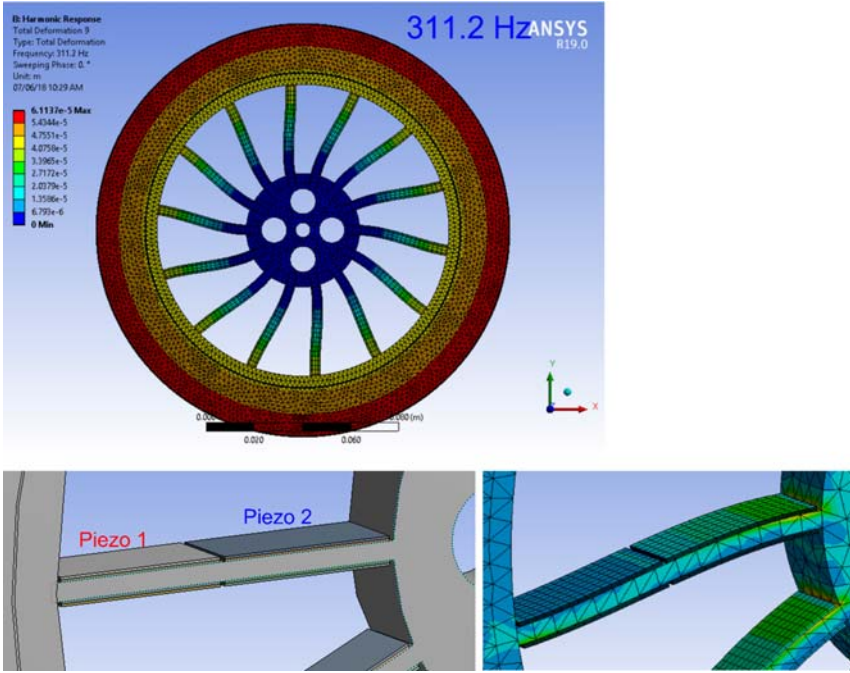


FIGURE 8.7 Piezoelectric FEA model.

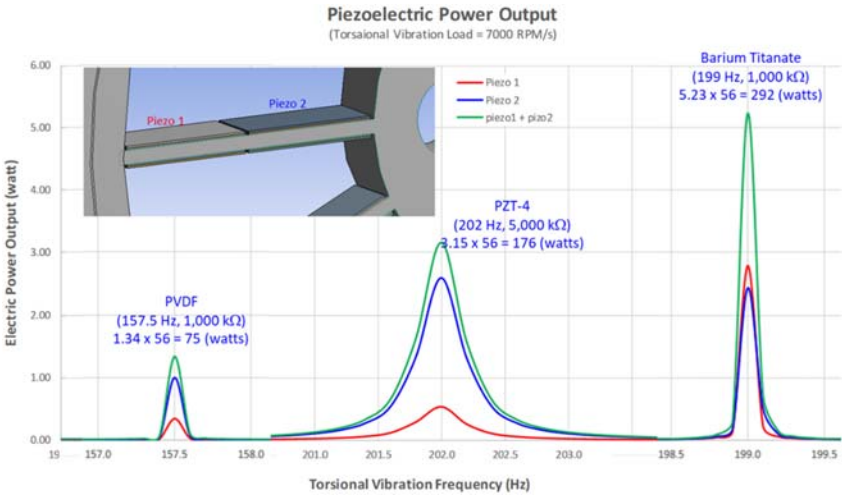


FIGURE 8.8 Effects of piezo-material properties on power output.

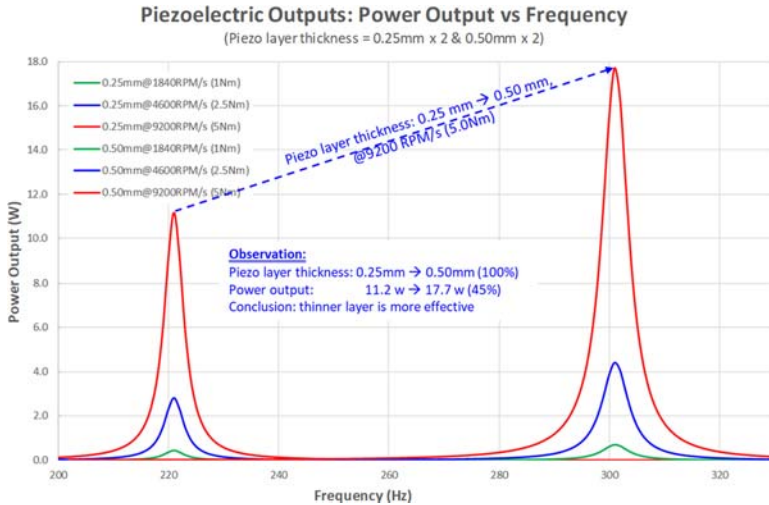


FIGURE 8.9 Effects of piezo layer thickness, on power output.

harvesting performance is proportional to highest damping performance; (3) The natural frequency of the device can be tuned to the system resonance frequency for max damping and harvesting; (4) Reduced damping requirement on the rubber component; and (5) All current rubber damper and viscous damper on the market do not harvest torsional vibration energy. The concept of the piezoelectric vibration energy harvester/damper can be used in manufacturing processes, where the mechanical linear or torsional vibrations need to be controlled to achieve both the optimal and sustainable manufacturing processes.

### 8.3 Thermoelectric technology in sustainable manufacturing

Waste heat sources are widely available for harvesting in manufacturing processes. The global total waste heat released in industrial and chemical processes is equivalent to almost 72% of all electrical energy produced in the year 2016, and about 63% of this waste heat is the low-grade waste heat (Forman et al., 2016). Thermal energy harvesting has been extensively researched in the past years, with the focus on Thermoelectric Generator (TEG) (Johnson et al., 2008), as TEG has a number of promising features, such as simpler structure, no moving parts and no vibration, continuous solid-state quite operation for many years, good scalability, no chemical reaction, and no toxic residuals (Zeb et al., 2017).

Thermal energy harvesting turns heat into electricity using either thermoelectric or pyroelectric effects (Sebald et al., 2009). In the thermoelectric energy harvesting, the thermoelectric effect produces a *permanent* voltage when there is a large temperature gradient, which requires huge heat flows. In the pyroelectric energy harvesting, pyroelectric effect produces a *temporary* voltage when there is a time varying temperature, which is hard to find. In other words, the thermoelectric effect uses temperature changing over distance and the pyroelectric effect uses temperature changing over time. If the temperature stays constant at the new level, the pyroelectric voltage gradually disappears.

### 8.3.1 Thermoelectric effects

The thermoelectric effect includes three effects: Seebeck effect, Peltier effect, and Thomson effect. It is often called the Peltier-Seebeck effect. The *Seebeck effect* directly converts the thermal energy into the electric energy, and the *Peltier effect* reversibly converts the electric energy into the thermal energy.

**Seebeck Effect:** In 1821, German-Estonian physicist Thomas Johann Seebeck discovered that a voltage difference is created between two different conductors N and P that are subjected a temperature gradient  $\Delta T$ . The heat flow  $Q$  in the conductors results in the diffusion or flow of charge carriers from the hot side to the cold side and leaves their oppositely charged nuclei at the hot side, which produces a thermoelectric voltage  $V$  (Kong et al., 2014).

$$V = \int_{T_1}^{T_2} [S_N(T) - S_P(T)] dT$$

where  $S_N$  and  $S_P$  are Seebeck coefficients of conductors N and P, and  $T_1$  and  $T_2$  are temperatures at two sides. The Seebeck coefficient is the thermopower in the unit of  $V/K$  or  $\mu V/K$  and is a function of temperature and material property, which measures the induced thermoelectric voltage at the given temperature gradient  $\Delta T$  and the entropy per charge carrier. The *Seebeck effect* is used for power generation and the device is called TEG, as shown in Fig. 8.10.

**Peltier Effect:** In 1834, French physicist Jean-Charles Peltier discovered that a junction of two different conductors N and P applied with a voltage  $V$  causes heat that is generated at one side and absorbed at the other side depending on the direction of the current. The heat  $\dot{Q}$  absorbed or generated is proportional to the current (Kong et al., 2014).

$$\dot{Q} = (\eta_N - \eta_P)I$$

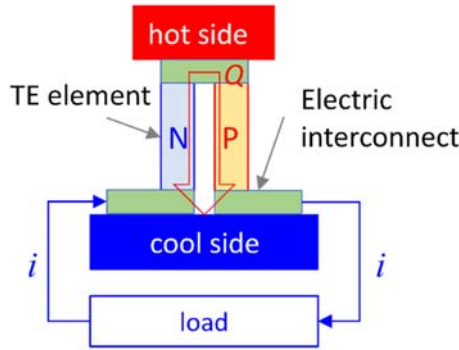


FIGURE 8.10 Thermoelectric generator (TEG).

where  $\eta_N$  and  $\eta_P$  are Peltier coefficients of conductors  $N$  and  $P$ , respectively. The Peltier coefficient represents the amount of heat flow through the material. The *Peltier effect* is used for cooling and heating and the device is called thermoelectric cooler (TEC), as shown in Fig. 8.11.

**Thomson Effect:** In 1851, Scottish-Irish physicist William Thomson, better known as Lord Kelvin, observed that a current-carrying conductor with a temperature gradient between two sides either dissipates or absorbs heat, that is, either heating or cooling (Kong et al., 2014).

$$Q = \rho J^2 - \mu J \frac{dT}{dx}$$

where  $Q$  is heat generated per unit volume of the material,  $J$  is current density,  $\rho$  is resistivity of the material,  $\mu$  is the Thomson coefficient, and  $dT/dx$  is the temperature gradient. The first term is Joule heating and the second term is the Thomson heating. In 1854, Lord Kelvin found the first

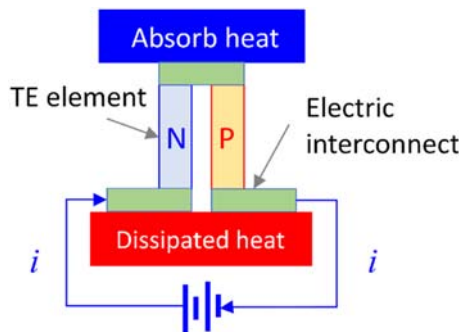


FIGURE 8.11 Thermoelectric cooler (TEC).

Thomson relation between the Thomson coefficient  $\mu$  and Seebeck coefficient  $S$  (Kong et al., 2014).

$$\mu = T \frac{dS}{dT}$$

and the second Thomson relation,

$$\eta = S \cdot T$$

where  $\mu$  is Thomson coefficient,  $S$  is Seebeck coefficient,  $\eta$  is Peltier coefficient, and  $T$  is absolute temperature ( $^{\circ}\text{K}$ ).

**Figure of Merit  $ZT$ :** The dimensionless figure of merit  $ZT$  is defined by the following (Kong et al., 2014):

$$ZT = \frac{\sigma S^2 (T_2 + T_1)}{2k}$$

where  $\sigma$  is electrical conductivity,  $k$  is thermal conductivity, and  $S$  is Seebeck coefficient.

$ZT$  determines the efficiency of thermoelectric effect. A larger  $ZT$  indicates a greater thermodynamic efficiency and can be used to compare the potential efficiency of the devices with different thermoelectric materials. The key parameters are the physical transport properties of thermoelectric materials, including thermal conductivity, electric conductivity, and thermoelectric coefficients (Seebeck coefficient or Peltier coefficient) as well as energy conversion efficiency in terms of figure-of-merit  $ZT$ . Ideally, a high Seebeck (or Peltier) coefficient, high electrical conductivity, and low thermal conductivity are desired for a TEG (or TEC), as a high thermal gradient at the junction can be easily maintained on low thermal conductivity. P- and N- elements are connected electrically in series and thermally in parallel.

Both TEG and TEC do not have the moving parts, which allow continuous operation for many years. TEC heating and cooling are reversible. However, one major drawback is that thermoelectric energy conversion efficiency is very low, around 4%–6%. The latest development has shown up to 10%.

### 8.3.2 Thermoelectric energy harvesting

Thermoelectric energy harvesting technology has been intensively investigated in automotive industry with the focus mainly on TEG for waste heat recovery in vehicles. As TEG is a solid-state device, directly converts heat to electricity, has no moving parts, operates quietly, requires low maintenance, BMW, Ford, GM, Fiat, Porsche, and many other auto OEMs have developed their thermoelectric applications for the wasted thermal energy harvesting, including (1) an integrated TEG exhaust heat

system to harvest exhaust heat, (2) an integrated TEG radiator to harvest wasted heat energy from a cooling system, (3) a thermoelectric-PCM heat exchanger (TPHX) to integrate the heat exchanger function, thermal energy harvesting function using TEG, and the thermal energy storage (TES) function using PCM all together into a single device as a general thermal management technology that can be applied to all kind of heat exchangers for automotive and many other industries. In addition, the TPHX reversible functionality can switch its functions between as a “Thermoelectric Generator (Seebeck)” and as a “Thermoelectric Cooler/Heater (Peltier).” This reversible functionality provides the flexibility for an electric vehicle battery cooling/heating thermal management system in single coolant circuit.

In 2012, BMW and Ford have developed a high-temperature TEG as shown in Fig. 8.12 (Crane et al., 2013). The TEGs were successfully integrated and tested on two passenger vehicles: a BMW X6 and a Lincoln MKT to harvest the waste thermal energy from the exhaust heat. On the test bench, over 700W of power was produced. Over 600W of power was

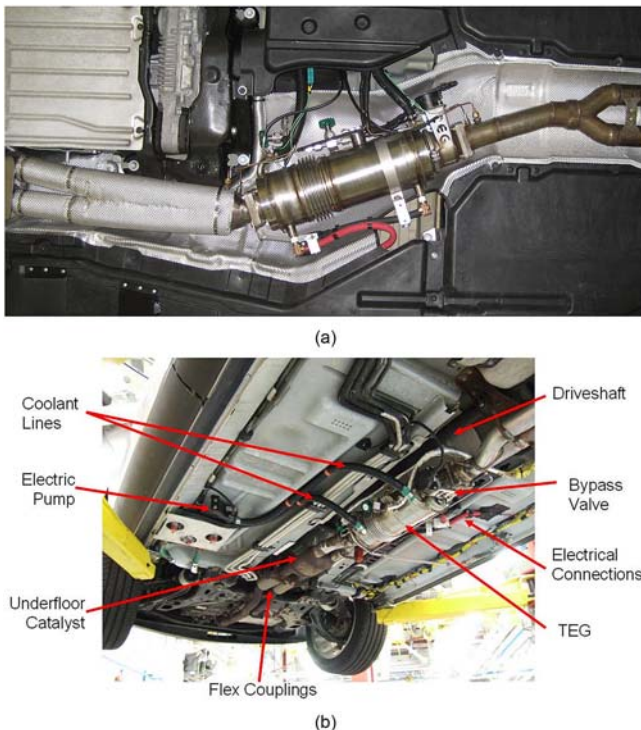


**FIGURE 8.12** TEGs installed in (A) BMW X6 and (B) Lincoln MKT. Used with permission from Crane, D., LaGrandeur, J., Jovovic, V. et al., 2013. TEG on-vehicle performance and model validation and what it means for further TEG development. *Journal of Electronic Materials* 42, 1582–1591, Springer Nature.

produced in on-vehicle tests. The success of this work has led to a follow-on US DOE-sponsored TE waste heat recovery program for passenger vehicles focused on addressing key technical and business-related topics that are meant to enable TEGs to be considered as a viable automotive product in the future (Crane et al., 2013).

### 8.3.3 Thermal energy harvesting in sustainable manufacturing

A huge amount of waste heat energy is available in industrial processes, which is usually defined as heat rejected in industrial processes, including iron and steel, chemicals and petrochemicals, etc. Waste heat is usually included in a thermal carrier such as exhaust gas, cooling air/water, hot oil, hot steel products, etc. According to Eurostat (2021), the final energy consumption in the EU in 2019 was 935 Mtoe. The industry sector accounted for 25.6% of the total energy consumption in EU. Chemical and steel industries were the largest consumers, followed by paper, nonmetallic minerals, and food; five sectors represent about two thirds of the total energy consumption in industry sector. Different industry sectors have different heat demands. Food, tobacco, textiles, and leather industries have heat demand up to 100°C, pulp and paper industries up to 500°C, and manufacturing metals, iron and steel, and nonmetallic minerals demand heat above 500°C (Papapetrou et al., 2018). It is estimated that the energy losses in industrial processes represent 20%–50% of the total energy consumption of industry sector in the form of waste heat included in exhaust gases, cooling air/liquid, etc., according to the SPIRE Roadmap (2020). The comparison of the useful energy and energy losses in industry sectors in the US in Fig. 8.13 shows the great potential of harvesting waste heat energy in industry processes.

Waste heat is a by-product common to all manufacturing processes. Harvesting waste heat energy in manufacturing processes represents a great opportunity to reduce the energy consumption for sustainable manufacturing processes. However, thermoelectric energy harvesting technology faces a major challenging for its very low thermoelectric energy conversion efficiency around 4%–6% and latest up to 10%. Significant R&D efforts are required to further develop emerging and innovative technologies to significantly improve thermoelectric energy conversion efficiency and cost-effectiveness for economic sustainability — the economic returns of waste heat recovery technology with a “reasonable” payback period ( $\ll$  3 years). Since most sectors have a low-grade waste heat as shown in Fig. 8.14, R&D efforts are driven by the need to develop the techniques to convert low-grade waste heat into electricity with high thermoelectric energy conversion efficiency. In addition, efficient heat energy storage technologies will play a

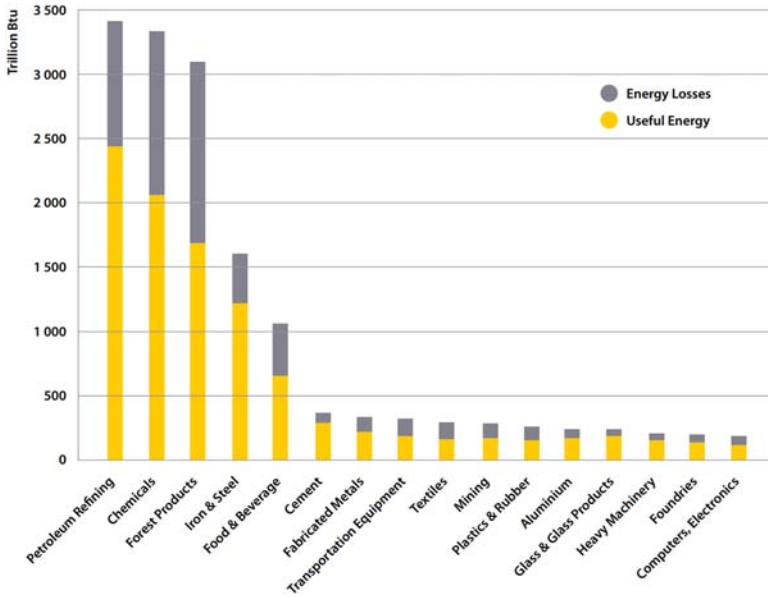


FIGURE 8.13 Overview of energy losses within sectors. Used with the permission from SPIRE ROADMAP. 2020. Sustainable Process Industry through Resource and Energy Efficiency (SPIRE).

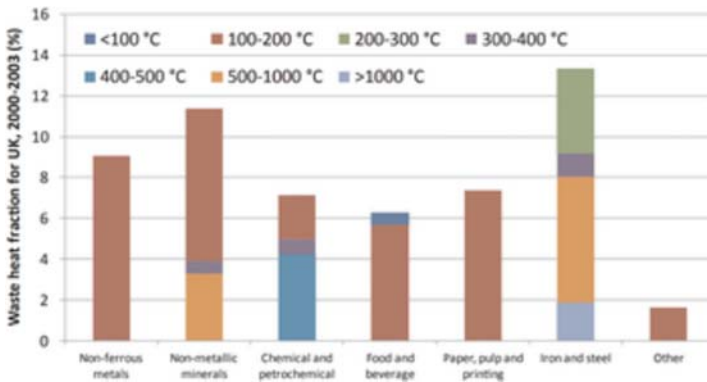


FIGURE 8.14 Waste heat fraction per industrial sector and temperature level for UK industry for the period 2000–2003. Used with permission from Papapetrou, M., Kosmadakis, G., Cipollina, A., Commare, U.L., Micale, G., 2018. Industrial waste heat: estimation of the technically available resource in the EU per industrial sector, temperature level and country. *Applied Thermal Engineering*, 138, 207–216. <https://reader.elsevier.com/reader/sd/pii/S1359431117347919?token=3DCC52EB508158323FA60DB2AF5F2811AF8213FE9B4076FB00B37B4E37C7DD1D1C6A623162CE9F184EA5D5ED5857DAFF&originRegion=us-east-1&originCreation=20220622165343>, Elsevier.

significant role as well, allowing harvested waste energy to be effectively stored for the use when need to balance temporal fluctuations on energy demands.

## 8.4 Other energy harvesting technologies in sustainable manufacturing

---

Beside the piezoelectric and thermoelectric energy harvesting technologies discussed above, there are many other energy harvesting technologies available. A brief introduction to some of them is given below (Akinaga, 2020; Almanza et al., 2016).

### 8.4.1 Pyroelectric technology in sustainable manufacturing

Pyroelectric effect generates temporary voltage from time-varying temperature. The pyroelectric effect describes that a temperature change  $\Delta T$  in a material induces a change in polarization of the material to generate electric current or voltage (Kong et al., 2014). It is analogous to the piezoelectric effect. The difference is that in pyroelectric effect, the change in polarization is caused by temperature changing over time, while in piezoelectric effect, the change in polarization is caused by mechanical stress. Pyroelectric coefficient  $p = \Delta P / \Delta T$  is a parameter to measure the pyroelectric efficiency of the material (Kong et al., 2014).

There are two types of pyroelectric effects: The first is primary pyroelectric effect, where only the change in polarization due to temperature change contributes to pyroelectric effect. It is constant strain pyroelectric effect. The other is secondary pyroelectric effect, where the change in polarization due to thermal stress or mechanical deformation of a material caused by thermal expansion makes an additional contribution to pyroelectric effect, through piezoelectric effect. Therefore, the total pyroelectric effect equals to the summation of primary pyroelectric coefficient and secondary pyroelectric coefficient (Kong et al., 2014).

Pyroelectric energy harvesting is receiving renewed interest for converting waste energy into electricity. Pyroelectricity requires time-varying temperature as inputs, which is not widely available in manufacturing processes and produces small power outputs, which is a drawback for waste energy harvesting. But pyroelectric materials are stable at high temperature even above 1200°C, which makes possible high temperature energy harvesting from iron and steel processes, in addition, high temperature also increases thermodynamic efficiency. This is a key advantage of pyroelectrics over thermoelectric. Since pyroelectric waste energy harvesting technology is plagued by inefficiencies and availability of time-varying temperature sources, R&D efforts are driven by the need to develop technologies to efficiently convert high temperature waste heat.

### 8.4.2 Electromagnetic energy harvesting

The electromagnetic mechanism can be used to convert kinetic energy into electrical energy extremely efficiently. Based on Faraday's law of electromagnetic induction discovered by scientist Michael Faraday in 1831, an electric current is induced to flow in the wire when moving a magnet inside a coil of wire or an electric potential difference is induced between the two ends of the conductor when passing this conductor through a magnetic field. In most generator applications, the circuit includes a coil of multiple turns of wire and the magnetic field is generated by permanent magnets. The voltage induced in an  $N$ -turn coil from a relative motion between a coil and a magnet is given by [Beeby et al. \(2009\)](#).

$$V = -\frac{d\Phi}{dt} = -N\frac{d\phi}{dt}$$

where  $V$  is the voltage induced,  $\phi$  is the average flux linkage per turn, and  $\Phi$  is the total flux linkage of the  $N$ -turn coil.

Most generators in the world are based on Faraday's law of electromagnetic induction to convert the mechanical kinetic energy of the rotor to electricity from large-scale power generation to small car generators to recharge batteries. Electromagnetic generators can also be used to harvest waste energy in manufacturing processes, where a magnet coil mechanical-to-electrical converter can be used to harvest waste mechanical vibration energy.

### 8.4.3 Electrostatic energy harvesting

Electrostatic energy harvesters convert mechanical energy into electrical energy using a variable capacitor structure to generate a capacitance variation and electric charges from a relative motion between two plates of a charged variable capacitor, where two plates are separated by air or dielectric materials. Electrostatic energy harvesters require a polarization source to work and include two categories ([Boisseau et al., 2012](#)): (1) Electret-free electrostatic harvesters that use the charges–discharges cycles of the capacitor for mechanical–electricity energy conversion, e.g., charge-constrained cycles and voltage-constrained cycles. In addition, it requires an active electronic circuit to manage the charge cycle for the synchronization with the capacitance variation, which greatly complicates the management circuit and (2) Electret-based electrostatic harvesters that add the electret layers on the two plates of the variable capacitor for the polarization of the plates. Electrets are electrically charged dielectric materials in a quasipermanent electric polarization state and able to keep the polarization on the capacitor for years.

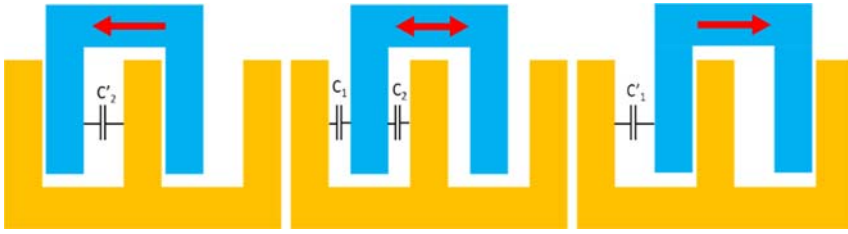


FIGURE 8.15 Basic capacitor shapes for electrostatic converters (Boisseau et al., 2012).

Electrostatic energy harvesters offer the possibility to decouple the mechanical structure and the converter.

A basic variable capacitive structure used in electrostatic energy harvesters is shown in Fig. 8.15. Both piezoelectric and electrostatic energy harvesters are usually used for small-scale energy harvesters ( $<1-10 \text{ cm}^3$ ) and electromagnetic converters are usually used for larger devices (Boisseau et al., 2012). The electrostatic energy harvesting can be applied in manufacturing processes to harvest mechanical vibration energy.

#### 8.4.4 Thermomagnetic energy harvesting

Manufacturing processes release substantial quantities of waste heat, most of which is low-grade heat. Low-grade waste heat represents a great resource for thermal energy harvesting. But harvesting low-grade heat is challenging due to low thermodynamic efficiency and very few technologies available today to convert low-grade waste heat into electricity. At present, harvesting low-grade waste heat mainly relies on thermoelectric technology. Comparing to various thermal energy harvesting technologies available for harvesting low-grade heat, the thermomagnetic effect offers a promising alternative. In addition, thermomagnetic energy harvesters have no moving parts.

Thermomagnetic energy harvesting is based on a cyclic change of magnetization with temperature using thermomagnetic material (TMM) to induce a voltage. In a thermomagnetic circuit as shown in Fig. 8.16 (Dzekan et al., 2021), the TMM is used as a thermal valve to change the magnetic flux  $\Phi$ , which is created by a permanent magnet, during hot-cold temperature cycling. At low temperatures, the TMM has a high  $M_{\text{cold}}$ , which allows magnetic flux  $\Phi$  through a closed magnetic circuit. At high temperatures, the TMM has a low  $M_{\text{hot}}$ , which reduces magnetic flux  $\Phi$ . This magnetic flux  $\Phi$  change due to temperature fluctuation converts magnetic energy  $E_M$  into electrical energy to induce a voltage in an induction coil, which is wound around the soft magnetic yoke. The energy

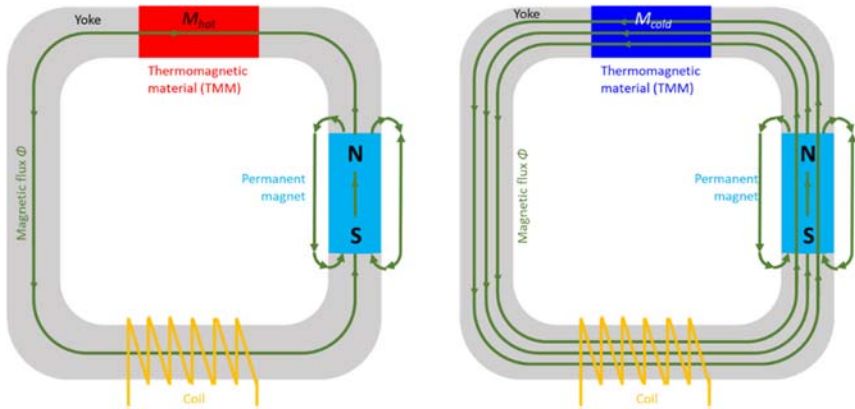


FIGURE 8.16 Thermomagnetic energy harvester (Dzekan et al., 2021).

efficiency can be defined as the ratio between the useful output and the related energy input. The TMM efficiency is given by Dzekan et al. (2021).

$$\eta = \frac{E_m}{Q_{in}} = \frac{\mu_0 \Delta MH}{Q_{in}}$$

where  $E_m$  is magnetic energy,  $Q_{in}$  is thermal input energy,  $\mu_0$  is the magnetic field constant,  $M$  is magnetization, and  $H$  is magnetic field.

### 8.4.5 Triboelectric energy harvesting

The triboelectric energy harvesting has gained much attention in the past decade as indicated by a large number of studies published (Thainirarn et al., 2020; Logothetis et al., 2017). The triboelectric effect converts mechanical energy into electric energy from friction or temporary contact between two different triboelectric materials. When two triboelectric materials come into contact, a charge transfer occurs, one triboelectric material is positively charged and the other negatively charged, which creates an electronic potential difference between them. The triboelectric mechanism is based on the coupling effect of contact electrification and electrostatic induction, which is the phenomenon of electrification by contact of two objects that become spontaneously charged (Thainirarn et al., 2020). In addition to its simple and economical production, the triboelectric generator has a high output power and great efficiency. For example, at a speed of  $0.2 \text{ m s}^{-1}$  and with a vertical force of  $9.8 \text{ N}$ , the PA6 triboelectric TEG produced a maximum open circuit voltage of  $800 \text{ V}$  and the PTFE TEG  $1000 \text{ V}$  (Logothetis et al., 2017).

### 8.4.6 Sensors and IIoT in sustainable manufacturing

The industrial sector is the largest user of energy and accounts for 37% of the total global energy consumption in 2017 (IEA, 2019). Any energy efficiency improvement in manufacturing processes could make a significant contribution to environmental sustainability. Manufacturing processes such as metal forming processes are usually a very nonlinear, time-varying multivariable system. An intelligent on-line self-learning adaptive control technique based on an artificial neural network back-propagation paradigm was proposed by the author for the real-time analysis and control (Jia, 1998). This intelligent control system includes four major subsystems, the first is the smart sensors system, which is used to continuously measure real-time process parameters, the second is the wireless communication network system, which is used to transfer the real-time data to controller, the third is the artificial neuron network controller, which is used for the real-time dynamical process analysis, optimization, and control, and the last is smart actuators.

In this intelligent control system, the waste energy harvesting technologies play a very important role. Waste heat energy and mechanical vibration energy released in manufacturing processes are harvested to power the wireless sensors and Industrial IoT network system, which provides great advantages and benefits, (1) no battery or wired power supply is required for smart sensors, (2) such wireless sensors can be placed practically anywhere as no battery or power wiring is required, (3) sensors are wirelessly connected to the controller, and (4) wireless sensor networks are usually less cost due to easier maintenance and more flexible configuration. Wireless sensors and Industrial IoT network integrated with ANNs and waste energy harvesting technologies pave the way for the real-time intelligent control for sustainable manufacturing processes.

In fact, energy harvesting is highly related to smart manufacturing operations, which require many sensors for the real-time measurements of process parameters. These sensors are usually wireless and ubiquitous. Regularly replacing the batteries throughout a large manufacturing operation is not practical or even impossible as some sensors may not be accessible easily. From this perspective, the waste energy harvesting technology could enable more intelligence in large-scale manufacturing operations, which in turn improve the energy efficiency. Therefore, the waste energy harvesting technologies contribute to sustainable manufacturing far beyond the immediate waste energy it harvested (Roundy et al., 2019).

## 8.5 Conclusion

The industrial sector is the largest energy consumer and accounts for about one third of the total global energy consumption. It is estimated that the global total energy losses in the form of waste heat in industrial processes are equivalent to almost 72% of all electrical energy produced in the year 2016 (IEA, 2019; Forman et al., 2016). Heat losses from manufacturing processes reflect a significant loss of efficiency. Reducing the total energy consumption in manufacturing processes is a fundamental requirement for sustainable manufacturing. Improving the overall energy efficiency in manufacturing processes is the very first step toward the goal of the reduction of the total energy consumption. However, for the energy efficiency, there is a fundamental limit set by the laws of thermodynamics, which cannot be achieved in a real-life practice. Thus, harvesting waste energy becomes an essential step for further improving the energy efficiency for sustainable manufacturing processes. Recovering even a fraction of this waste energy would have a great impact to both environmental sustainability and economic sustainability. The waste energy harvesting technologies discussed in this chapter play a very important role in the recovery of waste energy for sustainable manufacturing. There are many waste heat sources and mechanical vibration sources available in manufacturing processes. Piezoelectric, electromagnetic, electrostatic, etc., can be used to harvest mechanical vibration energy into electricity, and thermoelectric, pyroelectric, thermomagnetic, etc., can be used to convert thermal energy into electricity. It is expected that the waste energy harvesting technologies and applications will have a great advancement in the next 5–10 years.

## References

- Akinaga, H., 2020. Recent advances and future prospects in energy harvesting technologies. *Japanese Journal of Applied Physics* 59, 110201. <https://doi.org/10.35848/1347-4065/abfa0>.
- Almanza, M., Pasko, A., Bartok, A., Mazaleyrat, F., Lobue, M., 2016. Thermal Energy Harvesting: Thermomagnetic versus Thermoelectric Generator, 7th International Conference on Magnetic Refrigeration at Room Temperature. *Thermag VII*, Turin, Italy ffaal-01395695.
- Beeby, S.P., O'Donnell, T., 2009. Electromagnetic energy harvesting. In: Priya, S., Inman, D.J. (Eds.), *Energy Harvesting Technologies*. Springer, Boston, MA. [https://doi.org/10.1007/978-0-387-76464-1\\_5](https://doi.org/10.1007/978-0-387-76464-1_5).
- Boisseau, S., Despesse, G., Seddik, B.A., 2012. Electrostatic Conversion for Vibration Energy Harvesting, *Small-Scale Energy Harvesting*. Mickael Lallart, IntechOpen. <https://doi.org/10.5772/51360>. <https://www.intechopen.com/chapters/40640>.
- Crane, D., LaGrandeur, J., Jovovic, V., et al., 2013. TEG on-vehicle performance and model validation and what it means for further TEG development. *Journal of Electronic Materials* 42, 1582–1591.

- Cullen, J.M., Allwood, J.M., Borgstein, H., 2011. Reducing energy demand: what are the practical limits? *Journal of Environmental Science & Technology* 45 (4), pp1711–1718.
- Dzekan, D., Waske, A., Nielsch, K., Fähler, S., 2021. Efficient and affordable thermomagnetic materials for harvesting low grade waste heat. *APL Materials* 9. <https://aip.scitation.org/doi/10.1063/5.0033970>.
- Eurostat, Energy Statistics—an Overview, 2021. <https://ec.europa.eu/eurostat/statistics-explained/SEPDF/cache/29046.pdf>.
- Fawkes, S., Oung, K., Thorpe, D., 2016. Best Practices and Case Studies for Industrial Energy Efficiency Improvement – an Introduction for Policy Makers. UNEP DTU Partnership, Copenhagen. <https://europa.eu/capacity4dev/file/31409/download?token=kOYq705T>.
- Forman, C., Muritala, I.K., Pardemann, R., Meyer, B., 2016. Estimating the global waste heat potential. *Renewable and Sustainable Energy Reviews* 57, 1568–1579. <https://doi.org/10.1016/j.rser.2015.12.192>.
- IEA, 2019. World Energy Balances, an Overview. [https://iea.blob.core.windows.net/assets/8bd626f1-a403-4b14-964f-f8d0f61e0677/World\\_Energy\\_Balances\\_2019\\_Overview.pdf](https://iea.blob.core.windows.net/assets/8bd626f1-a403-4b14-964f-f8d0f61e0677/World_Energy_Balances_2019_Overview.pdf).
- Ikeda, T., 1996. *Fundamentals of Piezoelectricity*. Oxford University Press, New York.
- Jeon, Y.B., Sood, R., Kim, S.-G., 2005. MEMS power generator with transverse mode thin film PZT. *Sensors and Actuators A: Physical*. 122, 16–22.
- Jia, Z., 1998. An Integrated Analysis and Design Method for Metal Forming Processes. Ph.D. dissertation, Ohio University, USA.
- Jia, Z., Litens Automotive Group, 2021. Torsional Vibration Damper and Method of Making Same, United States Patent US11,028,897B2, United States Patent and Trademark Office. June 8, 2021. <https://patents.google.com/patent/US11028897B2/en?q=US11%2c028%2c897B2>.
- Johnson, I., Choate, W.T., Davidson, A., 2008. Waste Heat Recovery. Technology and Opportunities in U.S. Industry, United States. <https://doi.org/10.2172/1218716>. Web.
- Kong, L.B., Li, T., Hng, H.H., Boey, F., Zhang, T., Li, S., 2014. *Waste Energy Harvesting, Mechanical and Thermal Energies*. Springer, New York.
- Logothetis, I., Vassiliadis, S., Stiores, E., 2017. Triboelectric effect in energy harvesting. *IOP Conference Series: Materials Science and Engineering* 10 254, 042021. <https://doi.org/10.1088/1757-899X/254/4/042021>.
- Narayanan, R.G., Gunasekera, J.S., 2019. *Sustainable Material Forming and Joining*. CRC Press, New York.
- Papapetrou, M., Kosmadakis, G., Cipollina, A., Commare, U.L., Micale, G., 2018. Industrial waste heat: estimation of the technically available resource in the EU per industrial sector, temperature level and country. *Applied Thermal Engineering* 138, 207–216.
- Rafique, S., 2018. *Piezoelectric Vibration Energy Harvesting, Modeling & Experiments*. Springer AG.
- Roundy, S., Kim, M., Lee, G.Y., et al., 2019. Preface for the special issue of energy harvesting. *International Journal of Precision Engineering and Manufacturing-Green Technology* 6, 669–670. <https://doi.org/10.1007/s40684-019-00150-0>.
- Sebald, G., Guyomar, D., Agbossou, A., 2009. On thermoelectric and pyroelectric energy harvesting. *Smart Materials and Structures* 18 (7pp), 125006. <https://doi.org/10.1088/0964-1726/18/12/125006>.
- SPIRE ROADMAP, 2020. Sustainable Process Industry through Resource and Energy Efficiency. SPIRE.
- Thainiramit, P., Yingyong, P., Isarakorn, D., 2020. Impact-Driven Energy Harvesting: Piezoelectric versus Triboelectric Energy Harvesters, Sensors. MDPI. [https://www.researchgate.net/publication/344737334\\_Impact-Driven\\_Energy\\_Harvesting\\_Piezoelectric\\_Versus\\_Triboelectric\\_Energy\\_Harvesters](https://www.researchgate.net/publication/344737334_Impact-Driven_Energy_Harvesting_Piezoelectric_Versus_Triboelectric_Energy_Harvesters).
- Yang, A., Zhou, S., Zu, J., Inman, D., 2018. High-performance piezoelectric energy harvesters and their applications. *Joule* 2 (4), 642–697.

Zeb, K., Ali, S.M., Khan, B., Mehmood, C.A., Tareen, N., Din, W., Farid, U., Haider, A., 2017. A survey on waste heat recovery: electric power generation and potential prospects within Pakistan. *Renewable and Sustainable Energy Reviews* 75, 1142–1155. <https://doi.org/10.1016/j.rser.2016.11.096>. This page intentionally left blank

# Sustainability performance evaluation in manufacturing: theoretical and practical perspectives

---

*N. Harikannan, and S. Vinodh*

Department of Production Engineering, National Institute of Technology,  
Tiruchirappalli, Tamil Nadu, India

## 9.1 Literature and state of art

---

Sustainability in manufacturing intends to develop environmentally friendly products at lower cost. Holistic sustainable economic and environmental procedures are applied for the development of product and services in sustainable manufacturing (Akbar and Irohara, 2018). Generally, manufacturing process involves the transformation of available resources to the market ready output goods. The systems also cause detrimental effects on both ecosystems and environment through climate change, global warming, and carbon footprints. The sustainability concept was practiced in manufacturing to meet the emerging challenges and to create environmentally and economically consistent systems. As manufacturing industries are shifting toward the era of Industry 4.0, the digital technologies of the fourth industrial revolution can make it possible to efficiently distribute resources and solve the full potential of sustainability in manufacturing (Dubey et al., 2019). When environmental impact increases, sustainability in manufacturing becomes a greater cause for concern. Hence, sustainability assessment in manufacturing sector is of paramount importance. The purpose of the study is to carry out sustainability assessment for developing product by choosing less environmental impact material, with limited resource consumption and eco-friendly designs and to upgrade the manufacturing systems to

international sustainability values. For sustainability assessment of manufacturing process, a conceptual model is established. The experts provide data input for assessment. As a solution strategy, grey-based approach is used, and overall performance index is determined. Grey Performance Importance Index (GPII) is computed for each attribute and weaker attributes are identified based on GPII. More realistic implications are derived. The research study objectives are as follows:

- Derivation of conceptual model for sustainability assessment of manufacturing performance firm
- Assessment of sustainability index
- Recognition of weaker attributes that hinder the manufacturing sustainability, and
- Suggestions to improve the sustainable manufacturing performance.

[Veleva and Ellenbecker \(2001\)](#) considered the assessment of sustainable manufacturing performance. The authors presented 22 indicators and an eight-step model for implementing sustainable measures in manufacturing systems. They also discussed the strengths and weakness of the assessment methodology. Top management support, strong government policies, and consumers pressures were identified as key factors for effective sustainable manufacturing.

[Krajnc and Glavič \(2003\)](#) presented indicators with dimensions for evaluating sustainable manufacturing. Practical guidelines for achieving sustainability in manufacturing industries were also suggested. The indicators act as design metrics for evaluating the company's level of sustainability and for finding better potential choices.

[Singh et al. \(2014\)](#) evaluated sustainability of Small and Medium Enterprises (SMEs) in manufacturing sector using a model build on fuzzy inference system. Considering the uniqueness of SMEs, a catalog of 21 manufacturing sustainability metrics for SMEs has been established. Weaker areas were recognized using fuzzy model in order to make suitable decision for boosting the economy.

[Jayakrishna et al. \(2016\)](#) developed a model of graph theory to quantify the efficiency and interrelationship among an organization's sustainability enablers, for quantitatively assessing the organization's sustainable manufacturing practices. The organization's standard of sustainable production practices was determined by Comprehensive Assessment Index with the best case and worst case values.

[De et al. \(2020\)](#) discussed Data Envelopment Analysis (DEA)-based model for analyzing the combined effect of lean with sustainability practices on SMEs competitiveness. SMEs were classified for efficiency based on the application of the framework. The inefficient SMEs are

suggested for improvement using qualitative methods. The framework was demonstrated for applicability with a case.

[Song et al. \(2019\)](#) adopted a distance-to-target approach for computing the sustainability of manufacturing systems. The selected data-based method is consistent, inclusive, neutral, efficient, and easy to implement and overcome the limitations of other assessment methods. Nine sustainability indicators considering various manufacturing systems are developed. The case study involving both traditional manufacturing and cyber manufacturing systems is considered for the applicability of the methodology. The workload differences do not influence the indicator values developed by the framework and assessment can be used to compare different cases.

[Ahmad et al. \(2019\)](#) developed weight-based inclusive sustainability indicators for the food manufacturing industry in Malaysia. The study considered 57 indicators based on expert opinion from industries through the Delphi method. The study suggested that Malaysian food manufacturing industries consider social sustainability most important contrast to environmental and economic point of sustainability, and moreover on the basis of global priority analysis, the top-ranked sustainable indicators were identified as electricity consumption, raw material usage, and cost of raw materials. Based on the applicability score, 25 indicators are termed as more relevant indicators with greater priority to social indicators followed by environmental and economic indicators.

[Henao et al. \(2019\)](#) presented a review on the outcome of lean manufacturing on sustainable performance. The review study included 69 papers. They categorized the papers based on the effect of lean manufacturing on operations performance, environmental performance, and social performance of sustainability. The outcome of the review suggested that lean manufacturing supports operational performance of sustainability much better than environmental and social performances, but still lacks empirical evidence.

[Huang et al. \(2018\)](#) proposed an index-based approach for broadly assessing the performance of sustainable manufacturing both in the manufacturing line and at company levels. The detailed sustainability metrics were developed considering pillars of sustainability, 6R concepts, and life cycle practices. The metrics are hierarchically organized. The applicability of the developed index is demonstrated for a manufacturing company.

[Agrawal and Vinodh \(2019\)](#) performed sustainability assessment of additive manufacturing processes. They considered 54 attributes, 18 criteria, and 3 enablers. Grey-based approach was employed for evaluation. The opinions from the experts were employed to estimate the overall grey performance index (OGPI) indicating the sustainability level of the

process. To create meaningful insights to the practitioners, the weaker attributes were determined using grey performance importance index.

Hartini et al. (2020) performed a sustainability assessment in the furniture manufacturing industry based on lean and sustainable concepts. The developed framework integrated Delphi method with sustainable-value stream mapping and analytical hierarchy process (AHP) to determine a single manufacturing sustainability index score. 11 indicators are selected through the Delphi method and are assessed through sustainable VSM. The weights of the indicators are determined using AHP. The single index enables the decision makers to consider both sustainability and productivity for sustainable manufacturing. The critical indicators are identified as quality, safety level, HR training, and material consumption.

Felsberger et al. (2020) proposed a structural model for the implementation of Industry 4.0 for the survival of the firm's existence with new real-time capabilities and competencies for the achievement of a sustainable competitive advantage. Six European manufacturing companies are considered for case study research. They developed seven theoretical research propositions to show the interrelations between firm's dynamic capabilities, Industry 4.0, and dimensions of sustainability. The complete understanding of dynamic capabilities fosters influence of Industry 4.0 on the triple bottom line of the sustainability aspects. The conclusion also enables financial decisions in Industry 4.0 implementation.

Saxena et al. (2020) assessed the impacts of manufacturing decisions on sustainable performance. The traditional triple bottom line sustainability metrics are considered with other metrics like quality, time, and flexibility. The proposed framework firstly assesses and roughly ranks the alternative process plans based on the information from computer-aided technologies system along with resource availability and market demands. Secondly, Technique for Order of Preference by Similarity to Ideal Solution is employed for the evaluation of highly ranked process plans with respect to the selected criteria. Nearness to the ideal solution varied based on comparative importance of sustainability dimensions and are demand dependent.

Kravchenko et al. (2020) suggested a systematic hypothetical-deductive-based technique for the indicator selection for analyzing circular economy performance strategies. The procedure is dynamic and flexible to aid in the sustainability concerned decision-making process. The procedure is user friendly permitting customization of indicators suitable to circular economy strategies and business processes objectives.

Sartal et al. (2020) presented the evolution of sustainable manufacturing methods and metrics over time for sustainability performance assessment. The potential sustainable manufacturing compatibility with Industry 4.0 value creation has been studied. They highlighted that technologies of Industry 4.0 highly support economic and

environmental dimensions rather than social dimensions of sustainable manufacturing.

Machado et al. (2020) conducted systematic review on the impact of sustainable manufacturing on Industry 4.0 development. 35 papers were considered for the study to identify the synergy linking sustainable manufacturing and Industry 4.0. Conceptual framework was developed considering the technological supports of Industry 4.0 with principles and dimensions of sustainable manufacturing. The authors suggested that although synergies exist between the two paradigms, they lack maturity.

Cai and Lai (2021) proposed an innovative approach for sustainability benchmark assessment to prevail over the challenges of the previous assessment methods for manufacturing systems. The constructs of the sustainability index system focused on the economy, energy, and environment-oriented assessments. The model promotes hierarchization and performance quantification. The practicability of the proposed insight for sustainability assessment has been demonstrated with a case study.

The present study focused on developing suitable sustainability assessment indicators for manufacturing processes. Grey-based approach is used due to the availability of incomplete information for assessment.

## 9.2 Methodology

---

Through literature survey, 48 sustainability-related indicators have been identified in manufacturing process related to environmental, societal, and economical aspects. 48 indicators have been classified into 12 criteria. Grey-based approach has been used as solution approach for evaluation. The input for sustainability evaluation model is derived from discussion with experts and also from literature review. The step-by-step procedure of grey-based approach is shown below with a brief description. Grey-based theory was originally developed by Deng (1982). It is widely used for problem domains with uncertainty and with insufficient information (Ji Shukla et al., 2014).

Definition 1. The grey number is represented by a set of upper bound and lower bound values. The accurate value of the grey number is unclear. Grey number can be illustrated as follows:

$$\otimes G = G \begin{matrix} \bar{\mu} \\ \underline{\mu} \end{matrix} \quad (9.1)$$

The fundamental laws governing the operation of grey numbers have been referred from Ram Matawale et al. (2014). Let two grey numbers be

$\otimes G_1 = [\underline{G}_1, \overline{G}_1]$  and  $\otimes G_2 = [\underline{G}_2, \overline{G}_2]$ , then the subsequent equation provides the length of the grey number:

$$L(\otimes G_1) = [\overline{G} - \underline{G}] \quad (9.2)$$

For any two grey numbers  $\otimes G_1 = [\underline{G}_1, \overline{G}_1]$  and  $\otimes G_2 = [\underline{G}_2, \overline{G}_2]$ , the grey possibility degree of  $\otimes G_1 \leq \otimes G_2$  can be determined as follows (Ji Shukla et al., 2014):

$$P\{\otimes G_1 \leq \otimes G_2\} = \frac{\max\left\{0, L^* - \max\left(0, \overline{G}_1 - \underline{G}_2\right)\right\}}{L^*} \quad (9.3)$$

where  $L^* = L(\otimes G_1) + L(\otimes G_2)$ .

For position relationship, there occur four possible cases of grey possibility degree:

- (1)  $P\{\otimes G_1 \leq \otimes G_2\} = 0.5$ , if  $\otimes G_1 = \otimes G_2$ .
- (2)  $P\{\otimes G_1 \leq \otimes G_2\} = 1$ , if  $\otimes G_2 > \otimes G_1$ .
- (3)  $P\{\otimes G_1 \leq \otimes G_2\} = 0$ , if  $\otimes G_2 < \otimes G_1$ .
- (4) If intercrossing exists between two grey numbers,  $\otimes G_1$  and  $\otimes G_2$ , when  $P\{\otimes G_1 \leq \otimes G_2\} > 0.5$ , it means that  $\otimes G_2$  is larger than  $\otimes G_1$ , signified as  $\otimes G_2 > \otimes G_1$ . When  $P\{\otimes G_1 \leq \otimes G_2\} < 0.5$ , it means that  $\otimes G_2$  is smaller than  $\otimes G_1$  signified as  $\otimes G_2 < \otimes G_1$  Ram Matawale et al. (2014).

Following are the six steps used in grey approach:

- 1 Determination of the suitable linguistic scale for evaluating the performance rating and weights of the evaluation model.
- 2 Approximation of the experts data of rating and weights.
- 3 Evaluation of the performance rating for criteria and enabler.
- 4 Determination of the overall grey performance index (OGPI).
- 5 Determination of grey performance importance index (GPII).
- 6 Estimation of grey possibility degree and attribute ranking.

The linguistic variable scales used for weights and ratings are mentioned in Tables 9.1 and 9.2, respectively (Ram Matawale et al., 2014). The above discussed steps are further explained in the next section.

### 9.3 Case study

Through the literature, 48 indicators (attributes) have been selected for sustainability assessment of manufacturing. The selected attributes are comprehensive and applicable from TBL perspective of sustainability.

**TABLE 9.1** Linguistic scale for weights of enablers, criteria, and attributes.

<b>Weight</b>	<b>Linguistic scale</b>
Very low (VL)	[0.0, 0.1]
Low (L)	[0.1, 0.3]
Medium low (ML)	[0.3, 0.4]
Medium (M)	[0.4, 0.5]
Medium high (MH)	[0.5, 0.6]
High (H)	[0.6, 0.9]
Very high (VH)	[0.9, 1.0]

The conceptual model was developed considering the environment, economy, and social aspects of sustainability in the manufacturing processes. The model consists of 48 attributes which are classified into 12 criteria and are grouped with 3 enablers. Environment enablers comprise 5 criteria with 14 attributes. Economic enabler includes 4 criteria with 21 attributes, while 3 criteria with 13 attributes are included under social enabler. The conceptual sustainability assessment model has been presented in [Table 9.3](#).

Sustainability of the manufacturing firm is evaluated using grey-based approach. For diagnosing group decision-making problems with uncertainty and incomplete data, grey approach is an effective tool.

**TABLE 9.2** Linguistic scale for attributes rating.

<b>Rating</b>	<b>Linguistic scale</b>
Very poor (VP)	[0, 1]
Poor (P)	[1, 3]
Fairly poor (FP)	[3, 4]
Fair (F)	[4, 5]
Fairly good (FG)	[5, 6]
Good (G)	[6, 9]
Very good (VG)	[9, 10]

TABLE 9.3 Conceptual model for sustainability evaluation.

Enablers	Criteria	Attributes	References
Environment (E <sub>1</sub> )	Footprint (C <sub>1,1</sub> )	Carbon footprint (A <sub>1,1,1</sub> )	Jamil et al. (2020) Henao et al. (2019) Thirupathi et al. (2019)
		Air footprint (A <sub>1,1,2</sub> )	Jamil et al. (2020) Henao et al. (2019)
		Water footprint (A <sub>1,1,3</sub> )	Jamil et al. (2020) Belgin et al. (2020) Henao et al. (2019) Thirupathi et al. (2019)
	Consumption (C <sub>1,2</sub> )	Water consumption (A <sub>1,2,1</sub> )	Saxena et al. (2020) Arianpoor et al. (2020)
		Material consumption (A <sub>1,2,2</sub> )	Hartini et al. (2020) Felsberger et al. (2020) Arianpoor et al. (2020)
		Energy consumption (A <sub>1,2,3</sub> )	Felsberger et al. (2020) Saxena et al. (2020) Arianpoor et al. (2020)
		Renewable energy consumption (A <sub>1,2,4</sub> )	Hartini et al. (2020) Saxena et al. (2020) Arianpoor et al. (2020)
	Acidification/ eutrophication (C <sub>1,3</sub> )	Water eutrophication (A <sub>1,3,1</sub> )	Jamil et al. (2020) Henao et al. (2019)
		Air acidification (A <sub>1,3,2</sub> )	Jamil et al. (2020) Henao et al. (2019)
	Disposal (C <sub>1,4</sub> )	Disposal of generated waste (A <sub>1,4,1</sub> )	Hartini et al. (2020) Saxena et al. (2020) Arianpoor et al. (2020)
		Material recovery (A <sub>1,4,2</sub> )	Belgin et al. (2020) Hartini et al. (2020) Kravchenko et al. (2020)

TABLE 9.3 Conceptual model for sustainability evaluation.—cont'd

Enablers	Criteria	Attributes	References
Economy (E <sub>2</sub> )	Pollution (C <sub>1,5</sub> )	Land-filled products (A <sub>1,4,3</sub> )	Sartal et al. (2020) Henao et al. (2019)
		Hazardous substances (A <sub>1,5,1</sub> )	Sartal et al. (2020) Arianpoor et al. (2020) Jamil et al. (2020) Thirupathi et al. (2019)
		Greenhouse gases (A <sub>1,5,2</sub> )	Arianpoor et al. (2020) Jamil et al. (2020) Huang et al. (2018)
	Financial performance (C <sub>2,1</sub> )	Net profit (C <sub>2,1,1</sub> )	Hartini et al. (2020) Arianpoor et al. (2020) Ahmad et al. (2019)
		Return on investment (C <sub>2,1,2</sub> )	Arianpoor et al. (2020) Henao et al. (2019)
		Cost saved (C <sub>2,1,3</sub> )	Felsberger et al. (2020) Henao et al. (2019)
		Manufacturing cost (C <sub>2,2</sub> )	Material cost (C <sub>2,2,1</sub> )
	Machinery cost (C <sub>2,2,2</sub> )		Henao et al. (2019) Ahmad et al. (2019)
	Energy cost (C <sub>2,2,3</sub> )		Jamil et al. (2020) Henao et al. (2019) Ahmad et al. (2019)
	Labor cost (C <sub>2,2,4</sub> )		Jamil et al. (2020) Henao et al. (2019) Ahmad et al. (2019)
	Operational and capital cost (C <sub>2,2,5</sub> )		Jamil et al. (2020) Hartini et al. (2020) Henao et al. (2019)
	Waste treatment cost (C <sub>2,2,6</sub> )		Kamble et al. (2020), Santos et al. (2019)
	Process (C <sub>2,3</sub> )	Cycle time (C <sub>2,3,1</sub> )	Jamil et al. (2020) Huang et al. (2018)

*Continued*

TABLE 9.3 Conceptual model for sustainability evaluation.—cont'd

Enablers	Criteria	Attributes	References
Societal (E <sub>3</sub> )	Product (C <sub>2,4</sub> )	Setup time (C <sub>2,3,2</sub> )	Jamil et al. (2020) Huang et al. (2018)
		Process flexibility (C <sub>2,3,3</sub> )	Henao et al. (2019) Kamble et al. (2020)
		Level of automation (C <sub>2,3,4</sub> )	Felsberger et al. (2020)
		Process visualization and control (C <sub>2,3,5</sub> )	Qian et al. (2019) Edgar and Pistikopoulos (2018)
		Machine life prediction (C <sub>2,3,6</sub> )	He et al. (2019) Kumar et al. (2019) Zhang et al. (2018)
		Information security and privacy (C <sub>2,3,7</sub> )	O'Donovan et al. (2019) Khalid et al. (2018) Kamble et al. (2020)
		Process quality (C <sub>2,4,1</sub> )	Felsberger et al. (2020) Ahmad et al. (2019) Henao et al. (2019)
		Product quality (C <sub>2,4,2</sub> )	Felsberger et al. (2020) Ahmad et al. (2019) Henao et al. (2019)
		Traceability (C <sub>2,4,3</sub> )	Felsberger et al. (2020)
		Transparency (C <sub>2,4,4</sub> )	Felsberger et al. (2020)
	Product customization (C <sub>2,4,5</sub> )	Kamble et al. (2020)	
	Employee (C <sub>3,1</sub> )	Employee satisfaction (C <sub>3,1,1</sub> )	Hartini et al. (2020) Huang et al. (2018) Thirupathi et al. (2019)
		Health and safety (C <sub>3,1,2</sub> )	Sartal et al. (2020) Saxena et al. (2020) Huang et al. (2018) Thirupathi et al. (2019)

TABLE 9.3 Conceptual model for sustainability evaluation.—cont'd

Enablers	Criteria	Attributes	References
	Training (C <sub>3,2</sub> )	Labor productivity (C <sub>3,1,3</sub> )	Arianpoor et al. (2020) Huang et al. (2018) Henao et al. (2019)
		Physical load index (C <sub>3,1,4</sub> )	Jamil et al. (2020) Huang et al. (2018) Henao et al. (2019)
		Employee anxiety (C <sub>3,1,5</sub> )	Roldan et al. (2019c) Kamble et al. (2020)
		Noninvasive interaction (C <sub>3,1,6</sub> )	Kamble et al. (2020)
		Employee morale (C <sub>3,1,7</sub> )	Kamble et al. (2020), Tortorella et al. (2020)
		Education (C <sub>3,2,1</sub> )	Felsberger et al. (2020) Hartini et al. (2020) Saxena et al. (2020) Huang et al. (2018)
		Innovation (C <sub>3,2,2</sub> )	Felsberger et al. (2020) Henao et al. (2019)
	Customer (C <sub>3,3</sub> )	Problem-solving skills enhancement (C <sub>3,2,3</sub> )	Felsberger et al. (2020) Henao et al. (2019) Huang et al. (2018)
		Customer satisfaction (C <sub>3,3,1</sub> )	Arianpoor et al. (2020) Ahmad et al. (2019) Song et al. (2019)
		Customer complaints (C <sub>3,3,2</sub> )	Arianpoor et al. (2020) Ahmad et al. (2019) Song et al. (2019)
		Real-time monitoring of customer order (C <sub>3,3,3</sub> )	Qu et al. (2019) Petrillo et al. (2019)

### 9.3.1 Determination of the suitable linguistic scale for evaluating the performance rating and weights of the assessment model

The individual subjective opinion is always related with vagueness and moreover it is difficult to fix the precise numeric score for the vague attribute. Linguistic variables have been used to overcome this difficulty. Input data sheet have been sent to four domain experts who have competencies in sustainable manufacturing systems. The four experts ( $E_1, E_2, E_3, E_4$ ) have provided the inputs for ratings and weights for each attribute for assessment and are presented in Table 9.4. The four experts have also provided the weights of different criteria and enablers and are shown in Tables 9.5 and 9.6.

### 9.3.2 Approximation of the expert's data of rating and weights

The input data required for sustainability assessment of manufacturing systems are obtained from four domain experts. The expert opinion may vary from one another. In order to reduce the variability and to make as a single value, approximation has been done with the collected data. The data approximation has been done with the following equation and has been applied for both weight and rating approximation. The approximated weight and rating of attributes are shown in Table 9.7.

$$\otimes W_j = \frac{1}{n} \left[ \otimes W_j^1 + \otimes W_j^2 + \otimes W_j^3 + \dots + \otimes W_j^n \right], \quad (9.4)$$

Where operator  $\otimes$  represents grey number,  $n$  represents the number of experts,  $\otimes W_j$  denotes the approximate weight for the  $j$ th enabler, and  $\otimes W_j^n$  denotes the weight given by the  $n$ th expert to the  $j$ th enabler.

### 9.3.3 Evaluation of the performance rating for criteria and enabler

The rating for each criterion, that is the performance rating for the second level, can be determined using the subsequent equation:

$$R_{i,j} = \frac{\sum_{k=1}^p (W_{i,j,k} \otimes R_{i,j,k})}{W_{i,j,k}} \quad (9.5)$$

where  $p$  is the number of attributes related to  $j$ th criterion;  $R_{i,j}$  is the approximated performance rating of  $j$ th criterion of  $i$ th enabler;  $W_{i,j,k}$  and  $R_{i,j,k}$  are the approximated weight and approximated rating related to  $A_{i,j,k}$  attribute.

TABLE 9.4 Rating and weights of each attribute as given by the experts.

Attributes	Rating	E <sub>1</sub>	E <sub>2</sub>	E <sub>3</sub>	E <sub>4</sub>	Weights	E <sub>1</sub>	E <sub>2</sub>	E <sub>3</sub>	E <sub>4</sub>
A <sub>1,1,1</sub>	R <sub>1,1,1</sub>	G	FG	FG	G	W <sub>1,1,1</sub>	H	MH	MH	H
A <sub>1,1,2</sub>	R <sub>1,1,2</sub>	FG	G	G	FG	W <sub>1,1,2</sub>	MH	M	MH	M
A <sub>1,1,3</sub>	R <sub>1,1,3</sub>	FG	G	FG	G	W <sub>1,1,3</sub>	M	MH	M	MH
A <sub>1,2,1</sub>	R <sub>1,2,1</sub>	F	FG	FG	F	W <sub>1,2,1</sub>	M	MH	M	M
A <sub>1,2,2</sub>	R <sub>1,2,2</sub>	FG	G	FG	G	W <sub>1,2,2</sub>	MH	M	M	MH
A <sub>1,2,3</sub>	R <sub>1,2,3</sub>	FG	G	FG	F	W <sub>1,2,3</sub>	H	M	MH	M
A <sub>1,2,4</sub>	R <sub>1,2,4</sub>	FG	G	G	FG	W <sub>1,2,4</sub>	MH	H	MH	H
A <sub>1,3,1</sub>	R <sub>1,3,1</sub>	FG	G	G	FG	W <sub>1,3,1</sub>	MH	M	MH	M
A <sub>1,3,2</sub>	R <sub>1,3,2</sub>	FG	G	G	FG	W <sub>1,3,2</sub>	MH	M	M	MH
A <sub>1,4,1</sub>	R <sub>1,4,1</sub>	FG	G	G	G	W <sub>1,4,1</sub>	MH	M	MH	M
A <sub>1,4,2</sub>	R <sub>1,4,2</sub>	FG	G	FG	FG	W <sub>1,4,2</sub>	MH	MH	M	M
A <sub>1,4,3</sub>	R <sub>1,4,3</sub>	FG	G	FG	G	W <sub>1,4,3</sub>	M	MH	M	MH
A <sub>1,5,1</sub>	R <sub>1,5,1</sub>	FG	F	FG	F	W <sub>1,5,1</sub>	MH	M	MH	M
A <sub>1,5,2</sub>	R <sub>1,5,2</sub>	F	FG	FG	F	W <sub>1,5,2</sub>	M	MH	M	MH
A <sub>2,1,1</sub>	R <sub>2,1,1</sub>	FG	G	G	FG	W <sub>2,1,1</sub>	H	MH	MH	H
A <sub>2,1,2</sub>	R <sub>2,1,2</sub>	G	FG	FG	G	W <sub>2,1,2</sub>	H	MH	MH	H
A <sub>2,1,3</sub>	R <sub>2,1,3</sub>	G	FG	G	FG	W <sub>2,1,3</sub>	M	MH	M	MH
A <sub>2,2,1</sub>	R <sub>2,2,1</sub>	FG	G	G	FG	W <sub>2,2,1</sub>	M	MH	M	MH
A <sub>2,2,2</sub>	R <sub>2,2,2</sub>	FG	G	FG	G	W <sub>2,2,2</sub>	MH	M	M	MH
A <sub>2,2,3</sub>	R <sub>2,2,3</sub>	FG	G	G	FG	W <sub>2,2,3</sub>	M	MH	MH	M
A <sub>2,2,4</sub>	R <sub>2,2,4</sub>	F	F	FG	F	W <sub>2,2,4</sub>	M	ML	M	ML
A <sub>2,2,5</sub>	R <sub>2,2,5</sub>	FG	F	F	FP	W <sub>2,2,5</sub>	ML	M	M	ML
A <sub>2,2,6</sub>	R <sub>2,2,6</sub>	FG	G	G	FG	W <sub>2,2,6</sub>	M	MH	MH	M
A <sub>2,3,1</sub>	R <sub>2,3,1</sub>	G	FG	G	FG	W <sub>2,3,1</sub>	M	MH	M	MH
A <sub>2,3,2</sub>	R <sub>2,3,2</sub>	FG	F	FG	F	W <sub>2,3,2</sub>	M	ML	ML	M
A <sub>2,3,3</sub>	R <sub>2,3,3</sub>	FG	G	FG	F	W <sub>2,3,3</sub>	M	MH	MH	M
A <sub>2,3,4</sub>	R <sub>2,3,4</sub>	F	FG	FG	F	W <sub>2,3,4</sub>	M	MH	H	MH
A <sub>2,3,5</sub>	R <sub>2,3,5</sub>	F	FG	F	FG	W <sub>2,3,5</sub>	MH	M	M	MH
A <sub>2,3,6</sub>	R <sub>2,3,6</sub>	FG	G	FG	F	W <sub>2,3,6</sub>	M	MH	M	MH
A <sub>2,3,7</sub>	R <sub>2,3,7</sub>	F	FG	G	FG	W <sub>2,3,7</sub>	MH	M	MH	M

Continued

TABLE 9.4 Rating and weights of each attribute as given by the experts.—cont'd

Attributes	Rating	E <sub>1</sub>	E <sub>2</sub>	E <sub>3</sub>	E <sub>4</sub>	Weights	E <sub>1</sub>	E <sub>2</sub>	E <sub>3</sub>	E <sub>4</sub>
A <sub>2,4,1</sub>	R <sub>2,4,1</sub>	G	FG	G	F	W <sub>2,4,1</sub>	M	MH	MH	M
A <sub>2,4,2</sub>	R <sub>2,4,2</sub>	FG	G	FG	FG	W <sub>2,4,2</sub>	MH	H	MH	H
A <sub>2,4,3</sub>	R <sub>2,4,3</sub>	FG	G	FG	G	W <sub>2,4,3</sub>	M	MH	MH	M
A <sub>2,4,4</sub>	R <sub>2,4,4</sub>	FG	F	FG	G	W <sub>2,4,4</sub>	M	MH	M	H
A <sub>2,4,5</sub>	R <sub>2,4,5</sub>	G	G	FG	G	W <sub>2,4,5</sub>	MH	M	MH	H
A <sub>3,1,1</sub>	R <sub>3,1,1</sub>	G	VG	G	VG	W <sub>3,1,1</sub>	H	MH	H	MH
A <sub>3,1,2</sub>	R <sub>3,1,2</sub>	G	FG	G	VG	W <sub>3,1,2</sub>	H	MH	H	M
A <sub>3,1,3</sub>	R <sub>3,1,3</sub>	VG	G	FG	FG	W <sub>3,1,3</sub>	H	M	MH	M
A <sub>3,1,4</sub>	R <sub>3,1,4</sub>	G	FG	F	FG	W <sub>3,1,4</sub>	MH	M	M	MH
A <sub>3,1,5</sub>	R <sub>3,1,5</sub>	F	G	FG	G	W <sub>3,1,5</sub>	MH	M	M	MH
A <sub>3,1,6</sub>	R <sub>3,1,6</sub>	FG	G	G	FG	W <sub>3,1,6</sub>	M	MH	M	MH
A <sub>3,1,7</sub>	R <sub>3,1,7</sub>	G	FG	FG	G	W <sub>3,1,7</sub>	M	MH	MH	M
A <sub>3,2,1</sub>	R <sub>3,2,1</sub>	G	FG	FG	F	W <sub>3,2,1</sub>	MH	M	MH	M
A <sub>3,2,2</sub>	R <sub>3,2,2</sub>	FG	G	FG	F	W <sub>3,2,2</sub>	M	MH	MH	M
A <sub>3,2,3</sub>	R <sub>3,2,3</sub>	G	FG	G	FG	W <sub>3,2,3</sub>	MH	H	MH	H
A <sub>3,3,1</sub>	R <sub>3,3,1</sub>	G	FG	FG	G	W <sub>3,3,1</sub>	MH	H	MH	MH
A <sub>3,3,2</sub>	R <sub>3,3,2</sub>	G	FG	FG	G	W <sub>3,3,2</sub>	M	MH	MH	M
A <sub>3,3,3</sub>	R <sub>3,3,3</sub>	FG	G	FG	G	W <sub>3,3,3</sub>	H	MH	MH	H

For example:

$$R_{1,3} = \frac{[(W_{1,3,1} \otimes R_{1,3,1}) \times (W_{1,3,2} \otimes R_{1,3,2})]}{[W_{1,3,1} + W_{1,3,2}]}$$

$$R_{1,3} = \frac{[(0.45, 0.55) \times (5.5, 7.5)] + [(0.45, 0.55) \times (5.5, 7.5)]}{[(0.45, 0.55) + (0.45, 0.55)]}$$

$$R_{1,3} = (4.500, 9.166)$$

The weights and calculated performance ratings for criteria have been shown in Table 9.8.

The rating for each enabler that is the performance rating for the first level can be determined using the subsequent equation:

$$R_i = \frac{\sum_{k=1}^q (W_{i,j} \otimes R_{i,j})}{W_{i,j}} \tag{9.6}$$

TABLE 9.5 Weights of each criterion as given by the experts.

Criteria	Weight	E <sub>1</sub>	E <sub>2</sub>	E <sub>3</sub>	E <sub>4</sub>
C <sub>1,1</sub>	W <sub>1,1</sub>	H	MH	H	H
C <sub>1,2</sub>	W <sub>1,2</sub>	MH	H	H	MH
C <sub>1,3</sub>	W <sub>1,3</sub>	MH	M	M	MH
C <sub>1,4</sub>	W <sub>1,4</sub>	H	M	M	H
C <sub>1,5</sub>	W <sub>1,5</sub>	MH	MH	M	MH
C <sub>2,1</sub>	W <sub>2,1</sub>	H	VH	H	MH
C <sub>2,2</sub>	W <sub>2,2</sub>	MH	H	MH	H
C <sub>2,3</sub>	W <sub>2,3</sub>	H	MH	MH	H
C <sub>2,4</sub>	W <sub>2,4</sub>	M	MH	M	MH
C <sub>3,1</sub>	W <sub>3,1</sub>	MH	H	MH	H
C <sub>3,2</sub>	W <sub>3,2</sub>	H	MH	MH	H
C <sub>3,3</sub>	W <sub>3,3</sub>	H	M	MH	H

where  $q$  is the number of criteria related to  $i$ th enabler;  $R_i$  is the approximated performance rating of  $i$ th enabler;  $W_{i,j}$  and  $R_{i,j}$  are the approximated weight and computed rating related to  $C_{i,j}$  criterion.

For example:

$$R_3 = \frac{[(W_{3,1} \otimes R_{3,1}) \times (W_{3,2} \otimes R_{3,2}) \times (W_{3,3} \otimes R_{3,3})]}{[W_{3,1} + W_{3,2} + W_{3,3}]}$$

$$R_3 = \frac{\{(0.55, 0.75) \times (4.666, 10.132)\} + \{(0.55, 0.75) \times (3.770, 9.462)\} + \{(0.525, 0.725) \times (4.246, 9.713)\}}{\{(0.55, 0.75) + (0.55, 0.75) + (0.525, 0.725)\}}$$

$$R_3 = (3.087, 13.376)$$

The weights and calculated performance ratings for enablers are shown in Table 9.9.

TABLE 9.6 Weights of each enabler as given by the experts.

Enablers	Weight	E <sub>1</sub>	E <sub>2</sub>	E <sub>3</sub>	E <sub>4</sub>
E <sub>1</sub>	W <sub>1</sub>	H	MH	MH	H
E <sub>2</sub>	W <sub>2</sub>	M	MH	M	H
E <sub>3</sub>	W <sub>3</sub>	MH	M	M	MH

TABLE 9.7 Approximated weight and rating of attributes.

Attributes	Weight	Approximated weight expressed in grey number	Rating	Approximated rating expressed in grey number
$A_{1,1,1}$	$W_{1,1,1}$	(0.55, 0.75)	$R_{1,1,1}$	(5.5, 7.5)
$A_{1,1,2}$	$W_{1,1,2}$	(0.45, 0.55)	$R_{1,1,2}$	(5.5, 7.5)
$A_{1,1,3}$	$W_{1,1,3}$	(0.45, 0.55)	$R_{1,1,3}$	(5.5, 7.5)
$A_{1,2,1}$	$W_{1,2,1}$	(0.425, 0.525)	$R_{1,2,1}$	(4.5, 5.5)
$A_{1,2,2}$	$W_{1,2,2}$	(0.45, 0.55)	$R_{1,2,2}$	(5.5, 7.5)
$A_{1,2,3}$	$W_{1,2,3}$	(0.475, 0.625)	$R_{1,2,3}$	(5.0, 6.5)
$A_{1,2,4}$	$W_{1,2,4}$	(0.55, 0.75)	$R_{1,2,4}$	(5.5, 7.5)
$A_{1,3,1}$	$W_{1,3,1}$	(0.45, 0.55)	$R_{1,3,1}$	(5.5, 7.5)
$A_{1,3,2}$	$W_{1,3,2}$	(0.45, 0.55)	$R_{1,3,2}$	(5.5, 7.5)
$A_{1,4,1}$	$W_{1,4,1}$	(0.45, 0.55)	$R_{1,4,1}$	(5.75, 8.25)
$A_{1,4,2}$	$W_{1,4,2}$	(0.45, 0.55)	$R_{1,4,2}$	(5.25, 6.75)
$A_{1,4,3}$	$W_{1,4,3}$	(0.45, 0.55)	$R_{1,4,3}$	(5.5, 7.5)
$A_{1,5,1}$	$W_{1,5,1}$	(0.45, 0.55)	$R_{1,5,1}$	(4.5, 5.5)
$A_{1,5,2}$	$W_{1,5,2}$	(0.45, 0.55)	$R_{1,5,2}$	(4.5, 5.5)
$A_{2,1,1}$	$W_{2,1,1}$	(0.55, 0.75)	$R_{2,1,1}$	(5.5, 7.5)
$A_{2,1,2}$	$W_{2,1,2}$	(0.55, 0.75)	$R_{2,1,2}$	(5.5, 7.5)
$A_{2,1,3}$	$W_{2,1,3}$	(0.45, 0.55)	$R_{2,1,3}$	(5.5, 7.5)
$A_{2,2,1}$	$W_{2,2,1}$	(0.45, 0.55)	$R_{2,2,1}$	(5.5, 7.5)
$A_{2,2,2}$	$W_{2,2,2}$	(0.45, 0.55)	$R_{2,2,2}$	(5.5, 7.5)
$A_{2,2,3}$	$W_{2,2,3}$	(0.45, 0.55)	$R_{2,2,3}$	(5.5, 7.5)
$A_{2,2,4}$	$W_{2,2,4}$	(0.35, 0.45)	$R_{2,2,4}$	(4.25, 5.25)
$A_{2,2,5}$	$W_{2,2,5}$	(0.35, 0.45)	$R_{2,2,5}$	(4.0, 5.0)
$A_{2,2,6}$	$W_{2,2,6}$	(0.45, 0.55)	$R_{2,2,6}$	(5.5, 7.5)
$A_{2,3,1}$	$W_{2,3,1}$	(0.45, 0.55)	$R_{2,3,1}$	(5.5, 7.5)
$A_{2,3,2}$	$W_{2,3,2}$	(0.35, 0.45)	$R_{2,3,2}$	(4.5, 5.5)
$A_{2,3,3}$	$W_{2,3,3}$	(0.45, 0.55)	$R_{2,3,3}$	(5.0, 6.5)
$A_{2,3,4}$	$W_{2,3,4}$	(0.50, 0.65)	$R_{2,3,4}$	(4.5, 5.5)
$A_{2,3,5}$	$W_{2,3,5}$	(0.45, 0.55)	$R_{2,3,5}$	(4.5, 5.5)

TABLE 9.7 Approximated weight and rating of attributes.—cont'd

Attributes	Weight	Approximated weight expressed in grey number	Rating	Approximated rating expressed in grey number
$A_{2,3,6}$	$W_{2,3,6}$	(0.45, 0.55)	$R_{2,3,6}$	(5.0, 6.5)
$A_{2,3,7}$	$W_{2,3,7}$	(0.45, 0.55)	$R_{2,3,7}$	(5.0, 6.5)
$A_{2,4,1}$	$W_{2,4,1}$	(0.45, 0.55)	$R_{2,4,1}$	(5.25, 7.25)
$A_{2,4,2}$	$W_{2,4,2}$	(0.55, 0.75)	$R_{2,4,2}$	(5.25, 6.75)
$A_{2,4,3}$	$W_{2,4,3}$	(0.45, 0.55)	$R_{2,4,3}$	(5.5, 7.5)
$A_{2,4,4}$	$W_{2,4,4}$	(0.475, 0.625)	$R_{2,4,4}$	(5.0, 6.5)
$A_{2,4,5}$	$W_{2,4,5}$	(0.50, 0.65)	$R_{2,4,5}$	(5.75, 8.25)
$A_{3,1,1}$	$W_{3,1,1}$	(0.55, 0.75)	$R_{3,1,1}$	(7.5, 9.5)
$A_{3,1,2}$	$W_{3,1,2}$	(0.525, 0.725)	$R_{3,1,2}$	(6.5, 8.5)
$A_{3,1,3}$	$W_{3,1,3}$	(0.475, 0.625)	$R_{3,1,3}$	(6.25, 7.75)
$A_{3,1,4}$	$W_{3,1,4}$	(0.45, 0.55)	$R_{3,1,4}$	(5.0, 6.5)
$A_{3,1,5}$	$W_{3,1,5}$	(0.45, 0.55)	$R_{3,1,5}$	(5.25, 7.25)
$A_{3,1,6}$	$W_{3,1,6}$	(0.45, 0.55)	$R_{3,1,6}$	(5.5, 7.5)
$A_{3,1,7}$	$W_{3,1,7}$	(0.45, 0.55)	$R_{3,1,7}$	(5.5, 7.5)
$A_{3,2,1}$	$W_{3,2,1}$	(0.45, 0.55)	$R_{3,2,1}$	(5.0, 6.5)
$A_{3,2,2}$	$W_{3,2,2}$	(0.45, 0.55)	$R_{3,2,2}$	(5.0, 6.5)
$A_{3,2,3}$	$W_{3,2,3}$	(0.45, 0.75)	$R_{3,2,3}$	(5.5, 7.5)
$A_{3,3,1}$	$W_{3,3,1}$	(0.525, 0.675)	$R_{3,3,1}$	(5.5, 7.5)
$A_{3,3,2}$	$W_{3,3,2}$	(0.45, 0.55)	$R_{3,3,2}$	(5.5, 7.5)
$A_{3,3,3}$	$W_{3,3,3}$	(0.55, 0.75)	$R_{3,3,3}$	(5.5, 7.5)

### 9.3.4 Determination of the overall grey performance index

The sustainability index of the manufacturing performance is determined using the OGPI. The following equation is used to calculate the OGPI:

$$\text{OGPI} = \frac{\sum_{i=1}^r (W_i \otimes R_i)}{W_i} \quad (9.7)$$

where  $r$  is the number of enablers;  $W_i$  and  $R_i$  are the approximated weight and computed rating corresponding to  $E_i$  enabler.

TABLE 9.8 Approximated weight and calculated rating of each criterion.

Criteria	Weight	Approximated weight expressed in grey number	Rating	Approximated rating expressed in grey number
$C_{1,1}$	$W_{1,1}$	(0.575, 0.825)	$R_{1,1}$	(4.310, 9.568)
$C_{1,2}$	$W_{1,2}$	(0.55, 0.75)	$R_{1,2}$	(3.994, 8.789)
$C_{1,3}$	$W_{1,3}$	(0.45, 0.55)	$R_{1,3}$	(4.50, 9.166)
$C_{1,4}$	$W_{1,4}$	(0.50, 0.70)	$R_{1,4}$	(4.499, 9.165)
$C_{1,5}$	$W_{1,5}$	(0.475, 0.575)	$R_{1,5}$	(3.681, 6.722)
$C_{2,1}$	$W_{2,1}$	(0.65, 0.85)	$R_{2,1}$	(4.158, 9.919)
$C_{2,2}$	$W_{2,2}$	(0.55, 0.75)	$R_{2,2}$	(4.125, 8.445)
$C_{2,3}$	$W_{2,3}$	(0.55, 0.75)	$R_{2,3}$	(3.915, 7.717)
$C_{2,4}$	$W_{2,4}$	(0.45, 0.55)	$R_{2,4}$	(4.125, 9.318)
$C_{3,1}$	$W_{3,1}$	(0.55, 0.75)	$R_{3,1}$	(4.666, 10.132)
$C_{3,2}$	$W_{3,2}$	(0.55, 0.75)	$R_{3,2}$	(3.770, 9.462)
$C_{3,3}$	$W_{3,3}$	(0.525, 0.725)	$R_{3,3}$	(4.246, 9.713)

OGPI is computed by using Eq. (9.7):

$$\text{OGPI} = \frac{[(W_1 \otimes R_1) \times (W_2 \otimes R_2) \times (W_3 \otimes R_3)]}{[W_1 + W_2 + W_3]}$$

$$\text{OGPI} = \frac{\{(0.55, 0.75) \times (3.145, 11.688)\} + \{(0.475, 0.625) \times (3.096, 11.671)\} + \{(0.45, 0.55) \times (3.087, 13.376)\}}{\{(0.55, 0.75) + (0.475, 0.625) + (0.45, 0.55)\}}$$

$$\text{OGPI} = (2.384, 15.876)$$

OGPI value is found to be (2.384, 15.876), representing the sustainability index of the manufacturing process.

### 9.3.5 Determination of GPII

Once OGPI is calculated, it is also required to identify and examine the impediments for the sustainability index improvement. GPII can be used to identify the improvement domains. GPII can be determined for each attribute by means of Eq. (9.8) and associates both the performance rating and importance weight corresponding to that attribute. Higher value of GPII for an attribute indicates higher contribution toward sustainability.

$$\text{GPII}_{i,j,k} = W'_{i,j,k} \otimes R_{i,j,k} \quad (9.8)$$

TABLE 9.9 Approximated weight and calculated rating of each enabler.

Enabler	Weight	Approximated weight expressed in grey number	Rating	Approximated rating expressed in grey number
$E_1$	$W_1$	(0.55, 0.75)	$R_1$	(3.145, 11.689)
$E_2$	$W_2$	(0.475, 0.625)	$R_2$	(3.096, 11.671)
$E_3$	$W_3$	(0.45, 0.55)	$R_3$	(3.087, 13.376)

$$W'_{i,j,k} = \left[ (1, 1) - (W_{i,j,k}) \right] \quad (9.9)$$

where  $GPII_{i,j,k}$  is the GPII value corresponding to  $A_{i,j,k}$  attribute.  $W_{i,j,k}$  and  $R_{i,j,k}$  are the approximated weight and approximated rating related to  $A_{i,j,k}$  attribute.

For example,

$$\begin{aligned} GPII_{2,1,1} &= W'_{2,1,1} \otimes R_{2,1,1} \\ GPII_{2,1,1} &= [(0.25, 0.45) \times (5.5, 7.5)] \\ GPII_{2,1,1} &= (1.375, 3.375) \end{aligned}$$

### 9.3.6 Estimation of grey possibility degree and attribute ranking

In order to evaluate the individual performance rating of each attribute, GPII values are ranked. Poorly performing attributes are identified through raking and require much attention for boosting the overall sustainability. After determining GPII value of each attribute, grey possibility degree is computed for each attribute by comparing each attributes GPII value with ideal GPII value which is the maximum value among all the attributes GPII value. Smaller value of grey possibility degree of attribute indicates the attribute higher performance toward sustainability. The ideal GPII value from Table 9.10 is  $(\otimes G_2) = (2.587, 4.537)$ .

The grey possibility degree can be determined by means of Eq. (9.3).

For example, the grey possibility degree for the attribute  $(A_{2,1,1})$  is as follows:

$$A_{2,1,1} = \frac{\max \{0, L^* - \max(0, \bar{G}_1 - G_2)\}}{L^*}$$

where  $L^* = L(\otimes G_1) + L(\otimes G_2)$ .

GPII for  $A_{2,1,1} = (\otimes G_1) = (1.375, 3.375)$

TABLE 9.10 Computed GPII, Grey possibility degree and Ranking order of each attribute.

Sustainability Attributes	Rating ( $R_{i,j,k}$ )	Weight ( $W_{i,j,k}$ )	$W'$ $W'_{i,j,k} = [(1, 1) - (W_{i,j,k})]$	GPII	Grey possibility degree	Ranking order
$A_{1,1,1}$	(5.5, 7.5)	(0.55, 0.75)	(0.25, 0.45)	(1.375, 3.375)	0.801	16
$A_{1,1,2}$	(5.5, 7.5)	(0.45, 0.55)	(0.45, 0.55)	(2.475, 4.125)	0.573	2
$A_{1,1,3}$	(5.5, 7.5)	(0.45, 0.55)	(0.45, 0.55)	(2.475, 4.125)	0.573	2
$A_{1,2,1}$	(4.5, 5.5)	(0.425, 0.525)	(0.475, 0.575)	(2.137, 3.162)	0.807	17
$A_{1,2,2}$	(5.5, 7.5)	(0.45, 0.55)	(0.45, 0.55)	(2.475, 4.125)	0.573	2
$A_{1,2,3}$	(5.0, 6.5)	(0.475, 0.625)	(0.375, 0.525)	(1.875, 3.412)	0.763	14
$A_{1,2,4}$	(5.5, 7.5)	(0.55, 0.75)	(0.25, 0.45)	(1.375, 3.375)	0.801	16
$A_{1,3,1}$	(5.5, 7.5)	(0.45, 0.55)	(0.45, 0.55)	(2.475, 4.125)	0.573	2
$A_{1,3,2}$	(5.5, 7.5)	(0.45, 0.55)	(0.45, 0.55)	(2.475, 4.125)	0.573	2
$A_{1,4,1}$	(5.75, 8.25)	(0.45, 0.55)	(0.45, 0.55)	(2.587, 4.537)	0.500	1
$A_{1,4,2}$	(5.25, 6.75)	(0.45, 0.55)	(0.45, 0.55)	(2.362, 3.712)	0.659	8
$A_{1,4,3}$	(5.5, 7.5)	(0.45, 0.55)	(0.45, 0.55)	(2.475, 4.125)	0.573	2
$A_{1,5,1}$	(4.5, 5.5)	(0.45, 0.55)	(0.45, 0.55)	(2.025, 3.025)	0.852	18
$A_{1,5,2}$	(4.5, 5.5)	(0.45, 0.55)	(0.45, 0.55)	(2.025, 3.025)	0.852	18
$A_{2,1,1}$	(5.5, 7.5)	(0.55, 0.75)	(0.25, 0.45)	(1.375, 3.375)	0.801	16
$A_{2,1,2}$	(5.5, 7.5)	(0.55, 0.75)	(0.25, 0.45)	(1.375, 3.375)	0.801	16
$A_{2,1,3}$	(5.5, 7.5)	(0.45, 0.55)	(0.45, 0.55)	(2.475, 4.125)	0.573	2
$A_{2,2,1}$	(5.5, 7.5)	(0.45, 0.55)	(0.45, 0.55)	(2.475, 4.125)	0.573	2
$A_{2,2,2}$	(5.5, 7.5)	(0.45, 0.55)	(0.45, 0.55)	(2.475, 4.125)	0.573	2
$A_{2,2,3}$	(5.5, 7.5)	(0.45, 0.55)	(0.45, 0.55)	(2.475, 4.125)	0.573	2
$A_{2,2,4}$	(4.25, 5.25)	(0.35, 0.45)	(0.55, 0.65)	(2.337, 3.412)	0.727	12
$A_{2,2,5}$	(4.0, 5.0)	(0.35, 0.45)	(0.55, 0.65)	(2.200, 3.250)	0.779	15
$A_{2,2,6}$	(5.5, 7.5)	(0.45, 0.55)	(0.45, 0.55)	(2.475, 4.125)	0.573	2
$A_{2,3,1}$	(5.5, 7.5)	(0.45, 0.55)	(0.45, 0.55)	(2.475, 4.125)	0.573	2
$A_{2,3,2}$	(4.5, 5.5)	(0.35, 0.45)	(0.55, 0.65)	(2.475, 3.575)	0.676	10
$A_{2,3,3}$	(5.0, 6.5)	(0.45, 0.55)	(0.45, 0.55)	(2.250, 3.575)	0.698	11
$A_{2,3,4}$	(4.5, 5.5)	(0.50, 0.65)	(0.35, 0.50)	(1.575, 2.750)	0.948	20

TABLE 9.10 Computed GPII, Grey possibility degree and Ranking order of each attribute.—cont'd

Sustainability Attributes	Rating ( $R_{i,j,k}$ )	Weight ( $W_{i,j,k}$ )	$W'$ $W'_{i,j,k} = [(1, 1) - (W_{i,j,k})]$	GPII	Grey possibility degree	Ranking order
$A_{2,3,5}$	(4.5, 5.5)	(0.45, 0.55)	(0.45, 0.55)	(2.025, 3.025)	0.852	17
$A_{2,3,6}$	(5.0, 6.5)	(0.45, 0.55)	(0.45, 0.55)	(2.250, 3.575)	0.698	11
$A_{2,3,7}$	(5.0, 6.5)	(0.45, 0.55)	(0.45, 0.55)	(2.250, 3.575)	0.698	11
$A_{2,4,1}$	(5.25, 7.25)	(0.45, 0.55)	(0.45, 0.55)	(2.362, 3.987)	0.609	4
$A_{2,4,2}$	(5.25, 6.75)	(0.55, 0.75)	(0.25, 0.45)	(1.312, 3.037)	0.878	19
$A_{2,4,3}$	(5.5, 7.5)	(0.45, 0.55)	(0.45, 0.55)	(2.475, 4.125)	0.573	2
$A_{2,4,4}$	(5.0, 6.5)	(0.475, 0.625)	(0.375, 0.525)	(1.875, 3.412)	0.763	14
$A_{2,4,5}$	(5.75, 8.25)	(0.50, 0.65)	(0.35, 0.50)	(2.012, 4.125)	0.621	6
$A_{3,1,1}$	(7.5, 9.5)	(0.55, 0.75)	(0.25, 0.45)	(1.875, 4.275)	0.612	5
$A_{3,1,2}$	(6.5, 8.5)	(0.525, 0.725)	(0.275, 0.475)	(1.787, 4.037)	0.655	7
$A_{3,1,3}$	(6.25, 7.75)	(0.475, 0.625)	(0.375, 0.525)	(2.343, 4.068)	0.597	3
$A_{3,1,4}$	(5.0, 6.5)	(0.45, 0.55)	(0.45, 0.55)	(2.250, 3.575)	0.698	11
$A_{3,1,5}$	(5.25, 7.25)	(0.45, 0.55)	(0.45, 0.55)	(2.362, 3.987)	0.609	4
$A_{3,1,6}$	(5.5, 7.5)	(0.45, 0.55)	(0.45, 0.55)	(2.475, 4.125)	0.573	2
$A_{3,1,7}$	(5.5, 7.5)	(0.45, 0.55)	(0.45, 0.55)	(2.475, 4.125)	0.573	2
$A_{3,2,1}$	(5.0, 6.5)	(0.45, 0.55)	(0.45, 0.55)	(2.250, 3.575)	0.698	11
$A_{3,2,2}$	(5.0, 6.5)	(0.45, 0.55)	(0.45, 0.55)	(2.250, 3.575)	0.698	11
$A_{3,2,3}$	(5.5, 7.5)	(0.45, 0.75)	(0.25, 0.55)	(1.375, 4.125)	0.673	9
$A_{3,3,1}$	(5.5, 7.5)	(0.525, 0.675)	(0.325, 0.475)	(1.787, 3.562)	0.738	13
$A_{3,3,2}$	(5.5, 7.5)	(0.45, 0.55)	(0.45, 0.55)	(2.475, 4.125)	0.573	2
$A_{3,3,3}$	(5.5, 7.5)	(0.55, 0.75)	(0.25, 0.45)	(1.375, 3.375)	0.801	16

$$\text{Ideal GPII} = (\otimes G_2) = (2.587, 4.537)$$

$$L(\otimes G_1) = 3.375 - 1.375 = 2.00$$

$$L(\otimes G_2) = 4.537 - 2.587 = 1.95$$

$$L^* = 3.95$$

$$A_{2,1,1} = \frac{\max \{0, 3.95 - \max (0, 3.375 - 2.587)\}}{3.95}$$

$$A_{2,1,1} = 0.801$$

Table 9.10 shows the computed GPII and grey possibility degree of each attribute.

## 9.4 Results

The sustainability assessment of the manufacturing process is computed using OGPI and the performance index is calculated as (2.384, 15.876) in terms of grey number. Euclidean distance method is applied to determine the sustainability level of manufacturing processes. This method measures the distance between OGPI and a range of sustainability levels. The sustainability level considered in the study comprise seven factors specifically very poor (VP), poor (P), fairly poor (FP), fair (F), fairly good (FG), good (G), and very good (VG). The sustainability level having the nearest distance with OGPI will be regarded as the sustainability level of manufacturing process.

The Euclidean distance between the two grey numbers  $\otimes G_1 = [\underline{G}_1, \overline{G}_1]$  and  $\otimes G_2 = [\underline{G}_2, \overline{G}_2]$  can be computed using the equation:

$$D(\otimes G_1, \otimes G_2) = \left[ \left( \underline{G}_1 - \underline{G}_2 \right)^2 + \left( \overline{G}_1 - \overline{G}_2 \right)^2 \right]^{1/2} \quad (9.10)$$

Using the above equation, the Euclidean distance between each sustainability level and OGPI is computed as shown below:

$$D(\text{OGPI}, \text{VP}) = [(2.384 - 0)^2 + (15.876 - 1)^2]^{1/2} = 15.065,$$

$$D(\text{OGPI}, \text{P}) = [(2.384 - 1)^2 + (15.876 - 3)^2]^{1/2} = 12.950,$$

$$D(\text{OGPI}, \text{FP}) = [(2.384 - 3)^2 + (15.876 - 4)^2]^{1/2} = 11.891,$$

$$D(\text{OGPI}, \text{F}) = [(2.384 - 4)^2 + (15.876 - 5)^2]^{1/2} = 10.995,$$

$$D(\text{OGPI}, \text{FG}) = [(2.384 - 5)^2 + (15.876 - 6)^2]^{1/2} = 10.216,$$

$$D(\text{OGPI}, G) = [(2.384 - 6)^2 + (15.876 - 9)^2]^{1/2} = 7.768,$$

$$D(\text{OGPI}, \text{VG}) = [(2.384 - 9)^2 + (15.876 - 10)^2]^{1/2} = 8.848.$$

Among all levels, the Euclidean distance between sustainability level “good” and “OGPI” is 7.768 and represents the nearest distance among all other levels.

Hence, the manufacturing processes are regarded to be good in terms of sustainability.

## 9.5 Summary and recommendations

The conceptual model for sustainability assessment of manufacturing performance has been developed from literature survey of manufacturing process. The model considered TBL aspect of sustainability namely environmental, societal, and economical with appropriate practical indicators. The sustainability assessment model considered 3 enablers, 12 criteria, and 48 attributes. The four experts have provided inputs for assessment. Grey-based technique is used to evaluate the sustainability performance. Grey-based approach serves as an operational tool to solve uncertain problem with limited amount of data. The overall grey performance index value representing the sustainability index is computed as (2.384, 15.876). To examine the level of sustainability of manufacturing process, Euclidean distance method has been utilized. Targets have been set in Euclidean approach as very poor (VP), poor (P), fairly poor (FP), fair (F), fairly good (FG), good (G), and very good (VG). The sustainability of the manufacturing process is found to be good (G) from Euclidean distance method. Carbon footprint, water consumption, renewable energy consumption, presence of hazardous substances, and greenhouse gases are identified as weaker attributes in environmental aspect of sustainability. Level of automation, process visualization, and control and product quality are the weaker attributes in economy aspects of sustainability. Customer satisfaction and real-time monitoring of customer order represent the weaker attributes in societal aspects of sustainability. To improve the sustainability of the manufacturing process, the manufacturers and practitioners should concentrate more on the weaker attributes. The present study has the uniqueness that provides strategies and improvement recommendations to boost the sustainability of manufacturing process. The improvement recommendations for the weaker areas along with the future opportunity are listed in [Table 9.11](#). The present study assists the practitioners to recognize the sustainability indicators of manufacturing process, computation of sustainability index, and identification of weaker areas. The study could help the industries

TABLE 9.11 Improvement recommendations and future work for recognized weaker areas.

Recognized weaker areas	Improvement recommendations/future work
<i>Environment aspects:</i>	
Carbon footprint	In future selecting suitable eco-friendly materials using life cycle assessment (LCA) can enhance sustainability by reducing carbon footprint.
Water consumption	A water measurement system can be installed in the manufacturing systems to assess the storage and consumption of water across all stages of manufacturing. Recycling and refinement of wastewater from manufacturing processes should be initiated to reduce environmental impacts.
Renewable energy consumption	Renewable energy consumption had to be monitored and has to be enhanced for sustainability benefits. An energy measurement system has to be installed across the industry.
Hazardous substances	Selection of less toxic substances with necessary properties is the scope for future work. Suitable disposal methods with less environmental impact have to be identified through LCA.
Greenhouse gases	Measures has to be taken to reduce the impact of greenhouse gas emissions by utilizing alternative sources of energy.
<i>Economic aspects:</i>	
Level of automation	Enhancing the level of automation will improve the dynamic skills leveraging the sustainable business processes and expand the current process capabilities.
Process visualization and control	Improvement in process visualization and control directs the system performance and operational efficiency through real-time data sharing and reduces the time delay.
Product quality	Product quality has to be improved to reduce the process scrap ensuring process stability toward sustainability.
<i>Societal aspects:</i>	
Real time monitoring of customer order	Adapting to smart manufacturing, digital strategies with real-time monitoring of customer requirements promotes lesser resource consumption across the value chain, enhancing sustainability.
Customer satisfaction	Increased customer satisfaction by eliminating unnecessary costs encourages wider societal growth and promotes sustainability.

and practitioners to evaluate the manufacturing process sustainability and to integrate with Industry 4.0 technologies for industrial value creation.

## References

- Akbar, M., Irohara, T., 2018. Scheduling for sustainable manufacturing: a review. *Journal of Cleaner Production* 205, 856–883.
- Ahmad, S., Wong, K.Y., 2019. Development of weighted triple-bottom line sustainability indicators for the Malaysian food manufacturing industry using the Delphi method. *Journal of Cleaner Production* 229, 1167–1182.
- Agrawal, R., Vinodh, S., 2019. Sustainability evaluation of additive manufacturing processes using grey-based approach. *Grey Systems: Theory and Application* 10 (4), 393–412.
- Arianpoor, A., Salehi, M., 2020. A framework for business sustainability performance using meta-synthesis. *Management of Environmental Quality: An International Journal* 32 (2), 175–192.
- Belgin, O., Balkan, D., 2020. Environmental performance assessment of manufacturing sectors. *Clean Technologies and Environmental Policy* 22, 1–11.
- Cai, W., Lai, K.H., 2021. Sustainability assessment of mechanical manufacturing systems in the industrial sector. *Renewable and Sustainable Energy Reviews* 135, 110169.
- Deng, J.L., 1982. Control problems of grey systems. *Systems & Control Letters* 1 (5), 288–294.
- Dubey, R., Gunasekaran, A., Childe, S.J., Papadopoulos, T., Luo, Z., Wamba, S.F., Roubaud, D., 2019. Can big data and predictive analytics improve social and environmental sustainability? *Technological Forecasting and Social Change* 144 (C), 534–545.
- De, D., Chowdhury, S., Dey, P.K., Ghosh, S.K., 2020. Impact of lean and sustainability oriented innovation on sustainability performance of small and medium sized enterprises: a data envelopment analysis-based framework. *International Journal of Production Economics* 219, 416–430.
- Edgar, T.F., Pistikopoulos, E.N., 2018. Smart manufacturing and energy systems. *Computers & Chemical Engineering* 114, 130–144.
- Felsberger, A., Qaiser, F.H., Choudhary, A., Reiner, G., 2020. The impact of Industry 4.0 on the reconciliation of dynamic capabilities: evidence from the European manufacturing industries. *Production Planning & Control* 1–24.
- Huang, A., Badurdeen, F., 2018. Metrics-based approach to evaluate sustainable manufacturing performance at the production line and plant levels. *Journal of Cleaner Production* 192, 462–476.
- Henaio, R., Sarache, W., Gómez, I., 2019. Lean manufacturing and sustainable performance: trends and future challenges. *Journal of Cleaner Production* 208, 99–116.
- He, Q.P., Wang, J., Shah, D., 2019. Feature space monitoring for smart manufacturing via statistics pattern analysis. *Computers & Chemical Engineering* 126 (C), 321–331.
- Hartini, S., Ciptomulyono, U., Anityasari, M., 2020. Manufacturing sustainability assessment using a lean manufacturing tool. *International Journal of Lean Six Sigma* 11 (5), 957–985.
- Ji Shukla, O., Soni, G., Anand, G., 2014. An application of grey based decision-making approach for the selection of manufacturing system. *Grey Systems: Theory and Application* 4 (3), 447–462.
- Jayakrishna, K., Vinodh, S., Anish, S., 2016. A Graph Theory approach to measure the performance of sustainability enablers in a manufacturing organization. *International Journal of Sustainable Engineering* 9 (1), 47–58.
- Jamil, N., Gholami, H., Saman, M.Z.M., Streimikiene, D., Sharif, S., Zakuan, N., 2020. DMAIC-based approach to sustainable value stream mapping: towards a sustainable manufacturing system. *Economic Research* 33 (1), 331–360.
- Krajnc, D., Glavič, P., 2003. Indicators of sustainable production. *Clean Technologies and Environmental Policy* 5 (3–4), 279–288.

- Khalid, A., Kirisci, P., Khan, Z.H., Ghrairi, Z., Thoben, K.D., Pannek, J., 2018. Security framework for industrial collaborative robotic cyber-physical systems. *Computers in Industry* 97, 132–145.
- Kumar, A., Chinnam, R.B., Tseng, F., 2019. An HMM and polynomial regression based approach for remaining useful life and health state estimation of cutting tools. *Computers & Industrial Engineering* 128, 1008–1014.
- Kravchenko, M., Pigosso, D.C., McAloone, T.C., 2020. A procedure to support systematic selection of leading indicators for sustainability performance measurement of circular economy initiatives. *Sustainability* 12 (3), 1–21.
- Kamble, S.S., Gunasekaran, A., Ghadge, A., Raut, R., 2020. A performance measurement system for industry 4.0 enabled smart manufacturing system in SMMEs—a review and empirical investigation. *International Journal of Production Economics* 229, 107853.
- Machado, C.G., Winroth, M.P., Ribeiro da Silva, E.H.D., 2020. Sustainable manufacturing in Industry 4.0: an emerging research agenda. *International Journal of Production Research* 58 (5), 1462–1484.
- O'Donovan, P., Gallagher, C., Leahy, K., O'Sullivan, D.T., 2019. A comparison of fog and cloud computing cyber-physical interfaces for Industry 4.0 real-time embedded machine learning engineering applications. *Computers in Industry* 110, 12–35.
- Petrillo, A., De Felice, F., Zomparelli, F., 2019. Performance measurement for world-class manufacturing: a model for the Italian automotive industry. *Total Quality Management and Business Excellence* 30 (7–8), 908–935.
- Qian, X., Tu, J., Lou, P., 2019. A general architecture of a 3D visualization system for shop floor management. *Journal of Intelligent Manufacturing* 30 (4), 1531–1545.
- Qu, Y.J., Ming, X.G., Liu, Z.W., Zhang, X.Y., Hou, Z.T., 2019. Smart manufacturing systems: state of the art and future trends. *International Journal of Advanced Manufacturing Technology* 103 (9–12), 3751–3768.
- Ram Matawale, C., Datta, S., Mahapatra, S.S., 2014. Lean metric appraisal: exploration of grey numbers set theory. *Grey Systems: Theory and Application* 4 (3), 400–425.
- Roldán, J.J., Crespo, E., Martín-Barrio, A., Peña-Tapia, E., Barrientos, A., 2019. A training system for Industry 4.0 operators in complex assemblies based on virtual reality and process mining. *Robotics and Computer-Integrated Manufacturing* 59, 305–316.
- Singh, S., Olugu, E.U., Fallahpour, A., 2014. Fuzzy-based sustainable manufacturing assessment model for SMEs. *Clean Technologies and Environmental* 16 (5), 847–860.
- Sartal, A., Bellas, R., Mejías, A.M., García-Collado, A., 2020. The sustainable manufacturing concept, evolution and opportunities within Industry 4.0: a literature review. *Advances in Mechanical Engineering* 12 (5), 1687814020925232.
- Song, Z., Moon, Y., 2019. Sustainability metrics for assessing manufacturing systems: a distance-to-target methodology. *Environment, Development and Sustainability* 21 (6), 2811–2834.
- Santos, J., Muñoz-Villamizar, A., Ormazábal, M., Viles, E., 2019. Using problem-oriented monitoring to simultaneously improve productivity and environmental performance in manufacturing companies. *International Journal of Computer Integrated Manufacturing* 32 (2), 183–193.
- Saxena, P., Stavropoulos, P., Kechagias, J., Salonitis, K., 2020. Sustainability assessment for manufacturing operations. *Energies* 13 (11), 1–19.
- Thirupathi, R.M., Vinodh, S., Dhanasekaran, S., 2019. Application of system dynamics modelling for a sustainable manufacturing system of an Indian automotive component manufacturing organisation: a case study. *Clean Technologies and Environmental Policy* 21 (5), 1055–1071.
- Tortorella, G.L., Cawley Vergara, A.M., Garza-Reyes, J.A., Sawhney, R., 2020. Organizational learning paths based upon industry 4.0 adoption: an empirical study with Brazilian manufacturers. *International Journal of Production Economics* 219 (C), 284–294.

- Veleva, V., Ellenbecker, M., 2001. Indicators of sustainable production: framework and methodology. *Journal of Cleaner Production* 9 (6), 519–549.
- Zhang, J., Wang, P., Yan, R., Gao, R.X., 2018. Long short-term memory for machine remaining life prediction. *Journal of Manufacturing Systems* 48, 78–86.

This page intentionally left blank

# Additive manufacturing including laser-based manufacturing

---

Soyeon Park<sup>1</sup>, Kaiyue Deng<sup>1</sup>, and Kun Kelvin Fu<sup>1,2</sup>

<sup>1</sup>Department of Mechanical Engineering, University of Delaware, Newark, DE, United States; <sup>2</sup>Center for Composite Materials, University of Delaware, Newark, DE, United States

## 10.1 Introduction and basic principles

### 10.1.1 What is additive manufacturing?

Following the International Organization for Standardization (ISO)/American Society for Testing and Materials (ASTM) terminology standard, additive manufacturing (AM) is the process of joining materials to make parts from 3D model data, usually layer upon layer, as opposed to subtractive manufacturing and formative manufacturing methodologies (ISO/ASTM 52900, (2021)). In these days, AM is also known as 3D printing in the public. The first AM is stereolithography invented by Chuck Hull in 1987 that uses ultraviolet (UV) light to solidify the light-sensitive liquid polymer. In 1980 and 1990s period, different types of AM emerged including fused filament fabrication (FFF) and selective laser sintering (SLS) (Wohlers et al. (2016)). In the beginning, AM with polymers was designed for rapid prototyping (Gibson et al. (2015)), but nowadays, AM has been developed for functional applications composed of various materials such as carbon nanomaterials, biomaterials, ceramics, and metals in a variety of industries (e.g., aerospace, robotics, biomedical, energy storage devices, electronics, and even food area). 3D printing has many advantages, including cost-effectiveness, design flexibility, and easy accessibility, and these benefits enable 3D printing

prominent manufacturing technologies to develop rapidly (Niaki et al. (2018)).

Recently, a sustainable manufacturing that produces product environmentally friendly by minimizing negative environmental impacts and conserving energy and natural resources has been a topic of interest for environmental issues. As increasing demand for the sustainable manufacturing, AM has also got a lot of attention. The conventional manufacturing is a subtractive method and produces products by removing materials through cutting, boring, drilling, and grinding from solid bulks. These processes consume excess materials and need longer time according to the complexity of geometry of structures, resulting in a higher cost. Different from the traditional methods, AM is a process by placing materials on a substrate, and the complexity itself does not affect both time and cost. Some 3D printing technologies (e.g., FFF and material jetting) require the use of support structures that should be removed or subtracted, but the amount of material subtracted is much less than the conventional processes.

### 10.1.2 The generic AM process

In 3D printing process, there are many steps from digital data to physical objects. These processes can be divided to three steps: development of product idea, preprocessing of model data, and printing and post-treatment process. Fig. 10.1 shows the overall process of 3D printing from development of product idea to post-treatment process.

#### (1) Development of product idea

A. CAD. Computer-aided design (CAD) file is used for a 3D graphics file format and contains 2D or 3D designs. All parts for

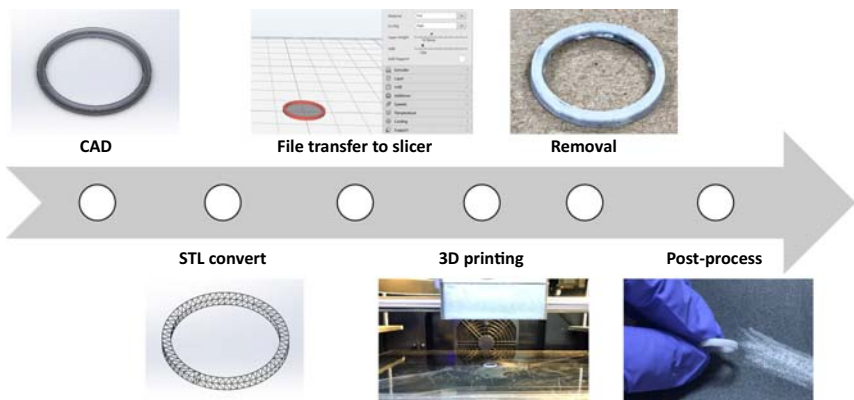


FIGURE 10.1 Overall process to print 3D object from digital data to physical part.

3D printing should be constructed with digital file using solid modeling software.

(2) Preprocessing of model data

**B. STL convert.** The generated CAD file is converted into standard triangle language (STL) file format in pre-processing of model data. STL file describes only the surface geometry of a three-dimensional object without any information of color, texture, or other common CAD model attributes. It just describes external closed surfaces of the original CAD model using triangle and gives the basis for calculation of slides. This STL format is the basis to 3D printing software.

**C. File transfer to slicer.** The STL file is transferred to slicing software to convert to printer commands in g-code format. The slicer divides a 3D object as a stack of flat layers for the 3D printer to generate the product layer by layer following the generated path. In this process, the manipulation for product details, including size, position, orientation of product, as well as printing conditions (e.g., nozzle temperature, printing speed, bed temperature), is possible in this procedure.

(3) Printing and post-treatment process

**D. Produce.** Once putting a G-code in the printer, an AM machine proceeds printing automatically. Monitoring of the machine might need to check product quality. If printed product shows some defects like warping, delamination, and cracks, troubleshooting printing parameters is required.

**E. Removal.** After the AM machine finished the printing, the printed part should be removed from the bed platform.

**F. Post-process.** The 3D object may require additional cleaning up steps such as removing supporters and unnecessary parts, polishing the surface, and painting for the final use. Sometimes products for mechanical parts require heat treatment to increase the bonding strength between the layers or reduce the porosity of the part, resulting in increasing strength and rigidity of the part.

### 10.1.3 Advantages and challenges of AM

AM can quickly turn concepts into 3D models or prototypes with just an idea and a 3D printer since it does not require any special tools and skills to make products. In addition to rapid prototyping, AM has a number of benefits, such as reduced resource and process, no or lower operator skills required, and less assembly steps that provides cost-effectiveness. With traditional manufacturing processes, whenever

making a new component or changing a part design, they require a new tool, mold, and jig. On the other hand, 3D printing does not require any physical changes of equipment or machine after redesigning the product in software. Moreover, 3D printing does not depend on labor skill due to simpleness and auto system of the process. The conventional processes such as molding, carving, and forming are tedious, difficult, and error prone so that these techniques need skilled labors and many experts for each process parts. In terms of resources, a lot of material may be consumed, and many wastes can be generated in the subtracting processes, but 3D printing fabricates products layer by layer without filling in unnecessary parts. The other advantage pointing out is the 3D printing ability to print integrated assembly by minimizing assemblies and welding steps, resulting in reduction in time and cost.

Although AM revolutionizes manufacturing and provides new insight and opportunities in various fields, several limitations still need to be developed. Although 3D printing produces some end-use products, the printed products might require post treatment such as polishing the surface and the heat treatment for quality of the final product that might take lots of time. In addition, manufacturing time is reduced due to reduced processes compared to traditional manufacturing methods, but printing speed itself is not so fast (around  $50\text{--}150\text{ mm h}^{-1}$  in the case of fused deposition modeling). Another limitation is lower manufacturing speed when producing large scale objects because 3D printing is difficult to produce large volume parts quickly due to heat generation that distorts final products. For example, the printing speed and maximum print size of stereolithography (SLA) using laser are around  $14\text{ mm h}^{-1}$  and  $27\text{--}750\text{ mm}$ . To overcome these limitations, digital light processing (DLP) using a projector to print 2D layers, continuous liquid interface production (CLIP) using oxygen permeable window or mobile oil, and high-area rapid printing (HARP) have been developed for a rapid printing process. The other challenge is lower mechanical properties of the printed products compared with those of objects using traditional processes. During 3D printing process, there is no external pressure to enhance the bonding between interlayers, resulting in the weakness in interlayer bonds. Therefore, the printed products mostly crack and fail at the weakest point where the layer adheres.

#### 10.1.4 AM technologies

There are various types of AM technologies we can choose, including FFF or FDM, stereolithography (SLA), and directed energy deposition (DED) depending on the material, process capabilities (accuracy and build size), and characteristics of the end part (physical and visual

properties). In this section, we will provide the overall printing process and mechanism, feedstock materials, and advantages/limitations of each 3D printing technologies to give general insight for choosing AM. Table 10.1 shows the brief information about AM processes (e.g., printing mechanism, material conditions, benefits, and limitations).

TABLE 10.1 The characteristics of additive manufacturing technologies.

		<b>Printing principle</b>	<b>Material state</b>	<b>Advantages</b>	<b>Disadvantages</b>
SLA		UV induced curing	Liquid photopolymer	High resolution	Low throughput and high cost
PBF		Heat induced Sintering	Powder shape of polymer, metal, and ceramic	Good for mass production and design flexibility	High cost, rough surface, and cavity generation
FFF/FDM		Extrusion	Polymer filament	Simplicity, low cost, and fast	Nozzle clogging and not outstanding quality
Jetting-based process	MJ	Drop-on-demand material, printing and heat or UV-assisted curing	Liquid photopolymer	High resolution, multi-material capabilities, and homogeneous properties	High cost and not suitable for structural applications
	BJ	Drop-on-demand binder printing	Powder shape of polymer, metal, and ceramic	Material and design flexibility, and good for mass production	Rough surface and cavity generation
DED		Heat induced melting	Metal powder or wire	No need for supports, good for part repair, and fast builds with rapid material deposition	Limited material use, and cavity generation
SL		Adhesion between sheets	Sheets of materials	Full color prints and relatively affordable	Low durability and need for support structures

## 10.2 Vat photopolymerization process (SLA)

Vat photopolymerization, which is also called stereolithography (SLA), uses photopolymers and initiates and cures the polymers with ultraviolet (UV) light. In general, UV and visible light radiation are used. This SLA using laser has high resolution between 6 and 140  $\mu\text{m}$ , and the printing speed and maximum print size are limited at 14  $\text{mm h}^{-1}$  and 27–750  $\text{mm}$ , respectively (Schmitdleithner et al. (2018)). SLA can be typically divided into top-down SLA and bottom-up SLA according to machine setup. In top-down SLA (Fig. 10.2A), UV light moves in the desired path and cures the photopolymer resin in the liquid bath by forming crosslinked networks. After printing a layer, the platform moves downward from the reaction zone with a certain layer thickness (25–100  $\mu\text{m}$ ), and uncured fresh resin replenishes the upper side of the printed layer. And then, the printer prints the next layer and repeats the processes until finishing the printing. Bottom-up SLA (Fig. 10.2B) is more common in these days due to high scalability in vertical direction compared to top-down one. The bottom-up SLA printers place the light source under the resin bath and the moving platform faces upside down. The resin bath has a transparent bottom with a coating, which allows the light of the laser to pass through but prevents the printed part from sticking to it. After printing a layer, the platform goes upward for detaching the printed layer from the bottom of the bath.

There are several printing methods depending on the projecting methods: DLP, two-photon polymerization (2 PP), and other advanced SLA (computed axial lithography (CAL), CLIP, and HARP).

- **Digital light processing (DLP)**

Digital light processing (DLP) projects 2D layer of UV light onto a liquid resin, as shown in Fig. 10.3A. The 2D image is created on the resin bath by

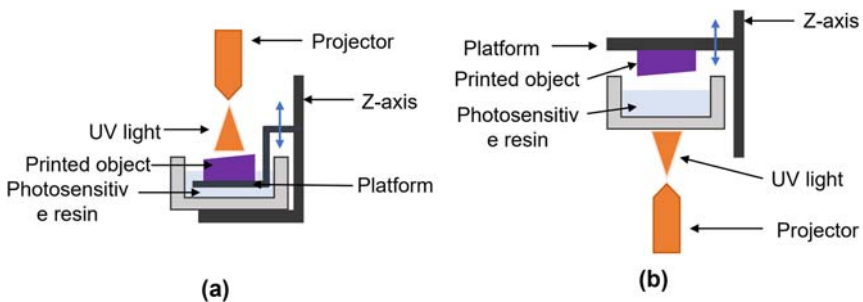


FIGURE 10.2 Schematic of the working principle of stereolithography printers (A) top-down and (B) bottom-up.

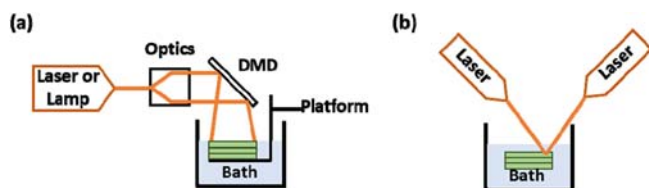


FIGURE 10.3 Schematic of various SLA techniques with different projecting methods (A) DLP and (B) 2 PP.

microscopically small mirror, called as digital micromirror device (DMD). DMD is the key part in DLP and consists of thousands of small mirrors that create the pattern of a layer onto the bottom of the resin bath, acting like a dynamic mask. Compared to the traditional SLA, DLP is faster with speeds between 25 and 150 mm h<sup>-1</sup>, but the resolution is larger due to the limited pixel size of the DMD. Other limitation of DLP is the boxy surface finish that the rectangular shape of voxels prevents smooth edges. The rough surface can be improved through post-processing such as sanding and grinding.

#### • Two-photon polymerization (2 PP)

Two-photon polymerization (2 PP) was proposed by Strickler et al. to enhance the resolution of SLA technology below 10 nm. Different from the conventional SLA, 2 PP triggers for solidification to take place inside the focal point region, called a volume pixel or voxel, as shown in Fig. 10.3B. Instead of UV light, it uses near-infrared (NIR) light with ultra-short pulse and twice the wavelength (i.e., half the energy) to cause the nonlinear light absorption. The NIR laser makes the resin to absorb two photons simultaneously that can trigger the same chemical reaction as a single UV photon. Due to the ability of 2 PP to cure some areas inside the resin bath, there is no need for layer-by-layer production, and 2 PP can create complex shape products. On the other hand, it is restricted to small geometries in the mm range and has a low print speed of up to a few mm/s.

#### • Advanced SLA

As mentioned before, SLA has slow printing speed, and only small products can be printed. There have been lots of research to overcome the limitations of SLA. The one of advanced examples is CAL (Kelly et al. (2019)). It illuminates a rotating volume of photosensitive resin with a dynamically evolving light pattern to improve the speed. CAL system utilizes a digital video projector to deliver light energy as a set of 2D images and the liquid resin exposed to the light from multiple angles

solidifies in the desired 3D geometry. Another example is CLIP (Tumbleston et al. (2015)). It uses oxygen permeable window to generate liquid interface where photopolymerization is inhibited, called dead zone. The last one is HARP (Niaki et al. (2018)). The HARP utilizes mobile oil to dissipate the generated heat and reduce adhesive forces. Both CLIP and HARP can dissipate the heat generated and reduce the process of lifting the printed part required to speed up printing.

### 10.3 Powder bed fusion process (PBF)

Powder bed fusion (PBF) (shown in Fig. 10.4) requires the feedstock in powder form to go through melting and fusion by heat sources, usually lasers and electron beams. According to the type of thermal sources, the PBF can be categorized as laser sintering (LS) and electron beam melting (EBM). In terms of processing materials, selective laser sintering (SLS) uses plastics, ceramics, etc., while direct metal laser sintering (DMLS) and selective laser melting (SLM) use metal or metal alloy. Engineering plastics (mostly nylon (PA11, PA12, filled nylon)) are one of the most commonly used materials in SLS due to its better productivity of functional prototypes. The difference between DMLS and SLM is whether metals are fully melted (i.e., SLM) or not (i.e., DMLS).

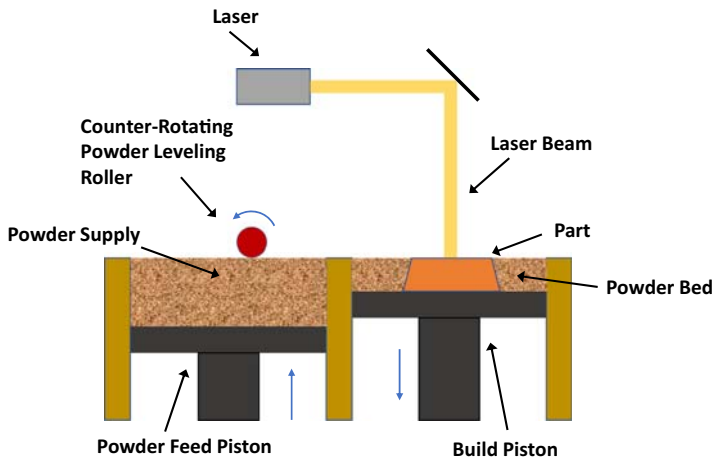


FIGURE 10.4 Schematic of PBF.

In PBF, the powder can act as a support to maintain the structural integrity of the part, minimizing the need to design additional support structures. One of limitations is that the surface of the printed product is rough and depends on the particle size of the powder and therefore requires post-processing to make it smooth (engineering product design). The powders excluded from the parts can be directly collected for future use, but recyclability is poor if powders are degraded caused by heating.

- **Selective laser sintering (SLS)**

Selective laser sintering (SLS) technique uses a basic structure of a PBF machine and targets a variety of materials in powder form, such as plastic, ceramic, and glass. The powder particle size is usually 0.075–0.1 mm, as said in [Gibson et al. \(2015\)](#). To prevent the powder from oxidizing, the build chamber is protected by inert gas, usually argon or nitrogen. As shown in [Fig. 10.4](#), the machine contains three main components: laser source, powder supply, and powder bed. The powder supply contains unused powder materials, and the leveling roller sweeps powders over the powder bed layer by layer, and these materials are preheated by IR heater to maintain surface temperature homogeneity. The computer-controlled CO<sub>2</sub> laser projects onto the surface layer of the powder bed and fuses the powder particles into a pattern as designed. Once a layer is finished, the leveling roller brings additional new powders from the powder supply, recoats the printed layer, and then repeats the operations.

- **Direct metal laser sintering (DMLS)**

Direct metal laser sintering (DMLS) process is used to partially melt metals. The power source is Nd:YAG laser (neodymium-doped yttrium aluminum garnet laser, typical wavelength: 1064 nm, infrared region). The process also takes place in inert chamber. Engineering materials are available for this mechanism, including Ti6Al4V, CoCrMo steel, NiCr alloy, etc., and particles size ranging from 20–40 microns are allowed in this process (identified in [Sun et al. \(2017\)](#)). Metal parts made from DMLS have no residual stress and can be exempt from heat treatment.

- **Selective laser melting (SLM)**

Selective laser melting (SLM) process fully melt metals, unlike the DMLS process, which partially melts (sintering) materials. The high powder-density laser melts each layer and allows the metallic powders to resolidify into dense parts. Density greater than 99% can be achieved for micron scale parts. The challenge is revealed in its limitation of printing complex shapes and overhang structures ([Song et al. \(2022\)](#)).

- **Electron beam melting (EBM)**

Unlike other PBF processes, electron beam melting (EBM) utilizes electron beam as the dominating power source to melt particles, so it adopts a different machine structure. As shown in Fig. 10.5, Electrons are formed into a collimated electron beam that is accelerated at a voltage of 60 kV within an electron beam column, focused by a focusing coil and controlled by a deflection coil (EWI (2018)). Compared with DMLS process, EBM machine has relatively limited build size,  $350 \times 350 \times 380$  mm for the largest EBM printer and EBM is expensive, costs greater than \$250,000.

## 10.4 Extrusion-based process (FDM or FFF)

Material extrusion process, often known as fused deposition modeling (FDM) or FFF, is one of the most common 3D printing processes since it is beginner friendly. In the case of FDM, it is the branded name owned by Stratasys, but FFF is its technical name. FFF technique commonly use thermoplastics, such as polylactic acid (PLA), acrylonitrile butadiene styrene (ABS), high-impact polystyrene (HIPS), nylon, polycarbonate (PC), and thermoplastic polyurethane (TPU). As shown in Fig. 10.6, in an

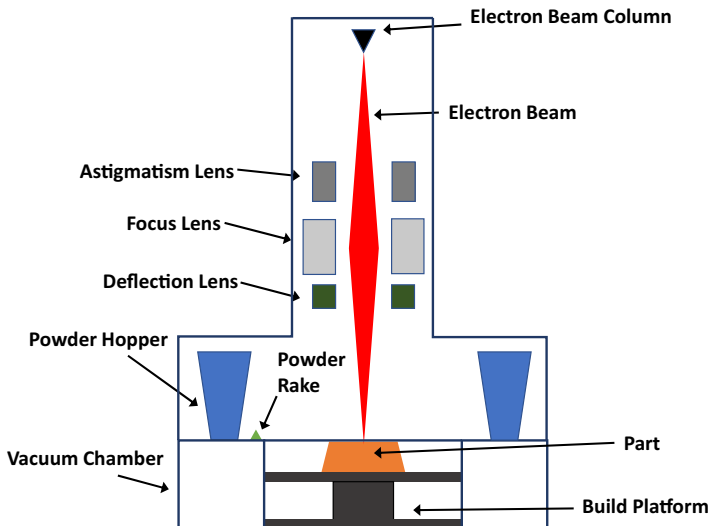


FIGURE 10.5 Schematic of EBM.

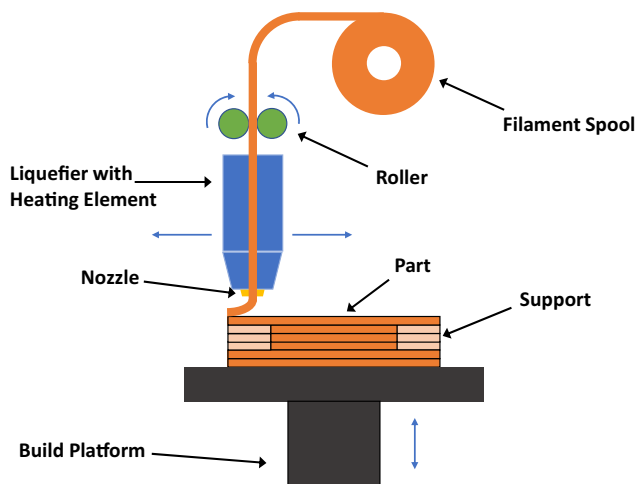


FIGURE 10.6 Schematic of FFF process.

FDM or FFF equipment, thermoplastic filaments are pushed down by rollers, liquefied by heating in the extrusion head, extruded from the print nozzle, and deposited on a platform or previously printed layers. If the overhang angle is greater than  $45^\circ$ , support structure is needed for sustaining shape of objects.

FFF or FDM has flexibility to replace material spools or cartridges on demand and various engineering polymers (e.g., polycarbonate (PC), polyethylene terephthalate glycol (PETG), and nylon) can be used for functional prototypes. In addition, it is convenient to remove support either by hand or water (Jadhav et al. (2017)). However, it has several issues of printing quality. One of them is that the printed samples have tendency of warping deformation. When earlier layers experience cooling earlier and newly deposited layers bring in temperature difference, it causes the inner stress for the samples to deform (Wang et al. (2007)). To prevent such deformation, the temperature control is needed. For instance, in order to minimize warping for the acrylonitrile butadiene styrene (ABS), the optimal chamber temperature is  $60\text{--}70^\circ\text{C}$ , and the bed temperature is  $90\text{--}100^\circ\text{C}$ . Another issue is the weak interlayer bonding, caused by heterogeneous temperature distribution in z-direction, results in limited mechanical properties (Stark (2016)). Furthermore, the staircase effect, geometric inaccuracies in which curved layers are flattened during printing, also induces poor interlayer bonding (Singamneni et al. (2010)).

## 10.5 Jetting-based process (material jetting (MJ) and binder jetting (BJ))

The material jetting (MJ) process (Fig. 10.7) is a derivative from 2D Inkjet printing process. The print head of a material jetting dispenses multiple droplets of preheated photopolymer resin. Before dispensing the photopolymer resin, the resin is heated up to 30–60 °C to obtain optimal viscosity, following in a line-wise order. The droplets are dispensed either in the continuous mode or drop on demand (DOD) mode (less than 10 kHz, identified in Miers et al. (2017)), and they are deposited onto the surface of the pattern via thermal or piezoelectric method. In the thermal inkjet method, vaporized bubbles generated by heat are the main factors to push the droplets from multiple nozzles. In the piezoelectric inkjet method, distortion caused by electric change squeezes the droplets from the ejection chamber (Furlani (2015)). Similar to the SLA printing mechanism, the deposited resin droplets undergo the photopolymerization step, where the pattern is cured and solidified with UV light. This step ensures the model with homogeneous mechanical and thermal properties. The technology displays high-resolution layer accuracy up to 16  $\mu\text{m}$  and can print upwards of 20  $\text{mm h}^{-1}$  per strip, and dimensional accuracy is minimized at  $\pm 0.1\%$  for large part printing. In addition, this process is also used in multimaterial printing and color printing (e.g., 3D System's colorjet Printing technology). Although there are many advantages, the weak bonding between deposited droplets negatively impacts the mechanical properties of the parts, and the form of small droplets lengthens the entire process.

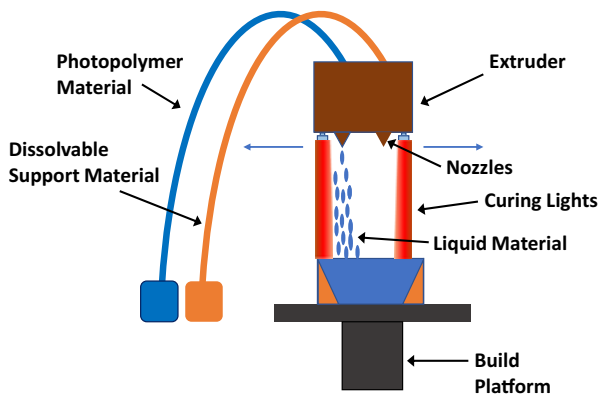


FIGURE 10.7 Schematic of MJ process.

Similar with MJ, Polyjet process is a multimaterial jetting process with patent owned by Stratasys, where droplets of resin are sprayed onto the build tray. This technology can use both rigid and stretchable photopolymers as building materials, and for supporting structures, it uses polyethylene and glycerin, which can be dissolved in proprietary chemical solutions. It is a similar method to Polyjet, but for the MultiJet process developed by 3D Systems, it uses paraffin wax as a support material that must be melted in the oven.

Binder Jetting (BJ) (Fig. 10.8) is also 2D Inkjet derivative, but different from MJ. It can use various feedstocks including ceramic, metal, and polymer (3D Hubs). For liquid binder, butyral resin, polyacrylic acid (PAA), and silicone are used (Ziaee et al. (2019)). Similar with the PBF, the powder roller feeds and levels the powder bed of the build platform in one layer thickness but differs in the bonding process where the binder is dispensed from the print head and forms adhesion on the powder bed. The dispensed spot is slightly heated to promote the cross-linking of the binder. After printing, the unbound powder is removed, and the printed green part is further processed with deboning and sintering (Ziaee et al. (2019)). This process is used to generate prototype parts, but post-processing steps slow down the total production time and increases cost.

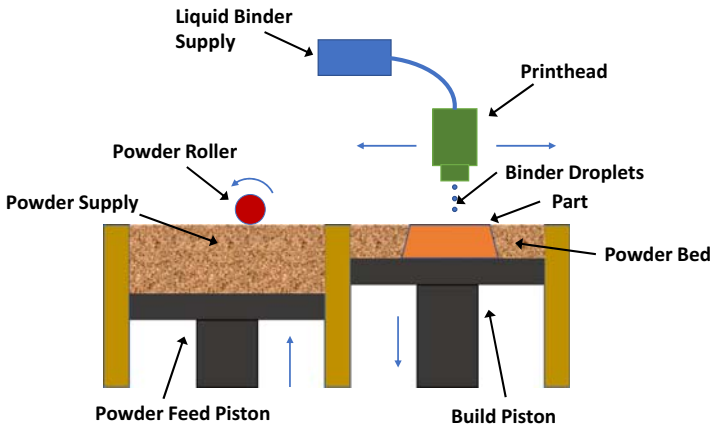


FIGURE 10.8 Schematic of BJ process.

## 10.6 Sheet lamination process (SL)

Sheet lamination (SL) is the process where thin layers of materials, including paper, polymer, ceramic, metal, or composite laminates are bonded together layer-by-layer. As shown in Fig. 10.9, the rolled laminates are conveyed to the build platform, stacked to previous layers, and cut to specific shapes by laser plotter. The layer thickness is determined by laminate thickness and machine process settings. Depending on the bonding method, the common sheet lamination process can be divided to laminated object manufacturing (LOM), ultrasonic additive manufacturing (UAM), and computer-aided manufacturing of laminated engineering materials (CAM-LEM). LOM is an original process of SL, where continuous paper rolls are supplied to the build platform, bonded with adhesives, profiled, and cross-hatched by laser. The thickness of each paper is around 0.07–0.2 mm (identified in Gibson et al. (2015)). It is an inexpensive and time-efficient process but requires post-processing to improve the part quality. UAM, also known as Ultrasonic Consolidation (UC), is the hybrid process (additive + subtractive) where ultrasonic welding bonds the metal foils on the heated build platform upwards of 200 °C. The rotating sonotrode, a typical tool used in ultrasonic machining, generates vibration at the interface and removes metal oxides. Meanwhile, the heated build platform results in the plastic deformation within the layer, which allows the metallurgical surface to bond closely. The model is milled by CNC during the process to add intricate features as designed. In this process, the part quality is assured by bonding and high-precision post-processing, and the staircase effect is minimized (Gibson et al.

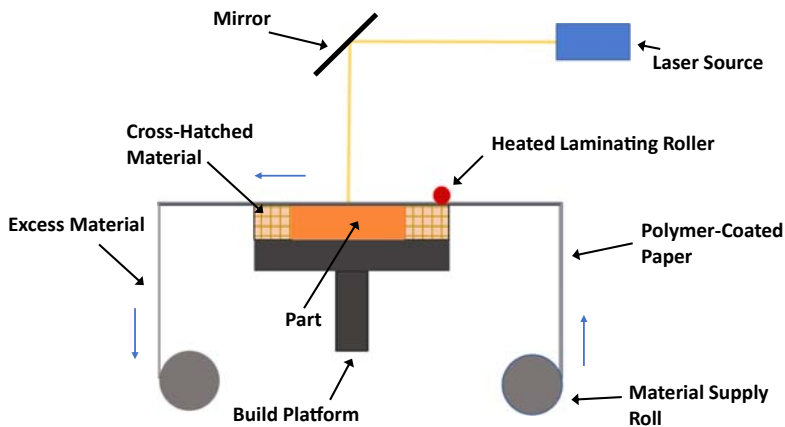


FIGURE 10.9 Schematic of SL process.

(2015)). CAM-LEM is the process where green ceramic parts and metal parts are formed through the sequence of laser cutting from ceramic or metal tape, stacking layer by layer and bonding. Then, the green part is placed in a furnace to remove binder. The staircase effect can be minimized by cutting the redundant section of the stacks.

## 10.7 Directed energy deposition process (DED)

Directed energy deposition (DED) process is a multiaxis computer numerical control (CNC)- or robotic-based process that uses arc, laser, plasma, and electron beam to melt the fed wire or powder onto deposits. A multiaxis (typically four or five axes) arm, where the deposition head is mounted on the end, starts the layer-by-layer patterning on the substrate. The dispensed material is then deposited to the melt pool of the pattern (0.25–1 mm in diameter, identified by Gibson et al. (2015)), which is generated by the energy source. The withdrawal of the energy source allows the pattern to solidify (at cooling rates of  $10^3$ – $10^5$  °C s<sup>-1</sup>) (Gibson et al. (2015)). The process takes place within a vacuum chamber with an inert gas to protect the molten pool. Due to the motion flexibility of the arm to tilt or turn, this technology can be applicable in repairing defective parts.

Depending on the form of material supply, the DED process can be further categorized into wire DED (Fig. 10.10A) and powder DED (Fig. 10.10B). Wire DED is developed by Sciaky. The material spools are fed through the wire feeder, similar to the extrusion-based process, and the wire is melted in the similar way to the welding process. This process is more applicable to the simple geometry, while the porosity is prone to occur in the large and delicate models (Gibson et al. (2015)). Powder DED, also called laser cladding or laser engineered net shaping (LENS), is a continuous laser-based process in which powders are injected together

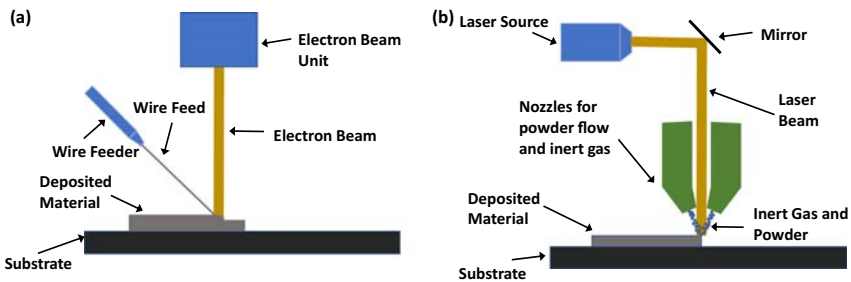


FIGURE 10.10 Schematic of (A) wire DED and (B) powder DED process.

with inert gas from the nozzles to the focus of the molten pool (Vartanian et al. (2018)). The powders can dynamically adjust the dimensional deviation and texture corrugation to ensure model accuracy, which is not easily achieved by wire DED. Furthermore, the multiple nozzles can increase the capability of printing intricate models. Compared with PBF process, the powder DED process is capable of building larger parts and the nozzles often feed the required amount of powder, which results in minimal material waste and minimal post-processing. In addition, if the multiple nozzles are used, DED will offer possibility of mixing different metals.

## 10.8 Hybrid manufacturing

With the growing interest in effective and flexible manufacturing, there have been several trials to combine different manufacturing processes in one step to reduce numerous process, involving transferring and setting up products. The one of limitations in AM is the surface integrity on specific surfaces, which often leads to the need of post-processing, especially in the case of metal 3D printing (Korpela et al. (2020)). Hybrid systems have been developed to handle this problem. The most popular example is the hybrid machine combining laser-assisted 3D printing for metal (e.g., DED and PBF) and computer numerical control (CNC) milling. Fig. 10.11 shows the combined process of laser-assisted PBF (building

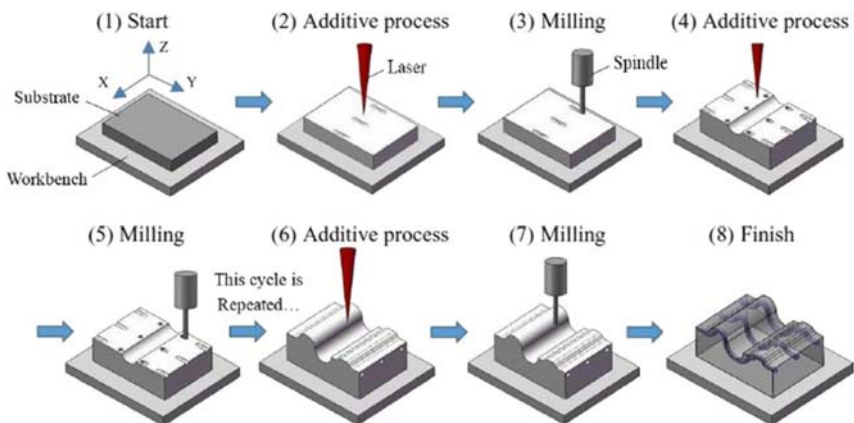


FIGURE 10.11 The schematic of hybrid manufacturing combining laser-assisted 3D printing and CNC milling. Used with permissions from Du, W., Bai, Q., and Zhang, B., 2016. *A Novel Method for Additive/Subtractive Hybrid Manufacturing of Metallic Parts. Procedia Manufacturing* 5, 1018–1030, ELSEVIER.

subpart on a substrate) and subtractive manufacturing (polishing surface and cutting for a final use) (Du et al., 2016). Once a substrate is fixed onto the workbench, a new part is built from powders as the laser beam scans across the surface of the powder bed (step 1-2). After several repeated scans, the laser tool is changed to a milling cutter to machine the part being built (step 3). The printing and milling steps are repeated for the finished product (step 4-8). The first research about this hybrid technology took place in the mid- to late-1990s by Klocke et al. (1996). The hybrid machine can solve the rough and stair stepping surface of a printed structure, which is one of the problems in metal 3D printing due to coarse materials and layer-by-layer printing process. In addition, the hybrid machining system enables not only high-quality surface finish associated with machining but also fast production of the 3D object with greater dimensional accuracy.

## 10.9 Post-treatment processes

### 10.9.1 Support material removal

The most common post-processing is support removal, as some angles of the structure may require supports to resist deformation. For example, if the overhang of the structure is more than  $45^\circ$ , supports are required. The support structures have lower density than the main build by having a lower in-fill percentage to make them easily removed. They have two standard shapes: tree-like support structure and liner/accordion support structure. The tree-like structures are tree-shaped support structures and designed to provide support at a specific point so that they are easy to be removed and consume less materials. Linear/accordion support structures look like pillars and bridges, respectively, and have a mesh-like design to provide comprehensive interconnected support for complex shapes. These supports can be made from the build material or a sacrificial material. In the case of the supports made of build material, various blades (e.g., needle nose plier, flush cutter, and knives) can be used to remove them. Once cutting is done, the surface of products might need subsequent sanding or polishing because it is easy to leave the witness marks where they were attached. To deal with the surface finish issue, the sacrificial materials become popular for use in support structures and these materials extend the design freedom and do not need extensive labor, as shown in Fig. 10.12 (Park et al. (2018)). In general, sacrificial materials are made of special filaments that can be dissolved in a chemical bath or water bath, to leave the main build perfectly intact. For instance, water soluble polymers such as polyvinyl alcohol (PVA) and Hydrofill can be used for PLA build materials, and as secondary materials for

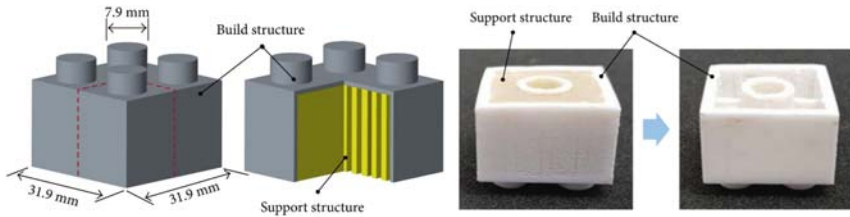


**FIGURE 10.12** The schematic of build and supporting structure and the removal of support materials composed of polyvinyl alcohol (PVA) from the printed products by dissolving them in water. Used with permissions from Park, S.J., Lee, J.E., Park, J.H., Lee, N.K., Lyu, M.-Y., Park, K., Koo, M.S., Cho, S.H., Son, Y., Park, S.-H., 2018, FDM-based 3D printed structure using hydrogen peroxide under ultrasonication. *Advances in Materials Science and Engineering* 2018, Article 3018761.

metals, alloys with lower melting temperature or alloys that can be chemically dissolved in a solvent are the most common. To speed up the process of dissolution, an ultrasonic chamber can be used.

### 10.9.2 Surface finishing

Another common post-treatment is surface texture improvement. The surface of the printed products may not be smooth due to stair-steps, powder adhesion, and witness mark attributed to the support removal process. Stair steps are inevitable in layer-by-layer manufacturing though these bump surfaces can be improved by minimizing the thickness of the layer. Powder adhesion generates in power-based process like PBF and DED. These rough surfaces can be controlled by manipulating part orientation, powder shape, and thermal control.

Various polishing processes are used depending on the desired surface finish of the printed polymer parts: sanding for smooth surface and bead blasting for mat surface. Sanding is straightforward method, but it is difficult for the parts with intricate surface and small details and can affect the overall accuracy of the printed one. During polishing surface, wet sand is recommended to prevent friction and heat build-up from damaging the products. Bead blasting is also commonly used for finishing process, and tiny beads of media are sprayed on the surface to remove layer lines. Although this method can be used for complicated objects, it has limitation of part size since the process is operated in an enclosed chamber. Both processes (sanding and bead blasting) are done by hand so that they cannot be mass finished. In case of the metal products, milling and vibratory systems are used. Milling is commonly used to finish surface as well as machining some parts. Vibratory system vibrates until the medium repeatedly impacts and polishes the parts. It is mainly used for metal parts even it can be used for ceramic and plastic materials because

the polishing medium must be softer than the component. Besides these ways, there are many methods of surface finishing including painting, heat treatment through hardening and thermal diffusion, and vapor smoothing that the surface of the printed product reacts with chemical vapors by removing visible layer lines.

### 10.9.3 Property enhancements

After 3D printing, additional thermal processing is required to enhance the printed product properties. This process is common in PBF and binder jetting, which are powder-based process since the fabricated products have many internal hollow cavities inside. In the case of binder jetting, the polymers inside the green products are removed during sintering, leading to porous structures and low mechanical properties. To deal with the porosity formation, a line is installed to inject materials into the pores inside the products during furnace processing. This system allows the infiltration of materials, resulting in a compact and finished component. It needs to be optimized to prevent shrinkage and distortion by controlling atmospheric pressure and temperature ramp. Fig. 10.13 shows the overall procedure of infiltration of bronze into steel products. After the part is

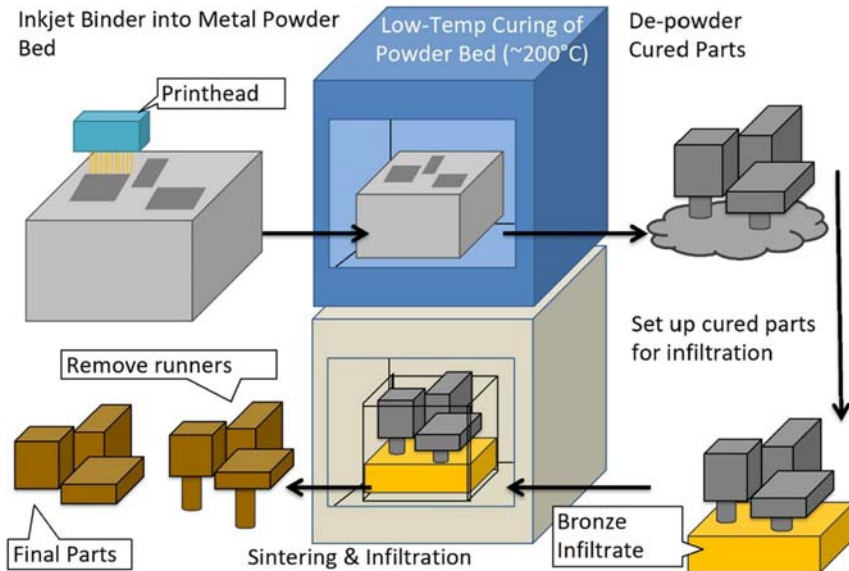


FIGURE 10.13 The overall process of BJ followed by curing, depowdering, and infiltration. Used with permissions from Mostafaei, A., Elliott, A.M., Barnes, J.E., Li, F., Tan, W., Cramer, C.L., Nandwana, P., Chmielus, M., 2021. Binder jet 3D printing - process parameters, materials, properties, modeling, and challenges. *Progress in Materials Science*, 119, Article 100707., Elsevier.

printed, it is cured at a low temperature, followed by an infiltration process at a high temperature (Mostafaei et al. (2021)). In the case of the PBF, thermal processing is mainly heat treatment to have microstructures and/or to relieve residual stresses.

The other technique for property enhancement is nonthermal techniques. When using photopolymers as feedstocks, the curing step is usually post-processed as polymerization does not complete during printing. In curing process, the printed products are exposed to UV or visible radiation to completely cure the surface and subsurface regions. Moreover, the products can be thermally cured at a low temperature to completely cure and improve mechanical properties.

#### 10.9.4 Machining

When printed parts require critical dimensions and fine features, additional machining may be needed to improve both dimensional accuracy and manufacturing speed. Industries requiring high functional and tolerance, such as automotive and medical products fabrication, require tight spaces. However, most AM can achieve up to  $\pm 0.005$  in, it is not enough for critical parts. A CNC machining is desired to get low tolerance down to  $\pm 0.002$  in through face milling, drilling in specific dimensions, and positional and alignment boring. The combination of AM for building and machining for finishing not only enables fast production but also gives more design flexibility. When operating additional processing, there are a few additional things to consider. At first, we should take account of how much additional materials are needed. Printed products should have enough layers for the tool. Another thing is the position that need to be machined since even 5-axis mills cannot reach some 3D-printed geometries. If a 3D-printed part requires machining, the tool reachable area must be considered during the design stage.

### 10.10 Sustainability issues in AM

As the demand for a sustainable future increase, 3D printing offers opportunities for more sustainable processes in many industries through design-optimized production. For being better sustainable manufacturing, research into waste reduction and disposal should be conducted to reduce environmental impact in AM. The management of failed prints and end-of-life products through recycling and the reusing of leftovers are good ways to reduce material costs and decrease demand for the frequent resupplying of parts by the supply chain.

### 10.10.1 Sustainability assessment of AM components

The growing interest in the sustainability of 3D printing has increased the demand for lifecycle evaluation of 3D-printed products. The printing design has a significant impact on the life cycle of printed products because printing parameters including fill pattern, print speed, nozzles, and environmental temperature affect product unity and product lifespan (Appelqvist et al. (2004); Ma et al. (2015)). Due to the complexity of considering the design stage in the life cycle evaluation of printed materials, life cycle evaluation of printed materials is still limited, and many studies are being conducted to close this gap by addressing the life cycle and design.

### 10.10.2 Energy demand and environment impact of AM

3D printing gives a net reduction of environmental impact compared to conventional machining, particularly in terms of material and energy consumption because of significantly decrease of the amount of waste generated in the process. In terms of energy consumption, there are increasing reports on the energy consumption of 3D printing. The report provided the number about the 3D printing energy consumption, such as 12–109 kWh/piece in DED, 0.007–1.25 kWh/piece in material extrusion, and 14.5–66.02 kWh/kg in PBF (Garcia et al. (2018)). The values and units vary, and even it is impossible to compare between them. The main reason is different 3D printing parameters including geometry, filling percentages, layer thickness and orientation, and supports. In terms of environmental impact, recently, the positive side but also the negative side of the environmental load of 3D printing has been reported. For example, some polymers used in 3D printing, such as ABS and PLA, can cause health problem by generating volatile organic compound (e.g., styrene, cyclohexanone, and butanol) (Wojtyla et al. (2017)) and ultrafine particle (Stephens et al. (2013)). The printed temperature plays a key part in particle emission, so more research is needed for better environmental sustainability.

### 10.10.3 Recycling/reusing of AM components

Recycling or reusing of AM component can further reduce environment impact. There have been many studies on the reuse of printed parts and the comparison of mechanical properties with printed parts using raw materials. In general, recycling processes include mechanical, thermal, and chemical recycling, but the following example shows different recycling method that is recycling 3D-printed composites using the reverse process of 3D printing. Composite materials are in demand in

industry because of their higher physical and mechanical properties compared to pure polymers, and a fully recyclable production for composites has been investigated for a better environmental effect. [Tian et al. \(2017\)](#) printed high-performance continuous carbon fiber reinforced thermoplastic composites (CFRTPs) on the base of recycling and remanufacturing of 3D-printed continuous carbon fiber–reinforced-PLA composites. The printed composite part is reproduced through the reverse process of 3D printing (remelting polymer with hot air gun and pulling the fiber out) and printed again. In this process, the fiber and polymer were recycled 100% and 73%, respectively. The remanufactured parts have no defected fibers and have good adhesion between fibers and polymers, resulting in higher tensile performance and flexural strength compared to original printed parts. In addition, this reverse process of 3D printing consumed  $67.7 \text{ MJ kg}^{-1}$  of energy in the recycling process, which is much lower than manufacturing virgin fibers. In the remanufacturing process (3D printing of recycled fiber),  $66 \text{ MJ kg}^{-1}$  was consumed. This energy consumption can be further reduced with optimized environmental control and higher printing speed.

#### 10.10.4 Reusing metal powder leftovers

Metal is one of popular feedstocks in AM including PBF, BJ, and DED. During 3D printing process, especially PBF, lots of metal powder leftovers remains in a powder bath. Most of leftover powders can be recycled through sieving, which is a one of general processing for the reuse them. After that, extra-processing is required because it is easy to have extra particles near the edge of a weld pool that fuse without attaching to the part. If these material chunks are used in the next printing, they will make internal gaps within the part. Besides the sieving, fresh powder is also mixed in the recycled powders for better mechanical properties of the final products since the materials used are aged after each printing.

The main concerns are effect of the previous printing on the leftover powders and material aging that affects the chemical properties of materials. The number of reusing leftovers is much depending on the material itself. Some materials can age quickly and are difficult to reuse the powder multiple times because of the oxidized surface of powders and the risk of porosity formation, resulting in the degradation of mechanical properties of the final 3D-printed objects. The oxidation can affect the powder melting rate under the laser, and the released oxygen is absorbed by the powders near the melting pool or is able to remain on the melted area, causing pores in the products after solidification. For example, [Gorji et al. \(2020\)](#) investigated stainless steel 316L powder, and the reused powder had a more than 10% increase in porosity and the printing with

this powder also increased the roughness of the powder surface around 28%, comparing with the new powder.

In industries, there are many attempts to recycle leftover powder as possible. One example is applying gas flow to filter out any byproducts generated during printing process. Another one is sealing the build platform for removing moisture, nitrogen, and oxygen during printing so that the chemical reactions might be minimized.

### 10.10.5 Recycling plastic waste

Plastics, which use polymers as a main ingredient, are widely used in daily products owing to their mass production and relatively low cost. Over decades, the production of plastic waste around the world has increased from 1.5 million metric tons in 1950 to 359 million metric tons in 2018, leading to environment pollution ([Shanmugam et al. \(2020\)](#)). Among various types of polymers (e.g., thermoplastics and thermosets), thermoplastics are easily recyclable due to no or low degradation of the polymer chain when melted down. The weaker interactions between polymer chains break, and their properties may not change in recycling process. The waste plastics or leftover thermoplastic materials can be recycled and used in the AM processes, especially FDM process. There are two methods to recycle the plastics that are mechanical recycling and chemical recycling. Mechanical recycling is most traditional method and is the process of collecting plastic wastes, washing, melting, and transforming the wastes into raw material for a new productive process. Chemical recycling is one of advanced recycling process, including pyrolysis and gasification and turns plastic polymers back into individual monomers so that they can be processed and remade into new materials for producing new products.

In FDM, thermoplastics such as polylactic acid (PLA), acrylonitrile butadiene styrene (ABS), polyethylene terephthalate (PET), and polyamide (PA) are commonly used as feedstocks, and these materials can be recycled as feedstocks for FDM through the simple mechanical recycling process. As one example, [Latko-Duralek et al. \(2019\)](#) processed the PET waste into filaments for 3D printing without the use of additives or modification to the polymer. The investigations for recycling PET are essential because PET waste is increasing daily due to increased use of packaging and bottles. The recycled filament had the capability for replacing commercial filament by showing comparable tensile strength and elongation. Another example is recycling ABS generated from failed/redundant 3D prints and raft/support material, which was studied by [Mohammed et al. \(2017\)](#). The ABS waste was granulated using a combination of crushing in a bench vice (for cutting large pieces into small pieces), direct cutting using wire cutters (for finer size reduction), and the

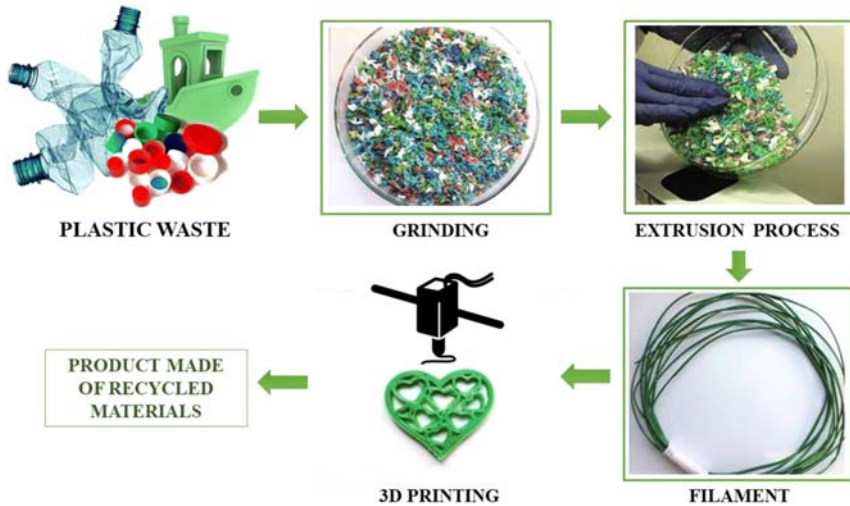


**FIGURE 10.14** A general the recycling process: recycling and grinding, filament extrusion and spooling, fused deposition modeling 3D printing, and the final products. *Used with permissions from Mikula, K., Skrzypczak, D., Izydorczyk, G., Warchol, J., Moustakas, K., Chojnacka, K., Witek-Krowiak, A., 2021. 3D printing filament as a second life of waste plastics-a review. Environmental Science and Pollution Research 28, 12321–12333, Springer Nature.*

use of modified paper shredder (for producing granules of ABS). Fig. 10.14 shows the general recycling processes from the waste granulation, filament extrusion to 3D printing for final products as a reference (Mikula et al. (2021)). Though the recycled ABS specimen exhibited the reduction in the tensile strength due to the degradation of polymer during the recycling, this can be reduced by optimizing the printing parameters.

## 10.11 Summary and future outlook

As an emerging sustainable manufacturing technology, the AM is revolutionizing the traditional manufacturing industry with a new methodology that is completely different from the subtractive manufacturing. As identified in Section 10.1, AM maximizes the utilization of material supplies by forming the patterns layer by layer. These unique manufacturing principles enable the creation of complex products quickly and accurately. Although AM addresses the limitations of subtractive manufacturing, it can be difficult to replace subtractive manufacturing completely owing to its lower production speed and lower mechanical properties of the produced specimens. AM has evolved into many different printing mechanisms over the recent years, embracing a broad range of materials and aiming at faster speed production with high

quality and low waste. As introduced in [Section 10.8](#), AM has seven widely used fundamental mechanisms but also more new mechanisms are being developed with consistent efforts of the academia and the industry. Discussed in [Section 10.9](#), the post-processing at the end of the production procedure assures the model to be consistent with the digital design in geometry and quality, with support removal, surface finish, and property enhancement. The recyclability of materials discussed in [Section 10.10](#) is making the process more environmentally benign and cost effective, ensuring the goal of sustainable manufacturing.

In the future, AM technology will be adaptive to more materials, and the newly developed materials will be able to be produced via AM technology as research efforts of materials science continue. Large volume of production will make AM possible to replace the traditional manufacturing technologies, with all the existing limitations fully addressed. The future AM will cover all the aspects of the society, ranging from nanoscale to large scale, from general hobbyist to the critical industries such as aerospace and medical applications ([CLACONnect \(2020\)](#)). The huge expansion of the AM market is in the projection. The market size is predicted to possess \$21.50 billion globally by 2025, which is approximately four times than 2015 (reported by Frost and Sullivan's research team, (2016)). Therefore, it is important to consider the sustainability of AM so as not to affect further environmental loads.

The increasing number of research have been come out and reduce the limitations of sustainability assessments in 3D printing. As it mentioned above that 3D printing is more sustainable compared to the conventional manufacturing because of low production of waste. However, more research is needed to not only to further reduce the energy consumption by optimizing printing parameters and advanced guideline to assess the sustainability of 3D printing exactly. In addition, new studies have shown that extrusion printing using polymers negatively affects the environment by generating volatile organic compounds and ultrafine particles. More research in this area is needed to reduce these environmental loads. In the meanwhile, development of materials with better recyclability can make 3D printing more sustainable.

## References

- Appelqvist, P., Lehtonen, J.M., Kokkonen, J., 2004. Modeling in product and supply chain design: literature survey and case study. *Journal of Manufacturing Technology Management* 15, 675–686.
- CLACONnect, 2020. The Pros, Cons, and the Future of 3D Printing. <http://www.claconnect.com/resources/articles/2020/the-future-of-3d-printing#:~:text=The%20future%20of%203D%20printing%20in%20the%20future%2C,increase%2C%20the%20cost%20of%203D%20printers%20will%20decrease.>

- Du, W., Bai, Q., Zhang, B., 2016. A Novel Method for Additive/Subtractive Hybrid Manufacturing of Metallic Parts. *Procedia Manufacturing* 5, 1018–1030.
- EWI, 2018. Electron Beam Melting: From Powder to Part. <https://www.ewi.org> (accessed January 30, 2021).
- Furlani, E.P., 2015. Fluid mechanics for inkjet printing. In: *Fundamentals of Inkjet Printing*. Wiley-VCH Verlag GmbH & Co. KGaA, pp. 13–56.
- Garcia, F.L., Moris, V.A.D.S., Nunes, A.O., Silva, D.A.L., 2018. Environmental performance of additive manufacturing process – an overview. *Rapid Prototyping Journal* 1355–2546.
- Gibson, I., Rosen, D., Stucker, B., 2015. *Additive Manufacturing Technologies: 3D Printing, Rapid Prototyping, and Direct Digital Manufacturing*, second ed. Springer, New York.
- Gorji, N., O'Connor, R., Brabazon, D., 2020. X-ray tomography, AFM and nanoindentation measurements for recyclability analysis of 316L powders in 3D printing process. *Procedia Manufacturing* 47, 1113–1116.
- Jadhav, V.S., Wankhade, S.R., Road, B., 2017. A review: fused deposition modeling-A rapid prototyping process. *International Research Journal of Engineering and Technology (IRJET)* 4 (9), 523–527.
- Kelly, B.E., Bhattacharya, I., Heidari, H., Shusteff, M., Spadaccini, C.M., Taylor, H.K., 2019. Volumetric additive manufacturing via tomographic reconstruction. *Science* 363, 1075–1079.
- Klocke, I.F., Wirtz, D.I.H., Meiners, D.P.W., 1996. *Direct Manufacturing of Metal Prototypes and Prototype Tools*, 1996 International Solid Freeform Fabrication Symposium (sand).
- Korpela, M., Riikonen, N., Piili, H., Salminen, A., Nyhälä, O., 2020. Additive manufacturing—past, present, and the future. In: *Technical, Economic and Societal Effects of Manufacturing 4.0*. Springer International Publishing, pp. 17–41.
- Latko-Durałek, P., Dydek, K., Boczkowska, A., 2019. Thermal, rheological and mechanical properties of PETG/rPETG blends. *Journal of Polymers and the Environment* 27, 2600–2606.
- Ma, J., Kremer, G., 2015. A sustainable modular product design approach with key components and uncertain end-of-life strategy consideration. *International Journal of Advanced Manufacturing Technology* 85, 741–763.
- Miers, J.C., Zhou, W., 2017. Droplet formation at megahertz frequency. *AIChE Journal* 63 (6), 2367–2377.
- Mikula, K., Skrzypczak, D., Izydorczyk, G., Warchol, J., Moustakas, K., Chojnacka, K., Witek-Krowiak, A., 2021. 3D printing filament as a second life of waste plastics-a review. *Environmental Science and Pollution Research* 28, 12321–12333.
- Mohammed, M.I., Das, A., Gomez-Kervin, E., Wilson, D., Gibson, I., 2017. EcoPrinting: investigating the use of 100% recycled acrylonitrile butadiene styrene (ABS) for additive manufacturing, solid freeform fabrication 2017. In: *Processings of the 28th Annual International Solid Freeform Fabrication Symposium - An Additive Manufacturing Conference*, pp. 532–542.
- Mostafaei, A., Elliott, A.M., Barnes, J.E., Li, F., Tan, W., Cramer, C.L., Nandwana, P., Chmielus, M., 2021. Binder jet 3D printing - process parameters, materials, properties, modeling, and challenges. *Progress in Materials Science* 119, 100707. Article.
- Niaki, M.K., Nonino, F., 2018. *The Management of Additive Manufacturing*, 193–220. Springer International Publishing.
- Park, S.J., Lee, J.E., Park, J.H., Lee, N.K., Lyu, M.-Y., Park, K., Koo, M.S., Cho, S.H., Son, Y., Park, S.-H., 2018. FDM-based 3D printed structure using hydrogen peroxide under ultrasonication. *Advances in Materials Science and Engineering* 2018, 3018761. Article.
- Schmidleithner, C., Kalaskar, D.M., 2018. Stereolithography. In: *3D Printing*. InTechOpen.
- Shanmugam, V., Das, O., Neisiany, R.E., Babu, K., Singh, S., Hedenqvist, M., Berto, F., Ramakrishna, S., 2020. Polymer recycling in additive manufacturing: an opportunity for the circular economy. *Materials Circular Economy* 2, 1–11.

- Singamneni, S., Diegel, O., Huang, B., Gibson, I., Chowdhury, R., 2010. Curved layer fused deposition modeling. *Journal for New Generation Sciences* 8 (2), 95–107.
- Song, X., Zhai, W., Huang, R., Fu, J., Fu, M., Li, F., 2022. Metal-based 3D-printed micro parts & structures. *Encyclopedia of Materials: Metals and Alloys* 4, 448–461.
- Stark, M.S., 2016. Improving and Understanding Inter-filament Bonding in 3D-Printed Polymers, Chancellor's Honors Program Projects. University of Tennessee. [https://trace.tennessee.edu/utk\\_chanhonoproj/1997](https://trace.tennessee.edu/utk_chanhonoproj/1997) (accessed January 30, 2021).
- Stephens, B., Azimi, P., Orch, Z.E., Ramos, R., 2013. Ultrafine particle emissions from desktop 3D printers. *Atmospheric Environment* 79, 334–339.
- Sun, S., Brandt, M., Easton, M., 2017. Powder Bed Fusion Processes: An Overview, Laser Additive Manufacturing: Materials, Design, Technologies and Applications. Woodhead Publishing Series in Electronic and Optical Materials, pp. 55–77.
- Tian, X., Liu, T., Wang, Q., Dilmurat, A., Li, D., Ziegmann, G., 2017. Recycling and remanufacturing of 3D printed continuous carbon fiber reinforced PLA composites. *Journal of Cleaner Production* 142, 1609–1618.
- Tumbleston, J.R., Shirvanyants, D., Ermoshkin, N., Januszewicz, R., Johnson, A.R., Kelly, D., Chen, K., Pinschmidt, R., Rolland, J.P., Ermoshkin, A., Samulski, E.T., DeSimone, J.M., 2015. Continuous liquid interface production of 3D objects. *Science* 347, 1349–1352.
- Vartanian, K., Brewer, L., Manley, K., Cobbs, T., 2018. Powder Bed Fusion vs Directed Energy Deposition Benchmark Study: Mid-size Part with Simple Geometry. Optomec Whitepaper.
- Wang, T.M., Xi, J.T., Jin, Y., 2007. A model research for prototype warp deformation in the FDM process. *International Journal of Advanced Manufacturing Technology* 33, 1087–1096.
- Wohlers, T., Gornet, T., 2016. History of Additive Manufacturing, Wohlers Report 2016.
- Wojtyla, S., Klama, P., Baran, T., 2017. Is 3D printing safe? Analysis of the thermal treatment of thermoplastics: ABS, PLA, PET, and nylon. *Journal of Occupational and Environmental Hygiene* 14 (6), D80–D85.
- Ziaee, M., Crane, N.B., 2019. Binder jetting: a review of process, materials, and methods. *Additive Manufacturing* 28, 781–801.

This page intentionally left blank

# Computer integrated sustainable manufacturing

---

*Steve Zhengjie Jia<sup>1</sup>, Jay S. Gunasekera<sup>2</sup>, and James Glancey<sup>2</sup>*

<sup>1</sup>Product Engineering, Litens Automotive Group, Toronto, ON, Canada;

<sup>2</sup>Mechanical Engineering, University of Delaware, Newark, DE, United States

## 11.1 Introduction to computer integrated manufacturing

---

Computer integrated manufacturing, popularly known as CIM, attempts to integrate the various functions of manufacturing using computers. These functions may include product design, analysis, optimization, production planning and control, manufacturing of individual components of the product, assembly, inspection, and quality control. Integration requires the understanding of the interrelationship among design, materials, various manufacturing processes, and the available resources such as equipment, personnel necessary, or outside sourcing. However, this book will only give a brief description of these technologies because there are many excellent books on this subject, and detailed description is outside the scope of this book.

As often stated in manufacturing textbooks, quality must be built into the product, thus reducing, or eliminating the need for expensive inspection and quality control. Also, costly product defects can be reduced or eliminated this way. Successful integration must be accomplished through computer aided design/manufacture/engineering (CAD/CAM/CAE) and optimization.

CIM system may consist of planning, design, scheduling, automation, manufacturing, inspection, packaging, warehousing, etc. The benefits of CIM such as product quality, optimizing the use of materials, equipment, energy, labor etc., have shown to be very high. Another advantage of CIM is the integration of all manufacturing functions using a single real-time

database for the entire organization. These data may include sales forecasting, CAD models, equipment capabilities, materials with their properties, manufacturing processes, finance, purchasing, sales, market analysis, and inventory.

## 11.2 CAD/CAM/CAE in sustainable manufacturing

CAD/CAM/CAE can be effectively used to design, analyze, and optimize manufacturing processes with the goal of reducing both thermal and mechanical energy, thus manufacturing parts with less pollution, and creating a path toward sustainability. CAD/CAM/CAE provides the integration of design, analysis, and manufacturing functions into a system, which is available to the user at his/her fingertips. In addition, other routine and monotonous (but important) tasks such as the preparation of bills of materials, costing, production scheduling, etc. may be performed automatically using the same computer network. Another major benefit in the use of CAD/CAM/CAE is reduced lead time from concept to design to manufacture. Product development cost can also be reduced dramatically because analysis such as the finite element method can be interfaced with design to arrive at the optimum design within a very short time.

### 11.2.1 Computer-aided design

2D, 2-1/2D or 3D geometric modeling of the product is typically done using a commercially available software such as AutoCAD, ProEngineer, SolidWorks, SolidEdge, and CATIA. 2D models may be useful in some sheet metal products, 2-1/2D in rotating parts or extrusions, and rolled products. 3D models are most common and are represented by wireframes, surface models and volume (or solid) models.

Wireframe models have solid (or dotted) lines representing edges of the product but may sometimes be ambiguous. Surface models have all visible surfaces and edges shown. Nonstraight or noncircular edges and surfaces can be represented by Bezier curves or B-splines. These methods use control points to define (and later modify the spline, if necessary) a polynomial curve or surface of a given order. If a control point in a Bezier curve is dragged/changed, the whole curve will get affected, whereas with the B-spline, a change of a control point will only affect it locally.

Solid models show visible edges and surfaces, but the data can describe the interior such as volume etc. They can be represented by swept volumes, boundary surfaces, or a combination of primitive solids, such as

blocks, cylinders etc. the dimensions can be represented as symbols and parametrically changed to modify the solid.

## 11.3 CAE in sustainable manufacturing

### 11.3.1 Introduction

Sustainable manufacturing has become a fundamental requirement nowadays. The manufacturing processes are now required to minimize the overall environmental impact to society under a life cycle perspective. The sustainability in manufacturing industry generally includes environmental sustainability, economic sustainability, and social sustainability. Sustainability is a concept and difficult to measure. Sustainability assessment in manufacturing processes is a multiobjective and interdisciplinary task and a great challenge due to its inherent complexity and uncertainty. A directly precise assessment or comparison of sustainability between different manufacturing processes can be very difficult. To achieve the sustainable manufacturing, energy consumption, water usage, and materials waste in manufacturing processes can be managed and reduced by (1) system-level eco-design and optimization of energy consumption, water usage, and materials waste through Product Lifecycle Assessment and Management. (2) Virtual manufacturing process development to reduce or eliminate the need for physical tests. (3) Integrated virtual-physical manufacturing process design and development methodology for sustainable manufacturing (Narayanan and Gunasekera, 2019).

Extensive research on manufacturing sustainability has been done in the past decades, focusing on how to use materials and resources effectively and how to reduce the energy consumption and material wastes in manufacturing processes effectively. The manufacturing processes should be designed, optimized, and controlled with environmental sustainability in mind to achieve high efficiency in energy consumption, minimum material waste, low cost, high quality, and minimum impact to society. The physical experiments have been widely used for the optimization of manufacturing processes for many years. However, physical experiments in manufacturing processes are usually very expensive in terms of both financial and environmental aspects and should be minimized and replaced by virtual experiments, whenever possible. Physical experiments should be used only for the confirmation of the predictions using virtual experiments or when virtual experiments are not applicable. Using virtual experiments to replace physical experiments whenever possible will deliver a great savings not only in time and costs but also in energy consumption and waste reduction to achieve sustainable manufacturing.

The computer-aided engineering (CAE), including finite element method (FEM), computational fluid dynamics (CFD), and multibody dynamics (MBD), is the most popular, powerful virtual experiment technique that has been widely used crossover manufacturing industry to optimize the manufacturing processes and product design and development for environmental and economic sustainability. CAE provides a multidisciplinary systematic approach to manufacturing sustainability to design and optimize manufacturing processes for sustainability and to understand the fundamental aspects of the problems in the analysis, design, and control of manufacturing processes. CAE can take many design and process parameters into account, such as the geometry and material of products and manufacturing equipment, manufacturing process conditions, mechanics of the equipment used, plant environment where the process is being conducted, etc. to investigate the complicated manufacturing process in a virtual experimental process. CAE has ability to control all the testing parameters for a truly parametric investigation virtually, which is usually very difficult for a physical experiment, analytical method, and theoretical analysis. Use of virtual experiments not only reduces the energy consumed in physical tests but also reduces the costs and shortens the time to market, thereby making the manufacturing process sustainable in terms of both environmental and economic sustainability.

In the past decade, many successful CAE applications for sustainable manufacturing have been reported. To reveal the importance of CAE technology in manufacturing sustainability, applications using FEM, CFD, MBD, and Multiphysics and Multidiscipline simulations for sustainable manufacturing are presented in the following sections.

## 11.3.2 Finite element method

### 11.3.2.1 Introduction to FEM

The finite element method (FEM) is a numerical technique that has been applied to a wide range of engineering problems. The FEM divides the geometry into many small pieces of elements by meshing process. The common points shared by multiple elements are called nodes. The FEM uses many different types of elements (Moaveni, 2020), such as 1D elements including linear element (2 nodes), quadratic element (3 nodes), and cubic element (4 nodes); 2D elements including rectangular element (4 nodes), quadratic quadrilateral element (8 nodes), linear triangular element (3 nodes), quadratic triangular element (6 nodes), and 3D elements including 4-node tetrahedral element, 10-node tetrahedral element, 8-node brick element, and 20-node brick element. Analysis using FEM is called finite element analysis (FEA). Most common FEA includes (1) Static FEA to predict displacements, strains, stresses, reaction forces, etc.; (2)

frequency studies to predict natural frequencies and the associated mode shapes; (3) thermal FEA to analyze temperature, temperature gradients, and heat flow based on heat generation, conduction, convection, radiation conditions; (4) topology optimization and shape optimization to search and identify the optimal design or solution for the given objectives and constraints with the least number of simulation runs; and (5) buckling simulations to predict the buckling failure. The FEM can easily take into account the complex geometries of products to accurately predict manufacturing process parameters. In metal forming processes, for example, those parameters can be forming load and distributions of stress, strain, strain-rate, displacement, velocity, temperature, etc. The details of the FEM theory can be found from many publications and are not discussed in detail here.

The FEA usually includes three steps. Step 1: Preprocessing, to create FEA models. First is to import, clean, and mesh the geometries being investigated and then to apply material properties, boundary conditions, and load conditions to the model. Step 2: Simulation, to submit FEA models to run simulations for solutions. The simulation is the most complicated numerical computation process. The convergence in nonlinear FEA simulations can be a very challenging task, which requires a good FEA knowledge and experience. High Performance Computing (HPC) systems have been often used to reduce computational time. Step 3: Post processing, to review and analyze the simulation results to confirm if the design and system meet the design expectations and functional requirements and if further modifications on the design and system are required for further improvements. For example, in a metal forming process analysis, an FE model is created in the preprocessing step to represent the forming process including billets, forming tools, and operation environments. The material properties, boundary conditions, and load conditions including mechanical and thermal loads are then applied to the FE model. A good knowledge of the metal forming process being investigated is very important to set up a proper model to represent the case for the simulation, and a good FEA modeling knowledge and experience is very important to balance between the accuracy of FE results and computational time, including the effective distribution of mesh density in high stress concentration areas, the reasonable simplification of detailed geometry features in noncritical regions of billet/tools, and the proper approximation of boundary/load conditions. In postprocessing, animation of the plastic deformation of the billet, load history, sectional plot, etc. can be used to provide a great insight into the forming process being studied.

The FEA plays an important role in sustainable manufacturing and has been extensively used to effectively solve problems in manufacturing industry to lower environmental impact from resource extraction and

energy consumption for both environmental sustainability and economic sustainability. A huge number of studies on various manufacturing processes using FEA have been reported by many researchers.

A few examples are given below to demonstrate the importance of FEA in sustainable manufacturing. The FEM has been used to investigate the die fill in a stream-lined die extrusion (Jia and Gunasekera, 1995) and the effects of the hydraulic pressure (residual strain and stresses) on the expansion of a thin-walled tube with longitudinal projections (Jia et al., 1996). Hadley Group, UK uses FEA to reduce the number of the traditional physical tests to achieve the sustainable cold rolling forming process for the improvement of the rolling product quality (English, 2013). The UltraSTEEL process, a patented cold roll forming process developed by Hadley, can be used to produce the strip steel for building and construction industries. Hadley invested \$30,000–\$150,000 to perform physical tests to understand and improve the mechanical and structural properties of the strip steel produced by the UltraSTEEL process, which is expensive in costs, materials wasted, and energy consumption. On the other hand, the complicated geometry formed by the UltraSTEEL process makes the analytical method impractical to accurately predict the performance and behavior. Hadley finally used nonlinear FEA to successfully solve this challenging task, which has resulted in the increase of \$4 million in sales (English, 2013). Another example is that Pilsen Steel, Czech Republic, a leading producer of castings, ingots, and forgings, uses nonlinear FEA to eliminate the multiple heating-cooling-reheating cycles in physical experiments to achieve the sustainable forging process (Tikal, 2013). The ingot cracking problem occurs during the forging process. The ingots were first cooled in water to between 500 and 600°C after casting, then placed in the forging furnace at 1100–1200°C, and late multiple cracks were found in the ingots during forging. In order to investigate the origin of the formation of longitudinal cracks in 34CrNiMo6 steel ingots in the forging process, Pilsen Steel has to investigate both the ingots heating process and the forging operation, which requires multiple times of heating-cooling-reheating cycles. This is an expansive investigation due to significantly high energy consumption. Pilsen Steel successfully solved this ingot cracking issue by using nonlinear FEA to analyze the thermal stress in the ingots during heating and to predict the parameters for the soaking process used to cool the ingots after casting before placed in the furnace. The problem was successfully solved by increasing the temperature of the ingot before the forging process and a significant heating/reheating energy was saved during the investigation, in which, FEA plays a critical role in this sustainable forging process (Tikal, 2013).

The FEA also has been widely used for the optimization of energy consumption in hot, warm, and cold forming processes. Forming

processes consume significant amount of energy. In hot forming, such as hot forging, hot rolling, and hot extrusion operations, the mechanical/electrical energy consumption during plastic deformation is significantly reduced due to the stock/billet preheating, but the thermal energy consumption in the stock/billet preheating accounts for a major portion of the total energy consumption. Almost all the thermal energy consumed in the preheating process is released back to the environment ultimately. The energy consumed in warm forming is at intermediate level for both preheating the stock and the plastic deformation. Use of warm forming or cold forming instead of hot forming can greatly reduce or even eliminate the thermal energy consumed in billet preheating and the thermal energy loss to the atmosphere. However, a great amount of mechanical/electrical energy is consumed in cold forming to achieve a same plastic deformation in hot forming operations because the forming load in cold forming is much higher than that in hot forming for the same plastic deformation. Due to this great mechanical/electrical energy consumption, a similar level of indirect environmental effect would have created during the energy generation. In addition, some annealing may be required between cold forming steps. This additional annealing consumes additional thermal energy in cold forming, which is not required in hot forming. On the other hand, since no recrystallization occurs in warm or cold forming, subsequent heat treatments to restore material properties is not needed as the original material properties are not greatly distorted, which reduces the total energy consumption over the operation. Therefore, there is a trade-off between the increased heating energy intake in hot forming process and increased mechanical energy consumption in cold forming process, and the total energy optimization should be achieved rather than focusing on energy consumed on one of the aspects. The trade-off should be carefully balanced to achieve total energy optimization for sustainable forming processes. The FEA is a very powerful tool and plays a key role in this optimization task.

### **11.3.2.2 Case study**

As a case study (with permission from Rob Mayer, President & CEO, Queen City Forging, Cincinnati, OH), nonlinear FEA has been successfully used by one of the authors of this Chapter and Fahad Al-Mufadi for the optimization of forging a rotating part for sustainable forging operations at Queen City Forging Co, Cincinnati, OH (Gunasekera et al., 2005).

The main objective of this case study was the optimization of a new preform dies design for any rotating part, so that the effective plastic strain in the dead metal zone (DMZ) of this part can be increased to a value greater than 0.5. These parts rotate at high speed thus creating very high centrifugal forces and high stresses in the part, and it is critical to control the forging parameters such as temperature and optimal die design. The yield

strength can also be increased by the optimization of the new die design since it increases the low effective plastic strain in the DMZ. This also leads to a uniform effective plastic strain throughout the formed product. The goal is to achieve the best mechanical properties through the forging of the two different rotating parts made from the alloys AA 2618 and AA 2014. In general, the main advantage of hot forging operation is gained by decreasing the inhomogeneities of the workpiece; porosities are eliminated from a cast billet, if any, because of fusion of macro or microcavities. However, all the bar stock sold to Queen City Forging Co. is subjected to sonic inspection, which virtually eliminates any significant inclusions or inhomogeneities. Another goal is the optimization of the Zener-Hollomon parameter,  $Z$ , by determining an optimal temperature and an average strain rate, in order to get an indication of the grain size of the material. The Zener-Hollomon parameter increases with an increase in the average strain rate, and the average strain rate increases with an increase in the effective plastic strain or decrease in forging time. The coarse columnar grains are replaced by smaller equiaxed, recrystallized grains that give an increase in ductility and toughness.

#### 11.3.2.2.1 Tool and die design

The design of the tool and die involve different parameters like die failure, die life, and characteristics of the designed die. The heating parameters employed in the process of forging, the material of the billet, and the material of the die and the recommendations of the die design like part line, draft, and radii are other concerns in tool and die design. Proper application of working pressures and proper die design ensures correct metal flow and the proper seating of the dies in the hammer or press. Potential defects such as underfill, laps could be minimized by good die design (including a provision for smooth progression in the shape of the forging from one die impression to the next, finishing the work in as little time as is practical), careful selection of die composition and hardness, and a forging technique that includes proper heating, any necessary descaling and correct die lubrication.

#### 11.3.2.2.2 Results and validation

An analysis of the preform die design was carried out, which would ultimately determine the workpiece to be manufactured. The die design analyzed was the one obtained from the best combinations (Fig. 11.1). This analysis was performed with the optimum work piece temperature, die temperature, and friction factor. It was done by increasing the minimum effective plastic strain and uniformity obtained and by comparing the range of values in the work piece. Also, the effect of increasing the number of revolutions of the press (i.e., increase die speed), on the strain rate, and on the applied force was studied. The data for dimension and

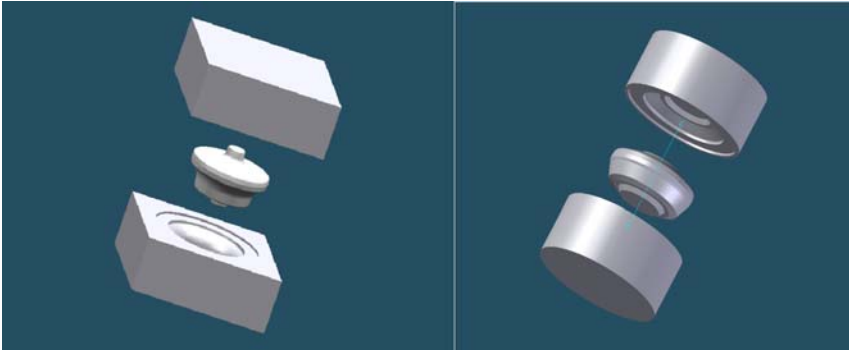


FIGURE 11.1 Model of final upper die, lower die, and the forging. Used with permission from Gunasekera, J.S., Mayer, R., Al-Mufadi, F., 2005. Case Study: Optimization of Forging a Rotating Part Using Computer Modeling at Queen City Forging Co. Cincinnati, OH.

the filling of the dies were obtained through experimentation and was compared to the data obtained through simulation in order to validate the work undertaken. Ten different preforms were designed and analyzed to obtain the final product in one and two preform stages. Only the final result is given here to limit the length of this case study. Fig. 11.2 shows the distribution of the plastic strain. Typically, when a cylindrical workpiece is forged, the DMZ is at the center of the top and bottom of the workpiece because of friction. That gives a low strain in that region. Here, the objective is to exceed 0.5 strain. The conical die at the first two hits make an indentation at the DMZ and increase the strain. The arrows show those two critical regions. The bottom edges also have lower strain because of the restriction from the geometry of the bottom die. But, that region had two earlier hits with conical die. The total strain has exceeded the 0.5 minimum strain required achieving the required fine grain size and maximizing the mechanical strength of the part.

The Zener–Hollomon parameter was optimized for the final stage to get an indication of the uniform smallest grain size by controlling the average strain rate and absolute temperature. In Fig. 11.3, it can be seen that  $Z$  is distributed within a fairly small range (or within an order of magnitude) for the AA 2618 specimen resulting in a fairly uniform microstructure. This is so because the power of both the lower and upper values for  $Z$  is the same;  $1.87 \times 10^{12} \leq Z \leq 3.48 \times 10^{12}$ . Similarly, it can be concluded that, for the AA 2014 specimen too,  $Z$  is nearly uniformly distributed, since the power of both the lower and the upper values for  $Z$  is the same,  $1.55 \times 10^{11} \leq Z \leq 2.17 \times 10^{11}$ .

$$Z = \dot{\epsilon} \exp\left(\frac{Q}{RT}\right)$$

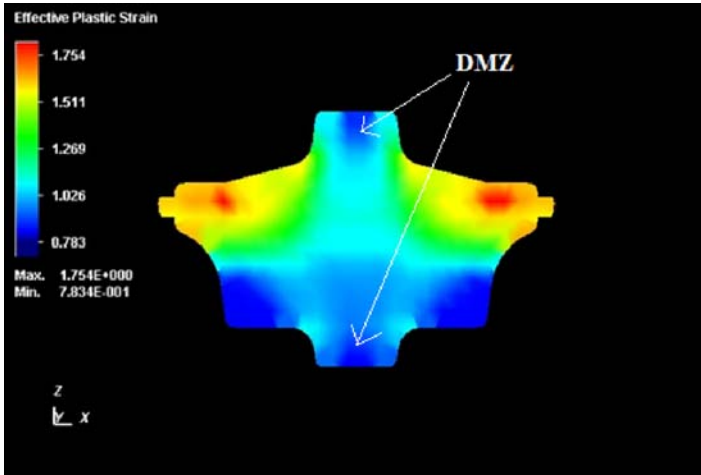


FIGURE 11.2 Effective plastic strain after using optimum preform. *Used with permission from Gunasekera, J.S., Mayer, R., Al-Mufadi, F., 2005. Case Study: Optimization of Forging a Rotating Part Using Computer Modeling at Queen City Forging Co. Cincinnati, OH.*

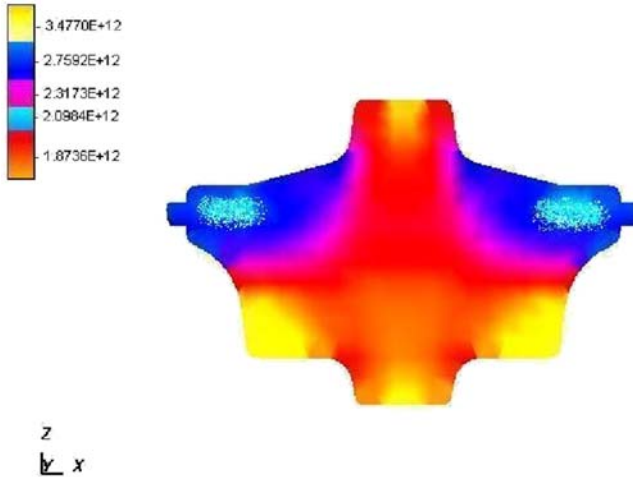


FIGURE 11.3 Distribution of Zener–Hollomon parameter. *Used with permission from Gunasekera, J.S., Mayer, R., Al-Mufadi, F., 2005. Case Study: Optimization of Forging a Rotating Part Using Computer Modeling at Queen City Forging Co. Cincinnati, OH.*

In the above expression,  $Q$  is the activation energy for deformation,  $161 \text{ kJ mol}^{-1}$ ,  $R$  is the universal gas constant,  $8.314 \text{ J mole}^{-1}\text{-K}$ , and  $T$  is the absolute temperature.

### 11.3.2.2.3 Validations of results

To substantiate the work carried out, the experimental results were compared to the ones obtained by simulation (Fig. 11.4). This comparison displayed the accuracy of the work and, hence, validated the case study. The dies were industrially fabricated for experimental work, which has been done in order to compare it with the simulation. All the parts from this study were successfully conducted at the Queen City Forging Co. The validation of the research requires the limiting tonnage capacity of the press, the workpiece's flow to the die, and the filling of the die cavities. The dimensions of the work piece and the filling of the die in the simulation were compared with the results of the actual experiment.

The dimensions of the part, obtained by simulation, were compared with that of actual experimentation, in order to see how good the results are. An actual product was obtained after the experimental work was carried out for all the three stages of the part forging. The correlation was within a few percent. Analysis through simulation is beneficial in many ways. Real-time results can be obtained in the simulation without actual experimentation. Simulation also reduces various experimental costs, saves money on materials, and eliminates valuable experimentation time, thus making the process sustainable.

The billet and the parts produced in the second stage and final stage at Queen City Forging Company are shown in Fig. 11.5. Fig. 11.6 shows a macrograph of the cross-section structure of the forged part indicating that the grains are distributed uniformly in the final stage. Fig. 11.7 shows the final finished part after five axis machining.

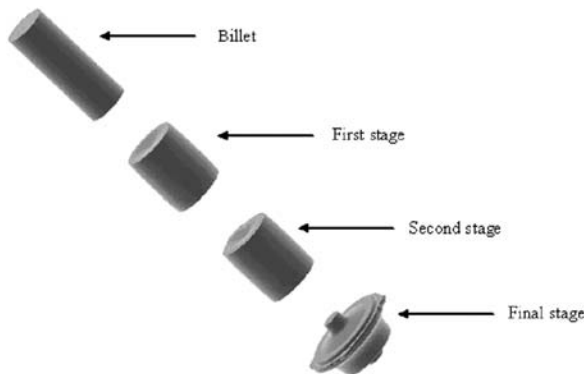


**FIGURE 11.4** Results obtained from simulated analysis for preform and final stages. *Used with permission from Gunasekera, J.S., Mayer, R., Al-Mufadi, F., 2005. Case Study: Optimization of Forging a Rotating Part Using Computer Modeling at Queen City Forging Co. Cincinnati, OH.*



**FIGURE 11.5** Results obtained for the preform and final stages. *Used with permission from Gunasekera, J.S., Mayer, R., Al-Mufadi, F., 2005. Case Study: Optimization of Forging a Rotating Part Using Computer Modeling at Queen City Forging Co. Cincinnati, OH.*



**FIGURE 11.6** Macrograph of forging cross-section structure. *Used with permission from Gunasekera, J.S., Mayer, R., Al-Mufadi, F., 2005. Case Study: Optimization of Forging a Rotating Part Using Computer Modeling at Queen City Forging Co. Cincinnati, OH.*

The results obtained by experimentation are closely confirmed by those obtained by simulation, hence, validating the theoretical part forging obtained by the finite volume method.

#### 11.3.2.2.4 Conclusions

The main objective of this research was the optimization of the new preform die design of any rotating part, which can increase the minimum effective plastic strain in the DMZ for strain homogenizing. This could lead to the improvement of the mechanical properties of the rotating part. Another primary concern of this study was to optimize Z in order to study

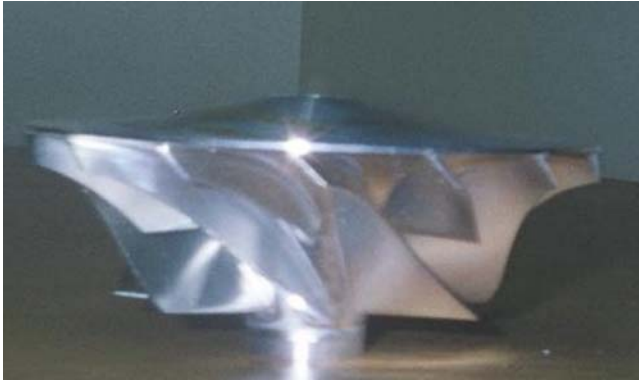


**FIGURE 11.7** Final 5-axis machined part (turbocharger impeller). *Used with permission from Gunasekera, J.S., Mayer, R., Al-Mufadi, F., 2005. Case Study: Optimization of Forging a Rotating Part Using Computer Modeling at Queen City Forging Co. Cincinnati, OH.*

the grain structure of the part. In addition, the die filling and die contact in the final stage for the chosen preform that satisfied the requirement for obtaining uniform plastic strain was verified. Through experimentation, the theoretical results obtained via finite volume method for the growth of the height, diameter, and filling of the die were validated.

This study was carried out in a systematic, step-by-step manner. Ten preform dies were designed on the computer (CAD) to analyze the effective plastic strain; the objective was to find the highest value for minimum effective plastic strain and also the minimum range (difference between maximum and minimum) for effective plastic strain in the workpiece. This minimum range indicates the most uniform effective plastic strain for a workpiece.

Of the 10 simulated designs, the best die preform design was chosen and tested using the three variables. The simulation run had a low friction factor, high die temperature, and high workpiece temperature. After the simulation was conducted,  $Z$  for the specimen was computed. Upon investigation into the methods through which  $Z$  could be increased, it was seen that an increase in the number of revolutions of the crank resulted in a higher strain rate, which, in turn, resulted in an increase in  $Z$ . Increasing  $Z$  reduces the grain size of the material. After producing forgings to the design optimized by computational modeling, forgings were sectioned and etched to reveal macrostructure, and specimens from various locations in the cross section were cut and mounted for microstructural examination. Empirical evidence obtained from the forged product demonstrated the validity of the simulation and modeling. An experimental rapid infrared heating techniques were also in use as part of this effort; extensive validation of metallurgical properties required ongoing

periodic destructive testing through the production lot. These examinations confirmed process stability, providing consistent results matching the model predictions. This study enabled Queen City Forging Company to successfully forge critical rotating parts without any defects and without too many trials.

### 11.3.3 Computational fluid dynamics

The computational fluid dynamics (CFD) is a branch of fluid mechanics and a numerical technique used to predict fluid flow, heat and mass transfer, chemical reactions, and related phenomena. CFD analysis is one of the key analysis methods used in engineering applications and has been applied to a wide range of engineering problems in many areas from aerodynamics and aerospace analysis to natural science and environmental engineering, industrial system design and analysis, fluid flows and heat transfer, etc. to predict the mass flow rate of coolant through water pump, forces on aircraft, weather patterns, etc. Basic CFD procedure includes three steps, Step 1: Preprocessing, first to create the geometry using CAD to define the fluid volume (fluid domain) and physical bounds of the problem and then to clean-up and mesh the fluid volume with uniform or nonuniform, structured or unstructured cells (elements), such as hexahedral, tetrahedral, prismatic, pyramidal, or polyhedral elements, and their combinations, and last to define the properties of the fluid materials and the boundary conditions at all the bounding surfaces of the fluid domain, and as well as the initial conditions in transient problems. The mesh quality in CFD has a great effect on the convergence and accuracy of the CFD results. The quality of CFD mesh is assessed by skewness, smoothness, and aspect ratio. The low skewness of CFD mesh is preferred. For smoothness in CFD mesh, the growth factor of 1.2 is recommended; Step 2: Simulation, to run the simulation to solve governing equations over a meshed model using numerical methods that turn partial differential equations into systems of linear equations to iteratively solve the problems for field values such as velocities, pressures, and temperatures. In the past decade, High Performance Computing (HPC) has been widely used to run CFD simulations; and Step 3: Post-processing, to perform the analysis and visualization of the simulation results, such as velocity, pressure, and temperature, etc. in relation to time and space.

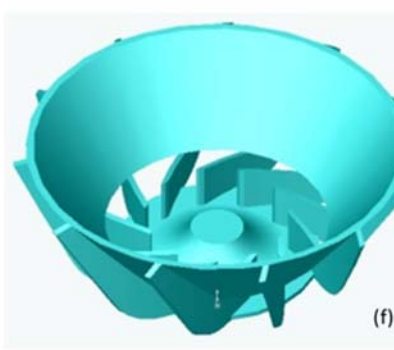
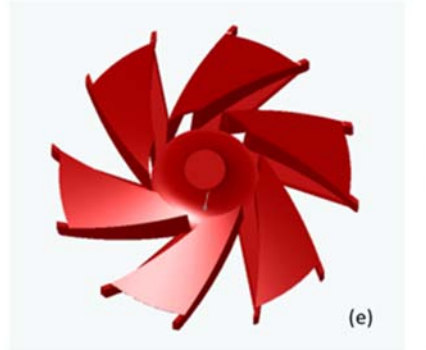
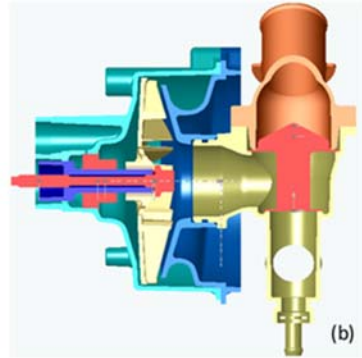
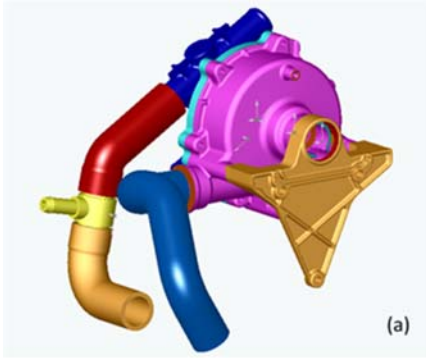
CFD has been used in many industries to reduce or eliminate the need for performing trial-and-error experimentation, including aerospace, automotive, biomedicine, chemical processing, heat ventilation air condition, hydraulics, power generation, sports and marine etc. for the design and optimization of products, equipment, and systems. Some typical CFD

application examples include the aerodynamics simulation of the flow over a vehicle or aircraft to predict drag, lift, and downforce; heat exchanger to predict heat transfer and pressure drop; and HVAC systems to assess and optimize the performance of ducts for energy consumption. A few examples of CFD applications are given below. Fig. 11.8 shows that CFD was used for the design and optimization of the water pump impeller. One existing design and seven different proposed designs of the impellers were virtually tested using CFD to compare their performance for the best design. Fig. 11.9 shows that CFD was used for the design and development of intake manifolds and valves. Significant savings were achieved by replacing physical tests with CFD virtual tests in terms of the costs, material waste, and energy consumption for both environmental and economic sustainability.

#### 11.3.4 Multibody dynamics

The multibody dynamics (MBD) generally refers the study of mechanical systems that consist of a set of rigid bodies and links connected each other by joints to restrict their relative motion. In MBD analysis, the equations of motion are numerically solved in the time domain with information of the mass, center of mass, inertia tensor of each rigid body, and interaction forces and constraints between bodies. The MBD has been widely used to investigate how a mechanical system (mechanism) works and behaviors under the influence of external forces and motions applied to the system, or what external forces and/or motions are required to make the mechanical system moves and behaviors as expected and designed. The MBD simulation provides a dynamic system-level analysis to understand how interconnected multiple moving parts interact with each other in a complex mechanical assembly system and to determine motions, forces, and interactions between multiple bodies, which are essential for engineering complex mechanisms. The MBD simulation can be used to predict the action/reaction loads generated by moving parts between them and to determine their motion, which are usually the fundamental information required in the product design and development, but it is very challenging and costly to obtain using physical tests. The MBD not only provides a powerful tool to solve the challenges of physical testing but also reduces or eliminates energy consumption and costs in physical testing to achieve sustainable manufacturing.

The typical MBD simulations include kinematic simulation to study the relative motion between bodies, dynamic simulation to study the action of forces on bodies in motion, static simulation to study the effects of forces on bodies in the absence of motion, quasi-static simulation, linear simulation, and their combination. The typical MBD analysis usually



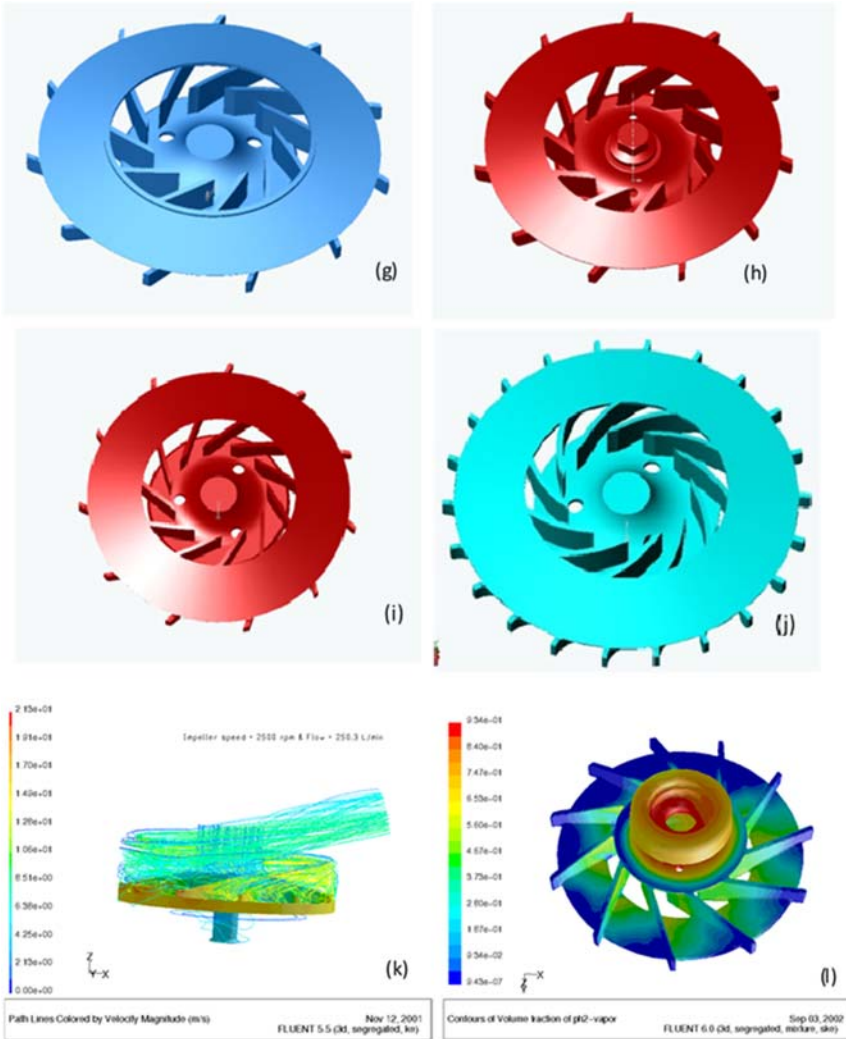


**FIGURE 11.8** Design and optimization of the water pump impeller using computational fluid dynamics. (A) Assembly, (B) section view of the pump assembly, (C) existing design, (D and E) wave design and variations, (F) cone design, (G, H, I) split design and variations, (J) final design—best performance, (K) path lines colored by velocity magnitude, and (L) cavitation analysis: the cavitation occurs at the seal area when inlet  $P \leq -11$  kPa for the given conditions.

requires the following information as inputs: mass, center of mass, and inertia tensor of rigid bodies; constraints such as joints and prescribed motions; various forces caused by springs, dampers, contact forces, frictions, gravity, and external forces; and initial conditions such as initial

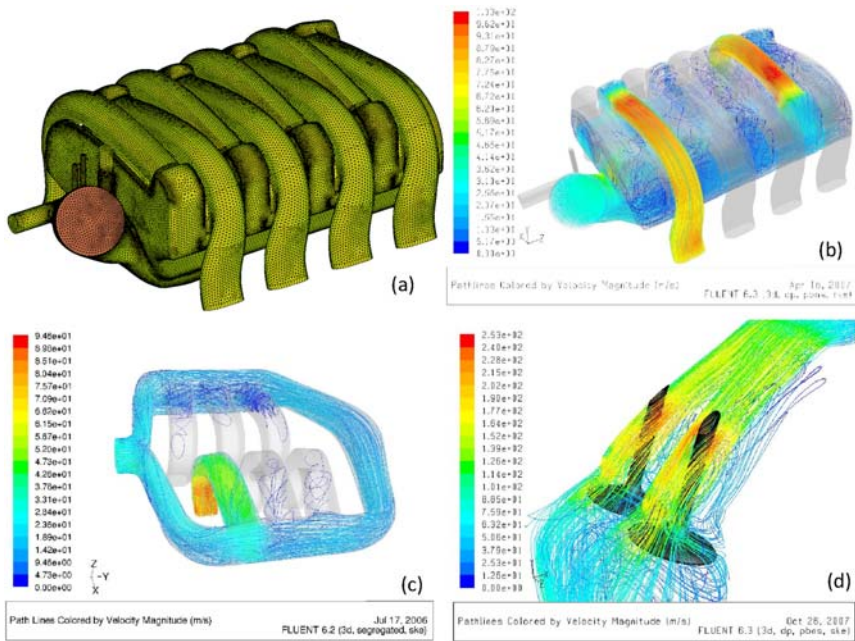


FIGURE 11.9 Development of intake manifold using computational fluid dynamics (CFD). (A) CFD mesh of intake manifold (8 ports), (B) path lines colored by velocity magnitude (intake manifold with eight ports), (C) path lines colored by velocity magnitude (intake manifold with six ports), and (D) path lines colored by velocity magnitude (valves).

position/velocity/orientation. The MBD analysis outputs usually are motions (position, velocity, and orientation) of rigid bodies and joint reaction forces, etc. The structural elements in MBD models are significantly simpler than that in detailed FEA models. Small time steps are required to reveal complex dynamical effects.

The MBD has a broad range of applications in many industries, including the applications for suspension systems, steering systems, brake systems, engines, drivetrains, etc., in automotive; pumps, robotic manipulators, conveyor belts, fork lifts, hydraulic control systems, wind turbines, solar panels, etc. in manufacturing and energy industry; landing gears, aircraft engines, space vehicles, mission-critical spacecraft mechanisms, etc., in aerospace & defense; and human locomotion, robotic limbs, sporting goods, bicycles, etc., in medical and consumer products. Fig. 11.10 shows an example, where the MBD was used to design and optimize the performance of the power lift gate. The goal is to achieve a very smooth opening and closing of the gate under many different conditions, including different gate geometries and environment temperature variations, road inclinations, motor speeds, costs, etc.

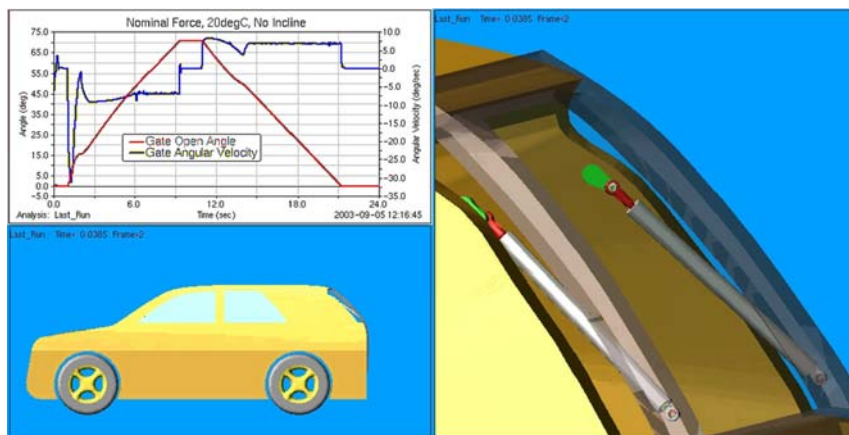


FIGURE 11.10 Performance optimization of the power lift gate using multibody dynamics.

### 11.3.5 Multiphysics and multidiscipline CAE analysis

Real-life manufacturing processes are usually multiphysics involving more than one simultaneously occurring physical fields, which challenges traditional CAE simulations since FEA, CFD, and MBD models do not share the same numerical foundation. In traditional CAE simulations, the design, development, and optimization of manufacturing products and processes are usually carried out by solving one physical phenomenon at a time and then importing the results into another CAE system to solve another physical phenomenon ([Multiphysics Learning & Networking, www.multiphysics.us/intro.html](http://www.multiphysics.us/intro.html)). Multiphysics research has increased significantly in the past 2 decades. Multiphysics simulations are the coupled simulation processes that involve multiple physical models or multiple simultaneous physical phenomena, based on a single computational framework for the modeling of multiple physical phenomena with fully coupled interaction constraints. Multiphysics simulations can be used to simulate and analyze multiple physical phenomena and behaviors at the same time, which enables co-simulation across the boundaries of engineering disciplines for system level modeling and analysis.

Typical multiphysics and multidiscipline simulations include (1) MBD-FEA motion/structural coupled analysis, where MBD provides efficient solutions to predict the kinematic behaviors such as displacements, velocities and accelerations and dynamic behaviors such as forces and moments of mechanical assemblies, and FEA provides detailed predictions of elastic/plastic deformation, strain, stress, and potential failure to gain insight into component behavior while taking into account all the

geometric, material and contact nonlinearities into account in FEA simulations. The MBD-FEA coupled simulation integrates MBD strength at system level analysis and FEA strength in nonlinear structure analysis at component-level together to provide a great capability to meet the demands on both higher accuracy and faster solution. (2) CFD-FEA fluid/structure interaction analysis, where CFD provides the pressure distributions on the structure that are used as the inputs of load conditions for FEA to predict the structural response. Thus, the influence of fluid pressures on the structure is taken into account to improve the accuracy in structural response prediction. (3) Thermo/mechanical coupled analysis, where the interactions and effects of temperature changes on structural responses are predicted, in addition to the prediction of the effects of structural mechanics and thermal conditions. There usually are two ways of coupling: the direct coupling of applying multiple physics to the model simultaneously and the chaining of passing load case results from one analysis to the next (**Multidisciplinary** <https://www.mscsoftware.com/application/multidiscipline>).

As an example, CFD/FEA interaction analysis was used for the design and optimization of a water pump impeller. The weld-line areas of the plastic impeller are the weakest areas and the max stresses in these areas must be verified to meet the acceptance criterion. In order to confirm the maximum stresses in these weld-line areas, first, a molding simulation is performed to predict the locations of the weld-line areas as shown in **Fig. 11.11B**; second, a CFD simulation is carried out to predict the pressure distribution on the surfaces of the impeller as shown in **Fig. 11.11C**; third, an FEA is conducted with the pressure distribution predicted using CFD as the input to predict the stress distribution in the impeller as shown in **Fig. 11.11D**; and lastly, to confirm the maximum stresses in the weld-line areas meet the acceptance criterion (**Fig. 11.11B, D**). In this CFD/FEA analysis, three different simulations are performed for the design and optimization of the impeller, instead of physical testing usually used in the design process, which greatly reduces the overall cost, material waste and energy consumption in the impeller design and development process to achieve sustainable manufacturing.

**Fig. 11.12** shows another example that MBD-FEA Motion/structural analysis was used for the design and development of the power lift gate. The load conditions predicted using MBD are used as the inputs in the FEA simulation to investigate the stress states in joint and shaft. The MBD-FEA simulations not only eliminate the physical testing to achieve sustainable manufacturing but also speed-up the design and development process.

### 11.3.6 Summary

A brief overview of CAE technology in sustainable manufacturing has been presented with numerous practical examples from industry and

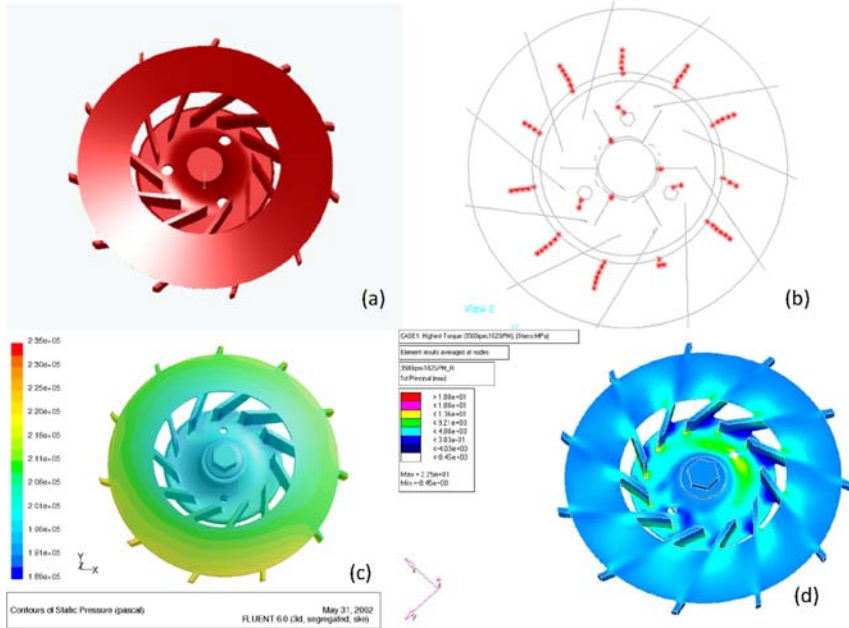


FIGURE 11.11 Computational fluid dynamics (CFD)/finite element analysis (FEA) for the design and optimization of a water pump impeller. (A) Computer-aided design (CAD) model of impeller, (B) weld-line locations predicted using Molding simulation, (C) pressure on impeller surface predicted using CFD, and (D) stress distribution predicted using FEA.

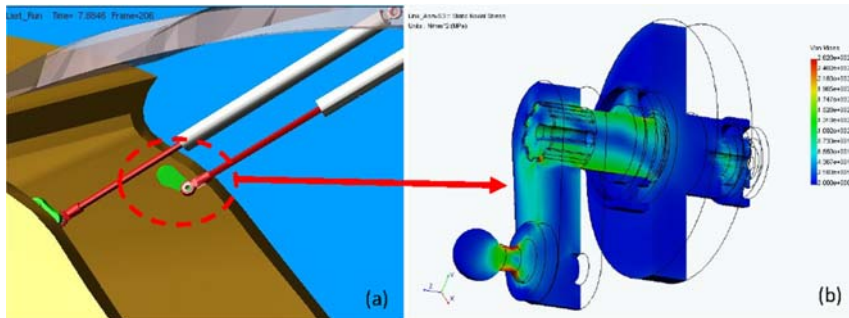


FIGURE 11.12 Multibody dynamics (MBD)-finite element analysis (FEA) simulations for the design and development of power lift gate. (A) MBD model and (B) FEA model.

research case studies. Applications using FEM, CFD, MBD, and multi-physics and multidiscipline simulations for the design, development, and optimization of manufacturing products, systems and processes have been briefly described. The FEA, CFD, MBD, etc. have been widely and

successfully used to optimize the manufacturing products, systems, and processes, especially multiphysics and multidiscipline simulations significantly improve the accuracy of the predictions, and greatly expand CAE application ranges to reduce or even eliminate physical testing. The CAE technology is a key to achieve the substantial reduction of energy consumption, material waste, and costs in manufacturing processes by the optimization of manufacturing products, systems, and processes and by the reduction or elimination of physical testing for sustainable manufacturing.

## References

- English, M., 2013. Simulation helps increase sales by \$4M - nonlinear FEA validates new cold roll forming process. *Simulating Reality Magazine III*, 2–3.
- Gunasekera, J.S., Mayer, R., Al-Mufadi, F., 2005. Case Study: Optimization of Forging a Rotating Part Using Computer Modeling at Queen City Forging Co, Cincinnati, OH.
- Jia, Z., Gunasekera, J.S., 1995. Computer simulation of hollow extrusion and drawing using 3D – FEM. In: *Proceedings of the 23rd North American Manufacturing Research Conference (NAMRC XXIII)*. Houghton, Michigan, USA, pp. 1–6.
- Jia, Z., Gunasekera, J.S., Dehghani, M., Ali, A.F., 1996. Simulation of hydraulic expansion of thin-walled tubes using the elastic-plastic FEM. In: *Proceedings of the Third Biennial Joint Conference on Engineering Systems Design and Analysis (ESDA'96)*, Montpellier, France, pp. 169–174.
- Moaveni, S., 2020. *Finite Element Analysis, Theory and Application with ANSYS*, fifth ed. Prentice Hall.
- Multidisciplinary <https://www.mssoftware.com/application/multidiscipline>.
- Multiphysics Learning & Networking, [www.multiphysics.us/intro.html](http://www.multiphysics.us/intro.html).
- Narayanan, R.G., Gunasekera, J.S., 2019. *Sustainable Material Forming and Joining*. CRC Press, New York.
- Tikal, F., 2013. Getting to the root cause of cracks - heat transfer analysis helps solve tough forging problem. *Simulating Reality Magazine III*, 4–5.

# Index

---

Note: 'Page number followed by "f" indicate figure and "t" indicate table.'

## A

Abrasive water jet machining  
(AJM/AJWM), 143

Accumulative roll bonding (ARB),  
164–165, 165f

Acrylonitrile butadiene styrene (ABS),  
307–308

Activated tungsten inert gas welding  
(A-TIG), 6

Activation energy, 175–176

Additive manufacturing (AM) process,  
7–9

- advantages and challenges, 287–288
- benefits, 7–9
- directed energy deposition (DED)  
process, 299–300
- 3D printing, 285
- energy consumption, 7–9
- energy demand and environment impact,  
305
- environmental impact, 7–9
- extrusion-based process, 294–295
- generic process, 286–287
- hybrid manufacturing, 300–301, 300f
- jetting-based process, 296–297
- limitation, 288
- metal powder leftovers reusing, 306–307
- model calculations, 7–9
- plastic waste recycling, 307–308
- posttreatment processes  
machining, 304
- property enhancements, 303–304
- support material removal, 301–302,  
302f
- surface finishing, 302–303
- powder bed fusion (PBF), 290–292
- recycling/reusing, 305–306
- sheet lamination process, 298–299
- stereolithography, 285
- sustainability assessment, 305
- sustainability issues, 304–308
- technologies, 288–289, 289t
- vat photopolymerization process,  
290–292
- waste management, 7–9

Adhesive bonding, 88–89, 91f

Agile process, 199

Air emission, foundry and metal casting  
process, 37

Aluminum alloy 2024 (Al-2024) materials  
hot working behavior, 187

- microstructural complexity, 189–190
- microstructures, 186–187, 187f
- narrow processing window, 189
- optimal processing windows, 188f
- plastic flow behavior, 189
- prior particle boundary (PPB) defects, 188
- steady state behavior, 187–188
- thermomechanical processing techniques,  
186
- whisker-matrix plastic flow behavior, 189

Aluminum foam fabrication, 2–3

Analytical hierarchy process (AHP), 260

Asymmetric rolling process, 167

Automotive component fabrication, 5–6

Axisymmetric compression tests, 216

## B

Binder jetting process, 297, 297f

Biodegradable lubricants, 70–72

## C

Cantilever piezoelectric energy harvester,  
238f

Carbon fiber–reinforced plastics (CFRP),  
65–66, 66f

Casting process, 3–4

Clean energy storage systems, foundry  
and metal casting industry, 40

CO<sub>2</sub> gas-shielded metal arc welding, 78

Computational fluid dynamics (CFD),  
326–327, 333f

Computer aided engineering (CAE)  
computational fluid dynamics, 326–327

- finite element method, 316–326
- manufacturing sustainability, 315
- multibody dynamics, 327–330
- multiphysics and multidiscipline,  
331–332
- physical experiments, 315

- Computer aided engineering (CAE)  
*(Continued)*  
 sustainability assessment, 315  
 virtual experiments, 315
- Computer-aided manufacturing of  
 laminated engineering materials  
 (CAM-LEM), 298–299
- Computer integrated manufacturing  
 (CIM) system  
 benefits, 313–314  
 computer-aided design, 314–315  
 functions, 313
- Computing-aided analyses  
 big data analytics, 15  
 cloud-based optimization, 15  
 computational power, 12–14  
 information models, 15  
 manufacturing simulations, 12–14  
 robots' usage, 15  
 smart manufacturing technologies, 12–14  
 sustainability analyzer, 14–15  
 sustainability metrics, 12–14  
 system-based modeling, 14–15  
 trials, 12–14  
 virtual machining model, 14–15
- Conceptual sustainability assessment  
 model, 264t–267t  
 attributes, 263t  
 Euclidean distance method, 278  
 expert's rating and weights, 268,  
 269t–270t  
 Grey Performance Importance Index  
 (GPII), 274–275  
 grey possibility degree and attribute  
 ranking, 275–278, 276t–277t  
 linguistic scale, 268  
 overall grey performance index (OGPI),  
 273–274, 278  
 performance rating, criteria and enabler,  
 268–271
- Conventional hot stamping process, 94f
- Coupled MQL (CSMQL) cooling method,  
 130
- Cross-rolling of sheets, 59–60, 59f
- Cryogenic cooling method, 114–115
- Cryogenic machining approaches, 119f  
 cryogenic fluids, 118  
 external cryogenic cooling, 119–120  
 indirect cryogenic cooling, 118–119  
 jet cooling approach, 118–119  
 precooling approach, 118–119  
 setup, 119–120, 119f
- Cryorolling process, 166, 166f
- Cyber-physical-system (CPS), 16
- D**
- Data Envelopment Analysis (DEA)-based  
 model, 258–259
- Decision support system, 2–3
- Design for Environment (DfE) approach,  
 206–207, 206f
- Design for Serviceability, 205
- Design for X (DFX) approach, 203
- Differential speed rolling (DSR), 58–59
- Digital light processing (DLP), 290, 291f
- Directed energy deposition (DED)  
 process, 299–300, 299f
- Direct metal deposition (DMD), 73–74
- Direct metal laser sintering (DMLS), 293
- Distance-to-target approach, 259
- Dry machining process, 114–116, 116f
- Dust collection, 39
- Dynamic material model (DMM)  
 processing mapping approach  
 apparent activation energy parameter,  
 174  
 conceptual, 175f  
 metallic system, 174–175  
 stability criteria, 174  
 strain-rate sensitivity parameter, 173  
 superposition mapping, 174–175  
 Ti–6Al–4V structurally porous materials,  
 216  
 effective strain-rate, 226  
 flow curves, 229–230  
 microstructure, 225–226  
 rolling processes, 226  
 stability maps, 224–225
- E**
- EcoInvent LCI database, 42
- ECO-Management and Audit Scheme  
 (EMAS), 41
- Electric discharge machining (EDM), 143
- Electric polarization, 236
- Electrochemical machining (ECM), 143
- Electromagnetic energy harvesting, 250
- Electron beam melting (EBM), 294
- Electron beam welding (EBW), 82
- Electrostatic energy harvesting, 250–251
- Energy harvesting technologies,  
 233–234
- Environmental Management System  
 (EMS), 41
- Environmental monitoring, measurement,  
 and control (EMMC), 41
- Equal channel angular extrusion (ECAE),  
 161–163, 162f

- Equal channel angular pressing (ECAP), 163
- Equal channel angular rolling (ECAR), 60
- Euclidean distance method, 278
- Explosion welding, 85
- Extended Producer Responsibility (EPR) laws, 197
- F**
- Figure of Merit ZT, 245
- Finite element method (FEM)
  - elements, 316–317
  - finite element analysis (FEA), 316–317
    - forming process, 318–319
    - ingot cracking problem, 318
    - metal forming process, 317
    - Pilsen Steel, 318
    - steps, 317
    - UltraSTEEL process, 318
  - metal forming processes, 316–317
  - Queen City Forging Co, case study, 319–326
    - cross-section structure, 324f
    - effective plastic strain, 322f
    - final 5-axis machined part, 325f
    - results and validation, 320–324
    - simulated analysis, 323f
    - tool and die design, 320
    - Zener–Hollomon parameter, 321, 322f
- Finite element model, 5
- Fluid lubricants, 69–70
- Flux core arc welding (FCAW), 80
- Foundry and metal casting process
  - air emissions, 33–34
  - cast product transport, 31–32
  - cleaning stage, 33
  - copper frog, 29
  - environmental issues, 32–34
  - ferrous and nonferrous, 30
  - finishing stage, 33
  - furnace, 30–31
  - gravity die casting process, 31
  - IoT and Industry 4.0, 43–46
  - inputs and outputs, 32f
  - machining operations, 31–32
  - management practices, 40–42
  - market potential, 29
  - melting, 33
  - metal composition, 31
  - mold preparation, 33
  - operations, 30–31
  - pollutant release, 33
  - preheated molten metal, 30–31
  - sand mold casting, 30
  - steps used, 30–31, 31f
  - sustainability assessment, 34, 42–43
  - sustainability concepts
    - green manufacturing, 38–39
    - lean concept, 38
    - new cupola injection system, 38–39
    - value stream mapping, 38–39
  - sustainability indicators
    - air emission, 37
    - economic aspects, 34–35
    - energy use, 36–37
    - environmental indicators, 35–36
    - environmental sustainability, 35
    - industrial sector, 35
    - material use, 37
    - social aspects, 34–35
    - solid waste, 37
    - structure, 36, 36f
    - wastewater, 37
    - water use, 37
  - sustainable manufacturing, 34–35
  - sustainable technologies, 39–40
  - technological advancements, 29
- Friction stir (FS)-assisted forging, 56–57
- Friction stir back extrusion, 55–56
- Friction stir processing (FSP), 62
- Friction stir welding (FSW), 6, 62–64, 86–88
  - formability improvement, 62
  - forming limit, 63f
- Friction welding, 86
- Friction welding of tube-to-tube plate using an external tool (FWTPET), 6
- Fused deposition modeling (FDM), 73–74, 294–295
- Fusion welding processes
  - CO<sub>2</sub> gas-shielded metal arc welding, 78
  - electron beam welding (EBW), 82
  - flux core arc welding (FCAW), 80
  - gas metal arc welding (GMAW), 78, 81t–82t
  - gas tungsten arc welding (GTAW), 78
  - laser beam welding (LBW), 82
  - plasma arc welding (PAW), 78–80
  - shielded metal arc welding (SMAW) process, 77–78
  - submerged arc welding (SAW), 80

**G**

- GaBi LCA tool, 42
- Gas metal arc welding (GMAW), 78, 81t–82t
- Gas tungsten arc welding (GTAW), 6, 78, 79t–80t
- Generic additive manufacturing (AM) process, 286–287
- Global joint topologies, 91f
- Gravity die casting process, 31
- Green cutting Fluid, 6–7
- Green lubrication, 69–73, 71t
- Green System Integration for Manufacturing Applications (Green SIMA), 15
- Grey number, 261–262
- Grey Performance Importance Index (GPII), 257–258, 274–275

**H**

- High heat input welding processes, 85
- High-pressure torsion (HPT)
  - equivalent strain, 163–164
  - fixture, 163
  - punch-die assembly, 163–164
  - schematic layout, 164f
- Hybrid additive manufacturing, foundry and metal casting industry, 40
- Hybrid laser-arc welding process, 92–95, 92f
- Hydroforming technology, 64–65

**I**

- Inclusive and sustainable industrial development (ISID), 95–97, 96t–97t
- Incremental sheet forming (ISF), 65–66, 66f
- Industry 4.0 technologies
  - cloud-based collaborative platform, 17–19
  - foundry and metal casting process, 43–46
  - lean manufacturing practices, 19
  - micro perspective, 16, 17f
  - NIST Smart manufacturing system, 16
  - product life cycle, 17–19
  - and sustainability, 17–19
  - sustainable development course implementation, 18t–19t
  - value stream map, 19
- Inorganic binders, 39
- Internet of Things (IoT) system, 16

- foundry and metal casting process, 43–46, 44f
- cyber-physical production systems, 46
- die casting industry, 43–44
- industrial IoT, 43
- machine learning techniques, 45–46
- rapid prototyping technologies, 46
- raw material handling, 45, 45f
- smart die casting model, 45–46

**J**

- Jetting-based process, 296–297

**K**

- Keyhole mode plasma arc welding process, 78–80

**L**

- Laminated object manufacturing (LOM) process, 298–299
- Laser beam machining (LBM), 143
- Laser beam welding (LBW), 82
- Laser direct deposition (LDD), 73–74
- Laser forming, 76, 77f
- Life cycle assessment (LCA), 34
- Life cycle inventory (LCI) databases, 34
- Linear friction welding (LFW), 86
- Low heat input solid-state welding, 85
- Lubricants, 69–73, 71t
- Lubricating and cooling systems., 136t

**M**

- Machining process
  - cryogenic cooling
    - drilling operation, 123–125
    - grinding, boring, and broaching operations, 127–128
    - milling operation, 125–127
    - turning operation, 123
  - cryogenic machining, 118–120
  - cutting fluids, 113–114, 135–137
  - dry machining, 115–116, 116f, 137–138
  - mineral oil usage, 138–140
  - minimum quantity lubrication machining, 116–117
  - minimum quantity lubrication (MQL) machining
    - drilling operation, 129
    - grinding operation, 130
    - milling operation, 129–130
    - turning operation, 128–129

- nonconventional machining processes, 133
  - optimization, 140–141, 142f
  - surface texturing tools, 120–122
    - drilling operation, 131–132
    - milling and grinding operations, 132–133, 133f
    - turning operation, 130–131
  - sustainable characteristics, 114–115, 115f
  - sustainable machining techniques, 114f
  - vegetable oils, 138–140, 140f
  - Magnetic pulse welding (MPW), 86
  - Magnetorheological fluid (MRF), 65
  - Manufacturing processes
    - additive manufacturing (AM), 3–4, 7–9
    - automotive component fabrication, 5–6
    - casting, 3–4
    - fusion and solid-state welding, 6
    - machining processes, 3–4
    - spent foundry sand (SFS) reuse, 4, 4f
    - sustainable machining, 6–7
  - Material forming and joining
    - adhesive bonding, 88–89
    - CO<sub>2</sub> emission, 53–55
    - extrusion and forging
      - bimetallic ring fabrication, 56–57, 58f
      - die design, 58
      - 3D printing methods, 55–56
      - finite element (FE) simulation, 55–56
      - friction stir back extrusion, 55–56
      - interface contact stress, 55–56
      - multistage cold forging process, 56–57
      - steering system output shaft, 56–57
    - flexible tooling, 67–69, 69f
    - fusion welding, 77–84
    - green lubrication, 69–73
    - hybrid joining, 92–95
    - inclusive manufacturing, 95–97
    - laser-based manufacturing, 73–76
      - direct metal deposition (DMD), 73–74
      - laser direct deposition (LDD), 73–74
      - laser forming, 76, 77f
      - powder bed fusion (PBF) method, 74–76
    - tool production, 73, 73f
  - mechanical joining
    - automotive applications, 88f
    - boron steels with aluminum, 89–90
    - fasteners, 88–89
    - material accumulation, 90, 90f
  - rolling strategies, 58–60
  - sheet stamping
    - friction stir processing (FSP), 62
    - friction stir welding (FSW), 62–64
    - hydroforming, 64–65
    - incremental sheet forming (ISF), 65–66
    - material grade replacement, 60–61
    - sandwich sheets, 66–67
    - strain rate sensitivity index, 61–62
    - warm forming, 61–62, 61f
  - solid-state welding, 85–88
  - sustainable joining process, 76–77
  - wire drawing, 58–60
- Material jetting process, 296f
- Materials development
  - activation energy, 175–176
  - aluminum alloy 2024 (Al-2024) materials, 186–190
  - aluminum extrusion industry
    - AL 6063 processing map, 180–181
    - extrusion die design configuration, 181, 181f
    - process improvement, 181–182, 182f
    - production method improvements, 180
  - classification, 158, 158f
  - manufacturing process, 156
  - material processing condition
    - optimization
    - original equipment manufacturers (OEMs), 167–168
    - product and process design, 168–169
    - selection and control, 168
    - supply chain, metal products, 168f
    - sustainability benefits, 167–168
  - material processing maps, 171–175
  - microstructural modification
    - accumulative roll bonding (ARB), 164–165
    - asymmetric rolling, 167
    - cryorolling, 166
    - equal channel angular extrusion (ECAE), 161–163
    - high-pressure torsion (HPT), 163–164
    - metal working process, 160
    - severe plastic deformation (SPD) process, 160–161
    - thermal and thermo-mechanical treatments, 159f
  - needs, 157–158
  - stability criterion
    - flow instabilities, 176–177
    - inhomogeneous deformation, 176–177
    - material instabilities, 176–177
    - strain rate, 179, 179f

- Materials development (*Continued*)
- strain-rate sensitivity (m) values, 177–178
  - stainless steel forging microstructure and property control, 191–192
  - sustainability cycle, 155f
  - workability and microstructural control
    - deformation process, 170
    - finite element predictions, 170
    - intrinsic workability, 171
    - material processing characteristics, 169–170
    - thermal gradients, 170
    - workpiece material, 170
  - workpiece behavior case study, 182–186
- Materials science, tetrahedron, 159f
- Mechanical waste energy sources, 235
- Microplasma welding process, 78–80
- Micro, small and medium enterprises (MSME), barriers, 9–10
- Minimum quantity lubrication (MQL), 6–7
- advancements, 137, 138f
  - coolant cost, 116–117
  - cooling method, 114–115
  - drawback, 116–117
  - external and internal, 138f
  - mist generation, 116–117, 117f
  - nanofluid MQL system, 116–117, 118f
  - setup, 116–117, 117f
  - small quantity lubrication, 116–117
- Mixed adhesive joint, 91–92
- Multibody dynamics (MBD), 327–330
- applications, 330
  - and finite element analysis (FEA)
    - simulations, 333f
  - mechanical system, 327
  - performance optimization, 331f
  - simulation, 327–330
- Multipoint forming, 68, 69f
- N**
- Nanofluid minimum quantity lubrication (MQL) machining, 116–117, 118f
- National Institute of Standards and Technology (NIST), 11–12
- New process development (NPD) process, 196, 201
- NIST Smart manufacturing system, 16
- Nonconventional machining processes, 133, 134t–135t, 143
- O**
- OpenLCA tool, 42
- Organic binders, 39
- Overall grey performance index (OGPI), 259–260, 273–274
- P**
- Paper-based packaging products, foundry and metal casting industry, 40
- Peltier effect, 243–244
- Perovskite solar cells, foundry and metal casting industry, 40
- Piezoelectric energy harvesting technology, 234
- FEA model, 240, 241f
  - harvester/damper mechanism, 240
  - mechanical energy, 237–239
  - patented damping device, 239–240, 239f
  - piezoelectric effects
    - electric polarization, 236
    - linear constitutive equations, 236–237
    - mechanical stresses, 235–236
  - power output, 241f
  - piezo layer thickness, 242f
  - piezo-material properties, 241f
  - thermoelectric technology, 242–249
  - torsional vibration (kinetic) energy, 239
  - torsional vibration energy harvester/damper, 240–242
- Plan-Do-Check-Act (PDCA), 41–42
- Plasma arc welding (PAW) process, 78–80
- Polyethylene terephthalate (PET), 307–308
- Polyjet process, 297
- Powder bed fusion (PBF), 74–76, 292f
- direct metal laser sintering, 293
  - electron beam melting (EBM), 294
  - selective laser melting, 293
  - selective laser sintering, 293
- Powder directed energy deposition (DED) process, 299–300
- Prior particle boundary (PPB) defects, 188
- Product development
- Agile process, 199
  - decision-making process, 201–202
  - Design for Environment (DfE), 206–207
  - Design for Safety and Quality, 205
  - Design for Serviceability, 205
  - design for X (DFX) approach, 203
  - end of life design
    - country and regional regulatory requirements, 208

- recyclability, 209
  - remanufacturing, 209
  - innovation strategy, 196
  - life cycles, 197f
    - concept phase, 196
    - decline, 198
    - growth and maturity stage, 198
    - material selections, 197
    - next generation product goals, 198
    - preplanning, 198
    - product introduction, 197
  - new process development (NPD) process, 201, 202f
  - novel products and ideas, 195
  - proactive feedback mechanism, 203
  - program release and launch, 202–203
  - remanufacturing, 207
  - stage gate process, 200f
    - business model, 200–201
    - concept development phase, 200
    - product launch, 201
    - program development stage, 201
    - technology management process, 210
  - Pulsating hydroforming, 65
  - Pyroelectric energy harvesting technology, 234, 249
- R**
- Renewable energy sources, 232–233
  - Resistance element welding (REW), 89–90
  - Rolled specimens, Ti–6Al–4V structurally porous materials
    - flow localization phenomena, 224f
    - gas pore characteristics, 222–223
    - microstructure, 227f–228f
    - stress state, 223, 224f
    - temperature distribution, 223, 225f–226f
  - Rooftop solar power, foundry and metal casting industry, 40
  - Rubber pad forming of sheets, 68–69
- S**
- Seebeck effect, 243
  - Selective laser melting, 293
  - Selective laser sintering, 293
  - Self-lubricating tool coating approach, 73
  - Severe plastic deformation (SPD) process
    - conventional metal forming process, 160
    - strain and nanostructures, 160–161
    - strengthening factors, 161
    - ultrafine grains (UFG), 161
  - Sheet lamination process, 298–299
  - Shielded metal arc welding (SMAW)
    - process, 77–78
  - SimaPro tool, 42
  - Single-point incremental sheet forming (ISF), 66f
  - Single roller drive rolling, 59
  - Smart human–robot SPR joining tool, 90
  - Solar sintered foams, 2–3
  - Solid lubricants, 69–70
  - Solid-state welding process, 6
    - explosion welding, 85
    - friction stir welding (FSW), 86–88
    - friction welding, 86
    - high heat input welding processes, 85
    - low heat input solid-state welding, 85
    - magnetic pulse welding (MPW), 86
    - ultrasonic welding, 85
  - Solid waste, foundry and metal casting process, 37
  - Spent foundry sand (SFS) reusage, 4, 4f
  - Stainless steel forging microstructure and property control, 191–192, 191f
  - Stereolithography (SLA), 285, 287
    - advanced, 291
    - bottom-up, 290
    - digital light processing (DLP), 291f
    - top-down, 290
    - two-photon polymerization (2 PP), 291
    - working principle, 290f
  - Strain rate sensitivity index, 61–62
  - Submerged arc welding (SAW) process, 80
  - Superalloys, 157
  - Surface models, 314
  - Surface texturing
    - derivative cutting mechanism, 120–121, 121f
    - drilling operation, 131–132
    - hybrid-textured tools, 121–122
    - milling and grinding operations, 132–133
    - single pattern textured tool, 121, 122f
    - turning operation, 130–131
  - Sustainability assessment, 7–9, 231–232
    - Data Envelopment Analysis (DEA)-based model, 258–259
    - Delphi method, 260
    - distance-to-target approach, 259
    - graph theory model, 258
    - Grey-based approach
      - conceptual model. *See* Conceptual sustainability assessment model
      - grey number, 261–262
      - grey possibility degree, 262

- Sustainability assessment (*Continued*)  
 solution approach, 261  
 Grey Performance Importance Index (GPII), 257–258  
 index-based approach, 259  
 Industry 4.0, 260–261  
 lean manufacturing, 259  
 linguistic scale, 263t  
 models, 11t  
 overall grey performance index (OGPI), 259–260  
 performance indicators, 10–11  
 research study objectives, 257–258  
 small and medium enterprises (SMEs), 258  
 small and medium size manufacturers (SMMs), 9–10  
 standards, 10–11  
 sustainability categorization, 12f  
 sustainability indicators (SIs), 10  
 systematic hypothetical deductive-based technique, 260  
 traditional triple bottom line sustainability metrics, 260  
 triple bottom line (TBL) approach, 11  
 weight-based inclusive sustainability indicators, 259
- Sustainability cycle, 155f
- Sustainability development education  
 academic community, 19–23  
 higher education and curriculum innovation, 19–23  
 mechanical engineering curricula, 20t–23t
- Sustainability evaluation process, 11–12, 13f
- Sustainability metrics, 12–14
- Sustainability Standards Accounting Board (SASB), 11
- Sustainable machining, 6–7
- Sustainable manufacturing (SM), definition, 1–2, 2f
- System Integration for Manufacturing Applications (SIMA) scheme, 15
- T**
- Thermal energy harvesting, 247–249  
 Thermal–mechanical joining, 89–90  
 Thermoelectric cooler (TEC), 244f  
 Thermoelectric energy harvesting technology  
 global total waste heat, 242  
 thermal energy harvesting, 247–249  
 thermoelectric applications, 245–246  
 thermoelectric effect, 243–245  
 thermoelectric generator (TEG), 242, 244f, 246–247  
 Thermoelectric generator (TEG), 244f  
 Thermomagnetic energy harvesting, 251–252, 252f  
 Thomson effect, 244–245  
 Ti–6Al–4V structurally porous materials  
 ANTARES FEA application  
 automatic remeshing control, 220–224  
 constitutive equation, 216–220  
 elemental velocity field, 219  
 general stress, 220  
 numerical calculation, 220  
 ANTARES interface  
 material behavior modeling, 221  
 microstructure comparisons, 221–222, 222f–223f  
 rolled specimens, 222–224  
 axisymmetric compression tests, 216  
 blistering formation, 213–215  
 constitutive behavior model, 216  
 deformation processing routes, 213–215  
 dynamic material model processing map, 224–230  
 dynamic material model (DMM)  
 processing map, 216  
 finite element method (FEM), 213–215  
 flow curves, 217t–218t  
 flow stress, 216, 219t  
 forming model, 215–216  
 rheological behavior, 215–216  
 Titanium-6242, 182–183, 183f  
 flow stress, 184f  
 microstructures, 182–183, 183f  
 processing map, 184–186, 185f  
 Triboelectric energy harvesting, 252  
 Triple bottom line (TBL) approach, 11  
 Tungsten inert gas welding (TIG), 6  
 Two-part adhesive system, 91–92  
 Two-photon polymerization (2 PP), 291
- U**
- Ultrafine grains (UFG), 161  
 Ultrasonic additive manufacturing (UAM)  
 process, 298–299  
 Ultrasonic consolidation (UC), 298–299  
 UltraSTEEL process, 318  
 Unit manufacturing process (UMP), 34

Unit manufacturing processes (UMPs),  
10–11

Unit Process Life Cycle Inventory  
(UPLCI), 34

## V

Vat photopolymerization process. *See*  
Stereolithography (SLA)

Vegetable oil-based lubricants, 70–72

Ventilation systems, foundry and metal  
casting industry, 39

Virtual machining model, 14–15

Volatile organic compounds (VOCs)  
reduction, foundry and metal  
casting industry, 39

## W

Waste energy harvesting  
electromagnetic energy harvesting, 250  
electrostatic energy harvesting, 250–251  
energy harvesting technologies, 233–234  
piezoelectric technology  
energy harvesting, 237–238

piezoelectric effects, 235–237  
sustainable manufacturing, 238–242

pyroelectric technology, 249

sensors and IIoT, 253

thermoelectric technology, 242–249

thermomagnetic energy harvesting,  
251–252

triboelectric energy harvesting, 252

waste energy, 234–235

Wastewater, foundry and metal casting  
process, 37

Water usage, foundry and metal casting  
industry, 39

Weight-based inclusive sustainability  
indicators, 259

Wireframe models, 314

World total final energy consumption,  
231–232, 232f

## Z

Zener–Hollomon parameter, 321

This page intentionally left blank

# SUSTAINABLE MANUFACTURING PROCESSES

EDITED BY

**R. GANESH NARAYANAN**  
**JAY S. GUNASEKERA**

*Sustainable Manufacturing Processes* provides best practice advice on sustainable manufacturing methods, with examples from industry as well as important supporting theory. In the current manufacturing industry, processes and materials are developed with close reference to sustainability issues, with an outward look to optimum production efficiency and reduced environmental impact. Important topics such as the use of renewable energy, reduction of material waste and recycling, reduction in energy and water consumption, and reduction in emissions are all discussed, along with broad coverage of deformation and joining technologies, computational techniques, and computer-aided engineering. In addition, a wide range of traditional and innovative manufacturing technologies are covered, including friction stir welding, incremental forming, abrasive water jet machining, laser beam machining, sustainable foundry, porous material fabrication by powder metallurgy, laser and additive manufacturing, and thermoelectric and thermomagnetic energy harvesting.

This book is a key reference for students and researchers with backgrounds in mechanical, industrial, materials and manufacturing engineering, and electronic production, with a keen interest in the relationship between manufacturing and sustainability. It will also aid engineers presently working in the manufacturing industry.

## Key Features

- Features practical case studies from industry experts
- Explains methods for reducing waste in foundry, machining, forming, and additive manufacturing
- Details sustainable product development and energy harvesting strategies
- Provides a detailed examination on how sustainability is measured in manufacturing

## About the Editors

**R. Ganesh Narayanan**, Professor, Department of Mechanical Engineering, Indian Institute of Technology Guwahati, Guwahati, India

**Jay S. Gunasekera**, Adjunct Professor, Department of Mechanical Engineering, University of Delaware, Newark, DE, USA.



**ACADEMIC PRESS**

An imprint of Elsevier  
[elsevier.com/books-and-journals](http://elsevier.com/books-and-journals)

ISBN 978-0-323-99990-8



9 780323 999908